EXPERIMENTAL STUDY OF THE STATIC AND DYNAMIC CHARACTERISTICS OF A LONG (L/D=0.75) SMOOTH ANNULAR SEAL OPERATING UNDER TWO-PHASE (LIQUID/GAS) CONDITIONS WITH THREE INLET PRESWIRL CONFIGURATIONS

A Thesis

by

DUNG LE TRAN

Submitted to the Office of Graduate and Professional Studies of
Texas A&M University
in partial fulfillment of the requirements for the degree of

MASTER OF SCIENCE

Chair of Committee,	Dara W. Childs
Committee Members,	Luis A. San Andrés
	Wayne N. P. Hung
Head of Department,	Andreas A. Polycarpou

May 2018

Major Subject: Mechanical Engineering

ABSTRACT

The thesis presents measured results for rotordynamic coefficients and leakage of a long annular smooth seal (*L/D*=0.75, *D*=114.686 mm, and C_r=0.200 mm) tested with a mixture of silicone oil (PSF-5cSt) and air. Due to the difficulties in (a) making 2-phase homogeneous mixtures with gas volume fraction (GVF) in a range of 10 to 92% and (b) operating the test rig, the tests are carried out for two operation ranges: (1) pure- and mainly-oil conditions (inlet GVF≤10%) and (2) pure- and mainly-air conditions (inlet liquid volume fraction (LVF) ≤8%). Leakage mass flow rate $\dot{m}$ and rotordynamic coefficients are measured, and the effect of changing inlet GVF/LVF, pressure drop/pressure ratio (PD/PR), ω, and inlet preswirl are studied. The test results are compared with predictions from a bulk-flow-model developed in 2011.

Under pure- and mainly-oil conditions, the test seal is centered, the seal exit pressure is maintained at 6.89 bar-g while the fluid inlet temperature is controlled within 37.8-40.6^{o}C. The test seal is tested with 3 inlet preswirl inserts (zero, medium, and high), 3 speeds (3, 4, and 5 krpm), 6 inlet GVFs (0%, 2%, 4%, 6%, 8%, and 10%), and 3 PDs (27.6, 34.5, and 41.4 bars) for the zero-preswirl insert, and 2 PDs (20.7 and 27.6 bars) for the medium- and high-preswirl inserts. The targeted test matrix is not completed for the medium- and high-preswirl inserts at PD≥27.6 bar due to the test-rig stator's dynamic instability.

Both predictions and measurements show a significant drop in measured and predicted direct stiffness *K* as a result of injecting air into the oil flow at PD=41.4 bar for the zero preswirl and at PD=27.6 bar for the medium and high preswirls. Since the flows are in a transitional regime, an increase of friction factor with increasing Reynolds number (*Re*), due to a GVF increment, potentially causes a reverse Lomakin effect, causing a drop in *K*. A drop in *K* could

decrease the rotor's critical speed, reduce the onset speed of instability, and cause dynamic instability. As predicted and measured, increasing inlet preswirl significantly increases cross coupled stiffness k and whirl-frequency ratio and decreases effective damping C_{eff}, which decrease the seal's stabilizing properties. The results obtained from K and k potentially relate to the instability issue (subsynchronous vibration) on the high-differential-pressure helico-axial multiphase pump, reported in 2013.

Under pure- and mainly-air conditions, due to the rig-stator's dynamic instability, tests were only conducted for the zero-preswirl insert. The test seal is centered, and inlet pressure is maintained at 62.1 bar-g. The supplied oil temperature is maintained within 35 to 37.8°C. The seal is tested with 3 PRs (0.6, 0.5, and 0.4 - corresponding to PD of 24.8, 31.1 and 37.3 bar), 3 speeds (5, 10, and 15 krpm), and 5 inlet LVFs (0%, 2%, 4%, 6%, and 8%).

As oil is injected into the air flow, measurements show an increasing trend of dynamic stiffness coefficient K_Ω for PR=0.4 and a minimum K_Ω at inlet LVF=2% for PR=0.6 and 0.5. However, predictions show no change at PR=0.4 and a drop at PR=0.5 and 0.6. With representative operating conditions for a compressor balance-piston seal (PR=0.5, ω=15 krpm, and the exciting frequency range 98-137 Hz), measured C_{eff} is significantly higher than predicted. As inlet LVF increases, predictions show a drop of the seal's stabilizing capacity (predicted C_{eff} decreased). However, measurements show the lowest measured C_{eff} is at inlet LVF=2%.

Smooth seals are not used in centrifugal compressors. The data presented here are mainly for examining the previously developed model. From the same rig, test results for tooth-on-stator labyrinth seals were recently reported. Future testing, under mainly-gas conditions, could consider different seal types, such as, hole-pattern and pocket damper seals which are used widely in compressors.

DEDICATION

This dissertation work is dedicated to my family.

ACKNOWLEDGMENTS

First and foremost, I would like to express my sincere thanks to Dr. Childs for giving me the opportunity to work at the Turbomachinery Laboratory and his invaluable support and guidance in my research.

I would also like to thank Dr. San Andrés and Dr. Hung for graciously serving on my committee.

Sincere thanks to Stephen Phillips for the technique support on the test cell, and Ray Mathews for the help in the machine shop.

Special thanks to fellow graduate research assistants Min Zhang, Hari Shrestha, J.J. Thiele. Many thanks to the undergraduate assistants Keaton Hruzek and Kyle Miller.

Finally, I want to thank my parents, my wife, and my sisters for their unfailing love and support.

CONTRIBUTORS AND FUNDING SOURCES

Contributors

This work was supported by a thesis committee consisting of Professor Dara Childs and Professor Luis San Andrés of the Department of Mechanical Engineering and Associate Professor Wayne Hung of the Department of Manufacturing and Mechanical Engineering Technology.

Funding Sources

Funding for this research was provided by the Turbomachinery Research Consortium (TRC), Texas A&M Turbomachinery Laboratory, from 09/2015 to 05/2017.

NOMENCLATURE

$\boldsymbol{A}_{ij}$	Fourier transforms of the stator acceleration in *i* direction due to a shake in *j* direction [L/T^2]
c	Cross-coupled damping coefficient [FT/L]
C	Direct damping coefficient [FT/L]
C_{eff}	Effective damping [FT/L]
C_{ij}	Damping coefficients [FT/L]
C_r	Seal radial clearance [L]
D	Seal inner diameter [L]
$\boldsymbol{D}_{ij}$	Fourier transforms of the relative displacement of the stator to the rotor in *i* direction due to a shake in *j* direction [L]
f_{Seal_X}, f_{Seal_Y}	Seal's reaction forces acting on the rotor in *X* and *Y* directions [F]
$\boldsymbol{F}_{ij}$	Fourier transforms of the excitation force in *i* direction due to a shake in *j* direction [F]
GVF	Gas volume fraction, defined by Eq. (8) [-]
H	Seal film thickness [L]
$\boldsymbol{H_{ij}}$	Complex dynamic stiffness coefficients introduced in Eq. (19) [F/L]
k	Cross-coupled stiffness coefficient [F/L]
k_Ω	Cross-coupled dynamic stiffness, defined by Eq. (37) [F/L]
$\bar{k}$	Average of k_Ω over a range of excitation frequencies
K	Direct stiffness coefficient [F/L]
K_{eff}	Effective stiffness [F/L]
K_{ij}	Stiffness coefficients [F/L]

K_Ω	Direct dynamic stiffness, defined by Eq. (36) [F/L]
L	Seal length [L]
m_q	Cross-coupled virtual mass coefficient [M]
$\dot{m}$	Mass flow rate [M/T]
M	Direct virtual mass coefficient [M]
Ma	Mach number [-]
M_{ij}	Virtual mass coefficients [M]
$[\boldsymbol{M}_S]$	Stator-mass coefficient matrix [M]
M_{sij}	Mass coefficients of the stator assembly [M]
P	Pressure [F/L^2]
PD	Pressure drop, PD=inlet pressure P_i-exit pressure P_e [F/L^2]
P_{gi}	Gas pressure at seal inlet [F/L^2]
PR	Pressure ratio, PR=P_e/P_i [-]
P_V	Liquid vapor pressure [F/L^2]
$\dot{Q}$	Volume flow rate [L^3/T]
Re	Reynolds number [-]
Re_a	Axial Reynolds number [-]
Re_θ	Circumferential Reynolds number [-]
S	Liquid surface tension per unit length [F/L]
T	Temperature [T]
V_a	Axial bulk-flow velocity [L/T]
V_θ	Circumferential bulk-flow velocity [L/T]
$V_{\theta 0}$	Circumferential velocity of the fluid at the seal inlet [L/T]

WFR	Whirl Frequency Ratio [-]
x, *y*	Relative displacements of the stator to the rotor in *X* and *Y* directions [L]
μ	Viscosity [FT/L^2]
γ	Specific Heat Ratio [-]
ξ	Empirical entrance loss coefficient [-]
ρ	Density [M/L^3]
ω	Rotor speed [T^{-1}]
Ω	Excitation frequency [T^{-1}]

Subscripts

X, *Y*	*X* and *Y* directions of the coordinate system defined in Fig. 17.
e	Seal exit condition
i	Seal inlet condition
l	Liquid component
g	Gas component

Acronyms

GVF	Gas Volume Fraction
LVF	Liquid Volume Fraction, LVF=1-GVF
SSV	Subsynchronous Vibration

TABLE OF CONTENTS

LIST OF FIGURES

LIST OF TABLES

1. INTRODUCTION

Multiphase pumping and wet-gas-compression technologies offer more choices for subsea and downhole applications to reduce costs.

Multiphase pump (MPP) units have been installed onshore, offshore, subsea and downhole for trials. MPPs can be used to overcome pressure from downstream resistance or to initiate a well flow during startup [1]. They subsequently reduce the cost by 30% compared to a conventional system with a gas-separation unit [2]. But, the challenge is to design a robust machine that can be operated in extreme cases in which gas volume fraction (GVF) varies from 0 to 100%. There are a number of new pump designs catered for those extreme services, for example, helico-axial-pump or multivane-impeller designs [1]. Based on experience, pump rotordynamic behavior is a key issue for a smooth mechanical operation. Bibet et al. [3] reported a subsynchronous vibration (SSV) for a high boost helico-axial multiphase pump, which has a differential pressure of 150 bar. The problem was due to de-stabilizing forces at the balance piston operating under a multiphase flow.

Similar to multiphase pump services, wet-gas compression offers an attractive benefit from an economic view. It reduces weight and size of a compressor footprint, and consequently brings down installation costs. However, operations under 2-phase flow operations probably affect compressors' rotordynamic stability which is highly related to compressors' balance-piston seals.

Therefore, measuring rotordynamic behavior of annular seals, i.e., inter-stage seals, impeller-eye seals, or balance piston seals, operating under multiphase flows in pumps and compressors is necessary to design such machines in extreme service conditions. Annular seals have been used widely in turbomachinery applications, as shown in Fig. 1, to restrict secondary leakage or to reduce thrust loads on rotor assemblies. Annular seals, i.e., smooth seals, labyrinth seals, pocket damper seals, honey comb seals, etc., are typically selected based on their service or application. Smooth seals are mainly employed in centrifugal pumps, not compressors.

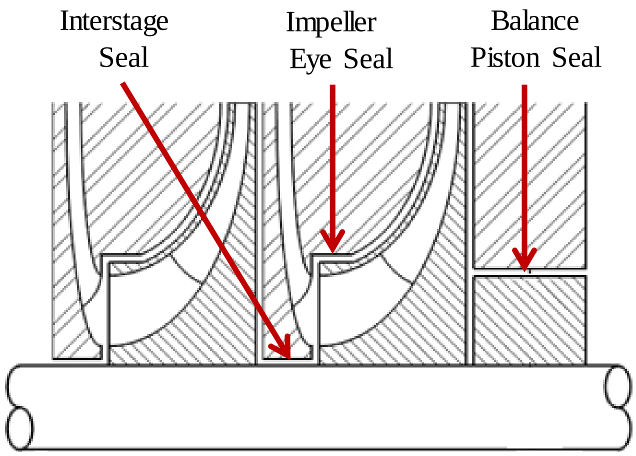

Figure 1 Annular seals in a multistage centrifugal pump

Although smooth annular pump seals have geometry similar to a plain journal bearing, their flow structure and pressure development are different. Due to the Lomakin effect from the high-pressure difference crossing a seal, smooth seals can produce a large stiffening effect [4]. On the other hand, a circumferential flow inside the seal could produce undesired cross-coupled dynamic force which affects seal stability. Hence, smooth seals have a significant influence on rotordynamic behaviors of centrifugal pumps.

Following Childs [5,6], the reaction forces produced by a centered annular seal are modeled by the following rotordynamic-coefficient model:

$$-\begin{Bmatrix} f_{Seal\_X} \\ f_{Seal\_Y} \end{Bmatrix} = \begin{bmatrix} K & k \\ k & K \end{bmatrix} \begin{Bmatrix} x \\ y \end{Bmatrix} + \begin{bmatrix} C & c \\ c & C \end{bmatrix} \begin{Bmatrix} \dot{x} \\ \dot{y} \end{Bmatrix} + \begin{bmatrix} M & m_q \\ m_q & M \end{bmatrix} \begin{Bmatrix} \ddot{x} \\ \ddot{y} \end{Bmatrix} \quad (1)$$

For two-phase flow, those coefficients might be dependent on excitation frequency, Ω. Equation (1) can be re-written as,

$$-\begin{Bmatrix} f_{Seal\_X} \\ f_{Seal\_Y} \end{Bmatrix} = \begin{bmatrix} K(\Omega) & k(\Omega) \\ -k(\Omega) & K(\Omega) \end{bmatrix} \begin{Bmatrix} x \\ y \end{Bmatrix} + \begin{bmatrix} C(\Omega) & c(\Omega) \\ -c(\Omega) & C(\Omega) \end{bmatrix} \begin{Bmatrix} \dot{x} \\ \dot{y} \end{Bmatrix} + \begin{bmatrix} M(\Omega) & m_q(\Omega) \\ -m_q(\Omega) & M(\Omega) \end{bmatrix} \begin{Bmatrix} \ddot{x} \\ \ddot{y} \end{Bmatrix} \quad (2)$$

The reaction forces in Eq. (2) can be resolved into circumferential and radial components, as shown in Fig. 2. For a rotor precessing at frequency Ω with a radius of e_o, the two force components are:

$$\frac{F_r}{e_o} = K_{eff} = K(\Omega) + c(\Omega)\Omega - M(\Omega)\Omega^2 \quad (3)$$

$$-\frac{F_\theta}{e_o} = C_{eff}\Omega = -k(\Omega) + C(\Omega)\Omega + m(\Omega)\Omega^2 \quad (4)$$

where, F_r is the seal reaction force in the radial direction, defining the effective stiffness K_{eff}, which resists radial motions, F_θ is the seal reaction force in circumferential direction, defining the effective damping C_{eff} which indicates the seal's stabilizing capability.

In the past, most research on multiphase flow of annular seals focused on cryogenic flows for rocket engines where a phase change of the fluid produces 2-phase flow. As a need to operate turbomachines under multiphase-flow applications, there have been a few studies working on modeling and experiment to investigate rotordynamic behavior of annular seals under multiphase-flow conditions for commercial centrifugal pumps and compressors. This thesis follows that line. It deals with two-phase flow that is a mixture of a gas and a liquid and does not involve a change of phase.

There are not many studies on mixed-flow conditions for annular seals. The following paragraphs discuss existing issues of operation with mixed flows in turbomachines and then summarize the past and current studies on mixed flows for turbomachinery applications, especially for annular seals.

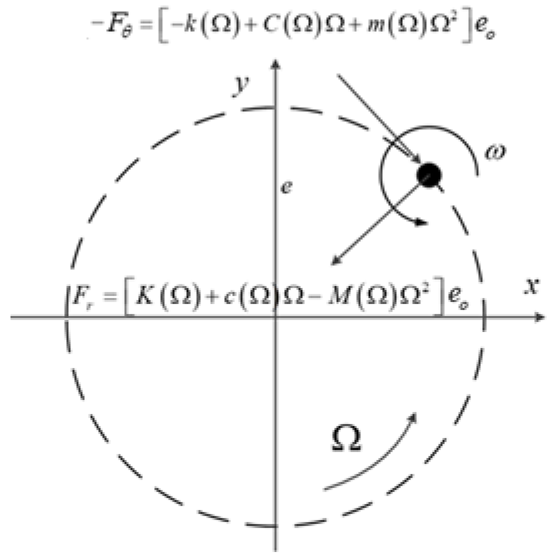

Figure 2 Seal forces on a forward precessing rotor

1.1 Operational Issues under Multiphase Flows in Turbomachinery

1.1.1 Wet-gas Compression Applications

In 2005, Brenne et al. [7] presented the performance test results of a single-stage centrifugal compressor under wet-gas conditions. The test covered typical flow conditions as in gas/condensate field production in the North Sea, i.e., GVF ranging from 97 to 100% for a mixture of hydrocarbon gas and hydrocarbon condensate. The compressor was designed to handle 4332 kg/min flow rate of dry gas hydrocarbon (molecule weight of 18.49), and was not designed for wet-gas services. The design inlet and discharge pressures are 130.2 bar and 161.8

bar, respectively. Under wet-gas operating conditions, there were two schemes of introducing liquid-gas mixture into the compressor inlet, namely, (a) droplet mist flows or (b) uniform liquid film at the inlet pipe surface. During the test at a speed of 9651 rpm, GVF ranging from 97 to 100%, with a suction pressure of 70 bar, the machine performed well in both liquid injection schemes. However, a sign of peak SSV at one-half of the running speed, appeared when the suction was brought down to 30 bar at a GVF of 97% (with a gas quality of 0.530). The SSV disappeared when GVF was increased to 98% (with a gas quality of 0.62). Brenne et al. [7] believed the entrainment of liquid into annular-impeller-eye and balance-piston labyrinth seals were likely the cause of the SSV.

In 2011, Griffin and Maier [8] reported a design in which the centrifugal compressor was incorporated with a turbo separator for wet-gas compression applications. The compressor was operated at 37.9-bar inlet pressure and speeds of 12 to 13.5 krpm. The log dec was increasing as liquid/gas mass ratio was increasing. Interestingly, liquid injection showed a positive impact on stability.

As reported in 2014 by Bertoneri et al. [9], GE had been collaborating with South West Research Institute to examine a wet-gas compressors' performance due to demands from subsea applications. The following discussion summarizes the key findings, focusing on rotordynamic performance, from the wet-gas testing campaign. The phase I test was completed in 2010, and subsequently the phase III was completed in 2013.

In 2011, Ransom et al. [10] reported the first set of test results from Phase I of the wet-gas test campaign. The paper focused on the mechanical performance of a two-stage compressor operating with a suction pressure of 20 bar-a and GVF ranging from 95 to 99.5%. The test was conducted with air and water. The compressor ran smoothly under dry compression. However, a low-frequency axial vibration started increasing once water was injected. The authors thought that the two-phase flow had a significant influence on rotordynamic behaviors of impeller-eye and shaft labyrinth seals. They believed that as water was injected and entered the balance-piston labyrinth seal, it occupied the cavity, between the seal and the rotor, and reduced the balance piston seal's ability to balance the thrust force.

In 2014, Bertoneri et al. [9] continued reporting the result of the wet-gas test campaign in Phase III. In this phase, rotordynamic stability and seals were assessed based on the previous test's observation at the balance-piston labyrinth seal, reported in [10]. A mixture of air and water with liquid volume fraction (LVF) ranging from 0 to 3% at the compressor inlet was tested. Tests were conducted with a direct injection of water into the compressor annular labyrinth seals, i.e., the impeller eye seals, the balance piston seal, and the shaft-end seals, as well.

In 2014, Vannini et al. [11] reported in detail the rotordynamic performance of the two-stage centrifugal compressor, introduced by Bertoneri et al. [9], operating under wet-gas conditions. At high flow rates, operating with a suction pressure of 10 bar-a and a speed of 13.5 krpm, as LVF level increased, the authors reported SSV at about 0.45 times the running frequency (0.45Xrev). The authors believed the source of the SSV came from the balance-piston labyrinth seal where liquid was trapped inside the seal. Interestingly, the SSV disappeared as nitrogen was injected into the balance-piston labyrinth seal.

As a solution, a pocket damper seal (PDS) was proposed to replace the tooth-on-stator labyrinth in the balance-piston position. Figure 3 shows both the labrinth seal and the PDS. As suggested by the authors, PDS would break the circumferential flow and as a consequence remove SSV. The result of this implementation showed a very small overall vibration, i.e., reducing from 20 μm to a few microns only, and there was no sign of SSV. A detailed computational fluid dynamic (CFD) study to compare the effect of the labyrinth seal and the PDS on the rotordynamic behavior was presented by Vannini et al. [12] in 2015, and it agreed with Vannini et al. [11].

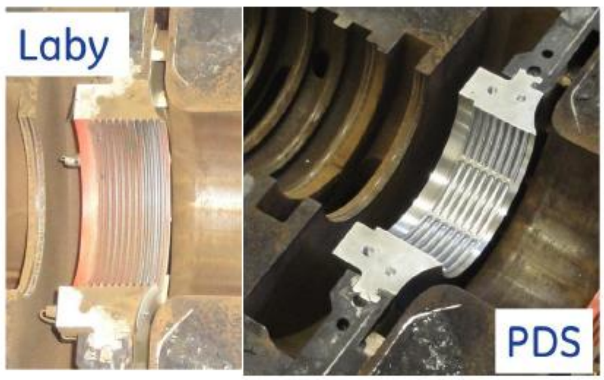

Figure 3 Labyrinth seal and pocket damper seal on the balance piston position. Reprinted with permission from [11]

In 2015, Vannini et al. [12] conducted a CFD study to further validate the experimental results observed by Vannini et al. [11]. Even though the experiment was conducted at LVF up to 3% in the main stream, the actual LVF in the seal was much higher than in the main stream. The author stated that it was reasonable to assume a 30% LVF entering the piston seal. CFD simulations were performed for high liquid loading conditions, LVF = 30% for both the labyrinth seal and the pocket damper seal. As observed, liquid tended to be trapped inside the labyrinth seal's cavity, i.e., up to 50% of the cavity filled with water, while the LVF inside the PDS was always smaller than 30% (no actual volume each seal had was given). The authors thought this could explain the SSV observed in [11] for the labyrinth seal case. The more fluid that accumulated in the seal cavity, the more inertia was generated in a tangential direction. An interesting observation obtained by CFD simulation was, in the case of PDS, there was an opposite direction circulation of the liquid w.r.t. the rotor's rotational direction. Further simulation also showed that, for a flooded situation, the PDS could empty faster than the labyrinth seal. CFD successfully simulated the scenario of SSV developed in the labyrinth seal under 2-phase flow condition. Simulations showed that, for wet-compression service, a tooth-on-stator labyrinth seal was not a good choice for a balance piston seal.

1.1.2 Multiphase Pumping Applications

A case of rotordynamic instabiltiy of a helico-axial multiphase pump was reported in 2013 by Bibet et al. [3]. It was the first helico-axial pump designed with a balance piston. The pump could generate a high differential pressure of 150 bar. A smooth surface that could handle solid particles or multiphase fluid was selected for the balance piston. The authors performed a CFD evaluation for the balance piston design with three segments separated by swirl brake rows between segments, shown in Fig. 4. They believed a low swirl factor could maximize the Lomakin effect and increase direct stiffness for the balance piston. The test was then performed on a 1.8 MW 13-stage helico-axial multiphase pump, with the balance-piston design shown in Fig. 4, running at 4,600 rpm with 2 different mixtures, namely, one with low viscosity – a mixture of water and nitrogen, another one with higher viscosity – a mixture of mineral oil and air. The pump performed well, both hydraulically and mechanically for a low viscosity mixture at a 30% GVF and a 150-bar pressure difference. However, the authors reported SSV for some cases where the pump operated at relatively low differential pressures in the higher-viscosity mixture. In cases of SSV, balance-piston rotordynamic simulation showed that the whirl frequency ratio was greater than 1, and the damping ratio was negative. They concluded that the destabilizing force happened at the balance piston. A different balance piston design for higher-viscosity mixture was proposed and tested with good rotordynamic performance; however, no detail of the new design was given in the paper.

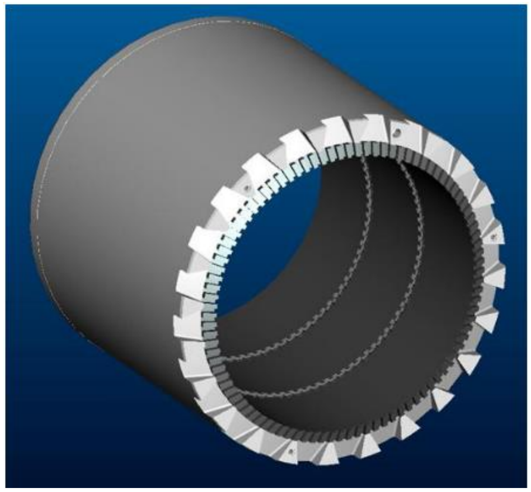

Figure 4 Balance piston design. Reprinted with permission from [3]

1.2 Multiphase Flow Research: Cases of Mixtures of Gas and Liquid

1.2.1 Experimental Studies

One of the first experiments for annular seals in multiphase flow was conducted by Iwatsubo and Nishino [13] in 1994 which investigated the static and dynamic behaviors of annular seals in turbopumps. The smooth seal tested was long (L/D=1, D=70mm, C_r=0.5mm), running up to 3.5 krpm with a mixture of air and water with GVF to 70%. The tests determined the effect of void ratios, inlet pressures, spin speeds, and preswirl velocities on the dynamic forces generated by the seal. The paper showed that, as the void ratio increased, all direct and cross-coupled force coefficients, i.e., stiffness, damping, and added mass coefficients, dropped.

In 2015, San Andrés et al. [14] introduced a multiphase test rig and reported experimental results, including leakage and force coefficients for a short annular seal (L/D=0.36, D=127 mm, and C_r=0.127 mm). The fluid was a mixture of ISO-VG10 oil and air. No shaft rotation was performed in their experiment. The results showed that mass flow rate increased, as expected, as LVF increased. For dynamic-force responses at inlet pressure of 2 bar-a and LVF to 4%, the real part of the direct dynamic stiffness [$Re(\boldsymbol{H}_{xx})$ and $Re(\boldsymbol{H}_{yy})$] was well fitted with a $(K - M\Omega^2)$ curve, while the imaginary part was not a linear function of excitation frequency [$Im(\boldsymbol{H}_{xx})$ and $Im(\boldsymbol{H}_{yy}) \neq C\Omega$]. The paper then compared the measured results with a prediction based on San Andrés's research [15] in 2011. The prediction provided good agreement about leakage and pure-gas dynamic stiffness; however, the dynamic stiffness at mixing conditions was not well predicted.

In 2016, Voigt et al. [16] presented a collaborative work between the Technical University of Denmark and Lloyd's Register Consulting. The aim was to develop a test facility to investigate the rotordynamic coeffcients for annular seals operating under multiphase flows (mixtures of air and water). The rig used an active magnetic bearing (AMB) approach to provide perturbation to test seals. The paper detailed the calibration for a Hall sensor system used by the AMB system to measure excitation force – a new technology trend. The rig would be used to validate CFD results, presented by Voigt et al. [17] in 2016 . The CFD covered two extreme ranges of air-water mixtures (LVF=0%, 3%, 5% and GVF=0%, 3%, 5%) with a smooth seal (L=83 mm, D=110 mm, and C_r=0.3 mm). Overall, the CFD results showed a clear drop of the direct damping as the percentage of gas increased; however, there was a linear relationship between the real parts of direct dynamic stiffness and excitation frequency for GVF = 0%, 3%, and 5%. This contradicted the previous experimental results presented in San Andrés [4] and Childs [5], where for pump seals, the real parts of direct dynamic stiffness is a quadratic function of exciation frequency, i.e., $Re(\boldsymbol{H}_{ii}) = K - M\Omega^2$. The future experimental results from the rig presented in [16] would be a good reference to validate the CFD study.

In 2017, San Andrés and Lu [18] presented static and dynamic results in the same test rig as presented in [14] but with shaft rotation. A [*K*][*C*][*M*] model in which [*K*], [*C*], and [*M*] were frequency-independent modeled the pure-oil condition cases well, but not for a mixture where the seal's direct dynamic stiffness $Re(\boldsymbol{H}_{ii})$ increases with excitation frequency Ω. The results showed a decrease of the direct damping coefficient and the cross-coupled dynamic stiffness when GVF increased; the lower the GVF, the larger the effective damping. In general, the predictions for force coefficients based on the bulk-flow model developed by San Andrés [15] showed a good agreement for GVF to 60%. For GVF>60%, the predicted results of the force coefficients were lower than measured.

In 2017, Zhang et al. [19] published a set of test results in the multiphase test rig used here. The tests were for a smooth seal (*L/D*=0.65, *D*=89.306 mm, and C_r=0.188 mm) under mainly-air (wet-gas) mixtures of air and silicone oil (PSF 5cSt). Tests were performed for an inlet pressure of 62.1 bar-g, speeds to 20 krpm, inlet LVF ranging from 0 to 8%, and PR of 0.43, 0.5, and 0.57. The paper reported a slight drop in leakage mass flow when inlet LVF increased to 2%, and then the leakage increased eventually as inlet LVF increased from 2 to 8%. On the other hand, the cross-coupled dynamic stiffness peaked at inlet LVF=2%, while direct dynamic stiffness decreased as inlet LVF increased. The results for damping and effective damping were also reported. The authors then compared the measurements with the prediction from the bulk-flow model code developed by San Andrés [15]. In general, the predicted leakage and damping coefficients matched well with the measurements; however, the code did not predict well the dynamic stiffness and the effective damping in mixture conditions.

1.2.2. Modeling Studies

Several models have been developed to study leakage and rotordynamic behavior of annular seals under cryogenic-flow conditions, but not for two-phase flows that are mixtures of a gas and a liquid.

San Andrés [15] developed a model to examine an effect of bubbly mixtures on the rotordynamic characteristics of annular smooth seals. The model was developed for flow mixtures from all-liquid to all-gas. The fluid mixture was assumed to be homogenous. Calculations presented for an example mixture of nitrogen gas and light oil (ISO VG2) was examined for a smooth seal (L=87.6mm, D=116.8mm, C_r=0.1267mm). In general, the predictions showed a drop in leakage and power loss when the liquid content increased. The seal's force coefficients were strongly influenced by excitation frequency. The laminar-to-turbulent-flow transition was a key influence on these coeffiecients. The cross-coupled dynamic stiffness and direct damping tended to decrease as GVF increased. As GVF changed, the direct dynamic stiffness showed both hardening and softening effects, i.e. increasing or decreasing stiffness as excitation frequency increased.

In 2011, Arghir et al. [20] predicted the influence of bubbly flows, i.e., GVF ranging from 0.1% - 10%, on textured annular seals by using a two-control-volume bulk-flow model. An example of a textured seal, with L=35 mm, D=76.5 mm, and C_r=0.100 mm, was used to examine the effect of bubbly flow. The results showed a frequency dependency at high GVF for stiffness, damping and added mass. The added mass, stiffness, and cross-coupled damping coefficient dropped as GVF increased; whereas, direct damping increased.

2. OBJECTIVES

Zhang [21] previously presented measurements for a smooth seal (*L/D*=0.65, *D*=88.9 mm) with a range of radial clearances (C_r=0.188, 0.163, and 0.140 mm) using a mixture of gas and liquid. In [21], under pure- and mainly-liquid conditions (inlet GVF≤10%), the speed was in a range of 5 to 15 krpm; and under pure- and mainly-air conditions (inlet LVF≤8%), the speed was in a range of 10 to 20 krpm. However, in this thesis, the test rig is changed to determine the impact of changing the preswirl on a smooth seal (*L/D*=0.75, *D*=114.686 mm, and C_r=0.200 mm) using a mixture of gas and liquid. The detailed work covers the following tasks:

1. Modify the existing seal housing to accommodate the test with a number of inlet preswirl inserts.
2. Perform experiments and data analysis to investigate the effect of changing inlet GVF/LVF, pressure drop or pressure ratio (PD/PR), rotor speed, and inlet preswirl on leakage mass flow rate and rotordynamic coefficients of a smooth annular seal.
3. Compare measured results to the predictions from *XLHseal_mix* code, developed by Dr. San Andrés at Texas A&M University, to validate his predictive model, presented in [15], for a smooth annular seal operating under a mixture of gas and liquid.

The balance of this thesis covers:

- Section 3 describes the test rig set up.
- Section 4 discusses experimental procedure.
- Section 5 presents pure- and mainly-oil measured results, including leakage and rotordynamic coefficients.

- Section 6 compares predictions and measurements for pure- and mainly-oil testing conditions.
- Section 7 presents pure- and mainly-air measured results, including leakage and rotordynamic coefficients.
- Section 8 compares predictions and measurements for pure- and mainly-air testing conditions.
- Section 9 summarizes and concludes the research works and results.

3. TEST RIG DESCRIPTION

The original test rig was designed to test high-speed hydrostatic bearing at the Turbomachinery Laboratory at Texas A&M University, described in detail by Childs and Hale [22] in 1994. It was then transformed into the annular-gas-seal test stand, as described by Dawson et al. [23] in 2001. To accommodate a testing program of mixed flow test conditions, the rig was modified from the air-annular seal test stand by PhD candidates, Min Zhang and James Mclean, and a research engineer, Stephen Phillips, under the supervision of Dr. Dara Childs. This modification is described by Zhang [21], and Zhang et al. [19]. Mainly-air mixtures are limited to inlet LVF=10%, because the gas-oil mixer is unable to supply the required oil flowrates through the nozzles in the existing mixer. It could possibly be fixed by redesigning to increase the number of nozzles or change the nozzle type to allow for more oil flow. For mainly-oil test conditions, the stator becomes dynamically unstable for inlet GVF≥12%.

3.1 Experimental Set-up

Figure 5 shows the piping and instrumentation diagram (P&ID) of the 2-Phase-Annular-Seal-Stand (2PASS) test rig. It includes 5 main sections which form a closed loop: air-supply section, oil-supply and return section, mainly-oil mixing section, mainly-air mixing section, and test section. The following paragraphs describe each of sections in detail.

3.1.1 Air-Supply Section

The air-supply section is highlighted in the top dotted box in Fig. 5. Depending on usage, pure- or mainly-air test conditions are performed at a pressure of 62 bar-g at the tested seals' inlet. Inlet air is filtered with a particulate filter and a coalescing filter before entering the mainly-oil mixing or mainly-air mixing sections. A main control valve (V6) is installed downsteam from the two filters to control air pressure supplied to the main test section. A rupture disk is in place, down-stream of the valve V6, to prevent line over-pressure above 129.4 bar-a in the test rig itself. There are 2 flow meters with 2 different ranges to improve measurement accuracy; namely, one for measuring air flow in pure- and mainly-air conditions, another used in pure- and mainly-oil conditions. Thermocouples and pressure transducers are installed before and after flow meters for measuring temperature and pressure, respectively. After passing through the flow meter, air goes into either the mainly-oil mixing section (for pure- or mainly oil testing conditions), or the mainly-air mixing section (for pure- or mainly-air testing conditions).

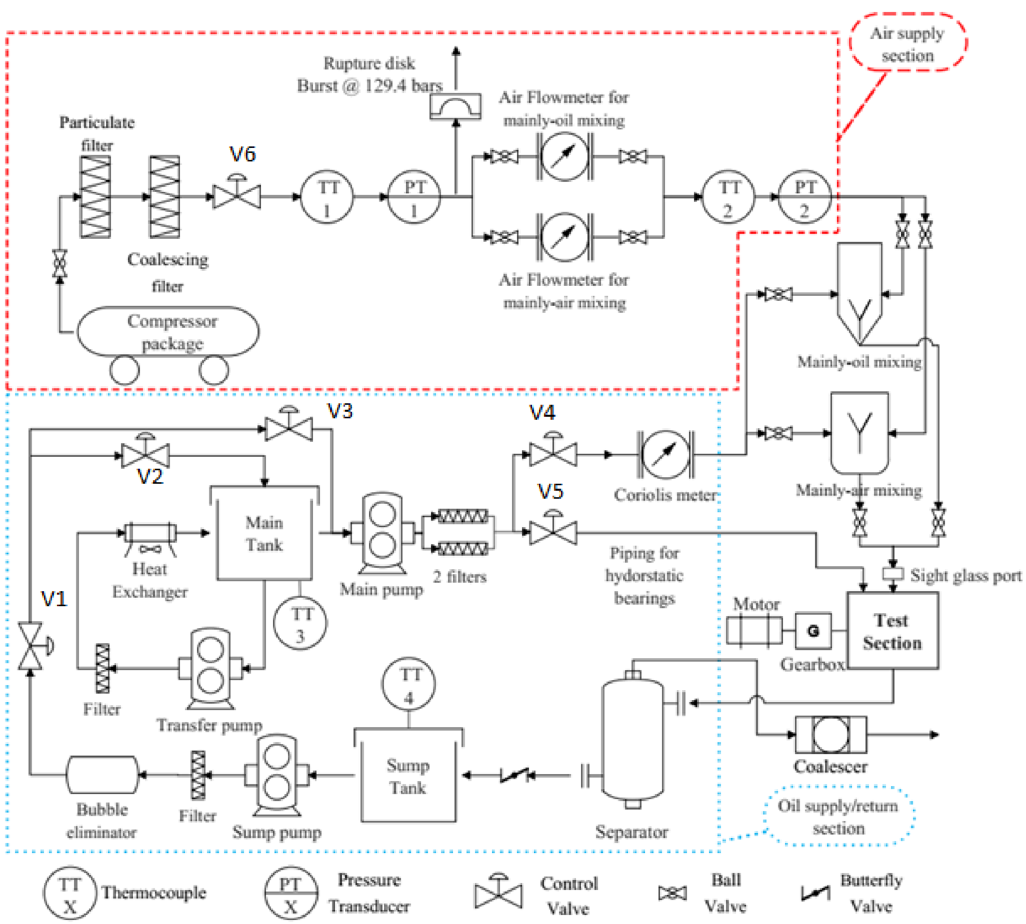

Figure 5 Piping and instrumentation diagram of the 2-Phase-Annular-Seal-Stand (2PASS). Republished with permission of ASME, from [19]; permission conveyed through Copyright Clearance Center, Inc.

3.1.2 Oil-Supply & Return Section

The oil-supply and return section is highlighted in the bottom dotted box in Fig. 5. First, a mixture of oil and air from the test section, including oil from the hybrid-bearing return (two high-stiffness hybrid bearings are used in the test section to support the spinning rotor) is collected by a separator. From the separator, collected oil is sent to a sump tank using gravity, while the wet air goes through a coalescer for a second time before air can be returned to the atmosphere. The sump tank's level is maintained by a sump pump. A bubble eliminator is installed after the sump pump to further remove dissolved-gas components. Hot oil from the sump pump either enters the main tank for heat removal or goes directly to a main pump. A transfer pump is used to circulate the oil in the main tank through a heat exchanger, which is controlled to maintain a specified temperature for oil in the main tank. A combination of hot oil from the sump pump and cold oil from the main tank is adjusted, using the control valves V2 and V3, to maintain a required temperature before being pumped back to the test section using the main pump. Filters are installed after all pumps. Oil temperature at the main tank and the sump tank are monitored using thermocouples. Oil from the main pump is supplied to the hybrid bearings and the mainly-oil or mainly-air mixing sections by using control valves V5 and V4, respectively. Oil flow entering the mixing section is measured by a Coriolis meter. All control valves are controlled using 4-20mA analog output from a National Instrument module.

3.1.3 Mainly-Oil Mixing Section

In mainly-oil testing conditions, the mixture is produced using spargers to inject air bubbles into the oil flow stream. While the compressed air flows through the porous surface of the spargers, the silicone oil flows through the annulus between the spargers and pipes. Two spargers are installed in a tee where air and oil input are coming as shown in P&ID of the mainly-oil mixing section in Fig. 6. To monitor pressures of air and oil input, pressure transducers are installed just before mixing.

Table 1 describes physical properties of the spargers. According to the guideline from the manufacturer [24], for an injector inside a pipeline with liquid moving 0.3-3 m/sec (which applies for current testing), the maximum velocity (V) across porous media should be 3 m/sec. For a typical air flow rate ($\dot{Q}$) of 1.0 ACFM in the current testing conditions, the porous diffuser must have a minimum surface area (A) of

$$A = \frac{\dot{Q}}{V} = \frac{0.02832\ m^3/\min}{3.048\ m/\min} = 0.00929\ m^2 \tag{5}$$

According to the sizing guidance, an injector with a porous outer diameter of 25.4 mm and a porous length of 215.9 mm, was selected in this setup. It has more than 0.0158 m^2 of surface area. As mentioned in [24], when an injector is sized correctly, a bubble size of approximately 5-15 μm will be achieved in a clear water solution. The silicone oil used here has a surface tension of 0.0197 N/m, which is approximately 1/3 that of water [25]; so, a bubble size of approximately 1.67-5 μm or 0.8-2.5% of the seal's radial clearance is expected in a mixture of silicone oil and air.

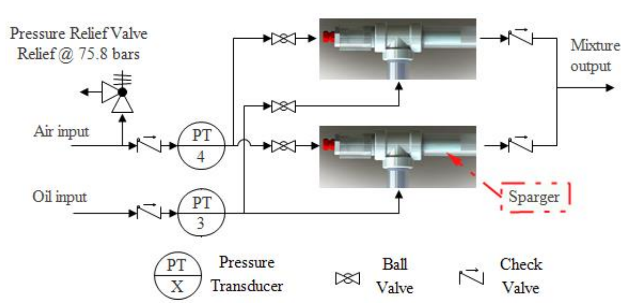

Figure 6 P&ID of mainly-oil mixing section. Reprinted with permission from [21]

Table 1 Properties of the sparger

Name	Mott 850-Series sintered porous metal element
Porous outer diameter (mm)	25.4
Wall thickness (mm)	3.2
Porous length (mm)	215.9
Nominal length without fitting (mm)	304.8
Media grade (μm)	10
Material	316L stainless steel

3.1.4 Mainly-Air Mixing Section

Figure 7 is a sectional view of the oil-gas mixer used for mainly-air mixing conditions. There are three main chambers, namely, the air chamber, the oil chamber, and the mixing chamber. Silicone oil enters the oil chamber and then flows to 9 spray nozzles through 9 injection tubes. Properties of the spray nozzle are described in Tab. 2. From the spray nozzle, atomized liquid droplets are sent to the mixing chamber where they meet compressed air coming from the air chamber.

Zhang [21] performed an experiment with an acrylic chamber to inspect the mixing performance and determine the liquid droplet size. Due to limited capability of the acrylic chamber, the experiment was only conducted at a 5.5-bar-g pressure. A high-speed camera with a sample rate of 8,300 frames/sec was used. The mixer performed well for a mixture of air and water with a GVF of 97% at 25^{o}C where the water droplet size was about 0.25mm. Zhang [21] then estimated the droplet size for actual testing condition where silicone oil is injected into compressed air at 25^{o}C and 62 bar-g which are similar to the test condition reported in this thesis. He predicted a diameter of about 6.2 μm. This bubble size was approximately 3% of the seal's radial clearance used in this thesis.

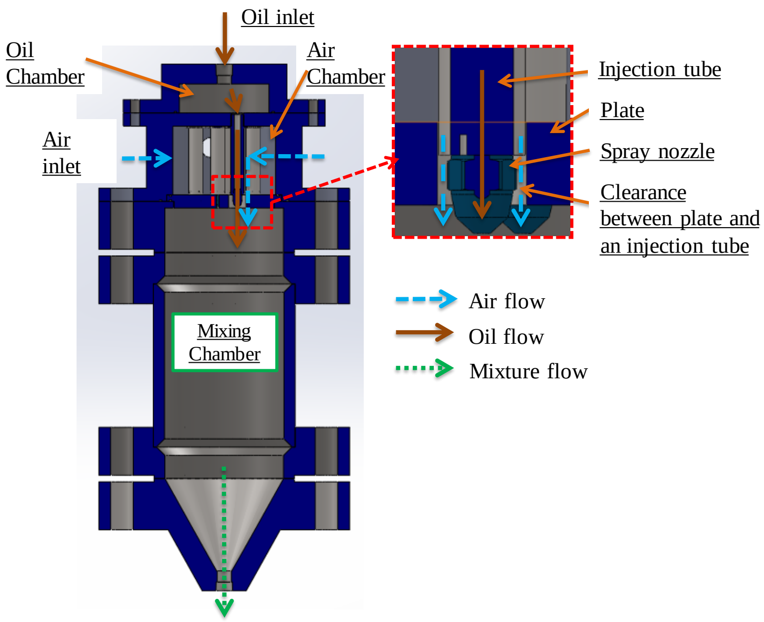

Figure 7 Sectional view of the oil-gas mixer. Republished with permission of ASME, from [19]; permission conveyed through Copyright Clearance Center, Inc.

Table 2 Properties of the spray nozzle

Type	Hollow cone spray nozzle
Model	1/4KKBP200S303
Standard pressure (bar)	3
Spray angle (º)	55±5
Spray capacity (l/min)	2±0.1

3.1.5 Test Section

Figure 8 depicts a section view of the test rig. The test section's rotor is supported by two high-stiffness hybrid bearings. A lube oil pressure of 62 bar-g is supplied by the oil-supply section to the hybrid bearings. The rotor is driven by a 112-kW electric motor and a Lufkin Gearbox which has a gear ratio of 6.96:1. A variable-speed drive is connected to the test section's motor. Zhang [21] discussed an additional gear pump for the gearbox, so the rotor speed could be operated at a low speed, i.e., 3 krpm, as operating in this study.

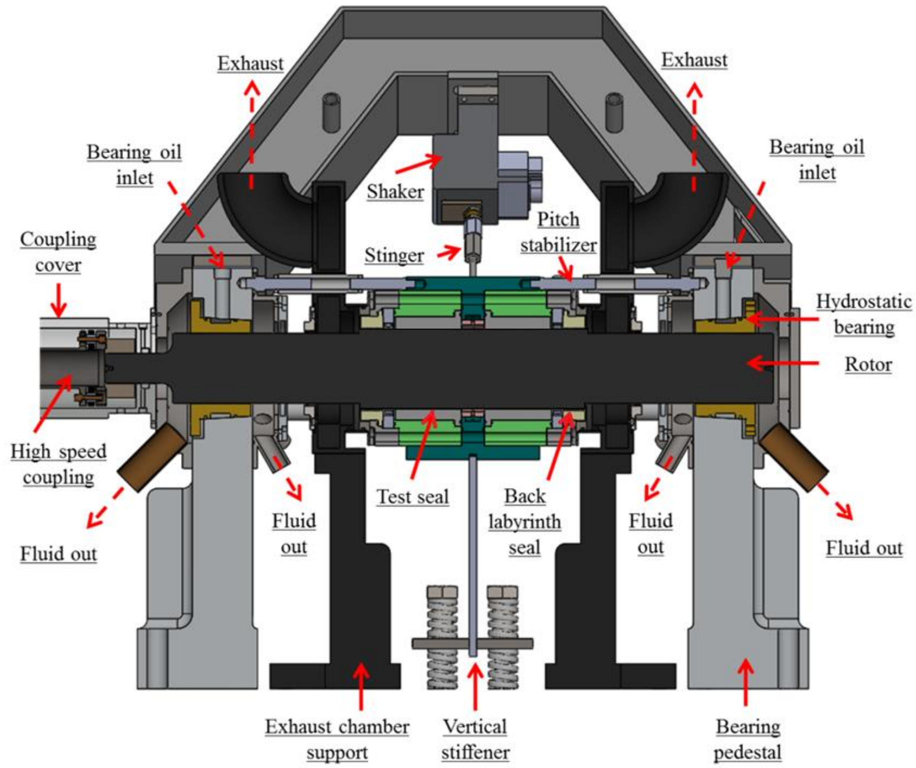

Figure 8 Section view of the test section. Republished with permission of ASME, from [19]; permission conveyed through Copyright Clearance Center, Inc.

Figure 9 provides photographs of the test rig. The stator assembly is supported by four horizontal cables, two on each side, and a vertical stiffener. This modification was added by Picardo and Childs [26] and Mehta and Childs [27] to eliminate stator static and dynamic instabilities. Three pairs of pitch stabilizers are installed axially in an equilateral triangle pattern in the front and back planes of the stator assembly. They are used to align the test seal and the rotor, so a uniform clearance can be achieved circumferentially and axially. The hydraulic shakers, connected to the stator assembly via two orthogonally oriented stingers at forty-five degrees from vertical in the angular direction, control the static position of the stator and excite the stator with a pseudo-random waveform excitation. Data are recorded for deriving dynamic force coefficients, including: acceleration components of the stator by accelerometers, shaking force components from force transducers attached to the stingers, and relative displacement components between stator/seal and the rotor through proximity probes.

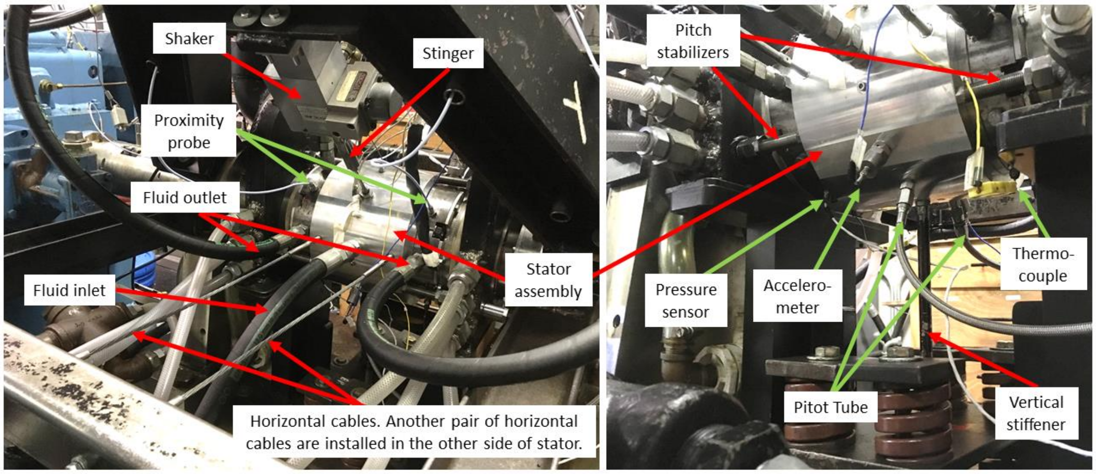

Figure 9 Photograph of the test section

Figure 10 shows an outer view of the stator assembly, indicating locations of proximity probes, inlet pressure transducer and thermocouple, accelerometers, and shaker stingers.

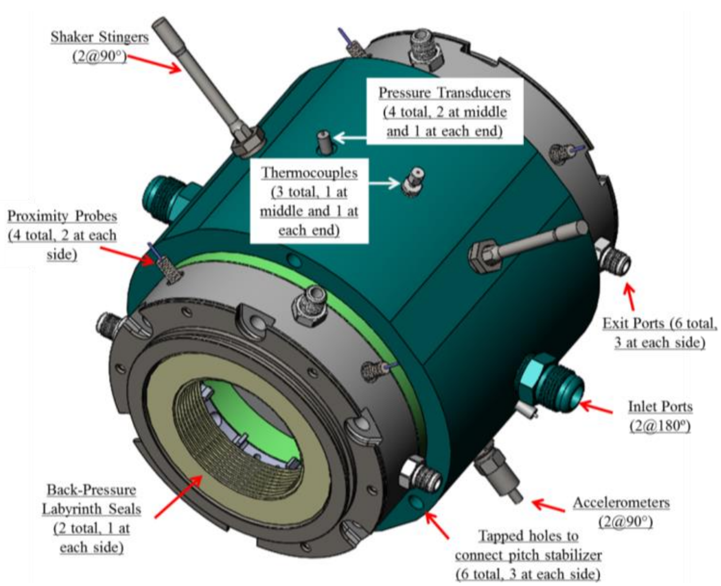

Figure 10 3-D model of the stator assembly. Reprinted with permission from [21]

Figure 11 is a cross sectional view of the stator housing. The clearance between the rotor and the seal are exaggerated for a clear visualization of the flow path inside the stator assembly. Fluid flow enters from the two inlet ports at the middle plane. A stator assembly accommodates two identical smooth seals. Fluid goes through the clearance between the rotor and the seals and exits at radial exit ports, three on each end. A back-pressure valve is provided downstream of the exit ports and back pressure labyrinth seals of the stator assembly to build up back pressure. Since the back-pressure labyrinth seals are short and have swirl brakes and much larger clearance w.r.t. the test seal, their effect on the dynamic force coefficients is negligible.

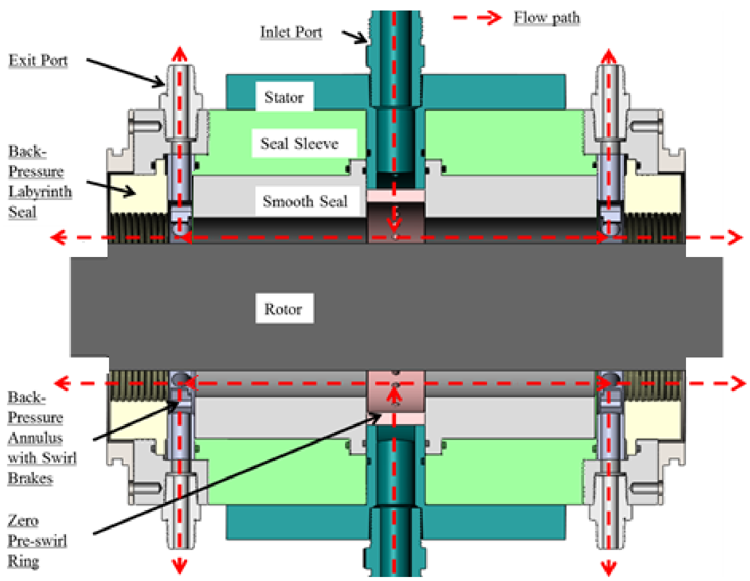

Figure 11 Cross section of stator housing. Republished with permission of ASME, from [19]; permission conveyed through Copyright Clearance Center, Inc.

Zhang [21] presented his work for a smooth seal under a mixture of air and silicon oil, with only a zero-preswirl insert. However, in this thesis, the tests are performed at three fluid inlet preswirl levels, namely: zero, medium, and high. Three inserts with three preswirl levels, shown in Fig. 12, are inserted in the inlet annulus housing to introduce different levels of inlet preswirl. The zero preswirl ring has 30 radial through holes (diameter of 3.57 mm) pointed radially towards the center of the hole; whereas the medium preswirl ring has 32 radial through holes (diameter of 3.30 mm), and the high preswirl has 32 radial through holes (diameter of 2.38 mm) inclined at an angle.

Each inserted ring has a pitot tube and a static pressure orifice which are connected to different pressure transmitters to measure the difference between the stagnation pressure P_t and static pressure P_s at the seal inlet. Figure 13 shows an example installation, on the zero-preswirl configuration, of a pitot tube and a static pressure orifice. The circumferential velocity of test fluid upstream from the seal inlet is

$$V_\theta = [2(P_t - P_s)/\rho]^{1/2} \tag{6}$$

where, ρ is the test fluid density.

The preswirl ratio is calculated based on the fluid's circumferential velocity w.r.t. the shaft surface's velocity.

$$preswirl = \frac{V_\theta}{R\omega} \tag{7}$$

where, R is the rotor's radius and ω is the rotor speed in rad/s.

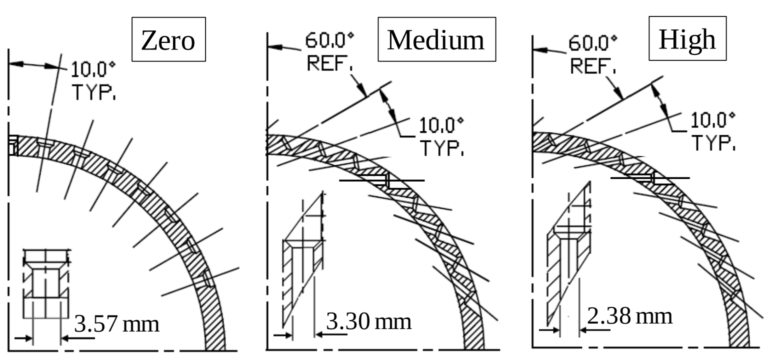

Figure 12 Cross section of fluid preswirl rings

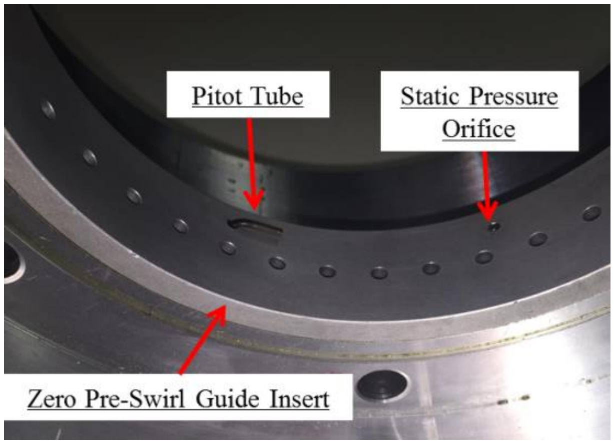

Figure 13 Pitot tube and static pressure orifice on the zero-preswirl ring. Reprinted with permission from [21]

3.2 Instrumentation

Instruments installed are described in Sec. 3.1. Static uncertainties for flow and density measurements, reported by Zhang [21], are shown in Tab. 3. Static uncertainties for instruments in the test section, reported by Kurtin et al. [28], are given in Tab. 4.

Table 3 Static uncertainties for volume/mass flow rates and oil density

Parameter	Uncertainty
Air Volumetric Flow Rate for Mainly-Air Conditions	0.305 ACFM (0.52 m^3/h)
Air Volumetric Flow Rate for Mainly-Oil Conditions	0.0414 ACFM (0.0703 m^3/h)
Liquid Mass Flow	0.11 kg/min (0.24 lbs/min)
Liquid Density	0.18 kg/m^3 (6.5x10^{-6}lbs/in^3)

Table 4 Static uncertainties for instruments in the test section

Parameter	Uncertainty
Pressure	0.06 bar (0.838 psi)
Temperature	3.1°C (5.613°F)
Pitot Tube Differential Pressure	0.0032 bar (1.276 in-H_2O)

3.3 Test Fluid

3.3.1 Silicone Oil (PSF 5cSt)

Silicone oil (PSF 5cSt) is the test fluid. It has low viscosity and behaves like a Newtonian fluid [25,29]. Table 5 presents the specification and data of Silicone oil (PSF 5cSt) [25].

Figure 14 shows the depenency of silicone oil (PSF 5cSt)'s viscosity on temperature. The point data are retrieved from the silicone oil datasheet, and an exponential-curved fit is used to estimate the oil kinematic viscosity as a function of the seal's inlet temperature. This information is used to estimate Reynolds number in Chapters 5 and 7 and provides inputs for predictions in Chapters 6 and 8.

Table 5 Silicone oil specifications and data

Chemical Name	Polydimethylsiloxane
Appearance	Clear, colorless, odorless
Viscosity-Temperature Coefficient	0.54
Viscosity @ 25 ºC (cSt)	5
Specific Gravity	0.918
Flash Point (ºC)	135
Pour Point (ºC)	-90
Vapor Pressure @ 25°C (Pa)	133.3
Thermal Expansion (m^3/ m^3·ºC)	0.00109
Thermal Conductivity @25ºC (W/m·K)	1.172
Surface Tension (N/m)	0.0197
Boiling Point (ºC)	>200

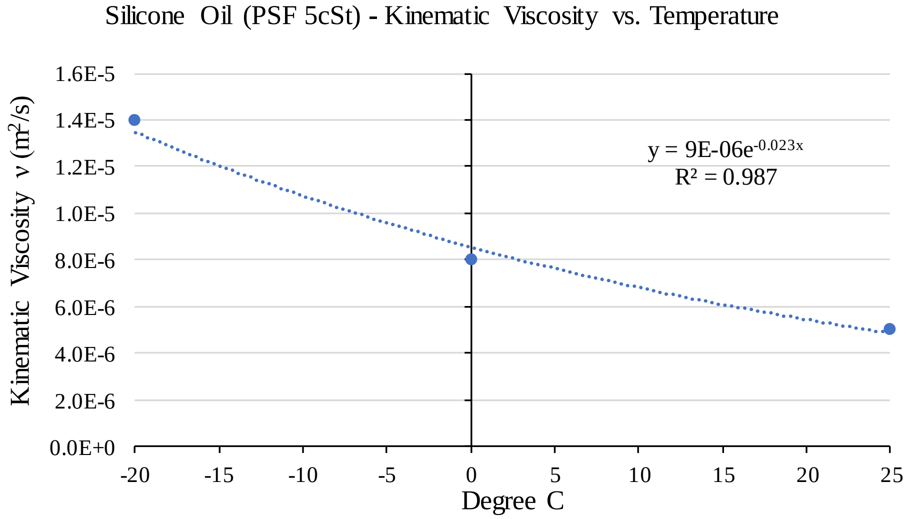

Figure 14 Silicone oil kinematic viscosity vs. temperature

3.3.2 Test Fluid Properties

The test fluid is a two-phase homogenous mixture of air and silicone oil (PSF 5cSt). For each test case, inlet fluid is observed through a sight glass before entering into the test seal to assure homogenity.

From Diaz [31], for a bubbly mixture of a Newtonian incompressible liquid and an ideal gas in equilibrium (homogenous, quasi-static, and isothermal), the local GVF at any point in the seal is solely a function of the local pressure P,

$$\mathrm{GVF} = \frac{1}{1 + \frac{P - (P_V + 2S/C_r)}{P_{gi}}\left(\frac{1}{\mathrm{GVF}_i} - 1\right)} \tag{8}$$

where, P_V is the liquid vapor pressure, P_{gi} is the gas pressure at the seal inlet, S is the liquid surface tension per unit length, C_r is the radial clearance, GVF_i is the GVF at the seal inlet.

According to San Andrés [15], since the magnitude of (P_v+2S/C_r) is negligible (only a few millibars for oil), the local GVF is simplified as

$$\mathrm{GVF} = \frac{1}{1 + \frac{P}{P_{gi}}\left(\frac{1}{\mathrm{GVF}_i} - 1\right)} \tag{9}$$

Gas volume fraction at seal inlet GVF_i is defined as

$$\mathrm{GVF}_i = \frac{\dot{Q}_{gi}}{\dot{Q}_{gi} + \dot{Q}_{li}} \tag{10}$$

where, $\dot{Q}_{gi}$ and $\dot{Q}_{li}$ are the volume flow rates of gas and liquid at seal inlet, respectively.

For silicone oil, inlet volume flow rate is determined by using data from the Coriolis meter

$$\dot{Q}_{li} = \frac{\dot{m}_l}{\rho_l} \tag{11}$$

where, $\dot{m}_l$ and ρ_l are the mass flow rate and density of the oil measured by the Coriolis meter.

For inlet-gas volume flow rate,

$$\dot{Q}_{gi} = \dot{Q}_{FM}\,\frac{P_{FM} T_i}{T_{FM} P_i} \tag{12}$$

where, $\dot{Q}_{FM}$ is turbine flowmeter, P_{FM} and T_{FM} are the pressure and temperature measured immediately downstream of the turbine flowmeters, and P_i and T_i are the pressure and temperature measured at the seal inlet.

a. Mixture density

According to Tao, et al. [30], the mixture density is defined as

$$\rho = \rho_g \mathrm{GVF} + \left(1 - \mathrm{GVF}\right)\rho_l \tag{13}$$

where, ρ_l denotes the liquid density, ρ_G is the gas density, and GVF is gas volume fraction.

Supplied gas is assumed as an ideal gas with the following state equation to calculate a gas density

$$\rho_g = \frac{P}{Z\Re_g T} \tag{14}$$

where, Z is the gas compressibility factor, $\Re_g$ is the gas constant, P is the pressure, and T denotes the temperature.

b. Mixture viscosity

There are several viscosity models for two-phase homogenous mixtures, and they provide significant difference in prediction for both static and dynamic characteristics of a seal. In this thesis, the model of Fourar and Bories [32] is used.

$$\mu = (1-\mathrm{GVF})\mu_l + \mathrm{GVF}\mu_\mathrm{g} + 2\sqrt{\mathrm{GVF}(1-\mathrm{GVF})\mu_l\mu_g} \tag{15}$$

It is implemented by *XLHseal_mix* program, which produces prediction results for a comparison in this thesis.

3.4 Test Seals

Figure 15 is a drawing of the test seal. The nomial length and inner diameter of the test seal are 85.700-85.725 mm (3.374-3.375 inches) and 114.7064-114.7191 mm (4.5160-4.5165 inches), respectively. The seals are made from 6061 T6 Aluminum with a surface finish of 0.4 μm (16 μin). They are pressed into the seal sleeve. A three-point gauge with an accuracy of 0.00254 mm (0.0001 inches) is used to measure the seal inner diameter (ID) at room temperature when the seals are pressed inside the seal sleeve. The dimensions are shown in Tab. 6. There are two sets of data, corresponding to the two test seals, and the measurements are done at three planes, namely, inlet, middle, and oulet planes. In each plane, the three-point-gauge measurements are repeated every 60°-rotation steps.

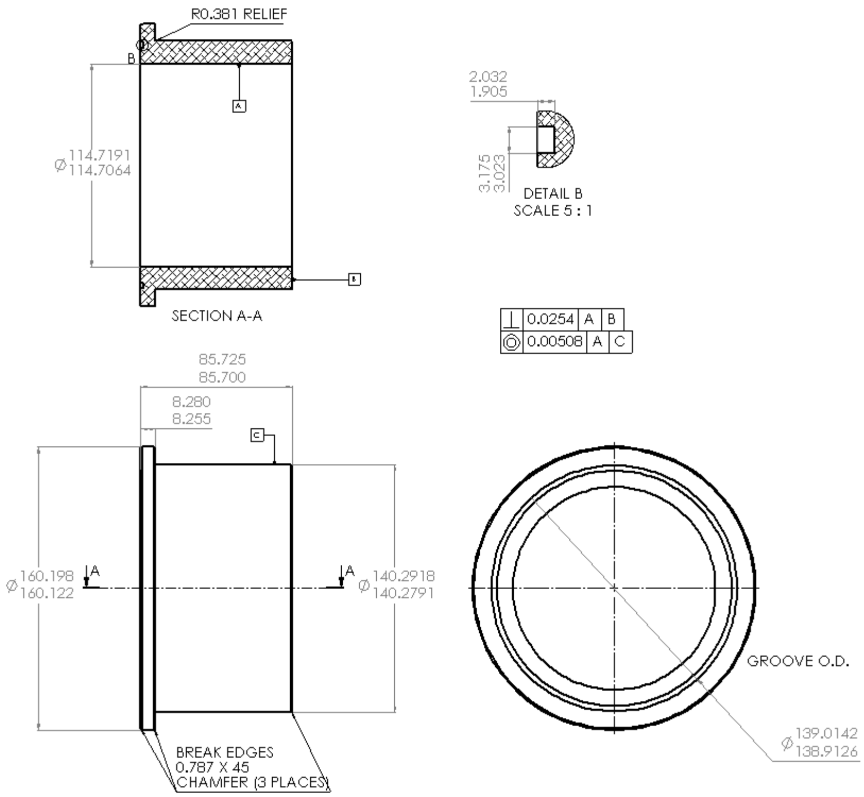

Figure 15 Test smooth seal (dimensions in mm)

Table 6 Seal ID dimensions

	Angle	**Inlet**		**Middle**		**Outlet**	
		(inch)	**(mm)**	**(inch)**	**(mm)**	**(inch)**	**(mm)**
Seal 1	0^o	4.5154	114.691	4.5154	114.690	4.5155	114.695
	60^o	4.5153	114.689	4.5153	114.689	4.5155	114.694
	120^o	4.5154	114.690	4.5154	114.690	4.5155	114.693
	Avg.	**4.5154**	**114.690**	**4.5153**	**114.690**	**4.5155**	**114.694**
Seal 2	0^o	4.5151	114.683	4.5151	114.683	4.5150	114.681
	60^o	4.5149	114.678	4.5149	114.679	4.5151	114.684
	120^o	4.5151	114.683	4.5151	114.683	4.5151	114.683
	Avg.	**4.5150**	**114.681**	**4.5150**	**114.682**	**4.5151**	**114.682**

3.5 Test Rotor

Figure 16 shows the test rotor's dimensions. It is made from 304 SS with a surface finish of 0.00254 mm (0.0001 inches) at the test-seal journal. Radial clearances are documented in Tab. 7.

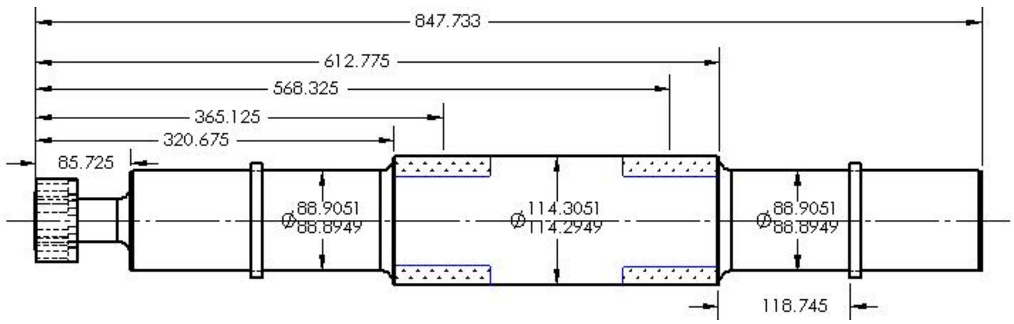

Figure 16 Test rotor (dimensions are in mm)

Table 7 Nominal radial clearances

Seal	Inlet Plane		Middle Plane		Outlet Plane	
	(inch)	(mm)	(inch)	(mm)	(inch)	(mm)
Seal 1	0.0076	0.1926	0.0077	0.1964	0.0078	0.1973
Seal 2	0.0076	0.1930	0.0076	0.1922	0.0076	0.1939

4. EXPERIMENTAL PROCEDURE

4.1 Parameter Identification

This dynamic parameter-identification approach was discussed in detail by Mehta and Childs [27]. The equation of motion for the stator is

$$\boldsymbol{F} - M_S \boldsymbol{A} = \boldsymbol{F_S} \tag{16}$$

where, $\boldsymbol{F_S}$ is seal reaction force given by Eq. (1), $\boldsymbol{F}$ is the applied excitation force, $\boldsymbol{A}$ is the stator's acceleration, and M_s is the stator mass in the *X*-*Y* coordinate system, as shown in Fig. 17.

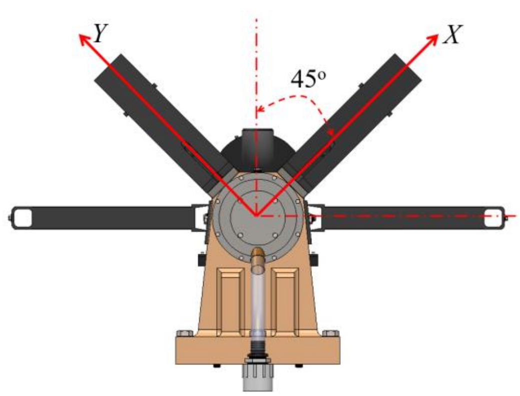

Figure 17 *X*-*Y* coordinate system

The stator is excited in *X* and *Y* directions, alternately. By using a Fourier transform, Eq. (16) can be transformed into the frequency domain as

$$\begin{bmatrix} \boldsymbol{F_{XX}} & \boldsymbol{F_{XY}} \\ \boldsymbol{F_{YX}} & \boldsymbol{F_{YY}} \end{bmatrix} - \left[M_S\right] \begin{bmatrix} \boldsymbol{A_{XX}} & \boldsymbol{A_{XY}} \\ \boldsymbol{A_{YX}} & \boldsymbol{A_{YY}} \end{bmatrix} = \begin{bmatrix} \boldsymbol{H_{XX}}(\Omega) & \boldsymbol{H_{XY}}(\Omega) \\ \boldsymbol{H_{YX}}(\Omega) & \boldsymbol{H_{YY}}(\Omega) \end{bmatrix} \begin{bmatrix} \boldsymbol{D_{XX}} & \boldsymbol{D_{XY}} \\ \boldsymbol{D_{YX}} & \boldsymbol{D_{YY}} \end{bmatrix} \tag{17}$$

where, $\boldsymbol{F_{ij}}$ are the Fourier transforms of the excitation forces, $[M_S]$ is the stator-mass coefficient matrix, $\boldsymbol{A_{ij}}$ are the Fourier transforms of the stator accelerations, $\boldsymbol{D_{ij}}$ are the Fourier transforms of the relative displacements of the stator to the rotor, and $\boldsymbol{H}_{ij}$ are the dynamic stiffness coefficients.

The subscript ij denotes the measured value in the i direction due to the excitation in the j direction.

$[M_S]$ is defined by,

$$[M_S] = \begin{bmatrix} M_{sXX} & M_{sXY} \\ M_{sYX} & M_{sYY} \end{bmatrix} \tag{18}$$

where, M_{sij} are mass coefficients of the stator assembly in the X-Y frame. Since X-Y coordinate system is symmetrical about the vertical axis, $M_{sXX} \approx M_{sYY}$, and $M_{sXY} \approx M_{sYX} \approx 0$.

$[M_S]$ is identified via baseline shakes, where the seal housing in the test section, as described in Sec. 3.1.5, is excited without fluid and shaft rotation using the hydraulic shakers.

If seal stiffness, damping, and virtual mass coefficients in Eq. (1) are frequency-independent, $\boldsymbol{H}_{ij}$ in Eq. (17) can be represented as

$$\boldsymbol{H}_{ij} = \left(K_{ij} - \Omega^2 M_{ij}\right) + \boldsymbol{j}\Omega C_{ij}, \;\; \boldsymbol{j} = \sqrt{-1} \tag{19}$$

$$\mathrm{Re}(\boldsymbol{H}_{ij}) = \left(K_{ij} - \Omega^2 M_{ij}\right) \tag{20}$$

$$\mathrm{Im}(\boldsymbol{H}_{ij}) = \Omega C_{ij} \tag{21}$$

where, K_{ij}, C_{ij}, and M_{ij} are the frequency-independent seal stiffness, damping, and virtual mass coefficients, and Ω are excitation frequencies.

4.2 Repeatability Analysis

The repeatability analysis provides an assessment on data consistency. During tests, excitation forces are applied alternatively in X and Y directions by the hydraulic shakers with a pre-programed waveform, consisting of an ensemble of pseudo-random frequencies [33]. The frequencies range from 10 Hz to 140 Hz with increments of 10 Hz. A factor of 1000/1024 is multiplied times the test frequencies to avoid electrical noise at 60/120/180 Hz. The waveform lasts 0.1024 seconds. In pure- or mainly-oil testing conditions, for each shake, the waveform is produced 640 times in sequence along each direction; whereas, for cases of pure- or mainly-air testing conditions, the waveform is produced 1280 times sequentially along each direction. Component of the exciting forces, stator acceleration, relative displacement between seal and rotor are captured during each shake. The results are then divided into 10 groups in each direction. Each group in pure- or mainly-oil conditions then contains data of 64 periods; while each group in pure- or mainly-air conditions contains data of 128 periods, which are then converted from time-domain to frequency domain by Fourier Transforms. Each of the 10 groups of data in one direction is combined with each of the 10 groups in the other direction forming 100 complex force [$\boldsymbol{F}$], acceleration [$\boldsymbol{A}$], and relative displacement [$\boldsymbol{D}$] matrices, respectively, to derive 100 matrices of dynamic-stiffness-coefficient matrices [$\boldsymbol{H}$] using Eq. (17). The repeatability values of dynamic-stiffness can be calculated from their standard deviations, and are graphically depicted by error bars in each dynamic-stiffness-coefficient plot.

5. MEASURED RESULTS FOR PURE- AND MAINLY-OIL TESTING

5.1 Baseline Data

A baseline dry shake is performed with no testing fluid flow and no shaft rotation to determine a contribution of the supporting structure to actual testing results. The back-pressure labyrinth seals are short (28.58 mm) and have swirl brakes and much larger clearance (0.254 mm) w.r.t. the test seal, their effect on the dynamic force coefficients is negligible. Equation (22) shows a relationship between total repeatability σ_{total}, the test data repeatability σ_{test}, and the baseline data repeatability $\sigma_{baseline}$, which is calculated in the same way as in Sec. 4.2.

$$\sigma_{total} = \sqrt{\sigma_{baseline}^2 + \sigma_{test}^2} \tag{22}$$

The total repeatability is shown by the error bar in result figures.

Figure 18 shows dynamic-stiffness coefficients which include imaginary and real parts for the dry shake baseline of the high-preswirl insert.

Figure 19 presents example dynamic-stiffness coefficients, before subtracting baseline results, for a case of pressure drop (PD) = 20.7 bar, inlet GVF = 0%, ω = 5 krpm, and with the high-preswirl insert.

Figure 20 shows results of the case in Fig. 19 after subtracting the baseline results, shown in Fig. 18. The real and imaginary parts of dynamic-stiffness coefficients for pure- and mainly-oil testing conditions in general can be represented by the following equations with fitting index R^2 around 0.99:

$$\mathrm{Re}(\boldsymbol{H_{ij}}) = K_{ij} - M_{ij}\Omega^2 \tag{23}$$

$$\mathrm{Im}(\boldsymbol{H_{ij}}) = C_{ij}\Omega\,, \tag{24}$$

K_{ij}, M_{ij}, and C_{ij} are constant and could be rendered from curve-fitting using Eqs. (23) and (24) (The curve-fitted results are shown in Appendix E).

From the test results, K_{ij}, M_{ij}, and C_{ij} are close to identical in *X* and *Y* directions; therefore stiffness, damping, virtual mass coefficients are averaged as

$$K = \frac{K_{XX} + K_{YY}}{2} \tag{25}$$

$$k = \frac{K_{XY} - K_{YX}}{2} \tag{26}$$

$$C = \frac{C_{XX} + C_{YY}}{2} \tag{27}$$

$$c = \frac{C_{XY} - C_{YX}}{2} \tag{28}$$

$$M = \frac{M_{XX} + M_{YY}}{2} \tag{29}$$

$$m_q = \frac{M_{XY} - M_{YX}}{2} \tag{30}$$

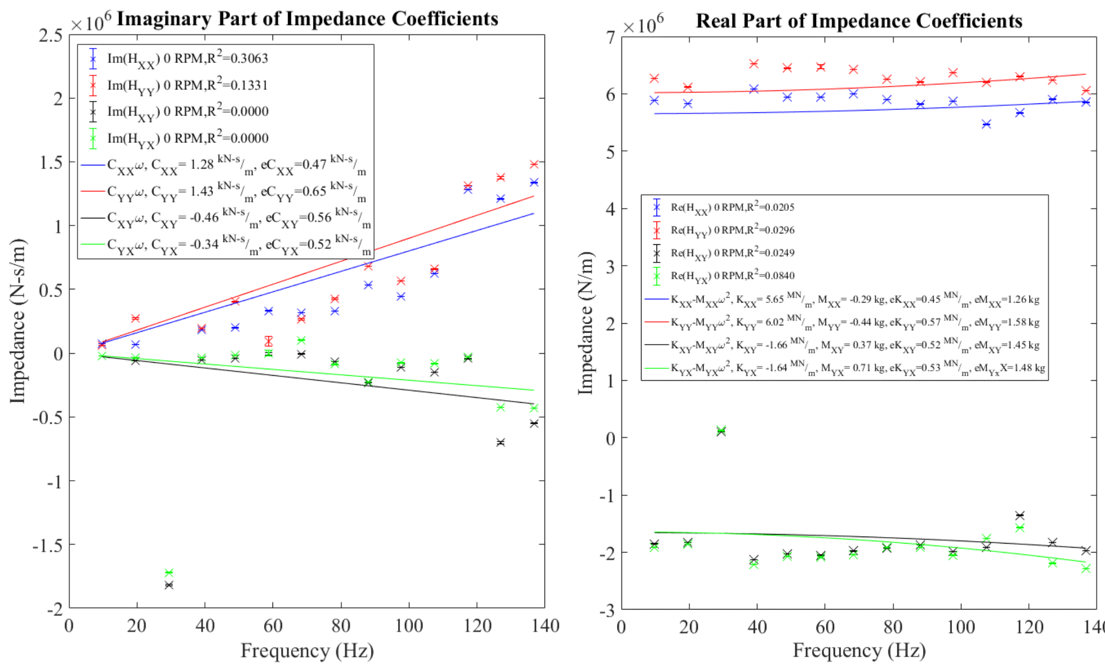

Figure 18 Dynamic-stiffness coefficients for the dry shake baseline of the high-preswirl insert

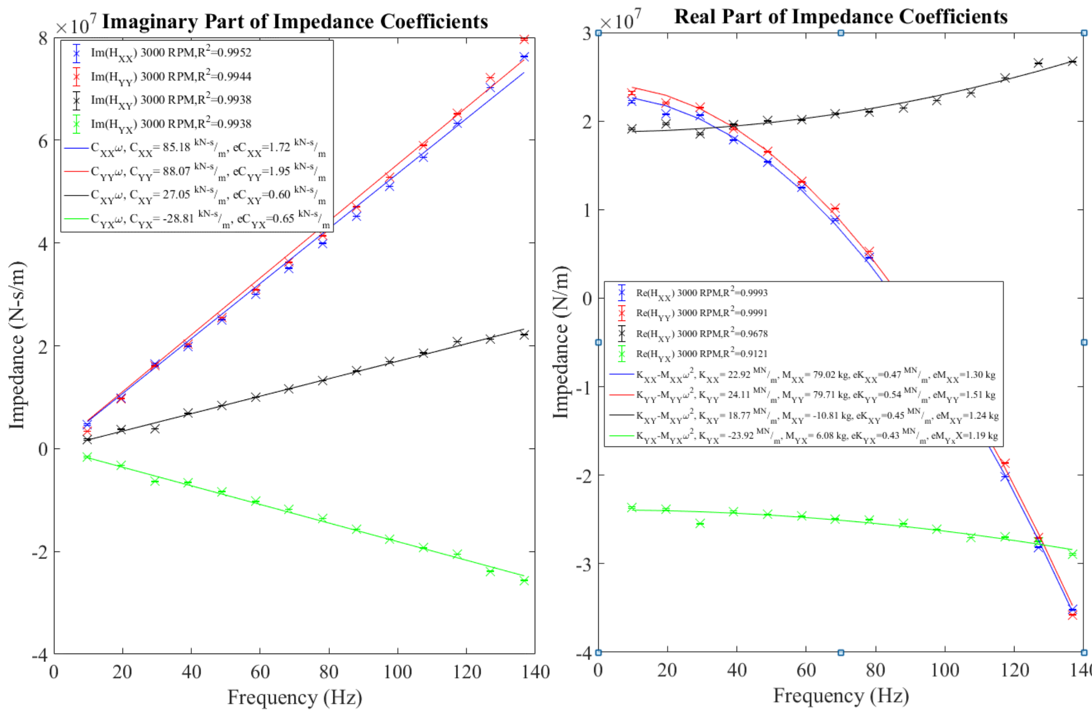

Figure 19 Dynamic-stiffness coefficients for a typical oil case (PD=20.7 bar, inlet GVF=0%, ω=3krpm, and with the high-preswirl insert) before subtracting the baseline data

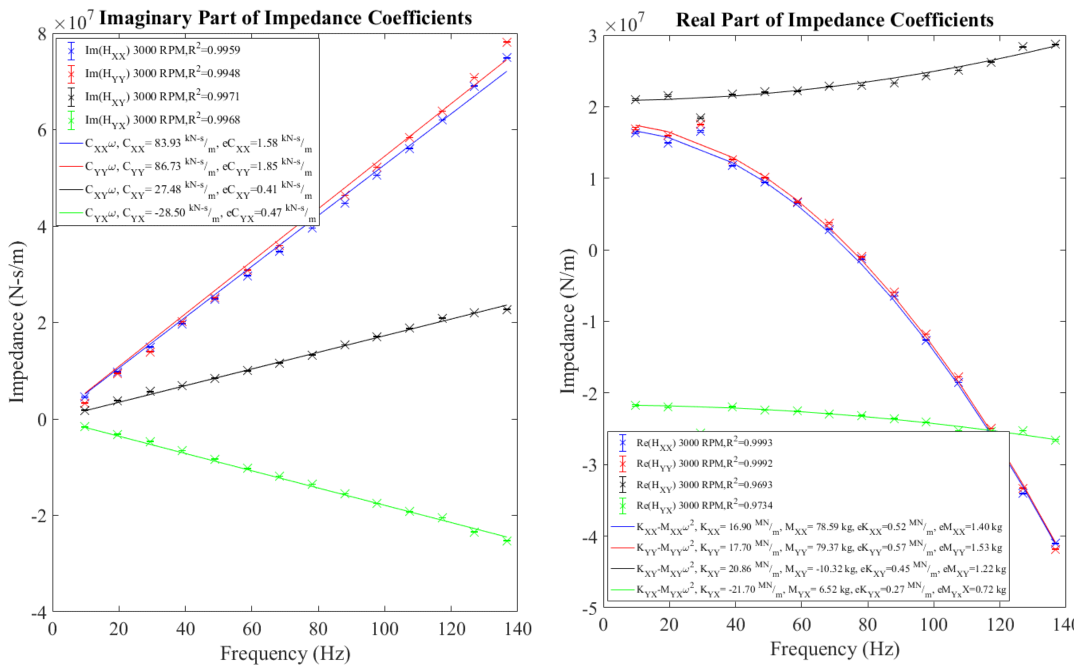

Figure 20 Dynamic-stiffness coefficients for a typical oil case (PD=20.7 bar, inlet GVF=0%, ω=3krpm, and with the high-preswirl insert) after subtracting the baseline data

5.2 Test Matrix

For pure- and mainly-oil test conditions, the test seal is centered, the seal exit pressure is maintained at 6.89 bar-g while the fluid inlet temperature is controlled within 37.8-40.6°C. Tests are performed for one radial clearance and three preswirl inserts. The **targeted** test matrix covers:

- 6 inlet GVFs: 0, 2, 4, 6, 8, and 10%
- 3 rotor speeds (ω): 3, 4, and 5 krpm
- 4 pressure drops (PD): 20.7, 27.6, 34.5, and 41.4 bar
- 3 positive-preswirl inserts: zero, medium, and high

The intention is to perform the test with 4 PDs, 3 speeds, for a range of inlet GVF from 0 to 10%, with 3 preswirl inserts. With the zero-preswirl insert, the back-pressure valve is almost closed fully, but could not produce a PD of 20.7 bar. With the medium- and high-preswirl inserts, the stator is moving even without excitations and dynamically unstable at PD≥27.6 bar.

For the medium-preswirl insert, at PD=27.6 bar, inlet GVF=4%, and ω=5 krpm, the system is stable with no external excitations applied; but it becomes unstable with applied excitation forces. A similar outcome is observed for cases at the same PD, inlet GVF=6%, and ω=3 and 4 krpm; however, at ω=5 krpm, the stator starts moving even without excitation forces. At PD=34.5 bar, under pure-oil conditions, the shaft is whirling as long as the rotor is spinning. A similar instability, as seen with the medium-preswirl insert, is observed for the high-preswirl insert at PD=27.6 and 34.5 bar. Therefore, in this thesis, the test matrix is limited up to PD of 27.6 bar for the medium- and high-preswirl inserts, and the speed is limited up to 5 krpm. All performed test conditions are listed in Tab. 8.

Zhang [21] reported a similar instability of the rig when he performed tests for a smooth seal (L/D=0.65, D=89.306 mm) with three clearances (C_r=0.188, 0.163, and 0.140 mm), under pure- and mainly-oil conditions with no intentional fluid pre-rotation provided. In his tests, the stator instability occurred at almost cases of speeds in a range of 5 to 15 krpm for C_r=0.163 and 0.140 mm. With C_r=0.140 mm, at PD=48.3 bar, inlet GVF=4%, and ω=5 krpm, the rotor was spinning unstably when the stator was excited by hydraulic shakers, and eventually an instability happened with no external excitations at inlet GVF=6%. Zhang [21] showed there were signs of sub-synchronous vibration for cases at PD=48.3 bar, ω of 5 krpm, and inlet GVF of 0 and 2%, where the instability was believed due to negative direct stiffness coefficients which dropped the stator's first natural frequency.

Table 8 Test conditions with pure-oil or mainly-oil mixtures

Pressure Drop (PD)	Inlet GVF (%)	Zero Preswirl (krpm)			Medium Preswirl (krpm)			High Preswirl (krpm)		
20.7 bar	0	Back Pressure Valve's constraint			3	4	5	3	4	5
	2				3	4	5	3	4	5
	4				3	4	5	3	4	5
	6				3	4	5	3	4	5
	8				3	4	5	3	4	5
	10				3	4	5	3	4	5
27.6 bar	0	3	4	5	3	4	5	3	4	5
	2	3	4	5	3	4	5	3	4	5
	4	3	4	5	3	4	Dynamically unstable. The seal housing was moving	3	4	5
	6	3	4	5				3	4	
	8	3	4	5				3	4	
	10	3	4	5				3		
34.5 bar	0	3	4	5						
	2	3	4	5						
	4	3	4	5						
	6	3	4	5						
	8	3	4	5						
	10	3	4	5						
41.4 bar	0	3	4	5						
	2	3	4	5						
	4	3	4	5						
	6	3	4	5						
	8	3	4	5						
	10	3	4	5						

Zhang [21] reported bad mixing quality in the same test facility for inlet GVF≥10%. In this thesis's tests, by observing through a sight glass at the seal-inlet entrance, the mixing quality is normal for all performed tests where inlet GVF goes to 10%.

The inlet preswirl ratios, defined in Eq. (7), are determined for each test case, and are shown in Fig. 21. The uncertainty of preswirl ratio measurement, shown in Tab. 13 (Appendix

C) or by error bars in Fig. 21, is a resultant of the uncertainties of the measurements of pitot tube differential pressure, liquid density, and gas density.

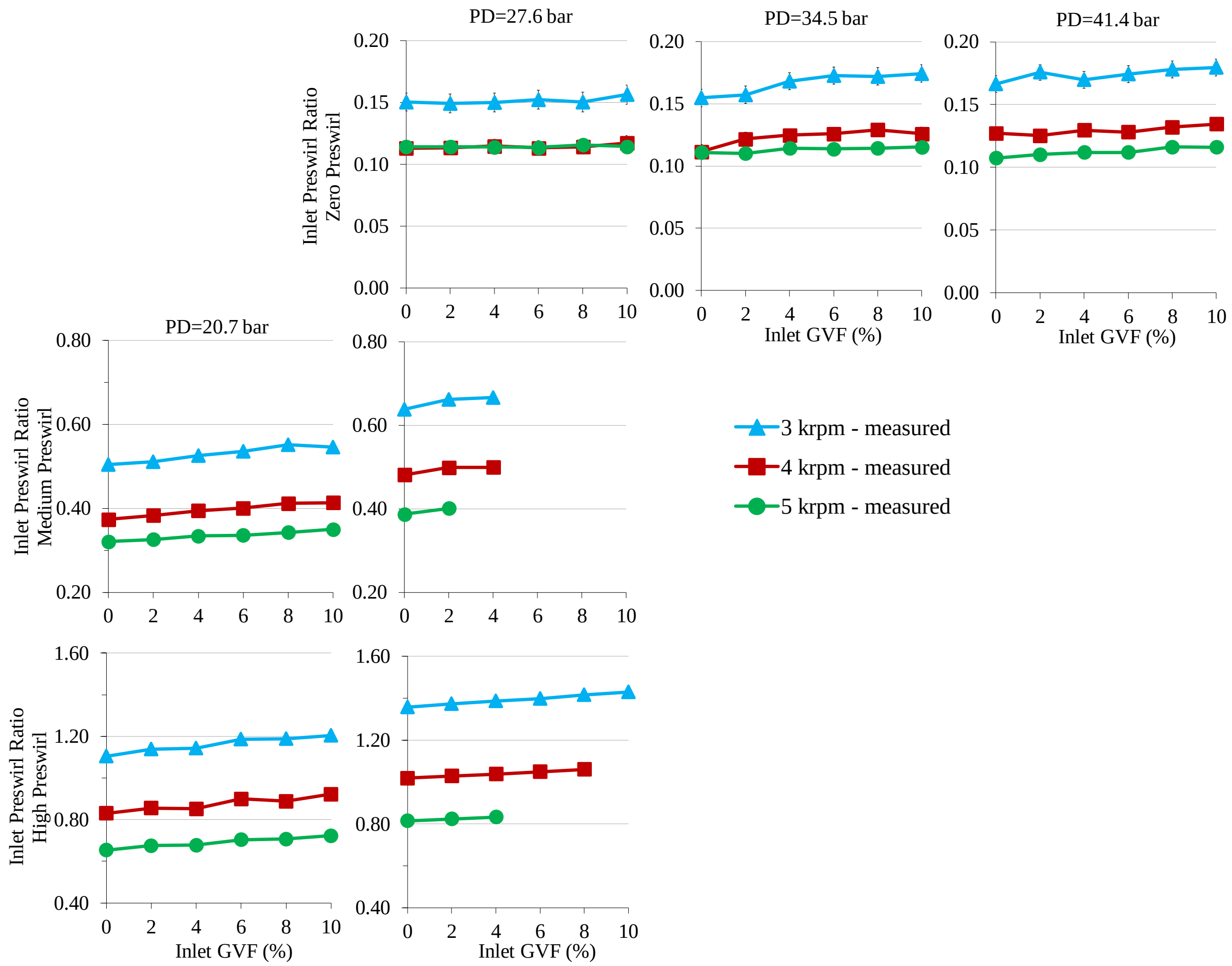

Figure 21 Measured preswirl ratio at seal inlet under pure- or mainly-oil conditions

The preswirl ratio is not necessarily equal to zero with the zero-preswirl insert due to the shaft rotation. The higher the shaft speed, the lower the inlet preswirl ratio. The effect of changing PD on inlet preswirl ratio is minimal for the zero-preswirl insert, but stronger for the medium- and high-preswirl inserts. Increasing PD increases the inlet preswirl ratio, via an increase of flow rate. The preswirl ratio slightly increases with increasing inlet GVF. As expected, preswirl ratio increases as the preswirl insert is changed from zero to medium, or from medium to high.

5.3 Leakage Mass Flow Rate

Figure 22 shows the mass flow rate $\dot{m}$ versus inlet GVF for four PD values, three preswirl inserts, and three ω values. The rows and columns are arranged by preswirl inserts and PD values, respectively.

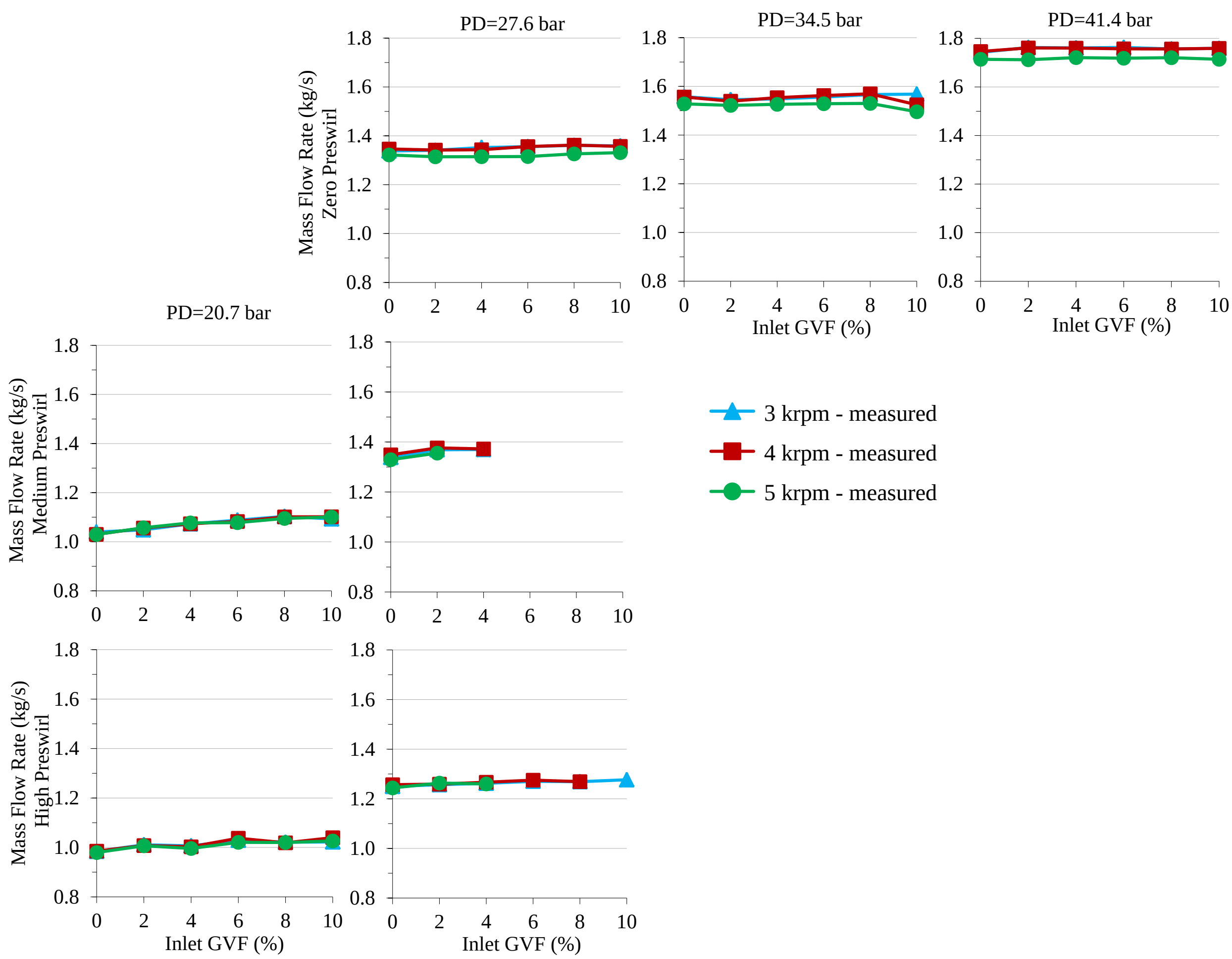

Figure 22 Measured $\dot{m}$ vs. inlet GVF under pure- or mainly-oil conditions

Following the top row for the zero-preswirl insert,

- As inlet GVF increasing from 0 to 10%, measured $\dot{m}$ barely changes. As seen from Eqs. (13) and (15), when GVF goes up, both effective density and effective viscosity decrease. Decreasing effective viscosity can increase $\dot{m}$, while decreasing effective density can decrease $\dot{m}$. Therefore, the insignificant change of measured $\dot{m}$ as inlet GVF increases implies that the effects of decreasing effective viscosity and decreasing effective density on $\dot{m}$ are comparable.
- Increasing PD increases $\dot{m}$. $\dot{m}$ increases by a factor of 1.15 and 1.3 as PD increasing from 27 to 34.5 bar, and from 27 to 41.4 bar, respectively. A similar tendency was obtained by Iwatsubo et al. [35] for pure-liquid conditions and by Zhang [21] for pure- and mainly liquid condition.
- There is an insignificant change of $\dot{m}$ between ω of 3 and 4 krpm, but when ω increases from 4 to 5 krpm, $\dot{m}$ drops by 1.5-3%. This tendency of drop in $\dot{m}$ as ω increases is similar to the results shown in Jolly et al. [34] and Iwatsubo et al. [35], where only pure-liquid conditions were tested, and in Zhang [21] where the tests covered both pure- and mainly-liquid conditions.

Following the middle row for the medium-preswirl insert,

- At PD=20.7 bar, increasing inlet GVF from 0 to 10% increases $\dot{m}$ by a factor of 1.07. At PD=27.6 bar, as inlet GVF increases from 0 to 4% at ω=3 and 4 krpm or inlet GVF increases from 0 to 2% at ω=5 krpm, $\dot{m}$ increases by about 2%. The increase of measured $\dot{m}$ implies that as a consequence of increasing GVF, the decrease of the effective viscosity has more impact on $\dot{m}$ than the decrease of the effective density.
- The higher the PD, the higher $\dot{m}$. $\dot{m}$ increases by 28-30% when PD increases from 20.7 to 27.6 bar.

- The effect of changing ω on $\dot{m}$ is insignificant. The change of $\dot{m}$ is less than 1% when increasing ω from 3 to 5 krpm.

For the high-preswirl insert in the bottom row,

- At PD=20.7 bar, an increase of inlet GVF from 0 to 10% increases $\dot{m}$ by 5%. At PD=27.6 bar, $\dot{m}$ increases by 2.1%, 1%, and 1.3% as GVF increases, from 0 to 10% at ω=3 krpm, from 0 to 8% at ω=4 krpm, and from 0 to 4% at ω=5 krpm, respectively.
- Increasing PD increases $\dot{m}$, specifically, $\dot{m}$ increases by 24-28% when PD increases from 20.7 to 27.6 bar.
- The effect of changing ω from 3 to 5 krpm on $\dot{m}$ is insignificant.

The impact of changing preswirl on $\dot{m}$ is based on the performance at PD=20.7 and 27.6 bar, as shown in the first and second columns in Fig. 22.

- At PD=20.7 bar, there is a drop in $\dot{m}$, by 4-7%, when changing from the medium- to high-preswirl insert.
- At PD=27.6 bar, as changing inlet preswirl from zero to medium, there is no change of $\dot{m}$ at inlet GVF=0%; however, $\dot{m}$ increases slightly, by 2%, at inlet GVF=2% and 4%. When inlet preswirl further increases from medium to high, $\dot{m}$ drops by 6-8% at inlet GVF=0-4%. Iwatsubo et al. [35], in his pure-liquid tests, reported an insensitivity of $\dot{m}$ on preswirl ratio where only three preswirl velocities were tested, namely, negative, zero, and positive preswirl ratio. Their results agreed with the measured results here for cases of GVF=0%, PD=27.6 bar, with changing from the zero- to medium-preswirl insert. At PD=27.6 bar, the effect of changing ω on $\dot{m}$ becomes weaker with a change of inlet preswirl from zero to medium, but remains

unchanged as inlet preswirl further increases from medium to high. At PD=27.6 bar, with the zero-preswirl insert, $\dot{m}$ only changes with changing ω at ω≥4 krpm; however, with the medium- and high-preswirl inserts, there is no change of $\dot{m}$ with changing ω from 3 to 5 krpm.

5.4 Reynolds Number and Flow Status

Reynolds number *Re* is defined as,

$$Re = \sqrt{Re_\theta^2 + Re_a^2} \tag{31}$$

where, Re_θ is the bulk-flow circumferential Reynolds number, and Re_a is the bulk-flow axial Reynolds number.

The fluid's bulk-flow circumferential velocity, density, and viscosity vary from inlet to exit. Assuming the fluid's circumferential velocity is half of the rotor's surface speed, $D_r\omega/4$, Re_θ is

$$Re_\theta = \frac{\rho C_r D_r \omega}{4\mu} \tag{32}$$

where, ρ is the mixture density, μ is the mixture viscosity, D_r is the rotor diameter, and C_r is the radial clearance. ρ and μ are calculated by Eqs. (13) and (15), respectively.

Re_a is related to $\dot{m}$ by,

$$Re_a = \frac{\rho}{\mu} V_a C_r = \frac{\rho}{\mu} \frac{\dot{m}}{\rho C_r \pi D_r} C_r = \frac{\dot{m}}{\mu \pi D_r} \tag{33}$$

Figure 23 shows the inlet *Re* versus inlet GVF for a range of PD values, three ω values, and three preswirl inserts. In general, for all three preswirl configurations, inlet *Re* slightly increases as inlet GVF increases from 0 to 10%. Increasing PD or ω increases inlet *Re*. As an effect of changing inlet preswirl, inlet *Re* decreases but not significantly as changing from zero to medium or from medium to high.

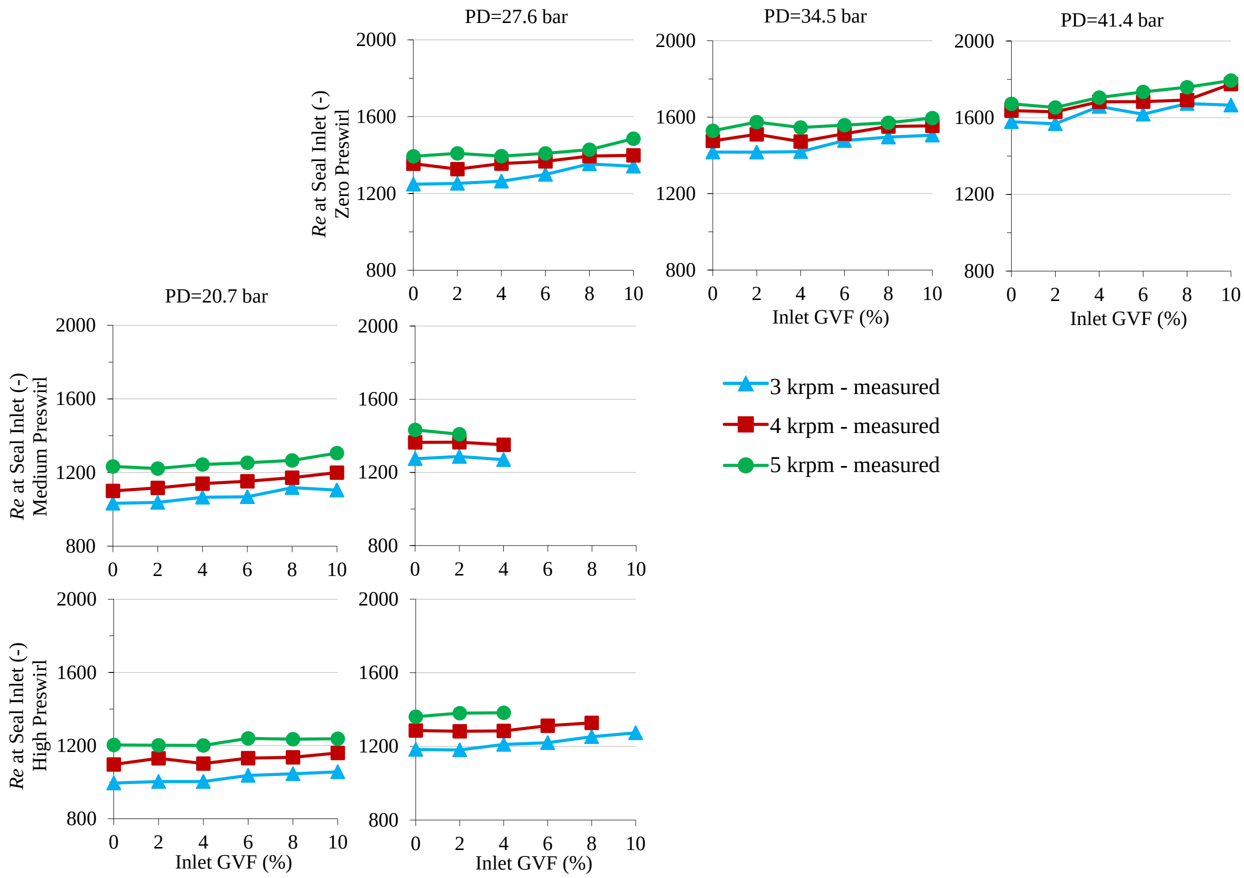

Figure 23 Measured *Re* at seal inlet vs. inlet GVF under pure- or mainly-oil conditions

Figure 24 shows the exit *Re* versus inlet GVF for a range of PD values, three ω values, and three preswirl inserts. The exit *Re* follows similar trends as with the inlet *Re* when inlet GVF, PD, ω, or preswirl change. The impact of changing GVF on the exit *Re* is more moderate compared to on the inlet *Re*. In general, exit *Re* values are higher than inlet *Re*.

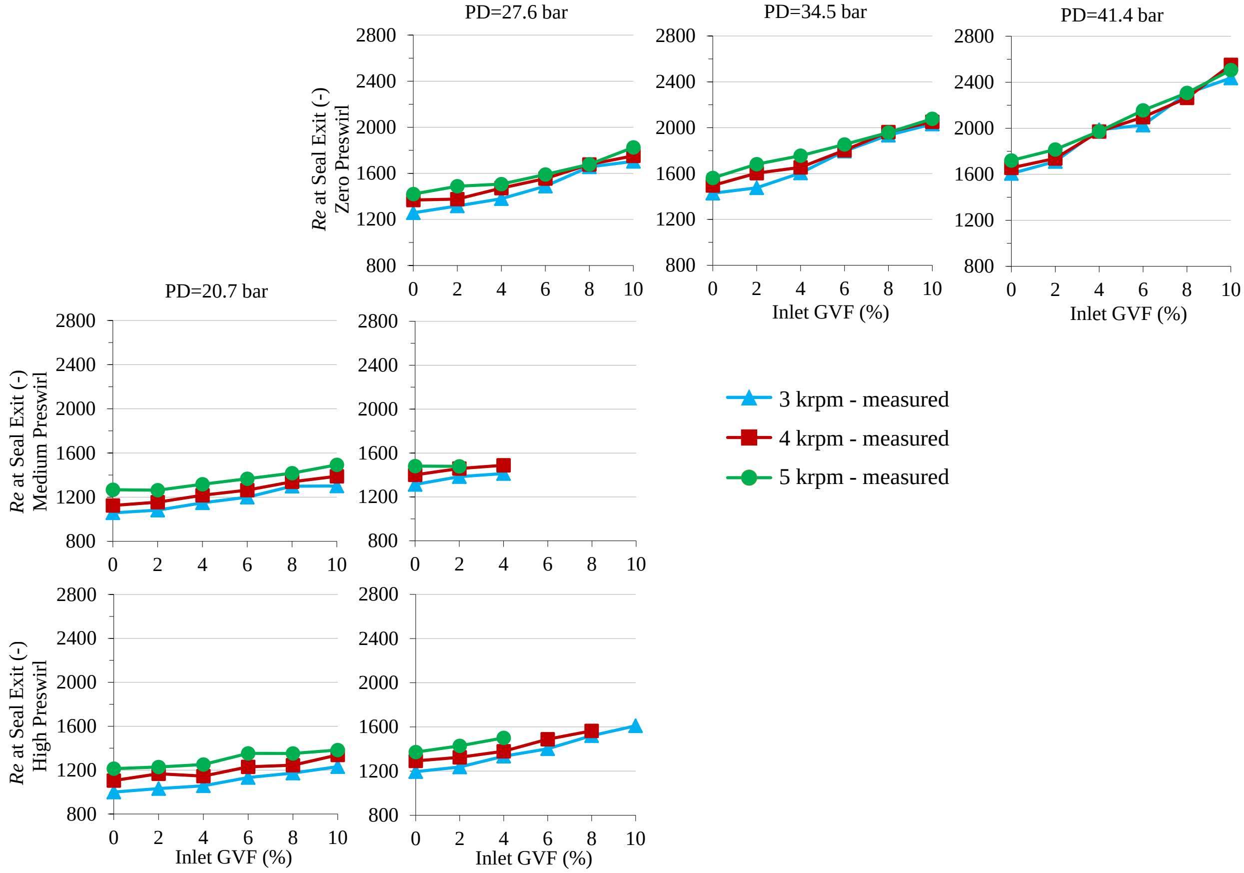

Figure 24 Measured *Re* at seal exit vs. inlet GVF under pure- or mainly-oil conditions

The Reynolds numbers are in ranges of 1000 to 1800 and 1000 to 2600 at the seal's inlet and the seal's exit, respectively. According to Zirkelback and San Andrés [36], for liquid-annular pressure seals, *Re* range for transitional flow is 1000 < *Re* < 3000, while laminar flow and turbulent flow exist with *Re* < 1000 and *Re* > 3000, respectively. Assume that, the effect of *Re* on flow status for mainly-liquid conditions with inlet GVF≤10% is comparable to cases at pure-liquid conditions; therefore, with *Re* in ranges of 1000 to 1800 and 1000 to 2600 at the seal's inlet and the seal's exit, respectively, the flow for all testing cases in this thesis is likely in a transitional state between laminar and turbulent flows.

5.5 Direct Stiffness Coefficient

Figure 25 shows *K* versus the inlet GVF for a range of PD values, three speeds, and three preswirl inserts.

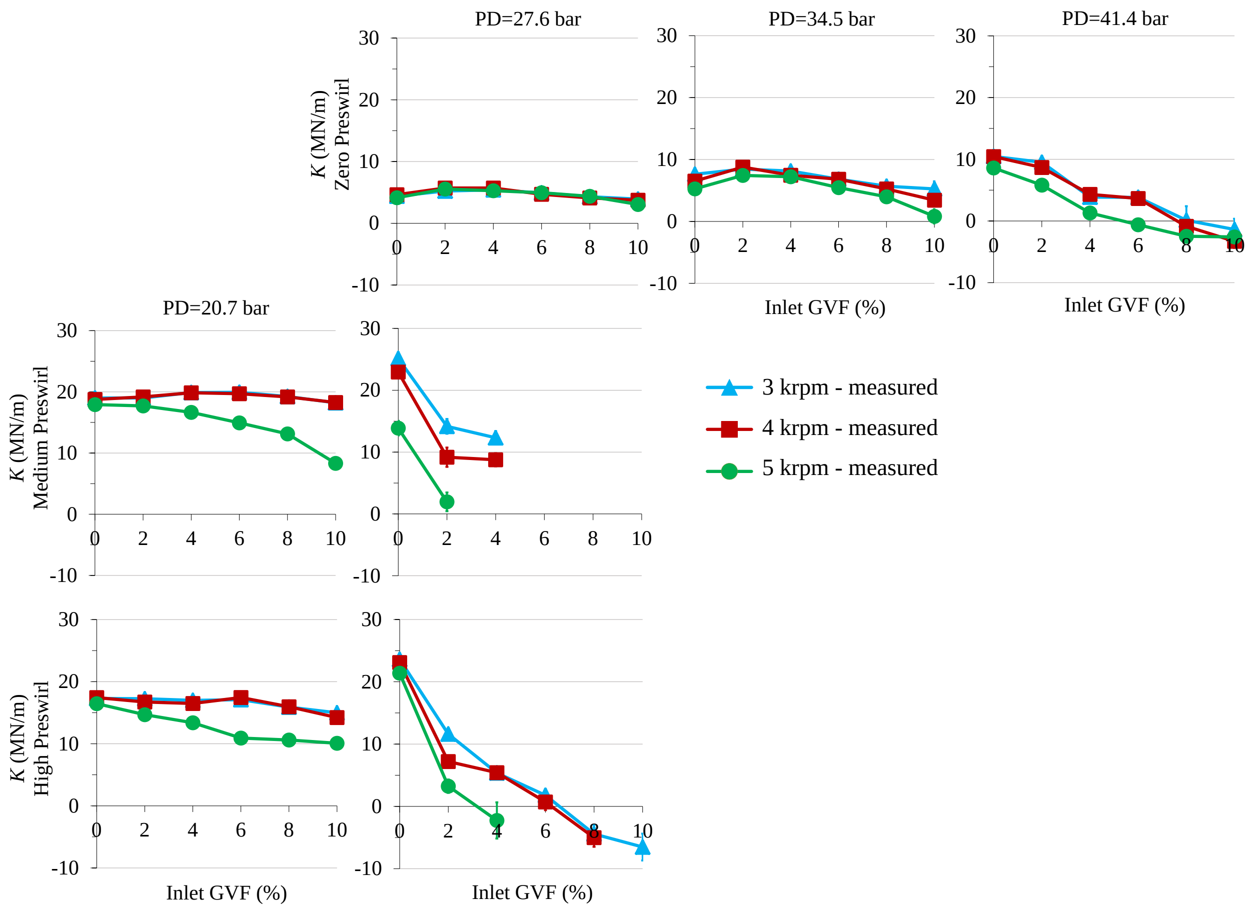

Figure 25 Measured *K* vs. inlet GVF under pure- or mainly-oil conditions

The top row shows the results for the zero-preswirl insert.

- At PD=27.6 or 34.5 bar, as inlet GVF increases from 0 to 10%, *K* increases by 30% and reaches a peak at inlet GVF around 2-4% and then drops as inlet GVF further increases. On the other hand, at PD=41.4 bar, *K* drops immediately as air is injected, and even becomes negative at inlet GVF=10%. The tendency of drop in *K* as inlet

GVF increases is more obvious when PD increases. The higher the PD, the more quickly *K* drops. The tendency of drop in *K* as inlet GVF increases was seen in measurements done by Iwatsubo and Nishino [13] but no detailed explanation was given.

- At inlet GVF=0% (pure-oil conditions), increasing PD increases *K*. However, at inlet GVF≥2%, (mainly-oil conditions), *K* increases when PD increases from 27.6 to 34.5 bar, and then drops as PD further increases to 41.4 bar.
- *K* is a weak function of ω at PD=27.6 bar; however, at higher PD values, *K* remains unchanged with increasing ω from 3 to 4 krpm, but further increasing ω from 4 to 5 krpm decreases *K*. As the effect of increasing ω, Iwatsubo and Nishino [13] also reported a drop in *K* for a mixed flow.

Reynolds number plot as shown in Figs. 23 and 24 might explain the phenomena of dropping *K* as observed for the zero-preswirl insert. According to the discussion in Sec. 5.4, the flow for tested cases is likely in a transitional phase between laminar and turbulent. In transitional regime, as *Re* increases, friction factor initially drops and then increases [36]. If friction factor increases with increasing *Re*, the Lomakin effect reverses and reduces direct stiffness values, and that could explain the trend of *K* decreasing as inlet GVF or PD increases.

The results obtained from *K* potentially relate to the instability issue on the high-differential-pressure helico-axial multiphase pump, reported by Bibet et al. [3]. The pump was designed to operate at a 150-bar differential pressure, running at 4600 rpm with multiphase fluid with 30% GVF. The authors reported SSV with multiphase flows and for relatively low differential pressures when operating at a higher viscosity fluid. With a WFR of more than 1 and the mode shape with a negative damping ratio showing the highest amplitude at the drive end, they believed a destabilizing force impacted on the pump shaft at the balance piston location. Introducing a higher viscosity fluid and running at a relatively low differential pressures might cause a transitional flow in the balance-piston seal. The flow in the transitional regime reverses the Lomakin effect and reduces *K* drastically under 2-phase flow, as seen from the test result of *K* shown in Fig. 25 for the zero-preswirl insert at PD=41.5 bar. A drop in *K* could decrease the rotor's critical speed, reduce the onset speed of instability and cause dynamic instability.

The middle row presents the measurements for the medium-preswirl insert.

- At PD=20.7 bar and ω=3 or 4 krpm, *K* increases slightly as inlet GVF increases from 0 to 6%, and then slightly declines as inlet GVF further increases to 10%. At the same PD (20.7 bar) and ω=5 krpm, a downward trend of *K* occurs much earlier, and *K* drops steadily as air is injected; i.e., *K* decreases by 54% as inlet GVF increases from 0 to 10%. At PD=27.6 bar, *K* falls immediately as inlet GVF increases from 0 to 2% (a similar observation as seen in the zero-preswirl configuration at PD=41.4 bar), and potentially becomes negative as inlet GVF approached 6%. This drop in *K* may have dropped the stator natural frequencies and causes the stator to become unstable at higher inlet GVF testing conditions with the medium-preswirl insert.
- Increasing PD increases *K* at pure-liquid conditions, except the case of ω=5 krpm, but drops *K* at inlet GVF≥2%.
- At PD=20.7 bar and inlet GVF=0%, *K* remains unchanged when ω increases; however, at inlet GVF≥2%, *K* remains unchanged as ω increases from 3 to 4 krpm, but drops as ω further increases to 5 krpm. At PD=27.6 bar, *K* drops steadily when ω increases from 3 to 5 krpm.

The bottom row shows measured *K* with the high-preswirl insert.

- At PD=20.7 bar and ω=3 and 4 krpm, *K* increases slightly with increasing inlet GVF from 0 to 6%, and then drops as inlet GVF further increases to 10%; however, at ω=5 krpm, *K* decreases steadily, by about 34%, with increasing inlet GVF from 0 to 6%, and then changes insignificantly as inlet GVF further increases to 10%. At PD=27.6 bar, *K* decreases significantly as inlet GVF increases, and drops below zero at inlet GVF=4% for cases at ω=5 krpm and at inlet GVF=8% for cases at ω=3 and 4 krpm.
- Changing PD has different impacts on *K* between pure- and mainly oil conditions. As PD increases from 20.7 to 27.6 bar, at inlet GVF=0%, *K* increases, but at inlet GVF≥2%, *K* decreases.
- As ω increases, *K* remains unchanged at inlet GVF=0%, but at inlet GVF≥2%, *K* only drops with increasing ω from 4 to 5 krpm, except a case at PD=27.6 bar and inlet GVF=2% where *K* drops even with increasing ω from 3 to 4 krpm.

With the medium- and high-preswirl inserts, the drop in *K* at PD=27.6 bar when inlet GVF increases is unlikely due to a transition between laminar and turbulent flows that is seen in cases of the zero-preswirl insert at PD=41.4 bar. At PD=27.6 bar, inlet and exit *Re*, seen in Figs. 23 and 24, for different preswirl inserts are almost similar; however, the drop in *K* as inlet GVF increases is not significant for the zero-preswirl insert, but it is moderate for the cases of the medium- and high-preswirl inserts.

The effect of changing only inlet preswirl is shown in the first and second columns of Fig. 25 for conditions at PD=20.7 and 27.6 bar, respectively.

- At PD=20.7 bar, changing from the medium- to high-insert preswirl decreases *K*, except the case at ω=5 krpm and inlet GVF=10% where the change of *K* is insignificant.

- At PD=27.6 bar, as changing from zero- to medium-preswirl insert, at ω =3 and 4 krpm, *K* increases for cases of inlet GVF of 0-4%; but at ω of 5 krpm, the increment of *K* occurs only at inlet GVF=0% and it starts dropping at inlet GVF≥2%. As inlet preswirl further increases from medium to high, there are drops in *K* at ω=3 and 4 krpm, even though the drop at inlet GVF=0% is insignificant; however, at ω=5 krpm, measurements show a significant drop in *K* at inlet GVF=0% but a slight increase at inlet GVF=2%.

5.6 Cross-Coupled Stiffness Coefficient

Figure 26 shows *k* of the test seal versus inlet GVF for a range of PD values, three speeds, and three preswirl inserts. The magnitude of *k* is comparable to *K* shown in Fig. 25.

Following the top row for the zero-preswirl insert,

- As inlet GVF increasing from 0 to 10%, *k* increases by 5%, 9%, and 20% at PDs of 27.6, 34.5, and 41.4 bar, respectively.
- As PD increases, *k* slightly increases with an increment of PD from 27.6 to 34.5 bar. The increment of *k* is more significant as PD further increases from 34.5 to 41.4 bar.
- *k* is a weak function of ω as ω changing from 3 to 4 krpm. However, *k* increases significantly as ω further increases from 4 to 5 krpm; i.e., *k* increases by 30-40% as ω increases from 4 to 5 krpm. For 2-phase flow conditions (mainly-liquid), Iwatsubo and Nishino [13] observed *k* to be insensitive with changing ω for ω≤3.5 krpm at high GVF; while in Zhang‘s tests [21], as ω increased from 5 to 15 krpm, the increase of *k* was significant. Those results are reconfirmed here.

The middle row shows the measurements for the medium-preswirl insert.

- At PD=20.7 bar, as inlet GVF increases from 0 to 10%, at ω=3 and 4 krpm, *k* slightly increases by 5%; while at ω=5 krpm, *k* increases significantly by a factor of 1.3. At PD=27.6 bar, with increasing inlet GVF from 0 to 2%, *k* increases by a factor of 1.14, 1.18, and 1.16 at ω=3, 4, and 5 krpm, respectively. As inlet GVF further increases from 2 to 4% at PD=27.6 bar, *k* at ω=3 and 4 krpm slightly drops.
- Increasing PD increases from 20.7 to 27.6 bar increases *k* significantly.
- Concerning the impact of increasing ω from 3 to 4 krpm, *k* changes insignificantly; however, as ω further increases from 4 to 5 krpm, *k* increases significantly.

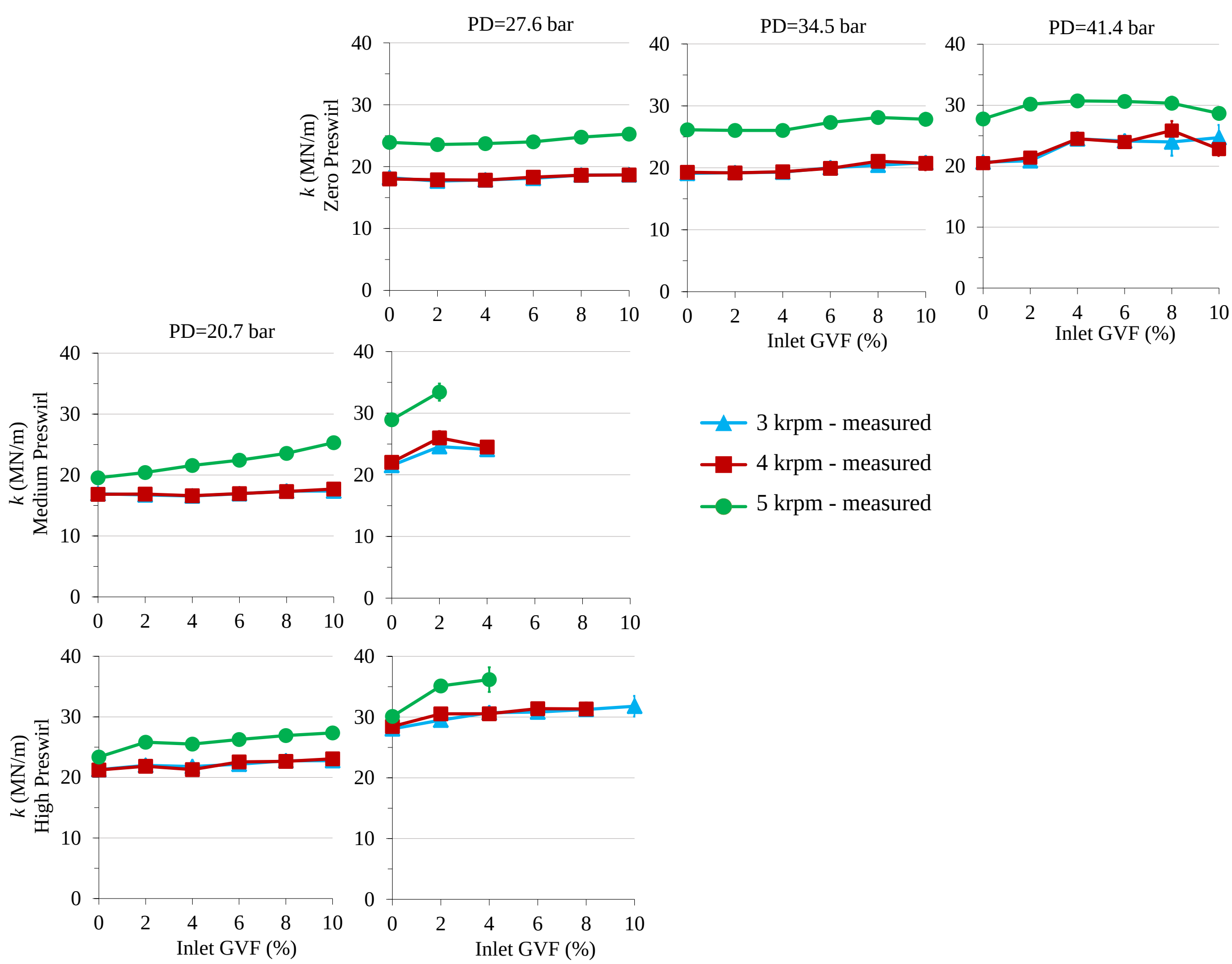

Figure 26 Measured *k* vs. inlet GVF under pure- or mainly-oil conditions

The bottom row presents the measurements for the high-preswirl insert.

- With increasing inlet GVF from 0 to 10%, *k* at ω=3 and 4 krpm increases slightly, while *k* at ω=5 increases significantly.
- *k* increases as PD increases from 20.7 to 27.6 bar.
- As the impact of increasing ω, there is an insignificant change of *k* with increasing ω from 3 to 4 kprm; however, a further increase in ω from 4 to 5 krpm increases *k* slightly at GVF=0% and significantly at GVF≥2%.

The increment of preswirl tends to increase cross-coupled components. As inlet preswirl increases, *k* increases, as expected. At PD=20.7 bar, shown in the first column, when changing from medium to high-preswirl insert, *k* increases by 30% at ω=3 and 4 krpm and by 20% at ω=5 krpm. At PD=27.6 bar, shown in column 2, *k* increases by 20-40% and 20-30% as changing preswirl inserts from zero to medium and from medium to high, respectively. The above effect of changing preswirl on *k* confirms the results done previously by Iwatsubo et al. [35] where only pure-liquid conditions were tested.

As seen from the results of *k*, shown in Fig. 26, at PD=27.6 bar, for the medium preswirl case, *k* increases rapidly with increasing inlet GVF at ω=5 krpm, significantly more rapidly than at ω=4 krpm. A similar result holds at high preswirl. However, for the zero-preswirl insert, *k* values are smaller and increase slowly with increasing GVF. *k* also increases moderately with increasing PD for the medium- and high-preswirl insert. In Bibet et al. [3], the variation of speed (from 1.5 to 4.6 krpm), inlet GVF and PD might cause *k* increased significantly and would cause instability.

5.7 Direct Damping Coefficient

Figure 27 shows *C* versus inlet GVF for a range of PD values, three speeds, and three preswirl inserts.

Following the zero-preswirl insert, shown in the top row, increasing inlet GVF from 0 to 10% increases *C* by 7%, 11%, 20% for PD of 27.6, 34.5, 41.4 bar, respectively. *C* increases as PD increases; i.e., *C* increases by 11-15% and 9-18% when PD increases from 27.6 to 34.5 bar and from 34.5 to 41.4 bar, respectively. There is an insignificant increase of *C* due to increasing ω; i.e., less than 3% when ω increases from 3 to 5 krpm. That tendency of *C* as an effect of changing ω was also reported by Iwatsubo and Nishino [13] (with ω up to 3.5 krpm) for pure- and mainly-liquid test conditions.

The measurements for the medium-preswirl insert are shown in the middle row. Increasing inlet GVF from 0 to 10% increases *C*. *C* tends to increase significantly as PD increases from 20.7 to 27.6 bar. The impact of changing ω is different at different PD. At PD=20.7 and GVF=0%, *C* remains unchanged with increasing ω from 3 to 5 krpm; however, as inlet GVF increases, *C* still remains unchanged with increasing ω from 3 to 4 krpm, but increases as ω further increases to 5 krpm. At PD=27.6 bar, *C* increases as ω increases.

The bottom row presents the measurement for the high-preswirl insert. Increasing inlet GVF increases *C*. *C* increases significantly as PD increases from 20.7 to 27.6 bar. At inlet GVF=0%, *C* changes insignificantly as the impact of changing ω. At inlet GVF≥2%, the impact of increasing ω from 3 to 4 krpm is insignificant, except at PD=27.6 bar and inlet GVF=2% where there is an increase of *C* as ω increases from 3 to 4 krpm. *C* increases with increasing ω from 4 to 5 krpm.

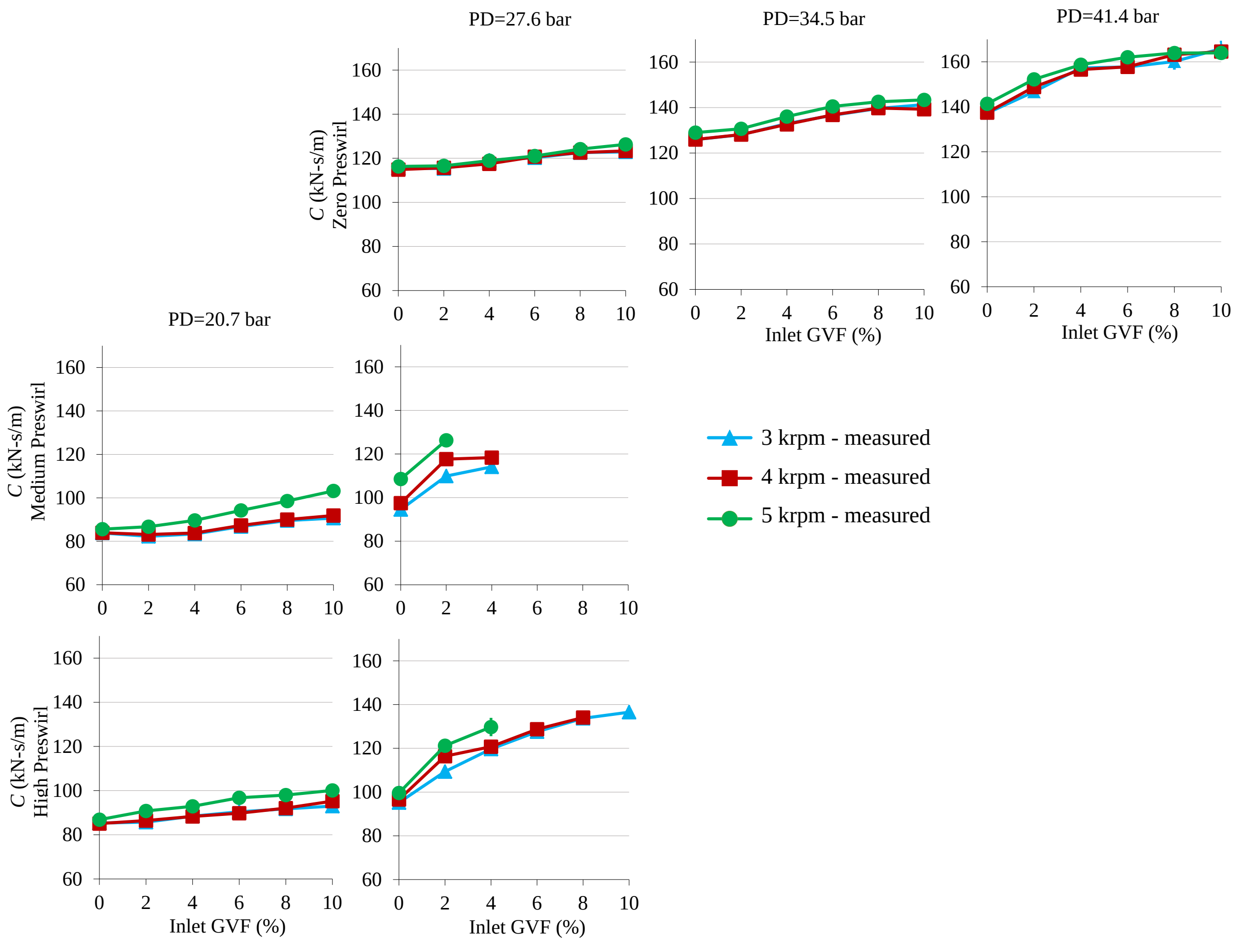

Figure 27 Measured *C* vs. inlet GVF under pure- or mainly-oil conditions

The effect of changing inlet preswirl ratio on *C* is shown in the first and second columns. At PD=20.7 bar, changing from the medium- to high-preswirl insert has a weak impact on *C* values; i.e., increases *C* by a factor of 1.05. At PD=27.6 bar, as changing from the zero- to medium-preswirl insert, there is a slight drop of *C* at inlet GVF=0%; however, at inlet GVF=2% and 4%, *C* remains unchanged at ω=4 kprm, slightly increases at ω=5 krpm, and slightly decreases at ω=3 krpm. At PD=27.6 bar, *C* changes insignificantly as changing from the medium- to high-preswirl insert, except a drop of 9% for the case at ω=5 krpm and inlet GVF=0%.

At PD=20.7 or 27.6 bar, changing from the medium- to high-preswirl insert does not change the behavior or impact of increasing inlet GVF on *C*. However, at PD=27.6 bar, changing from the zero- to medium-preswirl insert changes the impact of increasing inlet GVF on *C*. At PD=27.6 bar, with the zero-preswirl insert, *C* increases slowly as inlet GVF increases; but with the medium-preswirl insert, *C* increases rapidly as inlet GVF increases from 0 to 2% and then slowly increases (at ω=3 and 4 krpm) as inlet GVF further increases to 4%.

5.8 Cross-Coupled Damping Coefficient

Figure 28 shows *c* versus inlet GVF for a range of PD values, three speeds, and three preswirl inserts.

For the zero-preswirl insert, shown in the top row in Fig. 28,

- Increasing inlet GVF decreases *c*. At PD=27.6 bar, *c* drops steadily with increasing inlet GVF from 0 to 10%. However, at PD=34.5 and 41.5 bar, *c* drops as inlet GVF increases, but then changes insignificantly with changing inlet GVF at GVF≥8% and inlet GVF≥4%, respectively.
- As PD increases from 27.6 to 34.5 bar, at ω=3 and 4 krpm, *c* remains unchanged at inlet GVF=0-4% and decreases slightly at inlet GVF≥6%; however, at ω=5 krpm, *c* decreases slightly at inlet GVF=0-10%. With increasing PD further from 34.5 to 41.4 bar, *c* changes insignificantly at inlet GVF=0%, but decreases significantly at inlet GVF≥2%.
- There is an insignificant change of *c* with increasing ω from 3 to 4 krpm; however, increasing ω from 4 to 5 krpm increases *c*, except at PD=41.4 bar and inlet GVF=2% where *c* remains unchanged as ω increases from 3 to 5 krpm.

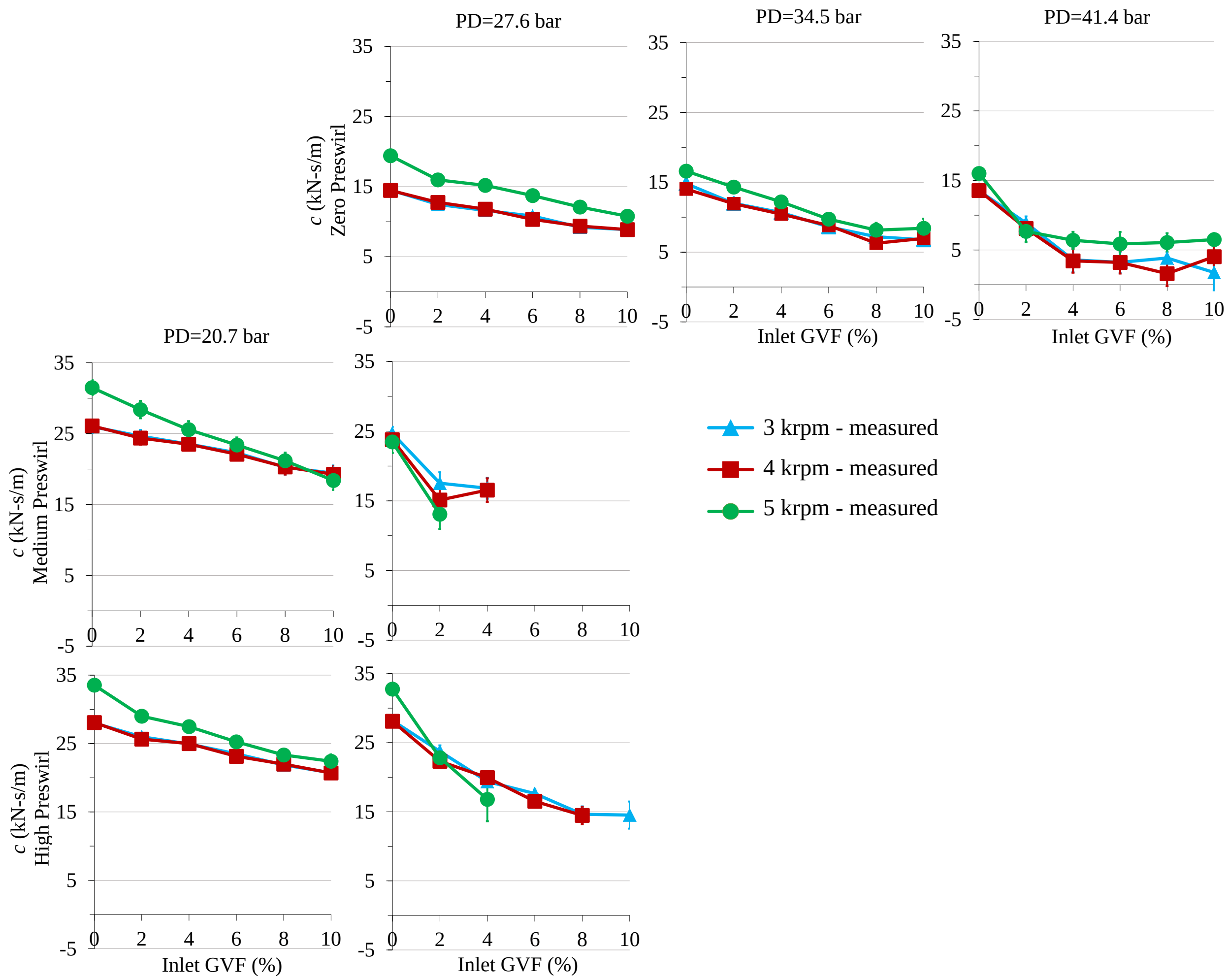

Figure 28 Measured *c* vs. inlet GVF under pure- or mainly-oil conditions

For the medium-preswirl insert, shown in the middle rows in Fig. 28,

- At PD=20.7 bar, increasing inlet GVF drops *c* steadily. At 27.6 bar, *c* drops with increasing inlet GVF from 0 to 2%; however, further increasing inlet GVF from 2 to 4% slightly increases *c* at ω=4 krpm, but slightly decreases *c* at ω=3 krpm.
- *c* drops as PD increases from 20.7 to 27.6 bar.
- At PD=20.7 bar, *c* changes insignificantly with increasing ω from 3 to 4 krpm; but further increasing ω from 4 to 5 krpm increases *c* at inlet GVF=0-8% and decreases *c*

at inlet GVF=10%. At PD=27.6 bar, with increasing ω from 3 to 5 krpm, *c* remains unchanged at inlet GVF=0%, but decreases at inlet GVF=2%. At PD=27.6 bar and inlet GVF=4%, *c* remains unchanged as ω increases from 3 to 4 krpm.

The measurements for the high-preswirl insert are shown in the bottom row.

- Increasing inlet GVF decreases *c*.
- With increasing PD from 20.7 to 27.6 bar, *c* remains unchanged at inlet GVF=0% but decreases at inlet GVF≥2%.
- At PD=20.7 bar, *c* changes insignificantly as ω increases from 3 to 4 krpm, but increases as ω further increases to 5 krpm. At PD=27.6 bar, *c* remains unchanged with increasing ω from 3 to 4 krpm; and as ω further increases to 5 krpm, *c* increases at inlet GVF=0%, remains unchanged at inlet GVF=2%, and drops at inlet GVF=4%.

The impact of changing inlet preswirl on *c* is shown in the first and second columns in Fig. 28. As the inlet preswirl ratio increased, *c* increases. At PD=20.7 bar, the increment is small, about 5-7%, when changing from the medium- to high-preswirl insert. At PD=27.6 bar, there are increases of *c* as changing inlet preswirl from zero to medium and from medium to high; i.e., *c* increases by a factor of 1.65, in average when changing from the zero- to high-preswirl insert.

5.9 Direct Virtual Mass Coefficient

Figure 29 shows *M* versus inlet GVF for a range of PD values, three speeds, and different preswirl inserts.

Following the zero-preswirl insert, shown in the top row, increasing inlet GVF decreases *M*. As PD increases from 27.6 bar to 34.5 bar, *M* changes insignificantly at inlet GVF=0% and 2%, but drops at inlet GVF≥4%. With PD further increasing from 34.5 to 41.4 bar, *M* changes insignificantly at inlet GVF=0%, but drops significantly at inlet GVF≥2%. Changes on ω has no significant effect on *M*. The above tendencies were seen in the previous researches. For mainly-liquid tests with zero-preswirl insert, Zhang [21] reported a drop of *M* as inlet GVF or PD increased; while Iwatsubo and Nishino [13] concluded *M* was insignificantly changed as results of increasing ω up to 3.5 krpm - these trends matched with the results of the cases of the zero-preswirl insert here.

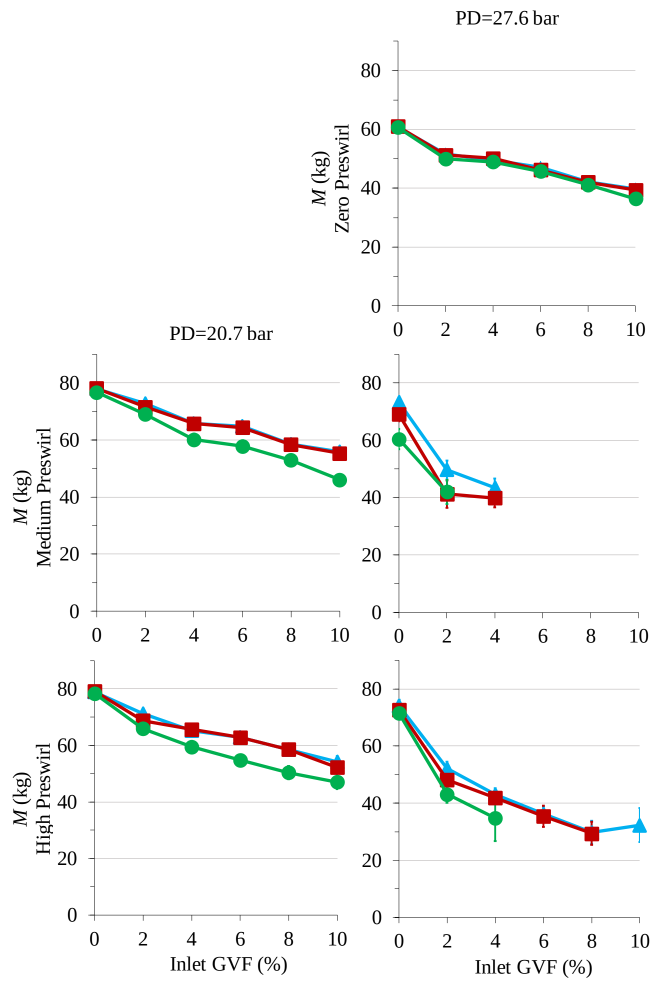

Figure 29 Measured *M* vs. inlet GVF under pure- or mainly-oil conditions

For the medium-preswirl insert, shown in the middle row, *M* drops when inlet GVF increases. Increasing PD decreases *M*, even at the pure-liquid condition (inlet GVF=0%). At

PD=20.7 bar, *M* is insensitive to a change of ω at ω≤4 krpm, and starts dropping when ω increases from 4 to 5 krpm; however, at PD=27.6 bar, *M* starts decreasing significantly when ω increases from 3 to 4 krpm, and from 4 to 5 krpm.

The bottom row shows *M* values for the high-preswirl insert. Increasing inlet GVF decreases *M*. As PD increases, *M* decreases. At inlet GVF=0%, *M* is insensitive with changing ω; however, at inlet GVF≥2%, *M* starts decreasing significantly as ω increases at ω≥4 krpm.

The impact of changing inlet preswirl on *M* is shown in the first and second columns in Fig. 29. At PD=20.7 bar, there is an insignificant effect of changing inlet preswirl from medium to high on *M*. At PD=27.6 bar and inlet GVF=0%, changing from the zero- to medium-preswirl insert or from the medium- to high-preswirl insert increases *M* significantly. However, at PD=27.6 bar and inlet GVF≥2%, *M* drops in changing from the zero- to medium-preswirl insert, but there is an insignificant change when moving from the medium- to high-preswirl insert, except a slight increase for the case at inlet GVF=2% and ω=4 krpm.

5.10 Cross-Coupled Virtual Mass Coefficient

Figure 30 shows m_q versus inlet GVF for a range of PD values, three speeds, and three preswirl inserts. Note that m_q can be negative. From Eq. (4), a negative value of m_q produces a destabilizing force.

By considering the uncertainty, the measured m_q values are close to zero for cases of the zero-preswirl insert (top row).

- At PD=27.6 and 34.5 bar, increasing inlet GVF generally increases m_q (less negative). At PD=41.4 bar and ω=3 and 4 krpm, increasing inlet GVF makes m_q be positive, but decreases m_q (more negative) at ω=5 krpm.

- Increasing PD from 27.6 to 34.5 bar has a little effect on m_q. Increasing PD from 34.5 to 41.4 bar switches m_q from negative to positive for most cases at ω=3 and 4 krpm (the seal force becomes stabilizing), but makes m_q more negative for cases at ω=5 krpm (making the seal force more destabilizing).
- There is insignificant different of m_q between ω=3 and 4 krpm; however, as ω increases from 4 to 5 krpm, m_q decreases (m_q more negative), resulting more destabilizing effect.

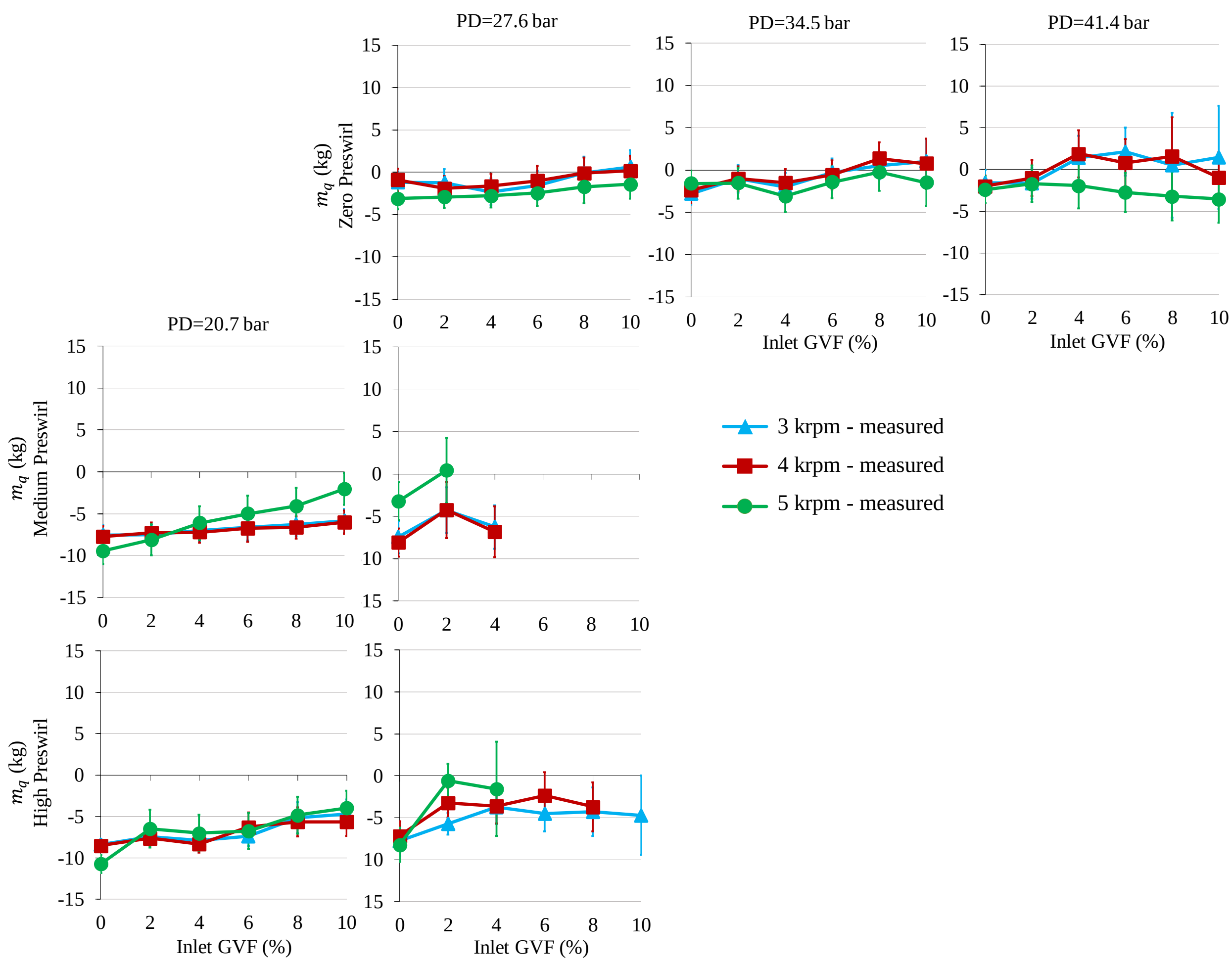

Figure 30 Measured m_q vs. inlet GVF under pure- or mainly-oil conditions

The cases of the medium-preswirl insert are shown in the middle row.

- Increasing inlet GVF increases m_q (less negative), making the seal force less destabilizing.
- As PD increases from 20.7 to 27.6 bar, at ω=5 krpm, m_q tends to increase (less negative); however, at ω=3 and 4 krpm, m_q tends to decrease (more negative) at inlet GVF=0%, but to increase (less negative) at GVF≥2%.
- There is an insignificant difference of m between ω=3 and 4 krpm. As ω increases from 4 to 5 krpm, at PD=20.7 bar, m_q tends to decrease (more negative) at inlet GVF=0% and 2%, but to increase (less negative) at inlet GVF≥4%; however, at PD=27.6 bar, m_q tends to increase (less negative).

The bottom row shows the cases of the high-preswirl insert. The impacts of changing inlet GVF, PD, and ω on m_q are similar to the cases of the medium-preswirl insert.

The impact of changing inlet preswirl on m_q is shown in the first and second columns. At PD=20.7 bar (first column), changing from the medium- to high-preswirl insert has a minimum impact on m_q at ω=3 and 4 krpm; however, at ω=5 krpm, m_q tends to decrease (more negative) for cases of inlet GVF≥6%. At PD=27.6 bar (second column), as changing from the zero- to medium-preswirl insert, m_q decreases (more negative) at ω=3 and 4 krpm (making the seal force more destabilizing), but slightly increases (less negative) at ω=5 krpm (making the seal force less destabilizing). As preswirl further increases from medium to high at PD=27.6, m_q changes insignificantly.

5.11 Whirl-Frequency Ratio

Due to finite values of m_q in the measurement, as shown in the Fig 30, whirl-frequency ratio (WFR) is defined using San Andrés [37]'s formulation (refer to Appendix A for the detailed formulation).

WFR is used as a system stability indicator. The lower the WFR, the better the system stability. According to Lund [38], the onset speed of instability (OSI) for a flexible rotor supported by hydrodynamic bearings with defined WFR is

$$OSI = \frac{\omega_{n1}}{WFR} \tag{34}$$

where, ω_{n1} is the first natural frequency of the rotor system. With a low WFR, the system's OSI would be high, resulting in increased stability.

Figure 31 shows WFR versus inlet GVF for a range of PD values, three speeds, and three preswirl inserts.

For the zero-preswirl insert, as shown in the top row of Fig. 31, WFR changes insignificantly with changing PD or inlet GVF. At ω=3 krpm, WFR is about 0.5, similar to a plain hydrodynamic bearing. At higher ω, i.e., 4 and 5 krpm, WFR drops and is about 0.3-0.4. Interestingly, WFR drops as ω increases (stability increased).

For the medium inlet preswirl (middle row), at PD=20.7 bar, WFR changes insignificantly as GVF increases; however, at PD=27.6 bar, WFR tends to drop slightly with increasing GVF. Increasing PD increases WFR. WFR drops as ω increases from 3 to 4 krpm; however, the drop in WFR with ω increasing from 4 to 5 krpm is insignificant.

The bottom row shows the results for the high-preswirl insert. At PD=20.7 bar, WFR is not a function of inlet GVF; however, at PD=27.6 bar, WFR decreases as GVF increases. As PD increases from 20.7 to 27.6 bar, WFR tends to increase at inlet GVF=0%, remains unchanged at inlet GVF=2% and 4%, but decreases slightly at inlet GVF≥6%. Interestingly, the higher the speed, the lower the WFR.

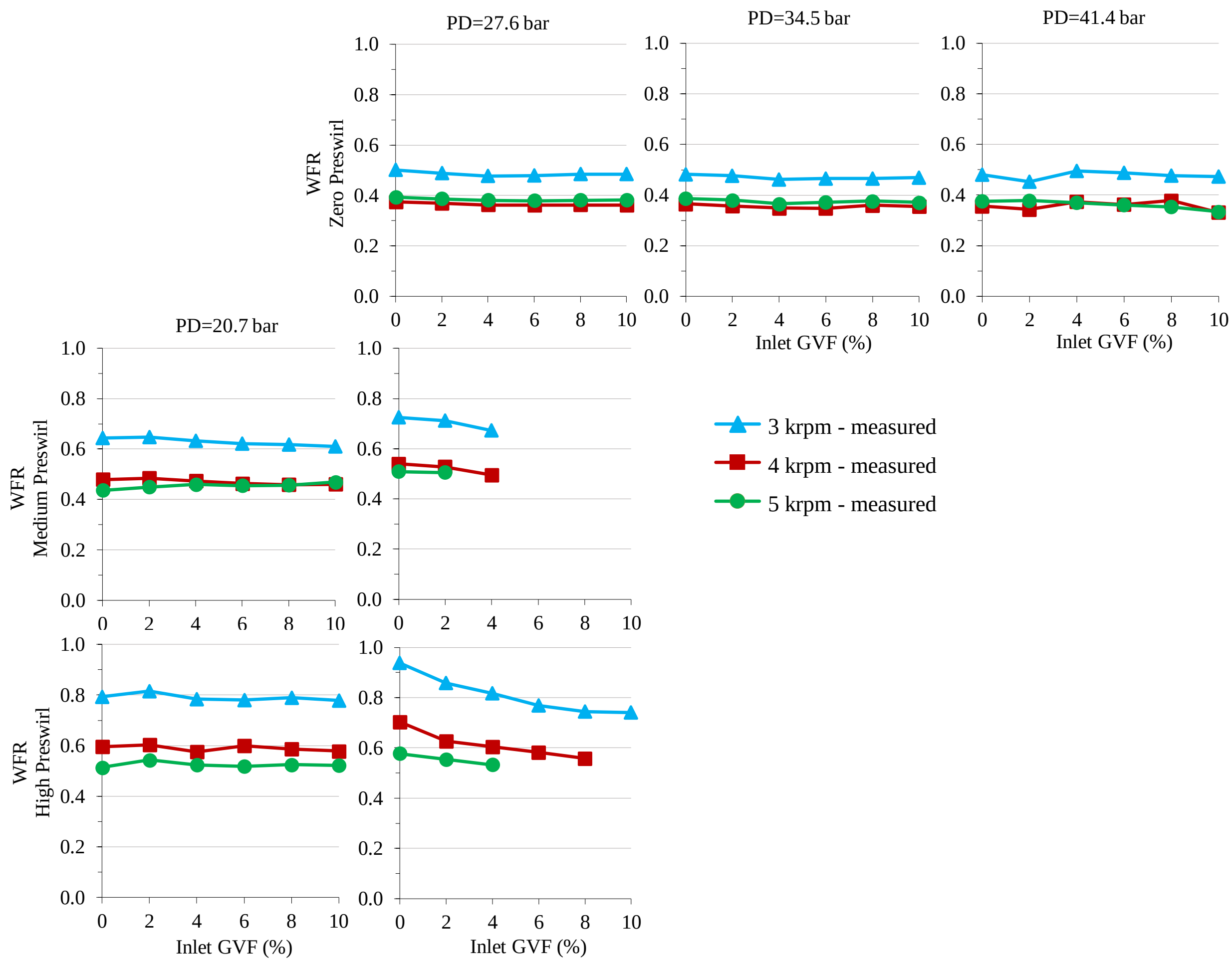

Figure 31 Measured WFR vs. inlet GVF under pure- or mainly-oil conditions

As expected, as the inlet preswirl ratio increases, WFR also increases (stability decreased). Comparing the results of WFR, shown in Fig. 31, and preswirl ratio (PSR), shown in Fig. 21, the ratio between WFR and PSR are 2.5, 1-1.25, and 0.5-0.8 for the zero-, medium-, and high-preswirl inserts, respectively.

5.12 Effective Damping

Effective damping C_{eff} for pure- or mainly-oil conditions is defined as

$$C_{eff} = C - \frac{k}{\omega} + m_q \omega \tag{35}$$

Increasing C_{eff} increases stability. Figure 32 shows C_{eff} versus inlet GVF for a range of PD values, three speeds, and three preswirl inserts.

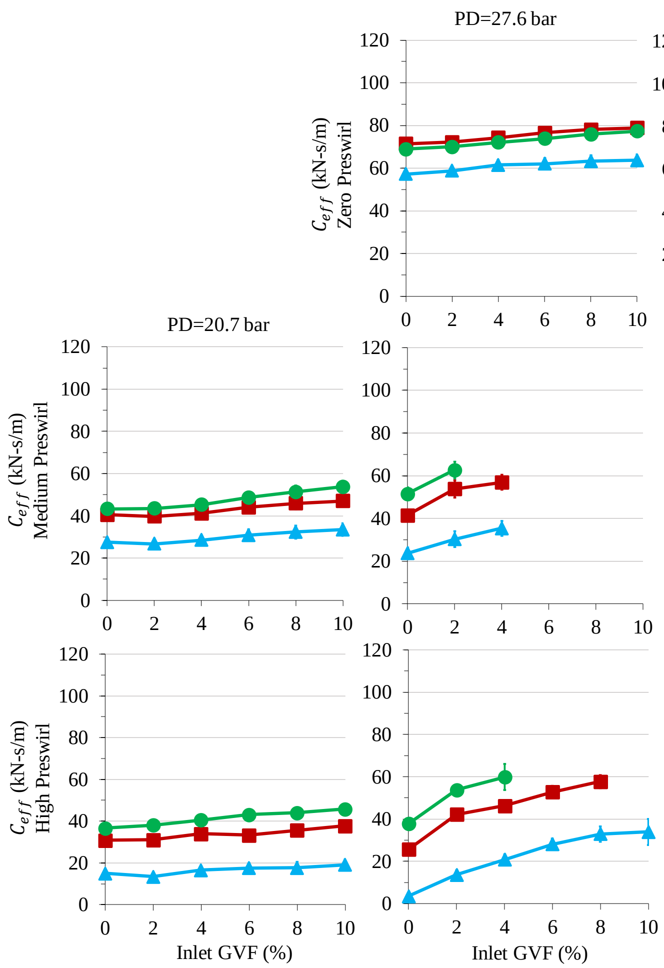

Figure 32 Measured C_{eff} vs. inlet GVF under pure- or mainly-oil conditions

For the zero-preswirl insert, as shown in the top row of Fig. 32, at PD=27.6 bar, C_{eff} is not a strong function of inlet GVF; however, at PD≥34.5 bar, C_{eff} increases as inlet GVF increases because increasing C has a greater impact than increasing k. Increasing PD increases C_{eff}. C_{eff} tends to increase as ω increases from 3 to 4 krpm, but then remains unchanged as ω further increases to 5 krpm.

The effect of inlet GVF, PD, and ω on C_{eff} for the medium-preswirl insert is shown in the middle row. C_{eff} slightly increases as GVF increases at PD=20.7 bar, but the increment of C_{eff} as the effect of increasing inlet GVF is more significant at PD=27.6 bar. At GVF=0%, increasing PD has an insignificant effect on C_{eff} at ω=4 and 5 krpm while it drops C_{eff} slightly at ω=3 krpm. However, at inlet GVF≥2%, increasing PD increases C_{eff}. C_{eff} tends to increase as ω increases.

The third row shows the cases of the high-preswirl insert. The impacts of changing inlet GVF, PD, and ω on m are similar to the cases of the medium-preswirl insert.

Interestingly, similar to the observation with WFR, C_{eff} increases as ω increases. Additionally, adding air increases C_{eff}. These are all signs of stability improvement.

The impact of changing inlet preswirl on C_{eff} is shown in the first and second columns. As the inlet preswirl ratio increases, C_{eff} tends to drop. At PD=20.7, C_{eff} decreases slightly when changing from the medium- to high-preswirl insert. At PD=27.6 bar, the drop is significant when changing from zero- to medium-preswirl or from medium- to high-preswirl. In general, increasing preswirl reduces stability.

6. PREDICTION VERSUS MEASUREMENTS FOR PURE- AND MAINLY-OIL CONDITIONS

Following the measurements as discussed in Chapter 5, this chapter provides comparisons between measured and predicted results for static and dynamic performances of the annular smooth seal operating under pure- and mainly-oil conditions, i.e., mixtures of air and silicone oil (PSF-5cSt). The predicted results are produced from the *XLHseal_mix* program which was developed based on a bulk-flow model introduced by San Andrés [15] in 2011. The program uses inputs listed below. Note that, during pure- and mainly-oil tests, the inlet temperature is maintained within 37.8 to 40.6^{o}C. Based on the measurement, an average value and standard deviation for the inlet temperature and liquid density in each preswirl insert are documented. The two parameters, inlet temperature and liquid density, are then used together with "Silicon oil kinematic viscosity vs. temperature" graph, as shown in Fig. 14, to calculate the liquid viscosity presented in Tab. 9. Inlet preswirl ratio, shown in Fig. 21, are also used as an input for predictions. Entrance pressure loss and exit pressure recovery factors are assumed to be 0.2 and 0, respectively.

The following differences between the predictive model and experiment need to be noted:

(1) The model assumes that the fluid's temperature remains constant in the seal clearance; however, due to power dissipation, the fluid's actual/measured temperature increases as the fluid flows through the seal. Table 11 in Appendix B shows the fluid's measured temperatures at the seal inlet and seal exit.

(2) The model assumes that the mixture is homogeneous in the seal clearance while the actual condition is unknown and may be different. Although the mixture is visually

inspected through a sight-glass view port shortly upstream of the inlet ports of the stator and a bubble size of approximately 1.67-5 μm or 0.8-2.5% of the seal's radial clearance is expected from the mainly-oil mixing section, the mixture might not remain homogeneous in the seal clearance due to piping configuration, the bubble coalescence, and centrifugal-inertia effects. The coalescence of fine bubbles could make larger bubbles. The centrifugal-inertia effect could lead to a stratified-flow.

Table 9 Liquid and gas properties used to run prediction code for pure- and mainly-oil conditions

	Zero-preswirl	**Medium-preswirl**	**High-preswirl**
Average supply temperature (°C)	38.62 (±0.55)	38.37 (±0.42)	38.55 (±0.34)
Liquid properties			
Viscosity (cP)	3.20	3.22	3.21
Density (kg/m3)	900.1 (±0.9)	898.3 (±0.7)	898.9 (±0.8)
Bulk-modulus (bar)	9987		
Surface tention/length (N/m)	0.0197		
Liquid vapor pressure (bar)	0.001		
Gas properties			
Gas constant, R_g (J/kg-C)	286.70		
Compressibility, Z	1.00		
Gas viscosity (cP)	0.0193		
Ratio specific heats	1.40		

6.1 Leakage Mass Flow Rate

Figure 33 compares predicted and measured $\dot{m}$ versus inlet GVF for a range of PD values, three preswirl inserts, and three ω values. The rows and columns are arranged by preswirl insert and PD, respectively.

The comparison for predicted and measured $\dot{m}$ with the zero-preswirl inert is shown in the top row of Fig. 33. Predicted $\dot{m}$ tends to decrease while measured $\dot{m}$ remains unchanged as inlet GVF increases. Both measurement and prediction show an increase in $\dot{m}$ with increasing PD and a slight drop of $\dot{m}$ as ω increases.

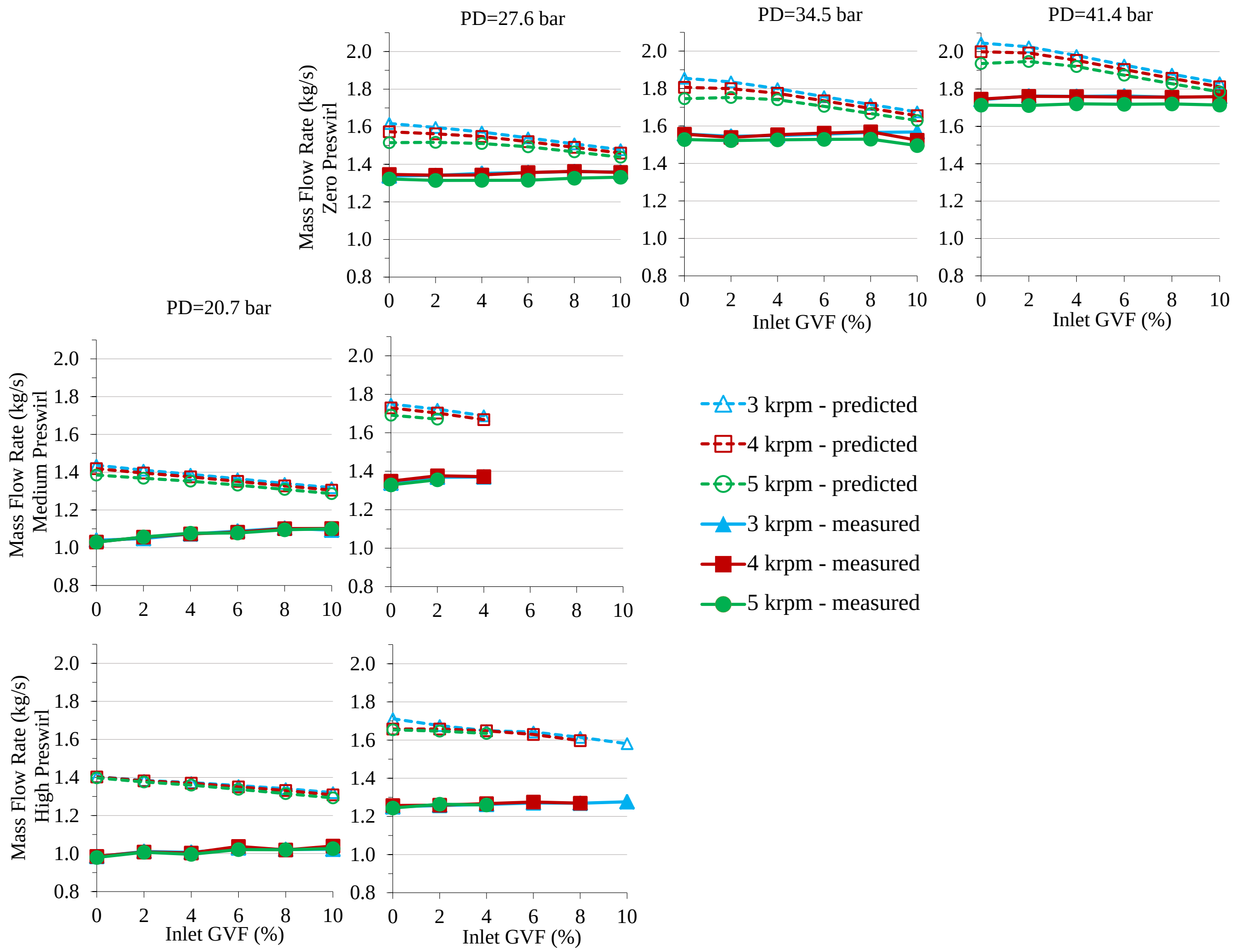

Figure 33 Predictions and measurements of $\dot{m}$ under pure- and mainly-oil conditions

The middle row shows the comparisons for the medium-preswirl insert. Measured $\dot{m}$ tends to increase slightly but prediction shows a drop when inlet GVF increases. Both predicted and measured $\dot{m}$ increase with increasing PD and change insignificantly with increasing ω from 3 to 5 krpm.

The high-preswirl insert's results are shown at the bottom row. As the impact of increasing GVF, measured $\dot{m}$ tends to stay constant while predicted $\dot{m}$ decreases. Both measured and predicted $\dot{m}$ increase as PD increases and remain unchanged as ω increases.

The impact of changing preswirl is shown in the first and second columns, corresponding to the cases at PD=20.7 and 27.6 bar. Generally, both measurement and prediction show little changes as inlet preswirl changes. At PD=20.7 bar, as the effect of changing preswirl from medium to high, predicted $\dot{m}$ remains unchanged, while measured $\dot{m}$ slightly decreases. At PD=27 bar, as changing inlet preswirl from zero to medium, predicted $\dot{m}$ tends to increase by 10%, while measured $\dot{m}$ remains unchanged. Changing from medium to high preswirl at PD=27 bar decreases $\dot{m}$, shown in both prediction and measurement.

In term of magnitude, the predicted $\dot{m}$ is higher than measured. Among three preswirl inserts, the code provides the best prediction for the zero-preswirl insert, especially at inlet GVF=10%. For the zero-preswirl insert, the predicted $\dot{m}$ is higher than measured by factors of less than 1.18 and 1.07 at inlet GVF=0% and 10%, respectively. For the medium- and high-preswirl inserts, the maximum discrepancy occurs at PD=20.7 bar and inlet GVF=0%, where the predicted $\dot{m}$ is larger than measured by a factor of 1.4.

6.2 Reynold Number and Flow Status

The comparison of predictions and measurements for inlet *Re* versus inlet GVF is shown in Fig. 34.

The top row presents the comparison for the zero-preswirl insert. The predicted inlet *Re* is a weak function of inlet GVF. Measurements show a similar tendency, except there is a slight increase as inlet GVF increases in a region of inlet GVF of 4-8%. As PD or ω increases, both predicted and measured inlet *Re* tends to increase.

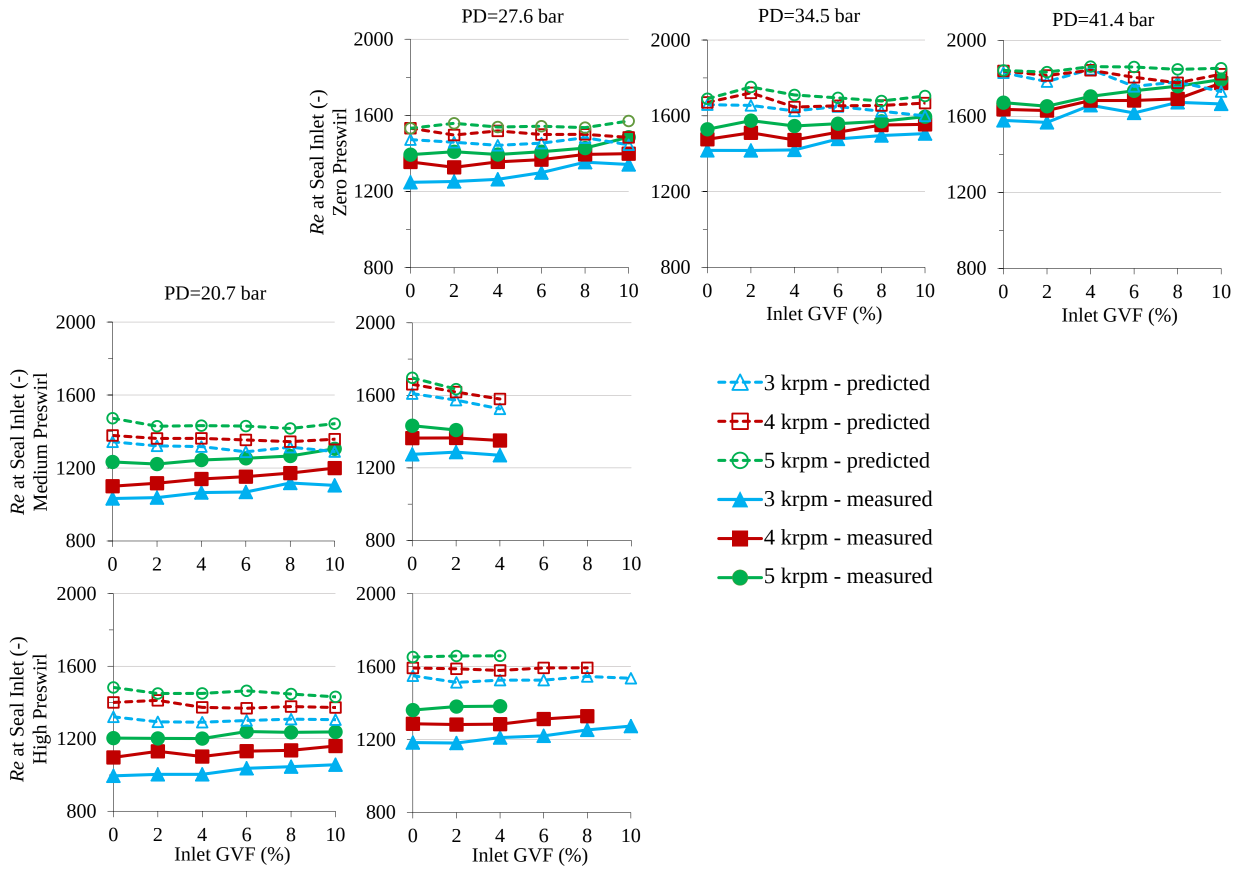

Figure 34 Predictions and measurements of inlet *Re* under pure- and mainly-oil conditions

The comparison between predictions and measurements for the medium-preswirl insert is shown in the middle row. The impact of changing inlet GVF on inlet *Re* is weak, shown on both measurements and predictions. At PD=20.7 bar, as inlet GVF increases, predicted inlet *Re* stays constant while measured values increase slightly. At PD=27.6 bar, measurements show an insignificant change of inlet *Re* while predicted values tend to drop slightly as inlet GVF increases. Both predictions and measurements show an increase of inlet *Re* with increasing PD or ω.

The comparison for the high-preswirl insert is shown in the bottom row. Both predictions and measurements show an insensitive change of inlet *Re* when inlet GVF increases, while increasing PD or ω increases inlet *Re*.

Both predictions and measurements show minor changes of inlet *Re* with the impact of increasing preswirl, as shown in the first and second columns. At PD=20.7 bar, measured and predicted inlet *Re* change insignificantly when increasing inlet preswirl from medium to high. A similar tendency is seen at PD=27.6 bar for a change of inlet preswirl from medium to high. At PD=27.6 bar, as changing from zero to medium preswirl, measured inlet *Re* remains unchanged while predictions show a slight increase.

In term of magnitude, predicted inlet *Re* is generally higher than measured, but they are reasonably close to each other. At the seal inlet, predicted and measured *Re* are in a range of 1300 to 1800 and 1000 to 1800, respectively.

Figure 35 compares prediction and measurement for exit *Re* versus inlet GVF. The top row presents the comparison for the zero-preswirl insert. Both predictions and measurements show increments of exit *Re* as increasing inlet GVF or PD. The impact of changing inlet GVF is predicted here much better than the cases with the inlet *Re*. As ω increases, measurements show a larger increment of exit *Re* while predicted exit *Re* only slightly increases.

The comparison for cases of the medium- and high-preswirl inserts are shown in the middle and bottom rows, respectively. Both predictions and measurements show increments of exit *Re* as increasing inlet GVF, PD or ω.

The impact of changing inlet preswirl on exit *Re* is shown in the first and second column of Fig. 35. Both predictions and measurements show an insignificant change of exit *Re* by changing inlet preswirl.

In term of magnitude, exit predicted *Re* is higher than measured, but they are reasonably close to each other. At the seal exit, predicted and measured *Re* are in a range of 1400 to 2600 and 1000 to 2600, respectively. The flows, in both predictions and measurements, are likely in transitional conditions.

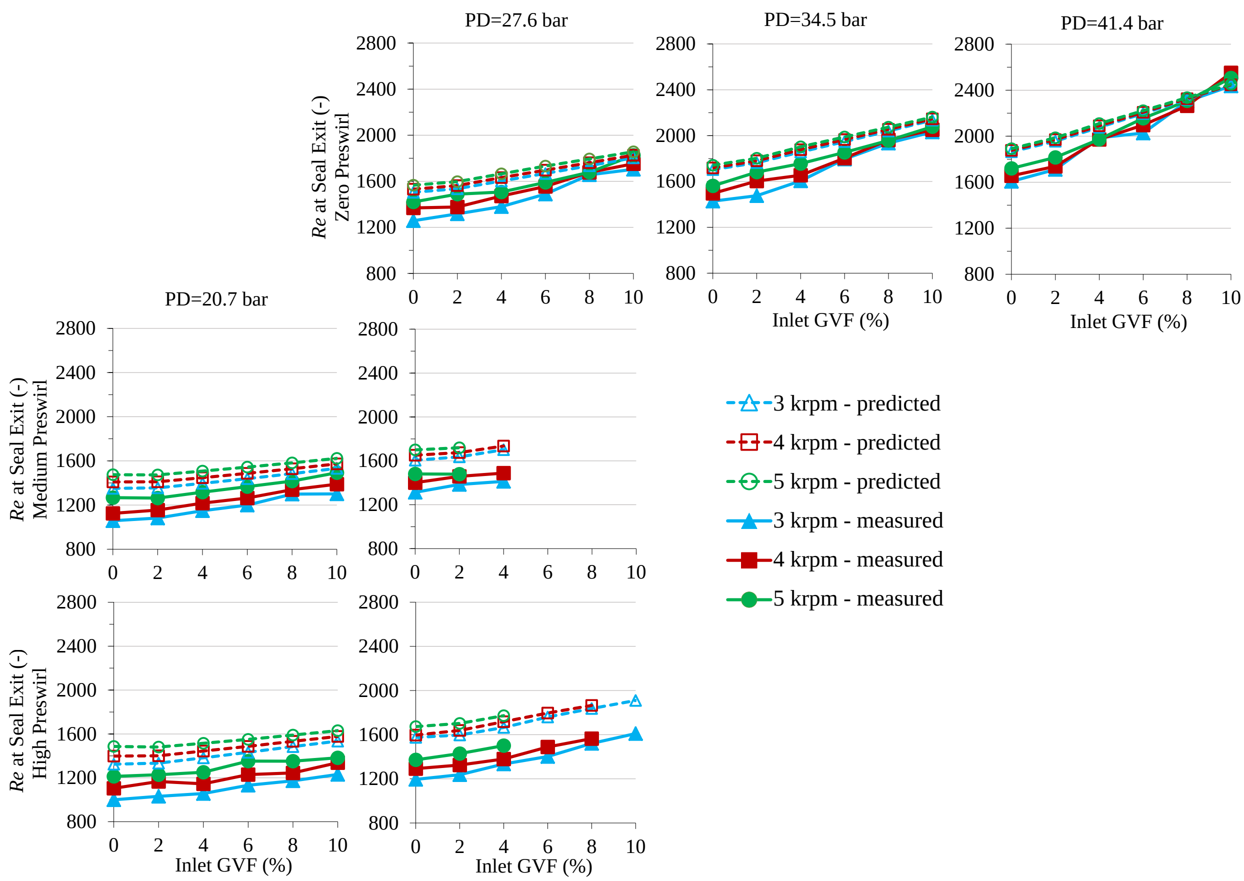

Figure 35 Predictions and measurements of exit *Re* under pure- and mainly-oil conditions

6.3 Direct Stiffness Coefficient

Figure 36 compares predicted and measured *K* versus inlet GVF for a range of PD values, three preswirl inserts, and three ω values.

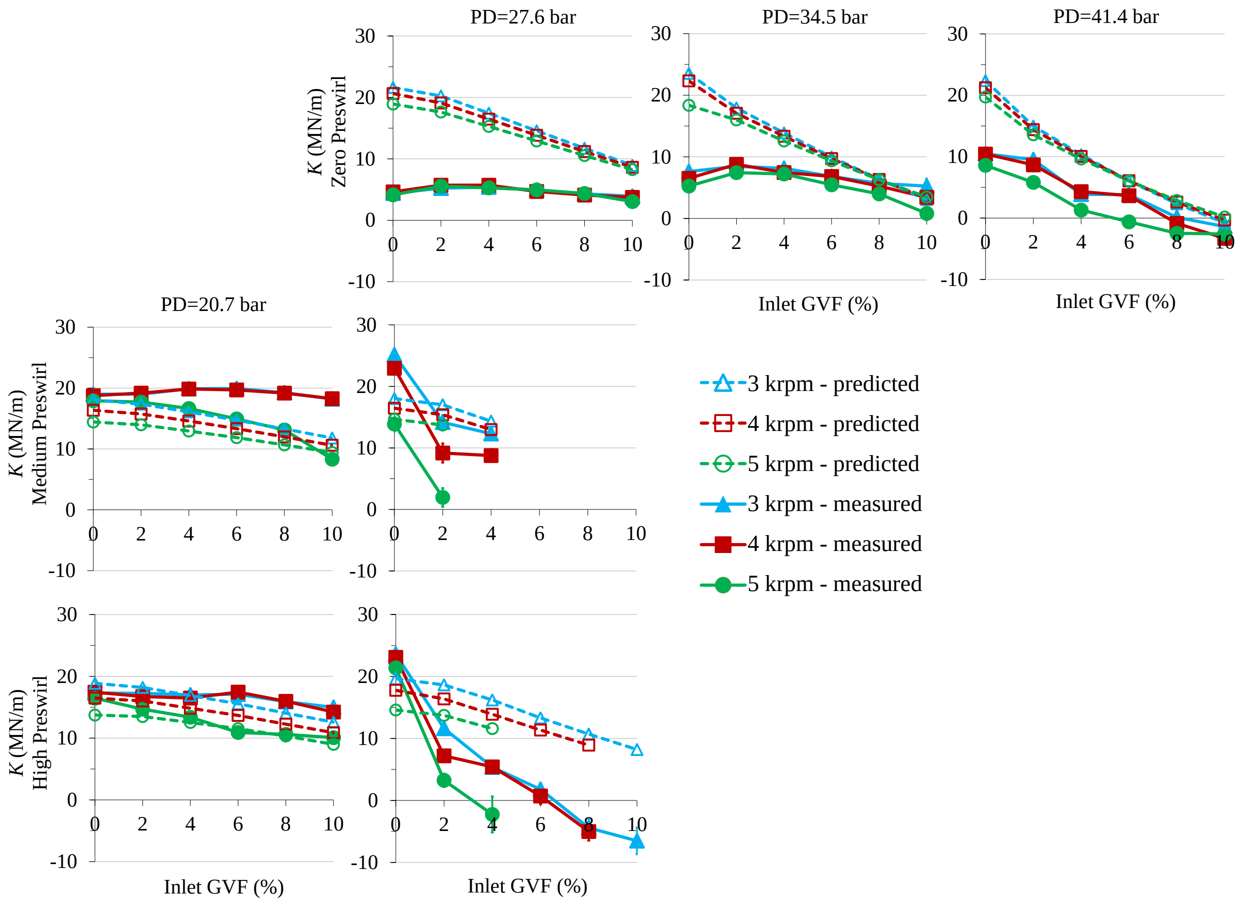

Figure 36 Predictions and measurements of *K* under pure- and mainly-oil conditions

The comparison for the zero-preswirl insert is shown in the top row.

- Predicted *K* tends to drop with increasing inlet GVF while measured *K* only shows that tendency strongly at PD=41.4 bar. At PD=27.6 bar, measured *K* changes insignificantly with changing inlet GVF, while at PD=34.5 bar, it increases slightly as inlet GVF increases from 0 to 2%, and then decreases as inlet GVF further increases from 2 to 10%.
- At pure-liquid condition (inlet GVF=0%), with increasing PD, the model predicts a slight increase of *K*, while measured *K* increases significantly. For mainly-liquid condition (inlet GVF≥2%), with PD increasing, predicted *K* tends to drop slightly at

inlet GVF=2% and significantly at inlet GVF≥4%; however, measurements show mixed trends. At inlet GVF≥2%, when PD increases from 27.6 to 34.5 bar, measured *K* shows a slight increase, but as PD further increases from 34.5 to 41.5 bar, measured *K* drops.

- In general, as ω increases from 3 to 5 krpm, predicted *K* tends to drop slightly at inlet GVF≤4% but it insignificantly changes at inlet GVF≥6%. On the other hand, for a range of operation ω from 3 to 5 krpm, measured *K* remains unchanged at PD=27.6 bar, and it only decreases as ω increases from 4 to 5 krpm at PD=34.5 and 41.4 bar.

The middle row shows the comparison between predictions and measurements for cases of the medium-preswirl insert.

- Predictions generally show a drop of *K* as inlet GVF increases; however, measured *K* only follows that tendency for cases of PD=27.6 bar and cases of ω=5 krpm at PD=20.7 bar. At PD=20.7 bar and ω=3 or 4 krpm, measured *K* changes insignificantly as inlet GVF changes.
- Predictions generally show insignificant change of *K* as PD increases from 20.7 to 27.6 bar. However, as PD increases, at inlet GVF=0%, measured *K* tends to increase at ω=3 and 4 krpm, and drops at ω=5 krpm; while at inlet GVF≥2%, measured *K* tends to drop.
- Predicted *K* drops when ω increases; however, measurements only show that tendency at PD=27.6 bar. At PD=20.7 bar, for cases of inlet GVF=0%, *K* remains unchanged from a range of ω of 3 to 5 krpm, while at inlet GVF≥2%, *K* only drops when ω increases from 4 to 5 krpm.

The comparison of predictions and measurements for the high-preswirl insert is shown in the bottom row:

- Both predictions and measurements show a drop of *K* as inlet GVF increases; however, at PD=27.6 bar, measurements show a more significant drop than predictions.
- At inlet GVF=0%, increasing PD from 20.7 to 27.6 bar does not affect predicted *K*, but increases measured *K*. However, at inlet GVF≥2%, while measured *K* significantly drops as PD increases, predicted *K* remains unchanged at inlet GVF=2-4% and only slightly decreases at GVF≥6%.
- At PD=20.7 bar, predicted *K* tends to drop as ω increases. However, at PD=20.7 bar and inlet GVF=0%, measured *K* is insensitive with changes of ω; and at inlet GVF≥2%, measured *K* tends to remain unchanged with increasing ω from 3 to 4 krpm, and only decreases as ω further increases to 5 krpm. At PD=27.6 bar, predicted *K* tends to drop as ω increases; however, measurements only show that tendency at inlet GVF=2%. At inlet GVF=0% and 4-10% and PD=27.6 bar, measured *K* remains unchanged with changes of ω at ω≤4 krpm and only decreases as ω further increases to 5 krpm.

As far as the impact of changing inlet preswirl on *K* is concerned, the comparison between measurements and predictions is shown in the first and second columns.

- At PD=20.7 bar, predicted *K* is a weak function of changing preswirl from medium to high, while the measurements show a slight drop.
- At PD=27.6 bar, as changing inlet preswirl from zero to medium, at inlet GVF=0%, predicted *K* tends to decrease while measured *K* tends to increase. At inlet GVF=2-

4%, measured *K* increases at ω=3 and 4 krpm and drops at ω=5 krpm, while predictions show a slight drop. As inlet preswirl further increases from medium to high, predictions show a slight increase; however, measurements show an increase only at ω=5 krpm, while at ω=3 and 4 krpm, measured *K* tends to drop.

Zhang [21] did tests with a zero-preswirl insert and performed a similar comparison of his measurements and predictions; however, the agreement between measurements and predictions as the impacts of changing inlet GVF, PD, and ω on *K* in his research was not as good as observed and presented here. In particular, as reported by Zhang [21], as the impact of changing ω, measured *K* was changing more significantly than predicted; and the tendency of measured *K* did not follow predictions as the impact of changing inlet GVF and PD.

6.4 Cross-Coupled Stiffness Coefficient

Figure 37 compares predicted and measured *k* versus inlet GVF for a range of PD values, three preswirl inserts, and three ω values.

The comparison between predictions and measurements for the zero-preswirl insert is shown in the top row:

- Both measured and predicted *k* are insensitive to changes of inlet GVF except at the transitions from inlet GVF=0 to 2%. For an increase of inlet GVF from 0 to 2%, at PD=27.6 bar, predicted *k* tends to increase slightly, but measured *k* remains unchanged; at PD=34.5 bar and ω=5 krpm, predicted *k* increases slightly while measurements do not change; at PD=41.4 bar, predicted *k* tends to drop slightly but measured *k* increases a little.
- As PD increases, both predicted and measured *k* tend to increase.

- Predictions show a steady increment of k as ω increases. The measured k follows a similar tendency as ω increases beyond 4 krpm; however, there is an insignificant change of measured k as ω increases from 3 to 4 krpm.

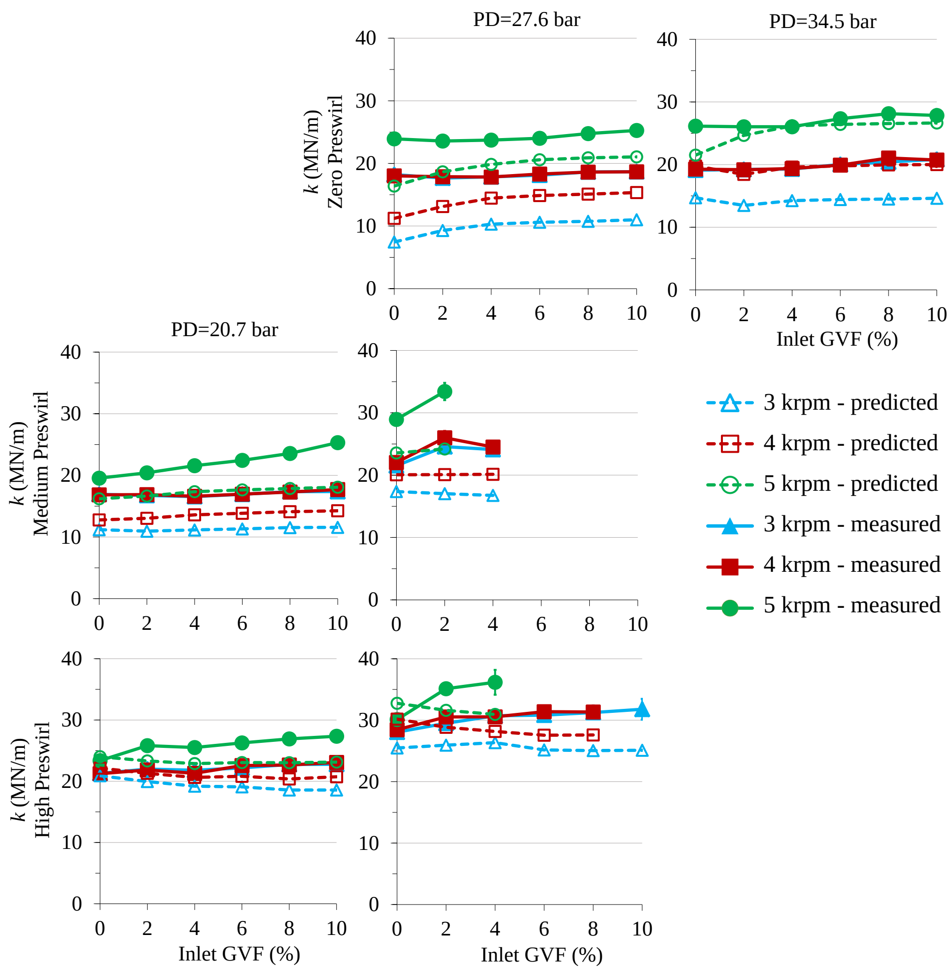

Figure 37 Predictions and measurements of *k* under pure- and mainly-oil conditions

The middle row presents results for the medium-preswirl insert.

- At PD=20.7 bar and ω=3 and 4 krpm, both predicted and measured k change insignificantly with changing inlet GVF; however, at ω=5 krpm, while predicted k tends to remain unchanged with increasing inlet GVF, measurements show an increase of *k*. At PD=27.6 bar, predictions show an insignificant impact of changing inlet GVF; however, measured *k* tends to increase with increasing inlet GVF from 0 to 2%, and then changes insignificantly as inlet GVF further increases.

- As PD increases, both predicted and measured *k* tend to increase.
- Predicted *k* increases steadily with increasing ω; but measured *k* changes insignificantly with increasing ω from 3 to 4 krpm, and only increases significantly as ω increases from 4 to 5 krpm.

The bottom row compares measurements and predictions for cases with the high-preswirl insert.

- At PD=20.7 and ω=3 and 4 krpm, both predictions and measurements show insignificant change of *k* with increasing inlet GVF; however, at ω=5 krpm, while predicted *k* tends to increase with increasing inlet GVF, measured *k* remains unchanged. At PD=27.6 bar and inlet GVF≥2%, both predictions and measurements show insignificant change of *k* with increasing inlet GVF. However, as inlet GVF increases from 0 to 2%, while measured *k* tends to increase, predictions show a slight drop at ω=4 and 5 krpm, and insignificant change at ω=3 krpm.
- As PD increases, both predicted and measured *k* tend to increase.
- Predicted *k* increases steadily with increasing ω; but measured *k* changes insignificantly with increasing ω from 3 to 4 krpm, and only increases significantly as ω increases from 4 to 5 krpm.

The comparison for the impact of changing inlet preswirl is shown in the first and second columns.

- At PD=20.7 bar, both measured and predicted *k* increase with changing from medium- to high-preswirl insert.
- At PD=27.6 bar, as inlet preswirl increases from zero to medium, both predictions and measurements show increases of *k*. When changing from the medium- to high-preswirl insert, predictions show a significant increase of *k*; however, measurements only show that tendency for cases at ω=3 and 4 krpm, while at ω=5 krpm, measured *k* changes insignificantly.

In term of magnitude, for the zero-preswirl insert, the predictions are within 1.05 times of the measurements at PD=34.5 and 41.4 bar and ω of 4 and 5 krpm. For the medium-preswirl insert, at PD=20.7 bar and 27.6 bar, the differences between measurements and predictions are less than 25% and 35%, respectively. With the high-preswirl insert, the errors are less than 10% and 16% at PD=20.7 and 27.6 bar, respectively.

In Zhang [21], as results were presented for a zero-preswirl insert, the agreement between measurements and predictions as an impact of changing PD on *k* in his research was not as good as observed and presented here. In particular, as reported by Zhang [21], for one of three tested clearances, concerning the impact of increasing PD on *k*, predicted *k* increased (similar tendency as seen in this thesis), while measured *k* remained unchanged.

6.5 Direct Damping Coefficient

Figure 38 compares predicted and measured *C* versus inlet GVF for a range of PD values, three preswirl inserts, and three ω values.

The top row compares predictions and measurements for the zero-preswirl insert.

- Predictions show small increments of *C* as inlet GVF increases, whereas that tendency only matches with measurements at PD=27.6 bar for all inlet GVF, at

PD=34.5 bar for inlet GVF≥6%, and at PD=41.4 bar for inlet GVF≥4%. At PD=34.5 bar for inlet GVF≤6%, and at PD=41.4 bar for inlet GVF≤4%, as increasing inlet GVF, measured *C* increases more significantly than predicted.

- As PD increases, both predicted and measured *C* tend to increase.
- Both measured and predicted *C* only increase slightly as ω increases from 3 to 5 krpm.

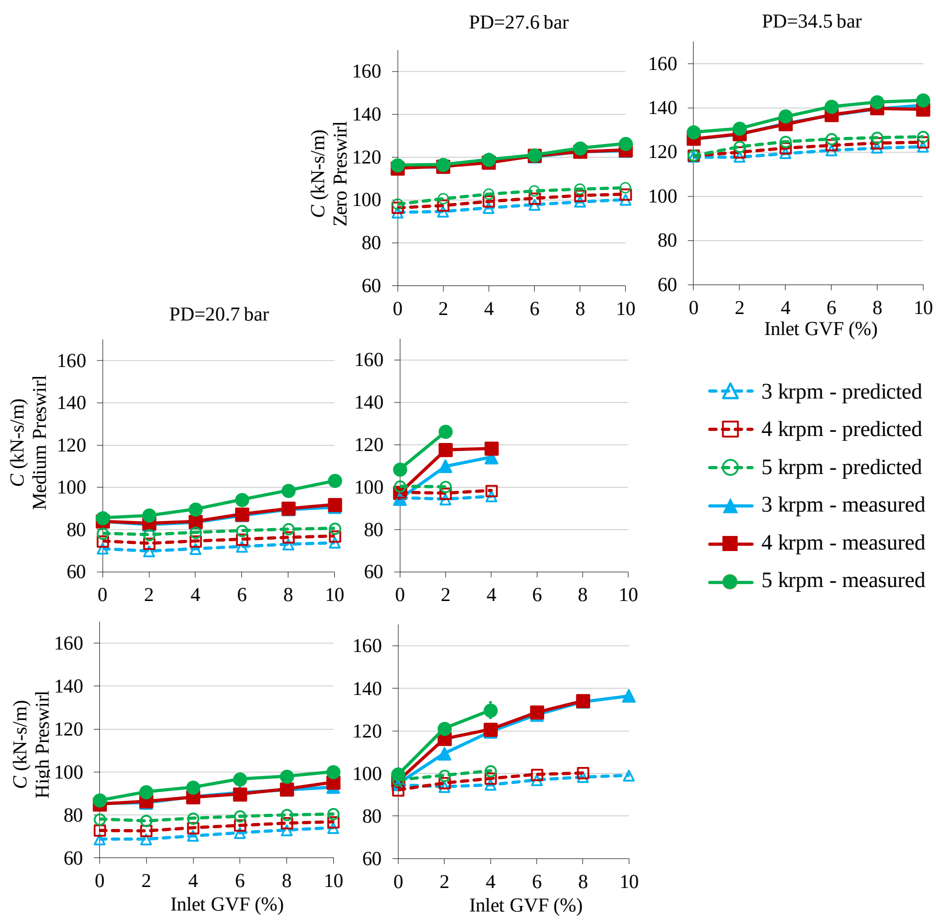

Figure 38 Predictions and measurements of *C* under pure- and mainly-oil conditions

Predicted and measured *C* for the medium-preswirl are compared, as shown in the middle row.

- At PD=20.7 bar, predictions show small increments of *C* as inlet GVF increases. However, measurements only show that tendency at ω=3 and 4 krpm for inlet GVF≤4%, and at ω=5 krpm for inlet GVF≤2%. At ω=3 and 4 krpm for inlet GVF≥4%, and at ω=5 krpm for inlet GVF≥2%, measured *C* increases more rapidly with increasing inlet GVF than predicted. At PD=27.6 bar, with increasing inlet GVF, measured *C* increases significantly while predicted *C* changes insignificantly.
- As PD increases, both predicted and measured *C* tend to increase.
- At PD=20.7 bar, predictions show steady increments of *C* as ω increases. However, at GVF=0%, measured *C* does not change with increasing ω, and at inlet GVF≥2%, measured *C* starts increasing with increasing ω from 4 to 5 krpm (measured *C* remains unchanged with increasing ω from 3 to 4 krpm). At PD=27.6 bar, prediction shows steady increments of *C* as ω increases; however, measurements only follow that tendency at inlet GVF≥2%, while at inlet GVF=0%, measured *C* remains unchanged with increasing ω from 3 to 4 krpm, and only increases as ω further increases to 5 krpm.

The bottom row compares predictions and measurements for the high-preswirl insert.

- Measured *C* increases more rapidly with increasing inlet GVF than predicted.
- As PD increases, both predicted and measured *C* tend to increase.
- At PD=20.7 bar, predictions show steady increments of *C* as ω increases. However, at inlet GVF=0%, measured *C* does not change with increasing ω, and at inlet GVF≥2%, measured *C* starts increasing with increasing ω from 4 to 5 krpm (measured *C* remains unchanged with increasing ω from 3 to 4 krpm). At PD=27.6 bar and inlet GVF=0%, predicted *C* tends to remain unchanged with increasing ω from 3 to 4

krpm, and to increase slightly as ω further increases to 5 krpm; however, measured *C* does not change with increasing ω. At PD=27.6 bar and inlet GVF=2%, measurements show steady increments of *C* with increasing ω; however, predicted *C* does not change with increasing ω from 3 to 4 krpm, and only increases slightly as ω increase from 4 to 5 krpm. At PD=27.6 bar and inlet GVF≥4%, both predictions and measurements show no difference between *C* at ω=3 and 4 krpm, and *C* starts increasing as ω increases from 4 to 5 krpm.

The impact of changing inlet preswirl on *C* is shown in the first and second columns. At PD=20.7 bar (first column), both measured and predicted *C* change insignificantly in changing from the medium- to high-preswirl insert. For cases of PD of 27.6 bar (second column), predictions show insignificant change of *C* when changing from the zero- to medium-preswirl; however, at inlet GVF=0%, measured *C* drops significantly, while at inlet GVF=2% and 4%, measured *C* remains unchanged at ω=4 krpm, slightly increases at ω=5 rpm and slightly drops at ω= 3krpm. In changing from the medium- to high-preswirl insert, at PD=27.6 bar, both predictions and measurements show insignificant changes, except there is a slightly drop of *C* at inlet GVF=0% and ω=5 krpm.

In term of magnitude, predicted *C* is lower than measured for most cases. The code provides fairly accurate *C* values for most cases at inlet GVF=0%. For the zero-preswirl insert, the measured results are higher than predicted by about 20% (max.). In the medium- and high-preswirl inserts, the maximum errors, which occurred mainly at PD=27.6 bar, are about 27% and 35%, respectively.

In Zhang [21] where prediction and measurement results for a zero-preswirl were presented, the agreement between measurements and predictions due to changing PD and ω on *C* was not as good as observed and presented here. In particular, as reported by Zhang [21], as an impact of changing ω on *C*, measurements changed much more than predicted; and the tendency of measured *C* did not follow prediction as the impact of changing PD.

6.6 Cross-Coupled Damping Coefficient

Figure 39 compares predicted and measured *c* versus inlet GVF for a range of PD values, three preswirl inserts, and three ω values.

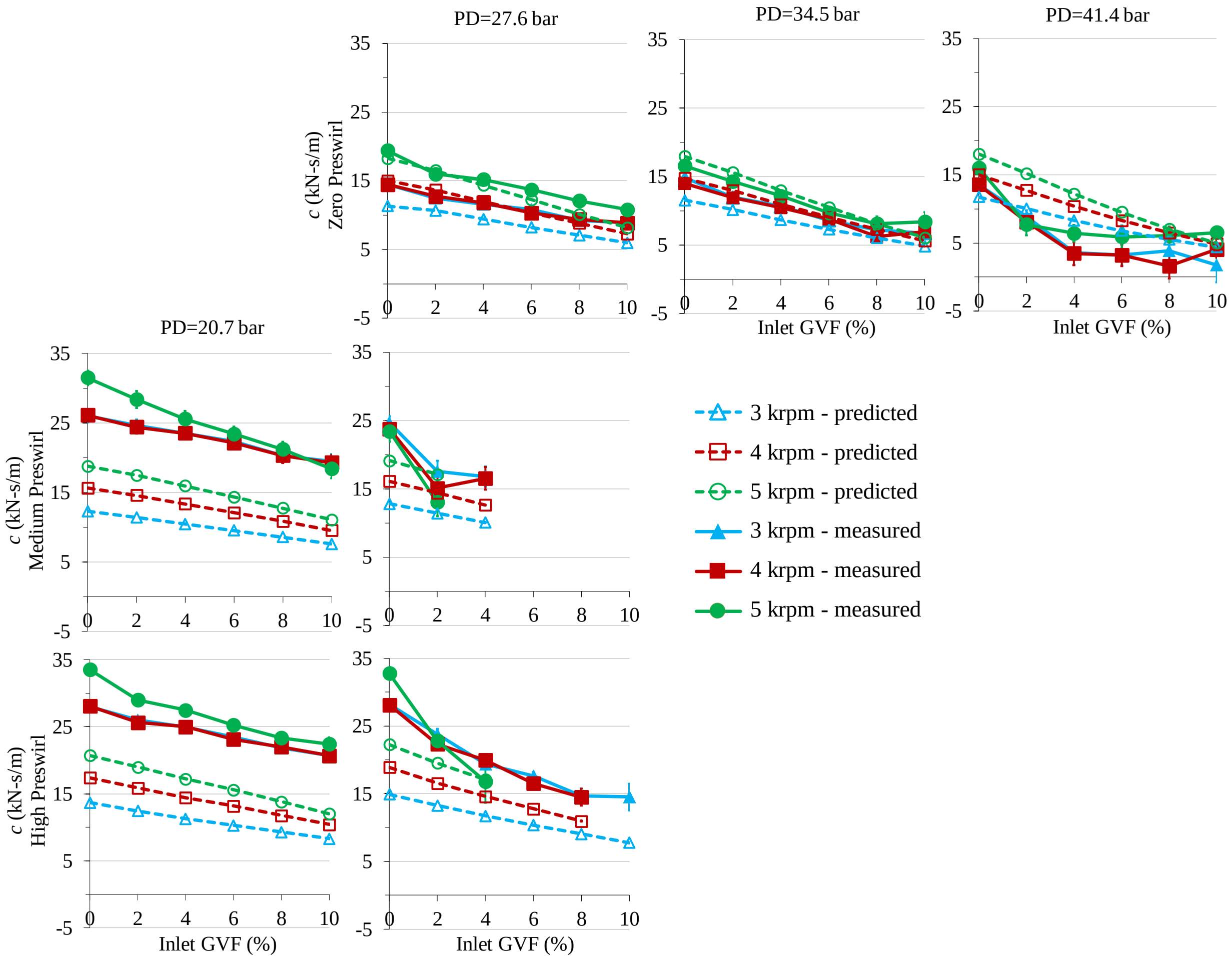

Figure 39 Predictions and measurements of *c* under pure- and mainly-oil conditions

The results for the zero-preswirl insert are shown in the first row.

- As inlet GVF increases, both predicted and measured results show a drop in *c*. At PD=27.6 and 34.5 bar, predictions and measurements show similar drop rates; whereas, at PD=41.4 bar, measured *c* first drops more rapidly than predicted, then converges to about the same values at inlet GVF=10%.
- With increasing PD from 27.6 to 34.5 bar, predicted *c* changes insignificantly, while measured *c* drops slightly. As PD further increases from 34.5 to 41.4 bar, prediction shows insignificant changes; however, measured *c* drops significantly at inlet GVF≥2%.
- In regard to changing ω, predicted *c* increases steadily with increasing ω at low inlet GVF, but converges to about the same values at inlet GVF=10%. Measured *c* values are about the same at ω=3 and 4 krpm, but increases with ω increasing from 4 to 5 krpm.

The middle row shows the comparison between measurements and predictions for the medium-preswirl insert.

- Both predictions and measurements show a drop in *c* as inlet GVF increases.
- In regard to changing PD, predicted *c* remains unchanged while measured *c* drops significantly as PD increases.
- For an impact of changing ω on *c*, prediction shows a significant increase of *c* as ω increases. At PD=20.7 bar, measured *c* values are about the same at ω=3 and 4 krpm. Increasing ω from 4 to 5 krpm increases measured *c*, but measured *c* values at ω=3, 4, and 5 krpm are converging at inlet GVF=10%. At PD=27.6 bar, at inlet GVF=0% and 4%, measured *c* remains unchanged with changing ω; but at inlet GVF=2%, measured *c* decreases as ω increases.

The comparison for the high-preswirl insert is presented in the bottom row.

- Both measurements and predictions show a drop of *c* as inlet GVF increases.
- In regard to the impact of increasing PD, predicted *c* tends to increase slightly at inlet GVF≤2% and changes insignificantly at inlet GVF≥4%; however, measured *c* remains unchanged at inlet GVF=0% and drops significantly at inlet GVF≥2%.
- In regard to changing ω, predicted *c* tends to increase as ω increases. However, at PD=20.7 bar, measured *c* values are about the same at ω=3 and 4 krpm, and only increase with increasing ω from 4 to 5 krpm. At PD=27.6 bar, measured *c* remains unchanged with increasing from 3 to 4 krpm, and as ω further increases to 5 krpm, measured *c* increases at inlet GVF=0%, remains unchanged at inlet GVF=2%, and drops at inlet GVF=4%.

The first and second columns compare predicted and measured *c* as the impact of changing inlet preswirl.

- At PD=20.7 bar (first column), both predictions and measurements show a small increase of *c* as changing from medium- to high-inlet preswirl.
- At PD=27.6 bar and inlet GVF=0%, when changing from the zero- to medium-preswirl insert, predicted *c* slightly increases at ω=3 and 4 krpm, and changes insignificantly at ω=5 krpm; while measurements show a significant increase. For cases of inlet GVF≥2% at PD=27.6 bar, changing preswirl from zero to medium increases both measured and predicted *c* slightly, except the case of inlet GVF=2% and ω of 5 krpm where measured *c* slightly drops while predicted *c* slightly increases. At PD=27.6 bar, further increasing preswirl from medium to high increases *c* moderately, both shown in prediction and measurement.

In term of magnitude, the model predicts accurately for most cases of the zero-preswirl insert and some cases at PD=27.6 bar for the medium- and high-preswirl inserts. However, at PD=20.7 bar, in cases of the medium- and high-preswirl inserts, measured *c* is higher than predicted by a factor of about 1.42.

In Zhang [21], as results were presented for a zero-preswirl insert, the agreement between measurements and predictions as the impact of changing ω on *c* in his research was not as good as observed and presented here. In particular, as reported by Zhang [21], with two tested clearances, with the impact of increasing ω on *c*, predicted *c* showed an increase (a similar tendency as seen here), while measured *c* dropped.

6.7 Direct Virtual Mass Coefficient

Figure 40 compares predicted and measured *M* versus inlet GVF for a range of PD values, three preswirl inserts, and three ω values.

The top row compares predictions and measurements for the cases of the zero-preswirl insert.

- Both predicted and measured *M* drop with increasing inlet GVF.
- In regard to the impact of changing PD, at GVF=0%, both measured and predicted M change insignificantly. At inlet GVF≥2%, with increasing PD, predicted *M* changes insignificantly while measurements show a drop in *M*.
- Both predictions and measurements show insignificant change of *M* in increasing ω from 3 to 5 krpm.

The middle row compares predictions and measurements for the cases of the medium-preswirl insert.

- Both predicted and measured *M* drop as inlet GVF increases.

- With changing PD, prediction shows insignificant changes in *M*; however, measured *M* tends to drop significantly.
- In regard to increasing ω from 3 to 5 krpm, at PD=20.7 bar and inlet GVF=0%, predicted and measured *M* remain unchanged. However, at PD=20.7 bar and inlet GVF≥2%, while predicted *M* remains unchanged with changing ω, measured *M* remains unchanged with increasing ω from 3 to 4 krmp, and increases as ω further increases to 5 krpm. At PD=27.6 bar, predicted *M* remains unchanged with increasing ω from 3 to 5 krpm; however, measurements show a drop in *M*.

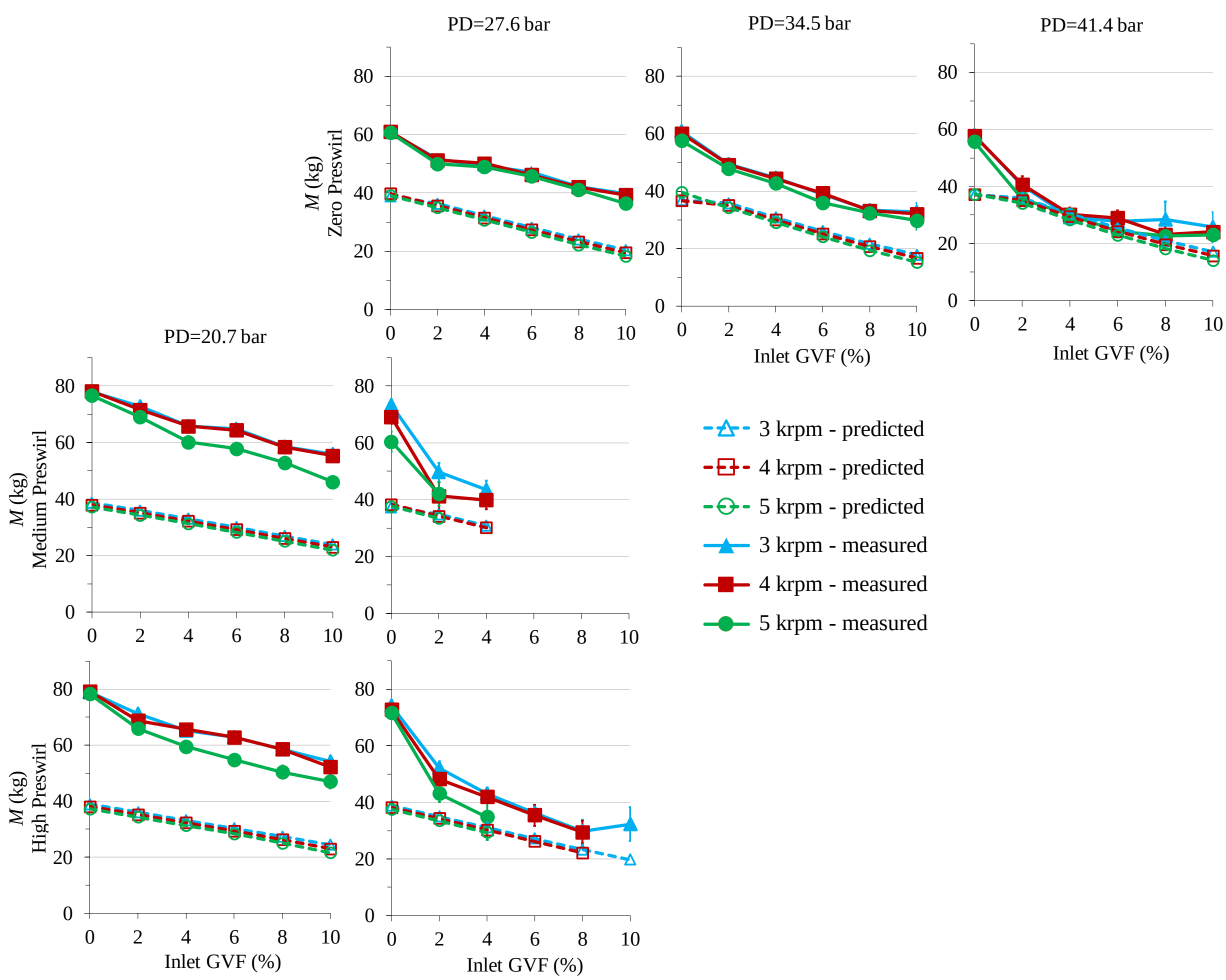

Figure 40 Predictions and measurements of *M* under pure- and mainly-oil conditions

The comparison between predictions and measurements for the high-preswirl insert is shown in the bottom row.

- Both predicted and measured *M* drop as inlet GVF increases.
- With changing PD, predictions show insignificant changes in *M*; however, measured *M* drops slightly at inlet GVF=0%, but significantly at inlet GVF≥2%.
- In regard to the impact of changing ω, at inlet GVF=0%, both predicted and measured *M* remain unchanged. However, at inlet GVF≥2%, while predicted *M* remains unchanged when changing ω, measured *M* remains unchanged with increasing ω from 3 to 4 krmp, and increases as ω further increases to 5 krpm.

The comparison between measurements and predictions with the impact of changing inlet preswirl is shown in the first and second columns.

- At PD=20.7 bar, shown in the first column, both predictions and measurements show insignificant change of *M* as increasing from medium to high inlet preswirl.
- At PD=27.6 bar, shown in the second column, with increasing inlet preswirl from zero to medium, predicted *M* remains unchanged while measurements show an increase at GVF=0% and a drop at inlet GVF≥2%. As inlet preswirl further increases from medium to high, both predictions and measurements show an insignificant change in *M*, except the case of inlet GVF=0% and ω=5 krpm, where measurements show an increase while predicted *M* remains unchanged.

In term of magnitude, predicted *M* is lower than measured. The maximum error occurs at PD=20.7 bar with the medium- and high-preswirl inserts; i.e., the measured *M* is almost two times larger than predicted *M*. The code predicts accurately *M* at PD=41.4 bar with the zero-preswirl cases; i.e., the error is less than 10%. Regarding the large discrepancy observed in some cases, Delgado [39] suggested a need of an appropriate model to make better predictions; i.e., a proper height of the oil supply chamber needs to be selected, based on the seal clearance to reproduce measured *M* values. In Childs et al. [40], for tests of a short (*L/D*=0.21) smooth laminar-liquid seal, the appropriate height for the flow region 1 was 10 to 15 times the seal clearance.

6.8 Cross-Coupled Virtual Mass Coefficient

Figure 41 compares predicted and measured m_q versus inlet GVF for a range of PD values, three preswirl inserts, and three ω values. As mentioned in Sec. 5.10, a negative value of m_q produces a destabilizing force.

The top row presents the comparison for the zero-preswirl insert

- As inlet GVF increases, predicted m_q decreases (destabilizing) while measured m_q increases (stabilizing), except there is a drop in measured m_q at PD=41.4 bar and ω=5 krpm
- There is an insignificant change of predicted m_q as PD increases; however, measured m_q tends to increase (less negative) and approaches zero with increasing PD, except the cases of ω=5 krpm where measured m_q drops (more negative) as PD increases from 34.5 to 41.4 bar.
- In regard to change of ω, predicted m_q tends to decrease slightly when increasing ω from 3 to 5 krpm; however, measurement shows insignificant changes when increasing ω from 3 to 4 krpm, and measured m_q decreases (more negative) as ω further increases to 5 krpm.

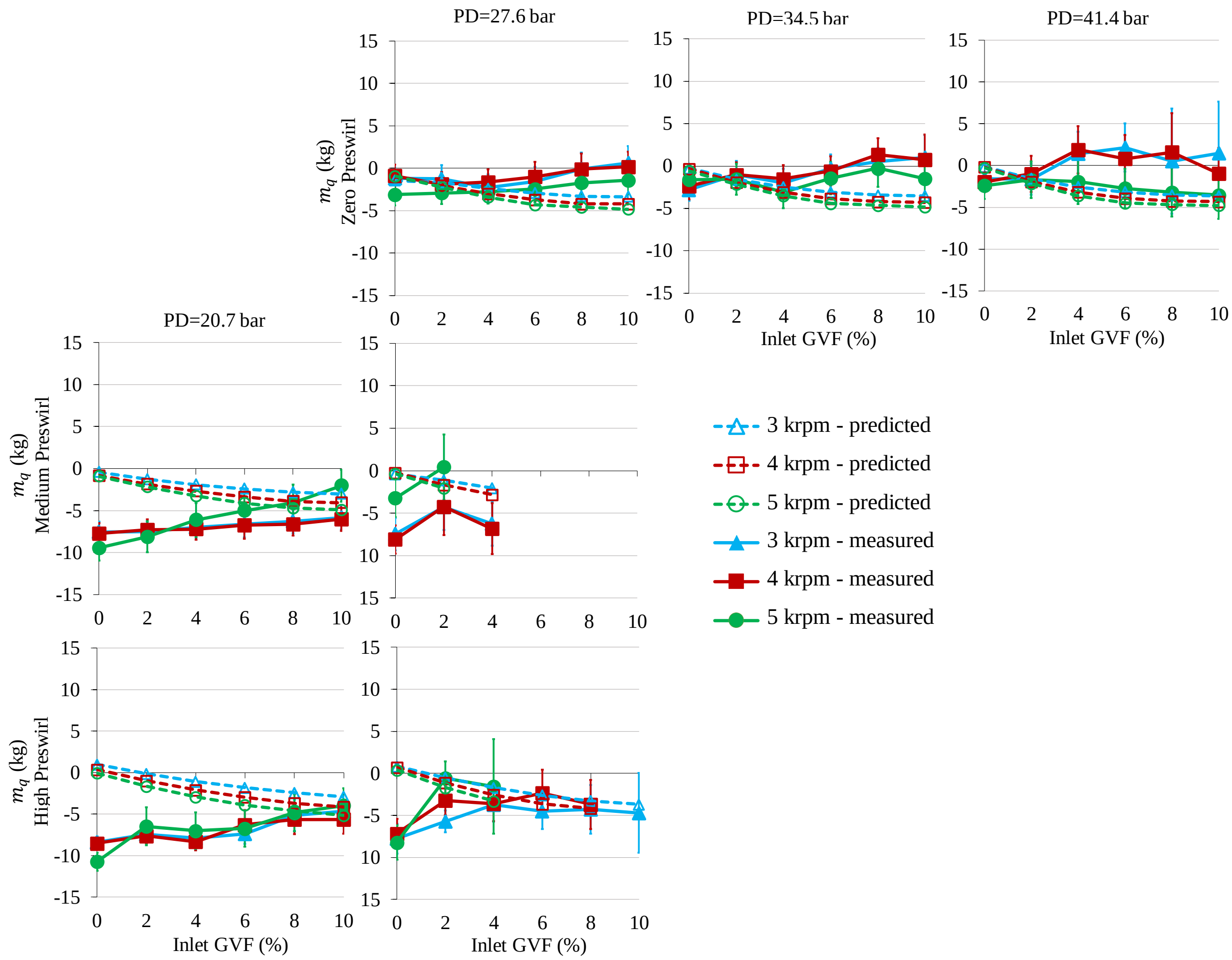

Figure 41 Predictions and measurements of m_q under pure- and mainly-oil conditions

The middle row shows the comparison between measurements and predictions for the medium-preswirl insert.

- In regard to the impact of changing inlet GVF, at PD=20.7 bar, as GVF increases, predicted m_q tends to decrease (more negative); however, measured m_q increases (less negative) at ω=5 krpm, but changes insignificantly at ω=3 and 4 krpm. At PD=27.6 bar, predicted m_q drops (more negative) as inlet GVF increases; but measurements show an increase of m_q as inlet GVF increases from 0 to 2%, then a drop (at ω=3 and 4 krpm, no measurement at ω=5 krpm) as inlet GVF increases from 2 to 4%.

- Predictions show insignificant change of predicted m_q with increasing PD; however, at ω=5 krpm, measured m_q increases (less negative), and at ω=3 and 4 krpm, measurements show a drop at inlet GVF=0%, an increase at inlet GVF=2%, and an insignificant change at inlet GVF=4%.
- In regard to the impact of changing ω, predicted m_q tends to decrease (more negative) with increasing ω; however, measured m_q remains unchanged when ω increases from 3 to 4 krpm and only changes as ω further increases from 4 to 5 krm. At PD=20.7 bar, as ω increases from 4 to 5 krpm, measured m_q tends to decrease (more negative) at inlet GVF=0% and 2%, but increases (less negative) at inlet GVF≥4%. At PD=27.6 bar, measured m_q increases (less negative) with increasing ω from 4 to 5 krpm.

The bottom row compares measurements and predictions for the cases of the high-preswirl insert.

- In regard to the impact of changing inlet GVF, predicted m_q tends to decrease (more negative) while measured m_q increases (less negative) as inlet GVF increases.
- While predicted m_q is insensitive to an increase of PD from 20.7 to 27.6 bar, the measurements show small increases (less negative) at inlet GVF=0%, 8% and 10% and significant increases at inlet GVF=2%, 4%, and 6%.
- As ω increases, predictions show a drop in m_q (more negative); however, measurements show insignificant changes at PD=20.7 bar and increases (less negative) at PD=27.6 bar.

In regard to the impact of changing preswirl, at PD=20.7 bar, both predictions and measurements show insignificant changes with increasing inlet preswirl from medium to high. At PD=27.6 bar, as inlet preswirl changes from zero to medium, predictions show no change;

however, measured m_q increases (less negative) at ω=5 krpm and drops (more negative) at ω=3 and 4 krpm. As inlet preswril further increases from medium to high, at PD=27.6 bar, predictions show no change, while measurements show small increases (less negative) at ω=3 and 4 krpm, and small decreases (more negative) at at ω=5 krpm.

6.9 Whirl-Frequency Ratio

Figure 42 compares predicted and measured whirl-frequency ratio (WFR), defined using San Andrés [37]'s formulation (refer to Appendix A for the detailed formulation), versus inlet GVF for a range of PD values, three preswirl inserts, and three ω values.

The top row compares predictions and measurements for the zero-preswirl insert.

- At inlet GVF=2-10%, both predicted and measured WFR are insensitive to changes of inlet GVF. However, with inlet GVF increases from 0 to 2%, measured WRF changes insignificantly while predictions show an increase at PD=27.6 bar, an insignificant change at PD=34.5 bar, and a decrease at PD=41.4 bar.
- In regard to the change of PD, measured WFR remains unchanged with increasing PD; however, predicted WFR increases significantly at inlet GVF=0%, but changes insignificantly at inlet GVF=2-10%.
- Measured WFR drops as ω increases from 3 to 4 krpm and remains unchanged with increasing ω from 4 to 5 krpm. However, as ω increases, predicted WFR increases slightly at PD=27.6 bar, and changes insignificantly at PD=34.5 and 41.5 bar.

The middle row compares measurements and predictions of WFR for the medium-preswirl insert.

- In regard to the impact of changing inlet GVF, at PD=20.7 bar, both predictions and measurements show minor changes of WFR with increasing inlet GVF. At PD=27.6

bar, with increasing inlet GVF, both predicted and measured WFR remain unchanged or drops slightly at ω=5 or 3 krpm, respectively; however, at ω=4 krpm, while predicted WFR stays constant with increasing inlet GVF, measured WFR drops slightly.

- When increasing PD from 20.7 to 27.6 bar, predicted and measured WFR increase.
- Concerning the impact of increasing ω, both predictions and measurements show a drop in WFR as ω increases from 3 to 4 krpm, and insignificant change as ω further increases to 5 krpm.

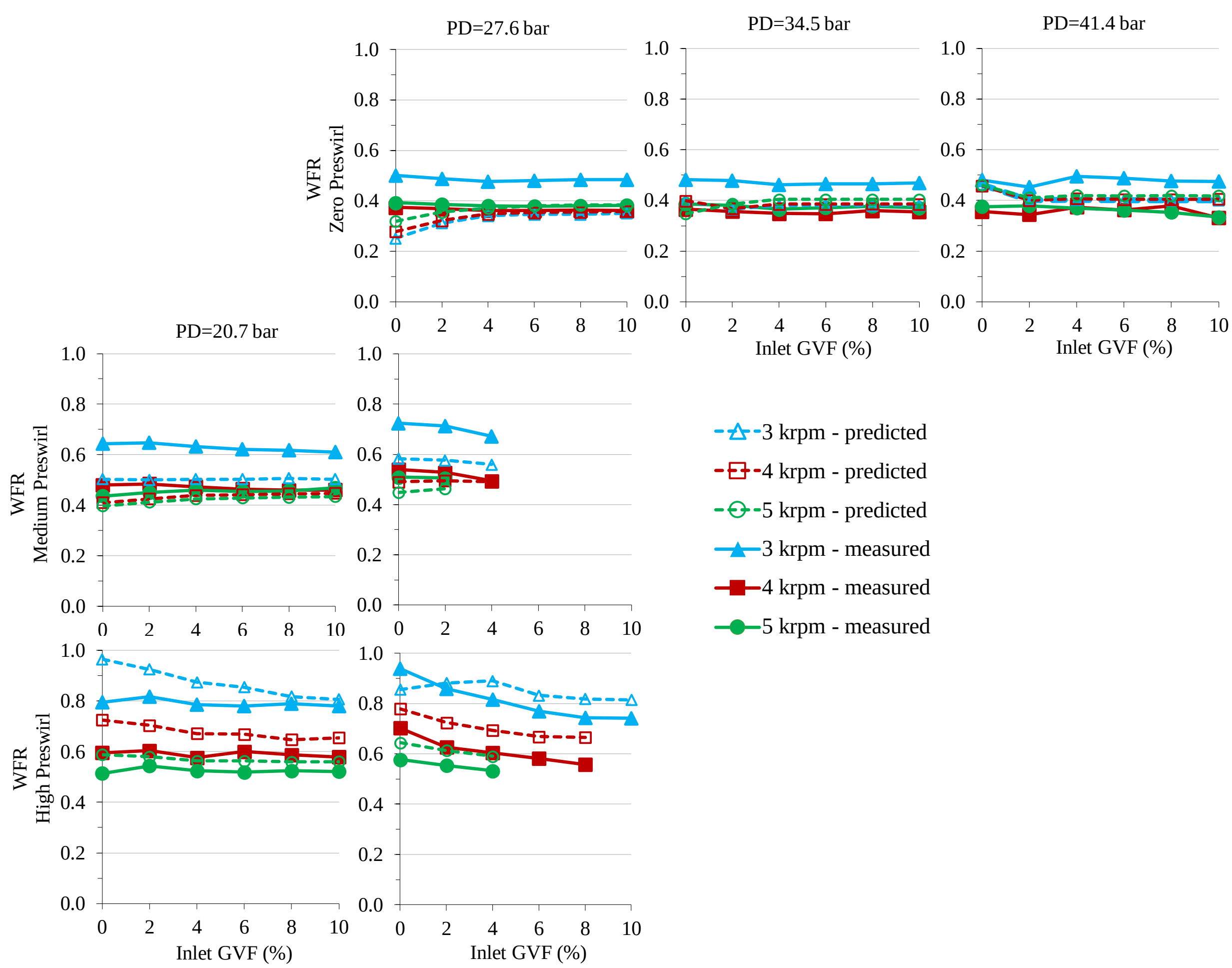

Figure 42 Predictions and measurements of WFR under pure- and mainly-oil conditions

The bottom row compares measurements and predictions of WFR for the high-preswirl insert.

- At PD=20.7 bar, with increasing inlet GVF, measured WFR changes insignificantly; whereas, predictions show a steady drop at ω=3 and 4 krpm and an insignificant change at ω=5 krpm. At PD=27.6 bar, both predictions and measurements show drops of WFR as inlet GVF increases at ω=4 and 5 krpm; however, at ω=3 krpm, while measured WFR tends to drop steadily, predicted WFR tends to increase slightly as inlet GVF increases from 0 to 4%, and then starts dropping as inlet GVF further increases.
- In regard to the impact of increasing PD, at inlet GVF=0%, both predictions and measurements show increments, except the case at ω=3 krpm where predicted WFR drops while measured WFR increases. At inlet GVF≥2%, predicted WFR changes insignificantly, while measured WFR remains unchanged at inlet GVF=2-6% and decreases slightly at inlet GVF=8% and 10%.
- Both predictions and measurements show a drop of WFR as ω increases.

The comparison between measurements and predictions with the impact of changing inlet preswirl is shown in the first and second columns. Both measured and predicted WFR increase significantly in changing from zero- to medium-preswirl insert or from medium- to high-preswirl insert.

6.10 Effective Damping

Figure 43 compares predicted and measured C_{eff}, defined in Eq. (35) ,versus inlet GVF for a range of PD values, three preswirl inserts, and three ω values.

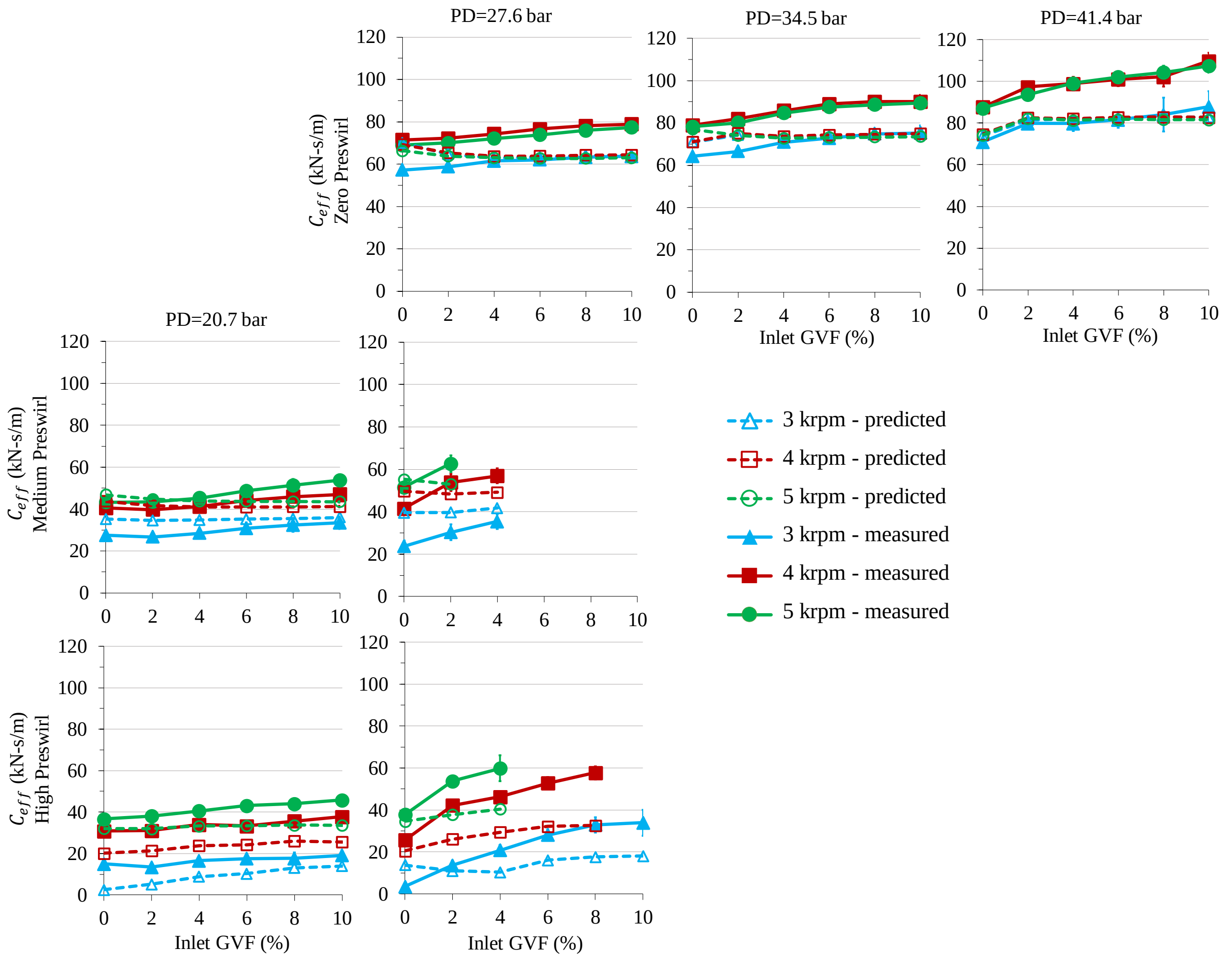

Figure 43 Predictions and measurements of C_{eff} under pure- and mainly-oil conditions

The top row shows a comparison between predictions and measurements for the zero-preswirl insert.

- In regard to the impact of changing inlet GVF on C_{eff}.

  - At PD=27.6 bar, as inlet GVF increases from 0 to 4%, predictions show a slight drop of C_{eff} while measured C_{eff} slightly increases. As inlet GVF further increases from 4 to 10% at PD=27.6 bar, both measurements and predictions show an insignificant change of C_{eff}.

- At PD=34.5 bar, as inlet GVF increases from 0 to 2%, predictions show a slight increase at ω=3 and 4 krpm and a slight drop at ω=5 krpm; and, predicted C_{eff} remains unchanged when inlet GVF further increases from 2 to 10%. On the other hand, measurements show a significant increase with increasing inlet GVF from 0 to 6%, but then measured C_{eff} stays constant as inlet GVF further increases to 10%.
- At PD=41.4 bar, both predicted and measured C_{eff} increase when increasing inlet GVF from 0 to 2%, and then change insignificantly when inlet GVF increases from 2 to 8%. However, with increasing inlet GVF from 8 to 10%, measured C_{eff} tends to increase slightly while predicted values remain unchanged.

- In regard to the impact of increasing PD, at inlet GVF=0%, measurements show a slight increase of C_{eff}; however, predicted C_{eff} slightly increases only at ω=3 and 4 krpm (at ω=5 krpm, as PD increases from 27.6 to 34.5 bar and from 34.5 to 41.4 bar, C_{eff} increases and then drops slightly, respectively). At inlet GVF≥2%, both predicted and measured C_{eff} increase with increasing PD
- In regard to the impact of increasing ω, predicted C_{eff} remains unchanged with increasing ω, except there is a slight increase of C_{eff} at PD=34.5 bar and inlet GVF=0% when ω increases from 4 to 5 krpm. Measured C_{eff} increases as increasing ω from 3 to 4 krpm; however, it remains unchanged as ω further increases to 5 krpm.

The middle row presents the comparison between measurements and predictions of the medium-preswirl insert:

- In regard to the impact of changing inlet GVF, at PD=20.7 bar and inlet GVF≤4%, both predictions and measurements show an insignificant change due to inlet GVF increasing; however, as inlet GVF increases from 4 to 10%, predicted C_{eff} stays constant, while measured C_{eff} increases slightly. At PD=27.6 bar, as inlet GVF increases, measured C_{eff} increases while predicted C_{eff} changes insignificantly.

- In regard to the impact of increasing PD, at inlet GVF=0%, with increasing PD from 20.7 to 27.6 bar, both predictions and measurements show a slight increase at ω=4 and 5 krpm; however, at ω=3 krpm, predicted C_{eff} deceases while measured C_{eff} increases. At inlet GVF≥2%, measured and predicted C_{eff} both increase with an increase of PD.
- Both predicted and measured C_{eff} increase with increasing ω from 3 to 5 krpm.

The bottom row shows a comparison between measurements and predictions of the high-preswirl insert:

- In regard to the impact of increasing inlet GVF, at PD=20.7 bar, measured C_{eff} changes insignificantly; however, predicted C_{eff} tends to increase at ω=3 and 4 krpm, and remains unchanged at ω=5 krpm. At PD=27.6 bar, at ω=4 and 5 krpm, both predicted and measured C_{eff} increases with increasing inlet GVF. However, at PD=27.6 bar and ω=3 krpm, measurements show a tendency of increasing as inlet GVF increases, whereas predicted C_{eff} does not change much as inlet GVF increases for a range of inlet GVF=0-4% and 6-10%, and predicted C_{eff} increases with increasing inlet GVF from 4 to 6%.
- In regard to the impact of increasing PD from 20.7 to 27.6 bar, at inlet inlet GVF=0% and ω=5 krpm, both predicted and measured C_{eff} remains unchanged; however, at ω=4 krpm, while predictions show no change, measurements show a drop, and at ω=3

krpm, predicted C_{eff} tends to increase, while measured C_{eff} drops. At inlet GVF≥2%, both predictions and measurements show an increase of C_{eff} as PD increases.

- Both predicted and measured C_{eff} increase with increasing ω from 3 to 5 krpm.

The comparison between measurements and predictions with the impact of changing inlet preswirl is shown in the first and second columns. Both measured and predicted C_{eff} drop as changing from zero- to medium-preswirl insert or from medium- to high-preswirl insert.

7. MEASURED RESULTS FOR PURE- AND MAINLY-AIR TESTING

As presented in Sec. 5.1, the test is started by determining the baseline result, and then the final complex dynamic stiffness coefficients are determined by subtracting the baseline result from the test result. Figure 44 shows an example of typical results for pure- or mainly-air test condition after subtracting the baseline results. The results include real and imaginary parts for dynamic stiffness coefficients $\boldsymbol{H}_{ij}$ for the case conducted at PR=0.4, inlet LVF=2%, ω= 15krpm, with the zero-preswirl insert. The real part Re($\boldsymbol{H}_{ij}$), is not fitted well with a quadratic function, shown in Eq. (20), to produce a stiffness coefficient K_{ij}, and a virtual-mass coefficient M_{ij}, as reflected by the associated R^2 values: 0.2690 for Re($\boldsymbol{H}_{XX}$), 0.8705 for Re($\boldsymbol{H}_{YY}$), 0.0004 for Re($\boldsymbol{H}_{XY}$), and 0.0753 for Re($\boldsymbol{H}_{YX}$). On the other hand, the imaginary part Im($\boldsymbol{H}_{ij}$), is linearly dependent on **Ω**, producing a damping coefficient C_{ij}. The linear curve-fitting produces R^2 around 0.995 for both Im($\boldsymbol{H}_{XX}$) and Im($\boldsymbol{H}_{YY}$) curves, while R^2 for Im($\boldsymbol{H}_{XY}$) and Im($\boldsymbol{H}_{YX}$) curves are relatively low since the magnitudes of Im($\boldsymbol{H}_{XY}$) and Im($\boldsymbol{H}_{YX}$) are small.

Therefore, the rotordynamic characteristics for cases of pure- or mainly-air conditions could be represented by the real impedance coefficients Re($\boldsymbol{H}_{ij}$), and the damping coefficient C_{ij} (The curve-fitted results are shown in Appendix E). The average value is chosen to represent the characteristic for each case since the values for Re($\boldsymbol{H}_{ij}$) and C_{ij} are close in *X* and *Y* directions.

$$K_{\Omega} = \frac{\mathrm{Re}(H_{XX}) + \mathrm{Re}(H_{YY})}{2} \tag{36}$$

$$k_{\Omega} = \frac{\mathrm{Re}(H_{XY}) - \mathrm{Re}(H_{YX})}{2} \tag{37}$$

$$C = \frac{C_{XX} + C_{YY}}{2} \tag{38}$$

$$c = \frac{C_{XY} - C_{YX}}{2} \tag{39}$$

K_Ω is the direct dynamic stiffness, k_Ω is the cross-coupled dynamic stiffness, C is the direct damping coefficient, and c is the cross-coupled damping coefficient. Zhang [21] had the same outcome for radial flow injection.

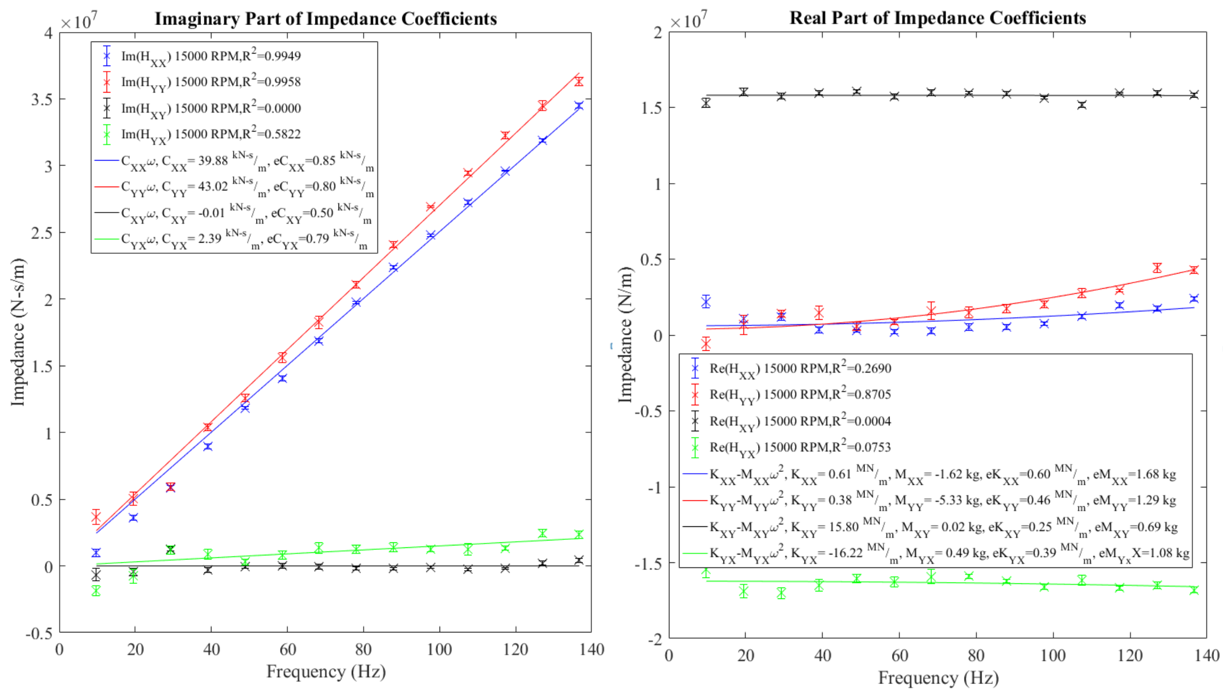

Figure 44 Complex dynamic stiffness for a typical mainly-air case (PR=0.4, inlet LVF=2%, ω=15krpm, and the zero-preswirl insert) after subtracting baseline data

7.1 Test Matrix

For pure- and mainly-air testing conditions, the inlet pressure is initially set at 62.1 bar-g. Due to dynamic instability of the stator, the inlet pressure is brought down to 19.3 bar-g for the medium and high preswirl inserts; however, the stator is still precessing at zero speed for LVF>0% - similar observations were reported by Zhang [21]. Therefore, the test is only conducted for the zero-preswirl insert with a 62.1-bar-g inlet pressure. The supplied oil temperature is maintained within 35 to 37.8°C. The test seal is centered, and no intentional fluid pre-rotation is provided (zero preswirl insert). The test matrix covers:

- 5 inlet LVFs: 0, 2, 4, 6, and 8%
- 3 rotor speeds (ω): 5, 10, and 15 krpm
- 3 pressure ratios (PR): 0.6, 0.5, and 0.4 (PD of 24.8, 31.1, and 37.3 bar, respectively)

The preswirl ratios, which would be used for running the prediction, are recorded for each case using pitot tube and static pressure orifice. Figure 45 shows the measured preswirl ratios for the zero-preswirl insert. The uncertainty of preswirl ratio measurement, shown in Tab. 14 (Appendix C) or by error bars in Fig. 45, is a resultant of the uncertainties of the measurements of pitot tube differential pressure, liquid density, and gas density. At PR=0.6, the preswirl ratios are around zero. As PR decreases (or PD increases), the preswirl ratios tend to increase at low inlet LVF conditions. At PR=0.5, the preswirl ratios increase slightly for cases at inlet LVF=0% and 2%, and further increase as PR drops from 0.5 to 0.4.

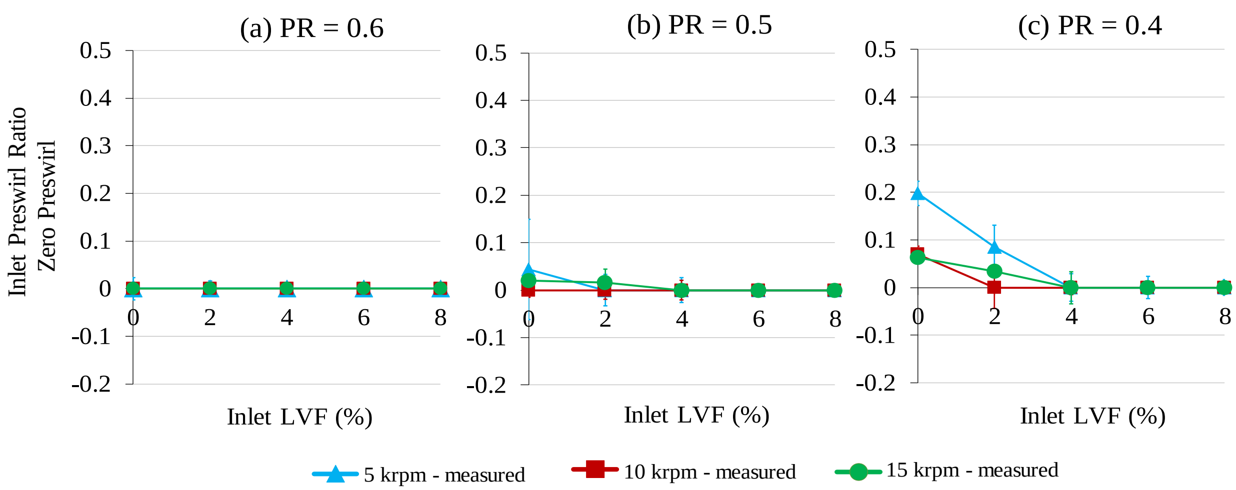

Figure 45 Measured preswirl ratio at seal inlet under pure- or mainly-air conditions for the zero-preswirl insert at: (a) PR=0.6, (b) PR=0.5, and (c) PR=0.4

7.2 Flow Status (Reynolds and Mach Numbers)

Reynolds number was calculated using Eqs. (31) - (33), as defined in Sec. 5.4.

Figure 46 shows inlet *Re* versus inlet LVF at three PR values and three ω values with the zero-preswirl insert. Inlet *Re* is in a range of 3,500 to 71,000, and it is likely in a turbulent regime according to Zirkelback and San Andrés [36]. Inlet *Re* tends to decrease with increasing inlet LVF. As PR decreases (PD increases) or ω increases, inlet *Re* increases.

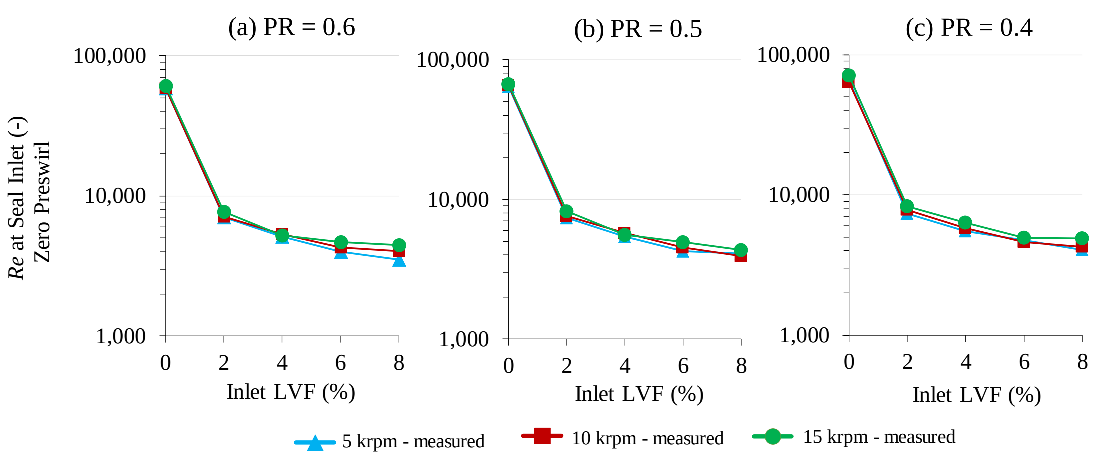

Figure 46 Measured *Re* at seal inlet under pure- or mainly-air conditions with the zero-preswirl insert at: (a) PR=0.6, (b) PR=0.5, and (c) PR=0.4

Similarly, Fig. 47 shows exit *Re* versus inlet LVF at three PR values and three ω values with the zero-preswirl insert. In general, exit *Re* is higher than inlet *Re* and in a range of 5,000 to 71,000 (a turbulent regime). Similar to inlet *Re*, as inlet LVF decreases, or ω increases, or PR decreases (PD increases), exit *Re* tends to increase.

Ma number is defined as

$$Ma = \sqrt{\frac{\left(\dfrac{\dot{m}}{2\pi R C_r \rho}\right)^2 + (R\omega/2)^2}{\gamma P/\rho}} \tag{40}$$

where ρ is density and γ is specific heat ratio. Figure 48 shows maximum *Ma* number (at the seal exit) versus ω at three PR values under pure-air conditions with the zero-preswirl insert.

In general, *Ma* changes insignificantly with changing ω and increases as PR drops (or PD increases). However, since *Ma* is in a range of 0.4 to 0.75, no choking occurs.

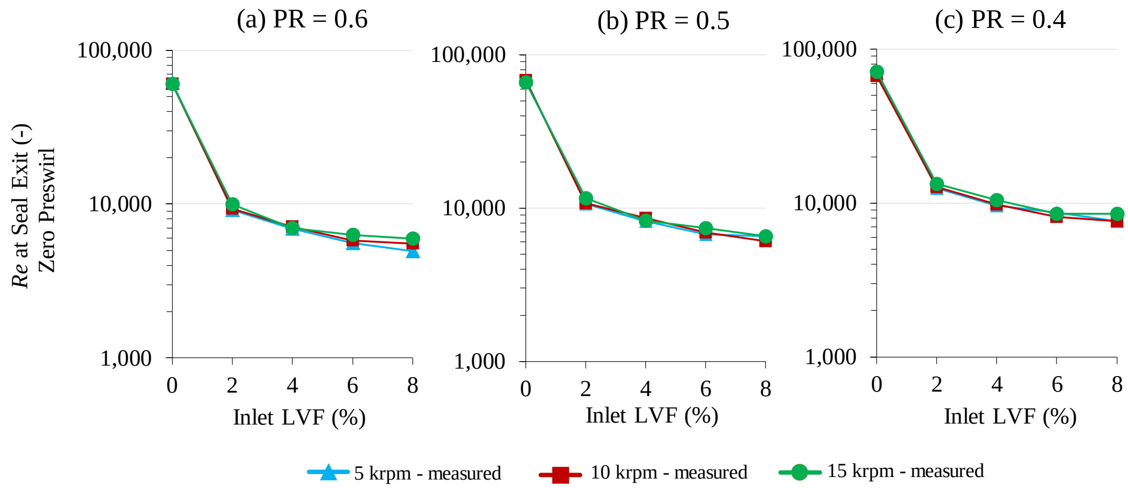

Figure 47 Measured *Re* at seal exit under pure- or mainly-air conditions with the zero-preswirl insert at: (a) PR=0.6, (b) PR=0.5, and (c) PR=0.4

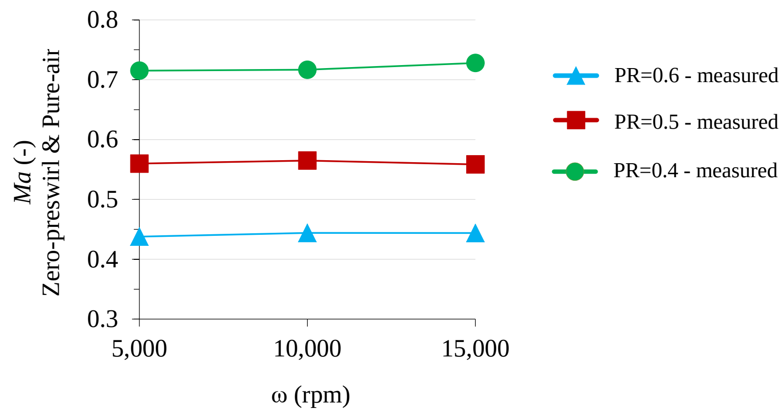

Figure 48 Measured maximum *Ma* number under pure-air conditions with the zero-preswirl insert

7.3 Leakage Mass Flow Rate

Figure 49 shows $\dot{m}$ versus inlet LVF at three PR values and three ω values with the zero-preswirl insert. $\dot{m}$ drops slightly, by 4-7%, as the inlet LVF increases from 0 to 2%, and then significantly increases by a factor of 1.40-1.44 when inlet LVF further increases from 2 to 8%.

As PR decreases from 0.6 to 0.4 (or PD increases from 24.8 to 37.3 bar), $\dot{m}$ increases by about 10%. These tendencies of $\dot{m}$ as functions of PR and inlet LVF are also observed in the measurements of Zhang [21].

The effect of changing ω is insignificant. There is a slight drop of $\dot{m}$ when ω increases from 5 to 15 krpm. Kerr [41] observed the same tendency for a smooth gas seal tested at pure-air conditions; while Zhang's results [21] also showed this trend for pure- and mainly-air conditions.

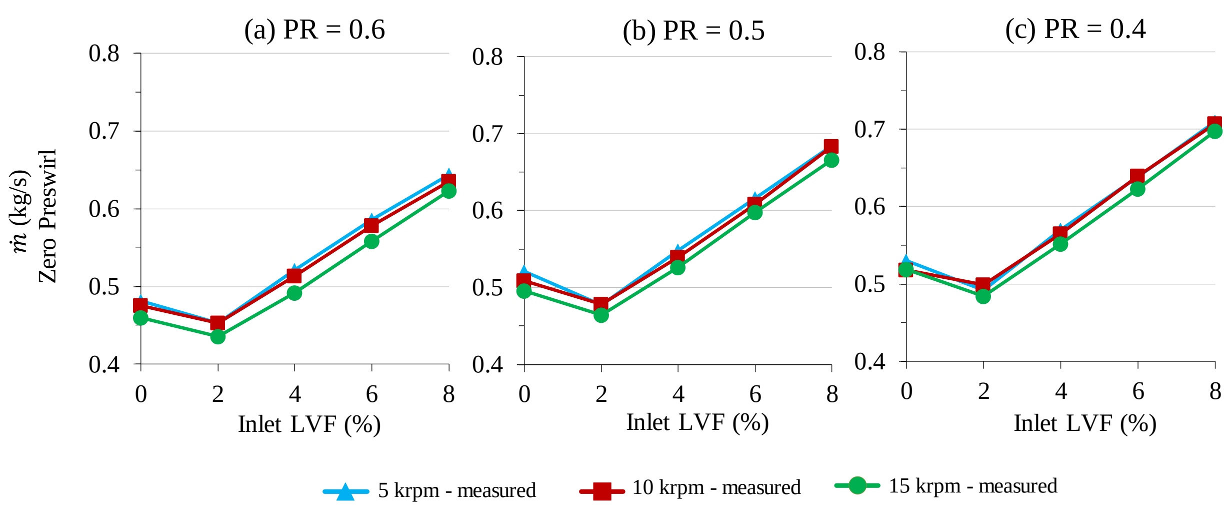

Figure 49 Measured $\dot{m}$ versus inlet LVF under pure- and mainly-air conditions for the zero-preswirl insert at: (a) PR=0.6, (b) PR=0.5, and (c) PR=0.4

7.4 Direct Dynamic Stiffness

Figure 50 shows K_{Ω} versus Ω with the zero-preswirl insert over three PRs, three ω values, and inlet LVF ranging from 0 to 8. K_{Ω} affects the system's natural frequency.

The effect of changing inlet LVF on K_Ω is different for different PR values:

- At PR=0.6 and 0.5, as inlet LVF increases from 0 to 8%, K_Ω is minimum at inlet LVF=2%; i.e., K_Ω drops as inlet LVF increases from 0 to 2%, and then increases when inlet LVF further increases.
- At PR=0.4, as inlet LVF increases from 0 to 8%, K_Ω increases. K_Ω is negative and about zero at inlet LVF=0%; however, it becomes positive as inlet LVF increases to above 2%.

The effect of changing ω is minimal for the tested ω range (5 to 15 krpm), which confirms Kerr‘s results [41] for gas-smooth-annular seals and Zhang's results [21] for pure- and mainly-air conditions (for ω up to 15 krpm). K_Ω at pure-air test changes insignificantly as ω increases from 5 to 15 krpm. Under mainly-air test (inlet LVF≥2%), there is a slight increase of K_Ω as ω increases, and the increase is more obvious at high LVF values.

The effect of changing PR is different for different inlet LVF values:

- At inlet LVF=0%, there is a continuous decreasing trend of K_Ω as PR decreases from 0.6 to 0.4 (PD increases from 24.8 to 37.3 bar). A similar tendency was reported by Kerr [41].
- At inlet LVF≥2%, K_Ω remains unchanged as PR drops from 0.6 to 0.5, and then decreased as PR further drops from 0.5 to 0.4. The effect of changing PR is weaker as inlet LVF increases. A similar tendency was reported by Zhang [21] for pure- and mainly-air test conditions.

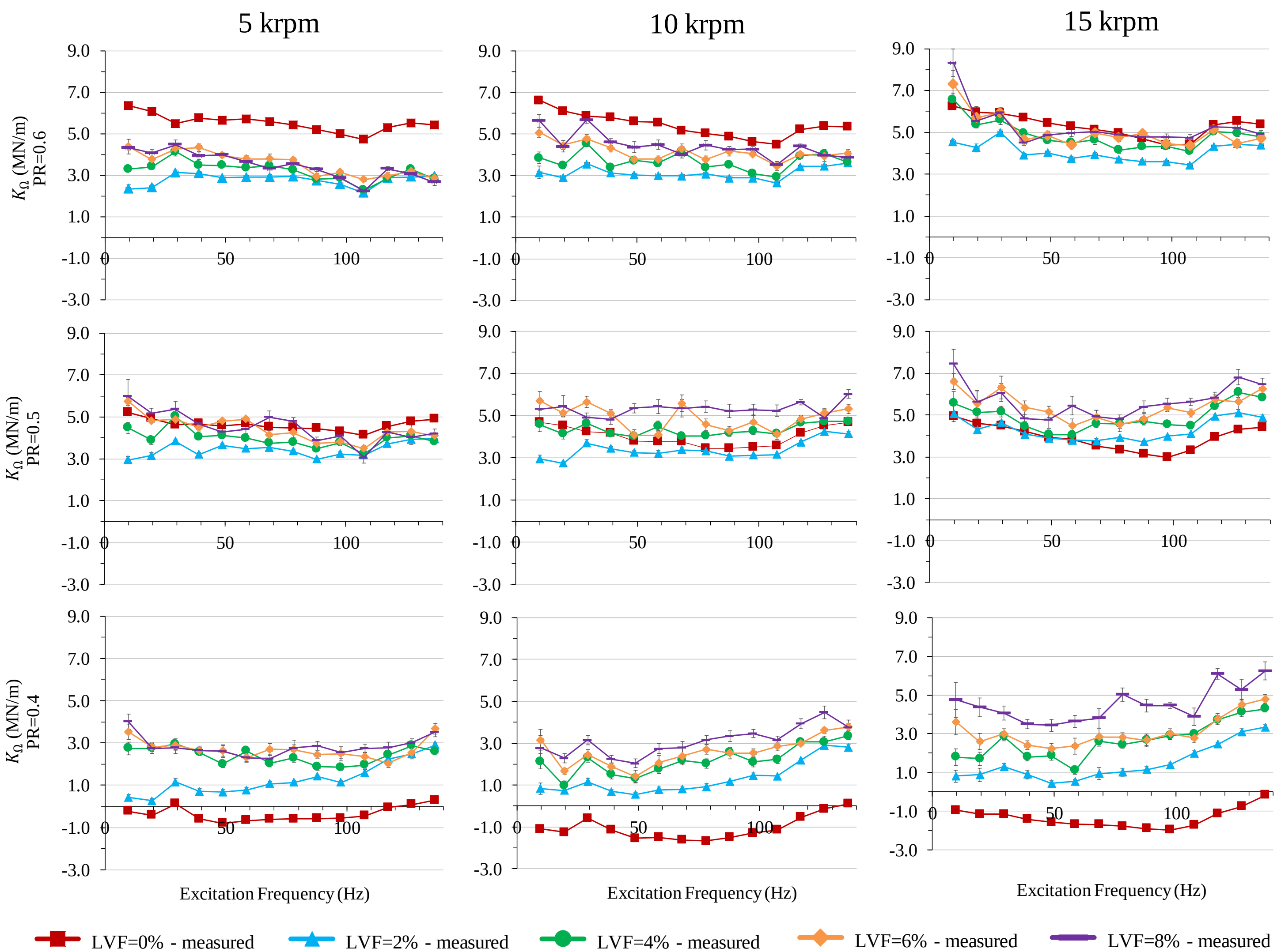

Figure 50 Measured K_Ω vs. Ω under pure- and mainly-air conditions for the zero-preswirl insert

7.5 Cross-Coupled Dynamic Stiffness

Figure 51 shows k_Ω versus Ω with the zero-preswirl insert over three PRs, three ω values, and inlet LVF ranging from 0 to 8%. k_Ω has direct contribution to a system's rotordynamic stability. There is very little frequency dependency of k_Ω, therefore, $\bar{k}$, an average value of k_Ω over the range of Ω, accounts for the test seal's cross-coupled stiffness.

Figure 52 shows $\bar{k}$ versus inlet LVF for three PR values and three ω values with the zero-preswirl insert.

At PR=0.6, increasing inlet LVF from 0 to 2% increases $\bar{k}$; however, as inlet LVF further increases, $\bar{k}$ tends to drop slightly at ω=15 krpm, while changes insignificantly at ω=5 and 10 krpm. As ω increases from 5 to 15 krpm, $\bar{k}$ increases significantly.

The impacts of changing inlet LVF and ω at PR=0.5 are similar to the cases at PR=0.6.

At PR=0.4, increasing inlet LVF from 0 to 2% increases $\bar{k}$, and $\bar{k}$ tends to drop with increasing inlet LVF from 2 to 4%; however, as inlet LVF further increases to 8%, $\bar{k}$ at ω=15 krpm drops slightly, while remains unchanged at ω=5 and 10 krpm. As ω increases from 5 to 15 krpm, at inlet LVF=0%, 4%, 6%, and 8%, $\bar{k}$ increases; however, at inlet LVF=2%, $\bar{k}$ remains unchanged with increasing ω from 5 to 10 krpm, and only increases as ω further increases to 15 krpm.

With decreasing PR from 0.5 to 0.4, $\bar{k}$ increases moderately at ω=15 krpm, slightly at ω=10 krpm, and remains unchanged at ω=5 krpm, except the case at inlet LVF=2% and ω=5 krpm where $\bar{k}$ increases significantly.

Zhang [21] reported similar tendencies of $\bar{k}$ or k_Ω as effects of changing ω, PR, and inlet LVF under pure- and mainly-air conditions.

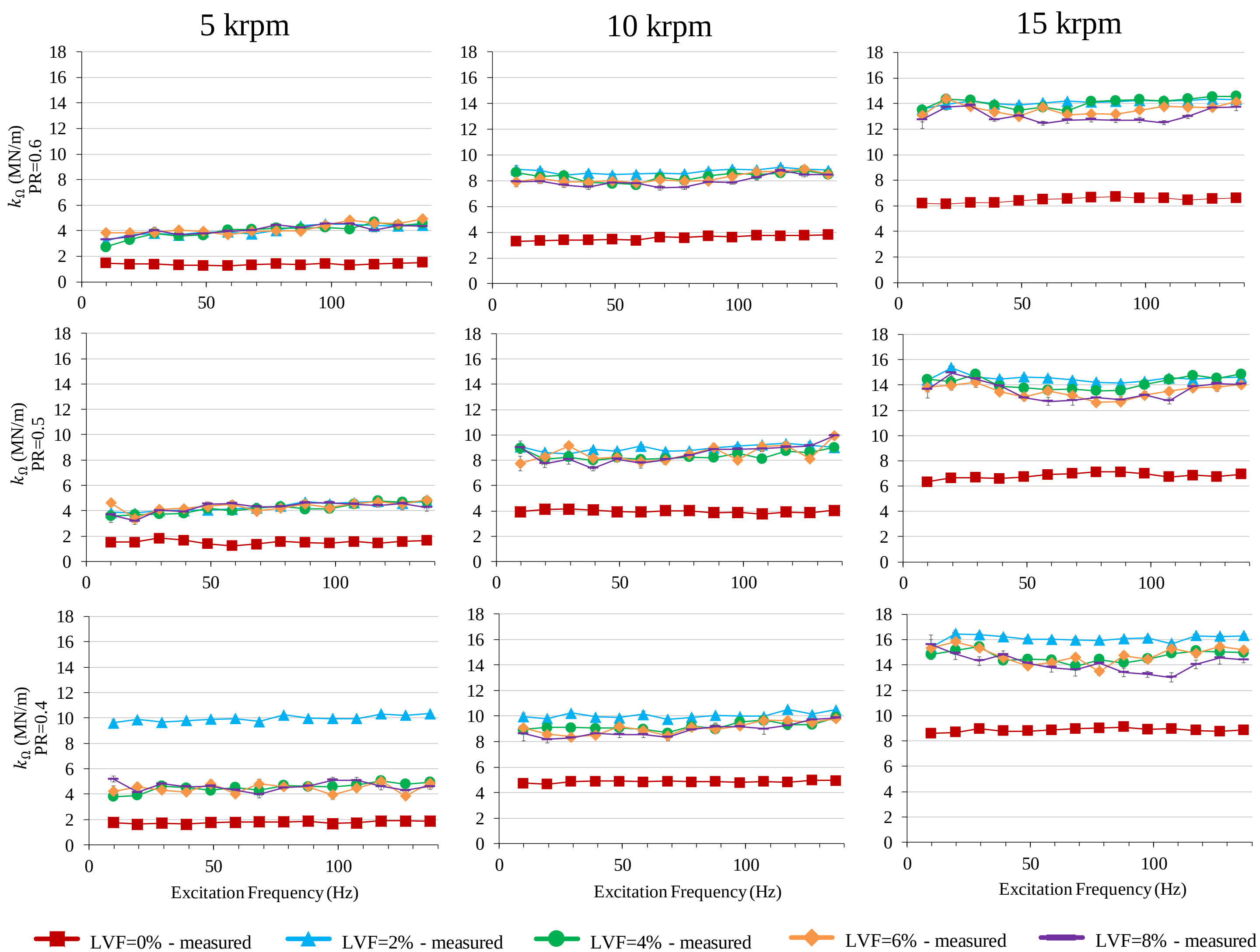

Figure 51 Measured k_Ω vs. Ω under pure- and mainly-air conditions for the zero-preswirl insert

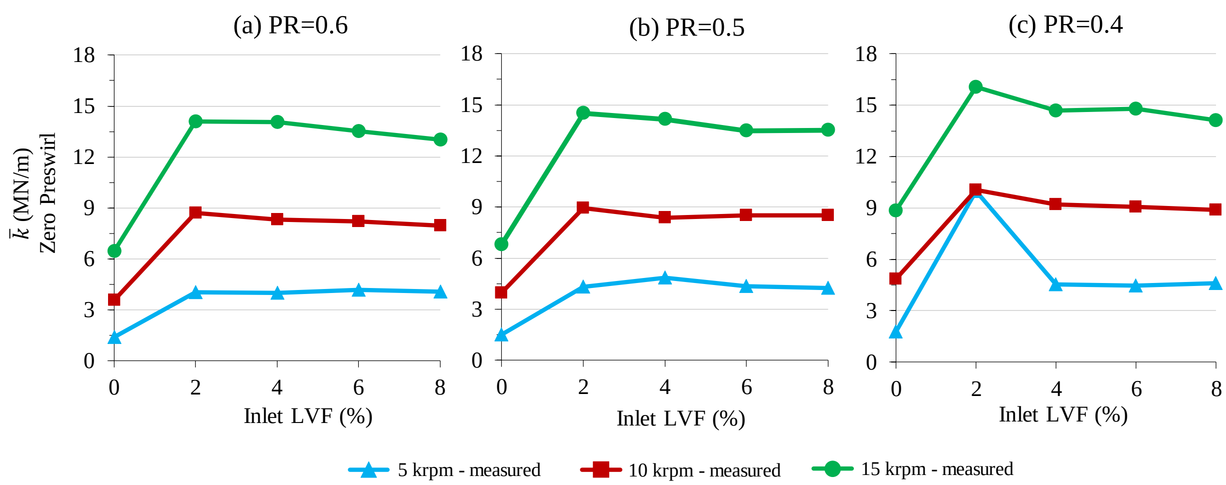

Figure 52 Measured $\bar{k}$ vs. inlet LVF under pure- and mainly-air conditions for the zero-prewirl insert at: (a) PR=0.6, (b) PR=0.5, and (c) PR=0.4

7.6 Direct Damping Coefficient

Figure 53 shows C versus inlet LVF for three PR values and three ω values with the zero-preswirl insert.

At PR=0.6, C increases rapidly with inlet LVF increasing from 0 to 2%, and steadily with inlet LVF further increasing to 8%. At inlet LVF=0%, C is a weak function of ω; however, at inlet LVF≥2%, C increases slightly as ω goes up from 5 to 10 krpm, but changes insignificantly as ω further increase to 15 krpm.

At PR=0.5, with increasing inlet LVF, C increases rapidly for an increase of inlet LVF from 0 to 2%, but then increases steadily with further increasing inlet LVF. There is no difference in C values at inlet inlet LVF=0% at different speeds; however, at inlet LVF≥2%, C increases as ω increases.

At PR=0.4 and ω=10 and 15 krpm, C tends to increase with increasing inlet LVF; however, at ω=5 krpm, C increases as inlet LVF increases from 0 to 2%, but then drops slightly as inlet LVF further increases to 4%, and increases again with increasing inlet LVF from 4 to

8%. *C* increases as ω increases, except the case at inlet LVF=2% where there is no change on *C* with increasing ω from 5 to 10 krpm, and *C* only increases as ω further increases to 15 krpm.

As PR decreases from 0.6 to 0.4 (PD increases from 24.8 to 37.3 bar), *C* increases by a factor of 1.2-1.3.

Zhang [21] reported similar tendencies of *C* as effects of changing PR under pure- and mainly-air conditions.

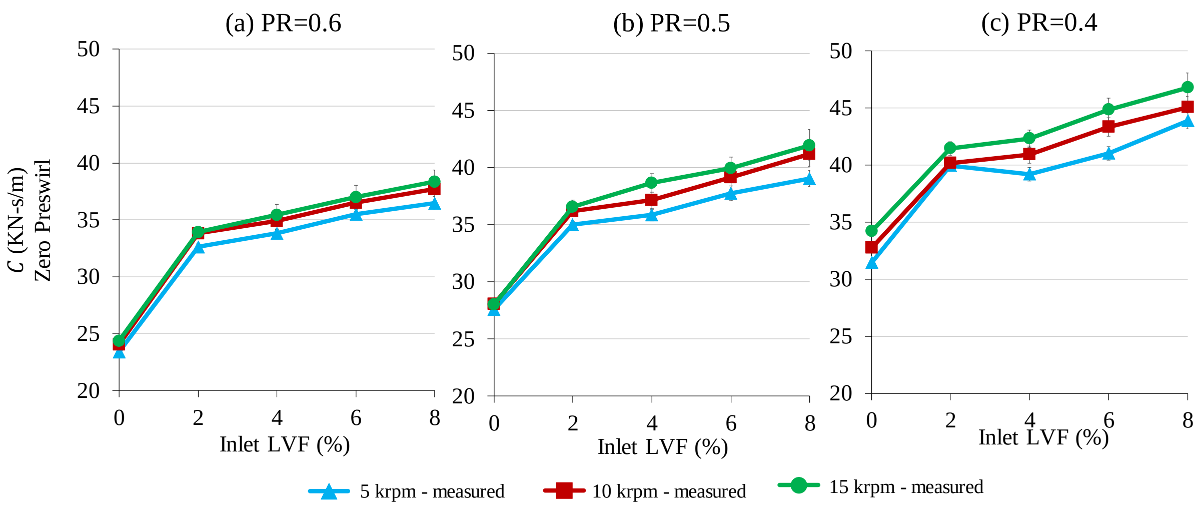

Figure 53 Measured *C* vs. inlet LVF under pure- and mainly-air conditions for the zero-preswirl insert at: (a) PR=0.6, (b) PR=0.5, and (c) PR=0.4

7.7 Cross-Coupled Damping Coefficient

Figure 54 shows *c* versus inlet LVF for three PR values and three ω values with the zero-preswirl insert.

At PR=0.6, in regard to change of inlet LVF, *c* changes insignificantly at ω=5 krpm; while at ω=10 and 15 krpm, *c* is a minimum at inlet LVF=2%. At inlet LVF=0%, *c* tends to increase with increasing ω; however, at inlet LVF≥2%, *c* increases with increasing ω from 5 to 10 krpm, but then stays constant as ω increases further.

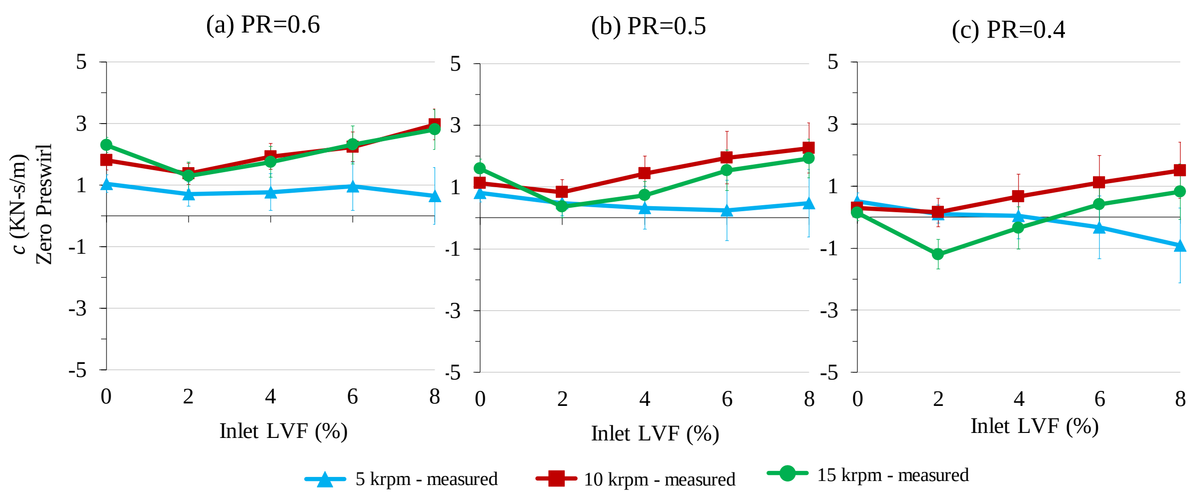

Figure 54 Measured *c* vs. inlet LVF under pure- and mainly-air conditions for the zero-preswirl insert at: (a) PR=0.6, (b) PR=0.5, and (c) PR=0.4

At PR=0.5, with the impact of changing inlet LVF, *c* is at minimum values at inlet LVF=2% for cases of ω=10 and 15 krpm and at inlet LVF=6% for cases of ω=5 krpm. In regard to the impact of changing ω, at inlet LVF=0% and 4-8%, increasing ω increases *c*; however, at inlet LVF=2%, *c* values at ω=5 and 15 krpm are the same and less than *c* value at ω=10 krpm.

At PR=0.4, with increasing inlet LVF, *c* at ω=5 krpm keeps dropping, while *c* at ω=10 and 15 krpm are minimum at inlet LVF=2%. In regard to the change of ω, at inlet LVF=0%, *c* remains unchanged; however, at inlet LVF≥2%, *c* tends to increase as ω increases from 5 to 10 krpm, and then drops as ω further increases from 10 to 15 krpm.

As the impact of decreasing PR (increasing PD), *c* decreases as a result of PR increments.

7.8 Effective Damping

Figure 55 shows C_{eff} versus Ω over three PRs, three ω values, and inlet LVF ranging from 0 to 8% with the zero-preswirl insert. As expected from Eq. (35), C_{eff}, switches from negative to positive as Ω increases. Cross-over frequency Ω_c is defined as the Ω value where C_{eff} changes from negative to positive. Increasing Ω_c decreases stability.

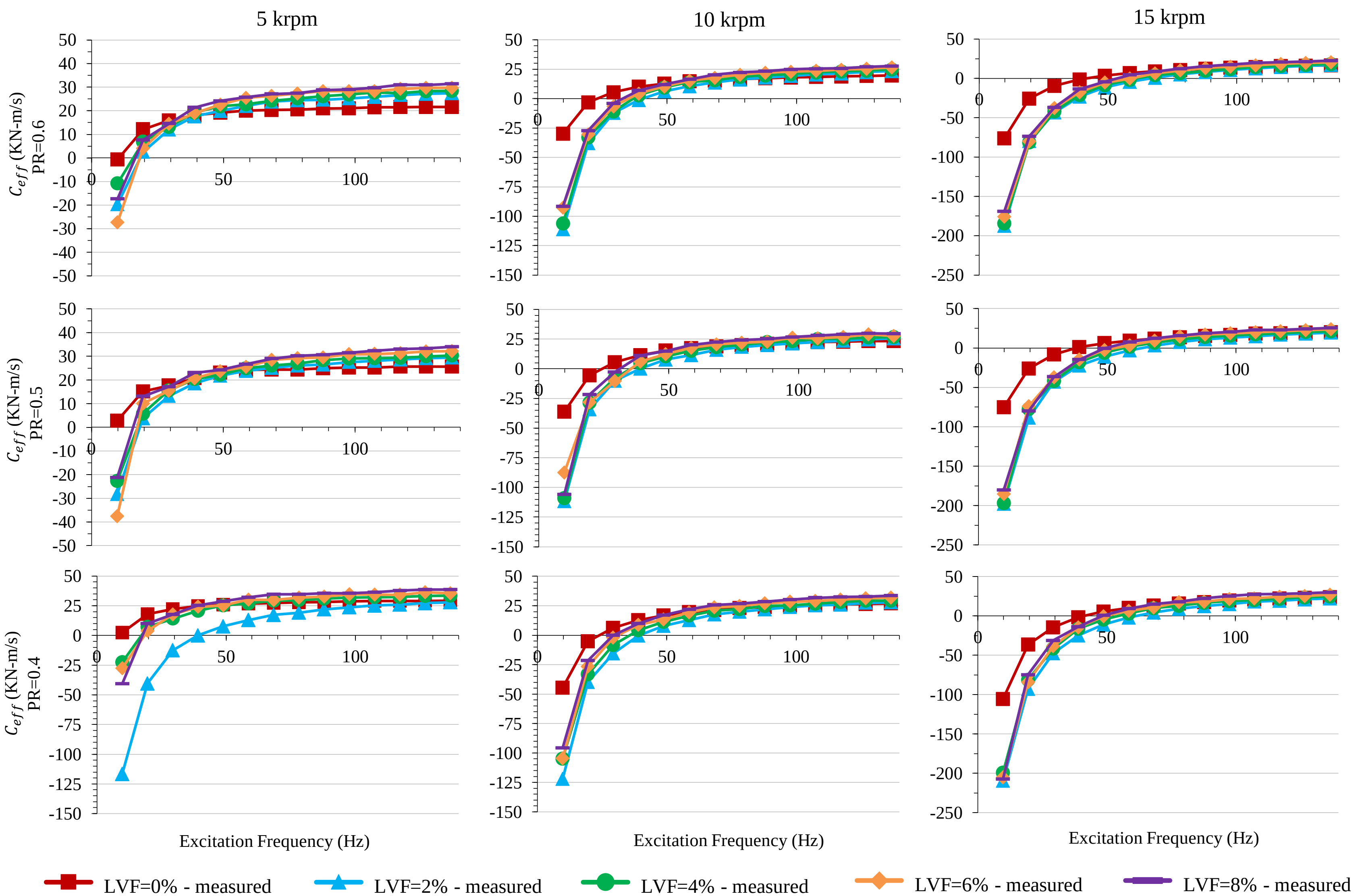

Figure 55 Measured C_{eff} vs. Ω under pure- and mainly-air conditions for the zero-preswirl insert

Figure 56 shows Ω_c versus inlet LVF for three PR values and three ω values with the zero-preswirl insert.

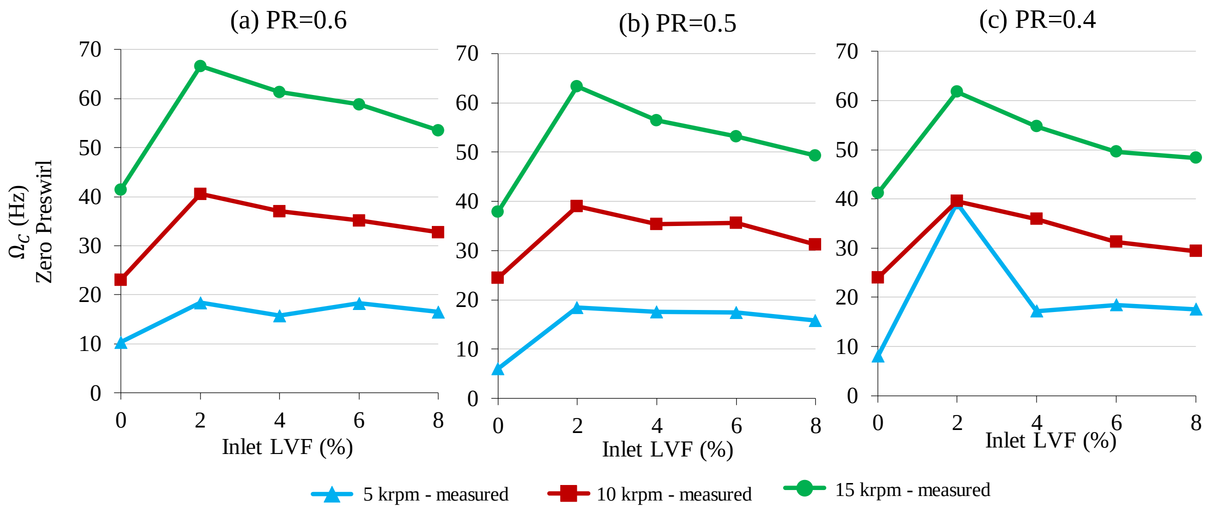

Figure 56 Ω_C versus inlet LVF under pure- and mainly-air cases for the zero-preswirl insert at: (a) PR=0.6, (b) PR=0.5, and (c) PR=0.4

At PR=0.6, increasing inlet LVF from 0 to 2% increases Ω_c (decreasing stability); however, as inlet LVF further increases, Ω_c tends to drop (increasing stability) at ω=10 and 15 krpm, while changes insignificantly at ω=5 krpm. As ω increases from 5 to 15 krpm, Ω_c increases significantly (decreasing stability).

The impacts of changing inlet LVF and ω at PR=0.5 are similar to the cases at PR=0.6.

At PR=0.4, increasing inlet LVF from 0 to 2% increases Ω_c. However, as inlet LVF further increases to 8%, Ω_c at ω=10 and 15 krpm drops; while at ω=5 krpm, Ω_c drops rapidly with increasing inlet LVF from 2 to 4% and then remains unchanged as inlet LVF further increases. As ω increases from 5 to 15 krpm, at inlet LVF=0%, 4%, 6%, and 8%, Ω_c increases; however, at inlet LVF=2%, Ω_c remains unchanged with increasing ω from 5 to 10 krpm, and only increases as ω further increases to 15 krpm.

With decreasing PR from 0.6 to 0.5, at inlet LVF=0%, Ω_c tends to drop slightly; however, at inlet LVF≥2%, Ω_c drops at ω=15 krpm, but changes insignificantly at ω=5 and 10 krpm. As PR further drops to 0.4, Ω_c changes insignificantly, except the case at inlet LVF=2% and ω=5 krpm, where there is a significant increase of Ω_c as PR decreases.

Both results of Ω_c, shown in Fig. 56, and $\bar{k}$, shown in Fig. 52, reflect stability. Increasing either Ω_c or $\bar{k}$ decreases stability. In regard to comparison results of Ω_c and $\bar{k}$, both have similar tendency of increasing (decreasing stability) as ω increases. With the impact of increasing inlet LVF, both Ω_c and $\bar{k}$ show similar trends; i.e., increase (decreasing stability) with increasing inlet LVF from 0 to 2%, and decrease (increasing a stability) or change insignificantly as inlet LVF further increases to 8%. Concerning the impact of decreasing PR, Ω_c and $\bar{k}$ have a similar tendency at ω=5 and 10 krpm (except the case at inlet LVF=2% and ω=5 krpm, where there is a significant increase as PR decreases from 0.5 to 0.4); however, at ω=15 krpm, Ω_c drops slightly while $\bar{k}$ increases slightly when PR decreases.

Zhang [21] reported similar tendencies of Ω_c as the impacts of changing ω and inlet LVF under pure- and mainly-air conditions.

Figure 57 shows the effect of inlet LVF on C_{eff} at PR=0.5 and ω=15 krpm (representative operating conditions for a compressor balance-piston seal) for the frequency range 98 Hz – 137 Hz (about 0.5ω). The frequency range is chosen to represent wet-gas compression on a compressor running at 15 krpm and PR=0.5 with the first natural frequency around 7500 rpm (125 Hz). C_{eff} is positive for all inlet LVFs, and tends to increase with increasing excitation frequency. As inlet LVF increases from 0 to 2%, C_{eff} drops (decreasing the stabilizing capability of the seal); however, it increases as inlet LVF further increases (increasing the stabilizing capability of the seal).

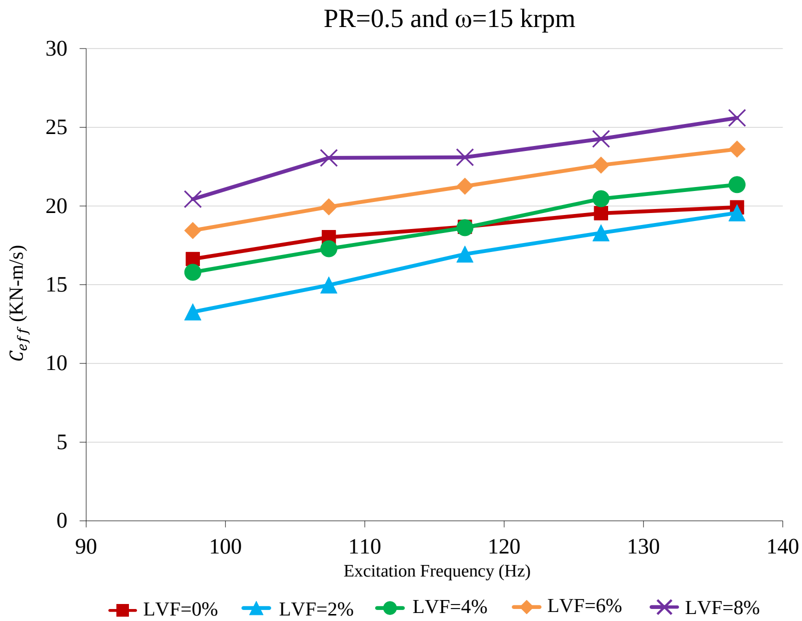

Figure 57 Measurements of C_{eff} vs. Ω at PR=0.5 and ω=15 krpm with the zero-preswirl insert for frequency range 98 Hz – 137 Hz

8. PREDICTIONS VERSUS MEASUREMENTS FOR PURE- AND MAINLY-AIR CONDITIONS

Following the measurements as discussed in Chapter 7, this chapter provides comparisons between measured and predicted results for static and dynamic performances of the annular smooth seal operating under pure- and mainly-air conditions, i.e. mixtures of air and silicone oil (PSF-5cSt), with the zero-preswirl insert. The predicted results are produced from the *XLHseal_mix* program which was developed based on a bulk-flow model introduced by San Andrés [15] in 2011. The code uses inputs listed below to obtain predicted results. Note that, during pure- and mainly-air tests, the supplied oil temperature is maintained within 35 to 37.8^{o}C. Inlet temperature, liquid density and liquid viscosity are presented in Tab. 10 to use for predictions. Entrance pressure loss and exit pressure recovery factors are assumed to be 0.2 and 0, respectively.

Table 10 Liquid and gas properties used for predictions for pure- and mainly-air conditions with the zero-preswirl insert

Average supply temperature (^{o}C)	23.11 (±4.89)
Liquid properties	
Viscosity (cP)	4.58 (avg.)
Density (kg/m3)	905.7 (±5.7)
Bulk-modulus (bar)	9987
Surface tension/length (N/m)	0.0197
Liquid vapor pressure (bar)	0.001
Gas properties	
Gas constant, R_g (J/kg-C)	286.70
Compressibility, Z	1.00
Gas viscosity (cP)	0.0193
Ratio specific heats	1.40

The following differences between the predictive model and experiment need to be noted:

(1) The model assumes that the fluid's temperature remains constant in the seal clearance; however, the fluid's actual/measured temperature throughout the seal may decrease (due to air expansion) or increase (due to power dissipation). Table 12 in Appendix B shows the fluid's measured temperatures at the seal inlet and seal exit.

(2) The model assumes that the mixture is homogeneous in the seal clearance while the actual condition is unknown and may be different. Although the mixture is visually inspected through a sight-glass view port shortly upstream of the inlet ports of the stator and a bubble size of approximately 6.2 μm or 3% of the seal's radial clearance is expected from the mainly-air mixing section, the mixture might not remain homogeneous in the seal clearance due to piping configuration, the bubble coalescence, and centrifugal-inertia effects. The coalescence of fine bubbles could make larger bubbles. The centrifugal-inertia effect could lead to a stratified-flow.

8.1 Flow Status (Reynolds and Mach Numbers)

Figure 58 compares measured and predicted inlet *Re*, defined in Eqs. (31) - (33), versus inlet LVF for three PR values and three speeds with the zero-preswirl insert. Measured inlet *Re* is in a range of 3,500 to 71,000, while predicted inlet *Re* is in a range of 3,000 to 71,000. Both predictions and measurements show a drop of inlet *Re* as inlet LVF increases, or PR increases (PD decreases), or ω decreases.

Figure 59 compares measured and predicted exit *Re*, defined in Eqs. (31) - (33), versus inlet LVF for three PR values and three speeds with the zero-preswirl insert. Measured exit *Re* is in a range of 5,000 to 71,000, while predicted exit *Re* is in a range of 4,000 to 80,000. Both predictions and measurements showed a drop of exit *Re* as inlet LVF increases, or PR increases (PD decreases), or ω decreases.

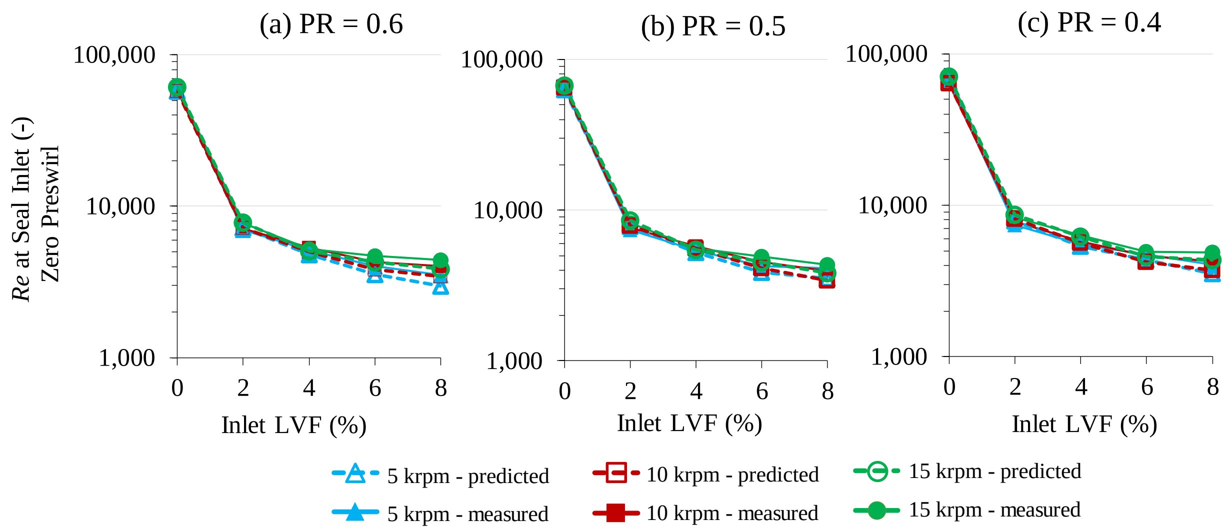

Figure 58 Predictions and measurements of inlet *Re* under pure- and mainly-air conditions with zero-preswirl insert at: (a) PR=0.6, (b) PR=0.5, and (c) PR=0.4

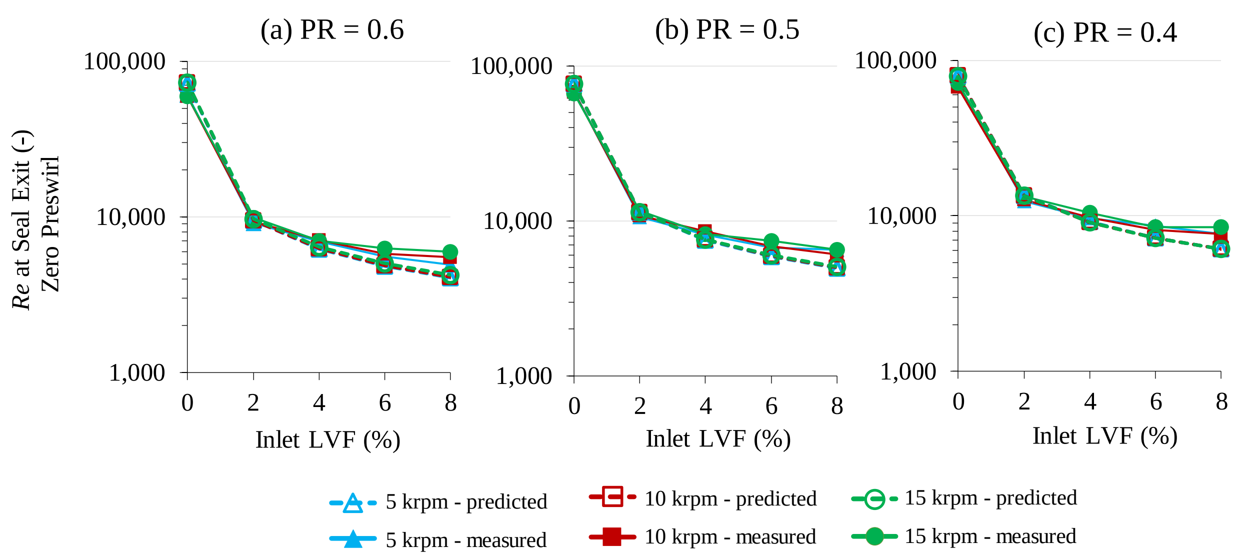

Figure 59 Predictions and measurements of exit *Re* under pure- and mainly-air conditions with zero-preswirl insert at: (a) PR=0.6, (b) PR=0.5, and (c) PR=0.4

Figure 60 compares maximum measured and predicted *Ma* number (at the seal exit), defined in Eq. (40) versus ω for three PR values with the zero-preswirl insert under pure-air conditions. Both predictions and measurements show an insignificant change of *Ma* number as ω increases. Predicted and measured *Ma* tend to increase as PR drops (or PD increases), however, both showed values less than 1 (no choking).

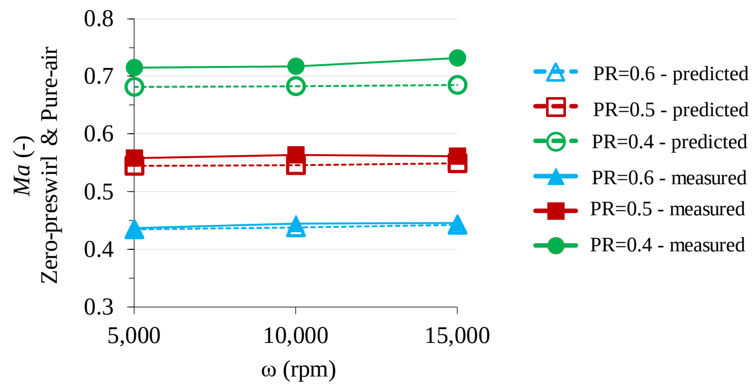

Figure 60 Predictions and measurements of maximum *Ma* number under pure-air conditions with zero-preswirl insert

8.2 Leakage Mass Flow Rate

Figure 61 compares measured and predicted $\dot{m}$ versus inlet LVF for three PR values and three speeds with the zero-preswirl insert.

At PR=0.6, in regard to changing inlet LVF, both predictions and measurements show a slight drop as inlet LVF increases from 0 to 2%, and an increase as inlet LVF further increases from 2 to 8%, even though the increasing measured rate is higher than predicted. Concerning the impact of increasing ω, while predicted $\dot{m}$ drops steadily, measured $\dot{m}$ remains unchanged at ω≤10 krpm, and only drops with increasing ω from 10 to 15 krpm.

At PR=0.5, for an increment of inlet LVF from 0 to 2%, predicted $\dot{m}$ remains unchanged, but measured $\dot{m}$ drops. With further increases of inlet LVF, both measured and predicted $\dot{m}$ show a same tendency of increasing. Both predictions and measurements show no change from the cases at PR=0.6 for the impact of changing ω on $\dot{m}$.

At PR=0.4, the impacts of changing inlet LVF and ω on $\dot{m}$ of both predictions and measurements are similar to the cases at PR=0.5.

Both predicted and measured $\dot{m}$ increase with dropping PR from 0.6 to 0.4.

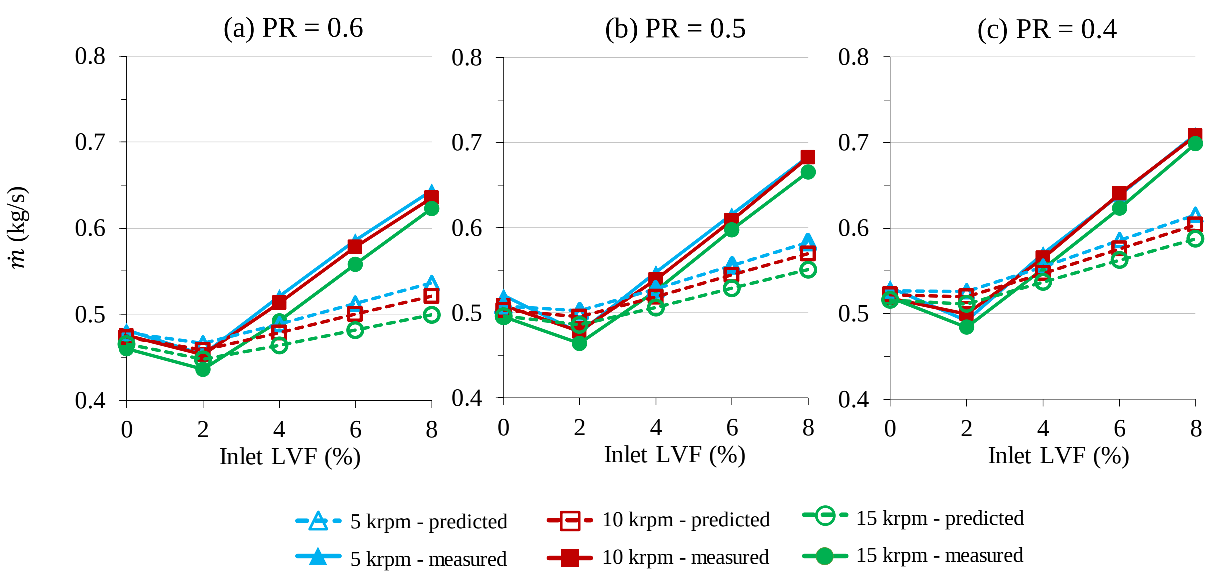

Figure 61 Predictions and measurements of $\dot{m}$ versus inlet LVF under pure- and mainly-air conditions for the zero-preswirl insert at: (a) PR=0.6, (b) PR=0.5, and (c) PR=0.4

8.3 Direct Dynamic Stiffness

Figure 62 compares measured and predicted K_Ω versus Ω for three PRs (rows) and three speeds (columns) over a range of inlet LVF with the zero-preswirl insert. As Ω increases, predicted K_Ω slightly drops; while measured K_Ω slightly drops at low Ω and then increases at high Ω.

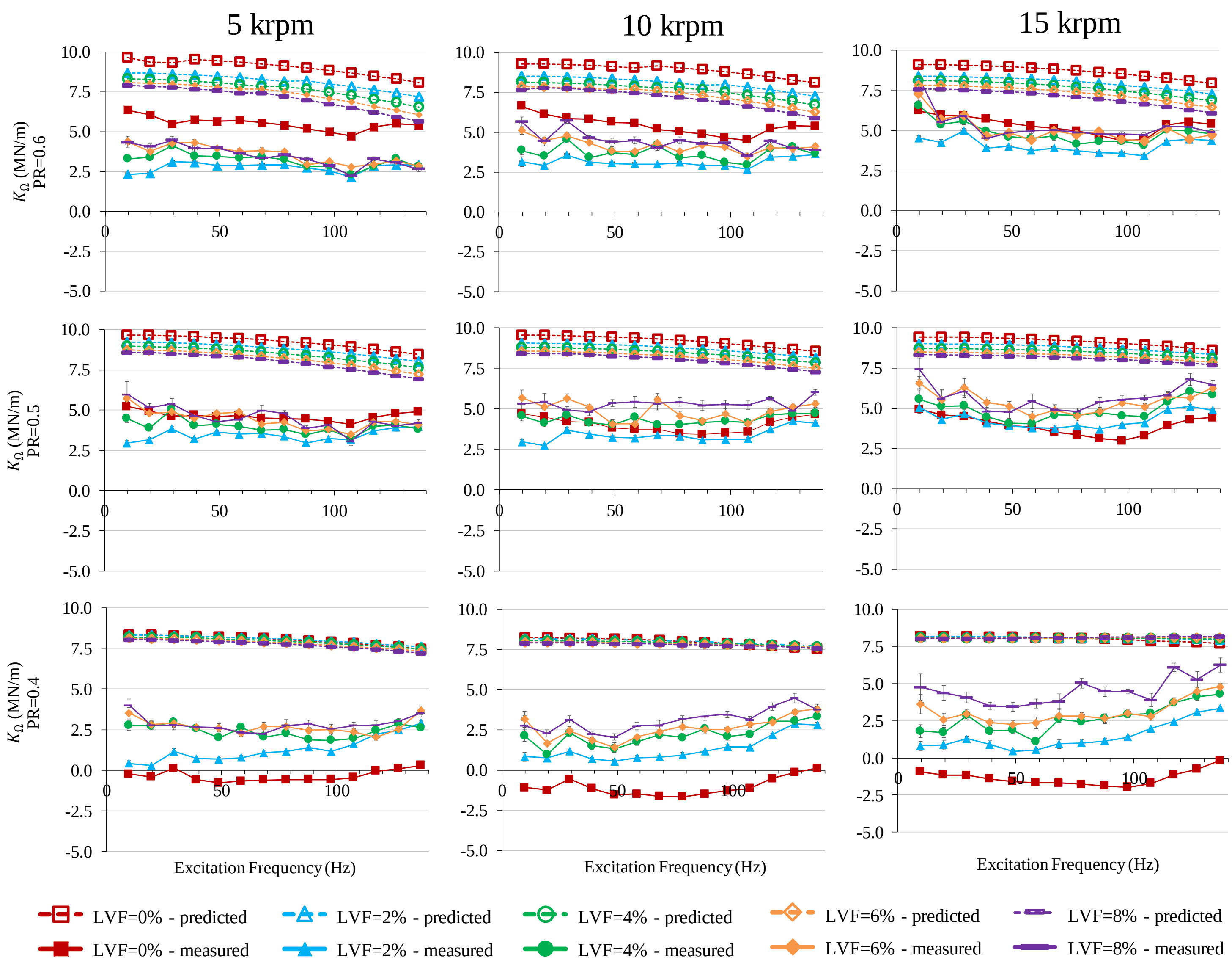

Figure 62 Predictions and measurements of K_Ω under pure- and mainly-air conditions for the zero-preswirl insert

At PR=0.6, predicted K_Ω drops with increasing inlet LVF; however, measured K_Ω tends to drop with increasing LVF from 0 to 2%, but then increases as inlet LVF further increases from 2 to 8%. In regard to the impact of changing ω, predicted K_Ω is insensitive to change in ω; however, measurements show an insignificant change at inlet LVF=0%, but increases at inlet LVF≥2%.

At PR=0.5 and ω=5 and 10 krpm, as inlet LVF increases, predictions show a drop of $K_{\Omega,}$ while measurements show a minimum K_Ω at inlet LVF=2%. However, at ω=15 krpm, while predicted K_Ω tends to drop with increasing inlet LVF, measurements show an increase. In regard to the impact of changing ω, as ω increases from 5 to 10 krpm, K_Ω at inlet LVF=0-4% changes insignificantly, while K_Ω at inlet LVF=6% and 8% slightly increases. With a further increase in ω to 15 krpm, K_Ω remains unchanged at inlet LVF=0%, but increases significantly at inlet LVF≥2%.

At PR=0.4, predicted K_Ω remains unchanged as LVF increases; however, measured K_Ω tends to increase as seen with cases at PR=0.5 and ω=15 krpm. With increasing ω from 5 to 10 krpm, both predictions and measurements show insignificant changes. As ω further increases to 15 krpm, predicted K_Ω remains unchanged, while measured K_Ω changes insignificantly at inlet LVF=0-6%, but increase slightly at inlet LVF=8%.

In regard to the impact of changing PR,

- At inlet LVF=0%, as PR drops from 0.6 to 0.5 (or PD increases from 24.8 to 31.1 bar) predicted K_Ω remains unchanged and only drops as PR further drops from 0.5 to 0.4 (or PD increases from 31.1 to 37.3 bar). On the other hand, measured $K_{\Omega,}$ tends to drop steadily with decreasing PR from 0.6 to 0.4 or PD increases from 24.8 to 37.3 bar)

- At inlet LVF≥2%, both predictions and measurements show a slight increase of K_{Ω} as PR drops from 0.6 to 0.5 (or PD increases from 24.8 to 31.1 bar) and then drops as PR further decreases from 0.5 to 0.4 (or PD increases from 31.1 to 37.3 bar).

8.4 Cross-Coupled Dynamic Stiffness

Figure 63 compares measured and predicted k_{Ω} versus Ω over three PRs (rows) and three speeds (columns) over a range of inlet LVF with the zero-preswirl insert.

There was very little frequency dependency of k_{Ω}, therefore, $\bar{k}$, an average value of k_{Ω} over a range of **Ω**, was used to describe the test seal's cross-coupled stiffness. Figure 64 shows $\bar{k}$ versus inlet LVF for three PR values and three ω values with the zero-preswirl insert.

At PR=0.6, as inlet LVF increases from 0 to 2%, both predicted and measured $\bar{k}$ tend to increase. With inlet LVF further increasing to 8%, predicted $\bar{k}$ increases; however, measured $\bar{k}$ drops slightly at ω=15 and 10 krpm, and remains unchanged at ω=5 krpm. As ω increases, both measured and predicted $\bar{k}$ increase.

At PR=0.5, the impacts of changing inlet LVF and ω on predicted and measured $\bar{k}$ are similar to the cases at PR=0.6.

At PR=0.4, both predicted and measured $\bar{k}$ tend to increase as inlet LVF increases from 0 to 2%; however, as inlet LVF increases from 2 to 4%, prediction shows increments while measurements show drops. With inlet LVF further increasing to 8%, predicted $\bar{k}$ increases; however, measured $\bar{k}$ changes insignificantly. As ω increases, both measured and predicted $\bar{k}$ increase, except the case at inlet LVF=2% where predicted $\bar{k}$ increases with increasing ω, but measured $\bar{k}$ remains unchanged with increasing ω from 5 to 10 krpm, and only increases as ω further increases to 15 krpm.

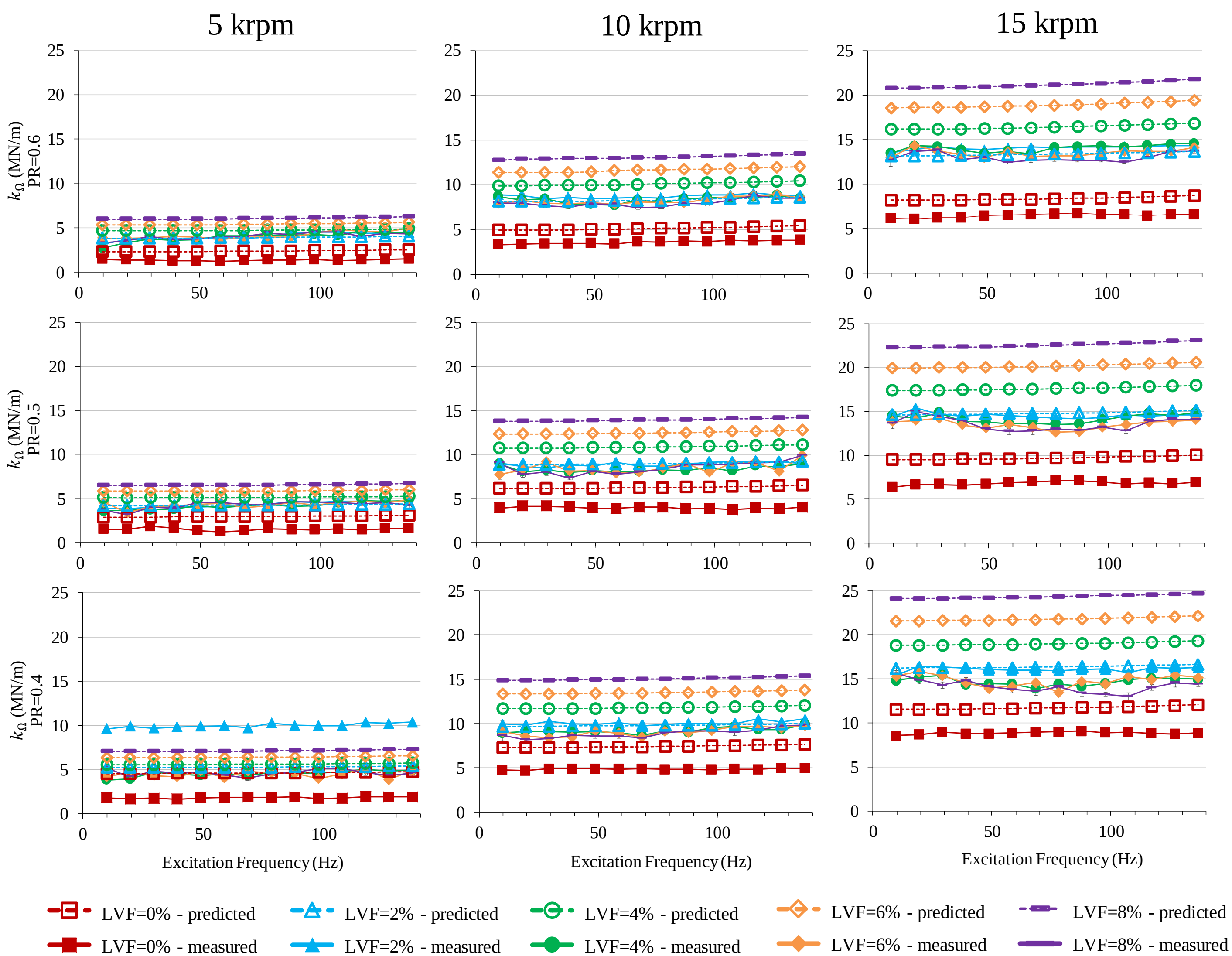

Figure 63 Predictions and measurements of k_Ω under pure- and mainly-air conditions for the zero-preswirl insert

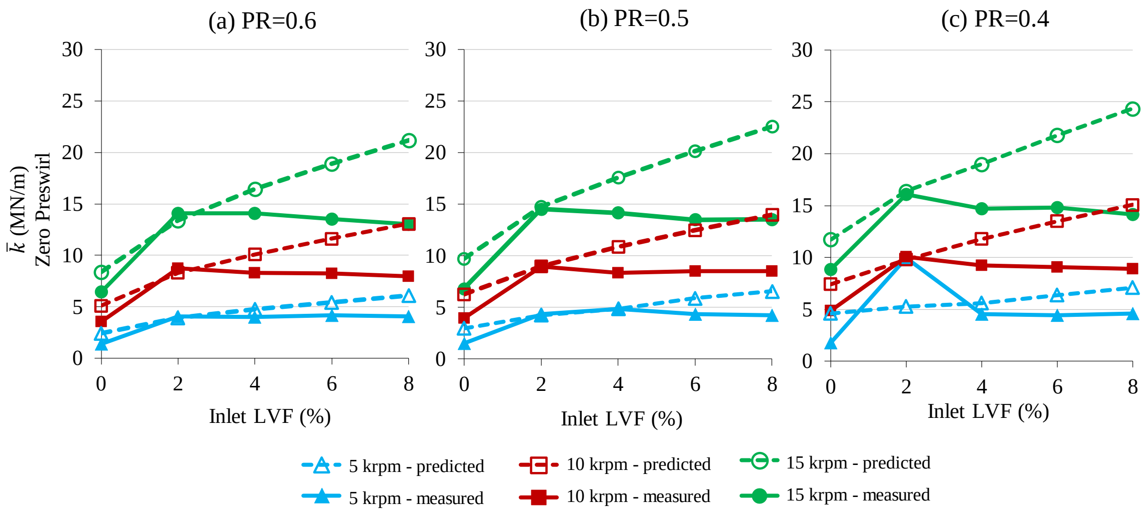

Figure 64 Predictions and measurements of $\bar{k}$ under pure- and mainly-air conditions for the zero-preswirl insert at: (a) PR=0.6, (b) PR=0.5, and (c) PR=0.4

In regard to the impact of decreasing PR, both predicted and measured $\bar{k}$ show little increase, except the case at inlet LVF=2% and ω=5 krpm when dropping PR from 0.5 to 0.4 where measured $\bar{k}$ increases significantly while predicted $\bar{k}$ remains unchanged.

8.5 Direct Damping Coefficient

Figure 65 compares measured and predicted *C* versus inlet LVF for three PR values and three speeds with the zero-preswirl insert.

At PR=0.6, with increasing inlet LVF, both predictions and measurements show increases; however, predicted *C* increases gradually, while measured *C* increases rapidly with increasing inlet LVF from 0 to 2% and then gradually increases as inlet LVF further increases. Concerning the impact of increasing ω, both predictions and measurements show insignificant change at inlet LVF=0% but slight increase at inlet LVF≥2%.

At PR=0.5, the impacts of changing inlet LVF on both predictions and measurements are similar to the cases at PR=0.6. With the impact of increasing ω, both predictions and measurements show insignificant change at inlet LVF=0%; however, at inlet LVF≥2%, even though both predicted and measured *C* tend to increase with increasing ω, the increment in measurements is larger than predicted.

At PR=0.4, regard to the impact of changing inlet LVF, predicted *C* tends to increase gradually; however, measured *C* increases rapidly with a change of inlet LVF from 0 to 2% and as inlet LVF further increases, measured *C* increases gradually for cases at ω=10 and 15 krpm, while dropping slightly before increasing again at ω=5 krpm. With increasing ω, predictions show insignificant changes, but measured *C* tends to increase as ω increases.

Prediction and measurement show a similar tendency of *C* as PR drops; i.e., there are moderate increases of *C* as PR drops from 0.6 to 0.4 (or PD increases from 24.8 to 37.3 bar).

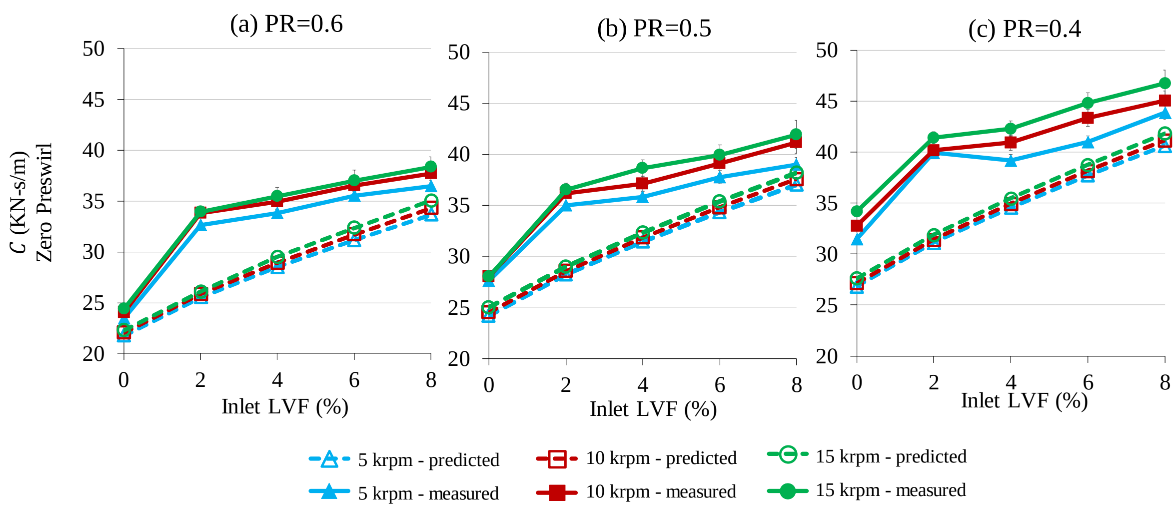

Figure 65 Predictions and measurements of *C* vs. inlet LVF LVF under pure- and mainly-air conditions for the zero-preswirl insert at: (a) PR=0.6, (b) PR=0.5, and (c) PR=0.4

8.6 Cross-Coupled Damping Coefficient

Figure 66 compares measured and predicted *c* versus inlet LVF over three PR values and three speeds with the zero-preswirl insert.

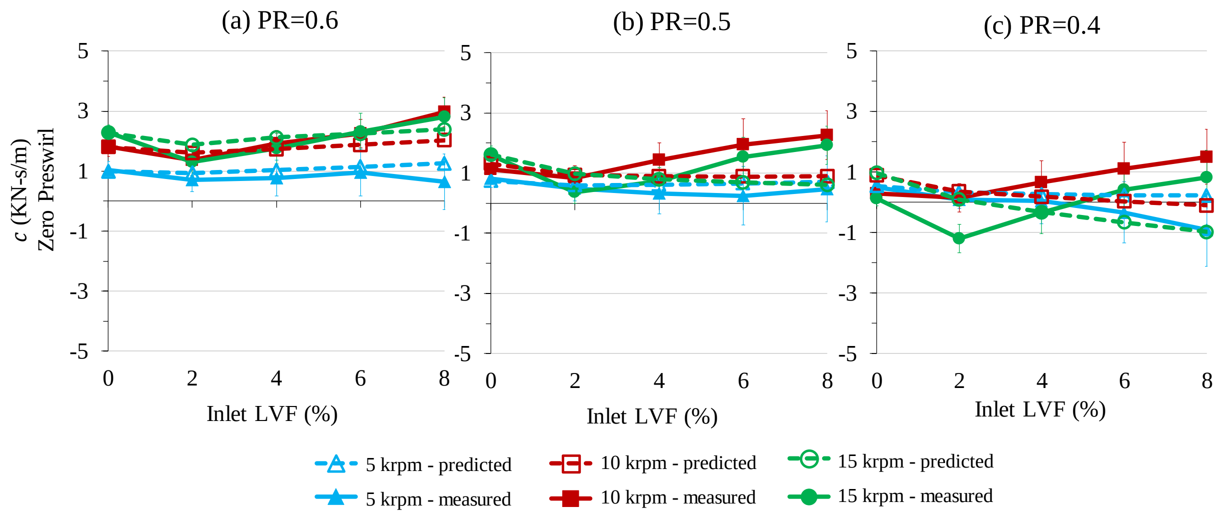

Figure 66 Predictions and measurements of *c* vs. inlet LVF under pure- and mainly-air conditions for the zero-preswirl insert at: (a) PR=0.6, (b) PR=0.5, and (c) PR=0.4

At PR=0.6 and ω=5 krpm, both predictions and measurements show minimum changes of *c* as inlet LVF increases from 0 to 8%. At ω=10 and 15 krpm, both predicted and measured *c* tend to drop slightly as inlet LVF increases from 0 to 2% and then increase as inlet LVF further increases to 8%. With increasing ω, predicted *c* increases, while measurements only show an increase of *c* as ω increases from 5 to 10 krpm. As ω further increases from 10 to 15 krpm, measured *c* changes insignificantly.

At PR=0.5 and ω=5 krpm, both predictions and measurements show a slight drop of *c* as inlet LVF increases from 0 to 8%. However, at ω=10 and 15 krpm, predicted *c* tends to drop as inlet LVF increases from 0 to 8%, but measured *c* drops, reaches a minimum value at inlet LVF=2% and then further increases as inlet LVF increases. Predicted *c* changes insignificantly as changing ω; however, as ω increases from 5 to 15 krpm, measured *c* is at a peak at ω=10 krpm.

At PR=0.4, the impacts of changing inlet LVF and ω on both predictions and measurements are similar to the cases at PR=0.5.

Both predictions and measurements show a drop of *c* as PR drops (or PD increases).

8.7 Effective Damping

Figure 67 compares measured and predicted Ω_c versus inlet LVF for three PR values and three ω values with the zero-preswirl insert.

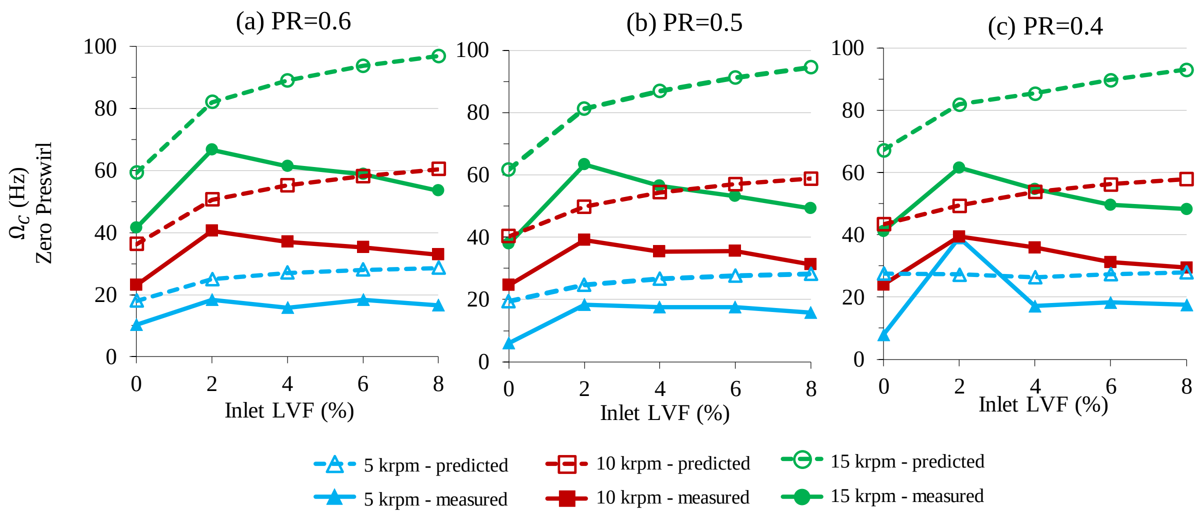

Figure 67 Predictions and measurements of Ω_C under pure- and mainly-air conditions for zero-preswirl insert at: (a) PR=0.6, (b) PR=0.5, and (c) PR=0.4

At PR=0.6, as inlet LVF increases from 0 to 2%, both predicted and measured Ω_c tend to increase. With a further increase in inlet LVF from 2 to 8%, at ω=5 krpm, both predictions and measurements show insignificant change of Ω_c; however, at ω=10 and 15 krpm, predicted Ω_c increases, while measured Ω_c tends to drop. As ω increases, measurements and predictions have the same tendency of increasing Ω_c.

At PR=0.5, the impacts of changing inlet LVF and ω on predicted and measured Ω_c are similar to the cases at PR=0.6.

At PR=0.4 and ω=10 and 15 krpm, as predicted, increasing inlet LVF increases Ω_c; however, measured Ω_c increases with increasing inlet LVF from 0 to 2%, but then decreases as inlet LVF further increases to 8%. At ω=5 krpm, predicted Ω_c remains unchanged, while measurements show a peak of Ω_c at inlet LVF=2% and a constant value of Ω_c at inlet LVF=4-8%. As ω increases, measurements and predictions both show increasing Ω_c, except the case at inlet LVF=2% where predicted Ω_c increases with increasing ω, but measured Ω_c remains unchanged with increasing ω from 5 to 10 krpm, and only increases as ω further increases to 15 krpm.

In regard to the impact of changing PR, both predicted and measured Ω_c show little or no change, except the case at inlet LVF=2% and ω=5 krpm with dropping PR from 0.5 to 0.4 where measured Ω_c increases significantly while predicted Ω_c remains unchanged.

Figure 68 compares predictions and measurements for the effect of inlet LVF on C_{eff} at PR=0.5 and ω=15 krpm for the frequency range 98 Hz – 137 Hz. Both predicted and measured C_{eff} are positive for all inlet LVFs, and tends to increase with increasing excitation frequency. Measured C_{eff} is significantly higher than predicted. As inlet LVF increases, predicted C_{eff} tends to drop (decreasing the stabilizing capability of the seal) and C_{eff} values at inlet LVF=2-8% converge at Ω=137 Hz. However, measured C_{eff} drops (decreasing the stabilizing capability of the seal) as inlet LVF increases from 0 to 2%, and then increases as inlet LVF further increases (increasing the stabilizing capability of the seal).

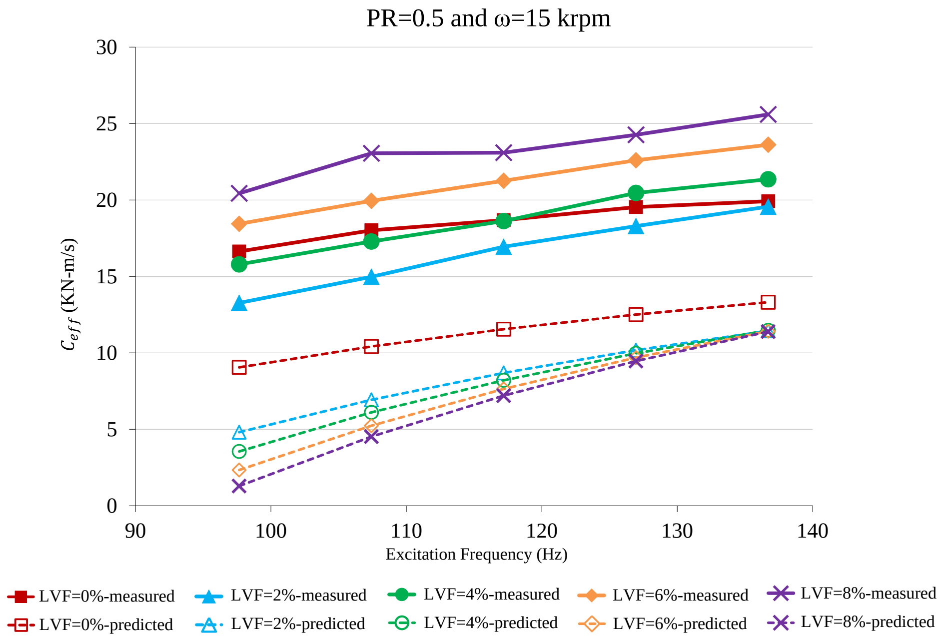

Figure 68 Predictions and measurements of C_{eff} at PR=0.5 and ω=15 krpm with the zero-preswirl insert for frequency range 98 Hz – 137 Hz

9. SUMMARY AND CONCLUSIONS

This thesis presents test results for rotordynamic coefficients and leakage of a long annular smooth seal (*L/D*=0.75, *D*=114.686 mm, and C_r=0.200 mm) tested with a mixture of silicone oil (PSF-5cSt) and air using the 2-phase annular-seal stand (2PASS) at the Texas A&M University Turbomachinery Laboratory. The impacts of changing PD/PR, ω, inlet GVF/LVF, and, mainly, inlet preswirl on the test seal's leakage mass flow $\dot{m}$ and rotordynamic coefficients are discussed. The test results are then compared with the bulk-flow-model prediction from *XLHseal_mix* developed by San Andrés [15].

Due to the difficulties in making 2-phase homogeneous mixtures with inlet GVF in a range of 10 to 92%, plus dynamic stability problems with the test-rig stator, the resultant test matrix covers two operation ranges: (1) pure- and mainly-oil conditions (inlet GVF≤10%) and (2) pure- and mainly-air conditions (inlet LVF≤8%). The following section summarizes the results for each operation range.

9.1 Pure- and Mainly-oil Conditions

The test seal is centered, the seal exit pressure is maintained at 6.89 bar-g while the fluid inlet temperature is controlled within 37.8-40.6°C. The test seal is tested with 3 inlet preswirl inserts (zero, medium, and high), 3 speeds (3, 4, and 5 krpm), 6 inlet GVFs (0%, 2%, 4%, 6%, 8%, and 10%), and 3 PDs (27.6, 34.5, and 41.4 bars) for the zero-preswirl insert, and 2 PDs (20.7 and 27.6 bars) for the medium- and high-preswirl inserts. The targeted test matrix was not completed for the medium- and high-preswirl inserts at PD≥27.6 bar due to the test-rig stator's instability.

Assuming that the effect of *Re* on flow status for mainly-oil conditions with inlet GVF≤10% is comparable to cases at pure-oil conditions; therefore, *Re* ranges of 1000 to 2600 are realized. According to Zirkelback and San Andrés [36], the flow for all testing cases is likely in a transitional state between laminar and turbulent flows.

9.1.1 Measurements vs. Predictions

The predicted and measured trends of $\dot{m}$ with changing inlet GVF do not agree. Predicted $\dot{m}$ decreases with increasing inlet GVF; however, measured $\dot{m}$ either remains unchanged or increases slightly. In regard to the impact of increasing PD, both predictions and measurements show an increasing $\dot{m}$. With an increasing ω, predicted and measured $\dot{m}$ slightly drop with the zero-preswirl insert, but change insignificantly with the medium- and high-preswirl inserts. Concerning changing inlet preswirl, both measurements and predictions show little change, but the tendencies are not the same. At PD=20.7 bar, changing inlet preswirl from medium to high slightly decreases measured $\dot{m}$, but predicted $\dot{m}$ remains unchanged. At PD=27.6 bar, when increasing inlet preswirl from zero to medium, predicted $\dot{m}$ tends to increase by 10%, while measured $\dot{m}$ remains unchanged. A further increase of inlet preswirl from medium to high at PD=27.6 bar decreases both measured and predicted $\dot{m}$.

Direct stiffness *K* contributes directly to the system's natural frequency. For all cases, predictions show a drop in *K* with increasing inlet GVF. However, with the zero-preswirl insert, increasing inlet GVF changes measured *K* insignificantly at PD=27.6 bar, but drops measured *K* at PD≥34.5 bar. For the medium- and high-preswirl insert, with increasing inlet GVF, measured *K* changes insignificantly at the cases of ω=3 and 4 krpm, PD=20.7 bar, but drops at the case of ω=5 krpm, PD=20.7 bar and the cases of PD=27.6 bar.

For the zero-preswirl insert, increasing PD does not change predicted *K* at inlet GVF=0%, but decreases predicted *K* at inlet GVF≥2%; however, measurements show mixed trends. Measured *K* increases significantly at inlet GVF=0%. At inlet GVF≥2%, measured *K* slightly increases when PD increases from 27.6 to 34.5 bar, but drops when PD further increases to 41.5 bar. For the medium-preswirl insert, at inlet GVF=0-4%, predictions generally show insignificant change of *K* as PD increases from 20.7 to 27.6 bar. However, as PD increases, at inlet GVF=0%, measured *K* tends to increase at ω=3 and 4 krpm, and drops at ω=5 krpm; while at inlet GVF≥2%, measured *K* tends to drop. For the high-preswirl insert, at inlet GVF=0%, increasing PD from 20.7 to 27.6 bar does not affect predicted *K*, but increases measured *K*. At inlet GVF≥2%, while measured *K* significantly drops as PD increases, predicted *K* remains unchanged at inlet GVF=2-4% and only slightly decreases at inlet GVF≥6%.

Concerning the impact of increasing ω on *K*, with the zero-preswirl insert, both measured and predicted *K* remain unchanged at PD=27.6 bar. At PD≥34.5 bar, while predicted *K* remains unchanged with increasing ω, measured *K* shows no changes when ω increases from 3 to 4 krpm, and drops with a further increase to 5 krpm. For the medium-preswirl insert, at PD=20.7 bar, increasing ω decreases predicted *K* steadily; but, measured *K* shows no change with increasing ω from 3 to 4 krpm, and decreases with a further increase of ω to 5 krpm. At PD=27.6 bar, both predictions and measurements show a decrease in *K* with increasing ω. For the high-preswirl insert, at both PD=20.7 and 27.6 bar, while predicted *K* steadily decreases with increasing ω, measured *K* shows an insignificant change with increasing ω from 3 to 4 krpm, and decreases with a further increase of ω to 5 krpm.

Regarding the impact of increasing inlet preswirl, at PD=20.7 bar, predicted *K* changes insignificantly with an increase of preswirl from medium to high, while the measurements show a slight drop. At PD=27.6 bar and inlet GVF=0%, increasing inlet preswirl from zero to medium decreases predicted *K*, but increases measured *K*. At PD=27.6 bar and inlet GVF=2-4%, in changing from the zero- to medium-preswirl inserts, measured *K* increases at ω=3 and 4 krpm and drops at ω=5 krpm, while predictions show a slight drop at all ω values. As inlet preswirl further increases from medium to high at PD=27.6 bar, predicted *K* slightly increases; however, measured *K* drops at ω=3 and 4 krpm, and increases at ω=5 krpm.

Cross-coupled stiffness *k* is a destabilizing rotordynamic component. Concerning the impact of increasing inlet GVF on *k*, in general, predicted *k* changes insignificantly; whereas, measured *k* increases. Both measurements and predictions show an increase of *k* with an increase of PD. Increasing ω steadily increases predicted *k*; however, measured *k* shows no change with increasing ω from 3 to 4 krpm, and increases with a further increase of ω from 4 to 5 krpm. Increasing inlet preswirl increases both predicted and measured *k*.

Direct damping *C* is a stabilizing rotordynamic component. Predictions show small increments of *C* as inlet GVF increases; whereas, measured *C* increases moderately. Increasing PD increases both measured and predicted *C*. Increasing ω increases predicted *C*. However, increasing ω from 3 to 4 krpm does not affect measured *C*, but a further increase of ω from 4 to 5 krpm increases measured *C*. When changing from the zero- to medium-preswirl insert (at PD=27.6 bar), predicted *C* remains unchanged. However, measured *C* drops at inlet GVF=0%; and at inlet GVF=2% and 4%, measured *C* remains unchanged at ω=4 kprm, slightly increases at ω=5 krpm, and slightly decreases at ω=3 krpm. Both measured and predicted *C* show an insignificant change with increasing inlet preswirl form medium to high (at PD=20.7 and 27.6 bar).

Whirl-frequency ratio (WFR) is used as a seal dynamic indicator. The lower the WFR, the better the seal's stabilizing properties. In general, predicted and measured WFR are close. Regarding the impact of increasing inlet GVF, both predictions and measurements show an insignificant change in WFR at inlet GVF=2-10% for the zero-preswirl insert and at inlet GVF=0-10% for the medium-preswirl insert. For the high-preswirl insert, as predicted, increasing inlet GVF drops WFR. However, with increasing inlet GVF, measurements show an insignificant change at PD=20.7 bar and a drop at PD=27.6 bar.

Regarding the impact of increasing PD on WFR, with the zero-preswirl insert, measurements show an insignificant change, while predictions show an increase at inlet GVF=0% and no change at inlet GVF≥2%. For the medium-preswirl insert, increasing PD from 20.7 to 27.6 bar increases both predicted and measured WFR. However, for the high-preswirl insert, predictions and measurements only agree well at inlet GVF=8% and 10% where there is an insignificant change of WFR with increasing PD.

For the zero-preswirl insert, at PD=27.6 bar, measured WFR drops as ω increases from 3 to 4 krpm and remains unchanged when increasing ω from 4 to 5 krpm; however, predicted WFR increases slightly with increasing ω. For the zero-preswirl insert, at PD=34.5 and 41.5 bar, predicted WFR changes insignificantly with increasing ω; but, measured WFR drops as ω increases from 3 to 4 krpm and remains unchanged with increasing ω from 4 to 5 krpm. For the medium- and high-preswirl insert, predicted and measured WFR show a drop with increasing ω. Concerning the impact of changing inlet preswirl, both measured and predicted WFR increase significantly (decreased stability) in changing from zero- to medium-preswirl insert or from medium- to high-preswirl insert.

Effective damping C_{eff} combines the effects of C and k on stability. Increasing C_{eff} increases stability. In general, as inlet GVF increases, measurements show a larger increase of C_{eff} than predicted. Concerning the impact of increasing ω, with the zero-preswirl insert, predictions show no change in C_{eff}, while measured C_{eff} shows an increase when increasing ω from 3 to 4 krpm, then no change when ω further increases to 5 krpm. For the medium- and high-preswirl inserts, both predicted and measured C_{eff} increase as ω increases. Regarding the impact of changing PD, for the zero-preswirl insert, predicted and measured C_{eff} increase with increasing PD. For the medium- and high-preswirl inserts, at inlet GVF≥2%, both predictions and measurements show an increase in C_{eff} when PD increases. Concerning the impact of changing inlet preswirl, both measured and predicted C_{eff} drop (decreased stability) in changing from the zero- to medium-preswirl insert or from the medium- to high-preswirl insert.

Recently, Zhang [21] presented measurements and predictions for a smooth seal (L/D=0.65, D=88.9 mm) with a range of radial clearances using a mixture of gas and liquid. The test results under pure- and mainly-oil conditions presented here, agree much better with predictions than from Zhang's results [21].

9.1.2 Conclusions for Mainly-Oil Results

Measurements and predictions under pure- and mainly-oil conditions lead to the following major conclusions:

(1) With the zero-preswirl insert, at the highest tested PD (41.4 bar), both predictions and measurements show a significant drop in K as a result of injecting air into the oil flow. This drop might be explained due to an increase of friction factor with increasing Re in the transitional flow regime. With the medium and high-preswirl insert, at the highest tested PD (27.6 bar), increasing inlet GVF also drops both

measured and predicted *K*, but the drop in measurements is more significant than predicted. However, this drop at the medium- and high-preswirl inserts is unlikely to be explained by a transition between laminar and turbulent flows because nominally the Reynolds number range is covered as with the radial-flow insert. The drop in *K* would drop the stator natural frequency and could cause the stator to become unstable at higher inlet GVF testing conditions with the medium- and high-preswirl inserts.

(2) With limited measurements performed on the medium-preswirl insert due to the test-rig's instability, no conclusion can be made concerning the impact of changing inlet preswirl from zero to medium on *K*. However, in increasing inlet preswirl from medium to high, both predictions and measurements show an insignificant effect on *K*.

(3) Increasing inlet GVF does not affect predicted *k*; whereas, measured *k* increases with increasing inlet GVF. As expected, increasing inlet preswirl increases both predicted and measured *k*. Increasing *k* increases the destabilizing force and could cause instability.

(4) Interestingly, injecting air shows a small increment in predicted *C*, but a moderate increase in measured *C*. Increasing *C* would help to improve stability. With increasing inlet preswirl from zero to medium, predicted *C* remains unchanged; but no conclusion can be made from limited measurement results due to the test-rig's instability. Both measured and predicted *C* show insignificant changes with increasing inlet preswirl from medium to high.

(5) As shown in both measurements and predictions, injecting air into the oil flow slightly increases C_{eff} and slightly decreases WFR, improving the seal's stabilizing

properties. For both predicted and measured, increasing inlet preswirl significantly increases WFR and decreases C_{eff}, decreasing the seal's stabilizing properties.

The results obtained from *K* and *k* potentially relate to the instability issue on the high-differential-pressure helico-axial multiphase pump, reported by Bibet et al. [3]. The pump was designed to operate at a 150-bar differential pressure, running at 4600 rpm with multiphase fluid with 30% GVF. The authors reported subsynchronous vibration with multiphase flows and for relatively low differential pressures when operating at a higher viscosity fluid. In cases of subsynchronous vibration, the balance-piston rotordynamic simulation showed that the whirl frequency ratio was greater than 1, and the damping ratio was negative. They concluded that the destabilizing force happened at the balance-piston seal. Introducing a higher viscosity fluid and running at a relatively low differential pressures might cause a transitional flow in the balance-piston seal. The flow in the transitional regime reverses the Lomakin effect and reduces *K* drastically under 2-phase flow, as seen from the test result of *K* shown in Fig. 36 for the zero-preswirl insert at PD=41.5 bar. A drop in *K* could decrease the rotor's critical speed, reduce the onset speed of instability and cause dynamic instability.

Additionally, as seen from the results of *k*, shown in Fig. 37, at PD=27.6 bar, for the medium preswirl case, *k* increases rapidly with increasing inlet GVF at ω=5 krpm, significantly more rapidly than at ω=4 krpm. A similar result holds at high preswirl. However, for the zero-preswirl insert, *k* values are smaller and increase slowly with increasing GVF. *k* also increases moderately with increasing PD for the medium- and high-preswirl insert. In Bibet et al. [3], the variation of speed (from 1.5 to 4.6 krpm), inlet GVF and PD might cause *k* to increase significantly and cause instability.

9.2 Pure- and Mainly-air Conditions

Under pure- and mainly-air conditions, due to the rig-stator's dynamic instability, tests were only conducted for the zero-preswirl insert. The test seal is centered, and inlet pressure is maintained at 62.1 bar-g. The supplied oil temperature is maintained within 35 to 37.8^{o}C. The seal is tested with 3 PRs (0.6, 0.5, and 0.4 - corresponding to PD of 24.8, 31.1 and 37.3 bar), 3 speeds (5, 10, and 15 krpm), and 5 inlet LVFs (0%, 2%, 4%, 6%, and 8%).

Measurements show inlet and exit *Re* in ranges of 3,500 to 71,000 and 5,000 to 71,000, respectively; therefore, according to Zirkelback and San Andrés [36], the flow is in the turbulent regime. Maximum *Ma* number, found at the seal exit, under pure-air conditions with the zero-preswirl insert is in a range of 0.4 to 0.75. Hence, no choking occurs.

9.2.1 Measurements vs. Predictions

Measured and predicted $\dot{m}$ increase as inlet LVF increases from 2 to 8%. Increasing inlet LVF from 0 to 2% decreases measured $\dot{m}$, while predicted $\dot{m}$ show a small drop at PR=0.6 and no change at PR=0.5 and 0.4. In regard to the impact of increasing ω from 5 to 15 krpm, both predicted and measured $\dot{m}$ drop slightly. Predicted and measured $\dot{m}$ increase when dropping PR from 0.6 to 0.4.

Due to the presence of liquid in mainly-air conditions, measured frequency-dependent behavior forced the use of frequency-dependent direct K_Ω and cross-coupled k_Ω dynamic stiffness coefficients. On the other hand, the imaginary components of the dynamic-stiffness coefficients could be fitted with frequency-independent direct *C* and cross-coupled *c* damping coefficients.

K_Ω provides the seal's centering forces on the rotor and affects the system's natural frequency. With increasing inlet LVF, predicted K_Ω drops at PR=0.6 and 0.5 (while measured K_Ω is minimum at inlet LVF=2%), and increases at PR=0.4 (while measured K_Ω remains unchanged). Predicted K_Ω changes insignificantly as ω increases. However, measurements show an insignificant or small increase for cases at inlet LVF≤4%, and a significant increase for cases at inlet LVF≥6%. At inlet LVF=0%, measured K_Ω drops as PR decreases, while predictions only show a drop as PR drops from 0.5 to 0.4. At inlet LVF≥2%, both predictions and measurements show a slight increase of K_Ω as PR drops from 0.6 to 0.5 and a decrease as PR drops further to 0.4.

k_Ω has a direct adverse contribution to a system's rotordynamic stability. There is largely negligible frequency dependency of k_Ω; therefore, $\bar{k}$, an average value of k_Ω over the range of Ω, accounts for the test seal's cross-coupled stiffness. Predicted $\bar{k}$ tends to increase steadily as inlet LVF increases. Measured $\bar{k}$ increases with increasing inlet LVF from 0 to 2%, but then either drops or remains unchanged with a further increase in inlet LVF. As ω increases, both measured and predicted $\bar{k}$ increase. Predicted and measured $\bar{k}$ show little or no change when PR drops, except at inlet LVF=2% and ω=5 krpm when dropping PR from 0.5 to 0.4. In this circumstance, measured $\bar{k}$ increases significantly while predicted $\bar{k}$ remains unchanged.

Increasing inlet LVF increases both measured and predicted *C*. However, predicted *C* increases gradually, while measured *C* increases rapidly with increasing inlet LVF from 0 to 2% and then gradually increases as inlet LVF further increases. With increasing ω, predictions show insignificant increases. However, measured *C* increases as ω increases, except at inlet LVF=0% and PR=0.5 and 0.6 where measured *C* does not change with changing speed. Both predictions and measurements show an increase in *C* as PR drops.

C_{eff} combines the destabilizing effect of k_Ω and the stabilizing effect of *C*. At low Ω, k_Ω dominates, and C_{eff} is negative (destabilizing). At high Ω, *C* dominates, and C_{eff} is positive (stabilizing). Cross-over frequency Ω_c is defined as the Ω value where C_{eff} changes from negative to positive, and the lower Ω_c, the better the system stability. With increasing inlet LVF, predicted Ω_c tends to increase considerably at ω=10 and 15 krpm, and little or insignificantly at ω=5 krpm. However, measurements show an increase in Ω_c with increasing inlet LVF from 0 to 2%, and a decrease or no change as inlet LVF further increases to 8%. Increasing ω increases both measured and predicted Ω_c. Predicted and measured Ω_c show little or no change with decreasing PR, except at LVF=2% and ω=5 krpm when dropping PR from 0.5 to 0.4. In this circumstance, measured Ω_c increases significantly while predicted Ω_c remains unchanged.

At PR=0.5 and ω=15 krpm (representative operating conditions for a compressor balance-piston seal), the exciting frequency range 98 Hz – 137 Hz (about 0.5ω) is chosen to examine the effect of changing inlet LVF on C_{eff}. Both predicted and measured C_{eff} are positive for all inlet LVF conditions, and tends to increase with increasing excitation frequency. Measured C_{eff} is significantly higher than predicted. As inlet LVF increases, predicted C_{eff} values tend to drop (decreasing the seal's stabilizing capability). However, measured C_{eff} drops (decreasing the seal's stabilizing capability) as inlet LVF increases from 0 to 2%, and then increases (increasing the seal's stabilizing capability) as inlet LVF further increases to 8%.

9.2.2 Conclusions for Mainly-Air Results

Measurements and predictions under pure- and mainly-air conditions lead to the following major conclusions:

(1) The seal's centering force is proportional to dynamic stiffness coefficient K_Ω. In general, as oil is injected into the air flow (inlet LVF increases from 0 to 8%), measurements show an increasing trend of K_Ω for PR=0.4 and a minimum K_Ω at inlet LVF=2% for PR=0.6 and 0.5. However, predictions show no change at PR=0.4 and a drop at PR=0.5 and 0.6. Decreasing the seal's centering force would decrease the

rotor's critical speed, reduce the onset speed of instability, and decrease the rotor's stability.

(2) Injecting a small amount of oil into the air flow (inlet LVF increases from 0 to 2%) increases Ω_c, decreasing the seal's stabilizing properties. However, as more oil is injected (inlet LVF increases from 2 to 8%), measurements and predictions do not agree; specifically, measured Ω_c decreases (stabilizing), while predicted Ω_c increases (destabilizing).

With representative operating conditions for a compressor balance-piston seal (PR=0.5, ω=15 krpm, and the exciting frequency range 98 Hz – 137 Hz), measured C_{eff} is significantly higher than predicted. As inlet LVF increases, predictions show a drop of the seal's stabilizing capacity (predicted C_{eff} decreased). However, measurements show the lowest stabilizing point (with the lowest measured C_{eff}) is at inlet LVF=2%.

Smooth seals are not used in centrifugal compressors. The data presented here are mainly for examining the correctness of the predictive model developed by San Andrés [15], and they are also a starting point to study impacts of mainly-gas conditions on compressors' annular seals. Shrestha [42] has recently reported test results for tooth-on-stator labyrinth seals. Future testing, under mainly-gas conditions, could consider different seal types, such as, hole-pattern seals and pocket damper seals which are used widely in compressors.

REFERENCES

[1] Gong, H., Falcone, G., Teodoriu, C., and Morrison, G. L., 2012, "Comparison of Multiphase Pumping Technologies for Subsea and Downhole Applications," *Oil and Gas Facilities*, **1**(1), pp. 36-46.

[2] Dal Porto, D. F., and Larson, L. A., 1997, "Multiphase-Pump Field Trials Demonstrate Practical Applications for the Technology, " SPE-36590-PA. *SPE Prod. & Oper.*, **12**(3), pp. 159-164.

[3] Bibet, P. J., Klepsvik, K. H., Lumpkin, V. A., and Grimstad, H., 2013, "Design and Verification Testing of a New Balance Piston for High Boost Multiphase Pumps," *Proc. 29th International Pump User Symposium*, Houston, TX.

[4] San Andrés, L., 2010, "Notes 12(a). Annular Pressure Seals," Modern Lubrication Theory, Texas A&M University Digital Libraries.

[5] Childs, D., 2013, *Turbomachinery Rotordynamics with Case Studies*, Minter Spring Publishing, Wellborn, Texas.

[6] Childs, D., 1993, *Turbomachinery Rotordynamics: Phenomena, Modeling, and Analysis*, Wiley Publishing, New York.

[7] Brenne, L., Bjørge, T., Gilarranz, J. L., Koch, J., and Miller, H., 2005, "Performance Evaluation of a Centrifugal Compressor Operating under Wet-Gas Conditions," *Proc. 34th Turbomachinery Symposium*, Houston, TX.

[8] Griffin, T., and Maier, W., 2011, "Demonstration of the Rotordynamic Effects of Centrifugal Liquid Separation and Gas Compression in an Oil-Free Integrated Motor-Compressor," *Proc. 40th Turbomachinery Symposium*, Houston, TX.

[9] Bertoneri, M., Wilcox, M., Toni, L., and Beck, G., 2014, "Development of Test Stand for Measuring Aerodynamic, Erosion, and Rotordynamic Performance of a Centrifugal Compressor Under Wet Gas Conditions," *Proc. ASME Turbo Expo 2014*, American Society of Mechanical Engineers, Düsseldorf, Germany.

[10] Ransom, D., Podesta, L., Camatti, M., Wilcox, M., Bertoneri, M., and Bigi, M., 2011, "Mechanical Performance of a Two Stage Centrifugal Compressor under Wet Gas Conditions," *Proc. 40th Turbomachinery Symposium*, Houston, TX.

[11] Vannini, G., Bertoneri, M., Del Vescovo, G., and Wilcox, M., 2014, "Centrifugal Compressor Rotordynamics in Wet Gas Conditions," *Proc. 43rd Turbomachinery Symposium*, Houston, TX.

[12] Vannini, G., Bertoneri, M., Nielsen, K. K., Iudiciani, P., and Stronach, R., 2015, "Experimental Results and CFD Simulations of Labyrinth and Pocket Damper Seals for Wet Gas Compression," *Proc. ASME Turbo Expo 2015*, American Society of Mechanical Engineers, Montreal, Quebec, Canada.

[13] Iwatsubo, T., and Nishino, T., 1994, "An Experimental Study on the Static and Dynamic Characteristics of Pump Annular Seals with Two Phase Flow," *Proc. Rotordynamic Instability Problems in High-Performance Turbomachinery*, pp. 49-64.

[14] San Andrés, L., Lu, X., and Liu, Q., 2015, "Measurements of Flowrate and Force Coefficients in a Short Length Annular Seal Supplied with a Liquid/Gas Mixture (Stationary Journal)," *Tribol. Trans.*, **59**(4), pp. 758-767.

[15] San Andrés, L., 2011, "Rotordynamic Force Coefficients of Bubbly Mixture Annular Pressure Seals," *J. Eng. Gas Turbines Power*, **134**(2), pp. 022503-022503-8.

[16] Voigt, A. J., Mandrum-Polsen, C., Nielsen, K. K., and Santos, I. F., 2016, "Design and Calibration of a Full Scale Active Magnetic Bearing Based Test Facility for Investigating Rotordynamic Properties of Turbomachinery Seals in Multiphase Flow," *Proc. ASME Turbo Expo 2016*, American Society of Mechanical Engineers, Seoul, South Korea.

[17] Voigt, A. J., Iudiciani, P., Nielsen, K. K., and Santos, I. F., 2016, "CFD Applied for the Identification of Stiffness and Damping Properties for Smooth Annular Turbomachinery Seals in Multiphase Flow," *Proc. ASME Turbo Expo 2016*, American Society of Mechanical Engineers, Seoul, South Korea.

[18] San Andrés, L., and Lu, X., 2017, "Leakage, Drag Power and Rotordynamic Force Coefficients of an Air in Oil (Wet) Annular Seal," *Proc. ASME Turbo Expo 2017*, American Society of Mechanical Engineers, Charlotte, NC, USA.

[19] Zhang, M., McLean, J., and Childs, D. W., 2017, "Experimental Study of the Static and Dynamic Characteristics of a Long Smooth Seal with Two-Phase, Mainly-air Mixtures," *J. Eng. Gas Turbines Power*, **139**(12), pp. 122504-122504-11.

[20] Arghir, M., Zerarka, A., and Pineau, G., 2011, "Rotordynamic Analysis of Textured Annular Seals With Multiphase (Bubbly) Flow," *Incas Bulletin*, **3**(3), pp. 3-13.

[21] Zhang, M., 2017, "Experimental Study of the Static and Dynamic Characteristics of a Long (L/D=0.65) Smooth Annular Seal Operating under Two-Phase (Liquid/Gas) Conditions," Ph.D. Thesis, Texas A&M University, College Station, TX.

[22] Childs, D., and Hale, K., 1994, "A Test Apparatus and Facility to Identify the Rotordynamic Coefficients of High-Speed Hydrostatic Bearings," *ASME Journal of Tribology*, **116**(2), pp. 337-344.

[23] Dawson, P. D., Childs, D. W., Holt, C. G., and Phillips, S. G., 2002, "Measurement Versus Predictions for the Dynamic Impedance of Annular Gas Seals: Part 1 – Test Facility and Apparatus," *J. Eng. Gas Turbines Power*, **124**(4), pp. 958-962.

[24] 2009, "Porous Injector Sizing," http://www.inyoprocess.com/images/Porous_inj/porous_sparger_sizing.pdf [Access Aug. 6,2017].

[25] "PSF-5cSt Pure Silicone Fluid," http://www.clearcoproducts.com/pdf/low-viscosity/NP-PSF-5cSt.pdf [Access Aug. 6,2017].

[26] Picardo, A., and Childs, D. W., 2004, "Rotordynamic Coefficients for a Tooth-on-Stator Labyrinth Seal at 70 Bar Supply Pressures: Measurements Versus Theory and Comparisons to a Hole-Pattern Stator Seal," *J. Eng. Gas Turbines Power*, **127**(4), pp. 843-855.

[27] Mehta, N., and Childs, D., 2013, "Measured Comparison of Leakage and Rotordynamic Characteristics for a Slanted-Tooth and a Straight-Tooth Labyrinth Seal," *J. Eng. Gas Turbines Power*, **136**(1), pp. 012501-012501-11.

[28] Kurtin, K. A., Childs, D., San Andrés, L., and Hale, K., 1993, "Experimental Versus Theoretical Characteristics of a High-Speed Hybrid (Combination Hydrostatic and Hydrodynamic) Bearing," *J. Tribol.*, **115**(1), pp. 160-168.

[29] "Low Viscosity Pure Silicone Fluids," http://www.clearcoproducts.com/pure-silicone-low-viscosity.html [Access Aug. 6,2017].

[30] Tao, L., Diaz, S., San Andrés, L., and Rajagopal, K. R., 1999, "Analysis of Squeeze Film Dampers Operating with Bubbly Lubricants," *J. Tribol.*, **122**(1), pp. 205-210.

[31] Diaz, S., 1999, "The Effect of Air Entrapment on the Performance of Squeeze Film Dampers: Experiments and Analysis," Ph.D. Thesis, Texas A&M University, College Station, TX.

[32] Fourar, M., and Bories, S., 1995, "Experimental Study of Air-Water Two-Phase Flow through a Fracture (Narrow Channel)," *Int. J. Multiphase Flow*, **21**(4), pp. 621-637.

[33] Stanway, R., Burrows, C., and Holmes, R., 1979, "Pseudo-Random Binary Sequence Forcing in Journal and Squeeze-Film Bearings," *ASLE Transactions*, **22**(4), pp. 315-322.

[34] Jolly, P., Hassini, A., Arghir, M., and Bonneau, O., "Experimental and Theoretical Rotordynamic Coefficients of Smooth and Round-Hole Pattern Water Fed Annular Seals," *Proc. ASME Turbo Expo 2014*, American Society of Mechanical Engineers, Düsseldorf, Germany.

[35] Iwatsubo, T., Sheng, B. C., and Matsumoto, T., 1988, "An Experimental Study on the Static and Dynamic Characteristics of Pump Annular Seals," NASA Conf. Pub. 3026, pp.229-252.

[36] Zirkelback, N., and San Andrés, L., 1996, "Bulk-Flow Model for the Transition to Turbulence Regime in Annular Pressure Seals," *Tribol. Trans.*, **39**(4), pp. 835-842.

[37] San Andrés, L. A., 1991, "Effects of Eccentricity on the Forced Response of a Hybrid Bearing," *Tribology Transactions*, **34**(4), pp. 537–544.

[38] Lund, J., 1966, "Self-Excited, Stationary Whirl Orbits of a Journal in a Sleeve Bearing," Ph.D. Thesis, Rensselaer Polytechnic Institute, Troy, NY.

[39] Delgado-Marquez, A., 2008, "A Linear Fluid Inertia Model for Improved Prediction of Force Coefficients in Grooved Squeeze Film Dampers and Grooved Oil Seal Rings," Ph.D Thesis, Texas A&M University.

[40] Childs, D. W., Rodriguez, L. E., Cullotta, V., Al-Ghasem, A., and Graviss, M., 2005, "Rotordynamic-Coefficients and Static (Equilibrium Loci and Leakage) Characteristics for Short, Laminar-Flow Annular Seals," *J. Tribol.*, **128**(2), pp. 378-387.

[41] Kerr, B., 2004, "Experimental and Theoretical Rotordynamic Coefficients and Leakage of Straight Smooth Annular Gas Seals," Master Thesis, Texas A&M University, College Station, TX.

[42] Shrestha, H., 2017, "Experimental Study of the Static and Dynamic Characteristics of a Long (L/D=0.75) Labyrinth Annular Seal Operating under Two-Phase (Liquid/Gas) Conditions," Master Thesis, Texas A&M University, College Station, TX.

APPENDIX A. WHIRL-FREQUENCY RATIO DEFINITION

The WFR (Φ) as formulated by San Andrés [37] which accounts for cross-coupled virtual-mass is defined as

$$\Phi^4 I_4 + \Phi^2 (I_2 - 1) + \Phi_o^2 = 0 \tag{41}$$

where I_2 and I_4 in Eq. (41) are

$$I_4 = \omega^2 \frac{I_1^2 + M_{XY} M_{YX}}{C_{XX} C_{YY} - C_{XY} C_{YX}} \tag{42}$$

$$I_2 = \frac{K_{XY} M_{YX} + K_{YX} M_{XY} - I_1 (K_{XX} + K_{YY}) + 2 K_{XY} I_1}{C_{XX} C_{YY} - C_{XY} C_{YX}} \tag{43}$$

and where I_1 in Eqs. (42) and (43) is

$$I_1 = \frac{C_{YX} M_{XY} + C_{XY} M_{YX}}{C_{XX} + C_{YY}} \tag{44}$$

and where Φ_o in Eq. (41) is

$$\Phi_o^2 = \frac{(K_{eq} - K_{XX})(K_{eq} - K_{YY}) - K_{XY} K_{YX}}{\omega^2 (C_{XX} C_{YY} - C_{XY} C_{YX})} \tag{45}$$

where K_{eq} in Eq. (42) is

$$K_{eq} = \frac{K_{XX} C_{YY} + K_{YY} C_{XX} - K_{XY} C_{YX} - K_{YX} C_{XY}}{C_{XX} + C_{YY}} \tag{46}$$

Table 11 Measured inlet and exit temperatures for pure- and mainly-oil cases

Inlet Preswirl Insert	PD (bar)	Inlet GVF (%)	3 krpm		4 krpm		5 krpm	
			T_i (ºC)	T_e (ºC)	T_i (ºC)	T_e (ºC)	T_i (ºC)	T_e (ºC)
Zero-Preswirl	27.6	0	38.2	38.6	39.1	39.6	38.1	39.0
		2	38.4	39.0	38.6	39.4	39.1	40.5
		4	38.2	38.8	39.1	39.6	38.5	39.4
		6	38.8	39.5	38.8	39.2	38.5	39.2
		8	39.7	40.5	38.9	39.6	38.5	39.4
		10	38.9	39.6	38.6	39.1	39.7	40.7
	34.5	0	38.0	38.4	37.9	38.5	37.8	38.8
		2	38.5	39.2	39.5	40.4	39.5	40.8
		4	38.0	38.5	37.7	38.5	38.3	39.6
		6	39.0	39.8	38.3	38.9	38.3	39.7
		8	38.7	39.8	38.6	39.8	38.1	39.7
		10	38.4	39.4	39.3	40.4	39.0	40.4
	41.4	0	38.4	39.2	38.3	38.9	38.0	39.3
		2	37.7	38.9	38.1	39.1	37.7	39.3
		4	39.7	41.4	39.0	40.3	38.6	40.2
		6	38.1	39.3	38.6	40.0	39.0	40.9
		8	39.0	40.6	38.2	39.4	39.1	40.9
		10	38.2	39.5	39.7	41.2	39.5	41.4
Medium-Preswirl	20.7	0	38.4	39.4	37.7	38.6	38.6	39.8
		2	38.6	39.6	38.0	38.9	38.0	39.2
		4	38.7	39.7	38.2	39.3	38.3	39.5
		6	38.0	39.1	38.2	39.3	38.4	39.7
		8	39.2	40.2	38.1	39.1	38.2	39.5
		10	38.6	39.6	38.9	40.0	39.1	40.3
	27.6	0	38.7	40.1	38.9	40.1	38.5	40.0
		2	38.5	39.8	38.5	39.6	37.6	38.9
		4	37.6	38.9	38.0	39.2	-	-
High-Preswirl	20.7	0	38.5	38.8	38.7	39.0	38.6	38.9
		2	38.3	38.4	39.7	40.4	38.3	39.0
		4	38.2	38.2	38.6	38.8	38.5	38.9
		6	38.5	38.4	38.5	38.9	39.0	40.5
		8	38.6	38.6	38.9	38.6	38.7	39.3
		10	38.5	38.9	38.7	39.3	38.3	38.5
	27.6	0	38.0	38.4	38.6	38.8	38.1	38.5
		2	37.9	38.3	38.7	39.0	38.7	39.2
		4	38.5	39.2	38.3	38.5	38.6	39.6
		6	38.1	38.7	38.7	39.4	-	-
		8	38.7	39.4	38.9	39.5	-	-
		10	38.8	39.4	-	-	-	-

Table 12 Measured inlet and exit temperatures for pure- and mainly-air cases

Inlet Preswirl Insert	PR	Inlet LVF (%)	5 krpm		10 krpm		15 krpm	
			T_i (ºC)	T_e (ºC)	T_i (ºC)	T_e (ºC)	T_i (ºC)	T_e (ºC)
Zero-Preswirl	0.6	0	14.7	10.2	15.9	12.7	18.5	18.0
		2	22.6	19.1	21.0	19.4	22.3	23.6
		4	27.3	24.8	26.5	25.5	20.6	22.3
		6	24.0	22.2	24.8	24.1	25.9	27.4
		8	24.4	23.3	28.4	28.2	29.3	31.0
	0.5	0	9.7	3.6	13.0	8.8	15.8	14.0
		2	22.0	17.8	22.8	20.2	23.6	24.4
		4	27.6	24.7	28.0	26.4	21.8	22.8
		6	25.1	23.1	25.4	24.1	26.5	27.8
		8	29.3	27.9	24.8	24.0	25.7	27.2
	0.4	0	18.2	11.5	19.4	14.4	12.3	9.5
		2	20.3	17.3	19.6	16.7	21.4	21.8
		4	25.6	22.9	26.6	24.6	27.2	28.1
		6	28.9	27.5	24.4	23.2	24.5	25.9
		8	26.6	25.6	27.1	26.5	30.8	32.4

Table 13 Measured preswirl ratios and uncertainties under pure- and mainly-oil conditions

Pressure Drop (PD)	Inlet GVF (%)	Zero Preswirl						Medium Preswirl						High Preswirl					
		3 krpm		4 krpm		5 krpm		3 krpm		4 krpm		5 krpm		3 krpm		4 krpm		5 krpm	
		U_o	δU_o	U_o	δU_o	U_o	δU_o	U_o	δU_o	U_o	δU_o	U_o	δU_o	U_o	δU_o	U_o	δU_o	U_o	δU_o
20.7 bar	0							0.504	0.002	0.374	0.002	0.321	0.001	1.104	0.001	0.830	0.001	0.654	0.001
	2							0.511	0.002	0.383	0.002	0.326	0.001	1.139	0.001	0.856	0.001	0.676	0.001
	4	-						0.525	0.002	0.394	0.002	0.334	0.001	1.143	0.001	0.852	0.001	0.677	0.001
	6							0.536	0.002	0.400	0.002	0.336	0.001	1.186	0.001	0.900	0.001	0.704	0.001
	8							0.551	0.002	0.411	0.002	0.343	0.001	1.188	0.001	0.888	0.001	0.708	0.001
	10							0.545	0.002	0.414	0.002	0.350	0.001	1.205	0.001	0.922	0.001	0.723	0.001
27.6 bar	0	0.151	0.007	0.113	0.005	0.114	0.003	0.639	0.002	0.481	0.001	0.387	0.001	1.358	0.001	1.019	0.001	0.815	0.000
	2	0.149	0.008	0.114	0.006	0.114	0.004	0.662	0.002	0.499	0.001	0.401	0.001	1.373	0.001	1.029	0.001	0.823	0.000
	4	0.150	0.008	0.115	0.006	0.114	0.004	0.667	0.002	0.499	0.001			1.386	0.001	1.038	0.001	0.833	0.001
	6	0.152	0.008	0.113	0.006	0.114	0.004							1.399	0.001	1.049	0.001		
	8	0.150	0.008	0.114	0.006	0.116	0.004							1.417	0.001	1.060	0.001		
	10	0.156	0.008	0.117	0.006	0.114	0.004							1.429	0.001				
34.5 bar	0	0.155	0.007	0.112	0.006	0.111	0.004												
	2	0.157	0.007	0.122	0.005	0.110	0.004												
	4	0.168	0.007	0.125	0.005	0.114	0.004												
	6	0.173	0.007	0.126	0.005	0.114	0.004												
	8	0.172	0.007	0.129	0.005	0.114	0.004												
	10	0.174	0.007	0.126	0.005	0.115	0.004						-						
41.4 bar	0	0.166	0.007	0.127	0.005	0.107	0.004												
	2	0.176	0.006	0.125	0.005	0.110	0.004												
	4	0.170	0.007	0.130	0.005	0.112	0.004												
	6	0.174	0.007	0.128	0.005	0.112	0.004												
	8	0.178	0.007	0.132	0.005	0.116	0.004												
	10	0.179	0.007	0.135	0.005	0.116	0.004												

Note: U_o - Preswirl ratio**, δU_o** - Uncertainty of preswirl ratio measurement

Table 14 Measured preswirl ratios and uncertainties under pure- and mainly-air conditions with the zero-preswirl insert

PR	Speed (krpm)	Inlet LVF (%)									
		0		2		4		6		8	
		U_o	δU_o	U_o	δU_o	U_o	δU_o	U_o	δU_o	U_o	δU_o
0.6	5	0.000	0.023	0.000	0.016	0.000	0.012	0.000	0.011	0.000	0.010
	10	0.000	0.012	0.000	0.008	0.000	0.006	0.000	0.006	0.000	0.005
	15	0.000	0.007	0.000	0.005	0.000	0.005	0.000	0.004	0.000	0.003
0.5	5	0.000	0.106	0.000	0.034	0.000	0.026	0.000	0.011	0.000	0.009
	10	0.000	0.015	0.000	0.019	0.000	0.020	0.000	0.005	0.021	0.005
	15	0.016	0.025	0.000	0.028	0.000	0.005	0.000	0.004	0.000	0.003
0.4	5	0.198	0.025	0.084	0.047	0.000	0.029	0.000	0.023	0.000	0.016
	10	0.070	0.017	0.000	0.044	0.000	0.014	0.000	0.009	0.000	0.008
	15	0.063	0.009	0.034	0.013	0.000	0.034	0.000	0.007	0.000	0.003

Note: U_o - Preswirl ratio**, δU_o -** Uncertainty of preswirl ratio measurement

Table 15 Raw data for the test seal at PD=27.6 bar, ω=3 krpm, and inlet GVF=0% with the zero-preswirl insert

Freq.	Re(H_{XX})	Re(H_{XY})	Re(H_{YX})	Re(H_{YY})	Im(H_{XX})	Im(H_{XY})	Im(H_{YX})	Im(H_{YY})	Re(eH_{XX})	Re(eH_{XY})	Re(eH_{YX})	Re(eH_{YY})	Im(eH_{XX})	Im(eH_{XY})	Im(eH_{YX})	Im(eH_{YY})
Hz	N/m	N/m	N/m	N/m	N/m	N/m	N/m	N/m	N/m	N/m	N/m	N/m	N/m	N/m	N/m	N/m
9.8	3.2E+06	1.5E+07	-2.1E+07	3.7E+06	7.1E+06	1.1E+06	-6.2E+05	6.3E+06	-1.2E+05	-9.4E+04	-8.4E+04	-1.1E+05	-8.8E+04	-7.5E+04	-1.3E+05	-6.4E+04
19.5	2.2E+06	1.5E+07	-2.1E+07	2.5E+06	1.4E+07	1.7E+06	-1.5E+06	1.4E+07	-4.7E+04	-5.7E+04	-6.8E+04	-1.1E+05	-6.6E+04	-4.8E+04	-8.1E+04	-6.0E+04
29.3	2.4E+06	1.5E+07	-2.2E+07	2.9E+06	2.0E+07	4.2E+06	-3.6E+05	1.9E+07	-1.4E+05	-8.5E+04	-1.4E+05	-1.6E+05	-8.6E+04	-6.8E+04	-1.1E+05	-7.4E+04
39.1	2.0E+05	1.5E+07	-2.2E+07	8.3E+05	2.8E+07	3.0E+06	-3.5E+06	2.9E+07	-1.0E+05	-9.1E+04	-8.5E+04	-7.6E+04	-9.9E+04	-8.7E+04	-3.8E+04	-5.2E+04
48.8	-2.0E+06	1.5E+07	-2.2E+07	-8.6E+05	3.4E+07	4.0E+06	-4.5E+06	3.5E+07	-1.1E+05	-1.8E+05	-6.6E+04	-1.1E+05	-1.2E+05	-1.0E+05	-9.4E+04	-6.8E+04
58.6	-4.2E+06	1.5E+07	-2.2E+07	-3.0E+06	4.1E+07	4.4E+06	-5.5E+06	4.2E+07	-8.0E+04	-7.6E+04	-1.8E+05	-8.4E+04	-6.8E+04	-9.3E+04	-1.3E+05	-7.5E+04
68.4	-7.4E+06	1.4E+07	-2.3E+07	-6.5E+06	4.8E+07	5.3E+06	-6.0E+06	5.0E+07	-1.9E+05	-1.7E+05	-1.6E+05	-3.2E+05	-2.9E+05	-1.9E+05	-2.8E+05	-2.5E+05
78.1	-1.1E+07	1.4E+07	-2.3E+07	-9.3E+06	5.6E+07	6.6E+06	-7.1E+06	5.7E+07	-1.3E+05	-6.1E+04	-9.1E+04	-1.9E+05	-1.4E+05	-1.5E+05	-1.0E+05	-1.4E+05
87.9	-1.3E+07	1.3E+07	-2.3E+07	-1.3E+07	6.3E+07	7.5E+06	-7.2E+06	6.4E+07	-8.7E+04	-4.6E+04	-5.7E+04	-1.4E+05	-1.1E+05	-1.0E+05	-8.2E+04	-5.6E+04
97.7	-1.8E+07	1.3E+07	-2.3E+07	-1.7E+07	7.0E+07	8.6E+06	-8.2E+06	7.1E+07	-1.4E+05	-4.6E+04	-8.9E+04	-9.6E+04	-9.8E+04	-1.6E+05	-1.1E+05	-1.2E+05
107.4	-2.4E+07	1.3E+07	-2.4E+07	-2.3E+07	7.6E+07	9.2E+06	-9.5E+06	7.9E+07	-1.0E+05	-1.2E+05	-1.5E+05	-2.0E+05	-1.4E+05	-1.6E+05	-1.1E+05	-1.8E+05
117.2	-2.8E+07	1.4E+07	-2.4E+07	-2.8E+07	8.5E+07	1.2E+07	-9.8E+06	8.6E+07	-8.7E+04	-1.5E+05	-7.3E+04	-1.2E+05	-1.2E+05	-6.7E+04	-9.5E+04	-1.0E+05
127.0	-3.5E+07	1.4E+07	-2.4E+07	-3.4E+07	9.2E+07	1.3E+07	-1.1E+07	9.5E+07	-7.1E+04	-1.8E+05	-9.0E+04	-2.9E+05	-1.0E+05	-1.3E+05	-1.0E+05	-1.5E+05
136.7	-4.2E+07	1.5E+07	-2.3E+07	-4.2E+07	9.9E+07	1.5E+07	-1.2E+07	1.0E+08	-1.2E+05	-1.1E+05	-1.2E+05	-1.8E+05	-1.5E+05	-1.5E+05	-1.7E+05	-1.1E+05

Table 16 Raw data for the test seal at PD=27.6 bar, ω=4 krpm, and inlet GVF=0% with the zero-preswirl insert

Freq.	Re(H_{XX})	Re(H_{XY})	Re(H_{YX})	Re(H_{YY})	Im(H_{XX})	Im(H_{XY})	Im(H_{YX})	Im(H_{YY})	Re(eH_{XX})	Re(eH_{XY})	Re(eH_{YX})	Re(eH_{YY})	Im(eH_{XX})	Im(eH_{XY})	Im(eH_{YX})	Im(eH_{YY})
Hz	N/m	N/m	N/m	N/m	N/m	N/m	N/m	N/m	N/m	N/m	N/m	N/m	N/m	N/m	N/m	N/m
9.8	4.0E+06	1.7E+07	-2.0E+07	3.9E+06	7.8E+06	1.0E+06	5.7E+05	7.6E+06	-9.3E+04	-1.3E+05	-1.5E+05	-1.6E+05	-1.4E+05	-6.7E+04	-1.6E+05	-9.2E+04
19.5	2.9E+06	1.6E+07	-2.0E+07	2.8E+06	1.4E+07	1.3E+06	-8.9E+05	1.4E+07	-8.0E+04	-9.6E+04	-1.2E+05	-1.3E+05	-1.6E+05	-9.7E+04	-1.0E+05	-5.9E+04
29.3	2.8E+06	1.6E+07	-2.1E+07	2.7E+06	2.0E+07	4.2E+06	1.3E+05	1.9E+07	-6.6E+04	-6.2E+04	-1.3E+05	-6.0E+04	-1.2E+05	-6.8E+04	-8.7E+04	-1.2E+05
39.1	7.2E+05	1.5E+07	-2.0E+07	8.2E+05	2.7E+07	2.4E+06	-3.1E+06	2.9E+07	-1.5E+05	-1.2E+05	-1.0E+05	-9.7E+04	-9.5E+04	-7.5E+04	-9.2E+04	-6.0E+04
48.8	-1.4E+06	1.5E+07	-2.0E+07	-8.6E+05	3.4E+07	3.4E+06	-3.9E+06	3.6E+07	-9.6E+04	-1.2E+05	-1.7E+05	-1.0E+05	-1.2E+05	-7.1E+04	-7.2E+04	-6.0E+04
58.6	-4.3E+06	1.5E+07	-2.1E+07	-3.1E+06	4.0E+07	4.4E+06	-5.6E+06	4.2E+07	-1.6E+05	-8.2E+04	-1.3E+05	-1.6E+05	-9.1E+04	-2.0E+05	-1.8E+05	-1.5E+05
68.4	-7.0E+06	1.4E+07	-2.2E+07	-6.9E+06	4.7E+07	4.6E+06	-6.7E+06	5.0E+07	-1.6E+05	-1.9E+05	-1.9E+05	-2.4E+05	-1.9E+05	-2.0E+05	-2.2E+05	-1.7E+05
78.1	-9.8E+06	1.4E+07	-2.1E+07	-9.2E+06	5.5E+07	5.7E+06	-7.9E+06	5.7E+07	-1.7E+05	-1.2E+05	-1.8E+05	-1.2E+05	-1.6E+05	-1.1E+05	-1.1E+05	-1.1E+05
87.9	-1.4E+07	1.4E+07	-2.2E+07	-1.3E+07	6.2E+07	6.8E+06	-7.8E+06	6.4E+07	-1.3E+05	-1.7E+05	-1.1E+05	-1.2E+05	-1.8E+05	-1.1E+05	-9.8E+04	-8.4E+04
97.7	-1.8E+07	1.4E+07	-2.2E+07	-1.6E+07	6.9E+07	7.6E+06	-8.9E+06	7.1E+07	-1.1E+05	-6.9E+04	-6.9E+04	-5.3E+04	-9.7E+04	-9.9E+04	-1.5E+05	-7.4E+04
107.4	-2.4E+07	1.3E+07	-2.4E+07	-2.2E+07	7.6E+07	8.9E+06	-1.0E+07	7.9E+07	-1.1E+05	-8.2E+04	-1.4E+05	-8.8E+04	-1.8E+05	-1.5E+05	-1.1E+05	-8.6E+04
117.2	-2.9E+07	1.4E+07	-2.4E+07	-2.8E+07	8.3E+07	1.1E+07	-1.1E+07	8.6E+07	-7.3E+04	-1.2E+05	-1.4E+05	-1.2E+05	-1.3E+05	-8.5E+04	-9.7E+04	-1.2E+05
127.0	-3.5E+07	1.5E+07	-2.2E+07	-3.3E+07	9.1E+07	1.2E+07	-1.3E+07	9.4E+07	-9.5E+04	-2.4E+05	-1.0E+05	-1.6E+05	-1.7E+05	-1.4E+05	-1.6E+05	-2.1E+05
136.7	-4.2E+07	1.5E+07	-2.3E+07	-4.1E+07	9.8E+07	1.3E+07	-1.4E+07	1.0E+08	-2.0E+05	-9.3E+04	-1.0E+05	-1.0E+05	-1.1E+05	-1.7E+05	-1.6E+05	-1.7E+05

Table 17 Raw data for the test seal at PD=27.6 bar, ω=5 krpm, and inlet GVF=0% with the zero-preswirl insert

Freq.	Re(H_{XX})	Re(H_{XY})	Re(H_{YX})	Re(H_{YY})	Im(H_{XX})	Im(H_{XY})	Im(H_{YX})	Im(H_{YY})	Re(eH_{XX})	Re(eH_{XY})	Re(eH_{YX})	Re(eH_{YY})	Im(eH_{XX})	Im(eH_{XY})	Im(eH_{YX})	Im(eH_{YY})
Hz	N/m	N/m	N/m	N/m	N/m	N/m	N/m	N/m	N/m	N/m	N/m	N/m	N/m	N/m	N/m	N/m
9.8	3.4E+06	2.5E+07	-2.2E+07	4.2E+06	7.2E+06	2.0E+06	-1.5E+05	6.7E+06	-1.8E+05	-1.8E+05	-9.3E+04	-1.4E+05	-1.5E+05	-1.6E+05	-1.7E+05	-1.5E+05
19.5	2.2E+06	2.5E+07	-2.4E+07	2.1E+06	1.4E+07	2.1E+06	-2.9E+06	1.5E+07	-1.7E+05	-1.5E+05	-1.1E+05	-1.2E+05	-1.3E+05	-1.5E+05	-9.5E+04	-8.2E+04
29.3	2.1E+06	2.5E+07	-2.5E+07	2.3E+06	2.1E+07	4.8E+06	-2.1E+06	2.0E+07	-9.6E+04	-1.2E+05	-1.3E+05	-1.3E+05	-1.3E+05	-8.8E+04	-1.1E+05	-7.0E+04
39.1	2.9E+05	2.5E+07	-2.4E+07	3.4E+05	2.8E+07	3.1E+06	-5.3E+06	2.8E+07	-8.0E+04	-9.5E+04	-7.5E+04	-7.8E+04	-9.8E+04	-9.0E+04	-9.9E+04	-9.1E+04
48.8	-1.6E+06	2.4E+07	-2.4E+07	-1.4E+06	3.5E+07	3.7E+06	-6.6E+06	3.5E+07	-9.9E+04	-8.1E+04	-1.9E+05	-1.1E+05	-1.4E+05	-1.0E+05	-1.2E+05	-1.5E+05
58.6	-4.2E+06	2.4E+07	-2.4E+07	-4.5E+06	4.1E+07	4.7E+06	-8.8E+06	4.2E+07	-1.2E+05	-1.2E+05	-2.5E+05	-1.1E+05	-1.4E+05	-9.1E+04	-1.5E+05	-1.5E+05
68.4	-7.0E+06	2.3E+07	-2.5E+07	-6.8E+06	4.9E+07	5.4E+06	-9.1E+06	4.9E+07	-1.3E+05	-9.4E+04	-1.9E+05	-1.5E+05	-1.4E+05	-1.8E+05	-1.0E+05	-2.1E+05
78.1	-9.6E+06	2.3E+07	-2.5E+07	-1.0E+07	5.7E+07	6.9E+06	-1.1E+07	5.7E+07	-1.7E+05	-1.5E+05	-1.7E+05	-1.2E+05	-2.2E+05	-1.7E+05	-1.2E+05	-1.3E+05
87.9	-1.4E+07	2.3E+07	-2.6E+07	-1.4E+07	6.3E+07	8.2E+06	-1.2E+07	6.4E+07	-1.1E+05	-2.0E+05	-1.1E+05	-1.3E+05	-1.8E+05	-8.7E+04	-9.6E+04	-9.8E+04
97.7	-1.8E+07	2.3E+07	-2.7E+07	-1.8E+07	7.0E+07	9.0E+06	-1.4E+07	7.1E+07	-7.9E+04	-1.5E+05	-1.2E+05	-5.6E+04	-1.4E+05	-1.2E+05	-1.2E+05	-1.5E+05
107.4	-2.4E+07	2.2E+07	-2.8E+07	-2.4E+07	7.8E+07	1.0E+07	-1.6E+07	7.9E+07	-1.3E+05	-7.0E+04	-1.6E+05	-1.2E+05	-1.6E+05	-1.7E+05	-1.9E+05	-9.9E+04
117.2	-2.8E+07	2.3E+07	-2.9E+07	-2.9E+07	8.5E+07	1.2E+07	-1.7E+07	8.7E+07	-2.1E+05	-1.3E+05	-8.2E+04	-1.4E+05	-9.1E+04	-1.7E+05	-1.4E+05	-1.1E+05
127.0	-3.4E+07	2.3E+07	-2.9E+07	-3.5E+07	9.3E+07	1.4E+07	-1.9E+07	9.5E+07	-1.3E+05	-1.8E+05	-1.9E+05	-2.1E+05	-1.2E+05	-1.4E+05	-1.8E+05	-1.3E+05
136.7	-4.1E+07	2.3E+07	-2.9E+07	-4.1E+07	1.0E+08	1.6E+07	-2.0E+07	1.0E+08	-1.3E+05	-1.8E+05	-1.6E+05	-1.3E+05	-1.2E+05	-1.9E+05	-1.8E+05	-1.6E+05

Table 18 Raw data for the test seal at PD=27.6 bar, ω=3 krpm, and inlet GVF=2% with the zero-preswirl insert

Freq.	Re(H_{XX})	Re(H_{XY})	Re(H_{YX})	Re(H_{YY})	Im(H_{XX})	Im(H_{XY})	Im(H_{YX})	Im(H_{YY})	Re(eH_{XX})	Re(eH_{XY})	Re(eH_{YX})	Re(eH_{YY})	Im(eH_{XX})	Im(eH_{XY})	Im(eH_{YX})	Im(eH_{YY})
Hz	N/m	N/m	N/m	N/m	N/m	N/m	N/m	N/m	N/m	N/m	N/m	N/m	N/m	N/m	N/m	N/m
9.8	5.0E+06	2.0E+07	-1.5E+07	2.8E+06	7.6E+06	1.0E+06	-7.8E+05	6.3E+06	-1.0E+05	-1.1E+05	-7.2E+04	-8.3E+04	-9.8E+04	-7.9E+04	-1.3E+05	-1.1E+05
19.5	4.3E+06	2.0E+07	-1.7E+07	2.0E+06	1.4E+07	1.1E+06	-2.0E+06	1.5E+07	-1.1E+05	-8.1E+04	-1.3E+05	-7.8E+04	-1.1E+05	-1.4E+05	-1.2E+05	-1.1E+05
29.3	4.5E+06	1.9E+07	-1.7E+07	2.3E+06	2.0E+07	3.2E+06	-6.4E+05	1.9E+07	-7.6E+04	-6.5E+04	-1.0E+05	-5.2E+04	-6.1E+04	-7.3E+04	-9.2E+04	-5.2E+04
39.1	3.7E+06	1.8E+07	-1.7E+07	1.8E+06	2.7E+07	9.0E+05	-3.5E+06	2.9E+07	-8.2E+04	-5.2E+04	-4.8E+04	-3.9E+04	-4.1E+04	-3.8E+04	-5.4E+04	-4.3E+04
48.8	1.6E+06	1.9E+07	-1.6E+07	-1.6E+05	3.4E+07	1.7E+06	-4.5E+06	3.5E+07	-9.5E+04	-5.3E+04	-4.0E+04	-5.3E+04	-4.8E+04	-5.9E+04	-5.2E+04	-5.3E+04
58.6	-1.4E+06	1.8E+07	-1.7E+07	-3.2E+06	4.0E+07	2.7E+06	-6.4E+06	4.2E+07	-6.8E+04	-1.1E+05	-1.1E+05	-6.2E+04	-6.4E+04	-6.8E+04	-7.1E+04	-5.3E+04
68.4	-3.7E+06	1.8E+07	-1.8E+07	-4.4E+06	4.7E+07	2.7E+06	-6.6E+06	4.9E+07	-1.3E+05	-9.4E+04	-1.4E+05	-9.1E+04	-9.7E+04	-5.6E+04	-1.0E+05	-2.0E+05
78.1	-5.2E+06	1.7E+07	-1.8E+07	-7.7E+06	5.5E+07	3.2E+06	-8.2E+06	5.7E+07	-7.8E+04	-6.4E+04	-1.0E+05	-1.0E+05	-5.8E+04	-8.2E+04	-7.7E+04	-5.4E+04
87.9	-8.7E+06	1.7E+07	-1.9E+07	-1.0E+07	6.1E+07	4.3E+06	-8.7E+06	6.4E+07	-1.2E+05	-7.9E+04	-7.0E+04	-4.1E+04	-7.5E+04	-8.4E+04	-8.6E+04	-6.1E+04
97.7	-1.2E+07	1.7E+07	-1.9E+07	-1.4E+07	6.9E+07	5.0E+06	-1.0E+07	7.1E+07	-6.8E+04	-7.5E+04	-5.0E+04	-4.3E+04	-5.6E+04	-7.9E+04	-7.4E+04	-4.3E+04
107.4	-1.8E+07	1.5E+07	-2.1E+07	-1.9E+07	7.6E+07	4.8E+06	-1.1E+07	7.8E+07	-9.2E+04	-8.1E+04	-8.7E+04	-1.1E+05	-1.5E+05	-7.7E+04	-7.3E+04	-8.8E+04
117.2	-2.1E+07	1.6E+07	-2.1E+07	-2.3E+07	8.3E+07	7.2E+06	-1.2E+07	8.6E+07	-6.1E+04	-1.0E+05	-6.0E+04	-1.0E+05	-5.5E+04	-5.8E+04	-7.2E+04	-2.1E+04
127.0	-2.7E+07	1.7E+07	-2.0E+07	-2.9E+07	9.2E+07	7.8E+06	-1.3E+07	9.4E+07	-7.9E+04	-1.1E+05	-1.2E+05	-7.5E+04	-7.2E+04	-1.1E+05	-8.2E+04	-1.1E+05
136.7	-3.4E+07	1.8E+07	-2.0E+07	-3.5E+07	1.0E+08	8.3E+06	-1.5E+07	1.0E+08	-1.6E+05	-9.0E+04	-6.2E+04	-7.7E+04	-1.1E+05	-1.5E+05	-1.2E+05	-1.0E+05

Table 19 Raw data for the test seal at PD=27.6 bar, ω=4 krpm, and inlet GVF=2% with the zero-preswirl insert

Freq.	Re(H_{XX})	Re(H_{XY})	Re(H_{YX})	Re(H_{YY})	Im(H_{XX})	Im(H_{XY})	Im(H_{YX})	Im(H_{YY})	Re(eH_{XX})	Re(eH_{XY})	Re(eH_{YX})	Re(eH_{YY})	Im(eH_{XX})	Im(eH_{XY})	Im(eH_{YX})	Im(eH_{YY})
Hz	N/m	N/m	N/m	N/m	N/m	N/m	N/m	N/m	N/m	N/m	N/m	N/m	N/m	N/m	N/m	N/m
9.8	5.6E+06	2.0E+07	-1.5E+07	3.2E+06	7.4E+06	9.8E+05	-8.7E+05	6.3E+06	-8.9E+04	-6.2E+04	-8.3E+04	-7.0E+04	-8.5E+04	-1.4E+05	-9.5E+04	-1.2E+05
19.5	5.0E+06	2.1E+07	-1.6E+07	2.3E+06	1.4E+07	1.3E+06	-2.4E+06	1.5E+07	-1.3E+05	-7.1E+04	-9.6E+04	-1.1E+05	-7.7E+04	-1.1E+05	-8.7E+04	-1.2E+05
29.3	4.7E+06	2.0E+07	-1.7E+07	2.8E+06	1.9E+07	3.5E+06	-9.3E+05	2.0E+07	-1.1E+05	-1.5E+05	-1.1E+05	-7.8E+04	-1.2E+05	-7.5E+04	-1.4E+05	-6.9E+04
39.1	4.0E+06	1.9E+07	-1.7E+07	2.1E+06	2.8E+07	8.1E+05	-3.9E+06	2.9E+07	-1.6E+05	-6.1E+04	-1.0E+05	-3.6E+04	-3.2E+04	-1.1E+05	-6.1E+04	-6.2E+04
48.8	2.2E+06	1.9E+07	-1.7E+07	5.9E+05	3.4E+07	1.9E+06	-4.8E+06	3.5E+07	-8.3E+04	-7.8E+04	-8.3E+04	-6.5E+04	-5.8E+04	-4.4E+04	-9.2E+04	-6.7E+04
58.6	-5.6E+05	1.8E+07	-1.7E+07	-2.4E+06	4.0E+07	2.7E+06	-6.6E+06	4.2E+07	-1.3E+05	-5.1E+04	-2.3E+05	-1.3E+05	-7.2E+04	-1.1E+05	-1.5E+05	-6.8E+04
68.4	-2.9E+06	1.9E+07	-1.8E+07	-3.9E+06	4.8E+07	2.8E+06	-6.8E+06	4.9E+07	-1.2E+05	-1.3E+05	-1.2E+05	-4.2E+04	-6.9E+04	-1.3E+05	-7.5E+04	-7.1E+04
78.1	-4.9E+06	1.8E+07	-1.8E+07	-7.0E+06	5.6E+07	3.1E+06	-8.3E+06	5.7E+07	-1.3E+05	-6.2E+04	-1.1E+05	-9.3E+04	-7.6E+04	-7.7E+04	-7.7E+04	-7.8E+04
87.9	-8.3E+06	1.8E+07	-1.9E+07	-9.8E+06	6.2E+07	4.2E+06	-9.0E+06	6.4E+07	-5.8E+04	-1.2E+05	-1.3E+05	-7.9E+04	-1.1E+05	-7.9E+04	-8.7E+04	-1.2E+05
97.7	-1.2E+07	1.7E+07	-1.9E+07	-1.3E+07	7.0E+07	5.0E+06	-1.1E+07	7.1E+07	-6.8E+04	-5.6E+04	-1.5E+05	-5.9E+04	-1.4E+05	-4.0E+04	-6.7E+04	-9.4E+04
107.4	-1.7E+07	1.6E+07	-2.1E+07	-1.9E+07	7.7E+07	4.7E+06	-1.2E+07	7.8E+07	-9.4E+04	-8.3E+04	-1.5E+05	-1.3E+05	-1.7E+05	-1.2E+05	-1.4E+05	-7.8E+04
117.2	-2.0E+07	1.7E+07	-2.1E+07	-2.2E+07	8.4E+07	7.2E+06	-1.2E+07	8.6E+07	-1.3E+05	-8.7E+04	-6.1E+04	-6.8E+04	-1.2E+05	-4.8E+04	-7.6E+04	-3.7E+04
127.0	-2.6E+07	1.8E+07	-2.1E+07	-2.8E+07	9.2E+07	7.9E+06	-1.3E+07	9.4E+07	-6.4E+04	-1.5E+05	-7.2E+04	-1.5E+05	-1.3E+05	-1.4E+05	-1.2E+05	-1.4E+05
136.7	-3.3E+07	1.8E+07	-2.1E+07	-3.5E+07	1.0E+08	9.1E+06	-1.4E+07	1.0E+08	-1.4E+05	-1.3E+05	-1.6E+05	-9.1E+04	-1.2E+05	-1.1E+05	-6.9E+04	-8.2E+04

Table 20 Raw data for the test seal at PD=27.6 bar, ω=5 krpm, and inlet GVF=2% with the zero-preswirl insert

Freq.	Re(H_{XX})	Re(H_{XY})	Re(H_{YX})	Re(H_{YY})	Im(H_{XX})	Im(H_{XY})	Im(H_{YX})	Im(H_{YY})	Re(eH_{XX})	Re(eH_{XY})	Re(eH_{YX})	Re(eH_{YY})	Im(eH_{XX})	Im(eH_{XY})	Im(eH_{YX})	Im(eH_{YY})
Hz	N/m	N/m	N/m	N/m	N/m	N/m	N/m	N/m	N/m	N/m	N/m	N/m	N/m	N/m	N/m	N/m
9.8	5.4E+06	2.8E+07	-1.9E+07	3.4E+06	7.4E+06	1.6E+06	-1.1E+06	5.8E+06	-1.1E+05	-1.2E+05	-9.2E+04	-6.4E+04	-1.2E+05	-1.1E+05	-1.0E+05	-1.2E+05
19.5	5.2E+06	2.7E+07	-2.1E+07	2.2E+06	1.4E+07	1.2E+06	-2.8E+06	1.4E+07	-7.3E+04	-1.4E+05	-6.9E+04	-8.7E+04	-1.3E+05	-6.5E+04	-1.2E+05	-1.2E+05
29.3	5.5E+06	2.7E+07	-2.2E+07	2.1E+06	2.0E+07	3.7E+06	-1.7E+06	1.9E+07	-7.7E+04	-9.5E+04	-1.2E+05	-1.2E+05	-1.5E+05	-7.8E+04	-1.3E+05	-5.6E+04
39.1	4.1E+06	2.6E+07	-2.2E+07	1.7E+06	2.8E+07	1.7E+06	-4.8E+06	2.9E+07	-1.0E+05	-6.7E+04	-8.8E+04	-7.7E+04	-5.7E+04	-7.8E+04	-6.9E+04	-6.2E+04
48.8	2.7E+06	2.6E+07	-2.1E+07	9.6E+04	3.4E+07	2.7E+06	-5.7E+06	3.5E+07	-6.7E+04	-6.6E+04	-1.1E+05	-8.8E+04	-1.1E+05	-7.9E+04	-1.3E+05	-8.1E+04
58.6	9.9E+04	2.6E+07	-2.2E+07	-3.3E+06	4.1E+07	3.5E+06	-7.9E+06	4.2E+07	-8.8E+04	-9.7E+04	-1.4E+05	-1.0E+05	-1.0E+05	-9.3E+04	-1.4E+05	-7.1E+04
68.4	-2.3E+06	2.5E+07	-2.3E+07	-4.7E+06	4.8E+07	3.7E+06	-8.6E+06	5.0E+07	-2.1E+05	-1.1E+05	-8.1E+04	-1.4E+05	-1.4E+05	-1.2E+05	-1.2E+05	-1.6E+05
78.1	-4.9E+06	2.5E+07	-2.3E+07	-7.5E+06	5.6E+07	4.9E+06	-1.0E+07	5.8E+07	-1.1E+05	-1.1E+05	-1.9E+05	-1.6E+05	-1.6E+05	-1.7E+05	-7.7E+04	-8.9E+04
87.9	-7.6E+06	2.5E+07	-2.4E+07	-1.0E+07	6.3E+07	5.9E+06	-1.1E+07	6.5E+07	-1.3E+05	-7.0E+04	-9.8E+04	-1.2E+05	-8.3E+04	-6.5E+04	-6.2E+04	-9.4E+04
97.7	-1.1E+07	2.5E+07	-2.4E+07	-1.3E+07	6.9E+07	6.7E+06	-1.2E+07	7.2E+07	-1.1E+05	-1.1E+05	-6.9E+04	-7.5E+04	-1.2E+05	-6.7E+04	-1.4E+05	-6.4E+04
107.4	-1.6E+07	2.4E+07	-2.5E+07	-1.8E+07	7.7E+07	6.8E+06	-1.4E+07	7.9E+07	-1.5E+05	-4.1E+04	-1.8E+05	-8.5E+04	-1.3E+05	-1.0E+05	-1.1E+05	-1.1E+05
117.2	-2.0E+07	2.4E+07	-2.6E+07	-2.1E+07	8.4E+07	8.8E+06	-1.5E+07	8.8E+07	-1.5E+05	-5.1E+04	-1.8E+05	-1.1E+05	-9.5E+04	-6.9E+04	-7.3E+04	-6.0E+04
127.0	-2.6E+07	2.5E+07	-2.6E+07	-2.7E+07	9.3E+07	1.1E+07	-1.7E+07	9.6E+07	-9.2E+04	-2.1E+05	-1.2E+05	-2.2E+05	-1.8E+05	-7.7E+04	-1.5E+05	-1.3E+05
136.7	-3.2E+07	2.6E+07	-2.7E+07	-3.4E+07	1.0E+08	1.1E+07	-1.8E+07	1.0E+08	-1.2E+05	-1.1E+05	-1.5E+05	-1.5E+05	-8.3E+04	-1.5E+05	-8.6E+04	-1.2E+05

Table 21 Raw data for the test seal at PD=27.6 bar, ω=3 krpm, and inlet GVF=4% with the zero-preswirl insert

Freq.	Re(H_{XX})	Re(H_{XY})	Re(H_{YX})	Re(H_{YY})	Im(H_{XX})	Im(H_{XY})	Im(H_{YX})	Im(H_{YY})	Re(eH_{XX})	Re(eH_{XY})	Re(eH_{YX})	Re(eH_{YY})	Im(eH_{XX})	Im(eH_{XY})	Im(eH_{YX})	Im(eH_{YY})
Hz	N/m	N/m	N/m	N/m	N/m	N/m	N/m	N/m	N/m	N/m	N/m	N/m	N/m	N/m	N/m	N/m
9.8	5.3E+06	2.0E+07	-1.4E+07	2.9E+06	8.0E+06	1.2E+06	-1.3E+06	6.1E+06	-8.4E+04	-6.5E+04	-9.7E+04	-1.2E+05	-5.4E+04	-7.9E+04	-1.3E+05	-1.2E+05
19.5	4.8E+06	2.1E+07	-1.6E+07	2.3E+06	1.5E+07	1.2E+06	-2.4E+06	1.5E+07	-1.1E+05	-7.3E+04	-1.3E+05	-1.3E+05	-5.4E+04	-8.8E+04	-1.4E+05	-1.1E+05
29.3	5.9E+06	2.0E+07	-1.7E+07	3.7E+06	2.0E+07	3.7E+06	-4.1E+05	1.9E+07	-9.6E+04	-5.9E+04	-1.1E+05	-4.9E+04	-9.0E+04	-5.4E+04	-5.7E+04	-6.2E+04
39.1	3.4E+06	2.0E+07	-1.6E+07	1.6E+06	2.7E+07	1.2E+06	-4.1E+06	2.8E+07	-5.3E+04	-3.5E+04	-8.8E+04	-5.6E+04	-6.7E+04	-4.2E+04	-8.4E+04	-6.7E+04
48.8	1.4E+06	2.0E+07	-1.6E+07	-4.9E+05	3.5E+07	1.6E+06	-4.8E+06	3.6E+07	-1.2E+05	-8.8E+04	-5.7E+04	-8.5E+04	-4.4E+04	-8.8E+04	-8.1E+04	-5.4E+04
58.6	-4.6E+05	1.9E+07	-1.7E+07	-2.8E+06	4.1E+07	2.2E+06	-6.2E+06	4.3E+07	-6.9E+04	-9.5E+04	-1.4E+05	-6.3E+04	-3.6E+04	-5.5E+04	-6.5E+04	-1.1E+05
68.4	-2.5E+06	1.9E+07	-1.8E+07	-3.6E+06	4.8E+07	2.3E+06	-6.4E+06	5.0E+07	-1.7E+05	-8.8E+04	-1.9E+05	-1.5E+05	-9.3E+04	-1.8E+05	-1.3E+05	-1.9E+05
78.1	-4.2E+06	1.8E+07	-1.8E+07	-7.1E+06	5.6E+07	3.1E+06	-7.8E+06	5.8E+07	-9.0E+04	-9.9E+04	-8.4E+04	-1.0E+05	-6.3E+04	-1.4E+05	-6.5E+04	-1.0E+05
87.9	-8.6E+06	1.8E+07	-1.9E+07	-9.8E+06	6.3E+07	4.4E+06	-8.4E+06	6.6E+07	-5.5E+04	-5.4E+04	-8.0E+04	-8.6E+04	-8.0E+04	-1.1E+05	-5.5E+04	-6.9E+04
97.7	-1.2E+07	1.8E+07	-1.9E+07	-1.3E+07	7.1E+07	5.0E+06	-9.5E+06	7.3E+07	-1.2E+05	-5.5E+04	-5.2E+04	-6.4E+04	-7.3E+04	-6.2E+04	-1.2E+05	-4.6E+04
107.4	-1.7E+07	1.7E+07	-2.0E+07	-1.9E+07	7.9E+07	4.1E+06	-1.1E+07	8.1E+07	-5.3E+04	-1.1E+05	-5.3E+04	-9.5E+04	-2.1E+05	-7.5E+04	-1.2E+05	-5.0E+04
117.2	-2.0E+07	1.8E+07	-2.1E+07	-2.1E+07	8.6E+07	5.8E+06	-1.1E+07	8.9E+07	-5.7E+04	-5.2E+04	-7.1E+04	-9.4E+04	-7.0E+04	-7.2E+04	-7.4E+04	-8.6E+04
127.0	-2.5E+07	1.9E+07	-2.0E+07	-2.7E+07	9.6E+07	6.9E+06	-1.2E+07	9.8E+07	-7.2E+04	-1.4E+05	-1.3E+05	-1.8E+05	-1.4E+05	-1.2E+05	-1.5E+05	-2.3E+05
136.7	-3.2E+07	2.0E+07	-2.0E+07	-3.3E+07	1.0E+08	7.1E+06	-1.3E+07	1.1E+08	-1.3E+05	-2.7E+05	-1.5E+05	-2.1E+05	-2.0E+05	-1.2E+05	-2.5E+05	-1.7E+05

Table 22 Raw data for the test seal at PD=27.6 bar, ω=4 krpm, and inlet GVF=4% with the zero-preswirl insert

Freq.	Re(H_{XX})	Re(H_{XY})	Re(H_{YX})	Re(H_{YY})	Im(H_{XX})	Im(H_{XY})	Im(H_{YX})	Im(H_{YY})	Re(eH_{XX})	Re(eH_{XY})	Re(eH_{YX})	Re(eH_{YY})	Im(eH_{XX})	Im(eH_{XY})	Im(eH_{YX})	Im(eH_{YY})
Hz	N/m	N/m	N/m	N/m	N/m	N/m	N/m	N/m	N/m	N/m	N/m	N/m	N/m	N/m	N/m	N/m
9.8	6.3E+06	2.1E+07	-1.4E+07	2.4E+06	7.7E+06	1.2E+06	-1.4E+06	6.0E+06	-9.9E+04	-7.1E+04	-7.3E+04	-7.2E+04	-8.1E+04	-1.3E+05	-1.2E+05	-1.2E+05
19.5	5.9E+06	2.2E+07	-1.5E+07	1.7E+06	1.4E+07	5.8E+05	-2.3E+06	1.5E+07	-1.5E+05	-8.8E+04	-7.0E+04	-1.2E+05	-1.0E+05	-1.3E+05	-1.5E+05	-6.6E+04
29.3	6.8E+06	2.0E+07	-1.7E+07	3.0E+06	2.0E+07	3.4E+06	-5.6E+05	2.0E+07	-7.7E+04	-6.6E+04	-6.8E+04	-3.8E+04	-7.7E+04	-7.3E+04	-4.6E+04	-3.2E+04
39.1	4.5E+06	2.0E+07	-1.5E+07	1.3E+06	2.7E+07	9.9E+05	-4.3E+06	2.8E+07	-4.1E+04	-6.7E+04	-5.3E+04	-4.6E+04	-5.4E+04	-3.4E+04	-7.8E+04	-5.5E+04
48.8	2.5E+06	2.0E+07	-1.6E+07	-8.8E+05	3.4E+07	1.3E+06	-5.3E+06	3.5E+07	-8.4E+04	-1.0E+05	-9.2E+04	-8.7E+04	-7.1E+04	-5.0E+04	-1.1E+05	-6.2E+04
58.6	5.0E+05	1.9E+07	-1.7E+07	-3.5E+06	4.1E+07	1.8E+06	-6.5E+06	4.3E+07	-9.4E+04	-8.5E+04	-9.4E+04	-9.4E+04	-9.0E+04	-1.1E+05	-1.0E+05	-7.1E+04
68.4	-1.7E+06	2.0E+07	-1.7E+07	-4.0E+06	4.8E+07	2.2E+06	-6.6E+06	4.9E+07	-1.3E+05	-1.4E+05	-8.9E+04	-1.1E+05	-1.2E+05	-9.5E+04	-5.6E+04	-6.2E+04
78.1	-3.4E+06	1.9E+07	-1.7E+07	-7.9E+06	5.6E+07	2.6E+06	-8.2E+06	5.8E+07	-5.4E+04	-6.6E+04	-3.9E+04	-7.8E+04	-7.3E+04	-7.6E+04	-8.8E+04	-4.4E+04
87.9	-7.6E+06	1.8E+07	-1.8E+07	-1.0E+07	6.2E+07	4.0E+06	-8.8E+06	6.6E+07	-9.2E+04	-6.6E+04	-6.9E+04	-8.6E+04	-5.5E+04	-7.0E+04	-7.0E+04	-6.4E+04
97.7	-1.1E+07	1.8E+07	-1.8E+07	-1.4E+07	6.9E+07	4.8E+06	-1.0E+07	7.3E+07	-7.9E+04	-3.6E+04	-8.8E+04	-6.9E+04	-7.0E+04	-4.8E+04	-5.1E+04	-5.1E+04
107.4	-1.6E+07	1.7E+07	-1.9E+07	-1.9E+07	7.7E+07	3.8E+06	-1.1E+07	8.0E+07	-9.7E+04	-1.2E+05	-7.3E+04	-8.7E+04	-8.8E+04	-9.6E+04	-6.4E+04	-8.1E+04
117.2	-1.9E+07	1.8E+07	-2.0E+07	-2.2E+07	8.5E+07	5.5E+06	-1.2E+07	8.9E+07	-1.3E+05	-6.3E+04	-1.5E+05	-8.0E+04	-4.6E+04	-5.5E+04	-9.7E+04	-7.1E+04
127.0	-2.5E+07	1.9E+07	-1.9E+07	-2.8E+07	9.3E+07	6.6E+06	-1.3E+07	9.7E+07	-1.0E+05	-1.9E+05	-1.3E+05	-9.9E+04	-6.1E+04	-5.5E+04	-1.0E+05	-1.5E+05
136.7	-3.2E+07	1.9E+07	-1.9E+07	-3.3E+07	1.0E+08	7.1E+06	-1.4E+07	1.1E+08	-1.3E+05	-5.6E+04	-2.1E+05	-1.4E+05	-6.2E+04	-1.5E+05	-1.9E+05	-8.6E+04

Table 23 Raw data for the test seal at PD=27.6 bar, ω=5 krpm, and inlet GVF=4% with the zero-preswirl insert

Freq.	Re(H_{XX})	Re(H_{XY})	Re(H_{YX})	Re(H_{YY})	Im(H_{XX})	Im(H_{XY})	Im(H_{YX})	Im(H_{YY})	Re(eH_{XX})	Re(eH_{XY})	Re(eH_{YX})	Re(eH_{YY})	Im(eH_{XX})	Im(eH_{XY})	Im(eH_{YX})	Im(eH_{YY})
Hz	N/m	N/m	N/m	N/m	N/m	N/m	N/m	N/m	N/m	N/m	N/m	N/m	N/m	N/m	N/m	N/m
9.8	4.7E+06	2.7E+07	-2.0E+07	3.2E+06	7.5E+06	1.3E+06	-6.8E+05	6.0E+06	-1.3E+05	-1.4E+05	-8.9E+04	-1.0E+05	-8.1E+04	-8.2E+04	-1.1E+05	-9.7E+04
19.5	4.2E+06	2.7E+07	-2.1E+07	2.1E+06	1.5E+07	9.7E+05	-2.7E+06	1.5E+07	-1.2E+05	-8.9E+04	-9.4E+04	-1.1E+05	-8.7E+04	-1.3E+05	-1.1E+05	-1.1E+05
29.3	5.4E+06	2.6E+07	-2.3E+07	3.2E+06	2.0E+07	4.5E+06	-1.1E+06	2.0E+07	-9.0E+04	-5.0E+04	-5.9E+04	-8.4E+04	-9.1E+04	-9.3E+04	-9.6E+04	-6.1E+04
39.1	3.5E+06	2.6E+07	-2.1E+07	1.4E+06	2.8E+07	2.6E+06	-4.7E+06	2.8E+07	-5.5E+04	-5.4E+04	-9.8E+04	-6.8E+04	-7.9E+04	-7.1E+04	-6.2E+04	-9.0E+04
48.8	1.6E+06	2.6E+07	-2.2E+07	-3.5E+05	3.5E+07	2.9E+06	-5.7E+06	3.6E+07	-1.2E+05	-5.8E+04	-9.2E+04	-9.1E+04	-6.8E+04	-1.1E+05	-7.6E+04	-1.0E+05
58.6	-1.7E+05	2.6E+07	-2.2E+07	-3.3E+06	4.2E+07	3.6E+06	-7.6E+06	4.3E+07	-6.8E+04	-6.0E+04	-1.0E+05	-6.0E+04	-6.5E+04	-7.2E+04	-8.8E+04	-6.7E+04
68.4	-1.8E+06	2.6E+07	-2.3E+07	-4.1E+06	4.9E+07	3.6E+06	-7.8E+06	5.0E+07	-8.5E+04	-1.1E+05	-9.0E+04	-7.5E+04	-1.2E+05	-1.2E+05	-9.9E+04	-9.0E+04
78.1	-4.3E+06	2.5E+07	-2.3E+07	-7.3E+06	5.6E+07	4.9E+06	-9.8E+06	5.8E+07	-8.1E+04	-9.7E+04	-1.1E+05	-1.0E+05	-1.1E+05	-6.6E+04	-6.3E+04	-8.0E+04
87.9	-8.0E+06	2.5E+07	-2.4E+07	-9.8E+06	6.3E+07	6.2E+06	-1.0E+07	6.6E+07	-5.9E+04	-9.6E+04	-6.2E+04	-7.7E+04	-5.6E+04	-4.2E+04	-7.8E+04	-6.8E+04
97.7	-1.2E+07	2.5E+07	-2.5E+07	-1.3E+07	7.1E+07	6.8E+06	-1.1E+07	7.3E+07	-1.1E+05	-7.9E+04	-4.8E+04	-3.9E+04	-6.0E+04	-6.2E+04	-4.2E+04	-4.7E+04
107.4	-1.6E+07	2.4E+07	-2.6E+07	-1.8E+07	7.9E+07	6.2E+06	-1.3E+07	8.1E+07	-9.9E+04	-4.2E+04	-8.0E+04	-5.9E+04	-8.8E+04	-1.2E+05	-1.2E+05	-8.7E+04
117.2	-2.0E+07	2.5E+07	-2.6E+07	-2.1E+07	8.6E+07	8.3E+06	-1.4E+07	9.0E+07	-6.4E+04	-5.5E+04	-7.3E+04	-7.9E+04	-9.1E+04	-1.0E+05	-4.8E+04	-6.6E+04
127.0	-2.6E+07	2.5E+07	-2.6E+07	-2.7E+07	9.5E+07	1.0E+07	-1.6E+07	9.7E+07	-7.6E+04	-1.1E+05	-6.5E+04	-1.6E+05	-5.7E+04	-9.4E+04	-6.3E+04	-1.5E+05
136.7	-3.2E+07	2.6E+07	-2.6E+07	-3.3E+07	1.0E+08	1.1E+07	-1.7E+07	1.1E+08	-9.6E+04	-8.4E+04	-1.7E+05	-1.1E+05	-7.7E+04	-8.2E+04	-7.8E+04	-8.3E+04

Table 24 Raw data for the test seal at PD=27.6 bar, ω=3 krpm, and inlet GVF=6% with the zero-preswirl insert

Freq.	Re(H_{XX})	Re(H_{XY})	Re(H_{YX})	Re(H_{YY})	Im(H_{XX})	Im(H_{XY})	Im(H_{YX})	Im(H_{YY})	Re(eH_{XX})	Re(eH_{XY})	Re(eH_{YX})	Re(eH_{YY})	Im(eH_{XX})	Im(eH_{XY})	Im(eH_{YX})	Im(eH_{YY})
Hz	N/m	N/m	N/m	N/m	N/m	N/m	N/m	N/m	N/m	N/m	N/m	N/m	N/m	N/m	N/m	N/m
9.8	5.5E+06	2.2E+07	-1.3E+07	2.2E+06	8.4E+06	1.9E+06	-1.5E+06	5.8E+06	-6.4E+04	-1.3E+05	-6.9E+04	-1.0E+05	-1.3E+05	-9.1E+04	-9.0E+04	-7.1E+04
19.5	5.7E+06	2.2E+07	-1.5E+07	2.0E+06	1.5E+07	5.5E+05	-2.2E+06	1.6E+07	-8.4E+04	-9.2E+04	-1.3E+05	-8.7E+04	-1.1E+05	-7.5E+04	-8.0E+04	-1.1E+05
29.3	6.2E+06	2.1E+07	-1.6E+07	2.9E+06	2.0E+07	3.9E+06	-3.6E+05	1.9E+07	-5.3E+04	-9.1E+04	-1.2E+05	-5.8E+04	-1.0E+05	-6.2E+04	-8.6E+04	-8.1E+04
39.1	3.8E+06	2.1E+07	-1.5E+07	5.1E+05	2.7E+07	1.1E+06	-4.2E+06	2.8E+07	-5.5E+04	-6.4E+04	-7.9E+04	-5.8E+04	-5.9E+04	-7.0E+04	-6.0E+04	-6.3E+04
48.8	2.3E+06	2.1E+07	-1.6E+07	-1.3E+06	3.5E+07	1.4E+06	-4.8E+06	3.6E+07	-1.1E+05	-1.2E+05	-1.2E+05	-4.3E+04	-1.0E+05	-7.9E+04	-5.2E+04	-6.8E+04
58.6	1.9E+05	2.0E+07	-1.6E+07	-3.8E+06	4.2E+07	2.0E+06	-6.1E+06	4.3E+07	-5.2E+04	-6.9E+04	-1.4E+05	-6.4E+04	-9.3E+04	-3.7E+04	-8.4E+04	-1.2E+05
68.4	-1.9E+06	2.0E+07	-1.7E+07	-4.4E+06	4.9E+07	1.9E+06	-6.6E+06	5.0E+07	-1.1E+05	-1.5E+05	-1.0E+05	-1.2E+05	-2.0E+05	-2.1E+05	-1.0E+05	-1.5E+05
78.1	-3.7E+06	2.0E+07	-1.7E+07	-8.1E+06	5.6E+07	2.8E+06	-8.0E+06	5.8E+07	-6.4E+04	-5.7E+04	-1.1E+05	-7.2E+04	-5.9E+04	-6.4E+04	-8.2E+04	-1.1E+05
87.9	-7.7E+06	1.9E+07	-1.8E+07	-1.0E+07	6.3E+07	3.9E+06	-8.3E+06	6.7E+07	-9.4E+04	-9.2E+04	-4.1E+04	-1.2E+05	-7.1E+04	-1.3E+05	-7.9E+04	-6.6E+04
97.7	-1.1E+07	1.9E+07	-1.8E+07	-1.3E+07	7.1E+07	4.3E+06	-9.0E+06	7.5E+07	-6.7E+04	-5.9E+04	-1.1E+05	-6.8E+04	-1.2E+05	-4.7E+04	-9.9E+04	-1.1E+05
107.4	-1.5E+07	1.8E+07	-1.9E+07	-1.9E+07	7.9E+07	3.3E+06	-1.1E+07	8.2E+07	-1.6E+05	-1.1E+05	-8.5E+04	-9.5E+04	-1.1E+05	-1.4E+05	-7.8E+04	-8.9E+04
117.2	-1.8E+07	1.9E+07	-1.9E+07	-2.1E+07	8.6E+07	4.8E+06	-1.1E+07	9.1E+07	-1.1E+05	-8.8E+04	-1.1E+05	-2.3E+04	-8.4E+04	-1.0E+05	-7.8E+04	-6.9E+04
127.0	-2.4E+07	2.0E+07	-1.8E+07	-2.7E+07	9.6E+07	5.7E+06	-1.2E+07	9.9E+07	-9.3E+04	-1.0E+05	-5.6E+04	-9.4E+04	-7.2E+04	-8.9E+04	-1.6E+05	-1.5E+05
136.7	-3.0E+07	2.0E+07	-1.8E+07	-3.2E+07	1.0E+08	5.2E+06	-1.3E+07	1.1E+08	-2.1E+05	-1.2E+05	-1.3E+05	-7.7E+04	-1.5E+05	-1.5E+05	-1.2E+05	-1.5E+05

Table 25 Raw data for the test seal at PD=27.6 bar, ω=4 krpm, and inlet GVF=6% with the zero-preswirl insert

Freq.	Re(H_{XX})	Re(H_{XY})	Re(H_{YX})	Re(H_{YY})	Im(H_{XX})	Im(H_{XY})	Im(H_{YX})	Im(H_{YY})	Re(eH_{XX})	Re(eH_{XY})	Re(eH_{YX})	Re(eH_{YY})	Im(eH_{XX})	Im(eH_{XY})	Im(eH_{YX})	Im(eH_{YY})
Hz	N/m	N/m	N/m	N/m	N/m	N/m	N/m	N/m	N/m	N/m	N/m	N/m	N/m	N/m	N/m	N/m
9.8	5.3E+06	2.2E+07	-1.4E+07	2.3E+06	8.3E+06	1.7E+06	-1.3E+06	6.1E+06	-1.6E+05	-1.4E+05	-1.2E+05	-7.9E+04	-9.1E+04	-1.3E+05	-8.5E+04	-1.4E+05
19.5	5.6E+06	2.2E+07	-1.5E+07	1.8E+06	1.5E+07	4.0E+05	-2.2E+06	1.6E+07	-9.2E+04	-1.0E+05	-9.8E+04	-1.2E+05	-1.1E+05	-7.7E+04	-1.1E+05	-8.0E+04
29.3	6.1E+06	2.1E+07	-1.6E+07	2.7E+06	1.9E+07	3.8E+06	-1.9E+05	1.9E+07	-7.1E+04	-8.3E+04	-1.0E+05	-9.1E+04	-1.1E+05	-8.5E+04	-8.8E+04	-7.5E+04
39.1	3.5E+06	2.1E+07	-1.5E+07	2.3E+05	2.7E+07	9.9E+05	-4.2E+06	2.8E+07	-3.5E+04	-5.1E+04	-7.2E+04	-1.0E+05	-4.9E+04	-4.2E+04	-5.0E+04	-5.8E+04
48.8	2.1E+06	2.1E+07	-1.6E+07	-1.5E+06	3.6E+07	1.4E+06	-4.7E+06	3.6E+07	-1.1E+05	-5.5E+04	-9.0E+04	-8.8E+04	-8.0E+04	-5.4E+04	-7.1E+04	-6.2E+04
58.6	1.4E+05	2.0E+07	-1.6E+07	-3.8E+06	4.2E+07	1.9E+06	-6.1E+06	4.4E+07	-4.6E+04	-1.0E+05	-1.0E+05	-1.2E+05	-6.0E+04	-9.8E+04	-7.9E+04	-7.4E+04
68.4	-1.9E+06	2.0E+07	-1.7E+07	-4.6E+06	4.9E+07	2.0E+06	-6.4E+06	5.0E+07	-1.9E+05	-1.5E+05	-8.9E+04	-1.1E+05	-7.5E+04	-1.5E+05	-9.9E+04	-1.1E+05
78.1	-3.7E+06	1.9E+07	-1.7E+07	-8.2E+06	5.6E+07	2.4E+06	-7.8E+06	5.9E+07	-3.6E+04	-9.6E+04	-5.8E+04	-1.3E+05	-7.0E+04	-6.4E+04	-7.1E+04	-9.8E+04
87.9	-7.5E+06	1.9E+07	-1.8E+07	-1.0E+07	6.3E+07	3.4E+06	-8.0E+06	6.8E+07	-9.4E+04	-1.0E+05	-7.5E+04	-7.4E+04	-1.2E+05	-9.0E+04	-7.9E+04	-1.2E+05
97.7	-1.1E+07	1.9E+07	-1.8E+07	-1.3E+07	7.1E+07	4.0E+06	-8.7E+06	7.6E+07	-4.4E+04	-6.9E+04	-5.1E+04	-1.2E+05	-4.4E+04	-8.5E+04	-6.2E+04	-4.3E+04
107.4	-1.5E+07	1.8E+07	-1.9E+07	-1.8E+07	7.9E+07	3.1E+06	-1.0E+07	8.3E+07	-5.1E+04	-1.2E+05	-8.5E+04	-1.2E+05	-1.6E+05	-6.1E+04	-1.1E+05	-7.7E+04
117.2	-1.8E+07	1.9E+07	-1.9E+07	-2.1E+07	8.7E+07	4.5E+06	-1.1E+07	9.2E+07	-5.9E+04	-7.0E+04	-5.6E+04	-7.3E+04	-7.0E+04	-5.2E+04	-4.0E+04	-5.9E+04
127.0	-2.4E+07	2.0E+07	-1.8E+07	-2.6E+07	9.5E+07	5.7E+06	-1.2E+07	1.0E+08	-1.1E+05	-1.7E+05	-1.1E+05	-1.4E+05	-9.4E+04	-1.1E+05	-1.3E+05	-7.6E+04
136.7	-3.0E+07	2.0E+07	-1.8E+07	-3.1E+07	1.0E+08	4.5E+06	-1.3E+07	1.1E+08	-1.8E+05	-2.2E+05	-1.8E+05	-1.5E+05	-1.8E+05	-1.0E+05	-1.0E+05	-1.4E+05

Table 26 Raw data for the test seal at PD=27.6 bar, ω=5 krpm, and inlet GVF=6% with the zero-preswirl insert

Freq.	Re(H_{XX})	Re(H_{XY})	Re(H_{YX})	Re(H_{YY})	Im(H_{XX})	Im(H_{XY})	Im(H_{YX})	Im(H_{YY})	Re(eH_{XX})	Re(eH_{XY})	Re(eH_{YX})	Re(eH_{YY})	Im(eH_{XX})	Im(eH_{XY})	Im(eH_{YX})	Im(eH_{YY})
Hz	N/m	N/m	N/m	N/m	N/m	N/m	N/m	N/m	N/m	N/m	N/m	N/m	N/m	N/m	N/m	N/m
9.8	4.4E+06	2.8E+07	-2.0E+07	2.8E+06	7.8E+06	2.0E+06	-1.3E+05	6.6E+06	-8.0E+04	-5.9E+04	-1.0E+05	-1.3E+05	-1.1E+05	-1.3E+05	-1.4E+05	-1.3E+05
19.5	5.2E+06	2.8E+07	-2.1E+07	2.1E+06	1.5E+07	7.6E+05	-2.1E+06	1.6E+07	-1.9E+05	-9.0E+04	-1.0E+05	-8.1E+04	-7.6E+04	-1.8E+05	-9.6E+04	-1.1E+05
29.3	5.8E+06	2.6E+07	-2.2E+07	2.6E+06	1.9E+07	4.5E+06	-1.1E+06	1.9E+07	-4.6E+04	-5.9E+04	-6.1E+04	-8.5E+04	-7.5E+04	-7.6E+04	-8.2E+04	-4.5E+04
39.1	3.5E+06	2.7E+07	-2.1E+07	4.3E+05	2.8E+07	2.3E+06	-4.6E+06	2.9E+07	-5.5E+04	-6.9E+04	-7.0E+04	-6.8E+04	-6.4E+04	-5.8E+04	-7.0E+04	-1.3E+05
48.8	2.6E+06	2.7E+07	-2.2E+07	-1.0E+06	3.6E+07	2.3E+06	-5.4E+06	3.6E+07	-3.2E+04	-1.0E+05	-6.7E+04	-9.0E+04	-8.6E+04	-3.5E+04	-5.7E+04	-6.6E+04
58.6	4.1E+05	2.6E+07	-2.2E+07	-3.1E+06	4.2E+07	3.6E+06	-7.0E+06	4.4E+07	-6.1E+04	-7.2E+04	-1.0E+05	-7.3E+04	-5.2E+04	-6.2E+04	-7.3E+04	-4.7E+04
68.4	-1.5E+06	2.7E+07	-2.3E+07	-4.5E+06	4.9E+07	3.6E+06	-8.0E+06	5.1E+07	-7.1E+04	-8.4E+04	-1.5E+05	-9.7E+04	-7.0E+04	-1.1E+05	-8.2E+04	-7.1E+04
78.1	-3.9E+06	2.6E+07	-2.3E+07	-7.3E+06	5.7E+07	4.5E+06	-9.1E+06	5.9E+07	-5.9E+04	-1.3E+05	-5.2E+04	-6.2E+04	-1.1E+05	-7.0E+04	-8.5E+04	-4.9E+04
87.9	-6.9E+06	2.6E+07	-2.4E+07	-1.0E+07	6.4E+07	5.4E+06	-9.7E+06	6.7E+07	-6.5E+04	-1.1E+05	-1.1E+05	-9.3E+04	-4.4E+04	-9.6E+04	-7.5E+04	-1.1E+05
97.7	-1.1E+07	2.6E+07	-2.5E+07	-1.3E+07	7.2E+07	6.3E+06	-1.0E+07	7.5E+07	-4.9E+04	-5.0E+04	-8.7E+04	-3.0E+04	-7.2E+04	-5.1E+04	-6.5E+04	-8.6E+04
107.4	-1.5E+07	2.4E+07	-2.5E+07	-1.8E+07	7.9E+07	5.8E+06	-1.2E+07	8.2E+07	-6.9E+04	-5.8E+04	-1.4E+05	-1.2E+05	-4.5E+04	-1.2E+05	-1.1E+05	-9.6E+04
117.2	-1.8E+07	2.6E+07	-2.6E+07	-2.1E+07	8.8E+07	7.7E+06	-1.3E+07	9.1E+07	-1.0E+05	-7.0E+04	-4.7E+04	-7.4E+04	-4.9E+04	-7.3E+04	-3.9E+04	-3.8E+04
127.0	-2.3E+07	2.6E+07	-2.4E+07	-2.5E+07	9.6E+07	8.9E+06	-1.4E+07	1.0E+08	-9.3E+04	-1.4E+05	-1.0E+05	-7.7E+04	-8.5E+04	-7.6E+04	-6.3E+04	-1.4E+05
136.7	-2.9E+07	2.7E+07	-2.4E+07	-3.0E+07	1.1E+08	8.5E+06	-1.5E+07	1.1E+08	-1.3E+05	-7.7E+04	-9.5E+04	-1.2E+05	-9.7E+04	-1.8E+05	-6.5E+04	-5.7E+04

Table 27 Raw data for the test seal at PD=27.6 bar, ω=3 krpm, and inlet GVF=8% with the zero-preswirl insert

Freq.	Re(H_{XX})	Re(H_{XY})	Re(H_{YX})	Re(H_{YY})	Im(H_{XX})	Im(H_{XY})	Im(H_{YX})	Im(H_{YY})	Re(eH_{XX})	Re(eH_{XY})	Re(eH_{YX})	Re(eH_{YY})	Im(eH_{XX})	Im(eH_{XY})	Im(eH_{YX})	Im(eH_{YY})
Hz	N/m	N/m	N/m	N/m	N/m	N/m	N/m	N/m	N/m	N/m	N/m	N/m	N/m	N/m	N/m	N/m
9.8	5.2E+06	2.5E+07	-1.3E+07	2.2E+06	8.2E+06	1.3E+06	-7.8E+05	6.3E+06	-1.2E+05	-2.0E+05	-1.1E+05	-1.6E+05	-1.4E+05	-9.8E+04	-1.4E+05	-1.5E+05
19.5	5.9E+06	2.4E+07	-1.4E+07	2.1E+06	1.6E+07	4.1E+05	-1.8E+06	1.6E+07	-1.5E+05	-1.5E+05	-8.5E+04	-1.1E+05	-1.7E+05	-1.2E+05	-1.5E+05	-8.7E+04
29.3	5.8E+06	2.2E+07	-1.5E+07	2.3E+06	2.0E+07	3.8E+06	-2.9E+05	1.9E+07	-8.7E+04	-1.1E+05	-5.1E+04	-6.3E+04	-8.0E+04	-7.3E+04	-8.4E+04	-3.5E+04
39.1	3.8E+06	2.2E+07	-1.4E+07	-1.4E+05	2.8E+07	6.8E+05	-3.8E+06	2.9E+07	-4.6E+04	-2.9E+04	-4.7E+04	-7.6E+04	-6.4E+04	-5.9E+04	-5.7E+04	-6.9E+04
48.8	2.4E+06	2.2E+07	-1.5E+07	-1.3E+06	3.6E+07	1.2E+06	-3.7E+06	3.7E+07	-1.1E+05	-8.6E+04	-8.0E+04	-7.2E+04	-7.2E+04	-6.2E+04	-9.7E+04	-7.8E+04
58.6	3.6E+05	2.2E+07	-1.5E+07	-4.0E+06	4.2E+07	2.2E+06	-5.6E+06	4.4E+07	-1.1E+05	-1.2E+05	-8.9E+04	-1.4E+05	-7.9E+04	-8.1E+04	-1.1E+05	-6.3E+04
68.4	-1.3E+06	2.2E+07	-1.6E+07	-4.3E+06	4.9E+07	1.1E+06	-6.0E+06	5.1E+07	-1.6E+05	-1.3E+05	-1.7E+05	-1.4E+05	-1.0E+05	-1.4E+05	-1.0E+05	-1.4E+05
78.1	-3.1E+06	2.1E+07	-1.5E+07	-8.6E+06	5.7E+07	1.7E+06	-8.1E+06	6.0E+07	-1.0E+05	-8.7E+04	-8.1E+04	-5.8E+04	-7.4E+04	-9.1E+04	-3.4E+04	-7.9E+04
87.9	-6.6E+06	2.1E+07	-1.7E+07	-1.1E+07	6.4E+07	2.5E+06	-8.1E+06	6.9E+07	-4.7E+04	-6.1E+04	-1.3E+05	-5.6E+04	-6.7E+04	-9.3E+04	-8.2E+04	-7.7E+04
97.7	-9.8E+06	2.1E+07	-1.7E+07	-1.3E+07	7.2E+07	3.2E+06	-8.7E+06	7.7E+07	-8.5E+04	-7.5E+04	-9.3E+04	-1.1E+05	-1.0E+05	-7.2E+04	-8.1E+04	-5.6E+04
107.4	-1.4E+07	1.9E+07	-1.8E+07	-1.8E+07	8.0E+07	2.2E+06	-9.8E+06	8.4E+07	-1.0E+05	-1.2E+05	-4.3E+04	-4.2E+04	-1.0E+05	-7.1E+04	-4.8E+04	-5.3E+04
117.2	-1.6E+07	2.1E+07	-1.8E+07	-2.0E+07	8.8E+07	3.5E+06	-1.0E+07	9.4E+07	-6.5E+04	-7.0E+04	-7.9E+04	-9.6E+04	-7.2E+04	-8.7E+04	-5.0E+04	-9.0E+04
127.0	-2.1E+07	2.1E+07	-1.6E+07	-2.4E+07	9.7E+07	4.3E+06	-1.1E+07	1.0E+08	-1.4E+05	-9.9E+04	-4.7E+04	-9.3E+04	-5.5E+04	-1.1E+05	-8.1E+04	-9.0E+04
136.7	-2.7E+07	2.1E+07	-1.6E+07	-2.7E+07	1.1E+08	3.8E+06	-1.1E+07	1.1E+08	-9.7E+04	-7.0E+04	-8.8E+04	-5.7E+04	-9.9E+04	-1.1E+05	-5.9E+04	-9.9E+04

Table 28 Raw data for the test seal at PD=27.6 bar, ω=4 krpm, and inlet GVF=8% with the zero-preswirl insert

Freq.	Re(H_{XX})	Re(H_{XY})	Re(H_{YX})	Re(H_{YY})	Im(H_{XX})	Im(H_{XY})	Im(H_{YX})	Im(H_{YY})	Re(eH_{XX})	Re(eH_{XY})	Re(eH_{YX})	Re(eH_{YY})	Im(eH_{XX})	Im(eH_{XY})	Im(eH_{YX})	Im(eH_{YY})
Hz	N/m	N/m	N/m	N/m	N/m	N/m	N/m	N/m	N/m	N/m	N/m	N/m	N/m	N/m	N/m	N/m
9.8	5.2E+06	2.4E+07	-1.3E+07	1.8E+06	8.1E+06	1.3E+06	-1.0E+06	6.1E+06	-1.3E+05	-1.6E+05	-9.5E+04	-1.4E+05	-1.0E+05	-9.6E+04	-1.5E+05	-1.5E+05
19.5	5.5E+06	2.3E+07	-1.5E+07	1.5E+06	1.6E+07	5.7E+05	-2.3E+06	1.6E+07	-7.3E+04	-1.1E+05	-1.1E+05	-9.4E+04	-9.6E+04	-1.2E+05	-1.0E+05	-1.2E+05
29.3	5.8E+06	2.2E+07	-1.6E+07	2.0E+06	2.0E+07	3.7E+06	-4.6E+05	1.9E+07	-1.2E+05	-4.4E+04	-6.8E+04	-5.0E+04	-6.3E+04	-1.1E+05	-8.1E+04	-9.7E+04
39.1	3.6E+06	2.2E+07	-1.5E+07	-3.3E+05	2.8E+07	8.1E+05	-3.8E+06	2.9E+07	-7.3E+04	-6.2E+04	-1.3E+05	-8.7E+04	-1.0E+05	-6.7E+04	-4.7E+04	-7.5E+04
48.8	2.2E+06	2.2E+07	-1.5E+07	-1.5E+06	3.6E+07	1.4E+06	-3.9E+06	3.7E+07	-1.7E+05	-7.5E+04	-8.8E+04	-9.3E+04	-9.3E+04	-9.3E+04	-1.1E+05	-1.3E+05
58.6	5.3E+05	2.2E+07	-1.5E+07	-4.4E+06	4.2E+07	1.9E+06	-5.8E+06	4.4E+07	-6.7E+04	-4.3E+04	-8.3E+04	-4.3E+04	-4.4E+04	-8.1E+04	-1.1E+05	-9.3E+04
68.4	-1.3E+06	2.2E+07	-1.6E+07	-4.7E+06	4.9E+07	1.3E+06	-6.0E+06	5.1E+07	-2.3E+05	-5.9E+04	-1.1E+05	-2.4E+05	-1.1E+05	-2.2E+05	-1.3E+05	-1.1E+05
78.1	-3.2E+06	2.1E+07	-1.5E+07	-8.6E+06	5.7E+07	1.8E+06	-8.0E+06	6.0E+07	-1.4E+05	-1.1E+05	-6.4E+04	-1.1E+05	-7.2E+04	-9.0E+04	-3.7E+04	-7.3E+04
87.9	-6.6E+06	2.1E+07	-1.7E+07	-1.1E+07	6.4E+07	2.6E+06	-8.2E+06	6.9E+07	-3.8E+04	-3.8E+04	-6.0E+04	-5.5E+04	-9.9E+04	-9.5E+04	-7.9E+04	-3.8E+04
97.7	-9.7E+06	2.0E+07	-1.7E+07	-1.3E+07	7.2E+07	3.2E+06	-8.6E+06	7.7E+07	-5.0E+04	-9.0E+04	-8.4E+04	-3.6E+04	-1.3E+05	-5.3E+04	-7.9E+04	-6.2E+04
107.4	-1.4E+07	1.9E+07	-1.9E+07	-1.8E+07	7.9E+07	2.1E+06	-9.8E+06	8.5E+07	-1.0E+05	-7.7E+04	-7.9E+04	-1.2E+05	-1.3E+05	-7.3E+04	-9.1E+04	-9.2E+04
117.2	-1.7E+07	2.0E+07	-1.8E+07	-2.0E+07	8.8E+07	3.7E+06	-1.0E+07	9.4E+07	-5.6E+04	-9.0E+04	-9.1E+04	-7.6E+04	-5.6E+04	-4.7E+04	-1.3E+05	-7.0E+04
127.0	-2.1E+07	2.0E+07	-1.7E+07	-2.4E+07	9.7E+07	4.7E+06	-1.1E+07	1.0E+08	-9.7E+04	-9.5E+04	-8.5E+04	-1.2E+05	-5.2E+04	-4.8E+04	-6.9E+04	-1.6E+05
136.7	-2.7E+07	2.0E+07	-1.6E+07	-2.7E+07	1.1E+08	4.0E+06	-1.1E+07	1.1E+08	-7.0E+04	-6.0E+04	-8.6E+04	-1.3E+05	-1.5E+05	-1.7E+05	-1.1E+05	-1.2E+05

Table 29 Raw data for the test seal at PD=27.6 bar, ω=5 krpm, and inlet GVF=8% with the zero-preswirl insert

Freq.	Re(H_{XX})	Re(H_{XY})	Re(H_{YX})	Re(H_{YY})	Im(H_{XX})	Im(H_{XY})	Im(H_{YX})	Im(H_{YY})	Re(eH_{XX})	Re(eH_{XY})	Re(eH_{YX})	Re(eH_{YY})	Im(eH_{XX})	Im(eH_{XY})	Im(eH_{YX})	Im(eH_{YY})
Hz	N/m	N/m	N/m	N/m	N/m	N/m	N/m	N/m	N/m	N/m	N/m	N/m	N/m	N/m	N/m	N/m
9.8	5.4E+06	3.0E+07	-1.9E+07	2.1E+06	8.0E+06	2.5E+06	-2.1E+05	7.0E+06	-1.3E+05	-1.4E+05	-1.1E+05	-8.9E+04	-1.3E+05	-1.3E+05	-1.1E+05	-1.2E+05
19.5	6.8E+06	3.0E+07	-2.0E+07	2.0E+06	1.6E+07	5.7E+05	-1.9E+06	1.6E+07	-8.5E+04	-1.7E+05	-9.6E+04	-1.5E+05	-1.7E+05	-1.3E+05	-1.5E+05	-1.2E+05
29.3	6.2E+06	2.8E+07	-2.2E+07	1.9E+06	2.0E+07	4.9E+06	-7.0E+05	1.9E+07	-4.3E+04	-3.5E+04	-6.1E+04	-8.1E+04	-6.9E+04	-5.9E+04	-8.8E+04	-5.5E+04
39.1	4.3E+06	2.8E+07	-2.1E+07	-6.6E+05	2.8E+07	1.6E+06	-4.4E+06	2.9E+07	-5.2E+04	-8.2E+04	-5.6E+04	-6.1E+04	-8.0E+04	-7.8E+04	-5.6E+04	-8.5E+04
48.8	3.2E+06	2.8E+07	-2.1E+07	-2.1E+06	3.6E+07	2.0E+06	-5.1E+06	3.7E+07	-9.4E+04	-7.2E+04	-1.1E+05	-6.0E+04	-8.3E+04	-6.4E+04	-5.1E+04	-6.1E+04
58.6	1.0E+06	2.8E+07	-2.1E+07	-4.3E+06	4.3E+07	3.6E+06	-6.5E+06	4.5E+07	-1.0E+05	-3.8E+04	-1.1E+05	-8.6E+04	-6.3E+04	-8.5E+04	-6.4E+04	-5.8E+04
68.4	-7.4E+05	2.9E+07	-2.3E+07	-5.6E+06	5.1E+07	3.0E+06	-7.2E+06	5.3E+07	-1.0E+05	-8.0E+04	-9.5E+04	-1.1E+05	-7.2E+04	-1.2E+05	-6.8E+04	-9.3E+04
78.1	-3.2E+06	2.7E+07	-2.2E+07	-8.0E+06	5.8E+07	3.9E+06	-8.5E+06	6.1E+07	-3.3E+04	-6.0E+04	-5.9E+04	-4.4E+04	-8.2E+04	-4.2E+04	-7.5E+04	-7.4E+04
87.9	-5.9E+06	2.8E+07	-2.4E+07	-1.1E+07	6.5E+07	4.7E+06	-8.8E+06	7.0E+07	-6.5E+04	-5.3E+04	-7.4E+04	-6.5E+04	-5.9E+04	-6.5E+04	-8.3E+04	-1.1E+05
97.7	-9.1E+06	2.8E+07	-2.4E+07	-1.2E+07	7.3E+07	5.7E+06	-9.3E+06	7.8E+07	-7.8E+04	-5.2E+04	-4.2E+04	-4.7E+04	-8.3E+04	-7.2E+04	-5.1E+04	-7.5E+04
107.4	-1.3E+07	2.6E+07	-2.5E+07	-1.7E+07	8.1E+07	4.8E+06	-1.1E+07	8.5E+07	-1.2E+05	-9.1E+04	-8.4E+04	-1.1E+05	-9.8E+04	-5.8E+04	-8.3E+04	-9.5E+04
117.2	-1.6E+07	2.7E+07	-2.5E+07	-1.9E+07	8.9E+07	6.5E+06	-1.2E+07	9.5E+07	-6.2E+04	-7.5E+04	-5.4E+04	-7.7E+04	-9.6E+04	-5.7E+04	-8.2E+04	-8.0E+04
127.0	-2.1E+07	2.8E+07	-2.3E+07	-2.3E+07	9.8E+07	7.8E+06	-1.2E+07	1.0E+08	-1.5E+05	-1.3E+05	-4.9E+04	-1.7E+05	-9.3E+04	-1.6E+05	-1.2E+05	-1.1E+05
136.7	-2.5E+07	2.8E+07	-2.3E+07	-2.7E+07	1.1E+08	6.8E+06	-1.3E+07	1.1E+08	-1.0E+05	-1.1E+05	-9.9E+04	-7.9E+04	-7.8E+04	-1.1E+05	-1.3E+05	-1.0E+05

Table 30 Raw data for the test seal at PD=27.6 bar, ω=3 krpm, and inlet GVF=10% with the zero-preswirl insert

Freq.	Re(H_{XX})	Re(H_{XY})	Re(H_{YX})	Re(H_{YY})	Im(H_{XX})	Im(H_{XY})	Im(H_{YX})	Im(H_{YY})	Re(eH_{XX})	Re(eH_{XY})	Re(eH_{YX})	Re(eH_{YY})	Im(eH_{XX})	Im(eH_{XY})	Im(eH_{YX})	Im(eH_{YY})
Hz	N/m	N/m	N/m	N/m	N/m	N/m	N/m	N/m	N/m	N/m	N/m	N/m	N/m	N/m	N/m	N/m
9.8	5.4E+06	2.4E+07	-1.3E+07	2.1E+06	8.7E+06	1.8E+06	3.3E+04	6.5E+06	-1.5E+05	-1.1E+05	-6.9E+04	-9.4E+04	-8.7E+04	-1.8E+05	-9.0E+04	-8.9E+04
19.5	6.2E+06	2.3E+07	-1.5E+07	1.2E+06	1.5E+07	5.7E+05	-1.9E+06	1.5E+07	-8.7E+04	-5.5E+04	-1.0E+05	-5.8E+04	-7.5E+04	-8.4E+04	-6.9E+04	-9.9E+04
29.3	6.1E+06	2.2E+07	-1.6E+07	1.6E+06	2.0E+07	4.1E+06	7.7E+04	1.9E+07	-9.4E+04	-7.7E+04	-4.5E+04	-7.7E+04	-9.8E+04	-6.0E+04	-1.1E+05	-4.3E+04
39.1	4.0E+06	2.2E+07	-1.5E+07	-8.4E+05	2.8E+07	9.0E+05	-3.3E+06	2.9E+07	-9.9E+04	-4.9E+04	-8.3E+04	-8.0E+04	-5.7E+04	-9.6E+04	-7.4E+04	-8.3E+04
48.8	2.5E+06	2.2E+07	-1.5E+07	-1.8E+06	3.6E+07	1.3E+06	-3.4E+06	3.7E+07	-1.2E+05	-7.3E+04	-8.2E+04	-8.7E+04	-1.4E+05	-8.8E+04	-7.8E+04	-5.6E+04
58.6	9.1E+05	2.1E+07	-1.5E+07	-4.7E+06	4.2E+07	2.2E+06	-5.1E+06	4.4E+07	-3.9E+04	-1.1E+05	-1.3E+05	-9.4E+04	-8.3E+04	-3.2E+04	-8.1E+04	-8.7E+04
68.4	-5.6E+05	2.2E+07	-1.6E+07	-4.6E+06	4.9E+07	6.5E+05	-5.5E+06	5.1E+07	-1.0E+05	-1.6E+05	-1.0E+05	-1.9E+05	-1.3E+05	-1.2E+05	-1.3E+05	-1.4E+05
78.1	-2.7E+06	2.1E+07	-1.5E+07	-9.0E+06	5.7E+07	1.5E+06	-7.9E+06	6.0E+07	-9.6E+04	-9.4E+04	-6.3E+04	-9.2E+04	-6.3E+04	-8.7E+04	-5.5E+04	-7.8E+04
87.9	-6.1E+06	2.1E+07	-1.7E+07	-1.1E+07	6.4E+07	2.2E+06	-7.9E+06	6.9E+07	-5.4E+04	-5.4E+04	-7.5E+04	-3.8E+04	-8.0E+04	-8.5E+04	-5.8E+04	-1.1E+05
97.7	-9.1E+06	2.1E+07	-1.7E+07	-1.4E+07	7.2E+07	2.9E+06	-8.7E+06	7.8E+07	-1.0E+05	-7.4E+04	-9.2E+04	-6.8E+04	-3.7E+04	-8.0E+04	-3.4E+04	-8.0E+04
107.4	-1.4E+07	1.9E+07	-1.8E+07	-1.8E+07	8.0E+07	1.6E+06	-9.7E+06	8.5E+07	-1.2E+05	-7.0E+04	-1.0E+05	-7.6E+04	-1.4E+05	-7.3E+04	-9.2E+04	-5.1E+04
117.2	-1.5E+07	2.0E+07	-1.8E+07	-1.9E+07	8.8E+07	3.3E+06	-1.0E+07	9.5E+07	-9.9E+04	-6.1E+04	-4.2E+04	-9.5E+04	-6.5E+04	-4.2E+04	-6.6E+04	-9.3E+04
127.0	-2.0E+07	2.0E+07	-1.5E+07	-2.3E+07	9.6E+07	4.0E+06	-1.0E+07	1.0E+08	-5.8E+04	-8.1E+04	-7.6E+04	-9.1E+04	-1.2E+05	-1.4E+05	-7.2E+04	-2.1E+05
136.7	-2.5E+07	2.0E+07	-1.5E+07	-2.5E+07	1.1E+08	3.1E+06	-1.2E+07	1.1E+08	-1.1E+05	-1.6E+05	-1.2E+05	-1.0E+05	-1.1E+05	-1.1E+05	-1.3E+05	-7.3E+04

Table 31 Raw data for the test seal at PD=27.6 bar, ω=4 krpm, and inlet GVF=10% with the zero-preswirl insert

Freq.	Re(H_{XX})	Re(H_{XY})	Re(H_{YX})	Re(H_{YY})	Im(H_{XX})	Im(H_{XY})	Im(H_{YX})	Im(H_{YY})	Re(eH_{XX})	Re(eH_{XY})	Re(eH_{YX})	Re(eH_{YY})	Im(eH_{XX})	Im(eH_{XY})	Im(eH_{YX})	Im(eH_{YY})
Hz	N/m	N/m	N/m	N/m	N/m	N/m	N/m	N/m	N/m	N/m	N/m	N/m	N/m	N/m	N/m	N/m
9.8	5.2E+06	2.3E+07	-1.3E+07	1.2E+06	8.0E+06	1.5E+06	-8.1E+05	6.1E+06	-8.5E+04	-1.4E+05	-1.1E+05	-1.2E+05	-1.5E+05	-1.4E+05	-9.6E+04	-1.2E+05
19.5	6.0E+06	2.3E+07	-1.5E+07	1.1E+06	1.6E+07	6.4E+05	-1.9E+06	1.5E+07	-1.5E+05	-5.9E+04	-7.5E+04	-1.1E+05	-7.8E+04	-1.3E+05	-8.1E+04	-8.0E+04
29.3	6.0E+06	2.2E+07	-1.6E+07	1.4E+06	2.0E+07	4.1E+06	-2.3E+05	2.0E+07	-1.1E+05	-1.0E+05	-9.0E+04	-1.0E+05	-1.0E+05	-7.3E+04	-7.8E+04	-7.0E+04
39.1	4.0E+06	2.2E+07	-1.5E+07	-9.5E+05	2.8E+07	8.6E+05	-3.4E+06	2.9E+07	-5.4E+04	-6.7E+04	-5.8E+04	-6.1E+04	-1.1E+05	-5.0E+04	-6.0E+04	-6.4E+04
48.8	2.5E+06	2.2E+07	-1.5E+07	-1.9E+06	3.6E+07	1.3E+06	-3.6E+06	3.7E+07	-1.1E+05	-1.1E+05	-8.5E+04	-6.8E+04	-9.4E+04	-5.4E+04	-7.8E+04	-5.0E+04
58.6	1.1E+06	2.2E+07	-1.5E+07	-4.9E+06	4.2E+07	1.8E+06	-5.4E+06	4.4E+07	-6.3E+04	-9.0E+04	-1.2E+05	-3.4E+04	-7.0E+04	-6.3E+04	-8.3E+04	-9.9E+04
68.4	-6.4E+05	2.2E+07	-1.6E+07	-4.9E+06	5.0E+07	3.0E+05	-5.7E+06	5.1E+07	-1.2E+05	-2.3E+05	-1.4E+05	-6.8E+04	-1.4E+05	-2.0E+05	-1.2E+05	-1.2E+05
78.1	-2.6E+06	2.1E+07	-1.5E+07	-9.0E+06	5.7E+07	1.4E+06	-7.8E+06	6.0E+07	-1.0E+05	-5.7E+04	-6.4E+04	-1.3E+05	-9.4E+04	-6.9E+04	-1.1E+05	-7.0E+04
87.9	-6.1E+06	2.1E+07	-1.7E+07	-1.1E+07	6.4E+07	2.2E+06	-7.9E+06	6.9E+07	-7.5E+04	-4.0E+04	-6.7E+04	-7.4E+04	-6.9E+04	-1.0E+05	-7.4E+04	-8.6E+04
97.7	-9.3E+06	2.1E+07	-1.7E+07	-1.4E+07	7.2E+07	2.8E+06	-8.7E+06	7.8E+07	-8.5E+04	-1.4E+05	-7.6E+04	-3.2E+04	-8.2E+04	-5.3E+04	-6.2E+04	-1.3E+05
107.4	-1.3E+07	1.9E+07	-1.9E+07	-1.8E+07	8.0E+07	1.7E+06	-9.9E+06	8.6E+07	-7.5E+04	-7.2E+04	-7.1E+04	-1.0E+05	-7.4E+04	-1.2E+05	-3.7E+04	-1.2E+05
117.2	-1.5E+07	2.0E+07	-1.8E+07	-1.9E+07	8.8E+07	3.3E+06	-9.9E+06	9.5E+07	-1.2E+05	-1.1E+05	-5.8E+04	-5.2E+04	-8.6E+04	-5.0E+04	-6.2E+04	-1.1E+05
127.0	-2.0E+07	2.0E+07	-1.6E+07	-2.2E+07	9.7E+07	4.1E+06	-1.0E+07	1.0E+08	-1.2E+05	-1.1E+05	-1.4E+05	-1.3E+05	-7.9E+04	-1.1E+05	-7.7E+04	-8.2E+04
136.7	-2.5E+07	2.0E+07	-1.6E+07	-2.5E+07	1.1E+08	3.4E+06	-1.1E+07	1.1E+08	-1.8E+05	-1.2E+05	-9.0E+04	-1.9E+05	-1.5E+05	-1.7E+05	-9.6E+04	-1.9E+05

Table 32 Raw data for the test seal at PD=27.6 bar, ω=5 krpm, and inlet GVF=10% with the zero-preswirl insert

Freq.	Re(H_{XX})	Re(H_{XY})	Re(H_{YX})	Re(H_{YY})	Im(H_{XX})	Im(H_{XY})	Im(H_{YX})	Im(H_{YY})	Re(eH_{XX})	Re(eH_{XY})	Re(eH_{YX})	Re(eH_{YY})	Im(eH_{XX})	Im(eH_{XY})	Im(eH_{YX})	Im(eH_{YY})
Hz	N/m	N/m	N/m	N/m	N/m	N/m	N/m	N/m	N/m	N/m	N/m	N/m	N/m	N/m	N/m	N/m
9.8	4.5E+06	3.0E+07	-2.0E+07	1.3E+06	7.9E+06	2.2E+06	-1.0E+05	6.9E+06	-3.2E+05	-3.5E+05	-1.6E+05	-2.0E+05	-2.5E+05	-2.5E+05	-1.5E+05	-9.7E+04
19.5	5.9E+06	3.0E+07	-2.1E+07	8.3E+05	1.7E+07	1.0E+06	-1.1E+06	1.6E+07	-1.3E+05	-1.7E+05	-1.5E+05	-1.5E+05	-1.8E+05	-1.7E+05	-1.4E+05	-1.8E+05
29.3	5.3E+06	2.9E+07	-2.3E+07	6.0E+05	2.1E+07	5.5E+06	1.3E+05	2.0E+07	-1.0E+05	-5.2E+04	-7.9E+04	-7.9E+04	-9.3E+04	-9.8E+04	-9.5E+04	-5.3E+04
39.1	3.6E+06	2.9E+07	-2.1E+07	-1.7E+06	2.9E+07	2.3E+06	-3.0E+06	3.0E+07	-3.4E+04	-5.2E+04	-1.1E+05	-1.0E+05	-4.3E+04	-7.0E+04	-8.2E+04	-8.0E+04
48.8	2.8E+06	2.9E+07	-2.2E+07	-3.6E+06	3.8E+07	2.6E+06	-4.0E+06	3.8E+07	-1.8E+05	-6.6E+04	-8.1E+04	-7.2E+04	-8.6E+04	-1.1E+05	-1.0E+05	-7.8E+04
58.6	5.6E+05	2.8E+07	-2.2E+07	-5.0E+06	4.3E+07	3.7E+06	-5.5E+06	4.6E+07	-7.1E+04	-7.7E+04	-1.2E+05	-1.0E+05	-9.5E+04	-1.3E+05	-1.1E+05	-8.3E+04
68.4	-1.1E+06	2.9E+07	-2.2E+07	-6.8E+06	5.1E+07	2.5E+06	-6.6E+06	5.4E+07	-8.5E+04	-9.3E+04	-8.0E+04	-1.0E+05	-5.1E+04	-8.7E+04	-1.2E+05	-1.5E+05
78.1	-2.7E+06	2.9E+07	-2.2E+07	-8.5E+06	5.9E+07	3.8E+06	-7.3E+06	6.2E+07	-1.3E+05	-9.4E+04	-6.2E+04	-4.2E+04	-9.1E+04	-9.9E+04	-7.0E+04	-8.8E+04
87.9	-5.7E+06	2.9E+07	-2.4E+07	-1.2E+07	6.6E+07	4.4E+06	-8.4E+06	7.1E+07	-9.4E+04	-1.2E+05	-9.0E+04	-1.0E+05	-8.0E+04	-9.7E+04	-1.2E+05	-7.9E+04
97.7	-8.7E+06	2.9E+07	-2.4E+07	-1.3E+07	7.4E+07	5.1E+06	-8.8E+06	8.0E+07	-1.3E+05	-7.0E+04	-9.4E+04	-5.5E+04	-5.4E+04	-5.2E+04	-4.4E+04	-5.9E+04
107.4	-1.2E+07	2.7E+07	-2.5E+07	-1.7E+07	8.2E+07	3.8E+06	-1.0E+07	8.8E+07	-8.4E+04	-8.7E+04	-9.7E+04	-5.2E+04	-4.4E+04	-4.6E+04	-1.1E+05	-8.3E+04
117.2	-1.4E+07	2.8E+07	-2.5E+07	-1.9E+07	9.0E+07	5.3E+06	-1.1E+07	9.7E+07	-5.9E+04	-3.2E+04	-9.1E+04	-3.6E+04	-4.7E+04	-7.6E+04	-6.8E+04	-4.6E+04
127.0	-1.8E+07	2.8E+07	-2.3E+07	-2.1E+07	9.8E+07	6.5E+06	-1.0E+07	1.0E+08	-9.5E+04	-1.1E+05	-6.5E+04	-1.5E+05	-8.0E+04	-1.2E+05	-8.5E+04	-1.4E+05
136.7	-2.4E+07	2.9E+07	-2.3E+07	-2.4E+07	1.1E+08	5.9E+06	-1.2E+07	1.2E+08	-1.3E+05	-9.8E+04	-1.4E+05	-1.4E+05	-8.3E+04	-9.9E+04	-7.0E+04	-1.0E+05

Table 33 Raw data for the test seal at PD=34.5 bar, ω=3 krpm, and inlet GVF=0% with the zero-preswirl insert

Freq.	Re(H_{XX})	Re(H_{XY})	Re(H_{YX})	Re(H_{YY})	Im(H_{XX})	Im(H_{XY})	Im(H_{YX})	Im(H_{YY})	Re(eH_{XX})	Re(eH_{XY})	Re(eH_{YX})	Re(eH_{YY})	Im(eH_{XX})	Im(eH_{XY})	Im(eH_{YX})	Im(eH_{YY})
Hz	N/m	N/m	N/m	N/m	N/m	N/m	N/m	N/m	N/m	N/m	N/m	N/m	N/m	N/m	N/m	N/m
9.8	5.6E+06	2.7E+07	-1.0E+07	7.1E+06	7.9E+06	1.7E+06	-1.4E+06	6.1E+06	-1.2E+05	-1.4E+05	-1.6E+05	-1.6E+05	-7.3E+04	-1.3E+05	-1.4E+05	-1.9E+05
19.5	4.9E+06	2.7E+07	-1.1E+07	6.3E+06	1.6E+07	1.5E+06	-3.6E+06	1.6E+07	-1.1E+05	-1.2E+05	-1.4E+05	-1.1E+05	-1.0E+05	-1.1E+05	-1.3E+05	-2.0E+05
29.3	4.2E+06	2.7E+07	-1.2E+07	6.8E+06	2.2E+07	4.5E+06	-2.8E+06	2.2E+07	-7.8E+04	-1.2E+05	-9.5E+04	-1.3E+05	-1.5E+05	-1.1E+05	-8.8E+04	-1.3E+05
39.1	2.5E+06	2.7E+07	-1.1E+07	5.4E+06	3.0E+07	1.6E+06	-6.3E+06	3.1E+07	-5.2E+04	-6.4E+04	-1.0E+05	-5.4E+04	-9.1E+04	-8.3E+04	-9.3E+04	-1.1E+05
48.8	2.4E+05	2.7E+07	-1.2E+07	3.9E+06	3.9E+07	1.8E+06	-8.0E+06	3.8E+07	-1.2E+05	-1.2E+05	-7.2E+04	-1.5E+05	-1.1E+05	-1.3E+05	-1.1E+05	-9.2E+04
58.6	-1.9E+06	2.6E+07	-1.3E+07	2.0E+05	4.5E+07	1.5E+06	-9.5E+06	4.5E+07	-9.7E+04	-1.9E+05	-1.1E+05	-1.2E+05	-1.3E+05	-1.6E+05	-1.5E+05	-1.2E+05
68.4	-4.9E+06	2.6E+07	-1.4E+07	-4.1E+05	5.3E+07	1.7E+06	-1.0E+07	5.2E+07	-2.0E+05	-2.4E+05	-2.5E+05	-2.5E+05	-3.0E+05	-2.1E+05	-2.2E+05	-1.6E+05
78.1	-6.4E+06	2.5E+07	-1.5E+07	-5.5E+06	6.2E+07	1.1E+06	-1.2E+07	6.0E+07	-1.7E+05	-1.2E+05	-1.1E+05	-1.5E+05	-7.8E+04	-1.1E+05	-1.1E+05	-1.1E+05
87.9	-1.2E+07	2.4E+07	-1.5E+07	-8.9E+06	6.9E+07	2.5E+06	-1.3E+07	6.9E+07	-1.0E+05	-7.6E+04	-9.8E+04	-9.1E+04	-1.1E+05	-8.6E+04	-7.0E+04	-1.4E+05
97.7	-1.6E+07	2.4E+07	-1.6E+07	-1.3E+07	7.8E+07	3.2E+06	-1.5E+07	7.6E+07	-1.6E+05	-1.3E+05	-9.5E+04	-5.4E+04	-1.4E+05	-9.6E+04	-1.3E+05	-1.2E+05
107.4	-2.0E+07	2.3E+07	-1.7E+07	-2.0E+07	8.6E+07	2.7E+06	-1.6E+07	8.3E+07	-2.3E+05	-1.5E+05	-1.2E+05	-2.3E+05	-1.1E+05	-8.9E+04	-1.8E+05	-8.3E+04
117.2	-2.4E+07	2.3E+07	-1.8E+07	-2.5E+07	9.4E+07	4.4E+06	-1.8E+07	9.2E+07	-1.9E+05	-1.1E+05	-1.1E+05	-5.1E+04	-1.2E+05	-1.7E+05	-8.2E+04	-9.9E+04
127.0	-3.0E+07	2.4E+07	-1.9E+07	-3.3E+07	1.0E+08	5.5E+06	-1.9E+07	1.0E+08	-1.4E+05	-1.4E+05	-1.1E+05	-1.1E+05	-1.5E+05	-1.9E+05	-1.2E+05	-2.8E+05
136.7	-3.8E+07	2.3E+07	-1.9E+07	-3.9E+07	1.1E+08	7.1E+06	-1.9E+07	1.1E+08	-3.0E+05	-1.9E+05	-2.0E+05	-1.4E+05	-1.2E+05	-1.7E+05	-1.6E+05	-2.0E+05

Table 34 Raw data for the test seal at PD=34.5 bar, ω=4 krpm, and inlet GVF=0% with the zero-preswirl insert

Freq.	Re(H_{XX})	Re(H_{XY})	Re(H_{YX})	Re(H_{YY})	Im(H_{XX})	Im(H_{XY})	Im(H_{YX})	Im(H_{YY})	Re(eH_{XX})	Re(eH_{XY})	Re(eH_{YX})	Re(eH_{YY})	Im(eH_{XX})	Im(eH_{XY})	Im(eH_{YX})	Im(eH_{YY})
Hz	N/m	N/m	N/m	N/m	N/m	N/m	N/m	N/m	N/m	N/m	N/m	N/m	N/m	N/m	N/m	N/m
9.8	7.5E+06	2.7E+07	-1.1E+07	3.4E+06	8.0E+06	1.2E+06	-1.2E+06	6.6E+06	-1.3E+05	-1.9E+05	-9.4E+04	-1.3E+05	-1.5E+05	-1.6E+05	-1.0E+05	-1.4E+05
19.5	6.7E+06	2.7E+07	-1.1E+07	2.7E+06	1.5E+07	1.0E+06	-3.4E+06	1.6E+07	-1.7E+05	-1.9E+05	-8.3E+04	-1.4E+05	-1.5E+05	-1.5E+05	-1.6E+05	-1.2E+05
29.3	6.2E+06	2.6E+07	-1.2E+07	2.5E+06	2.1E+07	4.6E+06	-2.5E+06	2.2E+07	-1.4E+05	-1.5E+05	-2.1E+05	-1.0E+05	-1.3E+05	-7.8E+04	-1.5E+05	-1.6E+05
39.1	3.6E+06	2.7E+07	-1.2E+07	1.5E+06	3.0E+07	1.4E+06	-6.6E+06	3.2E+07	-1.5E+05	-1.4E+05	-1.0E+05	-1.1E+05	-1.4E+05	-8.9E+04	-1.4E+05	-1.1E+05
48.8	1.5E+06	2.7E+07	-1.3E+07	4.2E+05	3.8E+07	9.2E+05	-8.5E+06	3.9E+07	-2.0E+05	-1.4E+05	-2.0E+05	-1.6E+05	-1.1E+05	-1.4E+05	-1.1E+05	-1.2E+05
58.6	-9.6E+05	2.6E+07	-1.3E+07	-3.8E+06	4.4E+07	1.9E+06	-1.0E+07	4.7E+07	-8.8E+04	-2.6E+05	-1.4E+05	-5.0E+04	-1.3E+05	-2.4E+05	-7.5E+04	-1.3E+05
68.4	-3.6E+06	2.6E+07	-1.5E+07	-3.7E+06	5.2E+07	2.3E+05	-9.7E+06	5.3E+07	-1.1E+05	-1.3E+05	-2.7E+05	-1.3E+05	-1.0E+05	-1.7E+05	-1.7E+05	-1.7E+05
78.1	-4.9E+06	2.4E+07	-1.5E+07	-8.4E+06	6.1E+07	4.0E+04	-1.2E+07	6.2E+07	-8.8E+04	-6.6E+04	-2.4E+05	-1.0E+05	-1.2E+05	-9.1E+04	-1.2E+05	-1.6E+05
87.9	-1.1E+07	2.5E+07	-1.6E+07	-1.2E+07	6.8E+07	1.6E+06	-1.3E+07	7.1E+07	-1.0E+05	-2.0E+05	-9.9E+04	-6.8E+04	-9.9E+04	-1.5E+05	-1.2E+05	-1.1E+05
97.7	-1.5E+07	2.4E+07	-1.7E+07	-1.6E+07	7.6E+07	2.1E+06	-1.5E+07	7.8E+07	-8.1E+04	-1.7E+05	-1.2E+05	-4.8E+04	-1.6E+05	-1.2E+05	-1.4E+05	-6.0E+04
107.4	-1.9E+07	2.2E+07	-1.8E+07	-2.2E+07	8.4E+07	1.7E+06	-1.6E+07	8.5E+07	-1.6E+05	-8.1E+04	-1.8E+05	-6.8E+04	-8.6E+04	-1.8E+05	-1.3E+05	-9.6E+04
117.2	-2.4E+07	2.3E+07	-1.9E+07	-2.7E+07	9.1E+07	3.4E+06	-1.7E+07	9.4E+07	-1.4E+05	-8.0E+04	-1.5E+05	-1.6E+05	-1.7E+05	-1.4E+05	-1.8E+05	-7.3E+04
127.0	-3.0E+07	2.3E+07	-1.9E+07	-3.4E+07	1.0E+08	4.8E+06	-1.8E+07	1.0E+08	-7.8E+04	-2.1E+05	-1.5E+05	-2.0E+05	-1.4E+05	-1.8E+05	-2.1E+05	-3.1E+05
136.7	-3.8E+07	2.3E+07	-1.9E+07	-4.0E+07	1.1E+08	6.3E+06	-1.9E+07	1.1E+08	-1.3E+05	-9.5E+04	-8.3E+04	-1.5E+05	-2.5E+05	-1.5E+05	-1.9E+05	-2.6E+05

Table 35 Raw data for the test seal at PD=34.5 bar, ω=5 krpm, and inlet GVF=0% with the zero-preswirl insert

Freq.	Re(H_{XX})	Re(H_{XY})	Re(H_{YX})	Re(H_{YY})	Im(H_{XX})	Im(H_{XY})	Im(H_{YX})	Im(H_{YY})	Re(eH_{XX})	Re(eH_{XY})	Re(eH_{YX})	Re(eH_{YY})	Im(eH_{XX})	Im(eH_{XY})	Im(eH_{YX})	Im(eH_{YY})
Hz	N/m	N/m	N/m	N/m	N/m	N/m	N/m	N/m	N/m	N/m	N/m	N/m	N/m	N/m	N/m	N/m
9.8	8.9E+06	3.4E+07	-1.8E+07	2.3E+06	8.8E+06	1.7E+06	2.6E+05	6.8E+06	-1.3E+05	-1.4E+05	-1.2E+05	-2.0E+05	-1.3E+05	-1.6E+05	-1.5E+05	-1.2E+05
19.5	6.9E+06	3.4E+07	-2.0E+07	2.4E+05	1.6E+07	2.0E+06	-2.4E+06	1.7E+07	-8.5E+04	-1.6E+05	-1.0E+05	-1.7E+05	-1.3E+05	-9.3E+04	-1.7E+05	-1.8E+05
29.3	6.1E+06	3.3E+07	-2.1E+07	-1.2E+04	2.2E+07	5.8E+06	-1.3E+06	2.2E+07	-1.3E+05	-1.5E+05	-1.1E+05	-1.2E+05	-1.9E+05	-1.8E+05	-1.6E+05	-1.3E+05
39.1	4.9E+06	3.3E+07	-2.0E+07	-2.2E+06	3.0E+07	2.0E+06	-5.3E+06	3.3E+07	-7.3E+04	-7.2E+04	-7.1E+04	-9.8E+04	-9.9E+04	-1.1E+05	-1.1E+05	-1.1E+05
48.8	3.3E+06	3.3E+07	-2.0E+07	-3.7E+06	3.8E+07	1.9E+06	-7.1E+06	4.1E+07	-9.8E+04	-9.4E+04	-8.2E+04	-9.8E+04	-1.3E+05	-1.0E+05	-1.3E+05	-9.0E+04
58.6	3.0E+05	3.2E+07	-2.1E+07	-6.4E+06	4.4E+07	3.4E+06	-9.3E+06	4.9E+07	-1.3E+05	-1.0E+05	-1.2E+05	-1.2E+05	-9.3E+04	-1.5E+05	-1.0E+05	-1.5E+05
68.4	-2.2E+06	3.2E+07	-2.2E+07	-8.4E+06	5.3E+07	9.8E+05	-1.1E+07	5.6E+07	-5.3E+04	-1.1E+05	-1.1E+05	-1.8E+05	-1.2E+05	-1.3E+05	-1.1E+05	-1.0E+05
78.1	-5.3E+06	3.0E+07	-2.1E+07	-1.1E+07	6.0E+07	2.8E+06	-1.3E+07	6.5E+07	-1.7E+05	-1.3E+05	-1.0E+05	-7.1E+04	-1.2E+05	-1.7E+05	-1.0E+05	-1.0E+05
87.9	-9.3E+06	3.1E+07	-2.3E+07	-1.5E+07	6.8E+07	3.9E+06	-1.3E+07	7.4E+07	-1.6E+05	-1.6E+05	-1.6E+05	-1.3E+05	-6.4E+04	-1.5E+05	-1.4E+05	-1.6E+05
97.7	-1.4E+07	3.1E+07	-2.3E+07	-1.8E+07	7.6E+07	5.2E+06	-1.5E+07	8.2E+07	-2.2E+05	-8.8E+04	-7.3E+04	-7.0E+04	-1.5E+05	-1.5E+05	-8.7E+04	-8.2E+04
107.4	-1.8E+07	2.9E+07	-2.4E+07	-2.3E+07	8.4E+07	4.5E+06	-1.6E+07	8.9E+07	-7.6E+04	-9.3E+04	-7.0E+04	-2.7E+05	-1.5E+05	-1.1E+05	-2.3E+05	-1.1E+05
117.2	-2.3E+07	3.0E+07	-2.5E+07	-2.8E+07	9.2E+07	6.4E+06	-1.9E+07	9.9E+07	-1.4E+05	-8.6E+04	-1.3E+05	-1.2E+05	-1.2E+05	-1.0E+05	-8.2E+04	-1.2E+05
127.0	-3.0E+07	2.9E+07	-2.4E+07	-3.4E+07	1.0E+08	8.6E+06	-2.0E+07	1.1E+08	-1.7E+05	-1.2E+05	-1.1E+05	-8.9E+04	-1.0E+05	-1.8E+05	-8.8E+04	-1.6E+05
136.7	-3.7E+07	2.9E+07	-2.6E+07	-3.9E+07	1.1E+08	8.9E+06	-2.1E+07	1.2E+08	-1.3E+05	-1.3E+05	-8.7E+04	-1.0E+05	-1.3E+05	-1.4E+05	-1.5E+05	-1.8E+05

Table 36 Raw data for the test seal at PD=34.5 bar, ω=3 krpm, and inlet GVF=2% with the zero-preswirl insert

Freq.	Re(H_{XX})	Re(H_{XY})	Re(H_{YX})	Re(H_{YY})	Im(H_{XX})	Im(H_{XY})	Im(H_{YX})	Im(H_{YY})	Re(eH_{XX})	Re(eH_{XY})	Re(eH_{YX})	Re(eH_{YY})	Im(eH_{XX})	Im(eH_{XY})	Im(eH_{YX})	Im(eH_{YY})
Hz	N/m	N/m	N/m	N/m	N/m	N/m	N/m	N/m	N/m	N/m	N/m	N/m	N/m	N/m	N/m	N/m
9.8	8.1E+06	2.8E+07	-9.9E+06	6.2E+06	8.4E+06	1.7E+06	-1.4E+06	6.2E+06	-6.9E+04	-1.3E+05	-1.3E+05	-1.8E+05	-1.5E+05	-1.6E+05	-8.2E+04	-1.1E+05
19.5	8.1E+06	2.8E+07	-1.1E+07	5.7E+06	1.6E+07	8.3E+05	-3.1E+06	1.6E+07	-1.2E+05	-8.2E+04	-1.6E+05	-1.8E+05	-8.1E+04	-1.7E+05	-1.5E+05	-1.2E+05
29.3	7.3E+06	2.8E+07	-1.2E+07	5.8E+06	2.2E+07	4.2E+06	-2.1E+06	2.2E+07	-8.3E+04	-7.2E+04	-1.4E+05	-8.8E+04	-1.3E+05	-1.0E+05	-1.3E+05	-1.1E+05
39.1	5.8E+06	2.7E+07	-1.1E+07	4.7E+06	3.1E+07	-1.1E+05	-5.5E+06	3.2E+07	-9.1E+04	-7.9E+04	-9.2E+04	-7.8E+04	-9.7E+04	-7.9E+04	-7.0E+04	-7.3E+04
48.8	3.9E+06	2.7E+07	-1.2E+07	4.5E+06	3.9E+07	4.7E+05	-6.6E+06	3.9E+07	-1.9E+05	-4.9E+04	-1.0E+05	-1.2E+05	-8.7E+04	-1.3E+05	-1.1E+05	-1.0E+05
58.6	2.4E+06	2.6E+07	-1.2E+07	1.2E+06	4.5E+07	6.9E+05	-7.9E+06	4.6E+07	-1.0E+05	-1.9E+05	-1.3E+05	-1.0E+05	-1.1E+05	-1.5E+05	-6.9E+04	-8.6E+04
68.4	5.8E+04	2.6E+07	-1.3E+07	1.5E+06	5.3E+07	-1.1E+04	-8.1E+06	5.3E+07	-9.5E+04	-1.8E+05	-1.0E+05	-1.3E+05	-7.5E+04	-1.4E+05	-1.8E+05	-1.0E+05
78.1	-1.8E+06	2.5E+07	-1.4E+07	-4.1E+06	6.1E+07	4.6E+04	-1.0E+07	6.2E+07	-1.5E+05	-9.9E+04	-8.3E+04	-5.0E+04	-1.4E+05	-9.8E+04	-8.5E+04	-1.1E+05
87.9	-6.2E+06	2.5E+07	-1.4E+07	-6.4E+06	6.9E+07	8.5E+05	-1.1E+07	7.1E+07	-6.6E+04	-1.6E+05	-5.2E+04	-8.9E+04	-6.4E+04	-1.0E+05	-1.2E+05	-4.4E+04
97.7	-9.7E+06	2.4E+07	-1.5E+07	-9.6E+06	7.7E+07	1.5E+06	-1.3E+07	7.9E+07	-9.6E+04	-1.3E+05	-9.3E+04	-9.6E+04	-8.4E+04	-5.9E+04	-1.1E+05	-4.9E+04
107.4	-1.4E+07	2.2E+07	-1.7E+07	-1.6E+07	8.5E+07	1.3E+06	-1.5E+07	8.6E+07	-1.6E+05	-1.5E+05	-1.2E+05	-1.0E+05	-1.5E+05	-7.7E+04	-1.3E+05	-8.7E+04
117.2	-1.6E+07	2.3E+07	-1.7E+07	-1.8E+07	9.4E+07	2.8E+06	-1.5E+07	9.6E+07	-1.4E+05	-4.9E+04	-1.5E+05	-1.1E+05	-5.5E+04	-9.7E+04	-6.3E+04	-1.0E+05
127.0	-2.2E+07	2.3E+07	-1.7E+07	-2.3E+07	1.0E+08	3.7E+06	-1.6E+07	1.0E+08	-1.5E+05	-1.2E+05	-1.0E+05	-1.4E+05	-8.0E+04	-1.3E+05	-4.1E+04	-1.6E+05
136.7	-2.9E+07	2.3E+07	-1.7E+07	-2.9E+07	1.1E+08	4.1E+06	-1.8E+07	1.1E+08	-1.6E+05	-1.9E+05	-1.6E+05	-1.5E+05	-9.9E+04	-2.0E+05	-1.3E+05	-8.6E+04

Table 37 Raw data for the test seal at PD=34.5 bar, ω=4 krpm, and inlet GVF=2% with the zero-preswirl insert

Freq.	Re(H_{XX})	Re(H_{XY})	Re(H_{YX})	Re(H_{YY})	Im(H_{XX})	Im(H_{XY})	Im(H_{YX})	Im(H_{YY})	Re(eH_{XX})	Re(eH_{XY})	Re(eH_{YX})	Re(eH_{YY})	Im(eH_{XX})	Im(eH_{XY})	Im(eH_{YX})	Im(eH_{YY})
Hz	N/m	N/m	N/m	N/m	N/m	N/m	N/m	N/m	N/m	N/m	N/m	N/m	N/m	N/m	N/m	N/m
9.8	8.1E+06	2.8E+07	-1.0E+07	6.8E+06	8.8E+06	1.3E+06	-1.2E+06	6.2E+06	-1.3E+05	-1.6E+05	-1.3E+05	-1.9E+05	-1.0E+05	-1.3E+05	-1.3E+05	-1.2E+05
19.5	7.7E+06	2.8E+07	-1.0E+07	6.1E+06	1.6E+07	9.1E+05	-3.0E+06	1.6E+07	-8.6E+04	-1.5E+05	-1.9E+05	-1.1E+05	-1.8E+05	-1.6E+05	-1.3E+05	-2.1E+05
29.3	7.4E+06	2.8E+07	-1.2E+07	5.7E+06	2.2E+07	3.9E+06	-2.1E+06	2.1E+07	-8.8E+04	-9.5E+04	-1.1E+05	-9.5E+04	-1.3E+05	-9.4E+04	-8.5E+04	-6.4E+04
39.1	6.0E+06	2.8E+07	-1.1E+07	5.4E+06	3.1E+07	-1.9E+05	-5.4E+06	3.2E+07	-6.3E+04	-6.5E+04	-1.4E+05	-1.4E+05	-7.2E+04	-8.5E+04	-1.2E+05	-1.2E+05
48.8	4.7E+06	2.7E+07	-1.2E+07	5.1E+06	3.9E+07	4.6E+05	-6.1E+06	3.9E+07	-1.0E+05	-1.4E+05	-1.3E+05	-1.1E+05	-6.8E+04	-9.6E+04	-1.3E+05	-1.4E+05
58.6	2.6E+06	2.6E+07	-1.1E+07	1.5E+06	4.5E+07	8.3E+05	-7.9E+06	4.6E+07	-8.5E+04	-2.2E+05	-1.5E+05	-9.4E+04	-6.9E+04	-9.4E+04	-1.2E+05	-1.4E+05
68.4	1.7E+05	2.6E+07	-1.3E+07	1.5E+06	5.2E+07	-3.9E+05	-8.3E+06	5.3E+07	-7.8E+04	-1.9E+05	-6.0E+04	-1.5E+05	-1.6E+05	-1.5E+05	-1.4E+05	-1.1E+05
78.1	-1.5E+06	2.6E+07	-1.3E+07	-3.4E+06	6.1E+07	-2.2E+05	-1.0E+07	6.2E+07	-1.3E+05	-8.7E+04	-7.6E+04	-8.5E+04	-1.3E+05	-1.1E+05	-9.0E+04	-1.8E+05
87.9	-5.9E+06	2.5E+07	-1.4E+07	-5.9E+06	6.9E+07	4.9E+05	-1.2E+07	7.1E+07	-7.0E+04	-7.1E+04	-5.6E+04	-1.5E+05	-1.2E+05	-3.8E+04	-7.4E+04	-9.6E+04
97.7	-9.5E+06	2.4E+07	-1.5E+07	-9.1E+06	7.8E+07	1.5E+06	-1.3E+07	7.9E+07	-1.4E+05	-6.0E+04	-8.9E+04	-5.3E+04	-3.0E+04	-1.0E+05	-1.4E+05	-7.7E+04
107.4	-1.4E+07	2.2E+07	-1.6E+07	-1.5E+07	8.6E+07	8.4E+05	-1.5E+07	8.6E+07	-8.5E+04	-8.6E+04	-1.3E+05	-7.7E+04	-1.1E+05	-9.9E+04	-9.9E+04	-1.3E+05
117.2	-1.6E+07	2.3E+07	-1.6E+07	-1.8E+07	9.3E+07	2.6E+06	-1.6E+07	9.6E+07	-6.7E+04	-1.1E+05	-5.3E+04	-1.0E+05	-1.4E+05	-8.1E+04	-1.0E+05	-9.7E+04
127.0	-2.2E+07	2.3E+07	-1.7E+07	-2.3E+07	1.0E+08	3.8E+06	-1.7E+07	1.0E+08	-1.1E+05	-1.1E+05	-1.3E+05	-1.0E+05	-1.3E+05	-2.0E+05	-1.4E+05	-1.0E+05
136.7	-2.9E+07	2.3E+07	-1.7E+07	-2.9E+07	1.1E+08	4.0E+06	-1.8E+07	1.1E+08	-2.1E+05	-1.5E+05	-1.6E+05	-1.3E+05	-1.3E+05	-2.6E+05	-1.4E+05	-2.1E+05

Table 38 Raw data for the test seal at PD=34.5 bar, ω=5 krpm, and inlet GVF=2% with the zero-preswirl insert

Freq.	Re(H_{XX})	Re(H_{XY})	Re(H_{YX})	Re(H_{YY})	Im(H_{XX})	Im(H_{XY})	Im(H_{YX})	Im(H_{YY})	Re(eH_{XX})	Re(eH_{XY})	Re(eH_{YX})	Re(eH_{YY})	Im(eH_{XX})	Im(eH_{XY})	Im(eH_{YX})	Im(eH_{YY})
Hz	N/m	N/m	N/m	N/m	N/m	N/m	N/m	N/m	N/m	N/m	N/m	N/m	N/m	N/m	N/m	N/m
9.8	6.6E+06	3.4E+07	-1.6E+07	6.5E+06	8.3E+06	2.3E+06	-1.4E+05	6.5E+06	-1.1E+05	-1.6E+05	-9.5E+04	-1.3E+05	-1.4E+05	-1.8E+05	-1.5E+05	-2.0E+05
19.5	6.4E+06	3.5E+07	-1.8E+07	5.8E+06	1.6E+07	1.5E+06	-2.8E+06	1.7E+07	-1.6E+05	-1.1E+05	-1.3E+05	-1.3E+05	-1.3E+05	-2.3E+05	-1.3E+05	-1.9E+05
29.3	5.6E+06	3.5E+07	-1.9E+07	5.5E+06	2.2E+07	4.4E+06	-2.1E+06	2.3E+07	-9.9E+04	-9.4E+04	-1.4E+05	-1.2E+05	-8.2E+04	-1.0E+05	-1.1E+05	-9.4E+04
39.1	3.8E+06	3.4E+07	-1.9E+07	4.0E+06	3.1E+07	7.5E+05	-5.7E+06	3.3E+07	-5.8E+04	-9.3E+04	-1.2E+05	-1.1E+05	-8.3E+04	-8.4E+04	-1.1E+05	-7.7E+04
48.8	2.8E+06	3.3E+07	-2.0E+07	3.6E+06	4.1E+07	6.6E+05	-6.4E+06	4.1E+07	-1.1E+05	-1.3E+05	-8.4E+04	-1.1E+05	-2.0E+05	-1.1E+05	-1.3E+05	-9.6E+04
58.6	1.3E+06	3.2E+07	-1.9E+07	1.3E+06	4.7E+07	2.3E+06	-7.8E+06	4.8E+07	-9.3E+04	-1.2E+05	-1.1E+05	-9.9E+04	-7.0E+04	-1.3E+05	-9.8E+04	-7.0E+04
68.4	-9.2E+05	3.3E+07	-2.1E+07	2.7E+05	5.4E+07	1.3E+06	-8.9E+06	5.5E+07	-1.3E+05	-9.7E+04	-1.1E+05	-9.6E+04	-1.0E+05	-1.0E+05	-1.4E+05	-1.5E+05
78.1	-3.3E+06	3.2E+07	-2.0E+07	-3.8E+06	6.2E+07	2.2E+06	-1.1E+07	6.3E+07	-1.4E+05	-9.2E+04	-9.2E+04	-1.0E+05	-1.1E+05	-1.6E+05	-8.4E+04	-9.1E+04
87.9	-7.4E+06	3.2E+07	-2.2E+07	-7.1E+06	7.0E+07	3.4E+06	-1.2E+07	7.3E+07	-1.3E+05	-1.0E+05	-5.8E+04	-8.2E+04	-8.2E+04	-1.5E+05	-1.2E+05	-1.4E+05
97.7	-1.1E+07	3.1E+07	-2.3E+07	-9.3E+06	7.9E+07	4.1E+06	-1.3E+07	8.2E+07	-1.2E+05	-1.2E+05	-2.4E+05	-8.9E+04	-9.5E+04	-8.0E+04	-8.0E+04	-1.4E+05
107.4	-1.5E+07	2.9E+07	-2.4E+07	-1.5E+07	8.7E+07	3.0E+06	-1.5E+07	8.8E+07	-1.1E+05	-1.3E+05	-1.3E+05	-1.2E+05	-1.1E+05	-1.5E+05	-1.4E+05	-1.5E+05
117.2	-1.8E+07	3.0E+07	-2.5E+07	-1.8E+07	9.5E+07	4.9E+06	-1.6E+07	9.8E+07	-1.3E+05	-1.2E+05	-4.4E+04	-4.7E+04	-5.6E+04	-8.5E+04	-8.7E+04	-1.2E+05
127.0	-2.3E+07	3.1E+07	-2.3E+07	-2.3E+07	1.0E+08	6.9E+06	-1.8E+07	1.1E+08	-1.7E+05	-7.2E+04	-5.7E+04	-1.7E+05	-6.7E+04	-1.1E+05	-6.6E+04	-1.1E+05
136.7	-3.0E+07	3.0E+07	-2.4E+07	-2.8E+07	1.1E+08	6.5E+06	-2.0E+07	1.2E+08	-2.5E+05	-8.5E+04	-6.0E+04	-7.7E+04	-1.2E+05	-9.8E+04	-5.6E+04	-1.2E+05

Table 39 Raw data for the test seal at PD=34.5 bar, ω=3 krpm, and inlet GVF=4% with the zero-preswirl insert

Freq.	Re(H_{XX})	Re(H_{XY})	Re(H_{YX})	Re(H_{YY})	Im(H_{XX})	Im(H_{XY})	Im(H_{YX})	Im(H_{YY})	Re(eH_{XX})	Re(eH_{XY})	Re(eH_{YX})	Re(eH_{YY})	Im(eH_{XX})	Im(eH_{XY})	Im(eH_{YX})	Im(eH_{YY})
Hz	N/m	N/m	N/m	N/m	N/m	N/m	N/m	N/m	N/m	N/m	N/m	N/m	N/m	N/m	N/m	N/m
9.8	7.3E+06	2.9E+07	-1.0E+07	6.4E+06	9.1E+06	1.1E+06	-1.7E+06	6.6E+06	-1.0E+05	-1.8E+05	-8.8E+04	-9.8E+04	-1.1E+05	-1.1E+05	-1.1E+05	-1.7E+05
19.5	7.1E+06	2.9E+07	-1.1E+07	6.2E+06	1.7E+07	-3.0E+05	-3.2E+06	1.7E+07	-6.8E+04	-1.8E+05	-1.2E+05	-1.4E+05	-2.4E+05	-2.0E+05	-9.7E+04	-9.8E+04
29.3	7.7E+06	2.7E+07	-1.2E+07	7.7E+06	2.2E+07	3.5E+06	-6.4E+05	2.1E+07	-1.0E+05	-1.0E+05	-8.1E+04	-8.8E+04	-1.3E+05	-9.1E+04	-1.3E+05	-9.6E+04
39.1	5.4E+06	2.7E+07	-1.0E+07	5.6E+06	3.1E+07	6.6E+05	-4.6E+06	3.1E+07	-6.8E+04	-8.0E+04	-6.1E+04	-7.2E+04	-1.3E+05	-8.6E+04	-6.0E+04	-5.9E+04
48.8	3.9E+06	2.8E+07	-1.1E+07	3.7E+06	4.0E+07	5.0E+05	-6.4E+06	3.9E+07	-1.2E+05	-1.2E+05	-1.6E+05	-1.2E+05	-1.4E+05	-5.3E+04	-1.5E+05	-1.4E+05
58.6	2.0E+06	2.7E+07	-1.1E+07	1.1E+06	4.7E+07	1.7E+06	-7.2E+06	4.7E+07	-9.2E+04	-9.0E+04	-8.9E+04	-1.5E+05	-1.5E+05	-1.9E+05	-8.5E+04	-1.5E+05
68.4	9.3E+05	2.7E+07	-1.3E+07	2.1E+06	5.5E+07	-1.4E+05	-7.7E+06	5.5E+07	-2.5E+05	-1.3E+05	-2.1E+05	-2.6E+05	-1.4E+05	-3.2E+05	-2.6E+05	-1.8E+05
78.1	-5.2E+05	2.6E+07	-1.4E+07	-2.5E+06	6.3E+07	-5.3E+04	-9.1E+06	6.4E+07	-8.4E+04	-7.4E+04	-1.2E+05	-7.7E+04	-1.4E+05	-1.2E+05	-1.0E+05	-1.4E+05
87.9	-4.8E+06	2.6E+07	-1.4E+07	-5.4E+06	7.1E+07	1.1E+06	-1.0E+07	7.3E+07	-3.4E+04	-1.2E+05	-4.9E+04	-6.7E+04	-1.1E+05	-9.6E+04	-5.3E+04	-1.1E+05
97.7	-7.9E+06	2.5E+07	-1.5E+07	-8.5E+06	8.0E+07	1.7E+06	-1.2E+07	8.2E+07	-4.7E+04	-1.2E+05	-1.1E+05	-1.2E+05	-7.9E+04	-7.1E+04	-2.0E+05	-5.2E+04
107.4	-1.2E+07	2.3E+07	-1.7E+07	-1.4E+07	8.8E+07	3.9E+05	-1.4E+07	8.9E+07	-1.3E+05	-1.3E+05	-2.0E+05	-9.6E+04	-1.3E+05	-1.4E+05	-1.3E+05	-1.9E+05
117.2	-1.4E+07	2.4E+07	-1.7E+07	-1.6E+07	9.7E+07	2.2E+06	-1.4E+07	9.9E+07	-7.7E+04	-1.4E+05	-8.4E+04	-1.6E+05	-2.9E+04	-8.0E+04	-9.1E+04	-1.0E+05
127.0	-2.0E+07	2.5E+07	-1.7E+07	-2.1E+07	1.1E+08	3.3E+06	-1.5E+07	1.1E+08	-8.2E+04	-1.7E+05	-1.6E+05	-1.6E+05	-1.2E+05	-2.6E+05	-1.6E+05	-1.4E+05
136.7	-2.6E+07	2.5E+07	-1.6E+07	-2.6E+07	1.2E+08	2.5E+06	-1.6E+07	1.2E+08	-7.6E+04	-1.3E+05	-2.0E+05	-8.5E+04	-7.1E+04	-8.7E+04	-1.0E+05	-1.3E+05

Table 40 Raw data for the test seal at PD=34.5 bar, ω=4 krpm, and inlet GVF=4% with the zero-preswirl insert

Freq.	Re(H_{XX})	Re(H_{XY})	Re(H_{YX})	Re(H_{YY})	Im(H_{XX})	Im(H_{XY})	Im(H_{YX})	Im(H_{YY})	Re(eH_{XX})	Re(eH_{XY})	Re(eH_{YX})	Re(eH_{YY})	Im(eH_{XX})	Im(eH_{XY})	Im(eH_{YX})	Im(eH_{YY})
Hz	N/m	N/m	N/m	N/m	N/m	N/m	N/m	N/m	N/m	N/m	N/m	N/m	N/m	N/m	N/m	N/m
9.8	6.4E+06	2.9E+07	-9.9E+06	6.0E+06	9.5E+06	7.9E+05	-1.7E+06	6.4E+06	-9.0E+04	-1.8E+05	-1.2E+05	-1.5E+05	-1.2E+05	-1.3E+05	-8.9E+04	-1.4E+05
19.5	6.5E+06	2.9E+07	-1.1E+07	5.9E+06	1.7E+07	-5.3E+05	-3.2E+06	1.7E+07	-1.3E+05	-1.5E+05	-1.1E+05	-1.5E+05	-1.0E+05	-1.3E+05	-1.6E+05	-1.3E+05
29.3	6.5E+06	2.7E+07	-1.2E+07	7.1E+06	2.2E+07	3.5E+06	-1.1E+06	2.1E+07	-1.5E+05	-8.3E+04	-1.2E+05	-5.5E+04	-1.2E+05	-1.3E+05	-6.9E+04	-1.0E+05
39.1	4.1E+06	2.7E+07	-1.1E+07	5.4E+06	3.1E+07	7.0E+05	-4.7E+06	3.1E+07	-7.3E+04	-7.2E+04	-5.1E+04	-7.1E+04	-1.2E+05	-7.0E+04	-8.7E+04	-4.1E+04
48.8	2.8E+06	2.8E+07	-1.1E+07	3.7E+06	4.0E+07	4.9E+05	-5.8E+06	3.9E+07	-8.3E+04	-1.0E+05	-1.9E+05	-1.0E+05	-1.8E+05	-1.2E+05	-1.2E+05	-1.4E+05
58.6	9.5E+05	2.7E+07	-1.1E+07	7.5E+05	4.7E+07	1.5E+06	-6.9E+06	4.7E+07	-6.2E+04	-1.6E+05	-1.3E+05	-8.0E+04	-1.3E+05	-1.7E+05	-1.3E+05	-2.6E+05
68.4	-1.9E+05	2.7E+07	-1.3E+07	2.1E+06	5.5E+07	-4.7E+05	-7.7E+06	5.4E+07	-2.5E+05	-2.9E+05	-1.7E+05	-1.2E+05	-1.9E+05	-2.1E+05	-2.5E+05	-1.6E+05
78.1	-1.9E+06	2.6E+07	-1.3E+07	-2.9E+06	6.3E+07	9.2E+03	-9.6E+06	6.4E+07	-9.2E+04	-1.6E+05	-1.4E+05	-7.7E+04	-9.4E+04	-1.1E+05	-7.7E+04	-1.1E+05
87.9	-6.1E+06	2.6E+07	-1.4E+07	-5.3E+06	7.1E+07	1.2E+06	-1.0E+07	7.3E+07	-8.6E+04	-1.8E+05	-8.5E+04	-1.7E+05	-1.3E+05	-9.6E+04	-1.1E+05	-1.6E+05
97.7	-9.2E+06	2.6E+07	-1.4E+07	-8.7E+06	8.0E+07	1.7E+06	-1.1E+07	8.2E+07	-1.1E+05	-8.1E+04	-1.1E+05	-9.1E+04	-6.4E+04	-7.8E+04	-8.5E+04	-8.6E+04
107.4	-1.3E+07	2.3E+07	-1.6E+07	-1.4E+07	8.9E+07	2.9E+05	-1.3E+07	8.8E+07	-7.3E+04	-7.3E+04	-1.8E+05	-1.8E+05	-2.0E+05	-7.8E+04	-1.4E+05	-7.3E+04
117.2	-1.5E+07	2.5E+07	-1.6E+07	-1.6E+07	9.7E+07	2.1E+06	-1.4E+07	9.8E+07	-6.2E+04	-4.4E+04	-1.2E+05	-1.0E+05	-1.4E+05	-6.0E+04	-9.7E+04	-9.4E+04
127.0	-2.0E+07	2.5E+07	-1.6E+07	-2.2E+07	1.1E+08	3.1E+06	-1.5E+07	1.1E+08	-3.5E+04	-2.8E+05	-6.9E+04	-1.8E+05	-1.6E+05	-1.2E+05	-1.4E+05	-1.7E+05
136.7	-2.6E+07	2.5E+07	-1.6E+07	-2.6E+07	1.2E+08	2.0E+06	-1.6E+07	1.2E+08	-1.5E+05	-1.6E+05	-7.5E+04	-1.3E+05	-9.7E+04	-1.2E+05	-8.6E+04	-9.6E+04

Table 41 Raw data for the test seal at PD=34.5 bar, ω=5 krpm, and inlet GVF=4% with the zero-preswirl insert

Freq.	Re(H_{XX})	Re(H_{XY})	Re(H_{YX})	Re(H_{YY})	Im(H_{XX})	Im(H_{XY})	Im(H_{YX})	Im(H_{YY})	Re(eH_{XX})	Re(eH_{XY})	Re(eH_{YX})	Re(eH_{YY})	Im(eH_{XX})	Im(eH_{XY})	Im(eH_{YX})	Im(eH_{YY})
Hz	N/m	N/m	N/m	N/m	N/m	N/m	N/m	N/m	N/m	N/m	N/m	N/m	N/m	N/m	N/m	N/m
9.8	6.5E+06	3.6E+07	-1.7E+07	6.6E+06	9.0E+06	1.0E+06	-6.9E+05	7.0E+06	-1.9E+05	-1.7E+05	-1.2E+05	-1.4E+05	-7.0E+04	-2.4E+05	-1.3E+05	-2.2E+05
19.5	6.2E+06	3.5E+07	-1.8E+07	6.5E+06	1.7E+07	-8.0E+05	-2.7E+06	1.7E+07	-1.2E+05	-1.8E+05	-1.5E+05	-1.7E+05	-1.5E+05	-1.5E+05	-1.5E+05	-1.9E+05
29.3	6.7E+06	3.3E+07	-1.9E+07	7.7E+06	2.2E+07	4.2E+06	-8.1E+05	2.2E+07	-1.2E+05	-9.7E+04	-9.6E+04	-1.5E+05	-1.1E+05	-1.1E+05	-8.4E+04	-6.9E+04
39.1	4.3E+06	3.3E+07	-1.9E+07	4.9E+06	3.2E+07	9.8E+05	-4.3E+06	3.2E+07	-1.3E+05	-7.6E+04	-9.4E+04	-1.3E+05	-1.0E+05	-1.1E+05	-1.2E+05	-1.1E+05
48.8	2.7E+06	3.4E+07	-1.9E+07	3.5E+06	4.1E+07	1.5E+06	-5.0E+06	4.1E+07	-8.2E+04	-1.2E+05	-1.1E+05	-8.5E+04	-1.8E+05	-1.1E+05	-1.1E+05	-1.1E+05
58.6	8.6E+05	3.3E+07	-1.9E+07	9.2E+05	4.8E+07	3.1E+06	-6.9E+06	4.9E+07	-9.1E+04	-1.5E+05	-9.7E+04	-1.2E+05	-7.7E+04	-1.0E+05	-1.0E+05	-8.8E+04
68.4	-1.7E+05	3.3E+07	-2.0E+07	1.2E+06	5.6E+07	1.3E+06	-7.5E+06	5.6E+07	-1.7E+05	-1.6E+05	-1.7E+05	-1.0E+05	-1.3E+05	-8.9E+04	-6.0E+04	-9.8E+04
78.1	-2.4E+06	3.2E+07	-2.0E+07	-2.8E+06	6.4E+07	2.3E+06	-9.3E+06	6.6E+07	-1.2E+05	-1.8E+05	-9.6E+04	-1.1E+05	-1.4E+05	-8.7E+04	-7.4E+04	-9.4E+04
87.9	-6.3E+06	3.2E+07	-2.2E+07	-5.5E+06	7.3E+07	3.6E+06	-1.0E+07	7.5E+07	-8.3E+04	-1.5E+05	-1.3E+05	-1.6E+05	-1.3E+05	-1.7E+05	-1.5E+05	-2.0E+05
97.7	-9.4E+06	3.2E+07	-2.3E+07	-7.6E+06	8.2E+07	4.6E+06	-1.1E+07	8.5E+07	-1.2E+05	-9.5E+04	-1.3E+05	-1.2E+05	-1.2E+05	-6.9E+04	-1.7E+05	-8.3E+04
107.4	-1.3E+07	3.0E+07	-2.4E+07	-1.2E+07	9.0E+07	3.3E+06	-1.2E+07	9.1E+07	-1.6E+05	-1.1E+05	-1.4E+05	-1.1E+05	-1.2E+05	-1.4E+05	-1.1E+05	-1.0E+05
117.2	-1.5E+07	3.2E+07	-2.4E+07	-1.5E+07	9.9E+07	4.9E+06	-1.3E+07	1.0E+08	-1.2E+05	-7.8E+04	-1.2E+05	-1.1E+05	-7.2E+04	-1.1E+05	-1.5E+05	-1.3E+05
127.0	-2.1E+07	3.3E+07	-2.3E+07	-2.0E+07	1.1E+08	6.8E+06	-1.4E+07	1.1E+08	-1.1E+05	-5.4E+04	-8.8E+04	-9.4E+04	-1.2E+05	-1.5E+05	-1.1E+05	-8.6E+04
136.7	-2.6E+07	3.3E+07	-2.4E+07	-2.4E+07	1.2E+08	5.3E+06	-1.5E+07	1.2E+08	-1.6E+05	-2.0E+05	-1.2E+05	-2.2E+05	-8.3E+04	-1.1E+05	-1.1E+05	-9.2E+04

Table 42 Raw data for the test seal at PD=34.5 bar, ω=3 krpm, and inlet GVF=6% with the zero-preswirl insert

Freq.	Re(H_{XX})	Re(H_{XY})	Re(H_{YX})	Re(H_{YY})	Im(H_{XX})	Im(H_{XY})	Im(H_{YX})	Im(H_{YY})	Re(eH_{XX})	Re(eH_{XY})	Re(eH_{YX})	Re(eH_{YY})	Im(eH_{XX})	Im(eH_{XY})	Im(eH_{YX})	Im(eH_{YY})
Hz	N/m	N/m	N/m	N/m	N/m	N/m	N/m	N/m	N/m	N/m	N/m	N/m	N/m	N/m	N/m	N/m
9.8	6.5E+06	3.0E+07	-9.9E+06	6.0E+06	9.3E+06	1.2E+06	-6.7E+05	7.6E+06	-2.5E+05	-3.9E+05	-1.6E+05	-1.7E+05	-1.6E+05	-1.8E+05	-2.1E+05	-3.3E+05
19.5	6.8E+06	3.0E+07	-1.1E+07	6.9E+06	1.7E+07	-7.7E+05	-1.7E+06	1.7E+07	-1.2E+05	-1.4E+05	-1.8E+05	-8.2E+04	-8.3E+04	-1.4E+05	-4.6E+04	-1.7E+05
29.3	6.1E+06	2.8E+07	-1.2E+07	7.1E+06	2.2E+07	3.4E+06	-2.2E+05	2.2E+07	-8.5E+04	-8.0E+04	-1.2E+05	-1.0E+05	-6.5E+04	-6.8E+04	-6.5E+04	-1.3E+05
39.1	4.1E+06	2.8E+07	-1.1E+07	4.8E+06	3.2E+07	2.3E+05	-4.1E+06	3.2E+07	-6.4E+04	-7.0E+04	-9.7E+04	-6.3E+04	-9.7E+04	-1.1E+05	-9.5E+04	-1.0E+05
48.8	2.8E+06	2.9E+07	-1.2E+07	3.9E+06	4.0E+07	4.9E+05	-4.2E+06	4.1E+07	-1.0E+05	-1.2E+05	-1.2E+05	-1.2E+05	-1.3E+05	-1.0E+05	-1.6E+05	-8.8E+04
58.6	7.1E+05	2.8E+07	-1.1E+07	8.7E+05	4.7E+07	2.2E+06	-6.3E+06	4.9E+07	-9.3E+04	-7.3E+04	-1.1E+05	-1.4E+05	-7.8E+04	-1.3E+05	-1.7E+05	-1.7E+05
68.4	-7.4E+05	2.8E+07	-1.3E+07	1.3E+06	5.6E+07	-1.0E+05	-7.0E+06	5.6E+07	-2.8E+05	-2.8E+05	-3.1E+05	-2.8E+05	-2.7E+05	-2.5E+05	-2.3E+05	-3.1E+05
78.1	-1.7E+06	2.7E+07	-1.3E+07	-2.6E+06	6.4E+07	-4.3E+05	-8.4E+06	6.6E+07	-1.2E+05	-9.6E+04	-1.3E+05	-1.6E+05	-1.7E+05	-1.2E+05	-2.0E+05	-9.3E+04
87.9	-5.5E+06	2.7E+07	-1.4E+07	-5.1E+06	7.3E+07	3.3E+05	-9.2E+06	7.6E+07	-7.4E+04	-1.1E+05	-9.3E+04	-1.3E+05	-6.4E+04	-1.1E+05	-1.8E+05	-5.0E+04
97.7	-8.1E+06	2.7E+07	-1.4E+07	-8.0E+06	8.2E+07	9.0E+05	-9.9E+06	8.5E+07	-1.4E+05	-3.5E+04	-1.9E+05	-1.4E+05	-8.9E+04	-7.8E+04	-1.2E+05	-9.8E+04
107.4	-1.2E+07	2.5E+07	-1.6E+07	-1.2E+07	9.0E+07	-3.1E+05	-1.2E+07	9.3E+07	-1.5E+05	-1.0E+05	-1.7E+05	-1.4E+05	-1.7E+05	-1.2E+05	-2.5E+05	-1.5E+05
117.2	-1.3E+07	2.6E+07	-1.6E+07	-1.4E+07	9.9E+07	9.7E+05	-1.1E+07	1.0E+08	-1.0E+05	-8.0E+04	-6.6E+04	-7.4E+04	-8.7E+04	-1.5E+05	-1.5E+05	-8.2E+04
127.0	-1.8E+07	2.6E+07	-1.4E+07	-1.8E+07	1.1E+08	2.2E+06	-1.2E+07	1.1E+08	-1.7E+05	-5.2E+04	-1.2E+05	-1.4E+05	-1.1E+05	-2.6E+05	-1.2E+05	-1.0E+05
136.7	-2.3E+07	2.5E+07	-1.4E+07	-2.1E+07	1.2E+08	1.3E+06	-1.3E+07	1.2E+08	-1.3E+05	-1.1E+05	-1.4E+05	-2.1E+05	-1.4E+05	-1.3E+05	-1.6E+05	-1.6E+05

Table 43 Raw data for the test seal at PD=34.5 bar, ω=4 krpm, and inlet GVF=6% with the zero-preswirl insert

Freq.	Re(H_{XX})	Re(H_{XY})	Re(H_{YX})	Re(H_{YY})	Im(H_{XX})	Im(H_{XY})	Im(H_{YX})	Im(H_{YY})	Re(eH_{XX})	Re(eH_{XY})	Re(eH_{YX})	Re(eH_{YY})	Im(eH_{XX})	Im(eH_{XY})	Im(eH_{YX})	Im(eH_{YY})
Hz	N/m	N/m	N/m	N/m	N/m	N/m	N/m	N/m	N/m	N/m	N/m	N/m	N/m	N/m	N/m	N/m
9.8	7.0E+06	3.1E+07	-9.8E+06	5.5E+06	9.4E+06	8.8E+05	-9.5E+05	7.2E+06	-1.4E+05	-2.0E+05	-1.7E+05	-1.7E+05	-1.1E+05	-1.9E+05	-8.8E+04	-2.0E+05
19.5	7.0E+06	2.9E+07	-1.1E+07	6.2E+06	1.7E+07	-3.8E+05	-2.1E+06	1.7E+07	-1.4E+05	-1.8E+05	-1.1E+05	-1.4E+05	-1.2E+05	-1.3E+05	-6.8E+04	-1.1E+05
29.3	6.3E+06	2.8E+07	-1.1E+07	6.7E+06	2.2E+07	3.6E+06	-5.7E+05	2.2E+07	-1.1E+05	-1.0E+05	-1.3E+05	-8.7E+04	-1.6E+05	-1.3E+05	-1.1E+05	-9.2E+04
39.1	4.0E+06	2.8E+07	-1.1E+07	4.3E+06	3.2E+07	5.0E+05	-4.4E+06	3.2E+07	-7.6E+04	-1.2E+05	-5.1E+04	-5.9E+04	-7.7E+04	-8.7E+04	-8.7E+04	-1.1E+05
48.8	3.4E+06	2.9E+07	-1.1E+07	3.6E+06	4.1E+07	1.9E+05	-4.5E+06	4.1E+07	-1.6E+05	-1.2E+05	-1.5E+05	-7.4E+04	-1.1E+05	-1.0E+05	-1.3E+05	-1.2E+05
58.6	1.1E+06	2.8E+07	-1.1E+07	5.5E+05	4.7E+07	2.0E+06	-6.6E+06	4.9E+07	-1.2E+05	-1.5E+05	-1.0E+05	-2.1E+05	-1.1E+05	-1.0E+05	-1.4E+05	-1.0E+05
68.4	1.3E+05	2.8E+07	-1.2E+07	7.1E+05	5.6E+07	-7.1E+05	-7.3E+06	5.6E+07	-3.1E+05	-2.2E+05	-1.7E+05	-3.0E+05	-2.1E+05	-2.5E+05	-2.1E+05	-2.7E+05
78.1	-1.3E+06	2.7E+07	-1.3E+07	-3.1E+06	6.5E+07	-7.0E+05	-8.8E+06	6.6E+07	-1.3E+05	-4.7E+04	-1.3E+05	-1.0E+05	-6.6E+04	-1.5E+05	-1.4E+05	-6.1E+04
87.9	-5.2E+06	2.7E+07	-1.4E+07	-5.6E+06	7.3E+07	6.9E+04	-9.4E+06	7.6E+07	-1.6E+05	-9.2E+04	-5.6E+04	-2.0E+05	-8.7E+04	-9.9E+04	-1.2E+05	-6.6E+04
97.7	-7.8E+06	2.7E+07	-1.4E+07	-8.4E+06	8.2E+07	9.0E+05	-1.0E+07	8.5E+07	-2.0E+05	-1.0E+05	-8.0E+04	-8.6E+04	-1.5E+05	-6.5E+04	-1.4E+05	-1.3E+05
107.4	-1.1E+07	2.4E+07	-1.6E+07	-1.3E+07	9.0E+07	-5.0E+05	-1.2E+07	9.3E+07	-1.8E+05	-8.9E+04	-1.3E+05	-1.3E+05	-1.0E+05	-1.5E+05	-9.4E+04	-1.2E+05
117.2	-1.3E+07	2.6E+07	-1.6E+07	-1.4E+07	9.9E+07	1.1E+06	-1.2E+07	1.0E+08	-1.4E+05	-9.3E+04	-1.1E+05	-8.3E+04	-9.4E+04	-1.0E+05	-1.2E+05	-1.3E+05
127.0	-1.8E+07	2.6E+07	-1.5E+07	-1.8E+07	1.1E+08	2.2E+06	-1.2E+07	1.1E+08	-1.6E+05	-1.0E+05	-1.9E+05	-1.8E+05	-8.7E+04	-1.2E+05	-7.4E+04	-8.9E+04
136.7	-2.3E+07	2.6E+07	-1.4E+07	-2.2E+07	1.2E+08	9.6E+05	-1.4E+07	1.2E+08	-2.1E+05	-8.7E+04	-1.2E+05	-1.2E+05	-1.2E+05	-1.5E+05	-1.4E+05	-1.4E+05

Table 44 Raw data for the test seal at PD=34.5 bar, ω=5 krpm, and inlet GVF=6% with the zero-preswirl insert

Freq.	Re(H_{XX})	Re(H_{XY})	Re(H_{YX})	Re(H_{YY})	Im(H_{XX})	Im(H_{XY})	Im(H_{YX})	Im(H_{YY})	Re(eH_{XX})	Re(eH_{XY})	Re(eH_{YX})	Re(eH_{YY})	Im(eH_{XX})	Im(eH_{XY})	Im(eH_{YX})	Im(eH_{YY})
Hz	N/m	N/m	N/m	N/m	N/m	N/m	N/m	N/m	N/m	N/m	N/m	N/m	N/m	N/m	N/m	N/m
9.8	4.6E+06	3.6E+07	-1.9E+07	5.4E+06	1.0E+07	3.4E+06	3.1E+05	1.0E+07	-1.7E+05	-2.1E+05	-2.4E+05	-2.5E+05	-8.4E+04	-2.1E+05	-1.6E+05	-3.9E+05
19.5	6.5E+06	3.5E+07	-1.9E+07	5.8E+06	1.7E+07	-2.8E+05	-1.7E+06	1.7E+07	-1.3E+05	-1.9E+05	-1.8E+05	-2.2E+05	-1.6E+05	-1.6E+05	-2.1E+05	-2.6E+05
29.3	4.7E+06	3.5E+07	-2.1E+07	6.9E+06	2.3E+07	6.1E+06	6.0E+05	2.3E+07	-2.2E+05	-1.2E+05	-1.5E+05	-9.9E+04	-1.5E+05	-2.2E+05	-1.7E+05	-1.8E+05
39.1	3.0E+06	3.4E+07	-2.0E+07	2.9E+06	3.2E+07	1.7E+06	-3.3E+06	3.3E+07	-6.9E+04	-6.6E+04	-7.2E+04	-1.0E+05	-8.8E+04	-8.3E+04	-1.4E+05	-1.2E+05
48.8	2.2E+06	3.5E+07	-2.1E+07	2.2E+06	4.3E+07	1.8E+06	-3.3E+06	4.3E+07	-1.4E+05	-1.1E+05	-7.8E+04	-1.5E+05	-1.2E+05	-1.4E+05	-2.6E+05	-8.6E+04
58.6	-1.9E+05	3.4E+07	-2.1E+07	-1.5E+05	4.8E+07	4.5E+06	-5.4E+06	5.1E+07	-1.2E+05	-7.1E+04	-1.2E+05	-1.7E+05	-3.3E+04	-1.1E+05	-1.4E+05	-1.2E+05
68.4	-5.4E+05	3.4E+07	-2.2E+07	-6.8E+05	5.7E+07	8.6E+05	-6.3E+06	5.9E+07	-6.4E+04	-1.0E+05	-8.0E+04	-1.4E+05	-1.4E+05	-5.8E+04	-1.9E+05	-1.3E+05
78.1	-2.4E+06	3.3E+07	-2.0E+07	-3.5E+06	6.6E+07	2.3E+06	-7.9E+06	6.9E+07	-1.6E+05	-9.2E+04	-9.6E+04	-1.6E+05	-5.2E+04	-1.3E+05	-1.3E+05	-1.8E+05
87.9	-6.4E+06	3.4E+07	-2.4E+07	-6.1E+06	7.4E+07	3.2E+06	-8.0E+06	7.9E+07	-6.3E+04	-7.7E+04	-1.5E+05	-6.7E+04	-1.3E+05	-1.6E+05	-7.8E+04	-1.0E+05
97.7	-9.4E+06	3.3E+07	-2.4E+07	-7.3E+06	8.4E+07	4.0E+06	-8.0E+06	8.8E+07	-1.1E+05	-1.0E+05	-1.0E+05	-8.3E+04	-7.0E+04	-5.6E+04	-1.0E+05	-1.1E+05
107.4	-1.2E+07	3.1E+07	-2.4E+07	-1.1E+07	9.2E+07	2.5E+06	-9.1E+06	9.6E+07	-1.1E+05	-1.4E+05	-1.4E+05	-9.6E+04	-1.3E+05	-7.9E+04	-1.5E+05	-8.9E+04
117.2	-1.4E+07	3.3E+07	-2.4E+07	-1.3E+07	1.0E+08	4.0E+06	-1.0E+07	1.1E+08	-1.1E+05	-1.2E+05	-4.3E+04	-7.9E+04	-1.2E+05	-7.3E+04	-5.9E+04	-9.1E+04
127.0	-1.8E+07	3.3E+07	-2.2E+07	-1.6E+07	1.1E+08	5.7E+06	-1.0E+07	1.2E+08	-9.9E+04	-1.4E+05	-9.5E+04	-2.0E+05	-1.2E+05	-1.6E+05	-1.1E+05	-1.7E+05
136.7	-2.3E+07	3.3E+07	-2.3E+07	-1.8E+07	1.2E+08	4.4E+06	-1.2E+07	1.3E+08	-1.4E+05	-9.0E+04	-2.0E+05	-1.0E+05	-5.0E+04	-1.3E+05	-1.0E+05	-1.4E+05

Table 45 Raw data for the test seal at PD=34.5 bar, ω=3 krpm, and inlet GVF=8% with the zero-preswirl insert

Freq.	Re(H_{XX})	Re(H_{XY})	Re(H_{YX})	Re(H_{YY})	Im(H_{XX})	Im(H_{XY})	Im(H_{YX})	Im(H_{YY})	Re(eH_{XX})	Re(eH_{XY})	Re(eH_{YX})	Re(eH_{YY})	Im(eH_{XX})	Im(eH_{XY})	Im(eH_{YX})	Im(eH_{YY})
Hz	N/m	N/m	N/m	N/m	N/m	N/m	N/m	N/m	N/m	N/m	N/m	N/m	N/m	N/m	N/m	N/m
9.8	6.8E+06	2.9E+07	-9.9E+06	4.7E+06	8.6E+06	1.6E+06	-7.4E+05	8.2E+06	-1.2E+05	-2.1E+05	-2.0E+05	-2.0E+05	-7.5E+04	-1.0E+05	-2.1E+05	-3.4E+05
19.5	6.2E+06	3.0E+07	-1.1E+07	5.7E+06	1.8E+07	7.2E+05	-1.6E+06	1.7E+07	-2.2E+05	-2.0E+05	-2.2E+05	-2.2E+05	-2.2E+05	-2.5E+05	-1.4E+05	-1.8E+05
29.3	6.2E+06	2.9E+07	-1.3E+07	4.8E+06	2.2E+07	4.0E+06	-1.5E+05	2.3E+07	-1.3E+05	-7.2E+04	-7.8E+04	-1.3E+05	-8.6E+04	-1.0E+05	-1.5E+05	-8.6E+04
39.1	3.7E+06	2.8E+07	-1.2E+07	3.2E+06	3.2E+07	6.1E+05	-3.7E+06	3.4E+07	-8.6E+04	-7.6E+04	-8.3E+04	-1.2E+05	-8.4E+04	-7.7E+04	-3.8E+04	-1.0E+05
48.8	2.3E+06	2.9E+07	-1.2E+07	3.0E+06	4.2E+07	1.0E+06	-3.9E+06	4.3E+07	-1.4E+05	-1.5E+05	-1.3E+05	-9.4E+04	-1.4E+05	-1.4E+05	-1.5E+05	-1.1E+05
58.6	4.7E+05	2.8E+07	-1.2E+07	2.8E+04	4.8E+07	2.3E+06	-5.2E+06	5.0E+07	-1.3E+05	-1.4E+05	-1.4E+05	-2.6E+05	-7.3E+04	-1.2E+05	-1.6E+05	-2.6E+05
68.4	-5.5E+05	2.8E+07	-1.4E+07	1.1E+06	5.7E+07	-9.2E+05	-5.7E+06	5.8E+07	-1.1E+05	-1.7E+05	-1.7E+05	-1.1E+05	-2.0E+05	-1.5E+05	-1.2E+05	-1.8E+05
78.1	-1.5E+06	2.8E+07	-1.3E+07	-3.1E+06	6.6E+07	-3.1E+05	-7.6E+06	6.8E+07	-1.2E+05	-8.2E+04	-1.4E+05	-1.1E+05	-8.0E+04	-1.7E+05	-8.5E+04	-2.0E+05
87.9	-5.2E+06	2.7E+07	-1.4E+07	-5.1E+06	7.5E+07	-2.0E+03	-7.2E+06	7.9E+07	-7.9E+04	-8.0E+04	-8.5E+04	-1.5E+05	-4.7E+04	-7.6E+04	-5.7E+04	-7.3E+04
97.7	-7.5E+06	2.8E+07	-1.4E+07	-6.8E+06	8.4E+07	5.8E+05	-8.0E+06	8.7E+07	-1.4E+05	-6.1E+04	-6.6E+04	-7.6E+04	-6.0E+04	-1.0E+05	-7.5E+04	-4.6E+04
107.4	-1.0E+07	2.5E+07	-1.5E+07	-1.1E+07	9.2E+07	-9.9E+05	-9.6E+06	9.5E+07	-2.2E+05	-1.2E+05	-1.3E+05	-9.2E+04	-1.2E+05	-1.4E+05	-6.7E+04	-1.1E+05
117.2	-1.2E+07	2.5E+07	-1.5E+07	-1.2E+07	1.0E+08	4.5E+05	-1.0E+07	1.1E+08	-1.6E+05	-1.6E+05	-1.3E+05	-1.4E+05	-1.3E+05	-9.5E+04	-4.1E+04	-8.2E+04
127.0	-1.5E+07	2.6E+07	-1.4E+07	-1.5E+07	1.1E+08	1.6E+06	-1.1E+07	1.1E+08	-1.7E+05	-2.9E+05	-1.2E+05	-1.1E+05	-1.6E+05	-1.7E+05	-1.3E+05	-1.6E+05
136.7	-2.1E+07	2.6E+07	-1.4E+07	-1.6E+07	1.2E+08	6.8E+05	-1.1E+07	1.3E+08	-2.3E+05	-1.1E+05	-1.3E+05	-2.0E+05	-1.2E+05	-9.8E+04	-1.4E+05	-1.4E+05

Table 46 Raw data for the test seal at PD=34.5 bar, ω=4 krpm, and inlet GVF=8% with the zero-preswirl insert

Freq.	Re(H_{XX})	Re(H_{XY})	Re(H_{YX})	Re(H_{YY})	Im(H_{XX})	Im(H_{XY})	Im(H_{YX})	Im(H_{YY})	Re(eH_{XX})	Re(eH_{XY})	Re(eH_{YX})	Re(eH_{YY})	Im(eH_{XX})	Im(eH_{XY})	Im(eH_{YX})	Im(eH_{YY})
Hz	N/m	N/m	N/m	N/m	N/m	N/m	N/m	N/m	N/m	N/m	N/m	N/m	N/m	N/m	N/m	N/m
9.8	6.3E+06	3.1E+07	-1.1E+07	4.7E+06	9.5E+06	2.1E+06	5.0E+05	9.8E+06	-2.5E+05	-3.9E+05	-1.3E+05	-1.5E+05	-1.5E+05	-2.1E+05	-1.9E+05	-3.0E+05
19.5	5.9E+06	3.0E+07	-1.2E+07	5.7E+06	1.7E+07	2.3E+05	-7.7E+05	1.8E+07	-1.4E+05	-2.0E+05	-1.5E+05	-1.3E+05	-1.9E+05	-1.9E+05	-9.8E+04	-1.7E+05
29.3	4.6E+06	2.8E+07	-1.4E+07	5.0E+06	2.2E+07	4.8E+06	6.1E+05	2.4E+07	-6.8E+04	-1.3E+05	-1.3E+05	-7.3E+04	-1.7E+05	-9.2E+04	-6.3E+04	-8.9E+04
39.1	3.1E+06	2.9E+07	-1.3E+07	2.4E+06	3.2E+07	7.2E+05	-3.3E+06	3.4E+07	-8.6E+04	-6.3E+04	-2.1E+05	-1.1E+05	-6.5E+04	-8.5E+04	-5.5E+04	-1.5E+05
48.8	1.6E+06	2.9E+07	-1.3E+07	2.5E+06	4.2E+07	1.0E+06	-2.8E+06	4.3E+07	-1.5E+05	-6.1E+04	-1.3E+05	-1.3E+05	-1.2E+05	-1.2E+05	-1.4E+05	-1.3E+05
58.6	-3.5E+05	2.8E+07	-1.4E+07	-3.0E+05	4.8E+07	2.3E+06	-4.6E+06	5.0E+07	-9.0E+04	-1.1E+05	-2.1E+05	-1.6E+05	-9.9E+04	-1.0E+05	-1.8E+05	-2.2E+05
68.4	-1.1E+06	2.8E+07	-1.5E+07	6.9E+05	5.7E+07	-1.1E+06	-5.0E+06	5.8E+07	-2.1E+05	-5.7E+04	-1.1E+05	-1.7E+05	-8.7E+04	-1.2E+05	-1.4E+05	-1.5E+05
78.1	-2.0E+06	2.7E+07	-1.3E+07	-3.0E+06	6.6E+07	-2.4E+05	-6.3E+06	6.8E+07	-1.3E+05	-1.2E+05	-1.1E+05	-2.0E+05	-1.8E+05	-1.8E+05	-1.7E+05	-1.1E+05
87.9	-6.2E+06	2.7E+07	-1.5E+07	-5.2E+06	7.5E+07	1.8E+05	-5.9E+06	7.9E+07	-9.3E+04	-1.3E+05	-1.5E+05	-1.6E+05	-1.1E+05	-4.4E+04	-1.9E+05	-7.8E+04
97.7	-8.4E+06	2.8E+07	-1.5E+07	-6.8E+06	8.4E+07	3.6E+05	-6.4E+06	8.8E+07	-1.2E+05	-7.0E+04	-1.3E+05	-1.2E+05	-1.0E+05	-9.1E+04	-1.8E+05	-7.1E+04
107.4	-1.1E+07	2.5E+07	-1.5E+07	-1.0E+07	9.3E+07	-9.3E+05	-8.0E+06	9.5E+07	-1.8E+05	-1.0E+05	-1.3E+05	-1.0E+05	-1.6E+05	-1.4E+05	-3.1E+05	-6.5E+04
117.2	-1.2E+07	2.6E+07	-1.6E+07	-1.2E+07	1.0E+08	4.3E+05	-9.1E+06	1.1E+08	-1.9E+05	-1.4E+05	-1.0E+05	-1.1E+05	-1.2E+05	-1.4E+05	-2.5E+05	-1.3E+05
127.0	-1.6E+07	2.6E+07	-1.3E+07	-1.6E+07	1.1E+08	1.4E+06	-9.9E+06	1.1E+08	-1.7E+05	-1.2E+05	-1.4E+05	-1.3E+05	-1.1E+05	-2.3E+05	-1.4E+05	-2.0E+05
136.7	-2.2E+07	2.6E+07	-1.4E+07	-1.6E+07	1.2E+08	7.2E+05	-1.1E+07	1.3E+08	-9.0E+04	-1.0E+05	-1.8E+05	-2.0E+05	-1.3E+05	-1.6E+05	-3.1E+05	-1.1E+05

Table 47 Raw data for the test seal at PD=34.5 bar, ω=5 krpm, and inlet GVF=8% with the zero-preswirl insert

Freq.	Re(H_{XX})	Re(H_{XY})	Re(H_{YX})	Re(H_{YY})	Im(H_{XX})	Im(H_{XY})	Im(H_{YX})	Im(H_{YY})	Re(eH_{XX})	Re(eH_{XY})	Re(eH_{YX})	Re(eH_{YY})	Im(eH_{XX})	Im(eH_{XY})	Im(eH_{YX})	Im(eH_{YY})
Hz	N/m	N/m	N/m	N/m	N/m	N/m	N/m	N/m	N/m	N/m	N/m	N/m	N/m	N/m	N/m	N/m
9.8	2.9E+06	3.8E+07	-2.0E+07	5.7E+06	1.1E+07	4.7E+06	1.4E+06	1.2E+07	-2.4E+05	-2.5E+05	-1.4E+05	-1.9E+05	-2.4E+05	-4.6E+05	-2.5E+05	-3.9E+05
19.5	4.3E+06	3.5E+07	-2.0E+07	6.0E+06	1.8E+07	-1.2E+06	-6.0E+05	1.7E+07	-1.2E+05	-2.0E+05	-1.4E+05	-1.5E+05	-1.5E+05	-1.4E+05	-1.5E+05	-2.1E+05
29.3	3.2E+06	3.5E+07	-2.2E+07	6.0E+06	2.5E+07	5.3E+06	2.0E+06	2.2E+07	-1.2E+05	-1.2E+05	-8.7E+04	-1.4E+05	-1.7E+05	-1.1E+05	-1.6E+05	-1.1E+05
39.1	1.9E+06	3.5E+07	-2.1E+07	1.8E+06	3.4E+07	1.6E+06	-2.3E+06	3.4E+07	-1.3E+05	-9.4E+04	-1.3E+05	-9.1E+04	-1.1E+05	-1.3E+05	-6.6E+04	-1.3E+05
48.8	8.4E+05	3.5E+07	-2.1E+07	8.4E+05	4.3E+07	1.8E+06	-2.8E+06	4.4E+07	-1.2E+05	-9.4E+04	-1.3E+05	-1.4E+05	-8.6E+04	-9.3E+04	-1.9E+05	-1.2E+05
58.6	-1.7E+06	3.4E+07	-2.2E+07	-1.3E+05	4.9E+07	3.9E+06	-4.4E+06	5.2E+07	-1.1E+05	-7.0E+04	-1.2E+05	-1.1E+05	-8.0E+04	-1.4E+05	-1.5E+05	-1.5E+05
68.4	-1.8E+06	3.4E+07	-2.2E+07	-2.8E+06	5.9E+07	2.3E+05	-6.1E+06	5.9E+07	-1.1E+05	-1.4E+05	-1.8E+05	-9.5E+04	-1.9E+05	-1.2E+05	-9.0E+04	-1.5E+05
78.1	-3.8E+06	3.4E+07	-2.1E+07	-3.9E+06	6.7E+07	2.7E+06	-6.4E+06	7.0E+07	-1.1E+05	-1.2E+05	-7.6E+04	-1.2E+05	-1.2E+05	-1.7E+05	-1.1E+05	-6.0E+04
87.9	-7.6E+06	3.4E+07	-2.4E+07	-7.0E+06	7.6E+07	3.1E+06	-6.5E+06	7.9E+07	-8.1E+04	-9.5E+04	-1.3E+05	-1.6E+05	-6.4E+04	-8.4E+04	-1.1E+05	-1.4E+05
97.7	-1.0E+07	3.4E+07	-2.4E+07	-7.3E+06	8.6E+07	3.3E+06	-6.0E+06	8.9E+07	-1.4E+05	-6.5E+04	-1.5E+05	-8.6E+04	-1.3E+05	-1.1E+05	-1.5E+05	-8.4E+04
107.4	-1.2E+07	3.2E+07	-2.5E+07	-1.0E+07	9.4E+07	2.5E+06	-7.4E+06	9.7E+07	-6.0E+04	-7.2E+04	-1.1E+05	-1.5E+05	-8.9E+04	-4.1E+04	-1.9E+05	-1.1E+05
117.2	-1.4E+07	3.3E+07	-2.5E+07	-1.2E+07	1.0E+08	3.7E+06	-8.9E+06	1.1E+08	-5.9E+04	-9.0E+04	-6.4E+04	-1.1E+05	-8.0E+04	-1.1E+05	-9.4E+04	-1.2E+05
127.0	-1.8E+07	3.3E+07	-2.2E+07	-1.4E+07	1.1E+08	4.4E+06	-8.6E+06	1.2E+08	-1.2E+05	-2.3E+05	-5.6E+04	-2.0E+05	-8.0E+04	-9.2E+04	-1.2E+05	-1.9E+05
136.7	-2.3E+07	3.3E+07	-2.3E+07	-1.5E+07	1.2E+08	3.2E+06	-1.0E+07	1.3E+08	-2.2E+05	-9.6E+04	-2.3E+05	-1.4E+05	-1.4E+05	-1.6E+05	-1.7E+05	-1.7E+05

Table 48 Raw data for the test seal at PD=34.5 bar, ω=3 krpm, and inlet GVF=10% with the zero-preswirl insert

Freq.	Re(H_{XX})	Re(H_{XY})	Re(H_{YX})	Re(H_{YY})	Im(H_{XX})	Im(H_{XY})	Im(H_{YX})	Im(H_{YY})	Re(eH_{XX})	Re(eH_{XY})	Re(eH_{YX})	Re(eH_{YY})	Im(eH_{XX})	Im(eH_{XY})	Im(eH_{YX})	Im(eH_{YY})
Hz	N/m	N/m	N/m	N/m	N/m	N/m	N/m	N/m	N/m	N/m	N/m	N/m	N/m	N/m	N/m	N/m
9.8	5.5E+06	2.9E+07	-1.2E+07	5.6E+06	8.2E+06	2.8E+06	5.3E+05	1.1E+07	-1.7E+05	-2.1E+05	-1.4E+05	-1.8E+05	-1.2E+05	-2.5E+05	-1.2E+05	-2.3E+05
19.5	5.3E+06	2.7E+07	-1.2E+07	5.9E+06	1.8E+07	-7.8E+05	-1.0E+06	1.8E+07	-2.8E+05	-1.3E+05	-9.6E+04	-3.2E+05	-2.1E+05	-3.1E+05	-3.4E+05	-1.1E+05
29.3	4.5E+06	2.7E+07	-1.4E+07	2.1E+06	2.1E+07	6.6E+06	-5.4E+05	2.5E+07	-1.8E+05	-1.5E+05	-1.4E+05	-7.8E+04	-2.4E+05	-1.6E+05	-1.2E+05	-1.2E+05
39.1	2.9E+06	2.7E+07	-1.4E+07	3.1E+06	3.2E+07	1.4E+06	-2.7E+06	3.4E+07	-9.6E+04	-8.9E+04	-1.4E+05	-7.5E+04	-1.3E+05	-7.5E+04	-9.9E+04	-9.3E+04
48.8	2.2E+06	2.7E+07	-1.4E+07	3.6E+06	4.2E+07	-6.7E+05	-2.1E+06	4.3E+07	-1.4E+05	-1.2E+05	-2.2E+05	-1.6E+05	-1.5E+05	-1.2E+05	-1.8E+05	-1.4E+05
58.6	-3.4E+05	3.1E+07	-1.5E+07	-3.3E+06	4.9E+07	2.0E+06	-5.1E+06	5.5E+07	-1.1E+05	-1.6E+05	-2.2E+05	-2.1E+05	-1.0E+05	-1.5E+05	-1.7E+05	-1.6E+05
68.4	-1.9E+06	2.7E+07	-1.6E+07	3.2E+06	5.7E+07	2.9E+06	-4.1E+06	5.9E+07	-6.8E+04	-1.1E+05	-1.5E+05	-1.7E+05	-1.1E+05	-1.8E+05	-1.2E+05	-1.6E+05
78.1	-1.4E+06	2.6E+07	-1.2E+07	-3.1E+06	6.6E+07	9.0E+05	-5.7E+06	6.6E+07	-1.0E+05	-1.8E+05	-1.2E+05	-2.1E+05	-1.0E+05	-1.0E+05	-1.4E+05	-1.2E+05
87.9	-5.5E+06	2.6E+07	-1.6E+07	-3.1E+06	7.4E+07	1.2E+06	-5.5E+06	8.1E+07	-9.7E+04	-8.8E+04	-1.4E+05	-1.5E+05	-9.7E+04	-1.6E+05	-9.2E+04	-1.4E+05
97.7	-8.1E+06	2.7E+07	-1.7E+07	-8.4E+06	8.4E+07	1.7E+06	-6.4E+06	9.2E+07	-1.4E+05	-2.0E+05	-1.7E+05	-1.9E+05	-1.0E+05	-1.6E+05	-2.0E+05	-9.9E+04
107.4	-1.1E+07	2.6E+07	-1.6E+07	-1.3E+07	9.3E+07	5.4E+05	-7.4E+06	9.7E+07	-1.9E+05	-7.9E+04	-1.4E+05	-7.5E+04	-3.0E+05	-1.4E+05	-1.9E+05	-1.2E+05
117.2	-1.2E+07	2.5E+07	-1.6E+07	-1.1E+07	1.0E+08	1.3E+06	-8.4E+06	1.1E+08	-8.1E+04	-1.6E+05	-1.4E+05	-1.7E+05	-1.3E+05	-8.0E+04	-1.4E+05	-8.4E+04
127.0	-1.4E+07	2.6E+07	-1.3E+07	-1.4E+07	1.1E+08	1.3E+06	-9.3E+06	1.2E+08	-1.6E+05	-2.7E+05	-9.2E+04	-1.7E+05	-2.2E+05	-3.8E+05	-2.0E+05	-2.9E+05
136.7	-2.0E+07	2.6E+07	-1.4E+07	-1.7E+07	1.2E+08	3.4E+06	-9.6E+06	1.3E+08	-3.1E+05	-2.4E+05	-2.1E+05	-1.7E+05	-1.6E+05	-4.0E+05	-1.4E+05	-1.5E+05

Table 49 Raw data for the test seal at PD=34.5 bar, ω=4 krpm, and inlet GVF=10% with the zero-preswirl insert

Freq.	Re(H_{XX})	Re(H_{XY})	Re(H_{YX})	Re(H_{YY})	Im(H_{XX})	Im(H_{XY})	Im(H_{YX})	Im(H_{YY})	Re(eH_{XX})	Re(eH_{XY})	Re(eH_{YX})	Re(eH_{YY})	Im(eH_{XX})	Im(eH_{XY})	Im(eH_{YX})	Im(eH_{YY})
Hz	N/m	N/m	N/m	N/m	N/m	N/m	N/m	N/m	N/m	N/m	N/m	N/m	N/m	N/m	N/m	N/m
9.8	5.1E+06	2.7E+07	-1.3E+07	2.3E+06	1.0E+07	4.5E+06	1.0E+06	1.1E+07	-1.9E+05	-2.3E+05	-2.1E+05	-2.6E+05	-1.6E+05	-2.2E+05	-1.0E+05	-1.5E+05
19.5	4.9E+06	2.8E+07	-1.4E+07	3.6E+06	1.9E+07	2.4E+06	4.4E+05	1.8E+07	-2.8E+05	-1.3E+05	-3.2E+05	-2.4E+05	-3.4E+05	-4.0E+05	-1.3E+05	-2.5E+05
29.3	4.2E+06	2.7E+07	-1.5E+07	3.3E+06	2.3E+07	6.2E+06	1.7E+06	2.3E+07	-1.1E+05	-7.2E+04	-1.4E+05	-8.4E+04	-1.0E+05	-8.4E+04	-1.2E+05	-1.3E+05
39.1	2.2E+06	2.6E+07	-1.5E+07	2.3E+05	3.2E+07	2.5E+06	-2.4E+06	3.4E+07	-1.2E+05	-5.4E+04	-2.4E+05	-1.1E+05	-1.1E+05	-1.2E+05	-6.3E+04	-1.5E+05
48.8	1.3E+06	2.6E+07	-1.5E+07	2.0E+05	4.2E+07	3.2E+06	-8.6E+05	4.3E+07	-1.6E+05	-9.6E+04	-1.5E+05	-1.0E+05	-8.8E+04	-8.1E+04	-1.8E+05	-1.2E+05
58.6	-1.4E+06	2.6E+07	-1.5E+07	-3.0E+06	4.8E+07	4.6E+06	-3.0E+06	4.9E+07	-8.5E+04	-1.3E+05	-1.7E+05	-1.3E+05	-6.8E+04	-1.2E+05	-1.3E+05	-1.8E+05
68.4	-2.5E+06	2.7E+07	-1.7E+07	-3.4E+06	5.6E+07	1.8E+06	-3.8E+06	5.9E+07	-1.3E+05	-9.0E+04	-3.1E+05	-1.3E+05	-1.3E+05	-9.2E+04	-2.3E+05	-1.8E+05
78.1	-2.3E+05	2.6E+07	-1.2E+07	-5.3E+06	6.5E+07	3.0E+06	-4.5E+06	6.8E+07	-9.6E+04	-1.4E+05	-1.3E+05	-8.0E+04	-1.6E+05	-1.1E+05	-1.5E+05	-9.9E+04
87.9	-7.3E+06	2.7E+07	-1.6E+07	-8.5E+06	7.4E+07	5.0E+06	-3.5E+06	7.9E+07	-9.8E+04	-6.7E+04	-9.6E+04	-9.9E+04	-1.1E+05	-1.4E+05	-1.3E+05	-5.4E+04
97.7	-9.9E+06	2.7E+07	-1.6E+07	-9.1E+06	8.4E+07	5.5E+06	-3.4E+06	8.8E+07	-1.2E+05	-1.3E+05	-2.0E+05	-1.2E+05	-2.6E+05	-9.3E+04	-1.1E+05	-1.2E+05
107.4	-1.2E+07	2.5E+07	-1.6E+07	-1.2E+07	9.3E+07	2.7E+06	-4.0E+06	9.5E+07	-1.4E+05	-1.0E+05	-2.2E+05	-1.0E+05	-1.9E+05	-2.0E+05	-1.4E+05	-1.6E+05
117.2	-1.3E+07	2.6E+07	-1.6E+07	-1.4E+07	1.0E+08	4.7E+06	-6.0E+06	1.1E+08	-4.5E+04	-8.5E+04	-1.1E+05	-7.1E+04	-2.0E+05	-1.2E+05	-1.2E+05	-6.5E+04
127.0	-1.5E+07	2.6E+07	-1.0E+07	-1.6E+07	1.1E+08	4.9E+06	-6.3E+06	1.1E+08	-6.0E+04	-1.3E+05	-8.3E+04	-1.5E+05	-8.6E+04	-1.2E+05	-1.3E+05	-2.2E+05
136.7	-2.3E+07	2.8E+07	-1.3E+07	-1.8E+07	1.2E+08	3.4E+06	-7.7E+06	1.3E+08	-1.4E+05	-1.5E+05	-2.3E+05	-1.8E+05	-1.4E+05	-6.9E+04	-2.7E+05	-1.0E+05

Table 50 Raw data for the test seal at PD=34.5 bar, ω=5 krpm, and inlet GVF=10% with the zero-preswirl insert

Freq.	Re(H_{XX})	Re(H_{XY})	Re(H_{YX})	Re(H_{YY})	Im(H_{XX})	Im(H_{XY})	Im(H_{YX})	Im(H_{YY})	Re(eH_{XX})	Re(eH_{XY})	Re(eH_{YX})	Re(eH_{YY})	Im(eH_{XX})	Im(eH_{XY})	Im(eH_{YX})	Im(eH_{YY})
Hz	N/m	N/m	N/m	N/m	N/m	N/m	N/m	N/m	N/m	N/m	N/m	N/m	N/m	N/m	N/m	N/m
9.8	7.0E+05	3.2E+07	-2.4E+07	8.5E+05	1.3E+07	6.8E+06	9.4E+05	1.1E+07	-2.5E+05	-2.5E+05	-2.6E+05	-2.0E+05	-2.3E+05	-2.4E+05	-3.4E+05	-4.4E+05
19.5	2.0E+06	3.4E+07	-2.3E+07	2.7E+06	2.1E+07	3.0E+06	9.5E+05	1.7E+07	-2.9E+05	-5.2E+05	-1.2E+05	-2.3E+05	-4.3E+05	-2.3E+05	-2.1E+05	-1.4E+05
29.3	6.3E+05	3.3E+07	-2.5E+07	1.5E+06	2.6E+07	8.2E+06	2.2E+06	2.3E+07	-1.3E+05	-1.0E+05	-1.2E+05	-1.1E+05	-1.2E+05	-1.1E+05	-9.6E+04	-1.1E+05
39.1	3.9E+04	3.2E+07	-2.3E+07	-6.3E+05	3.4E+07	3.7E+06	-1.4E+06	3.4E+07	-6.7E+04	-8.8E+04	-1.3E+05	-5.9E+04	-9.1E+04	-8.4E+04	-2.8E+04	-1.1E+05
48.8	-1.7E+06	3.1E+07	-2.5E+07	-2.9E+06	4.3E+07	4.4E+06	-2.5E+06	4.3E+07	-1.5E+05	-8.8E+04	-1.4E+05	-9.9E+04	-1.3E+05	-1.3E+05	-1.3E+05	-1.4E+05
58.6	-4.6E+06	3.1E+07	-2.5E+07	-3.2E+06	5.0E+07	5.8E+06	-2.9E+06	5.1E+07	-1.2E+05	-6.3E+04	-1.5E+05	-9.8E+04	-6.5E+04	-1.3E+05	-1.0E+05	-1.7E+05
68.4	-5.2E+06	3.0E+07	-2.5E+07	-6.2E+06	5.8E+07	3.8E+06	-4.0E+06	6.0E+07	-2.1E+05	-1.8E+05	-1.6E+05	-1.2E+05	-1.7E+05	-1.6E+05	-1.3E+05	-1.3E+05
78.1	-3.4E+06	3.2E+07	-2.3E+07	-6.3E+06	6.8E+07	5.7E+06	-1.9E+06	7.0E+07	-1.4E+05	-1.2E+05	-1.6E+05	-1.6E+05	-1.2E+05	-1.2E+05	-1.2E+05	-1.3E+05
87.9	-1.1E+07	3.1E+07	-2.6E+07	-1.0E+07	7.6E+07	7.2E+06	-3.6E+06	7.9E+07	-8.4E+04	-1.2E+05	-8.5E+04	-6.6E+04	-1.3E+05	-1.3E+05	-1.3E+05	-9.0E+04
97.7	-1.3E+07	3.3E+07	-2.7E+07	-1.1E+07	8.7E+07	8.0E+06	-2.9E+06	8.9E+07	-1.6E+05	-8.6E+04	-1.3E+05	-8.7E+04	-9.0E+04	-1.1E+05	-1.6E+05	-8.7E+04
107.4	-1.4E+07	3.1E+07	-2.7E+07	-1.3E+07	9.6E+07	6.3E+06	-3.7E+06	9.8E+07	-1.4E+05	-9.3E+04	-1.3E+05	-1.9E+05	-1.2E+05	-1.6E+05	-1.2E+05	-1.0E+05
117.2	-1.6E+07	3.3E+07	-2.5E+07	-1.5E+07	1.0E+08	8.2E+06	-4.6E+06	1.1E+08	-8.5E+04	-8.4E+04	-7.0E+04	-1.1E+05	-9.4E+04	-1.5E+05	-1.9E+05	-1.2E+05
127.0	-1.8E+07	3.4E+07	-2.2E+07	-1.4E+07	1.1E+08	8.1E+06	-3.4E+06	1.2E+08	-1.5E+05	-1.5E+05	-1.6E+05	-1.4E+05	-6.7E+04	-1.9E+05	-9.2E+04	-1.8E+05
136.7	-2.4E+07	3.5E+07	-2.3E+07	-1.8E+07	1.2E+08	6.6E+06	-6.8E+06	1.3E+08	-1.2E+05	-1.5E+05	-1.9E+05	-8.4E+04	-6.9E+04	-1.5E+05	-1.5E+05	-9.2E+04

Table 51 Raw data for the test seal at PD=41.4 bar, ω=3 krpm, and inlet GVF=0% with the zero-preswirl insert

Freq.	Re(H_{XX})	Re(H_{XY})	Re(H_{YX})	Re(H_{YY})	Im(H_{XX})	Im(H_{XY})	Im(H_{YX})	Im(H_{YY})	Re(eH_{XX})	Re(eH_{XY})	Re(eH_{YX})	Re(eH_{YY})	Im(eH_{XX})	Im(eH_{XY})	Im(eH_{YX})	Im(eH_{YY})
Hz	N/m	N/m	N/m	N/m	N/m	N/m	N/m	N/m	N/m	N/m	N/m	N/m	N/m	N/m	N/m	N/m
9.8	9.5E+06	3.3E+07	-7.3E+06	8.7E+06	9.6E+06	1.1E+06	-1.4E+06	6.3E+06	-2.4E+05	-3.0E+05	-1.4E+05	-2.7E+05	-1.5E+05	-3.0E+05	-1.7E+05	-1.9E+05
19.5	1.0E+07	3.4E+07	-8.0E+06	8.1E+06	1.7E+07	5.3E+05	-3.7E+06	1.7E+07	-1.8E+05	-2.8E+05	-1.4E+05	-1.1E+05	-1.7E+05	-1.5E+05	-1.9E+05	-2.4E+05
29.3	9.3E+06	3.3E+07	-8.8E+06	8.0E+06	2.4E+07	4.1E+06	-2.7E+06	2.3E+07	-1.5E+05	-1.4E+05	-1.1E+05	-1.3E+05	-1.5E+05	-1.4E+05	-1.4E+05	-1.6E+05
39.1	7.2E+06	3.2E+07	-8.3E+06	6.3E+06	3.3E+07	4.3E+05	-6.4E+06	3.3E+07	-1.2E+05	-1.5E+05	-1.5E+05	-1.3E+05	-1.7E+05	-9.9E+04	-1.9E+05	-1.6E+05
48.8	5.6E+06	3.3E+07	-8.9E+06	4.4E+06	4.1E+07	2.0E+05	-8.3E+06	4.2E+07	-6.8E+04	-2.0E+05	-1.8E+05	-1.4E+05	-1.5E+05	-1.4E+05	-1.4E+05	-1.1E+05
58.6	2.8E+06	3.3E+07	-9.0E+06	8.3E+05	4.9E+07	1.5E+06	-9.6E+06	5.1E+07	-1.1E+05	-3.0E+05	-1.4E+05	-1.8E+05	-1.4E+05	-1.7E+05	-1.4E+05	-8.7E+04
68.4	5.2E+05	3.3E+07	-1.1E+07	1.7E+06	5.7E+07	-1.1E+06	-1.1E+07	5.8E+07	-1.1E+05	-9.9E+04	-1.1E+05	-1.7E+05	-1.5E+05	-1.5E+05	-1.4E+05	-2.3E+05
78.1	-1.2E+06	3.1E+07	-1.1E+07	-3.6E+06	6.5E+07	-1.4E+06	-1.3E+07	6.8E+07	-1.9E+05	-1.2E+05	-1.6E+05	-1.3E+05	-9.8E+04	-1.1E+05	-1.3E+05	-1.7E+05
87.9	-6.5E+06	3.1E+07	-1.2E+07	-6.8E+06	7.4E+07	-1.8E+05	-1.5E+07	7.7E+07	-2.1E+05	-7.4E+04	-7.9E+04	-1.4E+05	-9.4E+04	-1.8E+05	-1.8E+05	-1.8E+05
97.7	-1.1E+07	3.0E+07	-1.3E+07	-1.1E+07	8.3E+07	2.4E+05	-1.7E+07	8.6E+07	-7.1E+04	-8.2E+04	-8.6E+04	-7.5E+04	-1.0E+05	-1.2E+05	-4.8E+04	-8.2E+04
107.4	-1.6E+07	2.8E+07	-1.5E+07	-1.7E+07	9.1E+07	-1.5E+06	-1.9E+07	9.3E+07	-7.5E+04	-1.0E+05	-1.5E+05	-1.1E+05	-2.4E+05	-1.6E+05	-1.6E+05	-1.4E+05
117.2	-1.9E+07	2.9E+07	-1.5E+07	-2.1E+07	9.9E+07	1.7E+05	-1.9E+07	1.0E+08	-1.2E+05	-4.4E+04	-1.2E+05	-1.0E+05	-8.5E+04	-1.3E+05	-1.7E+05	-8.4E+04
127.0	-2.6E+07	2.9E+07	-1.4E+07	-2.8E+07	1.1E+08	1.7E+06	-2.1E+07	1.1E+08	-1.7E+05	-2.2E+05	-5.6E+04	-1.2E+05	-9.4E+04	-2.1E+05	-7.6E+04	-1.3E+05
136.7	-3.4E+07	2.8E+07	-1.5E+07	-3.3E+07	1.2E+08	5.1E+05	-2.3E+07	1.2E+08	-8.0E+04	-2.2E+05	-2.8E+05	-3.2E+05	-2.0E+05	-1.9E+05	-1.1E+05	-2.1E+05

Table 52 Raw data for the test seal at PD=41.4 bar, ω=4 krpm, and inlet GVF=0% with the zero-preswirl insert

Freq.	Re(H_{XX})	Re(H_{XY})	Re(H_{YX})	Re(H_{YY})	Im(H_{XX})	Im(H_{XY})	Im(H_{YX})	Im(H_{YY})	Re(eH_{XX})	Re(eH_{XY})	Re(eH_{YX})	Re(eH_{YY})	Im(eH_{XX})	Im(eH_{XY})	Im(eH_{YX})	Im(eH_{YY})
Hz	N/m	N/m	N/m	N/m	N/m	N/m	N/m	N/m	N/m	N/m	N/m	N/m	N/m	N/m	N/m	N/m
9.8	9.9E+06	3.3E+07	-6.9E+06	9.1E+06	9.5E+06	8.8E+05	-1.6E+06	6.2E+06	-1.9E+05	-3.1E+05	-1.8E+05	-2.6E+05	-3.1E+05	-3.8E+05	-2.4E+05	-3.4E+05
19.5	9.5E+06	3.4E+07	-7.3E+06	8.9E+06	1.8E+07	9.7E+05	-3.2E+06	1.7E+07	-1.2E+05	-3.2E+05	-2.4E+05	-2.8E+05	-3.3E+05	-2.5E+05	-2.4E+05	-3.0E+05
29.3	8.9E+06	3.3E+07	-8.2E+06	8.2E+06	2.3E+07	4.1E+06	-3.1E+06	2.2E+07	-7.5E+04	-8.0E+04	-1.3E+05	-1.8E+05	-1.2E+05	-1.5E+05	-2.1E+05	-1.7E+05
39.1	6.6E+06	3.2E+07	-7.8E+06	6.2E+06	3.3E+07	4.4E+05	-6.8E+06	3.3E+07	-1.7E+05	-8.1E+04	-1.4E+05	-1.1E+05	-7.2E+04	-1.6E+05	-1.0E+05	-1.2E+05
48.8	5.5E+06	3.3E+07	-8.6E+06	4.7E+06	4.2E+07	4.3E+05	-8.2E+06	4.2E+07	-1.6E+05	-7.9E+04	-1.1E+05	-1.8E+05	-1.9E+05	-1.9E+05	-2.8E+05	-1.9E+05
58.6	2.4E+06	3.3E+07	-8.9E+06	8.0E+05	4.9E+07	1.9E+06	-9.7E+06	5.0E+07	-1.7E+05	-1.4E+05	-1.2E+05	-1.3E+05	-7.6E+04	-2.3E+05	-1.7E+05	-1.6E+05
68.4	-1.1E+05	3.3E+07	-1.0E+07	2.1E+06	5.7E+07	-9.1E+05	-1.1E+07	5.9E+07	-1.3E+05	-1.5E+05	-1.2E+05	-1.2E+05	-8.3E+04	-8.8E+04	-1.5E+05	-2.2E+05
78.1	-1.7E+06	3.1E+07	-1.1E+07	-3.0E+06	6.6E+07	-1.3E+06	-1.3E+07	6.8E+07	-7.7E+04	-2.3E+05	-1.7E+05	-1.9E+05	-2.1E+05	-1.2E+05	-1.0E+05	-1.3E+05
87.9	-7.2E+06	3.2E+07	-1.2E+07	-6.2E+06	7.4E+07	-7.7E+04	-1.5E+07	7.8E+07	-1.1E+05	-1.8E+05	-1.1E+05	-1.2E+05	-1.5E+05	-1.2E+05	-2.4E+05	-1.2E+05
97.7	-1.1E+07	3.0E+07	-1.2E+07	-1.0E+07	8.3E+07	1.9E+05	-1.7E+07	8.6E+07	-2.5E+05	-1.4E+05	-2.0E+05	-1.0E+05	-1.6E+05	-1.5E+05	-2.1E+05	-9.8E+04
107.4	-1.6E+07	2.8E+07	-1.4E+07	-1.6E+07	9.2E+07	-1.3E+06	-1.8E+07	9.2E+07	-1.5E+05	-8.6E+04	-1.9E+05	-1.0E+05	-2.2E+05	-1.3E+05	-2.4E+05	-1.1E+05
117.2	-1.9E+07	2.9E+07	-1.5E+07	-2.0E+07	1.0E+08	2.2E+04	-2.0E+07	1.0E+08	-6.7E+04	-1.4E+05	-1.9E+05	-1.6E+05	-4.0E+04	-1.2E+05	-2.0E+05	-7.7E+04
127.0	-2.6E+07	2.9E+07	-1.4E+07	-2.7E+07	1.1E+08	1.4E+06	-2.1E+07	1.1E+08	-8.3E+04	-1.9E+05	-2.0E+05	-2.6E+05	-2.4E+05	-1.8E+05	-1.1E+05	-1.3E+05
136.7	-3.4E+07	2.8E+07	-1.5E+07	-3.3E+07	1.2E+08	3.6E+05	-2.3E+07	1.2E+08	-2.2E+05	-1.6E+05	-1.6E+05	-1.2E+05	-1.2E+05	-9.4E+04	-1.2E+05	-1.5E+05

Table 53 Raw data for the test seal at PD=41.4 bar, ω=5 krpm, and inlet GVF=0% with the zero-preswirl insert

Freq.	Re(H_{XX})	Re(H_{XY})	Re(H_{YX})	Re(H_{YY})	Im(H_{XX})	Im(H_{XY})	Im(H_{YX})	Im(H_{YY})	Re(eH_{XX})	Re(eH_{XY})	Re(eH_{YX})	Re(eH_{YY})	Im(eH_{XX})	Im(eH_{XY})	Im(eH_{YX})	Im(eH_{YY})
Hz	N/m	N/m	N/m	N/m	N/m	N/m	N/m	N/m	N/m	N/m	N/m	N/m	N/m	N/m	N/m	N/m
9.8	8.1E+06	4.0E+07	-1.6E+07	8.3E+06	9.5E+06	2.9E+06	1.4E+05	8.6E+06	-1.6E+05	-2.6E+05	-1.7E+05	-2.6E+05	-3.1E+05	-5.1E+05	-1.6E+05	-2.6E+05
19.5	8.1E+06	4.0E+07	-1.6E+07	7.2E+06	1.7E+07	-3.1E+05	-2.7E+06	1.7E+07	-2.3E+05	-2.5E+05	-2.0E+05	-1.8E+05	-1.5E+05	-2.7E+05	-1.7E+05	-3.2E+05
29.3	6.5E+06	3.9E+07	-1.8E+07	7.0E+06	2.4E+07	4.8E+06	-2.1E+06	2.4E+07	-1.1E+05	-1.9E+05	-2.1E+05	-1.5E+05	-1.9E+05	-1.1E+05	-1.4E+05	-2.0E+05
39.1	5.0E+06	3.8E+07	-1.7E+07	4.2E+06	3.4E+07	1.0E+06	-6.4E+06	3.5E+07	-1.3E+05	-1.1E+05	-1.2E+05	-1.1E+05	-1.2E+05	-1.2E+05	-9.0E+04	-8.7E+04
48.8	3.6E+06	3.9E+07	-1.7E+07	2.9E+06	4.3E+07	1.3E+06	-8.0E+06	4.4E+07	-2.2E+05	-1.4E+05	-1.4E+05	-1.9E+05	-1.5E+05	-1.7E+05	-3.0E+05	-1.8E+05
58.6	4.4E+05	3.7E+07	-1.8E+07	-1.5E+05	4.9E+07	3.9E+06	-1.0E+07	5.2E+07	-1.5E+05	-2.6E+05	-1.6E+05	-2.1E+05	-1.1E+05	-1.5E+05	-1.8E+05	-2.1E+05
68.4	-1.0E+06	3.8E+07	-2.0E+07	-5.3E+05	5.9E+07	3.4E+05	-1.1E+07	6.0E+07	-1.3E+05	-7.9E+04	-1.6E+05	-1.9E+05	-5.2E+04	-1.5E+05	-2.2E+05	-1.6E+05
78.1	-3.6E+06	3.7E+07	-2.0E+07	-4.2E+06	6.8E+07	8.8E+05	-1.3E+07	7.0E+07	-5.5E+04	-1.2E+05	-2.1E+05	-1.4E+05	-1.8E+05	-1.2E+05	-1.5E+05	-1.3E+05
87.9	-8.7E+06	3.7E+07	-2.1E+07	-7.8E+06	7.6E+07	2.2E+06	-1.5E+07	8.0E+07	-1.4E+05	-1.0E+05	-2.0E+05	-1.5E+05	-1.5E+05	-8.5E+04	-3.0E+05	-1.1E+05
97.7	-1.3E+07	3.6E+07	-2.2E+07	-1.0E+07	8.5E+07	3.6E+06	-1.6E+07	8.8E+07	-2.0E+05	-1.1E+05	-1.9E+05	-1.5E+05	-9.0E+04	-1.7E+05	-8.6E+04	-1.7E+05
107.4	-1.8E+07	3.4E+07	-2.3E+07	-1.7E+07	9.4E+07	2.4E+06	-1.8E+07	9.5E+07	-7.5E+04	-1.1E+05	-7.1E+04	-1.2E+05	-1.7E+05	-9.2E+04	-2.2E+05	-1.7E+05
117.2	-2.0E+07	3.5E+07	-2.4E+07	-2.1E+07	1.0E+08	3.9E+06	-2.0E+07	1.1E+08	-1.1E+05	-2.0E+05	-1.7E+05	-9.2E+04	-2.0E+05	-1.2E+05	-7.6E+04	-1.8E+05
127.0	-2.7E+07	3.5E+07	-2.3E+07	-2.8E+07	1.1E+08	6.1E+06	-2.2E+07	1.1E+08	-9.8E+04	-1.2E+05	-7.9E+04	-1.8E+05	-9.3E+04	-2.5E+05	-1.7E+05	-2.2E+05
136.7	-3.4E+07	3.4E+07	-2.5E+07	-3.2E+07	1.2E+08	5.6E+06	-2.3E+07	1.2E+08	-1.3E+05	-2.2E+05	-1.9E+05	-2.6E+05	-2.2E+05	-2.3E+05	-2.3E+05	-1.5E+05

Table 54 Raw data for the test seal at PD=41.4 bar, ω=3 krpm, and inlet GVF=2% with the zero-preswirl insert

Freq.	Re(H_{XX})	Re(H_{XY})	Re(H_{YX})	Re(H_{YY})	Im(H_{XX})	Im(H_{XY})	Im(H_{YX})	Im(H_{YY})	Re(eH_{XX})	Re(eH_{XY})	Re(eH_{YX})	Re(eH_{YY})	Im(eH_{XX})	Im(eH_{XY})	Im(eH_{YX})	Im(eH_{YY})
Hz	N/m	N/m	N/m	N/m	N/m	N/m	N/m	N/m	N/m	N/m	N/m	N/m	N/m	N/m	N/m	N/m
9.8	9.1E+06	3.3E+07	-7.2E+06	8.9E+06	1.0E+07	8.2E+05	1.1E+05	8.3E+06	-8.1E+04	-1.9E+05	-1.7E+05	-2.3E+05	-1.9E+05	-2.3E+05	-1.2E+05	-2.2E+05
19.5	8.9E+06	3.3E+07	-7.9E+06	8.8E+06	1.8E+07	1.6E+05	-2.6E+06	1.8E+07	-1.7E+05	-2.3E+05	-1.2E+05	-1.6E+05	-2.0E+05	-2.3E+05	-1.5E+05	-1.6E+05
29.3	8.9E+06	3.2E+07	-1.1E+07	9.7E+06	2.4E+07	4.1E+06	-7.9E+05	2.6E+07	-7.1E+04	-1.4E+05	-1.3E+05	-2.2E+05	-1.9E+05	-1.8E+05	-2.0E+05	-8.7E+04
39.1	6.1E+06	3.1E+07	-9.5E+06	6.5E+06	3.3E+07	1.5E+06	-5.0E+06	3.5E+07	-1.7E+05	-1.2E+05	-1.8E+05	-1.4E+05	-1.1E+05	-1.6E+05	-1.0E+05	-1.5E+05
48.8	4.1E+06	3.2E+07	-1.1E+07	5.7E+06	4.4E+07	9.8E+05	-5.7E+06	4.5E+07	-2.4E+05	-1.8E+05	-1.4E+05	-1.2E+05	-3.1E+05	-2.2E+05	-1.5E+05	-1.3E+05
58.6	2.2E+06	3.2E+07	-1.2E+07	3.3E+06	5.1E+07	1.2E+06	-6.4E+06	5.5E+07	-2.0E+05	-1.4E+05	-1.8E+05	-2.5E+05	-1.1E+05	-1.2E+05	-1.6E+05	-1.2E+05
68.4	2.0E+06	3.2E+07	-1.2E+07	4.6E+06	6.0E+07	-1.4E+06	-7.2E+06	6.1E+07	-3.2E+05	-1.3E+05	-1.4E+05	-2.0E+05	-8.3E+04	-2.5E+05	-1.0E+05	-2.7E+05
78.1	1.4E+06	3.1E+07	-1.1E+07	4.0E+05	6.9E+07	-1.3E+06	-9.0E+06	7.2E+07	-1.0E+05	-1.4E+05	-1.2E+05	-2.6E+05	-1.0E+05	-1.5E+05	-1.3E+05	-1.8E+05
87.9	-4.2E+06	3.0E+07	-1.3E+07	-1.5E+06	7.8E+07	-2.2E+05	-9.4E+06	8.2E+07	-1.3E+05	-2.0E+05	-1.4E+05	-2.3E+05	-1.3E+05	-1.0E+05	-1.3E+05	-1.5E+05
97.7	-7.6E+06	3.0E+07	-1.4E+07	-3.6E+06	8.9E+07	-1.6E+05	-1.1E+07	9.2E+07	-1.5E+05	-1.5E+05	-2.0E+05	-7.1E+04	-1.5E+05	-1.1E+05	-1.7E+05	-2.1E+05
107.4	-1.1E+07	2.8E+07	-1.4E+07	-8.1E+06	9.8E+07	-1.1E+06	-1.2E+07	9.9E+07	-2.2E+05	-2.1E+05	-1.7E+05	-1.5E+05	-1.3E+05	-1.5E+05	-3.4E+05	-1.4E+05
117.2	-1.3E+07	2.9E+07	-1.5E+07	-1.0E+07	1.1E+08	5.1E+05	-1.3E+07	1.1E+08	-2.6E+05	-9.9E+04	-1.0E+05	-9.8E+04	-1.5E+05	-1.7E+05	-9.7E+04	-1.3E+05
127.0	-1.6E+07	2.9E+07	-1.3E+07	-1.5E+07	1.2E+08	8.5E+05	-1.5E+07	1.2E+08	-1.5E+05	-3.3E+05	-1.3E+05	-1.9E+05	-1.4E+05	-1.4E+05	-7.7E+04	-2.5E+05
136.7	-2.3E+07	3.0E+07	-1.5E+07	-1.9E+07	1.3E+08	-8.5E+05	-1.6E+07	1.3E+08	-1.4E+05	-2.1E+05	-2.4E+05	-1.7E+05	-2.9E+05	-1.5E+05	-2.0E+05	-3.1E+05

Table 55 Raw data for the test seal at PD=41.4 bar, ω=4 krpm, and inlet GVF=2% with the zero-preswirl insert

Freq.	Re(H_{XX})	Re(H_{XY})	Re(H_{YX})	Re(H_{YY})	Im(H_{XX})	Im(H_{XY})	Im(H_{YX})	Im(H_{YY})	Re(eH_{XX})	Re(eH_{XY})	Re(eH_{YX})	Re(eH_{YY})	Im(eH_{XX})	Im(eH_{XY})	Im(eH_{YX})	Im(eH_{YY})
Hz	N/m	N/m	N/m	N/m	N/m	N/m	N/m	N/m	N/m	N/m	N/m	N/m	N/m	N/m	N/m	N/m
9.8	9.4E+06	3.3E+07	-9.6E+06	7.9E+06	9.4E+06	2.9E+06	1.2E+05	1.1E+07	-1.5E+05	-2.2E+05	-1.7E+05	-2.9E+05	-1.1E+05	-1.9E+05	-1.7E+05	-2.1E+05
19.5	9.2E+06	3.1E+07	-1.1E+07	6.7E+06	1.9E+07	-3.6E+05	-2.0E+06	1.9E+07	-9.0E+04	-1.3E+05	-1.9E+05	-1.4E+05	-1.2E+05	-1.1E+05	-1.5E+05	-1.9E+05
29.3	8.6E+06	3.1E+07	-1.2E+07	3.6E+06	2.4E+07	5.3E+06	-1.1E+06	2.7E+07	-2.1E+05	-1.2E+05	-1.3E+05	-1.1E+05	-2.0E+05	-2.1E+05	-2.3E+05	-2.0E+05
39.1	6.3E+06	3.1E+07	-1.1E+07	5.3E+06	3.3E+07	1.8E+06	-3.6E+06	3.6E+07	-1.2E+05	-1.3E+05	-1.6E+05	-9.3E+04	-1.5E+05	-1.2E+05	-1.2E+05	-1.1E+05
48.8	5.3E+06	3.2E+07	-1.2E+07	5.5E+06	4.4E+07	-4.9E+05	-3.7E+06	4.5E+07	-2.3E+05	-1.9E+05	-1.3E+05	-2.6E+05	-1.5E+05	-1.9E+05	-2.4E+05	-1.0E+05
58.6	2.4E+06	3.3E+07	-1.3E+07	-4.5E+05	5.2E+07	1.2E+06	-6.4E+06	6.0E+07	-1.4E+05	-1.7E+05	-2.4E+05	-4.4E+05	-9.8E+04	-1.5E+05	-1.5E+05	-3.1E+05
68.4	1.5E+06	3.0E+07	-1.3E+07	4.7E+06	6.0E+07	1.5E+06	-5.9E+06	6.3E+07	-2.3E+05	-2.1E+05	-3.9E+05	-3.0E+05	-2.6E+05	-2.2E+05	-2.8E+05	-2.6E+05
78.1	1.3E+06	2.9E+07	-1.1E+07	-1.4E+06	6.9E+07	-2.5E+05	-7.5E+06	7.1E+07	-1.6E+05	-2.0E+05	-1.3E+05	-1.2E+05	-1.2E+05	-2.4E+05	-2.0E+05	-1.2E+05
87.9	-3.8E+06	2.9E+07	-1.5E+07	-1.6E+06	7.8E+07	-5.8E+05	-7.8E+06	8.5E+07	-1.5E+05	-2.2E+05	-1.4E+05	-1.3E+05	-8.7E+04	-7.6E+04	-1.3E+05	-2.6E+05
97.7	-6.7E+06	2.9E+07	-1.5E+07	-6.6E+06	8.8E+07	-1.4E+05	-8.9E+06	9.7E+07	-2.1E+05	-2.2E+05	-1.4E+05	-1.6E+05	-1.2E+05	-1.8E+05	-6.9E+04	-1.7E+05
107.4	-1.0E+07	2.9E+07	-1.6E+07	-1.2E+07	9.8E+07	-1.4E+06	-1.1E+07	1.0E+08	-8.7E+04	-1.4E+05	-2.4E+05	-1.8E+05	-1.9E+05	-1.2E+05	-2.0E+05	-3.5E+05
117.2	-1.2E+07	2.8E+07	-1.6E+07	-1.1E+07	1.1E+08	-2.7E+05	-1.2E+07	1.1E+08	-1.6E+05	-1.7E+05	-1.3E+05	-2.8E+05	-6.1E+04	-2.3E+05	-1.0E+05	-1.2E+05
127.0	-1.6E+07	3.0E+07	-1.4E+07	-1.9E+07	1.2E+08	3.0E+05	-1.4E+07	1.2E+08	-2.3E+05	-3.0E+05	-1.3E+05	-4.4E+05	-8.2E+04	-5.3E+05	-2.4E+05	-2.8E+05
136.7	-2.3E+07	2.9E+07	-1.5E+07	-2.2E+07	1.3E+08	1.6E+06	-1.4E+07	1.3E+08	-1.8E+05	-4.9E+05	-2.8E+05	-4.9E+05	-1.7E+05	-1.9E+05	-3.2E+05	-3.5E+05

Table 56 Raw data for the test seal at PD=41.4 bar, ω=5 krpm, and inlet GVF=2% with the zero-preswirl insert

Freq.	Re(H_{XX})	Re(H_{XY})	Re(H_{YX})	Re(H_{YY})	Im(H_{XX})	Im(H_{XY})	Im(H_{YX})	Im(H_{YY})	Re(eH_{XX})	Re(eH_{XY})	Re(eH_{YX})	Re(eH_{YY})	Im(eH_{XX})	Im(eH_{XY})	Im(eH_{YX})	Im(eH_{YY})
Hz	N/m	N/m	N/m	N/m	N/m	N/m	N/m	N/m	N/m	N/m	N/m	N/m	N/m	N/m	N/m	N/m
9.8	5.6E+06	3.8E+07	-2.0E+07	4.2E+06	1.2E+07	4.2E+06	1.9E+06	1.1E+07	-2.3E+05	-3.2E+05	-1.4E+05	-1.9E+05	-2.2E+05	-3.0E+05	-1.5E+05	-1.7E+05
19.5	5.8E+06	3.7E+07	-2.2E+07	3.0E+06	2.0E+07	1.7E+06	-2.1E+06	2.1E+07	-2.5E+05	-2.6E+05	-3.0E+05	-4.1E+05	-1.3E+05	-2.4E+05	-2.6E+05	-2.8E+05
29.3	5.4E+06	3.7E+07	-2.5E+07	6.1E+06	2.7E+07	6.2E+06	2.2E+06	2.9E+07	-2.2E+05	-5.6E+04	-3.9E+05	-2.0E+05	-1.4E+05	-2.4E+05	-1.4E+05	-3.1E+05
39.1	3.8E+06	3.6E+07	-2.3E+07	2.5E+06	3.6E+07	3.5E+06	-2.7E+06	3.9E+07	-1.5E+05	-1.3E+05	-2.0E+05	-1.8E+05	-1.2E+05	-1.9E+05	-1.7E+05	-1.6E+05
48.8	2.4E+06	3.8E+07	-2.5E+07	1.7E+06	4.6E+07	3.6E+06	-2.3E+06	4.9E+07	-1.7E+05	-1.5E+05	-2.0E+05	-9.3E+04	-1.1E+05	-1.2E+05	-1.2E+05	-1.9E+05
58.6	5.9E+05	3.6E+07	-2.5E+07	3.9E+05	5.3E+07	4.5E+06	-3.5E+06	5.8E+07	-1.7E+05	-8.9E+04	-3.4E+05	-1.4E+05	-1.8E+05	-1.7E+05	-1.3E+05	-2.0E+05
68.4	7.5E+05	3.7E+07	-2.5E+07	-5.8E+05	6.3E+07	8.1E+05	-4.1E+06	6.6E+07	-1.0E+05	-1.7E+05	-2.7E+05	-3.1E+05	-2.1E+05	-1.6E+05	-2.2E+05	-1.9E+05
78.1	-1.0E+06	3.6E+07	-2.3E+07	-1.2E+06	7.0E+07	2.8E+06	-3.9E+06	7.6E+07	-1.0E+05	-1.3E+05	-2.3E+05	-1.6E+05	-1.3E+05	-1.1E+05	-2.2E+05	-1.4E+05
87.9	-6.4E+06	3.6E+07	-2.6E+07	-4.7E+06	8.0E+07	3.5E+06	-5.2E+06	8.6E+07	-2.4E+05	-1.7E+05	-1.4E+05	-8.3E+04	-8.5E+04	-1.7E+05	-1.0E+05	-9.5E+04
97.7	-9.8E+06	3.6E+07	-2.7E+07	-5.5E+06	9.1E+07	4.3E+06	-3.9E+06	9.5E+07	-1.2E+05	-1.5E+05	-3.0E+05	-1.6E+05	-3.1E+05	-1.3E+05	-1.6E+05	-1.9E+05
107.4	-1.2E+07	3.5E+07	-2.6E+07	-8.7E+06	1.0E+08	2.5E+06	-5.7E+06	1.0E+08	-1.9E+05	-1.7E+05	-1.7E+05	-1.7E+05	-2.1E+05	-1.6E+05	-2.2E+05	-1.3E+05
117.2	-1.4E+07	3.6E+07	-2.6E+07	-1.2E+07	1.1E+08	4.5E+06	-7.7E+06	1.1E+08	-1.2E+05	-9.0E+04	-2.5E+05	-1.2E+05	-1.6E+05	-1.1E+05	-1.8E+05	-1.5E+05
127.0	-1.8E+07	3.7E+07	-2.4E+07	-1.6E+07	1.2E+08	5.0E+06	-8.3E+06	1.2E+08	-1.1E+05	-2.1E+05	-2.1E+05	-3.0E+05	-1.1E+05	-1.6E+05	-2.0E+05	-3.0E+05
136.7	-2.4E+07	3.7E+07	-2.7E+07	-1.9E+07	1.3E+08	2.0E+06	-1.0E+07	1.4E+08	-1.5E+05	-8.5E+04	-2.9E+05	-1.5E+05	-1.7E+05	-3.1E+05	-5.8E+04	-2.4E+05

Table 57 Raw data for the test seal at PD=41.4 bar, ω=3 krpm, and inlet GVF=4% with the zero-preswirl insert

Freq.	Re($\boldsymbol{H_{XX}}$)	Re($\boldsymbol{H_{XY}}$)	Re($\boldsymbol{H_{YX}}$)	Re($\boldsymbol{H_{YY}}$)	Im($\boldsymbol{H_{XX}}$)	Im($\boldsymbol{H_{XY}}$)	Im($\boldsymbol{H_{YX}}$)	Im($\boldsymbol{H_{YY}}$)	Re($\boldsymbol{eH_{XX}}$)	Re($\boldsymbol{eH_{XY}}$)	Re($\boldsymbol{eH_{YX}}$)	Re($\boldsymbol{eH_{YY}}$)	Im($\boldsymbol{eH_{XX}}$)	Im($\boldsymbol{eH_{XY}}$)	Im($\boldsymbol{eH_{YX}}$)	Im($\boldsymbol{eH_{YY}}$)
Hz	N/m	N/m	N/m	N/m	N/m	N/m	N/m	N/m	N/m	N/m	N/m	N/m	N/m	N/m	N/m	N/m
9.8	5.7E+06	3.1E+07	-1.6E+07	2.6E+06	1.3E+07	4.5E+06	1.8E+06	1.2E+07	-4.3E+05	-4.7E+05	-4.8E+05	-6.8E+05	-2.6E+05	-4.0E+05	-3.6E+05	-3.1E+05
19.5	4.9E+06	3.1E+07	-1.8E+07	3.8E+06	2.1E+07	2.4E+06	4.2E+05	2.2E+07	-5.7E+05	-1.2E+05	-1.1E+06	-7.0E+05	-3.2E+05	-7.2E+05	-2.9E+05	-1.0E+06
29.3	3.8E+06	3.0E+07	-1.9E+07	4.6E+06	2.7E+07	6.2E+06	2.6E+06	2.8E+07	-7.0E+05	-1.8E+05	-8.9E+05	-2.6E+05	-4.3E+05	-5.8E+05	-2.2E+05	-6.2E+05
39.1	1.3E+06	2.9E+07	-1.9E+07	1.4E+06	3.6E+07	2.4E+06	-1.5E+06	4.0E+07	-5.4E+05	-1.9E+05	-7.2E+05	-2.1E+05	-2.3E+05	-4.5E+05	-1.6E+05	-5.4E+05
48.8	-7.9E+05	3.0E+07	-2.1E+07	1.8E+06	4.9E+07	3.2E+06	1.7E+06	5.1E+07	-6.6E+05	-5.0E+05	-7.4E+05	-3.5E+05	-4.8E+05	-4.2E+05	-4.2E+05	-4.5E+05
58.6	-2.0E+06	3.0E+07	-1.9E+07	1.1E+06	5.5E+07	3.4E+06	-1.5E+06	5.7E+07	-6.7E+05	-2.1E+05	-7.0E+05	-2.2E+05	-3.3E+05	-3.7E+05	-2.3E+05	-3.3E+05
68.4	-2.8E+06	2.9E+07	-1.9E+07	-4.4E+05	6.3E+07	8.5E+05	-2.6E+06	6.6E+07	-4.3E+05	-5.3E+05	-5.9E+05	-5.7E+05	-3.6E+05	-2.2E+05	-2.9E+05	-2.6E+05
78.1	5.9E+05	2.9E+07	-1.4E+07	-2.2E+06	7.3E+07	1.0E+06	-2.5E+06	7.6E+07	-2.1E+05	-2.9E+05	-5.9E+05	-2.7E+05	-4.3E+05	-1.7E+05	-6.2E+05	-3.8E+05
87.9	-7.4E+06	2.9E+07	-2.0E+07	-4.9E+06	8.3E+07	1.7E+06	-1.9E+06	8.8E+07	-4.0E+05	-4.8E+05	-6.9E+05	-4.4E+05	-4.6E+05	-1.7E+05	-5.1E+05	-3.0E+05
97.7	-1.0E+07	3.0E+07	-2.0E+07	-5.3E+06	9.5E+07	2.7E+06	-1.1E+06	9.8E+07	-3.7E+05	-3.6E+05	-5.5E+05	-3.6E+05	-5.7E+05	-2.4E+05	-3.9E+05	-3.1E+05
107.4	-1.2E+07	2.8E+07	-1.9E+07	-8.4E+06	1.1E+08	4.6E+05	-1.8E+06	1.1E+08	-3.2E+05	-1.1E+05	-5.9E+05	-3.2E+05	-3.8E+05	-2.4E+05	-4.7E+05	-3.9E+05
117.2	-1.3E+07	2.8E+07	-2.0E+07	-1.1E+07	1.1E+08	2.0E+06	-4.4E+06	1.2E+08	-2.0E+05	-2.4E+05	-4.2E+05	-3.5E+05	-5.1E+05	-2.7E+05	-6.0E+05	-1.9E+05
127.0	-1.3E+07	2.9E+07	-1.5E+07	-1.2E+07	1.2E+08	5.9E+05	-4.1E+06	1.3E+08	-1.4E+05	-1.9E+05	-3.2E+05	-2.9E+05	-3.7E+05	-2.3E+05	-6.5E+05	-1.7E+05
136.7	-2.2E+07	3.1E+07	-1.7E+07	-1.4E+07	1.3E+08	8.0E+05	-5.6E+06	1.4E+08	-2.5E+05	-1.7E+05	-2.1E+05	-3.6E+05	-5.5E+05	-5.1E+05	-5.0E+05	-3.9E+05

Table 58 Raw data for the test seal at PD=41.4 bar, ω=4 krpm, and inlet GVF=4% with the zero-preswirl insert

Freq.	Re($\boldsymbol{H_{XX}}$)	Re($\boldsymbol{H_{XY}}$)	Re($\boldsymbol{H_{YX}}$)	Re($\boldsymbol{H_{YY}}$)	Im($\boldsymbol{H_{XX}}$)	Im($\boldsymbol{H_{XY}}$)	Im($\boldsymbol{H_{YX}}$)	Im($\boldsymbol{H_{YY}}$)	Re($\boldsymbol{eH_{XX}}$)	Re($\boldsymbol{eH_{XY}}$)	Re($\boldsymbol{eH_{YX}}$)	Re($\boldsymbol{eH_{YY}}$)	Im($\boldsymbol{eH_{XX}}$)	Im($\boldsymbol{eH_{XY}}$)	Im($\boldsymbol{eH_{YX}}$)	Im($\boldsymbol{eH_{YY}}$)
Hz	N/m	N/m	N/m	N/m	N/m	N/m	N/m	N/m	N/m	N/m	N/m	N/m	N/m	N/m	N/m	N/m
9.8	6.0E+06	3.2E+07	-1.4E+07	3.1E+06	1.2E+07	3.4E+06	1.5E+06	1.2E+07	-2.9E+05	-4.2E+05	-4.8E+05	-6.4E+05	-2.4E+05	-3.6E+05	-2.5E+05	-3.3E+05
19.5	5.7E+06	3.2E+07	-1.6E+07	4.3E+06	2.1E+07	1.6E+06	2.4E+04	2.2E+07	-4.7E+05	-3.8E+05	-6.2E+05	-4.4E+05	-2.2E+05	-4.1E+05	-2.5E+05	-5.5E+05
29.3	4.2E+06	3.1E+07	-1.8E+07	5.3E+06	2.7E+07	6.1E+06	2.9E+06	2.9E+07	-2.6E+05	-1.8E+05	-3.3E+05	-1.9E+05	-2.5E+05	-2.5E+05	-1.7E+05	-2.9E+05
39.1	1.7E+06	3.0E+07	-1.8E+07	1.5E+06	3.5E+07	2.0E+06	-1.9E+06	4.0E+07	-2.3E+05	-1.2E+05	-5.0E+05	-1.9E+05	-9.2E+04	-1.7E+05	-2.0E+05	-3.5E+05
48.8	-7.4E+05	3.1E+07	-1.9E+07	2.2E+06	4.8E+07	2.8E+06	1.0E+06	5.0E+07	-3.7E+05	-1.9E+05	-6.4E+05	-2.2E+05	-2.0E+05	-2.3E+05	-1.6E+05	-3.3E+05
58.6	-1.9E+06	3.1E+07	-1.8E+07	4.5E+05	5.4E+07	3.1E+06	-1.8E+06	5.7E+07	-3.1E+05	-8.5E+04	-5.4E+05	-1.3E+05	-2.2E+05	-2.1E+05	-2.1E+05	-3.1E+05
68.4	-2.5E+06	3.0E+07	-1.9E+07	3.1E+05	6.2E+07	2.9E+05	-3.1E+06	6.6E+07	-2.5E+05	-3.2E+05	-3.4E+05	-1.7E+05	-2.9E+05	-1.9E+05	-3.3E+05	-2.3E+05
78.1	8.3E+05	3.0E+07	-1.3E+07	-2.0E+06	7.2E+07	5.3E+04	-3.6E+06	7.7E+07	-3.2E+05	-1.8E+05	-4.9E+05	-2.3E+05	-2.5E+05	-2.0E+05	-3.6E+05	-3.3E+05
87.9	-7.8E+06	3.0E+07	-2.0E+07	-4.2E+06	8.4E+07	1.2E+06	-2.6E+06	8.8E+07	-2.1E+05	-1.3E+05	-3.3E+05	-2.1E+05	-2.4E+05	-1.4E+05	-3.0E+05	-1.9E+05
97.7	-9.9E+06	3.1E+07	-2.0E+07	-4.4E+06	9.4E+07	1.1E+06	-9.4E+05	9.8E+07	-8.3E+04	-1.5E+05	-2.6E+05	-1.9E+05	-2.3E+05	-1.4E+05	-3.8E+05	-1.4E+05
107.4	-1.2E+07	2.8E+07	-1.8E+07	-8.7E+06	1.0E+08	-2.1E+05	-2.8E+06	1.1E+08	-2.9E+05	-1.9E+05	-4.8E+05	-1.6E+05	-2.6E+05	-2.1E+05	-3.4E+05	-2.6E+05
117.2	-1.3E+07	2.9E+07	-1.9E+07	-1.1E+07	1.1E+08	7.3E+05	-5.4E+06	1.2E+08	-1.8E+05	-1.0E+05	-2.0E+05	-1.7E+05	-1.6E+05	-1.3E+05	-2.9E+05	-1.6E+05
127.0	-1.4E+07	2.9E+07	-1.4E+07	-1.3E+07	1.2E+08	4.5E+05	-5.1E+06	1.3E+08	-2.0E+05	-2.4E+05	-3.0E+05	-1.3E+05	-1.6E+05	-1.8E+05	-2.9E+05	-2.6E+05
136.7	-2.2E+07	3.1E+07	-1.6E+07	-1.4E+07	1.3E+08	-5.2E+05	-6.3E+06	1.4E+08	-1.5E+05	-2.0E+05	-2.8E+05	-1.3E+05	-2.0E+05	-3.3E+05	-4.7E+05	-2.8E+05

Table 59 Raw data for the test seal at PD=41.4 bar, ω=5 krpm, and inlet GVF=4% with the zero-preswirl insert

Freq.	Re(H_{XX})	Re(H_{XY})	Re(H_{YX})	Re(H_{YY})	Im(H_{XX})	Im(H_{XY})	Im(H_{YX})	Im(H_{YY})	Re(eH_{XX})	Re(eH_{XY})	Re(eH_{YX})	Re(eH_{YY})	Im(eH_{XX})	Im(eH_{XY})	Im(eH_{YX})	Im(eH_{YY})
Hz	N/m	N/m	N/m	N/m	N/m	N/m	N/m	N/m	N/m	N/m	N/m	N/m	N/m	N/m	N/m	N/m
9.8	2.1E+06	3.8E+07	-2.6E+07	1.5E+06	1.4E+07	4.8E+06	1.6E+06	1.2E+07	-2.6E+05	-3.3E+05	-3.6E+05	-4.6E+05	-2.2E+05	-2.9E+05	-3.5E+05	-3.0E+05
19.5	3.0E+06	3.6E+07	-2.6E+07	1.6E+06	2.1E+07	-7.8E+05	-3.3E+05	2.0E+07	-2.4E+05	-2.4E+05	-1.7E+05	-2.3E+05	-2.4E+05	-3.0E+05	-2.1E+05	-2.1E+05
29.3	6.4E+05	3.5E+07	-2.8E+07	2.6E+06	2.8E+07	6.2E+06	2.4E+06	2.7E+07	-2.5E+05	-2.2E+05	-2.9E+05	-2.3E+05	-2.0E+05	-1.9E+05	-2.4E+05	-2.0E+05
39.1	-7.7E+04	3.4E+07	-2.6E+07	-4.7E+05	3.8E+07	2.9E+06	-1.3E+06	3.8E+07	-1.3E+05	-1.1E+05	-1.5E+05	-9.3E+04	-8.3E+04	-1.3E+05	-9.2E+04	-1.7E+05
48.8	-2.1E+06	3.3E+07	-2.7E+07	-3.1E+06	4.6E+07	4.1E+06	-2.9E+06	4.9E+07	-2.4E+05	-1.5E+05	-1.8E+05	-2.2E+05	-1.8E+05	-1.7E+05	-2.0E+05	-2.0E+05
58.6	-4.6E+06	3.4E+07	-2.7E+07	-1.8E+06	5.4E+07	5.5E+06	-2.3E+06	5.8E+07	-8.2E+04	-1.0E+05	-1.7E+05	-1.5E+05	-1.5E+05	-1.2E+05	-1.7E+05	-1.2E+05
68.4	-4.3E+06	3.3E+07	-2.8E+07	-5.1E+06	6.4E+07	2.7E+06	-3.5E+06	6.7E+07	-2.3E+05	-2.0E+05	-2.1E+05	-1.8E+05	-9.3E+04	-1.4E+05	-1.4E+05	-1.7E+05
78.1	-5.1E+06	3.5E+07	-2.7E+07	-4.7E+06	7.5E+07	5.1E+06	-1.1E+06	7.8E+07	-1.8E+05	-9.7E+04	-1.0E+05	-1.3E+05	-1.6E+05	-1.3E+05	-1.7E+05	-2.5E+05
87.9	-1.0E+07	3.4E+07	-2.9E+07	-8.6E+06	8.4E+07	4.3E+06	-3.8E+06	8.7E+07	-1.1E+05	-1.9E+05	-1.5E+05	-6.4E+04	-1.5E+05	-1.3E+05	-8.5E+04	-1.6E+05
97.7	-1.3E+07	3.5E+07	-3.0E+07	-9.2E+06	9.5E+07	5.3E+06	-2.1E+06	9.9E+07	-1.3E+05	-1.2E+05	-1.5E+05	-9.2E+04	-1.7E+05	-7.3E+04	-1.9E+05	-1.3E+05
107.4	-1.4E+07	3.4E+07	-3.0E+07	-1.2E+07	1.1E+08	4.3E+06	-3.0E+06	1.1E+08	-1.9E+05	-1.3E+05	-2.4E+05	-1.7E+05	-2.3E+05	-1.1E+05	-2.7E+05	-2.6E+05
117.2	-1.6E+07	3.5E+07	-2.9E+07	-1.4E+07	1.1E+08	5.9E+06	-4.2E+06	1.2E+08	-2.4E+05	-1.5E+05	-2.1E+05	-1.4E+05	-1.4E+05	-1.5E+05	-1.9E+05	-1.9E+05
127.0	-1.8E+07	3.5E+07	-2.7E+07	-1.4E+07	1.2E+08	4.3E+06	-3.1E+06	1.3E+08	-1.5E+05	-5.1E+04	-1.9E+05	-1.3E+05	-8.2E+04	-1.9E+05	-2.9E+05	-1.2E+05
136.7	-2.4E+07	3.7E+07	-2.8E+07	-1.9E+07	1.3E+08	4.8E+06	-6.0E+06	1.5E+08	-1.8E+05	-8.4E+04	-2.1E+05	-2.0E+05	-1.2E+05	-2.6E+05	-2.2E+05	-9.3E+04

Table 60 Raw data for the test seal at PD=41.4 bar, ω=3 krpm, and inlet GVF=6% with the zero-preswirl insert

Freq.	Re(H_{XX})	Re(H_{XY})	Re(H_{YX})	Re(H_{YY})	Im(H_{XX})	Im(H_{XY})	Im(H_{YX})	Im(H_{YY})	Re(eH_{XX})	Re(eH_{XY})	Re(eH_{YX})	Re(eH_{YY})	Im(eH_{XX})	Im(eH_{XY})	Im(eH_{YX})	Im(eH_{YY})
Hz	N/m	N/m	N/m	N/m	N/m	N/m	N/m	N/m	N/m	N/m	N/m	N/m	N/m	N/m	N/m	N/m
9.8	5.7E+06	3.2E+07	-1.6E+07	3.9E+06	1.3E+07	4.4E+06	2.0E+06	1.2E+07	-3.1E+05	-2.4E+05	-3.0E+05	-3.5E+05	-1.5E+05	-3.6E+05	-2.1E+05	-3.1E+05
19.5	5.6E+06	3.2E+07	-1.7E+07	3.4E+06	2.1E+07	9.7E+05	7.3E+04	2.0E+07	-2.6E+05	-3.9E+05	-4.6E+05	-4.1E+05	-3.1E+05	-2.4E+05	-2.9E+05	-3.6E+05
29.3	3.7E+06	3.0E+07	-1.9E+07	3.6E+06	2.7E+07	6.0E+06	2.6E+06	2.8E+07	-2.1E+05	-1.5E+05	-3.1E+05	-2.3E+05	-2.6E+05	-1.9E+05	-2.0E+05	-1.9E+05
39.1	2.0E+06	2.9E+07	-1.8E+07	2.7E+05	3.6E+07	1.6E+06	-1.4E+06	3.9E+07	-2.1E+05	-1.1E+05	-2.9E+05	-2.1E+05	-1.2E+05	-1.8E+05	-1.7E+05	-1.5E+05
48.8	1.1E+05	2.9E+07	-1.9E+07	8.5E+05	4.8E+07	2.3E+06	6.8E+05	5.0E+07	-3.8E+05	-1.5E+05	-4.7E+05	-1.7E+05	-2.2E+05	-2.6E+05	-2.1E+05	-2.5E+05
58.6	-1.5E+06	3.0E+07	-1.9E+07	-2.4E+04	5.5E+07	2.5E+06	-1.5E+06	5.7E+07	-2.5E+05	-1.8E+05	-4.3E+05	-1.2E+05	-2.2E+05	-2.1E+05	-2.3E+05	-2.2E+05
68.4	-2.0E+06	2.9E+07	-1.9E+07	-1.4E+06	6.3E+07	6.5E+05	-2.5E+06	6.7E+07	-2.3E+05	-1.1E+05	-3.5E+05	-2.6E+05	-1.8E+05	-2.2E+05	-1.6E+05	-2.1E+05
78.1	6.7E+05	2.9E+07	-1.4E+07	-2.8E+06	7.3E+07	7.3E+05	-2.2E+06	7.7E+07	-2.5E+05	-1.5E+05	-1.6E+05	-1.1E+05	-1.5E+05	-1.9E+05	-2.0E+05	-1.9E+05
87.9	-6.6E+06	2.8E+07	-2.0E+07	-5.7E+06	8.4E+07	1.4E+06	-1.8E+06	8.9E+07	-3.4E+05	-1.6E+05	-3.0E+05	-1.3E+05	-1.8E+05	-1.5E+05	-2.0E+05	-1.2E+05
97.7	-9.3E+06	2.9E+07	-2.0E+07	-6.0E+06	9.5E+07	2.2E+06	-9.0E+05	9.9E+07	-2.0E+05	-6.9E+04	-2.4E+05	-1.5E+05	-1.9E+05	-8.9E+04	-4.6E+05	-1.0E+05
107.4	-1.0E+07	2.7E+07	-1.9E+07	-8.8E+06	1.1E+08	7.3E+04	-1.9E+06	1.1E+08	-1.4E+05	-1.6E+05	-1.9E+05	-1.9E+05	-2.2E+05	-1.7E+05	-2.4E+05	-1.7E+05
117.2	-1.2E+07	2.7E+07	-1.9E+07	-1.1E+07	1.1E+08	2.4E+06	-4.5E+06	1.2E+08	-1.1E+05	-1.0E+05	-1.4E+05	-1.8E+05	-1.8E+05	-1.2E+05	-2.6E+05	-2.3E+05
127.0	-1.2E+07	2.8E+07	-1.4E+07	-1.2E+07	1.2E+08	6.8E+05	-3.9E+06	1.3E+08	-1.2E+05	-2.2E+05	-2.1E+05	-2.1E+05	-1.7E+05	-1.7E+05	-4.0E+05	-2.0E+05
136.7	-2.0E+07	3.0E+07	-1.7E+07	-1.3E+07	1.3E+08	-3.0E+05	-5.8E+06	1.4E+08	-4.0E+05	-2.9E+05	-2.8E+05	-1.1E+05	-2.1E+05	-3.8E+05	-3.8E+05	-3.8E+05

Table 61 Raw data for the test seal at PD=41.4 bar, ω=4 krpm, and inlet GVF=6% with the zero-preswirl insert

Freq.	Re(H_{XX})	Re(H_{XY})	Re(H_{YX})	Re(H_{YY})	Im(H_{XX})	Im(H_{XY})	Im(H_{YX})	Im(H_{YY})	Re(eH_{XX})	Re(eH_{XY})	Re(eH_{YX})	Re(eH_{YY})	Im(eH_{XX})	Im(eH_{XY})	Im(eH_{YX})	Im(eH_{YY})
Hz	N/m	N/m	N/m	N/m	N/m	N/m	N/m	N/m	N/m	N/m	N/m	N/m	N/m	N/m	N/m	N/m
9.8	5.4E+06	3.3E+07	-1.5E+07	5.6E+06	1.3E+07	3.0E+06	2.5E+06	1.1E+07	-2.8E+05	-3.3E+05	-2.2E+05	-2.0E+05	-2.7E+05	-3.9E+05	-1.8E+05	-3.1E+05
19.5	3.9E+06	3.1E+07	-1.7E+07	4.6E+06	2.1E+07	1.5E+06	9.1E+05	2.1E+07	-2.9E+05	-3.7E+05	-1.7E+05	-2.5E+05	-3.7E+05	-3.1E+05	-2.6E+05	-3.0E+05
29.3	3.0E+06	3.0E+07	-1.9E+07	4.4E+06	2.6E+07	5.3E+06	2.6E+06	2.8E+07	-2.6E+05	-1.3E+05	-1.7E+05	-1.4E+05	-2.0E+05	-2.0E+05	-1.8E+05	-1.6E+05
39.1	1.5E+06	2.8E+07	-1.8E+07	8.5E+05	3.6E+07	1.0E+06	-1.3E+06	3.9E+07	-1.1E+05	-8.6E+04	-1.5E+05	-1.9E+05	-1.0E+05	-1.7E+05	-1.5E+05	-2.4E+05
48.8	-6.8E+05	2.9E+07	-1.9E+07	6.6E+05	4.7E+07	1.8E+06	5.2E+04	4.9E+07	-1.8E+05	-2.1E+05	-1.8E+05	-2.0E+05	-2.1E+05	-1.2E+05	-2.0E+05	-2.6E+05
58.6	-2.0E+06	2.9E+07	-1.9E+07	3.4E+05	5.4E+07	2.2E+06	-1.8E+06	5.7E+07	-9.0E+04	-1.3E+05	-2.2E+05	-1.7E+05	-1.4E+05	-2.2E+05	-1.5E+05	-1.0E+05
68.4	-3.2E+06	2.8E+07	-2.0E+07	-1.8E+06	6.3E+07	3.0E+05	-2.8E+06	6.7E+07	-3.9E+05	-1.9E+05	-3.6E+05	-2.0E+05	-3.7E+05	-1.6E+05	-2.2E+05	-4.1E+05
78.1	-5.7E+04	2.8E+07	-1.4E+07	-3.3E+06	7.3E+07	8.0E+05	-3.0E+06	7.7E+07	-1.5E+05	-1.9E+05	-1.2E+05	-2.6E+05	-1.0E+05	-2.5E+05	-3.3E+05	-2.0E+05
87.9	-7.9E+06	2.8E+07	-2.0E+07	-5.6E+06	8.3E+07	1.4E+06	-2.0E+06	8.9E+07	-1.4E+05	-2.5E+05	-1.2E+05	-1.3E+05	-1.5E+05	-2.0E+05	-2.3E+05	-1.4E+05
97.7	-1.0E+07	2.9E+07	-2.0E+07	-6.1E+06	9.4E+07	2.1E+06	-1.6E+06	9.9E+07	-2.9E+05	-6.9E+04	-1.5E+05	-2.0E+05	-1.7E+05	-1.1E+05	-2.2E+05	-9.8E+04
107.4	-1.2E+07	2.7E+07	-2.0E+07	-8.8E+06	1.1E+08	5.1E+05	-1.9E+06	1.1E+08	-1.3E+05	-1.7E+05	-2.1E+05	-2.5E+05	-1.0E+05	-9.8E+04	-1.7E+05	-1.3E+05
117.2	-1.3E+07	2.7E+07	-1.9E+07	-1.1E+07	1.1E+08	1.7E+06	-4.2E+06	1.2E+08	-1.4E+05	-1.9E+05	-2.2E+05	-2.1E+05	-1.7E+05	-1.1E+05	-1.6E+05	-9.8E+04
127.0	-1.3E+07	2.7E+07	-1.4E+07	-1.2E+07	1.2E+08	7.5E+05	-4.5E+06	1.3E+08	-2.6E+05	-1.8E+05	-1.7E+05	-2.9E+05	-1.8E+05	-2.6E+05	-3.1E+05	-2.1E+05
136.7	-2.0E+07	2.9E+07	-1.7E+07	-1.2E+07	1.3E+08	2.2E+05	-4.7E+06	1.4E+08	-2.9E+05	-1.6E+05	-2.6E+05	-1.7E+05	-2.5E+05	-2.2E+05	-2.5E+05	-4.7E+05

Table 62 Raw data for the test seal at PD=41.4 bar, ω=5 krpm, and inlet GVF=6% with the zero-preswirl insert

Freq.	Re(H_{XX})	Re(H_{XY})	Re(H_{YX})	Re(H_{YY})	Im(H_{XX})	Im(H_{XY})	Im(H_{YX})	Im(H_{YY})	Re(eH_{XX})	Re(eH_{XY})	Re(eH_{YX})	Re(eH_{YY})	Im(eH_{XX})	Im(eH_{XY})	Im(eH_{YX})	Im(eH_{YY})
Hz	N/m	N/m	N/m	N/m	N/m	N/m	N/m	N/m	N/m	N/m	N/m	N/m	N/m	N/m	N/m	N/m
9.8	-2.2E+06	3.3E+07	-2.7E+07	-9.9E+04	1.3E+07	6.8E+06	-2.3E+05	1.1E+07	-3.1E+05	-4.1E+05	-2.5E+05	-3.8E+05	-3.5E+05	-3.8E+05	-2.8E+05	-2.5E+05
19.5	-5.4E+05	3.1E+07	-2.8E+07	9.5E+05	1.9E+07	1.9E+06	-1.1E+06	2.1E+07	-3.1E+05	-3.8E+05	-1.4E+05	-2.9E+05	-3.4E+05	-3.2E+05	-2.7E+05	-1.8E+05
29.3	-2.7E+06	3.4E+07	-3.0E+07	1.3E+06	2.9E+07	8.0E+06	1.4E+06	2.7E+07	-3.1E+05	-1.4E+05	-3.1E+05	-2.0E+05	-2.3E+05	-2.6E+05	-2.2E+05	-2.3E+05
39.1	-2.9E+06	3.3E+07	-2.9E+07	-2.3E+05	3.9E+07	4.2E+06	-1.2E+06	3.9E+07	-2.7E+05	-1.5E+05	-1.6E+05	-2.4E+05	-1.1E+05	-2.1E+05	-1.9E+05	-1.2E+05
48.8	-4.6E+06	3.2E+07	-2.9E+07	-2.3E+06	4.7E+07	5.1E+06	-2.3E+06	4.8E+07	-2.4E+05	-1.3E+05	-2.0E+05	-1.4E+05	-1.8E+05	-1.6E+05	-1.7E+05	-2.2E+05
58.6	-6.4E+06	3.3E+07	-3.0E+07	-2.1E+06	5.6E+07	5.8E+06	-1.9E+06	5.9E+07	-2.4E+05	-2.2E+05	-2.2E+05	-2.0E+05	-1.5E+05	-1.5E+05	-1.7E+05	-1.9E+05
68.4	-6.2E+06	3.1E+07	-3.0E+07	-4.5E+06	6.5E+07	3.3E+06	-1.9E+06	6.8E+07	-2.5E+05	-1.6E+05	-1.7E+05	-1.6E+05	-1.7E+05	-1.4E+05	-2.4E+05	-1.6E+05
78.1	-5.1E+06	3.3E+07	-3.0E+07	-5.2E+06	7.7E+07	5.4E+06	6.3E+05	7.9E+07	-1.4E+05	-1.6E+05	-2.9E+05	-1.5E+05	-1.5E+05	-2.0E+05	-1.2E+05	-1.3E+05
87.9	-1.1E+07	3.2E+07	-3.1E+07	-8.1E+06	8.6E+07	5.2E+06	-2.3E+06	8.8E+07	-2.0E+05	-1.9E+05	-1.0E+05	-1.9E+05	-3.2E+05	-1.3E+05	-1.3E+05	-1.1E+05
97.7	-1.4E+07	3.4E+07	-3.2E+07	-8.8E+06	9.8E+07	6.2E+06	-1.0E+06	1.0E+08	-1.3E+05	-1.5E+05	-3.3E+05	-1.7E+05	-3.5E+05	-9.2E+04	-2.4E+05	-1.8E+05
107.4	-1.4E+07	3.2E+07	-3.2E+07	-1.1E+07	1.1E+08	5.0E+06	-7.7E+05	1.1E+08	-2.2E+05	-1.4E+05	-2.4E+05	-2.8E+05	-1.9E+05	-1.2E+05	-1.6E+05	-2.4E+05
117.2	-1.6E+07	3.4E+07	-3.0E+07	-1.3E+07	1.2E+08	6.9E+06	-2.1E+06	1.2E+08	-1.7E+05	-1.8E+05	-2.2E+05	-2.7E+05	-2.5E+05	-1.3E+05	-1.8E+05	-1.4E+05
127.0	-1.7E+07	3.4E+07	-2.8E+07	-1.1E+07	1.3E+08	5.8E+06	-9.2E+05	1.3E+08	-1.2E+05	-1.2E+05	-2.0E+05	-1.6E+05	-2.0E+05	-2.3E+05	-2.3E+05	-7.8E+04
136.7	-2.3E+07	3.7E+07	-2.8E+07	-1.4E+07	1.4E+08	4.7E+06	-3.9E+06	1.5E+08	-2.1E+05	-1.5E+05	-2.5E+05	-2.5E+05	-8.3E+04	-2.2E+05	-2.8E+05	-2.5E+05

Table 63 Raw data for the test seal at PD=41.4 bar, ω=3 krpm, and inlet GVF=8% with the zero-preswirl insert

Freq.	Re(H_{XX})	Re(H_{XY})	Re(H_{YX})	Re(H_{YY})	Im(H_{XX})	Im(H_{XY})	Im(H_{YX})	Im(H_{YY})	Re(eH_{XX})	Re(eH_{XY})	Re(eH_{YX})	Re(eH_{YY})	Im(eH_{XX})	Im(eH_{XY})	Im(eH_{YX})	Im(eH_{YY})
Hz	N/m	N/m	N/m	N/m	N/m	N/m	N/m	N/m	N/m	N/m	N/m	N/m	N/m	N/m	N/m	N/m
9.8	-1.9E+06	3.4E+07	-2.4E+07	8.0E+05	2.0E+07	1.3E+07	6.4E+06	1.7E+07	-6.7E+05	-9.4E+05	-5.2E+05	-4.8E+05	-5.8E+05	-5.0E+05	-4.4E+05	-4.9E+05
19.5	1.1E+07	3.0E+07	-1.7E+07	-9.0E+04	2.6E+07	-8.4E+06	4.7E+06	1.4E+07	-1.5E+06	-6.9E+05	-7.3E+05	-4.3E+05	-4.1E+05	-1.8E+06	-4.4E+05	-9.5E+05
29.3	1.8E+06	2.8E+07	-2.2E+07	-1.9E+06	3.0E+07	7.8E+06	4.3E+06	2.6E+07	-6.5E+05	-5.0E+05	-5.5E+05	-1.6E+05	-3.0E+05	-7.4E+05	-2.5E+05	-5.7E+05
39.1	4.4E+06	2.4E+07	-2.0E+07	-8.1E+06	3.8E+07	-5.4E+06	-1.4E+06	3.3E+07	-6.4E+05	-3.9E+05	-6.0E+05	-2.5E+05	-1.3E+05	-1.0E+06	-2.3E+05	-9.9E+05
48.8	-1.7E+06	2.0E+07	-2.4E+07	-7.8E+06	4.6E+07	4.3E+06	5.3E+05	4.9E+07	-3.4E+05	-8.5E+05	-3.0E+05	-3.3E+05	-4.0E+05	-3.8E+05	-1.8E+05	-2.9E+05
58.6	-3.6E+06	2.9E+07	-2.3E+07	-4.9E+06	5.5E+07	1.2E+06	-8.4E+05	5.5E+07	-4.3E+05	-3.8E+05	-5.0E+05	-3.4E+05	-2.4E+05	-4.1E+05	-2.4E+05	-2.5E+05
68.4	-2.9E+06	2.1E+07	-2.3E+07	-1.1E+07	6.3E+07	1.1E+06	-2.1E+06	6.6E+07	-3.9E+05	-6.0E+05	-5.0E+05	-2.5E+05	-2.5E+05	-2.5E+05	-2.4E+05	-2.6E+05
78.1	2.0E+06	2.3E+07	-1.7E+07	-1.1E+07	7.4E+07	5.6E+06	-1.2E+06	7.8E+07	-2.0E+05	-2.6E+05	-3.3E+05	-1.5E+05	-2.7E+05	-6.1E+05	-2.4E+05	-1.5E+05
87.9	-1.1E+07	2.2E+07	-2.4E+07	-1.5E+07	8.5E+07	4.3E+06	-1.6E+06	8.8E+07	-4.1E+05	-5.9E+05	-3.8E+05	-2.0E+05	-3.8E+05	-2.4E+05	-2.4E+05	-4.4E+05
97.7	-9.5E+06	2.6E+07	-2.3E+07	-1.3E+07	9.9E+07	5.1E+06	3.8E+05	9.8E+07	-2.9E+05	-4.5E+05	-2.9E+05	-1.7E+05	-4.5E+05	-2.2E+05	-2.7E+05	-2.7E+05
107.4	-1.4E+07	2.4E+07	-2.6E+07	-1.7E+07	1.1E+08	6.4E+06	2.8E+05	1.1E+08	-3.7E+05	-3.7E+05	-3.7E+05	-2.3E+05	-5.0E+05	-3.2E+05	-2.5E+05	-2.2E+05
117.2	-1.4E+07	2.5E+07	-2.4E+07	-1.8E+07	1.2E+08	5.0E+06	-1.5E+06	1.2E+08	-2.8E+05	-3.9E+05	-2.2E+05	-1.8E+05	-4.2E+05	-2.1E+05	-2.6E+05	-1.0E+05
127.0	-9.8E+06	2.9E+07	-1.7E+07	-1.7E+07	1.3E+08	4.4E+06	5.8E+03	1.3E+08	-1.2E+05	-1.6E+05	-2.7E+05	-1.2E+05	-4.0E+05	-1.8E+05	-3.5E+05	-3.2E+05
136.7	-1.9E+07	2.9E+07	-2.0E+07	-2.2E+07	1.4E+08	4.9E+06	-1.9E+06	1.5E+08	-2.5E+05	-4.9E+05	-3.4E+05	-4.8E+05	-6.4E+05	-3.7E+05	-3.5E+05	-1.2E+05

Table 64 Raw data for the test seal at PD=41.4 bar, ω=4 krpm, and inlet GVF=8% with the zero-preswirl insert

Freq.	Re(H_{XX})	Re(H_{XY})	Re(H_{YX})	Re(H_{YY})	Im(H_{XX})	Im(H_{XY})	Im(H_{YX})	Im(H_{YY})	Re(eH_{XX})	Re(eH_{XY})	Re(eH_{YX})	Re(eH_{YY})	Im(eH_{XX})	Im(eH_{XY})	Im(eH_{YX})	Im(eH_{YY})
Hz	N/m	N/m	N/m	N/m	N/m	N/m	N/m	N/m	N/m	N/m	N/m	N/m	N/m	N/m	N/m	N/m
9.8	-5.5E+06	2.9E+07	-2.1E+07	5.0E+06	1.3E+07	5.2E+06	2.5E+06	1.4E+07	-3.1E+05	-3.7E+05	-2.6E+05	-4.7E+05	-3.2E+05	-3.8E+05	-4.1E+05	-3.4E+05
19.5	-5.4E+06	2.7E+07	-2.3E+07	4.9E+06	2.2E+07	1.5E+06	1.4E+06	2.1E+07	-2.6E+05	-2.2E+05	-5.6E+05	-2.8E+05	-1.5E+05	-2.8E+05	-2.2E+05	-5.4E+05
29.3	-6.6E+06	2.8E+07	-2.6E+07	7.9E+06	3.0E+07	5.1E+06	4.3E+06	2.9E+07	-2.6E+05	-2.4E+05	-5.5E+05	-1.7E+05	-3.8E+05	-2.2E+05	-1.5E+05	-4.3E+05
39.1	-7.1E+06	2.5E+07	-2.5E+07	2.0E+06	3.8E+07	1.3E+06	-9.8E+05	3.9E+07	-3.1E+05	-1.3E+05	-3.4E+05	-2.2E+05	-1.9E+05	-2.0E+05	-2.2E+05	-2.3E+05
48.8	-1.1E+07	2.4E+07	-2.8E+07	2.4E+06	5.0E+07	4.1E+06	1.9E+06	5.1E+07	-2.5E+05	-2.5E+05	-5.2E+05	-2.1E+05	-1.9E+05	-1.6E+05	-2.6E+05	-2.8E+05
58.6	-1.0E+07	2.7E+07	-2.5E+07	3.0E+05	5.8E+07	1.6E+06	-1.0E+06	5.6E+07	-2.0E+05	-2.7E+05	-3.7E+05	-2.1E+05	-1.9E+05	-2.7E+05	-2.6E+05	-2.3E+05
68.4	-1.2E+07	2.4E+07	-2.6E+07	-3.6E+04	6.7E+07	2.0E+06	8.6E+04	6.6E+07	-2.8E+05	-2.3E+05	-2.3E+05	-2.5E+05	-2.9E+05	-3.3E+05	-2.8E+05	-1.8E+05
78.1	-6.5E+06	2.6E+07	-1.8E+07	-1.1E+06	7.8E+07	3.4E+06	-7.0E+05	8.0E+07	-1.8E+05	-2.0E+05	-4.0E+05	-2.0E+05	-1.6E+05	-1.3E+05	-2.5E+05	-3.8E+05
87.9	-1.6E+07	2.4E+07	-2.7E+07	-3.7E+06	8.9E+07	3.6E+06	1.7E+06	9.2E+07	-1.3E+05	-2.8E+05	-1.0E+05	-2.1E+05	-1.3E+05	-2.7E+05	-1.7E+05	-6.9E+04
97.7	-1.6E+07	2.6E+07	-2.5E+07	-1.4E+06	1.0E+08	3.3E+06	2.6E+06	1.0E+08	-3.7E+05	-7.7E+04	-1.7E+05	-1.6E+05	-1.5E+05	-1.3E+05	-2.2E+05	-1.7E+05
107.4	-1.9E+07	2.3E+07	-2.7E+07	-6.9E+06	1.1E+08	2.7E+06	2.3E+06	1.1E+08	-2.4E+05	-2.0E+05	-3.7E+05	-8.7E+04	-2.1E+05	-1.5E+05	-2.1E+05	-2.0E+05
117.2	-1.9E+07	2.5E+07	-2.5E+07	-7.2E+06	1.2E+08	5.2E+06	1.5E+06	1.2E+08	-1.2E+05	-1.5E+05	-3.0E+05	-1.3E+05	-1.5E+05	-1.4E+05	-2.5E+05	-1.5E+05
127.0	-1.7E+07	2.6E+07	-1.7E+07	-1.0E+07	1.3E+08	3.1E+06	1.5E+05	1.2E+08	-1.8E+05	-2.7E+05	-2.3E+05	-1.5E+05	-1.1E+05	-2.4E+05	-3.4E+05	-1.8E+05
136.7	-2.4E+07	2.9E+07	-2.0E+07	-9.5E+06	1.4E+08	2.4E+06	5.2E+05	1.4E+08	-2.5E+05	-2.7E+05	-4.5E+05	-2.2E+05	-1.9E+05	-2.9E+05	-6.7E+05	-3.2E+05

Table 65 Raw data for the test seal at PD=41.4 bar, ω=5 krpm, and inlet GVF=8% with the zero-preswirl insert

Freq.	Re(H_{XX})	Re(H_{XY})	Re(H_{YX})	Re(H_{YY})	Im(H_{XX})	Im(H_{XY})	Im(H_{YX})	Im(H_{YY})	Re(eH_{XX})	Re(eH_{XY})	Re(eH_{YX})	Re(eH_{YY})	Im(eH_{XX})	Im(eH_{XY})	Im(eH_{YX})	Im(eH_{YY})
Hz	N/m	N/m	N/m	N/m	N/m	N/m	N/m	N/m	N/m	N/m	N/m	N/m	N/m	N/m	N/m	N/m
9.8	-3.7E+06	3.2E+07	-3.1E+07	-4.7E+05	1.3E+07	4.5E+06	6.2E+04	9.8E+06	-3.0E+05	-8.1E+05	-3.4E+05	-3.3E+05	-6.6E+05	-7.4E+05	-4.5E+05	-6.7E+05
19.5	-5.8E+06	2.8E+07	-3.0E+07	-3.8E+05	1.9E+07	3.6E+06	-1.1E+06	2.0E+07	-5.7E+05	-3.9E+05	-2.0E+05	-2.4E+05	-2.6E+05	-5.2E+05	-2.6E+05	-2.6E+05
29.3	-5.2E+06	3.1E+07	-3.1E+07	5.6E+05	2.9E+07	6.8E+06	9.3E+05	2.7E+07	-3.8E+05	-2.3E+05	-3.1E+05	-2.1E+05	-2.3E+05	-3.0E+05	-2.9E+05	-2.7E+05
39.1	-5.1E+06	3.1E+07	-3.1E+07	6.4E+04	4.0E+07	3.6E+06	-9.0E+05	3.9E+07	-4.9E+05	-1.6E+05	-1.7E+05	-1.7E+05	-1.4E+05	-3.2E+05	-2.1E+05	-1.1E+05
48.8	-6.5E+06	2.8E+07	-3.0E+07	-2.0E+06	4.6E+07	4.7E+06	-1.3E+06	4.8E+07	-1.8E+05	-1.3E+05	-1.9E+05	-1.8E+05	-2.0E+05	-1.5E+05	-2.1E+05	-1.2E+05
58.6	-9.7E+06	3.1E+07	-3.2E+07	-1.8E+06	5.7E+07	5.6E+06	-1.1E+06	5.9E+07	-1.3E+05	-2.1E+05	-2.2E+05	-2.1E+05	-2.2E+05	-9.9E+04	-1.9E+05	-1.4E+05
68.4	-8.6E+06	2.9E+07	-3.2E+07	-5.4E+06	6.7E+07	4.4E+06	-2.4E+06	6.8E+07	-3.5E+05	-1.3E+05	-1.4E+05	-3.8E+05	-2.7E+05	-1.5E+05	-4.7E+05	-2.3E+05
78.1	-9.6E+06	3.0E+07	-3.3E+07	-6.7E+06	7.9E+07	7.2E+06	-7.0E+04	8.0E+07	-5.4E+05	-1.2E+05	-2.9E+05	-1.7E+05	-2.5E+05	-2.6E+05	-2.3E+05	-2.0E+05
87.9	-1.3E+07	2.9E+07	-3.3E+07	-9.2E+06	8.8E+07	6.5E+06	-1.8E+06	8.8E+07	-1.9E+05	-1.8E+05	-1.9E+05	-1.2E+05	-2.9E+05	-1.4E+05	-2.3E+05	-2.0E+05
97.7	-1.5E+07	3.1E+07	-3.5E+07	-1.0E+07	1.0E+08	7.6E+06	-7.0E+05	1.0E+08	-2.0E+05	-1.6E+05	-1.8E+05	-1.1E+05	-2.1E+05	-2.2E+05	-1.6E+05	-1.8E+05
107.4	-1.6E+07	3.0E+07	-3.4E+07	-1.2E+07	1.1E+08	6.1E+06	-5.7E+05	1.1E+08	-1.7E+05	-2.6E+05	-4.5E+05	-1.9E+05	-4.4E+05	-1.8E+05	-2.7E+05	-1.5E+05
117.2	-1.7E+07	3.1E+07	-3.3E+07	-1.2E+07	1.2E+08	8.4E+06	-5.8E+05	1.2E+08	-2.0E+05	-1.4E+05	-1.1E+05	-1.0E+05	-3.1E+05	-1.6E+05	-1.4E+05	-1.8E+05
127.0	-1.9E+07	3.3E+07	-3.1E+07	-1.0E+07	1.3E+08	6.8E+06	6.9E+05	1.3E+08	-9.0E+04	-2.1E+05	-1.3E+05	-2.5E+05	-1.7E+05	-2.1E+05	-1.8E+05	-1.5E+05
136.7	-2.3E+07	3.5E+07	-3.0E+07	-1.5E+07	1.4E+08	6.8E+06	-1.4E+06	1.5E+08	-2.5E+05	-1.3E+05	-1.7E+05	-1.5E+05	-2.0E+05	-3.3E+05	-2.9E+05	-2.0E+05

Table 66 Raw data for the test seal at PD=41.4 bar, ω=3 krpm, and inlet GVF=10% with the zero-preswirl insert

Freq.	Re(H_{XX})	Re(H_{XY})	Re(H_{YX})	Re(H_{YY})	Im(H_{XX})	Im(H_{XY})	Im(H_{YX})	Im(H_{YY})	Re(eH_{XX})	Re(eH_{XY})	Re(eH_{YX})	Re(eH_{YY})	Im(eH_{XX})	Im(eH_{XY})	Im(eH_{YX})	Im(eH_{YY})
Hz	N/m	N/m	N/m	N/m	N/m	N/m	N/m	N/m	N/m	N/m	N/m	N/m	N/m	N/m	N/m	N/m
9.8	-7.0E+06	3.1E+07	-2.5E+07	6.3E+06	1.7E+07	6.8E+06	5.2E+06	1.5E+07	-6.8E+05	-8.8E+05	-3.4E+05	-7.2E+05	-6.7E+05	-7.1E+05	-5.7E+05	-2.1E+05
19.5	3.1E+05	2.5E+07	-2.0E+07	1.5E+06	2.1E+07	-6.8E+06	-3.5E+05	1.5E+07	-6.2E+05	-2.5E+05	-4.4E+05	-2.7E+05	-1.8E+05	-5.4E+05	-2.9E+05	-4.0E+05
29.3	-4.9E+06	2.6E+07	-2.6E+07	3.0E+06	3.2E+07	3.5E+06	3.5E+06	2.7E+07	-4.5E+05	-2.9E+05	-5.4E+05	-2.2E+05	-3.0E+05	-3.2E+05	-2.1E+05	-3.1E+05
39.1	-3.2E+06	2.2E+07	-2.3E+07	1.5E+06	4.0E+07	-2.1E+06	1.1E+06	3.7E+07	-2.2E+05	-2.0E+05	-2.1E+05	-1.6E+05	-2.2E+05	-1.5E+05	-1.8E+05	-1.4E+05
48.8	-1.0E+07	2.1E+07	-2.6E+07	-2.3E+06	4.8E+07	4.3E+06	-7.1E+05	4.8E+07	-3.3E+05	-2.5E+05	-5.0E+05	-2.3E+05	-2.4E+05	-1.8E+05	-2.8E+05	-2.5E+05
58.6	-1.1E+07	2.4E+07	-2.7E+07	-2.4E+06	5.7E+07	1.7E+06	-1.1E+06	5.8E+07	-2.7E+05	-7.4E+04	-2.2E+05	-1.9E+05	-5.7E+04	-1.8E+05	-1.9E+05	-3.2E+05
68.4	-1.0E+07	2.0E+07	-2.5E+07	-5.2E+06	6.7E+07	2.6E+06	4.4E+05	6.8E+07	-4.7E+05	-3.9E+05	-4.6E+05	-2.8E+05	-7.9E+05	-2.4E+05	-3.5E+05	-3.3E+05
78.1	-5.8E+06	2.4E+07	-2.1E+07	-6.2E+06	8.0E+07	4.7E+06	2.2E+06	8.0E+07	-3.2E+05	-1.1E+05	-5.0E+05	-3.1E+05	-2.9E+05	-2.1E+05	-2.3E+05	-2.6E+05
87.9	-1.5E+07	2.1E+07	-2.8E+07	-9.4E+06	8.9E+07	4.4E+06	7.6E+05	9.1E+07	-2.7E+05	-3.4E+05	-1.7E+05	-1.6E+05	-1.9E+05	-1.8E+05	-1.3E+05	-1.3E+05
97.7	-1.5E+07	2.4E+07	-2.5E+07	-7.2E+06	1.0E+08	4.1E+06	3.9E+06	1.0E+08	-2.7E+05	-2.0E+05	-3.1E+05	-1.9E+05	-2.2E+05	-1.5E+05	-2.0E+05	-1.8E+05
107.4	-1.9E+07	2.1E+07	-2.9E+07	-1.0E+07	1.1E+08	4.2E+06	3.4E+06	1.1E+08	-3.0E+05	-2.1E+05	-2.6E+05	-2.7E+05	-3.6E+05	-1.2E+05	-2.7E+05	-1.4E+05
117.2	-1.8E+07	2.2E+07	-2.5E+07	-1.1E+07	1.2E+08	5.8E+06	2.2E+06	1.2E+08	-2.6E+05	-1.5E+05	-1.7E+05	-2.4E+05	-2.6E+05	-2.2E+05	-2.7E+05	-1.0E+05
127.0	-1.6E+07	2.6E+07	-2.0E+07	-9.3E+06	1.3E+08	4.2E+06	3.0E+06	1.3E+08	-1.8E+05	-1.6E+05	-5.0E+05	-2.1E+05	-3.2E+05	-2.2E+05	-7.4E+04	-3.9E+05
136.7	-2.3E+07	2.7E+07	-2.0E+07	-1.4E+07	1.4E+08	4.2E+06	7.1E+05	1.5E+08	-3.3E+05	-1.0E+05	-3.7E+05	-2.9E+05	-3.9E+05	-3.7E+05	-3.3E+05	-4.5E+05

Table 67 Raw data for the test seal at PD=41.4 bar, ω=4 krpm, and inlet GVF=10% with the zero-preswirl insert

Freq.	Re($\boldsymbol{H_{XX}}$)	Re($\boldsymbol{H_{XY}}$)	Re($\boldsymbol{H_{YX}}$)	Re($\boldsymbol{H_{YY}}$)	Im($\boldsymbol{H_{XX}}$)	Im($\boldsymbol{H_{XY}}$)	Im($\boldsymbol{H_{YX}}$)	Im($\boldsymbol{H_{YY}}$)	Re($\boldsymbol{eH_{XX}}$)	Re($\boldsymbol{eH_{XY}}$)	Re($\boldsymbol{eH_{YX}}$)	Re($\boldsymbol{eH_{YY}}$)	Im($\boldsymbol{eH_{XX}}$)	Im($\boldsymbol{eH_{XY}}$)	Im($\boldsymbol{eH_{YX}}$)	Im($\boldsymbol{eH_{YY}}$)
Hz	N/m	N/m	N/m	N/m	N/m	N/m	N/m	N/m	N/m	N/m	N/m	N/m	N/m	N/m	N/m	N/m
9.8	-6.6E+06	2.0E+07	-2.7E+07	9.3E+05	1.0E+07	-1.5E+06	-1.4E+06	8.5E+06	-3.3E+05	-3.8E+05	-4.6E+05	-2.7E+05	-4.7E+05	-3.3E+05	-3.6E+05	-2.6E+05
19.5	-9.1E+06	2.0E+07	-2.7E+07	-3.2E+04	2.0E+07	6.1E+05	-2.8E+06	2.0E+07	-3.3E+05	-2.8E+05	-2.5E+05	-1.5E+05	-3.2E+05	-2.5E+05	-1.7E+05	-2.1E+05
29.3	-7.2E+06	2.0E+07	-2.7E+07	1.2E+05	2.8E+07	3.3E+06	5.5E+05	2.6E+07	-3.6E+05	-2.1E+05	-2.4E+05	-2.4E+05	-3.5E+05	-1.9E+05	-2.8E+05	-2.2E+05
39.1	-7.6E+06	1.9E+07	-2.5E+07	1.9E+06	3.8E+07	1.0E+06	1.0E+06	3.7E+07	-1.6E+05	-1.1E+05	-1.8E+05	-2.1E+05	-1.9E+05	-1.0E+05	-3.7E+05	-1.9E+05
48.8	-8.5E+06	1.9E+07	-2.4E+07	-2.5E+06	4.7E+07	1.7E+06	-2.6E+06	4.6E+07	-2.2E+05	-1.4E+05	-2.9E+05	-1.9E+05	-2.1E+05	-2.1E+05	-2.3E+05	-2.5E+05
58.6	-8.3E+06	2.0E+07	-2.6E+07	-2.7E+06	6.0E+07	1.7E+06	-9.7E+04	5.9E+07	-7.4E+04	-1.5E+05	-2.5E+05	-3.2E+05	-9.9E+04	-7.3E+04	-2.2E+05	-8.3E+04
68.4	-1.2E+07	1.8E+07	-2.6E+07	-4.7E+06	6.8E+07	5.0E+06	1.1E+05	6.9E+07	-1.2E+05	-2.0E+05	-2.9E+05	-3.0E+05	-2.9E+05	-2.1E+05	-3.1E+05	-2.3E+05
78.1	-1.4E+07	1.9E+07	-3.0E+07	-7.4E+06	7.9E+07	5.2E+06	1.9E+06	7.8E+07	-2.8E+05	-3.3E+05	-2.5E+05	-2.2E+05	-2.4E+05	-1.1E+05	-2.5E+05	-1.5E+05
87.9	-1.3E+07	1.9E+07	-2.7E+07	-9.8E+06	8.7E+07	4.7E+06	-2.0E+06	8.8E+07	-1.2E+05	-1.7E+05	-1.2E+05	-9.9E+04	-2.3E+05	-1.2E+05	-1.8E+05	-6.9E+04
97.7	-1.6E+07	1.9E+07	-2.8E+07	-1.1E+07	9.8E+07	4.8E+06	-4.0E+05	1.0E+08	-2.2E+05	-2.1E+05	-2.3E+05	-8.5E+04	-2.3E+05	-2.2E+05	-1.7E+05	-9.0E+04
107.4	-2.0E+07	1.7E+07	-2.8E+07	-1.3E+07	1.1E+08	4.7E+06	-2.5E+06	1.1E+08	-3.7E+05	-1.8E+05	-3.0E+05	-1.3E+05	-2.0E+05	-2.6E+05	-1.7E+05	-3.4E+05
117.2	-2.0E+07	2.0E+07	-2.6E+07	-1.2E+07	1.2E+08	7.4E+06	1.1E+06	1.2E+08	-1.6E+05	-1.2E+05	-1.3E+05	-1.3E+05	-2.2E+05	-7.0E+04	-8.0E+04	-1.9E+05
127.0	-2.3E+07	2.2E+07	-2.7E+07	-1.1E+07	1.3E+08	7.0E+06	3.6E+06	1.4E+08	-2.0E+05	-3.3E+05	-2.1E+05	-2.3E+05	-2.2E+05	-3.6E+05	-7.2E+04	-1.8E+05
136.7	-2.4E+07	2.3E+07	-2.3E+07	-1.8E+07	1.4E+08	5.9E+06	-2.1E+04	1.5E+08	-1.6E+05	-1.5E+05	-1.9E+05	-1.8E+05	-3.6E+05	-4.0E+05	-3.3E+05	-3.6E+05

Table 68 Raw data for the test seal at PD=41.4 bar, ω=5 krpm, and inlet GVF=10% with the zero-preswirl insert

Freq.	Re($\boldsymbol{H_{XX}}$)	Re($\boldsymbol{H_{XY}}$)	Re($\boldsymbol{H_{YX}}$)	Re($\boldsymbol{H_{YY}}$)	Im($\boldsymbol{H_{XX}}$)	Im($\boldsymbol{H_{XY}}$)	Im($\boldsymbol{H_{YX}}$)	Im($\boldsymbol{H_{YY}}$)	Re($\boldsymbol{eH_{XX}}$)	Re($\boldsymbol{eH_{XY}}$)	Re($\boldsymbol{eH_{YX}}$)	Re($\boldsymbol{eH_{YY}}$)	Im($\boldsymbol{eH_{XX}}$)	Im($\boldsymbol{eH_{XY}}$)	Im($\boldsymbol{eH_{YX}}$)	Im($\boldsymbol{eH_{YY}}$)
Hz	N/m	N/m	N/m	N/m	N/m	N/m	N/m	N/m	N/m	N/m	N/m	N/m	N/m	N/m	N/m	N/m
9.8	-7.5E+06	2.8E+07	-3.3E+07	-4.4E+05	1.2E+07	1.5E+06	-6.9E+05	9.4E+06	-2.5E+05	-4.1E+05	-2.6E+05	-4.6E+05	-4.3E+05	-2.5E+05	-4.2E+05	-3.4E+05
19.5	-7.7E+06	2.7E+07	-3.1E+07	1.0E+06	2.1E+07	3.0E+06	2.3E+04	2.1E+07	-4.2E+05	-3.2E+05	-2.9E+05	-3.0E+05	-3.7E+05	-4.3E+05	-2.9E+05	-2.7E+05
29.3	-5.0E+06	2.7E+07	-3.0E+07	6.0E+05	2.9E+07	4.2E+06	-7.2E+05	2.6E+07	-2.1E+05	-3.4E+05	-3.7E+05	-3.5E+05	-3.7E+05	-1.3E+05	-3.9E+05	-3.0E+05
39.1	-5.0E+06	2.6E+07	-3.1E+07	1.3E+05	3.9E+07	1.7E+06	-1.7E+06	3.9E+07	-1.3E+05	-2.5E+05	-1.7E+05	-1.2E+05	-2.5E+05	-1.2E+05	-1.7E+05	-1.9E+05
48.8	-6.4E+06	2.5E+07	-2.9E+07	-6.9E+05	4.6E+07	3.3E+06	-4.0E+05	4.6E+07	-1.8E+05	-1.8E+05	-2.3E+05	-2.1E+05	-3.6E+05	-1.2E+05	-3.4E+05	-1.4E+05
58.6	-7.9E+06	2.7E+07	-3.0E+07	-2.8E+06	5.8E+07	4.1E+06	-1.0E+06	5.8E+07	-1.1E+05	-9.6E+04	-2.5E+05	-2.3E+05	-1.7E+05	-1.2E+05	-1.9E+05	-1.9E+05
68.4	-1.1E+07	2.5E+07	-3.2E+07	-3.8E+06	6.7E+07	6.6E+06	-1.5E+06	6.8E+07	-3.9E+05	-2.2E+05	-2.3E+05	-2.5E+05	-2.7E+05	-2.5E+05	-2.7E+05	-1.7E+05
78.1	-1.1E+07	2.7E+07	-3.4E+07	-6.7E+06	7.9E+07	7.6E+06	-7.0E+05	7.9E+07	-2.4E+05	-1.7E+05	-1.6E+05	-1.0E+05	-1.9E+05	-2.9E+05	-1.8E+05	-1.2E+05
87.9	-1.2E+07	2.6E+07	-3.2E+07	-7.5E+06	8.8E+07	6.8E+06	-1.8E+06	8.8E+07	-2.0E+05	-1.4E+05	-8.8E+04	-1.9E+05	-2.4E+05	-8.0E+04	-3.0E+05	-1.3E+05
97.7	-1.4E+07	2.7E+07	-3.3E+07	-9.9E+06	9.9E+07	7.7E+06	-2.1E+06	1.0E+08	-2.4E+05	-1.7E+05	-8.0E+04	-1.2E+05	-1.2E+05	-2.1E+05	-2.0E+05	-7.3E+04
107.4	-1.9E+07	2.7E+07	-3.5E+07	-1.2E+07	1.1E+08	7.2E+06	-1.6E+06	1.1E+08	-3.6E+05	-1.6E+05	-3.2E+05	-2.6E+05	-2.3E+05	-1.6E+05	-2.0E+05	-1.5E+05
117.2	-1.8E+07	2.9E+07	-3.2E+07	-1.2E+07	1.2E+08	9.4E+06	-1.6E+05	1.2E+08	-1.3E+05	-1.0E+05	-1.1E+05	-1.2E+05	-5.9E+04	-5.8E+04	-1.3E+05	-2.0E+05
127.0	-2.0E+07	3.2E+07	-3.2E+07	-1.1E+07	1.3E+08	8.9E+06	1.1E+06	1.4E+08	-1.3E+05	-2.7E+05	-1.6E+05	-3.3E+05	-1.6E+05	-1.5E+05	-1.1E+05	-2.1E+05
136.7	-2.2E+07	3.2E+07	-2.8E+07	-1.6E+07	1.4E+08	7.1E+06	-8.7E+05	1.5E+08	-2.5E+05	-3.6E+05	-1.4E+05	-2.6E+05	-1.6E+05	-3.4E+05	-3.5E+05	-3.0E+05

Table 69 Raw data for the test seal at PD=20.7 bar, ω=3 krpm, and inlet GVF=0% with the medium-preswirl insert

Freq.	Re(H_{XX})	Re(H_{XY})	Re(H_{YX})	Re(H_{YY})	Im(H_{XX})	Im(H_{XY})	Im(H_{YX})	Im(H_{YY})	Re(eH_{XX})	Re(eH_{XY})	Re(eH_{YX})	Re(eH_{YY})	Im(eH_{XX})	Im(eH_{XY})	Im(eH_{YX})	Im(eH_{YY})
Hz	N/m	N/m	N/m	N/m	N/m	N/m	N/m	N/m	N/m	N/m	N/m	N/m	N/m	N/m	N/m	N/m
9.8	1.7E+07	1.7E+07	-1.8E+07	1.9E+07	4.7E+06	1.7E+06	-1.1E+06	3.7E+06	-6.4E+04	-8.3E+04	-4.2E+04	-8.1E+04	-6.4E+04	-6.9E+04	-7.4E+04	-1.2E+05
19.5	1.6E+07	1.7E+07	-1.7E+07	1.7E+07	9.9E+06	3.2E+06	-2.7E+06	9.9E+06	-4.6E+04	-6.0E+04	-3.7E+04	-6.3E+04	-7.2E+04	-7.1E+04	-6.5E+04	-6.0E+04
29.3	1.6E+07	1.6E+07	-1.9E+07	1.8E+07	1.3E+07	6.9E+06	-2.5E+06	1.2E+07	-4.8E+04	-7.0E+04	-6.9E+04	-7.3E+04	-7.2E+04	-5.3E+04	-7.6E+04	-8.7E+04
39.1	1.3E+07	1.7E+07	-1.7E+07	1.5E+07	2.0E+07	6.3E+06	-6.1E+06	2.0E+07	-7.1E+04	-6.5E+04	-4.4E+04	-6.0E+04	-4.1E+04	-5.3E+04	-7.4E+04	-5.9E+04
48.8	1.1E+07	1.8E+07	-1.7E+07	1.3E+07	2.4E+07	7.9E+06	-7.7E+06	2.5E+07	-3.9E+04	-5.9E+04	-2.9E+04	-5.9E+04	-6.1E+04	-4.2E+04	-4.6E+04	-5.2E+04
58.6	8.0E+06	1.8E+07	-1.8E+07	9.3E+06	2.9E+07	9.4E+06	-9.6E+06	3.0E+07	-4.1E+04	-7.8E+04	-8.0E+04	-6.6E+04	-5.4E+04	-7.5E+04	-7.3E+04	-6.1E+04
68.4	4.4E+06	1.8E+07	-1.9E+07	6.0E+06	3.4E+07	1.0E+07	-1.1E+07	3.5E+07	-7.4E+04	-1.0E+05	-7.7E+04	-1.4E+05	-7.3E+04	-6.7E+04	-7.6E+04	-1.2E+05
78.1	5.8E+05	1.8E+07	-1.9E+07	1.3E+06	3.9E+07	1.2E+07	-1.2E+07	4.0E+07	-4.0E+04	-5.6E+04	-3.5E+04	-6.5E+04	-3.4E+04	-5.0E+04	-3.7E+04	-6.1E+04
87.9	-4.6E+06	1.9E+07	-1.9E+07	-3.7E+06	4.4E+07	1.4E+07	-1.4E+07	4.6E+07	-2.5E+04	-5.4E+04	-2.6E+04	-5.7E+04	-3.4E+04	-4.0E+04	-3.5E+04	-5.9E+04
97.7	-1.1E+07	1.9E+07	-1.9E+07	-9.4E+06	5.0E+07	1.5E+07	-1.6E+07	5.1E+07	-4.2E+04	-5.3E+04	-2.6E+04	-5.8E+04	-2.3E+04	-5.2E+04	-3.0E+04	-5.2E+04
107.4	-1.7E+07	2.0E+07	-2.0E+07	-1.6E+07	5.5E+07	1.7E+07	-1.8E+07	5.7E+07	-3.0E+04	-5.4E+04	-3.7E+04	-9.3E+04	-4.1E+04	-3.9E+04	-5.4E+04	-6.6E+04
117.2	-2.5E+07	2.1E+07	-2.0E+07	-2.3E+07	6.1E+07	1.9E+07	-2.0E+07	6.3E+07	-2.8E+04	-5.3E+04	-3.9E+04	-6.0E+04	-6.6E+04	-5.3E+04	-5.2E+04	-8.4E+04
127.0	-3.3E+07	2.4E+07	-1.8E+07	-3.3E+07	6.9E+07	2.0E+07	-2.3E+07	6.9E+07	-8.1E+04	-7.2E+04	-7.3E+04	-1.1E+05	-6.5E+04	-1.0E+05	-6.0E+04	-1.3E+05
136.7	-3.9E+07	2.4E+07	-2.3E+07	-3.9E+07	7.6E+07	2.1E+07	-2.6E+07	7.7E+07	-1.3E+05	-1.3E+05	-1.3E+05	-1.3E+05	-7.4E+04	-1.0E+05	-1.2E+05	-1.8E+05

Table 70 Raw data for the test seal at PD=20.7 bar, ω=4 krpm, and inlet GVF=0% with the medium-preswirl insert

Freq.	Re(H_{XX})	Re(H_{XY})	Re(H_{YX})	Re(H_{YY})	Im(H_{XX})	Im(H_{XY})	Im(H_{YX})	Im(H_{YY})	Re(eH_{XX})	Re(eH_{XY})	Re(eH_{YX})	Re(eH_{YY})	Im(eH_{XX})	Im(eH_{XY})	Im(eH_{YX})	Im(eH_{YY})
Hz	N/m	N/m	N/m	N/m	N/m	N/m	N/m	N/m	N/m	N/m	N/m	N/m	N/m	N/m	N/m	N/m
9.8	1.7E+07	1.7E+07	-1.7E+07	1.8E+07	4.7E+06	1.6E+06	-1.3E+06	3.7E+06	-5.2E+04	-8.5E+04	-7.3E+04	-8.9E+04	-3.6E+04	-6.2E+04	-5.7E+04	-6.8E+04
19.5	1.6E+07	1.7E+07	-1.7E+07	1.7E+07	1.0E+07	3.1E+06	-3.0E+06	9.9E+06	-3.9E+04	-6.1E+04	-3.3E+04	-7.3E+04	-4.0E+04	-4.4E+04	-1.1E+05	-1.0E+05
29.3	1.6E+07	1.6E+07	-1.9E+07	1.7E+07	1.3E+07	6.6E+06	-2.6E+06	1.3E+07	-4.5E+04	-6.5E+04	-7.6E+04	-8.8E+04	-4.7E+04	-6.7E+04	-4.9E+04	-6.5E+04
39.1	1.3E+07	1.7E+07	-1.7E+07	1.5E+07	2.0E+07	6.3E+06	-6.1E+06	2.0E+07	-2.0E+04	-4.9E+04	-4.7E+04	-6.8E+04	-6.9E+04	-4.9E+04	-4.8E+04	-5.6E+04
48.8	1.1E+07	1.8E+07	-1.8E+07	1.2E+07	2.4E+07	7.8E+06	-7.9E+06	2.5E+07	-3.5E+04	-7.1E+04	-2.3E+04	-4.9E+04	-3.3E+04	-4.7E+04	-3.5E+04	-6.8E+04
58.6	7.8E+06	1.8E+07	-1.8E+07	9.0E+06	2.9E+07	9.4E+06	-9.7E+06	3.0E+07	-3.1E+04	-7.4E+04	-5.2E+04	-7.2E+04	-5.9E+04	-6.7E+04	-7.9E+04	-1.1E+05
68.4	4.2E+06	1.8E+07	-1.8E+07	5.6E+06	3.4E+07	1.0E+07	-1.1E+07	3.5E+07	-7.6E+04	-1.1E+05	-7.6E+04	-1.1E+05	-8.5E+04	-1.0E+05	-7.6E+04	-1.1E+05
78.1	3.7E+05	1.8E+07	-1.9E+07	1.0E+06	3.9E+07	1.2E+07	-1.3E+07	4.0E+07	-3.4E+04	-5.2E+04	-2.9E+04	-7.8E+04	-5.3E+04	-4.5E+04	-4.9E+04	-9.5E+04
87.9	-4.8E+06	1.9E+07	-1.9E+07	-4.2E+06	4.4E+07	1.4E+07	-1.4E+07	4.6E+07	-3.6E+04	-4.4E+04	-3.2E+04	-6.3E+04	-3.0E+04	-4.3E+04	-4.8E+04	-8.8E+04
97.7	-1.1E+07	1.9E+07	-1.9E+07	-9.9E+06	4.9E+07	1.5E+07	-1.6E+07	5.2E+07	-2.7E+04	-5.2E+04	-3.1E+04	-7.1E+04	-4.3E+04	-4.1E+04	-5.3E+04	-1.0E+05
107.4	-1.7E+07	2.0E+07	-2.0E+07	-1.6E+07	5.5E+07	1.7E+07	-1.8E+07	5.8E+07	-3.2E+04	-7.4E+04	-2.9E+04	-8.6E+04	-7.1E+04	-6.2E+04	-5.4E+04	-9.5E+04
117.2	-2.5E+07	2.1E+07	-2.0E+07	-2.4E+07	6.1E+07	1.9E+07	-2.0E+07	6.3E+07	-3.6E+04	-4.5E+04	-3.0E+04	-9.2E+04	-5.7E+04	-6.0E+04	-6.8E+04	-1.0E+05
127.0	-3.3E+07	2.4E+07	-1.8E+07	-3.3E+07	6.9E+07	2.0E+07	-2.3E+07	6.9E+07	-4.8E+04	-7.1E+04	-4.0E+04	-9.1E+04	-6.2E+04	-8.3E+04	-8.0E+04	-1.5E+05
136.7	-3.9E+07	2.4E+07	-2.3E+07	-4.0E+07	7.6E+07	2.1E+07	-2.7E+07	7.7E+07	-9.3E+04	-9.6E+04	-1.2E+05	-1.6E+05	-8.4E+04	-8.5E+04	-1.4E+05	-1.6E+05

Table 71 Raw data for the test seal at PD=20.7 bar, ω=5 krpm, and inlet GVF=0% with the medium-preswirl insert

Freq.	Re(H_{XX})	Re(H_{XY})	Re(H_{YX})	Re(H_{YY})	Im(H_{XX})	Im(H_{XY})	Im(H_{YX})	Im(H_{YY})	Re(eH_{XX})	Re(eH_{XY})	Re(eH_{YX})	Re(eH_{YY})	Im(eH_{XX})	Im(eH_{XY})	Im(eH_{YX})	Im(eH_{YY})
Hz	N/m	N/m	N/m	N/m	N/m	N/m	N/m	N/m	N/m	N/m	N/m	N/m	N/m	N/m	N/m	N/m
9.8	1.6E+07	2.0E+07	-2.0E+07	1.8E+07	4.8E+06	1.6E+06	-1.1E+06	3.1E+06	-7.5E+04	-1.1E+05	-6.0E+04	-1.0E+05	-6.0E+04	-8.5E+04	-1.1E+05	-1.3E+05
19.5	1.5E+07	2.0E+07	-2.0E+07	1.7E+07	1.0E+07	3.5E+06	-3.3E+06	9.6E+06	-6.0E+04	-7.9E+04	-8.1E+04	-9.6E+04	-4.6E+04	-9.5E+04	-6.0E+04	-8.5E+04
29.3	1.5E+07	1.9E+07	-2.2E+07	1.7E+07	1.3E+07	7.7E+06	-3.2E+06	1.2E+07	-8.0E+04	-6.4E+04	-7.6E+04	-9.6E+04	-6.3E+04	-5.8E+04	-4.8E+04	-3.8E+04
39.1	1.2E+07	2.0E+07	-2.0E+07	1.3E+07	2.0E+07	7.6E+06	-7.3E+06	2.0E+07	-2.3E+04	-4.9E+04	-4.0E+04	-6.2E+04	-3.9E+04	-4.4E+04	-5.7E+04	-6.6E+04
48.8	9.4E+06	2.0E+07	-2.0E+07	1.1E+07	2.5E+07	9.1E+06	-9.3E+06	2.6E+07	-3.3E+04	-5.7E+04	-4.2E+04	-7.7E+04	-6.4E+04	-5.3E+04	-2.5E+04	-5.1E+04
58.6	6.8E+06	2.1E+07	-2.1E+07	8.2E+06	3.0E+07	1.1E+07	-1.2E+07	3.1E+07	-3.9E+04	-8.5E+04	-5.5E+04	-7.1E+04	-6.8E+04	-8.4E+04	-7.1E+04	-6.1E+04
68.4	3.5E+06	2.1E+07	-2.2E+07	4.7E+06	3.5E+07	1.3E+07	-1.4E+07	3.6E+07	-5.6E+04	-1.1E+05	-4.7E+04	-7.8E+04	-6.8E+04	-6.6E+04	-5.1E+04	-6.3E+04
78.1	-1.4E+05	2.1E+07	-2.2E+07	6.1E+05	4.0E+07	1.4E+07	-1.5E+07	4.1E+07	-3.1E+04	-4.1E+04	-5.2E+04	-6.4E+04	-4.4E+04	-4.1E+04	-5.5E+04	-9.4E+04
87.9	-5.0E+06	2.2E+07	-2.2E+07	-4.3E+06	4.5E+07	1.7E+07	-1.7E+07	4.7E+07	-5.0E+04	-4.7E+04	-5.7E+04	-9.3E+04	-5.5E+04	-6.8E+04	-5.6E+04	-7.9E+04
97.7	-1.1E+07	2.2E+07	-2.3E+07	-9.9E+06	5.1E+07	1.9E+07	-1.9E+07	5.2E+07	-2.8E+04	-4.5E+04	-3.7E+04	-8.2E+04	-5.0E+04	-5.2E+04	-5.5E+04	-6.4E+04
107.4	-1.7E+07	2.3E+07	-2.3E+07	-1.6E+07	5.6E+07	2.0E+07	-2.1E+07	5.8E+07	-3.1E+04	-6.1E+04	-4.0E+04	-6.9E+04	-1.1E+05	-7.5E+04	-4.0E+04	-6.2E+04
117.2	-2.5E+07	2.5E+07	-2.3E+07	-2.3E+07	6.3E+07	2.3E+07	-2.4E+07	6.4E+07	-7.6E+04	-6.0E+04	-5.0E+04	-7.8E+04	-7.4E+04	-6.9E+04	-4.9E+04	-7.7E+04
127.0	-3.4E+07	2.7E+07	-2.2E+07	-3.3E+07	7.0E+07	2.5E+07	-2.7E+07	7.0E+07	-4.6E+04	-7.8E+04	-6.5E+04	-7.6E+04	-1.2E+05	-7.6E+04	-6.7E+04	-7.1E+04
136.7	-3.9E+07	2.8E+07	-2.8E+07	-4.0E+07	7.8E+07	2.6E+07	-3.2E+07	7.8E+07	-5.4E+04	-1.0E+05	-7.4E+04	-1.7E+05	-1.5E+05	-6.2E+04	-1.2E+05	-1.7E+05

Table 72 Raw data for the test seal at PD=20.7 bar, ω=3 krpm, and inlet GVF=2% with the medium-preswirl insert

Freq.	Re(H_{XX})	Re(H_{XY})	Re(H_{YX})	Re(H_{YY})	Im(H_{XX})	Im(H_{XY})	Im(H_{YX})	Im(H_{YY})	Re(eH_{XX})	Re(eH_{XY})	Re(eH_{YX})	Re(eH_{YY})	Im(eH_{XX})	Im(eH_{XY})	Im(eH_{YX})	Im(eH_{YY})
Hz	N/m	N/m	N/m	N/m	N/m	N/m	N/m	N/m	N/m	N/m	N/m	N/m	N/m	N/m	N/m	N/m
9.8	1.7E+07	1.6E+07	-1.7E+07	1.9E+07	4.2E+06	1.6E+06	-1.2E+06	3.3E+06	-6.1E+04	-8.2E+04	-4.4E+04	-1.1E+05	-7.1E+04	-6.1E+04	-8.2E+04	-6.5E+04
19.5	1.6E+07	1.7E+07	-1.7E+07	1.8E+07	9.9E+06	3.1E+06	-2.9E+06	9.6E+06	-4.7E+04	-5.8E+04	-5.8E+04	-7.4E+04	-2.6E+04	-4.6E+04	-4.7E+04	-9.0E+04
29.3	1.7E+07	1.5E+07	-1.9E+07	1.8E+07	1.3E+07	6.8E+06	-2.5E+06	1.2E+07	-5.8E+04	-4.8E+04	-6.4E+04	-6.1E+04	-7.0E+04	-4.8E+04	-5.3E+04	-3.8E+04
39.1	1.4E+07	1.6E+07	-1.7E+07	1.5E+07	1.9E+07	6.2E+06	-5.9E+06	1.9E+07	-3.9E+04	-4.4E+04	-3.6E+04	-7.4E+04	-2.8E+04	-4.8E+04	-3.2E+04	-3.4E+04
48.8	1.2E+07	1.8E+07	-1.8E+07	1.3E+07	2.4E+07	7.5E+06	-7.6E+06	2.5E+07	-3.2E+04	-7.0E+04	-4.0E+04	-7.0E+04	-4.2E+04	-3.4E+04	-4.4E+04	-3.4E+04
58.6	8.8E+06	1.8E+07	-1.8E+07	9.9E+06	2.9E+07	9.0E+06	-9.2E+06	2.9E+07	-5.0E+04	-5.0E+04	-5.0E+04	-9.2E+04	-3.8E+04	-7.9E+04	-7.6E+04	-5.5E+04
68.4	5.2E+06	1.8E+07	-1.8E+07	6.9E+06	3.3E+07	1.0E+07	-1.0E+07	3.5E+07	-7.1E+04	-1.3E+05	-8.1E+04	-1.6E+05	-1.1E+05	-1.3E+05	-1.1E+05	-1.4E+05
78.1	1.7E+06	1.8E+07	-1.9E+07	2.6E+06	3.8E+07	1.1E+07	-1.2E+07	3.9E+07	-3.2E+04	-5.7E+04	-4.8E+04	-7.3E+04	-1.9E+04	-4.0E+04	-3.9E+04	-7.6E+04
87.9	-3.1E+06	1.9E+07	-1.9E+07	-2.2E+06	4.3E+07	1.3E+07	-1.4E+07	4.5E+07	-4.0E+04	-4.4E+04	-4.3E+04	-7.6E+04	-4.2E+04	-4.0E+04	-3.1E+04	-6.3E+04
97.7	-8.8E+06	1.9E+07	-1.9E+07	-7.6E+06	4.9E+07	1.5E+07	-1.6E+07	5.0E+07	-2.3E+04	-4.6E+04	-3.0E+04	-5.5E+04	-4.6E+04	-4.3E+04	-4.0E+04	-5.9E+04
107.4	-1.4E+07	1.9E+07	-2.0E+07	-1.3E+07	5.4E+07	1.6E+07	-1.7E+07	5.6E+07	-3.2E+04	-6.0E+04	-3.1E+04	-6.7E+04	-4.6E+04	-5.2E+04	-3.3E+04	-5.2E+04
117.2	-2.2E+07	2.1E+07	-2.0E+07	-2.0E+07	6.0E+07	1.8E+07	-1.9E+07	6.2E+07	-5.2E+04	-5.5E+04	-3.7E+04	-7.5E+04	-3.7E+04	-4.9E+04	-3.6E+04	-5.4E+04
127.0	-3.0E+07	2.3E+07	-1.8E+07	-2.9E+07	6.8E+07	1.9E+07	-2.2E+07	6.8E+07	-6.1E+04	-7.2E+04	-6.7E+04	-7.9E+04	-8.1E+04	-6.7E+04	-8.0E+04	-8.2E+04
136.7	-3.5E+07	2.3E+07	-2.3E+07	-3.5E+07	7.5E+07	1.9E+07	-2.5E+07	7.6E+07	-6.2E+04	-9.5E+04	-5.8E+04	-1.6E+05	-6.9E+04	-4.4E+04	-1.3E+05	-9.5E+04

Table 73 Raw data for the test seal at PD=20.7 bar, ω=4 krpm, and inlet GVF=2% with the medium-preswirl insert

Freq.	Re(H_{XX})	Re(H_{XY})	Re(H_{YX})	Re(H_{YY})	Im(H_{XX})	Im(H_{XY})	Im(H_{YX})	Im(H_{YY})	Re(eH_{XX})	Re(eH_{XY})	Re(eH_{YX})	Re(eH_{YY})	Im(eH_{XX})	Im(eH_{XY})	Im(eH_{YX})	Im(eH_{YY})
Hz	N/m	N/m	N/m	N/m	N/m	N/m	N/m	N/m	N/m	N/m	N/m	N/m	N/m	N/m	N/m	N/m
9.8	1.7E+07	1.7E+07	-1.8E+07	1.9E+07	4.0E+06	1.5E+06	-1.2E+06	3.5E+06	-6.1E+04	-8.6E+04	-6.1E+04	-1.2E+05	-2.8E+04	-4.2E+04	-8.4E+04	-7.7E+04
19.5	1.7E+07	1.7E+07	-1.8E+07	1.8E+07	1.0E+07	3.0E+06	-2.8E+06	9.7E+06	-3.2E+04	-6.0E+04	-5.3E+04	-1.1E+05	-4.1E+04	-5.6E+04	-4.5E+04	-9.5E+04
29.3	1.7E+07	1.5E+07	-1.9E+07	1.8E+07	1.3E+07	6.7E+06	-2.3E+06	1.2E+07	-4.8E+04	-3.8E+04	-5.4E+04	-7.1E+04	-3.7E+04	-4.5E+04	-4.9E+04	-6.5E+04
39.1	1.4E+07	1.6E+07	-1.7E+07	1.5E+07	1.9E+07	6.2E+06	-5.8E+06	2.0E+07	-3.7E+04	-6.7E+04	-5.5E+04	-8.1E+04	-3.7E+04	-4.8E+04	-4.6E+04	-5.2E+04
48.8	1.2E+07	1.8E+07	-1.8E+07	1.3E+07	2.4E+07	7.3E+06	-7.4E+06	2.5E+07	-3.6E+04	-4.5E+04	-6.0E+04	-6.3E+04	-4.3E+04	-5.3E+04	-3.5E+04	-5.1E+04
58.6	9.1E+06	1.8E+07	-1.8E+07	1.0E+07	2.9E+07	8.9E+06	-9.0E+06	3.0E+07	-3.5E+04	-7.6E+04	-5.8E+04	-8.8E+04	-7.3E+04	-5.8E+04	-5.5E+04	-2.7E+04
68.4	5.5E+06	1.8E+07	-1.9E+07	7.3E+06	3.4E+07	9.9E+06	-1.0E+07	3.5E+07	-7.2E+04	-1.1E+05	-9.0E+04	-1.3E+05	-1.1E+05	-1.2E+05	-8.0E+04	-1.3E+05
78.1	2.1E+06	1.8E+07	-1.9E+07	3.1E+06	3.9E+07	1.1E+07	-1.1E+07	4.0E+07	-3.9E+04	-5.0E+04	-3.1E+04	-6.5E+04	-7.9E+04	-5.5E+04	-4.4E+04	-3.6E+04
87.9	-2.6E+06	1.9E+07	-1.9E+07	-1.7E+06	4.3E+07	1.3E+07	-1.3E+07	4.5E+07	-5.3E+04	-5.6E+04	-1.9E+04	-5.8E+04	-4.7E+04	-4.8E+04	-4.5E+04	-4.5E+04
97.7	-8.2E+06	1.9E+07	-1.9E+07	-6.9E+06	4.9E+07	1.5E+07	-1.5E+07	5.1E+07	-3.8E+04	-4.1E+04	-1.8E+04	-5.2E+04	-5.6E+04	-5.2E+04	-4.2E+04	-4.5E+04
107.4	-1.4E+07	2.0E+07	-2.0E+07	-1.2E+07	5.5E+07	1.6E+07	-1.7E+07	5.7E+07	-3.6E+04	-6.2E+04	-2.9E+04	-6.9E+04	-7.5E+04	-6.7E+04	-5.3E+04	-4.4E+04
117.2	-2.1E+07	2.1E+07	-2.0E+07	-1.9E+07	6.1E+07	1.8E+07	-1.8E+07	6.2E+07	-9.4E+04	-5.0E+04	-2.5E+04	-6.0E+04	-9.8E+04	-7.5E+04	-3.6E+04	-6.3E+04
127.0	-2.9E+07	2.3E+07	-1.8E+07	-2.8E+07	6.9E+07	1.9E+07	-2.1E+07	6.8E+07	-4.3E+04	-8.0E+04	-6.8E+04	-1.1E+05	-1.3E+05	-8.1E+04	-5.6E+04	-7.8E+04
136.7	-3.4E+07	2.3E+07	-2.3E+07	-3.4E+07	7.7E+07	1.9E+07	-2.5E+07	7.7E+07	-7.2E+04	-9.5E+04	-7.5E+04	-1.5E+05	-1.4E+05	-8.5E+04	-1.3E+05	-1.4E+05

Table 74 Raw data for the test seal at PD=20.7 bar, ω=5 krpm, and inlet GVF=2% with the medium-preswirl insert

Freq.	Re(H_{XX})	Re(H_{XY})	Re(H_{YX})	Re(H_{YY})	Im(H_{XX})	Im(H_{XY})	Im(H_{YX})	Im(H_{YY})	Re(eH_{XX})	Re(eH_{XY})	Re(eH_{YX})	Re(eH_{YY})	Im(eH_{XX})	Im(eH_{XY})	Im(eH_{YX})	Im(eH_{YY})
Hz	N/m	N/m	N/m	N/m	N/m	N/m	N/m	N/m	N/m	N/m	N/m	N/m	N/m	N/m	N/m	N/m
9.8	1.6E+07	2.1E+07	-2.1E+07	1.9E+07	4.8E+06	-2.3E+05	-1.2E+06	2.7E+06	-6.8E+04	-1.2E+05	-6.4E+04	-9.1E+04	-1.2E+05	-1.1E+05	-7.4E+04	-1.0E+05
19.5	1.5E+07	2.2E+07	-2.1E+07	1.6E+07	1.1E+07	3.0E+06	-3.6E+06	9.5E+06	-6.2E+04	-1.2E+05	-1.2E+05	-1.5E+05	-8.8E+04	-9.6E+04	-1.2E+05	-1.0E+05
29.3	1.5E+07	2.0E+07	-2.1E+07	1.6E+07	1.3E+07	7.1E+06	-3.4E+06	1.2E+07	-8.0E+04	-1.5E+05	-9.3E+04	-1.0E+05	-1.3E+05	-1.1E+05	-6.4E+04	-5.9E+04
39.1	1.3E+07	2.0E+07	-2.0E+07	1.3E+07	1.9E+07	6.8E+06	-7.2E+06	2.0E+07	-6.1E+04	-8.7E+04	-3.9E+04	-7.0E+04	-1.3E+05	-9.9E+04	-5.4E+04	-4.7E+04
48.8	1.0E+07	2.2E+07	-2.1E+07	1.2E+07	2.5E+07	7.6E+06	-8.9E+06	2.6E+07	-5.5E+04	-9.5E+04	-6.2E+04	-1.1E+05	-6.5E+04	-6.6E+04	-5.7E+04	-6.6E+04
58.6	7.5E+06	2.2E+07	-2.1E+07	9.2E+06	3.0E+07	9.8E+06	-1.1E+07	3.1E+07	-4.5E+04	-1.0E+05	-6.8E+04	-9.3E+04	-1.3E+05	-1.2E+05	-7.0E+04	-7.1E+04
68.4	4.5E+06	2.3E+07	-2.2E+07	6.3E+06	3.6E+07	1.0E+07	-1.3E+07	3.7E+07	-5.5E+04	-1.4E+05	-5.5E+04	-9.5E+04	-1.4E+05	-1.0E+05	-4.9E+04	-6.9E+04
78.1	1.4E+06	2.2E+07	-2.2E+07	2.5E+06	4.0E+07	1.2E+07	-1.4E+07	4.2E+07	-4.1E+04	-1.0E+05	-4.8E+04	-8.3E+04	-1.5E+05	-9.4E+04	-5.9E+04	-4.7E+04
87.9	-3.1E+06	2.2E+07	-2.2E+07	-2.3E+06	4.5E+07	1.4E+07	-1.6E+07	4.7E+07	-6.8E+04	-1.1E+05	-4.9E+04	-1.0E+05	-1.4E+05	-1.2E+05	-4.8E+04	-6.4E+04
97.7	-8.6E+06	2.3E+07	-2.3E+07	-7.3E+06	5.1E+07	1.6E+07	-1.8E+07	5.3E+07	-7.9E+04	-1.2E+05	-5.7E+04	-6.6E+04	-1.0E+05	-8.4E+04	-2.8E+04	-4.4E+04
107.4	-1.4E+07	2.3E+07	-2.3E+07	-1.3E+07	5.7E+07	1.7E+07	-2.0E+07	5.9E+07	-4.6E+04	-8.6E+04	-6.6E+04	-1.1E+05	-8.5E+04	-1.0E+05	-5.7E+04	-7.5E+04
117.2	-2.2E+07	2.5E+07	-2.3E+07	-2.0E+07	6.3E+07	2.0E+07	-2.2E+07	6.5E+07	-3.7E+04	-5.5E+04	-3.1E+04	-8.0E+04	-7.5E+04	-8.5E+04	-2.6E+04	-5.1E+04
127.0	-2.9E+07	2.7E+07	-2.2E+07	-2.8E+07	7.1E+07	2.1E+07	-2.6E+07	7.1E+07	-8.6E+04	-1.1E+05	-5.4E+04	-9.0E+04	-1.6E+05	-9.1E+04	-6.4E+04	-7.1E+04
136.7	-3.3E+07	2.8E+07	-2.8E+07	-3.5E+07	8.0E+07	2.1E+07	-3.2E+07	8.1E+07	-6.2E+04	-7.4E+04	-1.2E+05	-7.2E+04	-1.2E+05	-9.6E+04	-4.7E+04	-1.0E+05

Table 75 Raw data for the test seal at PD=20.7 bar, ω=3 krpm, and inlet GVF=4% with the medium-preswirl insert

Freq.	Re(H_{XX})	Re(H_{XY})	Re(H_{YX})	Re(H_{YY})	Im(H_{XX})	Im(H_{XY})	Im(H_{YX})	Im(H_{YY})	Re(eH_{XX})	Re(eH_{XY})	Re(eH_{YX})	Re(eH_{YY})	Im(eH_{XX})	Im(eH_{XY})	Im(eH_{YX})	Im(eH_{YY})
Hz	N/m	N/m	N/m	N/m	N/m	N/m	N/m	N/m	N/m	N/m	N/m	N/m	N/m	N/m	N/m	N/m
9.8	1.8E+07	1.7E+07	-1.7E+07	2.0E+07	4.2E+06	9.0E+05	-1.2E+06	3.3E+06	-8.0E+04	-1.2E+05	-8.3E+04	-1.5E+05	-1.2E+05	-1.6E+05	-8.1E+04	-8.5E+04
19.5	1.7E+07	1.7E+07	-1.7E+07	1.8E+07	9.8E+06	2.5E+06	-2.8E+06	9.8E+06	-8.4E+04	-6.3E+04	-9.7E+04	-1.1E+05	-1.7E+04	-3.8E+04	-9.9E+04	-9.5E+04
29.3	1.8E+07	1.6E+07	-1.8E+07	1.9E+07	1.3E+07	5.9E+06	-2.7E+06	1.2E+07	-7.3E+04	-9.2E+04	-8.2E+04	-8.0E+04	-6.1E+04	-7.6E+04	-5.5E+04	-9.7E+04
39.1	1.5E+07	1.6E+07	-1.7E+07	1.6E+07	2.0E+07	4.7E+06	-6.2E+06	2.1E+07	-5.8E+04	-5.6E+04	-4.3E+04	-5.7E+04	-7.0E+04	-7.5E+04	-4.1E+04	-4.4E+04
48.8	1.3E+07	1.6E+07	-1.8E+07	1.6E+07	2.3E+07	6.9E+06	-7.1E+06	2.5E+07	-2.9E+04	-5.6E+04	-2.9E+04	-6.4E+04	-5.6E+04	-8.1E+04	-4.9E+04	-5.7E+04
58.6	1.0E+07	1.7E+07	-1.8E+07	1.2E+07	2.8E+07	8.9E+06	-8.8E+06	2.9E+07	-5.1E+04	-4.9E+04	-7.6E+04	-1.0E+05	-6.7E+04	-5.7E+04	-7.4E+04	-1.1E+05
68.4	6.6E+06	1.8E+07	-1.9E+07	9.0E+06	3.3E+07	9.7E+06	-1.0E+07	3.5E+07	-7.8E+04	-1.1E+05	-1.1E+05	-1.6E+05	-9.4E+04	-1.1E+05	-1.0E+05	-1.6E+05
78.1	3.4E+06	1.8E+07	-1.9E+07	5.0E+06	3.9E+07	1.1E+07	-1.1E+07	4.0E+07	-5.0E+04	-7.1E+04	-3.3E+04	-6.8E+04	-5.3E+04	-5.6E+04	-4.8E+04	-7.3E+04
87.9	-5.1E+05	1.8E+07	-1.9E+07	4.3E+05	4.4E+07	1.2E+07	-1.3E+07	4.6E+07	-3.5E+04	-8.1E+04	-4.2E+04	-6.7E+04	-7.3E+04	-4.8E+04	-4.3E+04	-8.8E+04
97.7	-5.0E+06	1.8E+07	-2.0E+07	-4.1E+06	5.0E+07	1.4E+07	-1.4E+07	5.1E+07	-3.3E+04	-6.1E+04	-2.6E+04	-7.9E+04	-7.0E+04	-6.4E+04	-6.9E+04	-9.2E+04
107.4	-9.9E+06	1.9E+07	-2.0E+07	-8.8E+06	5.5E+07	1.5E+07	-1.6E+07	5.7E+07	-2.5E+04	-5.6E+04	-2.1E+04	-7.3E+04	-4.1E+04	-6.5E+04	-4.2E+04	-7.3E+04
117.2	-1.7E+07	2.0E+07	-2.0E+07	-1.5E+07	6.1E+07	1.7E+07	-1.8E+07	6.3E+07	-1.8E+04	-4.2E+04	-6.7E+04	-8.8E+04	-4.9E+04	-5.3E+04	-4.9E+04	-1.1E+05
127.0	-2.4E+07	2.2E+07	-1.9E+07	-2.3E+07	6.8E+07	1.8E+07	-2.0E+07	6.8E+07	-6.6E+04	-7.5E+04	-3.1E+04	-1.4E+05	-5.8E+04	-8.6E+04	-1.1E+05	-1.5E+05
136.7	-2.9E+07	2.2E+07	-2.4E+07	-2.9E+07	7.6E+07	1.8E+07	-2.5E+07	7.7E+07	-8.2E+04	-9.5E+04	-1.2E+05	-1.5E+05	-8.9E+04	-9.7E+04	-1.0E+05	-1.7E+05

Table 76 Raw data for the test seal at PD=20.7 bar, ω=4 krpm, and inlet GVF=4% with the medium-preswirl insert

Freq.	Re(H_{XX})	Re(H_{XY})	Re(H_{YX})	Re(H_{YY})	Im(H_{XX})	Im(H_{XY})	Im(H_{YX})	Im(H_{YY})	Re(eH_{XX})	Re(eH_{XY})	Re(eH_{YX})	Re(eH_{YY})	Im(eH_{XX})	Im(eH_{XY})	Im(eH_{YX})	Im(eH_{YY})
Hz	N/m	N/m	N/m	N/m	N/m	N/m	N/m	N/m	N/m	N/m	N/m	N/m	N/m	N/m	N/m	N/m
9.8	1.8E+07	1.7E+07	-1.7E+07	2.0E+07	4.3E+06	1.1E+06	-1.0E+06	3.5E+06	-7.7E+04	-9.7E+04	-7.6E+04	-1.2E+05	-5.3E+04	-7.2E+04	-6.6E+04	-1.1E+05
19.5	1.7E+07	1.7E+07	-1.7E+07	1.8E+07	9.8E+06	2.5E+06	-2.7E+06	9.8E+06	-6.0E+04	-7.9E+04	-3.2E+04	-9.3E+04	-8.5E+04	-7.1E+04	-6.7E+04	-5.1E+04
29.3	1.7E+07	1.6E+07	-1.9E+07	1.9E+07	1.3E+07	5.8E+06	-2.6E+06	1.2E+07	-9.1E+04	-7.5E+04	-7.7E+04	-9.2E+04	-4.8E+04	-5.7E+04	-4.8E+04	-5.6E+04
39.1	1.5E+07	1.6E+07	-1.8E+07	1.6E+07	2.0E+07	5.0E+06	-6.2E+06	2.1E+07	-4.0E+04	-5.5E+04	-5.0E+04	-7.7E+04	-3.4E+04	-3.3E+04	-2.9E+04	-3.2E+04
48.8	1.3E+07	1.6E+07	-1.8E+07	1.6E+07	2.3E+07	7.2E+06	-6.9E+06	2.5E+07	-5.2E+04	-6.3E+04	-5.3E+04	-9.3E+04	-3.5E+04	-6.5E+04	-2.5E+04	-4.4E+04
58.6	1.0E+07	1.7E+07	-1.8E+07	1.2E+07	2.8E+07	8.9E+06	-8.7E+06	2.9E+07	-5.9E+04	-4.8E+04	-5.7E+04	-9.5E+04	-3.9E+04	-6.7E+04	-8.1E+04	-7.5E+04
68.4	6.6E+06	1.8E+07	-1.9E+07	9.0E+06	3.4E+07	9.8E+06	-1.0E+07	3.5E+07	-7.0E+04	-1.3E+05	-9.0E+04	-1.8E+05	-9.1E+04	-1.1E+05	-1.3E+05	-1.4E+05
78.1	3.4E+06	1.8E+07	-1.9E+07	4.8E+06	3.9E+07	1.1E+07	-1.1E+07	4.0E+07	-5.6E+04	-6.1E+04	-5.2E+04	-6.3E+04	-6.6E+04	-7.0E+04	-5.0E+04	-5.7E+04
87.9	-5.2E+05	1.8E+07	-1.9E+07	6.7E+05	4.4E+07	1.2E+07	-1.3E+07	4.6E+07	-3.1E+04	-6.2E+04	-2.4E+04	-7.5E+04	-4.7E+04	-5.6E+04	-4.1E+04	-6.0E+04
97.7	-5.1E+06	1.8E+07	-2.0E+07	-4.0E+06	5.0E+07	1.4E+07	-1.4E+07	5.1E+07	-2.8E+04	-5.3E+04	-3.4E+04	-7.7E+04	-6.1E+04	-4.5E+04	-2.6E+04	-4.8E+04
107.4	-1.0E+07	1.9E+07	-2.0E+07	-8.7E+06	5.5E+07	1.5E+07	-1.6E+07	5.8E+07	-3.8E+04	-5.8E+04	-2.1E+04	-5.2E+04	-7.3E+04	-7.3E+04	-5.4E+04	-4.2E+04
117.2	-1.7E+07	2.0E+07	-2.0E+07	-1.5E+07	6.1E+07	1.7E+07	-1.8E+07	6.3E+07	-5.9E+04	-6.2E+04	-4.6E+04	-6.7E+04	-1.0E+05	-6.0E+04	-6.2E+04	-3.8E+04
127.0	-2.4E+07	2.2E+07	-1.9E+07	-2.3E+07	6.9E+07	1.8E+07	-2.0E+07	6.8E+07	-4.3E+04	-9.5E+04	-4.1E+04	-7.4E+04	-1.7E+05	-6.4E+04	-6.4E+04	-9.4E+04
136.7	-2.9E+07	2.2E+07	-2.4E+07	-3.0E+07	7.7E+07	1.8E+07	-2.5E+07	7.7E+07	-7.7E+04	-1.2E+05	-1.3E+05	-1.7E+05	-1.5E+05	-9.7E+04	-1.1E+05	-1.4E+05

Table 77 Raw data for the test seal at PD=20.7 bar, ω=5 krpm, and inlet GVF=4% with the medium-preswirl insert

Freq.	Re(H_{XX})	Re(H_{XY})	Re(H_{YX})	Re(H_{YY})	Im(H_{XX})	Im(H_{XY})	Im(H_{YX})	Im(H_{YY})	Re(eH_{XX})	Re(eH_{XY})	Re(eH_{YX})	Re(eH_{YY})	Im(eH_{XX})	Im(eH_{XY})	Im(eH_{YX})	Im(eH_{YY})
Hz	N/m	N/m	N/m	N/m	N/m	N/m	N/m	N/m	N/m	N/m	N/m	N/m	N/m	N/m	N/m	N/m
9.8	1.5E+07	2.3E+07	-2.2E+07	1.9E+07	4.8E+06	-9.2E+05	-2.1E+06	3.5E+06	-1.1E+05	-1.7E+05	-1.3E+05	-1.5E+05	-8.4E+04	-7.9E+04	-7.5E+04	-1.0E+05
19.5	1.4E+07	2.4E+07	-2.1E+07	1.4E+07	1.1E+07	1.9E+06	-4.1E+06	9.1E+06	-1.0E+05	-2.0E+05	-9.0E+04	-1.4E+05	-9.4E+04	-8.4E+04	-7.6E+04	-8.9E+04
29.3	1.4E+07	2.2E+07	-2.1E+07	1.4E+07	1.4E+07	5.7E+06	-3.9E+06	1.2E+07	-7.5E+04	-1.3E+05	-1.4E+05	-2.1E+05	-8.8E+04	-8.3E+04	-7.0E+04	-7.0E+04
39.1	1.3E+07	2.2E+07	-2.1E+07	1.3E+07	2.1E+07	4.5E+06	-7.4E+06	2.2E+07	-9.4E+04	-1.5E+05	-1.3E+05	-1.4E+05	-9.6E+04	-1.0E+05	-6.9E+04	-8.7E+04
48.8	1.1E+07	2.3E+07	-2.2E+07	1.3E+07	2.5E+07	6.2E+06	-8.7E+06	2.8E+07	-8.4E+04	-2.0E+05	-1.3E+05	-1.7E+05	-9.3E+04	-7.3E+04	-6.3E+04	-6.6E+04
58.6	7.6E+06	2.3E+07	-2.1E+07	9.9E+06	3.0E+07	8.3E+06	-1.0E+07	3.1E+07	-7.7E+04	-1.5E+05	-7.4E+04	-1.2E+05	-8.4E+04	-1.0E+05	-9.9E+04	-8.6E+04
68.4	4.5E+06	2.4E+07	-2.3E+07	7.1E+06	3.6E+07	8.9E+06	-1.2E+07	3.8E+07	-7.1E+04	-1.1E+05	-8.7E+04	-1.1E+05	-8.6E+04	-7.8E+04	-1.2E+05	-9.3E+04
78.1	1.8E+06	2.4E+07	-2.2E+07	3.0E+06	4.2E+07	9.8E+06	-1.3E+07	4.3E+07	-9.7E+04	-1.6E+05	-1.1E+05	-2.0E+05	-1.2E+05	-1.0E+05	-1.3E+05	-9.6E+04
87.9	-1.6E+06	2.3E+07	-2.3E+07	-9.0E+05	4.8E+07	1.1E+07	-1.5E+07	4.9E+07	-9.6E+04	-1.4E+05	-3.8E+04	-1.2E+05	-1.1E+05	-1.4E+05	-1.1E+05	-8.7E+04
97.7	-5.9E+06	2.3E+07	-2.3E+07	-5.2E+06	5.3E+07	1.4E+07	-1.7E+07	5.5E+07	-8.5E+04	-1.1E+05	-5.1E+04	-1.2E+05	-8.7E+04	-1.4E+05	-9.9E+04	-8.4E+04
107.4	-1.0E+07	2.3E+07	-2.4E+07	-8.9E+06	5.9E+07	1.5E+07	-1.8E+07	6.2E+07	-1.0E+05	-1.1E+05	-8.7E+04	-9.6E+04	-8.9E+04	-1.5E+05	-7.3E+04	-1.5E+05
117.2	-1.7E+07	2.5E+07	-2.3E+07	-1.5E+07	6.5E+07	1.7E+07	-2.1E+07	6.7E+07	-9.0E+04	-7.6E+04	-5.5E+04	-9.2E+04	-7.8E+04	-1.5E+05	-7.8E+04	-8.3E+04
127.0	-2.4E+07	2.6E+07	-2.3E+07	-2.2E+07	7.2E+07	1.8E+07	-2.5E+07	7.3E+07	-9.0E+04	-1.3E+05	-9.6E+04	-1.1E+05	-1.5E+05	-1.9E+05	-1.1E+05	-2.1E+05
136.7	-2.8E+07	2.7E+07	-2.8E+07	-3.0E+07	8.2E+07	1.9E+07	-3.0E+07	8.3E+07	-1.4E+05	-9.7E+04	-1.6E+05	-1.1E+05	-7.8E+04	-1.2E+05	-1.2E+05	-1.5E+05

Table 78 Raw data for the test seal at PD=20.7 bar, ω=3 krpm, and inlet GVF=6% with the medium-preswirl insert

Freq.	Re(H_{XX})	Re(H_{XY})	Re(H_{YX})	Re(H_{YY})	Im(H_{XX})	Im(H_{XY})	Im(H_{YX})	Im(H_{YY})	Re(eH_{XX})	Re(eH_{XY})	Re(eH_{YX})	Re(eH_{YY})	Im(eH_{XX})	Im(eH_{XY})	Im(eH_{YX})	Im(eH_{YY})
Hz	N/m	N/m	N/m	N/m	N/m	N/m	N/m	N/m	N/m	N/m	N/m	N/m	N/m	N/m	N/m	N/m
9.8	1.8E+07	1.7E+07	-1.7E+07	2.0E+07	4.2E+06	6.9E+05	-1.5E+06	3.6E+06	-1.1E+05	-1.1E+05	-8.0E+04	-9.7E+04	-4.1E+04	-7.3E+04	-1.1E+05	-1.0E+05
19.5	1.7E+07	1.8E+07	-1.7E+07	1.8E+07	1.0E+07	1.7E+06	-3.0E+06	1.0E+07	-6.5E+04	-1.4E+05	-8.0E+04	-1.4E+05	-6.0E+04	-4.7E+04	-1.1E+05	-8.4E+04
29.3	1.8E+07	1.5E+07	-1.9E+07	1.9E+07	1.3E+07	5.4E+06	-2.6E+06	1.3E+07	-6.6E+04	-8.2E+04	-8.8E+04	-1.3E+05	-8.3E+04	-6.2E+04	-8.6E+04	-9.2E+04
39.1	1.5E+07	1.6E+07	-1.7E+07	1.7E+07	1.9E+07	5.7E+06	-5.7E+06	2.0E+07	-4.8E+04	-7.2E+04	-3.5E+04	-5.9E+04	-7.5E+04	-5.0E+04	-5.2E+04	-4.9E+04
48.8	1.3E+07	1.7E+07	-1.8E+07	1.4E+07	2.4E+07	6.7E+06	-7.3E+06	2.5E+07	-4.4E+04	-6.5E+04	-5.8E+04	-8.0E+04	-5.9E+04	-5.6E+04	-4.9E+04	-5.1E+04
58.6	1.0E+07	1.8E+07	-1.8E+07	1.2E+07	2.9E+07	8.3E+06	-8.8E+06	3.0E+07	-4.4E+04	-6.2E+04	-5.4E+04	-7.9E+04	-5.5E+04	-5.1E+04	-7.4E+04	-7.8E+04
68.4	7.3E+06	1.8E+07	-1.9E+07	9.4E+06	3.5E+07	9.0E+06	-9.7E+06	3.6E+07	-7.9E+04	-1.2E+05	-1.1E+05	-1.9E+05	-1.2E+05	-1.6E+05	-1.1E+05	-7.8E+04
78.1	4.4E+06	1.8E+07	-1.9E+07	5.8E+06	4.0E+07	1.0E+07	-1.0E+07	4.1E+07	-3.8E+04	-8.7E+04	-3.9E+04	-8.3E+04	-8.2E+04	-5.8E+04	-4.5E+04	-3.7E+04
87.9	3.9E+05	1.8E+07	-1.9E+07	1.5E+06	4.5E+07	1.2E+07	-1.2E+07	4.6E+07	-3.6E+04	-6.6E+04	-4.7E+04	-8.8E+04	-6.5E+04	-6.1E+04	-3.6E+04	-4.0E+04
97.7	-4.4E+06	1.9E+07	-2.0E+07	-3.6E+06	5.1E+07	1.3E+07	-1.4E+07	5.2E+07	-4.0E+04	-6.6E+04	-4.5E+04	-6.8E+04	-8.0E+04	-5.2E+04	-4.3E+04	-4.7E+04
107.4	-9.4E+06	1.9E+07	-2.1E+07	-8.8E+06	5.6E+07	1.4E+07	-1.5E+07	5.9E+07	-4.8E+04	-6.2E+04	-4.4E+04	-7.9E+04	-8.6E+04	-6.0E+04	-5.8E+04	-3.9E+04
117.2	-1.6E+07	2.0E+07	-2.0E+07	-1.5E+07	6.3E+07	1.6E+07	-1.6E+07	6.5E+07	-6.1E+04	-6.1E+04	-3.3E+04	-7.4E+04	-6.8E+04	-6.2E+04	-5.5E+04	-4.8E+04
127.0	-2.3E+07	2.2E+07	-1.9E+07	-2.2E+07	7.1E+07	1.7E+07	-1.9E+07	7.2E+07	-3.1E+04	-6.8E+04	-5.6E+04	-1.2E+05	-1.1E+05	-4.3E+04	-6.6E+04	-9.3E+04
136.7	-2.7E+07	2.2E+07	-2.4E+07	-2.8E+07	8.0E+07	1.7E+07	-2.3E+07	8.2E+07	-6.8E+04	-8.7E+04	-8.4E+04	-1.1E+05	-1.6E+05	-7.8E+04	-8.4E+04	-5.3E+04

Table 79 Raw data for the test seal at PD=20.7 bar, ω=4 krpm, and inlet GVF=6% with the medium-preswirl insert

Freq.	Re(H_{XX})	Re(H_{XY})	Re(H_{YX})	Re(H_{YY})	Im(H_{XX})	Im(H_{XY})	Im(H_{YX})	Im(H_{YY})	Re(eH_{XX})	Re(eH_{XY})	Re(eH_{YX})	Re(eH_{YY})	Im(eH_{XX})	Im(eH_{XY})	Im(eH_{YX})	Im(eH_{YY})
Hz	N/m	N/m	N/m	N/m	N/m	N/m	N/m	N/m	N/m	N/m	N/m	N/m	N/m	N/m	N/m	N/m
9.8	1.8E+07	1.7E+07	-1.7E+07	2.0E+07	4.3E+06	6.7E+05	-1.4E+06	3.8E+06	-7.8E+04	-1.1E+05	-4.6E+04	-1.0E+05	-6.6E+04	-8.7E+04	-7.9E+04	-9.4E+04
19.5	1.7E+07	1.8E+07	-1.7E+07	1.8E+07	1.0E+07	2.0E+06	-2.9E+06	1.0E+07	-6.7E+04	-1.3E+05	-1.1E+05	-1.9E+05	-7.4E+04	-7.0E+04	-6.2E+04	-8.3E+04
29.3	1.8E+07	1.5E+07	-1.9E+07	1.9E+07	1.3E+07	5.3E+06	-2.3E+06	1.3E+07	-7.7E+04	-1.5E+05	-6.6E+04	-1.3E+05	-5.8E+04	-4.8E+04	-8.1E+04	-8.2E+04
39.1	1.5E+07	1.6E+07	-1.7E+07	1.7E+07	1.9E+07	5.8E+06	-5.6E+06	2.0E+07	-5.4E+04	-8.8E+04	-7.1E+04	-1.4E+05	-7.6E+04	-7.9E+04	-4.6E+04	-4.7E+04
48.8	1.3E+07	1.7E+07	-1.8E+07	1.4E+07	2.4E+07	6.8E+06	-7.3E+06	2.5E+07	-4.2E+04	-1.1E+05	-4.1E+04	-8.6E+04	-4.9E+04	-6.8E+04	-4.9E+04	-7.6E+04
58.6	9.8E+06	1.8E+07	-1.8E+07	1.2E+07	3.0E+07	8.3E+06	-8.6E+06	3.0E+07	-4.7E+04	-8.5E+04	-5.0E+04	-7.4E+04	-5.8E+04	-5.7E+04	-6.6E+04	-5.9E+04
68.4	7.1E+06	1.8E+07	-1.9E+07	9.4E+06	3.5E+07	8.8E+06	-9.6E+06	3.7E+07	-9.6E+04	-1.2E+05	-7.3E+04	-2.0E+05	-1.1E+05	-1.6E+05	-1.5E+05	-1.9E+05
78.1	4.1E+06	1.8E+07	-1.9E+07	5.6E+06	4.0E+07	1.0E+07	-1.1E+07	4.1E+07	-2.3E+04	-7.8E+04	-5.3E+04	-1.3E+05	-1.2E+05	-6.6E+04	-5.0E+04	-6.1E+04
87.9	2.7E+05	1.9E+07	-1.9E+07	1.4E+06	4.5E+07	1.2E+07	-1.2E+07	4.7E+07	-3.1E+04	-9.4E+04	-3.4E+04	-9.0E+04	-7.6E+04	-6.5E+04	-5.0E+04	-5.7E+04
97.7	-4.6E+06	1.9E+07	-2.0E+07	-3.7E+06	5.1E+07	1.3E+07	-1.4E+07	5.2E+07	-3.7E+04	-6.9E+04	-3.9E+04	-5.3E+04	-8.4E+04	-9.3E+04	-3.1E+04	-4.5E+04
107.4	-9.4E+06	1.9E+07	-2.1E+07	-8.7E+06	5.7E+07	1.4E+07	-1.5E+07	5.9E+07	-3.0E+04	-5.8E+04	-5.0E+04	-6.2E+04	-6.6E+04	-7.2E+04	-3.8E+04	-7.3E+04
117.2	-1.6E+07	2.0E+07	-2.0E+07	-1.5E+07	6.3E+07	1.6E+07	-1.6E+07	6.6E+07	-7.2E+04	-3.9E+04	-4.2E+04	-7.9E+04	-9.5E+04	-1.1E+05	-4.0E+04	-4.2E+04
127.0	-2.3E+07	2.2E+07	-1.9E+07	-2.2E+07	7.2E+07	1.7E+07	-1.8E+07	7.2E+07	-6.6E+04	-7.9E+04	-3.2E+04	-7.7E+04	-1.4E+05	-1.6E+05	-7.8E+04	-9.5E+04
136.7	-2.7E+07	2.2E+07	-2.4E+07	-2.8E+07	8.1E+07	1.7E+07	-2.3E+07	8.2E+07	-7.1E+04	-1.0E+05	-6.0E+04	-8.8E+04	-1.7E+05	-1.3E+05	-1.0E+05	-8.4E+04

Table 80 Raw data for the test seal at PD=20.7 bar, ω=5 krpm, and inlet GVF=6% with the medium-preswirl insert

Freq.	Re(H_{XX})	Re(H_{XY})	Re(H_{YX})	Re(H_{YY})	Im(H_{XX})	Im(H_{XY})	Im(H_{YX})	Im(H_{YY})	Re(eH_{XX})	Re(eH_{XY})	Re(eH_{YX})	Re(eH_{YY})	Im(eH_{XX})	Im(eH_{XY})	Im(eH_{YX})	Im(eH_{YY})
Hz	N/m	N/m	N/m	N/m	N/m	N/m	N/m	N/m	N/m	N/m	N/m	N/m	N/m	N/m	N/m	N/m
9.8	1.3E+07	2.5E+07	-2.2E+07	1.5E+07	5.0E+06	-9.0E+05	-2.3E+06	4.8E+06	-1.3E+05	-2.4E+05	-1.1E+05	-1.7E+05	-1.5E+05	-1.5E+05	-1.1E+05	-1.6E+05
19.5	1.3E+07	2.6E+07	-2.0E+07	1.1E+07	1.1E+07	1.3E+06	-3.7E+06	9.8E+06	-8.7E+04	-1.6E+05	-1.1E+05	-1.8E+05	-6.6E+04	-8.7E+04	-1.1E+05	-1.1E+05
29.3	1.4E+07	2.3E+07	-2.1E+07	1.2E+07	1.4E+07	4.9E+06	-3.2E+06	1.3E+07	-8.8E+04	-1.4E+05	-1.4E+05	-1.4E+05	-9.9E+04	-1.3E+05	-6.7E+04	-8.5E+04
39.1	1.2E+07	2.4E+07	-2.0E+07	1.2E+07	2.1E+07	4.7E+06	-6.4E+06	2.2E+07	-9.1E+04	-2.2E+05	-1.2E+05	-1.8E+05	-8.7E+04	-8.0E+04	-8.2E+04	-8.6E+04
48.8	9.1E+06	2.5E+07	-2.1E+07	9.0E+06	2.6E+07	5.3E+06	-8.5E+06	2.8E+07	-9.3E+04	-1.9E+05	-1.0E+05	-2.2E+05	-1.5E+05	-8.6E+04	-1.5E+05	-9.9E+04
58.6	6.9E+06	2.5E+07	-2.1E+07	7.3E+06	3.2E+07	6.3E+06	-9.8E+06	3.3E+07	-5.1E+04	-1.5E+05	-1.2E+05	-1.4E+05	-1.0E+05	-1.0E+05	-1.1E+05	-9.2E+04
68.4	4.5E+06	2.6E+07	-2.3E+07	5.0E+06	3.8E+07	6.6E+06	-1.2E+07	4.2E+07	-8.6E+04	-1.9E+05	-7.9E+04	-2.0E+05	-9.5E+04	-8.8E+04	-1.4E+05	-1.2E+05
78.1	2.0E+06	2.5E+07	-2.1E+07	2.4E+06	4.3E+07	8.0E+06	-1.2E+07	4.5E+07	-6.8E+04	-9.6E+04	-8.2E+04	-1.5E+05	-8.6E+04	-1.1E+05	-1.0E+05	-7.7E+04
87.9	-1.8E+06	2.5E+07	-2.2E+07	-1.7E+06	4.8E+07	9.7E+06	-1.4E+07	5.1E+07	-5.9E+04	-1.4E+05	-7.1E+04	-2.0E+05	-7.5E+04	-8.1E+04	-1.5E+05	-9.9E+04
97.7	-6.4E+06	2.4E+07	-2.3E+07	-6.3E+06	5.4E+07	1.2E+07	-1.7E+07	5.7E+07	-4.7E+04	-1.3E+05	-3.2E+04	-1.8E+05	-8.0E+04	-1.3E+05	-1.2E+05	-1.2E+05
107.4	-1.1E+07	2.4E+07	-2.4E+07	-9.9E+06	6.0E+07	1.3E+07	-1.8E+07	6.5E+07	-6.8E+04	-8.7E+04	-5.6E+04	-1.6E+05	-1.0E+05	-1.5E+05	-1.6E+05	-1.5E+05
117.2	-1.8E+07	2.6E+07	-2.3E+07	-1.5E+07	6.7E+07	1.5E+07	-1.9E+07	7.1E+07	-6.5E+04	-1.3E+05	-9.4E+04	-1.6E+05	-9.2E+04	-1.8E+05	-1.3E+05	-1.6E+05
127.0	-2.4E+07	2.8E+07	-2.2E+07	-2.2E+07	7.6E+07	1.6E+07	-2.3E+07	7.8E+07	-9.0E+04	-1.3E+05	-1.3E+05	-1.8E+05	-1.3E+05	-1.0E+05	-1.9E+05	-1.7E+05
136.7	-2.7E+07	2.9E+07	-2.8E+07	-2.9E+07	8.6E+07	1.6E+07	-2.9E+07	8.9E+07	-1.3E+05	-1.8E+05	-2.0E+05	-2.4E+05	-1.5E+05	-1.3E+05	-2.0E+05	-2.7E+05

Table 81 Raw data for the test seal at PD=20.7 bar, ω=3 krpm, and inlet GVF=8% with the medium-preswirl insert

Freq.	Re(H_{XX})	Re(H_{XY})	Re(H_{YX})	Re(H_{YY})	Im(H_{XX})	Im(H_{XY})	Im(H_{YX})	Im(H_{YY})	Re(eH_{XX})	Re(eH_{XY})	Re(eH_{YX})	Re(eH_{YY})	Im(eH_{XX})	Im(eH_{XY})	Im(eH_{YX})	Im(eH_{YY})
Hz	N/m	N/m	N/m	N/m	N/m	N/m	N/m	N/m	N/m	N/m	N/m	N/m	N/m	N/m	N/m	N/m
9.8	1.8E+07	1.8E+07	-1.8E+07	2.0E+07	4.0E+06	-9.0E+04	-1.7E+06	4.3E+06	-6.5E+04	-6.0E+04	-7.9E+04	-9.8E+04	-1.6E+05	-1.4E+05	-1.0E+05	-1.6E+05
19.5	1.7E+07	1.8E+07	-1.7E+07	1.8E+07	1.0E+07	1.4E+06	-3.0E+06	1.0E+07	-6.7E+04	-1.1E+05	-8.4E+04	-1.9E+05	-9.9E+04	-9.8E+04	-8.5E+04	-8.2E+04
29.3	1.8E+07	1.6E+07	-1.9E+07	1.9E+07	1.3E+07	5.6E+06	-2.0E+06	1.2E+07	-6.5E+04	-1.3E+05	-8.0E+04	-1.5E+05	-6.2E+04	-9.6E+04	-9.3E+04	-9.1E+04
39.1	1.5E+07	1.6E+07	-1.7E+07	1.6E+07	1.9E+07	5.4E+06	-5.6E+06	2.0E+07	-6.7E+04	-1.0E+05	-2.2E+04	-6.6E+04	-7.1E+04	-5.1E+04	-3.4E+04	-6.7E+04
48.8	1.3E+07	1.8E+07	-1.8E+07	1.4E+07	2.5E+07	6.3E+06	-7.4E+06	2.6E+07	-6.2E+04	-1.3E+05	-7.5E+04	-1.3E+05	-7.2E+04	-6.0E+04	-4.8E+04	-5.9E+04
58.6	1.0E+07	1.8E+07	-1.8E+07	1.2E+07	3.0E+07	7.9E+06	-8.2E+06	3.1E+07	-5.6E+04	-8.6E+04	-8.6E+04	-1.5E+05	-8.6E+04	-8.8E+04	-6.4E+04	-4.8E+04
68.4	7.7E+06	1.8E+07	-2.0E+07	9.5E+06	3.5E+07	8.3E+06	-9.7E+06	3.8E+07	-1.0E+05	-2.0E+05	-1.5E+05	-1.5E+05	-9.9E+04	-1.1E+05	-1.2E+05	-2.1E+05
78.1	4.7E+06	1.8E+07	-2.0E+07	6.1E+06	4.1E+07	9.8E+06	-1.0E+07	4.3E+07	-5.0E+04	-8.0E+04	-6.3E+04	-1.0E+05	-7.2E+04	-7.8E+04	-9.6E+04	-7.4E+04
87.9	8.1E+05	1.9E+07	-2.0E+07	1.9E+06	4.6E+07	1.1E+07	-1.1E+07	4.8E+07	-2.3E+04	-9.7E+04	-4.8E+04	-9.4E+04	-6.1E+04	-8.9E+04	-7.1E+04	-7.0E+04
97.7	-3.7E+06	2.0E+07	-2.0E+07	-2.4E+06	5.3E+07	1.2E+07	-1.2E+07	5.5E+07	-5.0E+04	-7.1E+04	-4.8E+04	-8.9E+04	-5.4E+04	-6.5E+04	-5.7E+04	-7.6E+04
107.4	-7.4E+06	1.9E+07	-2.0E+07	-6.2E+06	5.9E+07	1.2E+07	-1.3E+07	6.2E+07	-8.5E+04	-7.4E+04	-8.4E+04	-7.4E+04	-8.4E+04	-8.7E+04	-8.0E+04	-1.0E+05
117.2	-1.4E+07	2.0E+07	-1.9E+07	-1.2E+07	6.5E+07	1.5E+07	-1.4E+07	6.7E+07	-9.6E+04	-7.5E+04	-9.7E+04	-6.6E+04	-7.3E+04	-1.0E+05	-2.9E+04	-5.0E+04
127.0	-2.0E+07	2.2E+07	-1.8E+07	-2.0E+07	7.3E+07	1.6E+07	-1.7E+07	7.4E+07	-9.8E+04	-1.7E+05	-9.0E+04	-1.2E+05	-6.0E+04	-1.3E+05	-3.9E+04	-7.5E+04
136.7	-2.3E+07	2.2E+07	-2.2E+07	-2.4E+07	8.3E+07	1.4E+07	-2.1E+07	8.6E+07	-6.1E+04	-1.0E+05	-6.5E+04	-2.0E+05	-7.0E+04	-1.6E+05	-1.7E+05	-2.2E+05

Table 82 Raw data for the test seal at PD=20.7 bar, ω=4 krpm, and inlet GVF=8% with the medium-preswirl insert

Freq.	Re(H_{XX})	Re(H_{XY})	Re(H_{YX})	Re(H_{YY})	Im(H_{XX})	Im(H_{XY})	Im(H_{YX})	Im(H_{YY})	Re(eH_{XX})	Re(eH_{XY})	Re(eH_{YX})	Re(eH_{YY})	Im(eH_{XX})	Im(eH_{XY})	Im(eH_{YX})	Im(eH_{YY})
Hz	N/m	N/m	N/m	N/m	N/m	N/m	N/m	N/m	N/m	N/m	N/m	N/m	N/m	N/m	N/m	N/m
9.8	1.8E+07	1.7E+07	-1.7E+07	2.0E+07	4.2E+06	2.5E+05	-1.4E+06	4.1E+06	-6.5E+04	-1.4E+05	-1.1E+05	-1.3E+05	-6.9E+04	-7.5E+04	-9.2E+04	-1.2E+05
19.5	1.7E+07	1.8E+07	-1.7E+07	1.8E+07	1.1E+07	1.5E+06	-3.2E+06	1.1E+07	-8.2E+04	-1.7E+05	-9.3E+04	-1.8E+05	-6.5E+04	-7.2E+04	-9.2E+04	-1.0E+05
29.3	1.8E+07	1.6E+07	-1.9E+07	1.9E+07	1.3E+07	5.7E+06	-1.8E+06	1.2E+07	-1.2E+05	-1.6E+05	-1.1E+05	-2.3E+05	-6.5E+04	-5.4E+04	-8.9E+04	-5.7E+04
39.1	1.5E+07	1.6E+07	-1.7E+07	1.6E+07	2.0E+07	5.4E+06	-5.7E+06	2.0E+07	-7.1E+04	-1.4E+05	-7.1E+04	-1.6E+05	-5.7E+04	-8.8E+04	-2.7E+04	-5.0E+04
48.8	1.3E+07	1.8E+07	-1.8E+07	1.4E+07	2.5E+07	6.5E+06	-7.5E+06	2.6E+07	-5.5E+04	-9.1E+04	-8.3E+04	-1.9E+05	-7.5E+04	-8.7E+04	-6.5E+04	-8.1E+04
58.6	1.0E+07	1.8E+07	-1.9E+07	1.2E+07	3.0E+07	8.1E+06	-8.3E+06	3.1E+07	-6.9E+04	-1.1E+05	-9.7E+04	-2.2E+05	-7.4E+04	-7.1E+04	-9.9E+04	-7.8E+04
68.4	7.7E+06	1.8E+07	-2.0E+07	9.3E+06	3.6E+07	8.4E+06	-9.8E+06	3.7E+07	-1.1E+05	-1.7E+05	-1.2E+05	-2.4E+05	-1.2E+05	-2.2E+05	-1.6E+05	-1.6E+05
78.1	4.7E+06	1.9E+07	-2.0E+07	5.9E+06	4.1E+07	9.9E+06	-1.0E+07	4.3E+07	-5.7E+04	-1.5E+05	-5.7E+04	-1.2E+05	-1.3E+05	-1.2E+05	-9.1E+04	-1.2E+05
87.9	7.7E+05	1.9E+07	-2.0E+07	1.7E+06	4.7E+07	1.1E+07	-1.1E+07	4.8E+07	-4.5E+04	-9.3E+04	-2.4E+04	-9.8E+04	-9.1E+04	-1.6E+05	-7.9E+04	-1.1E+05
97.7	-3.5E+06	2.0E+07	-2.0E+07	-2.5E+06	5.3E+07	1.2E+07	-1.2E+07	5.5E+07	-6.8E+04	-9.1E+04	-5.7E+04	-1.1E+05	-8.7E+04	-1.2E+05	-5.2E+04	-8.8E+04
107.4	-7.3E+06	2.0E+07	-2.1E+07	-6.2E+06	5.9E+07	1.2E+07	-1.3E+07	6.2E+07	-6.2E+04	-9.9E+04	-4.5E+04	-8.1E+04	-1.1E+05	-2.1E+05	-6.9E+04	-1.2E+05
117.2	-1.4E+07	2.1E+07	-2.0E+07	-1.2E+07	6.6E+07	1.5E+07	-1.4E+07	6.7E+07	-7.9E+04	-8.2E+04	-5.0E+04	-5.8E+04	-4.9E+04	-1.8E+05	-3.4E+04	-9.0E+04
127.0	-2.0E+07	2.2E+07	-1.8E+07	-2.0E+07	7.4E+07	1.6E+07	-1.7E+07	7.4E+07	-1.1E+05	-1.1E+05	-1.1E+05	-1.1E+05	-1.2E+05	-2.5E+05	-5.0E+04	-2.0E+05
136.7	-2.3E+07	2.2E+07	-2.2E+07	-2.4E+07	8.4E+07	1.4E+07	-2.2E+07	8.6E+07	-8.5E+04	-1.0E+05	-1.3E+05	-1.2E+05	-1.2E+05	-2.2E+05	-5.2E+04	-1.8E+05

Table 83 Raw data for the test seal at PD=20.7 bar, ω=5 krpm, and inlet GVF=8% with the medium-preswirl insert

Freq.	Re(H_{XX})	Re(H_{XY})	Re(H_{YX})	Re(H_{YY})	Im(H_{XX})	Im(H_{XY})	Im(H_{YX})	Im(H_{YY})	Re(eH_{XX})	Re(eH_{XY})	Re(eH_{YX})	Re(eH_{YY})	Im(eH_{XX})	Im(eH_{XY})	Im(eH_{YX})	Im(eH_{YY})
Hz	N/m	N/m	N/m	N/m	N/m	N/m	N/m	N/m	N/m	N/m	N/m	N/m	N/m	N/m	N/m	N/m
9.8	1.2E+07	2.7E+07	-2.2E+07	1.3E+07	4.9E+06	-1.1E+06	-2.2E+06	4.0E+06	-2.2E+05	-3.9E+05	-2.9E+05	-2.9E+05	-2.3E+05	-2.3E+05	-2.0E+05	-3.6E+05
19.5	1.2E+07	2.8E+07	-2.1E+07	9.1E+06	1.2E+07	7.7E+04	-4.3E+06	1.1E+07	-1.4E+05	-2.5E+05	-2.0E+05	-1.9E+05	-1.1E+05	-1.3E+05	-1.5E+05	-2.2E+05
29.3	1.4E+07	2.4E+07	-2.2E+07	1.2E+07	1.4E+07	4.1E+06	-2.6E+06	1.3E+07	-1.1E+05	-2.0E+05	-1.5E+05	-1.5E+05	-8.4E+04	-7.3E+04	-9.3E+04	-1.0E+05
39.1	1.0E+07	2.6E+07	-2.0E+07	1.0E+07	2.1E+07	3.7E+06	-6.0E+06	2.2E+07	-9.6E+04	-2.2E+05	-1.5E+05	-2.4E+05	-1.1E+05	-6.4E+04	-9.9E+04	-1.1E+05
48.8	7.9E+06	2.7E+07	-2.1E+07	6.9E+06	2.7E+07	4.3E+06	-8.1E+06	2.9E+07	-7.2E+04	-1.7E+05	-1.1E+05	-1.9E+05	-8.2E+04	-9.7E+04	-9.0E+04	-7.8E+04
58.6	6.4E+06	2.7E+07	-2.1E+07	5.4E+06	3.3E+07	5.1E+06	-9.8E+06	3.5E+07	-8.4E+04	-1.9E+05	-1.0E+05	-2.1E+05	-8.6E+04	-8.8E+04	-1.8E+05	-1.2E+05
68.4	3.4E+06	2.8E+07	-2.2E+07	2.9E+06	3.9E+07	6.8E+06	-1.2E+07	4.3E+07	-1.1E+05	-2.1E+05	-1.4E+05	-2.6E+05	-8.8E+04	-7.9E+04	-1.2E+05	-1.0E+05
78.1	2.0E+06	2.7E+07	-2.2E+07	8.5E+05	4.5E+07	6.5E+06	-1.2E+07	4.8E+07	-7.1E+04	-1.8E+05	-6.8E+04	-2.2E+05	-1.1E+05	-1.8E+05	-1.5E+05	-1.3E+05
87.9	-1.8E+06	2.6E+07	-2.2E+07	-2.7E+06	5.0E+07	8.1E+06	-1.3E+07	5.4E+07	-9.0E+04	-1.7E+05	-3.9E+04	-2.0E+05	-9.3E+04	-1.5E+05	-1.7E+05	-1.3E+05
97.7	-6.2E+06	2.6E+07	-2.3E+07	-7.0E+06	5.7E+07	9.6E+06	-1.5E+07	6.1E+07	-9.9E+04	-1.6E+05	-7.0E+04	-2.4E+05	-7.7E+04	-1.1E+05	-1.5E+05	-1.0E+05
107.4	-1.0E+07	2.6E+07	-2.4E+07	-9.5E+06	6.4E+07	1.0E+07	-1.6E+07	6.9E+07	-9.4E+04	-1.5E+05	-9.1E+04	-1.7E+05	-1.1E+05	-1.3E+05	-1.2E+05	-1.6E+05
117.2	-1.6E+07	2.7E+07	-2.2E+07	-1.4E+07	7.0E+07	1.3E+07	-1.7E+07	7.4E+07	-1.0E+05	-1.2E+05	-1.0E+05	-1.3E+05	-9.2E+04	-1.6E+05	-1.3E+05	-1.8E+05
127.0	-2.2E+07	3.0E+07	-2.2E+07	-2.2E+07	7.9E+07	1.3E+07	-2.2E+07	8.2E+07	-1.0E+05	-2.5E+05	-5.8E+04	-2.5E+05	-1.4E+05	-1.5E+05	-1.5E+05	-1.9E+05
136.7	-2.5E+07	3.0E+07	-2.6E+07	-2.8E+07	8.9E+07	1.4E+07	-2.7E+07	9.4E+07	-1.6E+05	-2.1E+05	-1.2E+05	-2.7E+05	-1.1E+05	-7.7E+04	-1.9E+05	-1.6E+05

Table 84 Raw data for the test seal at PD=20.7 bar, ω=3 krpm, and inlet GVF=10% with the medium-preswirl insert

Freq.	Re(H_{XX})	Re(H_{XY})	Re(H_{YX})	Re(H_{YY})	Im(H_{XX})	Im(H_{XY})	Im(H_{YX})	Im(H_{YY})	Re(eH_{XX})	Re(eH_{XY})	Re(eH_{YX})	Re(eH_{YY})	Im(eH_{XX})	Im(eH_{XY})	Im(eH_{YX})	Im(eH_{YY})
Hz	N/m	N/m	N/m	N/m	N/m	N/m	N/m	N/m	N/m	N/m	N/m	N/m	N/m	N/m	N/m	N/m
9.8	1.7E+07	1.7E+07	-1.7E+07	1.9E+07	4.1E+06	9.9E+04	-1.6E+06	4.7E+06	-1.1E+05	-1.7E+05	-6.7E+04	-1.3E+05	-1.2E+05	-1.1E+05	-1.1E+05	-1.7E+05
19.5	1.6E+07	1.9E+07	-1.7E+07	1.7E+07	1.1E+07	1.4E+06	-2.9E+06	1.1E+07	-8.1E+04	-1.7E+05	-9.6E+04	-2.2E+05	-7.2E+04	-9.2E+04	-1.2E+05	-9.1E+04
29.3	1.7E+07	1.6E+07	-1.8E+07	1.8E+07	1.3E+07	5.8E+06	-1.9E+06	1.2E+07	-8.2E+04	-1.5E+05	-1.0E+05	-1.8E+05	-8.5E+04	-8.6E+04	-1.1E+05	-6.2E+04
39.1	1.4E+07	1.7E+07	-1.7E+07	1.6E+07	2.0E+07	4.8E+06	-5.8E+06	2.0E+07	-5.8E+04	-1.4E+05	-7.6E+04	-1.5E+05	-8.4E+04	-8.5E+04	-5.0E+04	-7.1E+04
48.8	1.2E+07	1.8E+07	-1.7E+07	1.3E+07	2.5E+07	6.0E+06	-7.3E+06	2.6E+07	-5.0E+04	-1.4E+05	-9.1E+04	-1.2E+05	-8.0E+04	-9.1E+04	-1.2E+05	-1.2E+05
58.6	9.7E+06	1.9E+07	-1.8E+07	1.1E+07	3.0E+07	7.6E+06	-8.5E+06	3.2E+07	-7.6E+04	-1.5E+05	-9.8E+04	-1.6E+05	-8.8E+04	-9.9E+04	-8.8E+04	-1.2E+05
68.4	7.2E+06	1.9E+07	-1.9E+07	8.4E+06	3.6E+07	7.2E+06	-1.0E+07	3.9E+07	-8.0E+04	-1.9E+05	-8.0E+04	-2.2E+05	-1.7E+05	-2.2E+05	-1.6E+05	-2.3E+05
78.1	4.5E+06	1.9E+07	-1.9E+07	5.4E+06	4.1E+07	8.7E+06	-1.0E+07	4.3E+07	-6.0E+04	-1.3E+05	-1.1E+05	-1.2E+05	-9.0E+04	-1.5E+05	-9.3E+04	-8.4E+04
87.9	5.2E+05	2.0E+07	-2.0E+07	1.1E+06	4.7E+07	1.1E+07	-1.1E+07	4.9E+07	-6.4E+04	-1.4E+05	-6.0E+04	-1.1E+05	-9.8E+04	-1.1E+05	-9.3E+04	-8.4E+04
97.7	-3.6E+06	2.0E+07	-2.0E+07	-3.0E+06	5.3E+07	1.1E+07	-1.2E+07	5.5E+07	-7.3E+04	-1.4E+05	-7.4E+04	-1.7E+05	-7.4E+04	-1.3E+05	-6.6E+04	-8.4E+04
107.4	-7.3E+06	1.9E+07	-2.0E+07	-6.0E+06	5.9E+07	1.1E+07	-1.3E+07	6.3E+07	-6.9E+04	-8.1E+04	-1.0E+05	-9.2E+04	-8.8E+04	-1.7E+05	-6.0E+04	-9.5E+04
117.2	-1.3E+07	2.0E+07	-1.9E+07	-1.2E+07	6.6E+07	1.3E+07	-1.4E+07	6.8E+07	-1.1E+05	-5.9E+04	-1.3E+05	-7.4E+04	-5.3E+04	-1.4E+05	-5.3E+04	-9.1E+04
127.0	-2.0E+07	2.2E+07	-1.7E+07	-1.9E+07	7.4E+07	1.5E+07	-1.7E+07	7.5E+07	-6.1E+04	-1.4E+05	-6.9E+04	-2.5E+05	-7.6E+04	-9.3E+04	-1.1E+05	-1.0E+05
136.7	-2.2E+07	2.2E+07	-2.2E+07	-2.3E+07	8.4E+07	1.3E+07	-2.1E+07	8.7E+07	-1.2E+05	-1.5E+05	-1.5E+05	-1.5E+05	-1.3E+05	-2.3E+05	-1.9E+05	-3.1E+05

Table 85 Raw data for the test seal at PD=20.7 bar, ω=4 krpm, and inlet GVF=10% with the medium-preswirl insert

Freq.	Re(H_{XX})	Re(H_{XY})	Re(H_{YX})	Re(H_{YY})	Im(H_{XX})	Im(H_{XY})	Im(H_{YX})	Im(H_{YY})	Re(eH_{XX})	Re(eH_{XY})	Re(eH_{YX})	Re(eH_{YY})	Im(eH_{XX})	Im(eH_{XY})	Im(eH_{YX})	Im(eH_{YY})
Hz	N/m	N/m	N/m	N/m	N/m	N/m	N/m	N/m	N/m	N/m	N/m	N/m	N/m	N/m	N/m	N/m
9.8	1.7E+07	1.8E+07	-1.7E+07	2.0E+07	4.5E+06	2.8E+04	-1.8E+06	5.0E+06	-8.6E+04	-1.7E+05	-9.4E+04	-1.6E+05	-1.3E+05	-1.4E+05	-5.8E+04	-7.1E+04
19.5	1.7E+07	2.0E+07	-1.7E+07	1.7E+07	1.1E+07	1.2E+06	-3.2E+06	1.1E+07	-9.4E+04	-1.6E+05	-9.8E+04	-1.9E+05	-5.5E+04	-8.0E+04	-6.1E+04	-1.1E+05
29.3	1.8E+07	1.7E+07	-1.8E+07	1.8E+07	1.3E+07	5.9E+06	-2.2E+06	1.2E+07	-6.8E+04	-1.4E+05	-1.0E+05	-1.5E+05	-6.2E+04	-8.0E+04	-8.8E+04	-6.5E+04
39.1	1.4E+07	1.7E+07	-1.7E+07	1.5E+07	2.0E+07	4.7E+06	-6.0E+06	2.0E+07	-4.8E+04	-1.3E+05	-6.8E+04	-1.4E+05	-6.5E+04	-9.4E+04	-6.8E+04	-8.9E+04
48.8	1.3E+07	1.9E+07	-1.7E+07	1.3E+07	2.6E+07	5.6E+06	-7.7E+06	2.7E+07	-1.1E+05	-1.4E+05	-6.6E+04	-1.5E+05	-9.5E+04	-9.2E+04	-6.6E+04	-9.4E+04
58.6	1.0E+07	1.9E+07	-1.8E+07	1.1E+07	3.1E+07	7.3E+06	-8.7E+06	3.2E+07	-6.5E+04	-1.7E+05	-9.4E+04	-1.9E+05	-5.8E+04	-8.1E+04	-9.2E+04	-5.7E+04
68.4	7.5E+06	2.0E+07	-1.9E+07	8.0E+06	3.7E+07	6.8E+06	-1.1E+07	3.9E+07	-1.1E+05	-1.9E+05	-1.0E+05	-2.3E+05	-1.2E+05	-1.8E+05	-1.5E+05	-1.9E+05
78.1	4.8E+06	2.0E+07	-2.0E+07	5.2E+06	4.2E+07	8.6E+06	-1.0E+07	4.4E+07	-3.5E+04	-1.4E+05	-3.9E+04	-1.2E+05	-8.9E+04	-1.2E+05	-8.1E+04	-1.1E+05
87.9	1.1E+06	2.0E+07	-2.0E+07	8.9E+05	4.8E+07	1.0E+07	-1.2E+07	5.0E+07	-4.1E+04	-1.1E+05	-5.5E+04	-1.5E+05	-9.6E+04	-1.0E+05	-6.9E+04	-8.1E+04
97.7	-3.0E+06	2.1E+07	-2.0E+07	-3.0E+06	5.4E+07	1.1E+07	-1.3E+07	5.6E+07	-5.0E+04	-1.0E+05	-7.7E+04	-1.3E+05	-6.7E+04	-1.3E+05	-7.3E+04	-1.3E+05
107.4	-6.5E+06	2.0E+07	-2.1E+07	-5.8E+06	6.0E+07	1.1E+07	-1.3E+07	6.4E+07	-5.3E+04	-9.7E+04	-9.0E+04	-1.0E+05	-5.5E+04	-1.6E+05	-4.1E+04	-1.4E+05
117.2	-1.3E+07	2.1E+07	-2.0E+07	-1.2E+07	6.6E+07	1.3E+07	-1.4E+07	6.9E+07	-5.4E+04	-6.8E+04	-9.9E+04	-1.0E+05	-5.5E+04	-1.4E+05	-6.1E+04	-1.2E+05
127.0	-1.9E+07	2.2E+07	-1.8E+07	-1.8E+07	7.5E+07	1.4E+07	-1.7E+07	7.6E+07	-1.0E+05	-1.5E+05	-7.5E+04	-2.1E+05	-9.4E+04	-1.7E+05	-1.1E+05	-9.4E+04
136.7	-2.2E+07	2.2E+07	-2.2E+07	-2.3E+07	8.5E+07	1.2E+07	-2.2E+07	8.8E+07	-1.3E+05	-1.5E+05	-1.5E+05	-1.4E+05	-2.2E+05	-3.2E+05	-1.9E+05	-2.5E+05

Table 86 Raw data for the test seal at PD=20.7 bar, ω=5 krpm, and inlet GVF=10% with the medium-preswirl insert

Freq.	Re(H_{XX})	Re(H_{XY})	Re(H_{YX})	Re(H_{YY})	Im(H_{XX})	Im(H_{XY})	Im(H_{YX})	Im(H_{YY})	Re(eH_{XX})	Re(eH_{XY})	Re(eH_{YX})	Re(eH_{YY})	Im(eH_{XX})	Im(eH_{XY})	Im(eH_{YX})	Im(eH_{YY})
Hz	N/m	N/m	N/m	N/m	N/m	N/m	N/m	N/m	N/m	N/m	N/m	N/m	N/m	N/m	N/m	N/m
9.8	8.4E+06	3.0E+07	-2.0E+07	7.7E+06	4.5E+06	-6.2E+05	-1.3E+06	1.5E+06	-3.9E+05	-5.9E+05	-3.5E+05	-3.0E+05	-2.5E+05	-3.2E+05	-2.0E+05	-4.8E+05
19.5	9.7E+06	3.1E+07	-2.1E+07	6.0E+06	1.2E+07	-1.2E+06	-3.2E+06	9.9E+06	-1.3E+05	-3.3E+05	-2.0E+05	-1.7E+05	-2.2E+05	-2.0E+05	-1.4E+05	-3.0E+05
29.3	1.1E+07	2.8E+07	-2.3E+07	8.5E+06	1.5E+07	1.6E+06	-2.4E+06	1.5E+07	-1.6E+05	-3.0E+05	-2.4E+05	-2.4E+05	-1.6E+05	-1.2E+05	-1.2E+05	-1.8E+05
39.1	6.9E+06	3.0E+07	-2.0E+07	3.9E+06	2.3E+07	2.2E+06	-5.3E+06	2.2E+07	-1.3E+05	-3.1E+05	-3.1E+05	-4.3E+05	-1.1E+05	-7.2E+04	-1.2E+05	-2.7E+05
48.8	4.8E+06	3.0E+07	-2.0E+07	1.9E+06	2.9E+07	2.8E+06	-7.5E+06	3.0E+07	-1.3E+05	-3.0E+05	-2.5E+05	-4.7E+05	-1.8E+05	-1.4E+05	-1.6E+05	-1.7E+05
58.6	3.0E+06	3.1E+07	-2.1E+07	-9.1E+05	3.6E+07	3.9E+06	-9.6E+06	3.7E+07	-1.3E+05	-3.9E+05	-3.2E+05	-6.1E+05	-1.8E+05	-1.3E+05	-2.3E+05	-2.2E+05
68.4	8.7E+05	3.0E+07	-2.1E+07	-1.1E+06	4.0E+07	6.8E+06	-9.7E+06	4.3E+07	-1.1E+05	-2.1E+05	-2.2E+05	-3.3E+05	-1.1E+05	-9.9E+04	-1.9E+05	-3.2E+05
78.1	1.8E+04	3.0E+07	-2.2E+07	-4.3E+06	4.7E+07	4.3E+06	-1.1E+07	5.1E+07	-9.9E+04	-2.3E+05	-1.6E+05	-5.3E+05	-1.3E+05	-1.7E+05	-2.4E+05	-1.7E+05
87.9	-3.1E+06	2.9E+07	-2.3E+07	-6.6E+06	5.3E+07	4.7E+06	-1.3E+07	5.9E+07	-7.9E+04	-2.3E+05	-9.7E+04	-4.7E+05	-1.3E+05	-2.2E+05	-3.1E+05	-3.5E+05
97.7	-7.2E+06	2.8E+07	-2.3E+07	-9.7E+06	6.0E+07	6.5E+06	-1.4E+07	6.6E+07	-1.4E+05	-1.7E+05	-8.7E+04	-3.9E+05	-1.1E+05	-2.1E+05	-2.7E+05	-2.8E+05
107.4	-1.1E+07	2.9E+07	-2.3E+07	-1.4E+07	6.7E+07	8.6E+06	-1.6E+07	7.3E+07	-9.6E+04	-1.5E+05	-9.6E+04	-5.7E+05	-9.2E+04	-1.1E+05	-3.0E+05	-2.1E+05
117.2	-1.6E+07	2.9E+07	-2.2E+07	-1.7E+07	7.3E+07	1.0E+07	-1.6E+07	8.0E+07	-8.1E+04	-1.5E+05	-7.9E+04	-4.1E+05	-8.4E+04	-2.0E+05	-2.4E+05	-3.5E+05
127.0	-2.2E+07	3.4E+07	-1.9E+07	-2.6E+07	8.2E+07	1.2E+07	-2.2E+07	8.6E+07	-1.3E+05	-3.2E+05	-1.5E+05	-6.3E+05	-1.3E+05	-1.3E+05	-2.6E+05	-1.4E+05
136.7	-2.5E+07	3.1E+07	-2.4E+07	-2.8E+07	9.1E+07	1.2E+07	-2.5E+07	9.7E+07	-1.5E+05	-1.5E+05	-1.9E+05	-2.5E+05	-1.2E+05	-8.7E+04	-1.6E+05	-7.3E+04

Table 87 Raw data for the test seal at PD=27.6 bar, ω=3 krpm, and inlet GVF=0% with the medium-preswirl insert

Freq.	Re(H_{XX})	Re(H_{XY})	Re(H_{YX})	Re(H_{YY})	Im(H_{XX})	Im(H_{XY})	Im(H_{YX})	Im(H_{YY})	Re(eH_{XX})	Re(eH_{XY})	Re(eH_{YX})	Re(eH_{YY})	Im(eH_{XX})	Im(eH_{XY})	Im(eH_{YX})	Im(eH_{YY})
Hz	N/m	N/m	N/m	N/m	N/m	N/m	N/m	N/m	N/m	N/m	N/m	N/m	N/m	N/m	N/m	N/m
9.8	2.5E+07	2.1E+07	-2.2E+07	2.6E+07	3.1E+06	-3.1E+05	-6.7E+05	4.2E+06	-3.2E+05	-2.7E+05	-3.4E+05	-2.4E+05	-1.8E+05	-1.9E+05	-1.9E+05	-3.0E+05
19.5	2.3E+07	2.5E+07	-2.0E+07	2.2E+07	9.4E+06	2.2E+06	-3.2E+06	1.2E+07	-1.5E+05	-1.5E+05	-1.7E+05	-2.1E+05	-1.2E+05	-1.2E+05	-1.1E+05	-1.7E+05
29.3	2.3E+07	2.3E+07	-2.0E+07	2.2E+07	1.3E+07	6.0E+06	-3.1E+06	1.5E+07	-2.3E+05	-2.2E+05	-1.5E+05	-1.7E+05	-1.6E+05	-1.5E+05	-1.1E+05	-1.1E+05
39.1	1.9E+07	2.3E+07	-1.9E+07	2.1E+07	2.0E+07	5.1E+06	-7.1E+06	2.3E+07	-1.1E+05	-9.9E+04	-1.2E+05	-1.4E+05	-1.2E+05	-1.1E+05	-1.1E+05	-1.6E+05
48.8	1.7E+07	2.4E+07	-2.0E+07	1.8E+07	2.6E+07	6.0E+06	-9.3E+06	3.0E+07	-1.3E+05	-1.3E+05	-1.2E+05	-1.2E+05	-7.9E+04	-9.3E+04	-1.6E+05	-1.3E+05
58.6	1.5E+07	2.4E+07	-2.1E+07	1.6E+07	3.2E+07	7.8E+06	-1.1E+07	3.5E+07	-1.0E+05	-1.8E+05	-1.5E+05	-1.9E+05	-1.1E+05	-9.9E+04	-1.3E+05	-1.4E+05
68.4	1.1E+07	2.5E+07	-2.2E+07	1.3E+07	3.8E+07	8.4E+06	-1.4E+07	4.2E+07	-1.8E+05	-1.2E+05	-1.4E+05	-1.6E+05	-1.9E+05	-1.6E+05	-1.9E+05	-1.9E+05
78.1	8.6E+06	2.5E+07	-2.2E+07	8.9E+06	4.4E+07	9.6E+06	-1.4E+07	4.7E+07	-9.6E+04	-1.7E+05	-8.1E+04	-1.1E+05	-8.4E+04	-1.1E+05	-1.2E+05	-9.5E+04
87.9	3.2E+06	2.5E+07	-2.3E+07	3.9E+06	4.9E+07	1.2E+07	-1.6E+07	5.3E+07	-8.4E+04	-7.3E+04	-5.3E+04	-1.1E+05	-7.1E+04	-7.4E+04	-1.3E+05	-1.1E+05
97.7	-2.2E+06	2.5E+07	-2.4E+07	-1.4E+06	5.5E+07	1.3E+07	-1.7E+07	5.9E+07	-1.7E+05	-1.3E+05	-1.5E+05	-1.1E+05	-7.0E+04	-1.1E+05	-1.5E+05	-8.5E+04
107.4	-7.3E+06	2.5E+07	-2.5E+07	-5.9E+06	6.1E+07	1.3E+07	-1.8E+07	6.6E+07	-1.7E+05	-1.0E+05	-1.7E+05	-1.5E+05	-1.0E+05	-1.3E+05	-1.3E+05	-8.6E+04
117.2	-1.5E+07	2.6E+07	-2.4E+07	-1.4E+07	6.7E+07	1.5E+07	-2.0E+07	7.1E+07	-9.0E+04	-5.4E+04	-1.1E+05	-1.2E+05	-9.8E+04	-9.6E+04	-1.6E+05	-9.6E+04
127.0	-2.4E+07	2.8E+07	-2.2E+07	-2.2E+07	7.4E+07	1.6E+07	-2.4E+07	7.9E+07	-1.4E+05	-1.4E+05	-1.6E+05	-2.0E+05	-1.3E+05	-1.7E+05	-1.2E+05	-2.6E+05
136.7	-2.9E+07	2.9E+07	-2.7E+07	-3.0E+07	8.3E+07	1.6E+07	-2.8E+07	8.8E+07	-2.0E+05	-1.4E+05	-2.5E+05	-2.3E+05	-1.4E+05	-2.0E+05	-2.1E+05	-1.5E+05

Table 88 Raw data for the test seal at PD=27.6 bar, ω=4 krpm, and inlet GVF=0% with the medium-preswirl insert

Freq.	Re(H_{XX})	Re(H_{XY})	Re(H_{YX})	Re(H_{YY})	Im(H_{XX})	Im(H_{XY})	Im(H_{YX})	Im(H_{YY})	Re(eH_{XX})	Re(eH_{XY})	Re(eH_{YX})	Re(eH_{YY})	Im(eH_{XX})	Im(eH_{XY})	Im(eH_{YX})	Im(eH_{YY})
Hz	N/m	N/m	N/m	N/m	N/m	N/m	N/m	N/m	N/m	N/m	N/m	N/m	N/m	N/m	N/m	N/m
9.8	2.3E+07	2.3E+07	-2.2E+07	2.4E+07	2.8E+06	-7.4E+05	-2.9E+05	5.6E+06	-3.2E+05	-6.3E+05	-4.9E+05	-8.6E+05	-3.5E+05	-2.6E+05	-2.4E+05	-1.7E+05
19.5	2.1E+07	2.5E+07	-2.0E+07	1.9E+07	9.9E+06	2.5E+06	-3.4E+06	1.2E+07	-2.8E+05	-3.5E+05	-2.9E+05	-4.7E+05	-2.0E+05	-2.1E+05	-1.5E+05	-1.7E+05
29.3	2.1E+07	2.4E+07	-2.0E+07	2.0E+07	1.3E+07	5.5E+06	-2.3E+06	1.6E+07	-2.1E+05	-2.1E+05	-3.5E+05	-3.7E+05	-1.7E+05	-1.7E+05	-1.2E+05	-1.7E+05
39.1	1.8E+07	2.4E+07	-1.9E+07	2.0E+07	2.1E+07	5.3E+06	-6.3E+06	2.4E+07	-3.1E+05	-3.8E+05	-2.0E+05	-4.0E+05	-1.0E+05	-1.8E+05	-1.3E+05	-1.8E+05
48.8	1.5E+07	2.5E+07	-2.1E+07	1.6E+07	2.7E+07	6.2E+06	-9.1E+06	3.1E+07	-2.2E+05	-3.3E+05	-2.1E+05	-4.9E+05	-1.3E+05	-1.7E+05	-1.3E+05	-2.0E+05
58.6	1.2E+07	2.5E+07	-2.1E+07	1.4E+07	3.3E+07	7.7E+06	-1.1E+07	3.6E+07	-2.7E+05	-3.7E+05	-2.2E+05	-4.3E+05	-1.9E+05	-2.3E+05	-2.2E+05	-2.3E+05
68.4	9.1E+06	2.6E+07	-2.2E+07	1.1E+07	4.0E+07	8.7E+06	-1.3E+07	4.4E+07	-1.7E+05	-2.9E+05	-2.2E+05	-3.9E+05	-2.1E+05	-2.5E+05	-2.7E+05	-3.9E+05
78.1	7.3E+06	2.6E+07	-2.2E+07	8.1E+06	4.5E+07	9.3E+06	-1.4E+07	4.9E+07	-1.1E+05	-2.6E+05	-2.0E+05	-3.3E+05	-2.3E+05	-4.1E+05	-3.1E+05	-4.1E+05
87.9	2.4E+06	2.6E+07	-2.4E+07	3.8E+06	5.0E+07	1.1E+07	-1.5E+07	5.5E+07	-1.7E+05	-2.8E+05	-1.5E+05	-4.2E+05	-3.6E+05	-3.9E+05	-2.9E+05	-3.9E+05
97.7	-3.2E+06	2.6E+07	-2.4E+07	-2.0E+06	5.7E+07	1.3E+07	-1.7E+07	6.1E+07	-9.2E+04	-1.6E+05	-1.1E+05	-2.9E+05	-1.6E+05	-3.2E+05	-3.0E+05	-3.5E+05
107.4	-8.3E+06	2.7E+07	-2.5E+07	-6.2E+06	6.3E+07	1.3E+07	-1.7E+07	6.8E+07	-1.9E+05	-2.1E+05	-1.7E+05	-3.4E+05	-2.3E+05	-3.3E+05	-2.7E+05	-3.9E+05
117.2	-1.6E+07	2.8E+07	-2.4E+07	-1.4E+07	6.9E+07	1.5E+07	-1.9E+07	7.3E+07	-1.5E+05	-2.5E+05	-1.8E+05	-3.2E+05	-2.4E+05	-3.4E+05	-3.4E+05	-4.9E+05
127.0	-2.4E+07	3.0E+07	-2.1E+07	-2.3E+07	7.6E+07	1.5E+07	-2.4E+07	8.1E+07	-9.3E+04	-2.8E+05	-2.1E+05	-3.2E+05	-2.4E+05	-2.0E+05	-3.7E+05	-3.7E+05
136.7	-2.9E+07	3.0E+07	-2.7E+07	-3.0E+07	8.5E+07	1.5E+07	-2.7E+07	9.1E+07	-1.4E+05	-3.4E+05	-2.3E+05	-4.7E+05	-3.1E+05	-2.4E+05	-3.0E+05	-4.3E+05

Table 89 Raw data for the test seal at PD=27.6 bar, ω=5 krpm, and inlet GVF=0% with the medium-preswirl insert

Freq.	Re(H_{XX})	Re(H_{XY})	Re(H_{YX})	Re(H_{YY})	Im(H_{XX})	Im(H_{XY})	Im(H_{YX})	Im(H_{YY})	Re(eH_{XX})	Re(eH_{XY})	Re(eH_{YX})	Re(eH_{YY})	Im(eH_{XX})	Im(eH_{XY})	Im(eH_{YX})	Im(eH_{YY})
Hz	N/m	N/m	N/m	N/m	N/m	N/m	N/m	N/m	N/m	N/m	N/m	N/m	N/m	N/m	N/m	N/m
9.8	1.5E+07	3.3E+07	-2.7E+07	1.1E+07	2.8E+06	-2.9E+06	-3.6E+06	3.1E+06	-3.8E+05	-5.1E+05	-4.8E+05	-5.6E+05	-2.4E+05	-2.7E+05	-1.8E+05	-3.2E+05
19.5	1.5E+07	3.2E+07	-2.6E+07	8.6E+06	9.4E+06	-1.6E+05	-5.2E+06	1.2E+07	-2.4E+05	-3.6E+05	-4.6E+05	-4.1E+05	-2.0E+05	-1.2E+05	-1.7E+05	-3.7E+05
29.3	1.5E+07	3.0E+07	-2.7E+07	9.6E+06	1.3E+07	2.2E+06	-4.3E+06	1.7E+07	-2.6E+05	-3.3E+05	-5.1E+05	-3.2E+05	-2.2E+05	-1.6E+05	-2.1E+05	-3.6E+05
39.1	1.2E+07	3.3E+07	-2.5E+07	9.1E+06	2.3E+07	2.6E+06	-6.9E+06	2.8E+07	-3.2E+05	-4.2E+05	-4.7E+05	-4.4E+05	-2.1E+05	-1.6E+05	-3.0E+05	-3.9E+05
48.8	7.2E+06	3.2E+07	-2.7E+07	6.3E+06	2.8E+07	4.6E+06	-9.3E+06	3.6E+07	-3.0E+05	-4.0E+05	-3.3E+05	-3.9E+05	-2.2E+05	-1.0E+05	-3.6E+05	-3.0E+05
58.6	5.4E+06	3.4E+07	-2.6E+07	4.9E+06	3.6E+07	5.4E+06	-1.1E+07	4.2E+07	-3.3E+05	-4.0E+05	-3.4E+05	-4.6E+05	-2.4E+05	-2.8E+05	-4.0E+05	-3.2E+05
68.4	1.8E+06	3.3E+07	-2.7E+07	2.8E+06	4.2E+07	9.2E+06	-1.3E+07	5.0E+07	-3.2E+05	-3.9E+05	-3.2E+05	-4.0E+05	-1.5E+05	-1.8E+05	-3.6E+05	-3.2E+05
78.1	2.3E+06	3.4E+07	-2.5E+07	7.8E+05	5.1E+07	7.2E+06	-1.4E+07	5.5E+07	-2.2E+05	-3.8E+05	-1.8E+05	-3.9E+05	-2.4E+05	-3.3E+05	-2.9E+05	-2.2E+05
87.9	-2.7E+06	3.2E+07	-2.7E+07	-2.5E+06	5.6E+07	8.4E+06	-1.5E+07	6.3E+07	-3.0E+05	-2.3E+05	-2.1E+05	-4.2E+05	-2.1E+05	-3.5E+05	-4.9E+05	-2.8E+05
97.7	-9.0E+06	3.1E+07	-2.7E+07	-7.6E+06	6.2E+07	1.1E+07	-1.7E+07	6.9E+07	-3.5E+05	-1.8E+05	-1.7E+05	-4.5E+05	-1.6E+05	-3.6E+05	-4.8E+05	-3.9E+05
107.4	-1.3E+07	3.4E+07	-2.7E+07	-1.2E+07	7.0E+07	1.1E+07	-1.9E+07	7.7E+07	-4.0E+05	-2.0E+05	-1.9E+05	-5.0E+05	-2.0E+05	-3.6E+05	-5.7E+05	-3.0E+05
117.2	-2.1E+07	3.3E+07	-2.6E+07	-1.7E+07	7.7E+07	1.4E+07	-2.0E+07	8.2E+07	-2.2E+05	-1.8E+05	-1.1E+05	-4.2E+05	-2.7E+05	-2.9E+05	-4.3E+05	-3.3E+05
127.0	-2.7E+07	3.8E+07	-2.4E+07	-2.8E+07	8.4E+07	1.4E+07	-2.7E+07	9.1E+07	-2.1E+05	-3.0E+05	-1.7E+05	-5.8E+05	-2.7E+05	-1.9E+05	-5.2E+05	-3.5E+05
136.7	-3.2E+07	3.7E+07	-2.9E+07	-3.4E+07	9.4E+07	1.6E+07	-3.1E+07	1.0E+08	-2.0E+05	-2.8E+05	-2.3E+05	-4.8E+05	-2.7E+05	-1.1E+05	-6.5E+05	-2.8E+05

Table 90 Raw data for the test seal at PD=27.6 bar, ω=3 krpm, and inlet GVF=2% with the medium-preswirl insert

Freq.	Re(H_{XX})	Re(H_{XY})	Re(H_{YX})	Re(H_{YY})	Im(H_{XX})	Im(H_{XY})	Im(H_{YX})	Im(H_{YY})	Re(eH_{XX})	Re(eH_{XY})	Re(eH_{YX})	Re(eH_{YY})	Im(eH_{XX})	Im(eH_{XY})	Im(eH_{YX})	Im(eH_{YY})
Hz	N/m	N/m	N/m	N/m	N/m	N/m	N/m	N/m	N/m	N/m	N/m	N/m	N/m	N/m	N/m	N/m
9.8	1.4E+07	2.6E+07	-2.4E+07	1.0E+07	3.9E+06	-1.3E+06	7.5E+05	7.4E+06	-6.0E+05	-6.6E+05	-7.4E+05	-7.5E+05	-2.0E+05	-3.4E+05	-2.9E+05	-5.3E+05
19.5	1.3E+07	2.5E+07	-2.5E+07	1.2E+07	1.0E+07	3.5E+05	-7.7E+05	1.7E+07	-6.8E+05	-5.9E+05	-1.1E+06	-6.6E+05	-3.6E+05	-3.3E+05	-5.2E+05	-8.8E+05
29.3	1.4E+07	2.3E+07	-2.4E+07	1.3E+07	1.4E+07	4.1E+06	7.7E+05	2.1E+07	-1.0E+06	-6.4E+05	-7.7E+05	-5.1E+05	-3.0E+05	-4.4E+05	-7.8E+05	-6.2E+05
39.1	9.6E+06	2.5E+07	-2.3E+07	1.1E+07	2.2E+07	6.1E+06	-2.1E+06	3.1E+07	-9.3E+05	-6.2E+05	-9.8E+05	-7.0E+05	-2.4E+05	-3.9E+05	-7.7E+05	-7.9E+05
48.8	7.8E+06	2.7E+07	-2.3E+07	1.1E+07	3.0E+07	6.6E+06	-4.6E+06	3.7E+07	-8.9E+05	-5.9E+05	-6.0E+05	-8.2E+05	-3.1E+05	-4.2E+05	-7.9E+05	-5.1E+05
58.6	4.2E+06	2.9E+07	-2.4E+07	8.5E+06	3.8E+07	7.8E+06	-6.1E+06	4.3E+07	-9.3E+05	-3.7E+05	-6.9E+05	-4.5E+05	-4.2E+05	-6.4E+05	-7.6E+05	-6.3E+05
68.4	1.5E+06	2.7E+07	-2.4E+07	8.0E+06	4.4E+07	1.0E+07	-7.3E+06	4.9E+07	-8.8E+05	-3.6E+05	-4.9E+05	-7.5E+05	-4.4E+05	-5.3E+05	-8.4E+05	-4.6E+05
78.1	2.8E+06	3.0E+07	-2.2E+07	5.0E+06	5.3E+07	7.6E+06	-1.0E+07	5.5E+07	-8.1E+05	-3.0E+05	-4.0E+05	-6.6E+05	-6.8E+05	-5.5E+05	-7.7E+05	-3.8E+05
87.9	-4.2E+05	2.9E+07	-2.5E+07	2.0E+06	5.9E+07	8.1E+06	-1.1E+07	6.4E+07	-7.7E+05	-3.6E+05	-3.5E+05	-7.9E+05	-6.6E+05	-5.5E+05	-8.9E+05	-5.3E+05
97.7	-4.6E+06	2.8E+07	-2.5E+07	-1.4E+06	6.5E+07	9.1E+06	-1.2E+07	6.9E+07	-6.3E+05	-1.9E+05	-3.1E+05	-5.1E+05	-6.1E+05	-5.4E+05	-9.1E+05	-4.7E+05
107.4	-8.6E+06	3.1E+07	-2.3E+07	-5.2E+06	7.2E+07	9.7E+06	-1.2E+07	7.6E+07	-7.4E+05	-2.6E+05	-3.4E+05	-6.6E+05	-6.1E+05	-4.1E+05	-9.2E+05	-3.7E+05
117.2	-1.5E+07	3.0E+07	-2.4E+07	-1.0E+07	7.9E+07	1.1E+07	-1.4E+07	8.2E+07	-4.8E+05	-2.6E+05	-2.6E+05	-4.7E+05	-5.9E+05	-3.7E+05	-8.9E+05	-4.9E+05
127.0	-2.0E+07	3.4E+07	-1.9E+07	-1.9E+07	8.6E+07	1.0E+07	-1.8E+07	8.7E+07	-3.3E+05	-4.7E+05	-3.9E+05	-6.9E+05	-1.0E+06	-3.9E+05	-1.1E+06	-5.7E+05
136.7	-2.5E+07	3.1E+07	-2.4E+07	-2.2E+07	9.6E+07	1.2E+07	-2.1E+07	9.7E+07	-5.6E+05	-3.3E+05	-2.4E+05	-5.5E+05	-9.1E+05	-3.1E+05	-9.7E+05	-3.8E+05

Table 91 Raw data for the test seal at PD=27.6 bar, ω=4 krpm, and inlet GVF=2% with the medium-preswirl insert D

Freq.	Re(H_{XX})	Re(H_{XY})	Re(H_{YX})	Re(H_{YY})	Im(H_{XX})	Im(H_{XY})	Im(H_{YX})	Im(H_{YY})	Re(eH_{XX})	Re(eH_{XY})	Re(eH_{YX})	Re(eH_{YY})	Im(eH_{XX})	Im(eH_{XY})	Im(eH_{YX})	Im(eH_{YY})
Hz	N/m	N/m	N/m	N/m	N/m	N/m	N/m	N/m	N/m	N/m	N/m	N/m	N/m	N/m	N/m	N/m
9.8	1.1E+07	2.6E+07	-2.6E+07	4.3E+06	3.5E+06	-1.2E+06	1.4E+06	7.8E+06	-6.1E+05	-7.5E+05	-7.1E+05	-6.9E+05	-4.4E+05	-3.2E+05	-2.6E+05	-4.9E+05
19.5	9.7E+06	2.4E+07	-2.9E+07	6.9E+06	9.6E+06	3.4E+05	-9.2E+04	2.1E+07	-3.7E+05	-6.9E+05	-8.5E+05	-7.7E+05	-5.0E+05	-1.4E+05	-3.8E+05	-7.2E+05
29.3	8.5E+06	2.2E+07	-2.9E+07	8.6E+06	1.4E+07	4.0E+06	2.1E+06	2.5E+07	-4.6E+05	-5.2E+05	-6.8E+05	-8.2E+05	-3.5E+05	-3.6E+05	-4.1E+05	-4.7E+05
39.1	3.6E+06	2.4E+07	-2.6E+07	7.2E+06	2.3E+07	7.1E+06	-6.1E+05	3.4E+07	-6.6E+05	-6.1E+05	-4.7E+05	-9.9E+05	-3.3E+05	-4.3E+05	-4.8E+05	-3.1E+05
48.8	2.8E+06	2.7E+07	-2.6E+07	7.1E+06	3.2E+07	7.5E+06	-2.3E+06	4.1E+07	-6.8E+05	-5.7E+05	-5.3E+05	-1.0E+06	-3.6E+05	-4.6E+05	-4.7E+05	-3.7E+05
58.6	-1.7E+06	3.0E+07	-2.5E+07	6.1E+06	4.1E+07	8.9E+06	-2.6E+06	4.7E+07	-6.0E+05	-6.9E+05	-5.7E+05	-1.3E+06	-5.3E+05	-6.8E+05	-6.9E+05	-4.7E+05
68.4	-2.9E+06	2.8E+07	-2.6E+07	6.4E+06	4.8E+07	1.1E+07	-4.3E+06	5.4E+07	-7.4E+05	-3.9E+05	-2.4E+05	-8.3E+05	-3.8E+05	-5.2E+05	-5.8E+05	-3.8E+05
78.1	-1.2E+06	3.1E+07	-2.3E+07	3.8E+06	5.7E+07	8.0E+06	-6.5E+06	6.0E+07	-4.4E+05	-3.2E+05	-2.8E+05	-8.1E+05	-6.0E+05	-6.1E+05	-6.4E+05	-5.8E+05
87.9	-3.8E+06	3.1E+07	-2.6E+07	5.6E+05	6.4E+07	8.7E+06	-7.7E+06	6.7E+07	-4.2E+05	-2.8E+05	-3.3E+05	-9.4E+05	-5.2E+05	-6.3E+05	-5.7E+05	-5.9E+05
97.7	-6.7E+06	3.0E+07	-2.5E+07	-2.4E+06	7.0E+07	8.7E+06	-9.0E+06	7.4E+07	-3.0E+05	-3.2E+05	-2.7E+05	-8.8E+05	-5.0E+05	-6.1E+05	-6.1E+05	-8.7E+05
107.4	-1.2E+07	3.3E+07	-2.5E+07	-6.2E+06	7.7E+07	1.1E+07	-9.0E+06	8.0E+07	-2.4E+05	-5.6E+05	-4.8E+05	-1.1E+06	-5.2E+05	-5.4E+05	-6.5E+05	-8.6E+05
117.2	-1.7E+07	3.1E+07	-2.4E+07	-1.0E+07	8.3E+07	1.1E+07	-1.2E+07	8.6E+07	-4.7E+05	-3.0E+05	-3.1E+05	-7.1E+05	-4.2E+05	-5.2E+05	-4.4E+05	-9.3E+05
127.0	-2.0E+07	3.7E+07	-1.9E+07	-2.0E+07	9.3E+07	1.0E+07	-1.4E+07	9.1E+07	-3.9E+05	-4.0E+05	-2.7E+05	-7.6E+05	-7.0E+05	-5.2E+05	-6.5E+05	-8.9E+05
136.7	-2.6E+07	3.3E+07	-2.4E+07	-2.1E+07	1.0E+08	9.9E+06	-1.8E+07	1.0E+08	-4.0E+05	-3.0E+05	-3.2E+05	-4.7E+05	-4.7E+05	-2.6E+05	-6.5E+05	-9.0E+05

Table 92 Raw data for the test seal at PD=27.6 bar, ω=5 krpm, and inlet GVF=2% with the medium-preswirl insert

Freq.	Re(H_{XX})	Re(H_{XY})	Re(H_{YX})	Re(H_{YY})	Im(H_{XX})	Im(H_{XY})	Im(H_{YX})	Im(H_{YY})	Re(eH_{XX})	Re(eH_{XY})	Re(eH_{YX})	Re(eH_{YY})	Im(eH_{XX})	Im(eH_{XY})	Im(eH_{YX})	Im(eH_{YY})
Hz	N/m	N/m	N/m	N/m	N/m	N/m	N/m	N/m	N/m	N/m	N/m	N/m	N/m	N/m	N/m	N/m
9.8	1.2E+06	3.8E+07	-2.8E+07	4.1E+06	4.2E+06	-1.6E+06	6.1E+06	6.6E+06	-2.8E+05	-4.1E+05	-6.1E+05	-7.8E+05	-3.1E+05	-4.2E+05	-6.2E+05	-7.2E+05
19.5	3.4E+06	3.5E+07	-2.9E+07	1.6E+05	1.1E+07	-1.2E+06	1.5E+06	1.3E+07	-3.1E+05	-7.4E+05	-7.0E+05	-8.1E+05	-4.8E+05	-1.7E+05	-6.8E+05	-9.5E+05
29.3	3.9E+06	3.5E+07	-3.3E+07	-4.0E+05	1.6E+07	1.8E+06	2.2E+06	2.1E+07	-4.8E+05	-6.1E+05	-1.1E+06	-5.0E+05	-3.5E+05	-3.2E+05	-3.0E+05	-1.2E+06
39.1	-6.9E+05	3.9E+07	-2.9E+07	-6.9E+06	2.7E+07	2.4E+06	-3.4E+06	3.2E+07	-7.0E+05	-5.9E+05	-1.1E+06	-5.1E+05	-4.2E+05	-6.4E+05	-2.2E+05	-1.1E+06
48.8	-1.3E+06	3.8E+07	-2.9E+07	-5.6E+06	3.5E+07	1.2E+06	-2.8E+06	4.2E+07	-6.6E+05	-3.2E+05	-1.1E+06	-7.3E+05	-3.3E+05	-7.4E+05	-7.5E+05	-1.0E+06
58.6	-3.6E+06	4.1E+07	-3.0E+07	-7.6E+06	4.4E+07	2.4E+06	-4.8E+06	5.1E+07	-6.5E+05	-1.7E+05	-8.9E+05	-7.7E+05	-3.7E+05	-6.0E+05	-9.5E+05	-8.9E+05
68.4	-5.1E+06	3.5E+07	-3.0E+07	-5.1E+06	4.8E+07	4.7E+06	-4.8E+06	5.8E+07	-6.1E+05	-3.8E+05	-3.7E+05	-9.0E+05	-4.6E+05	-9.6E+05	-9.3E+05	-5.5E+05
78.1	-5.9E+06	3.9E+07	-2.9E+07	-9.8E+06	6.0E+07	3.7E+06	-8.8E+06	6.7E+07	-6.9E+05	-3.2E+05	-6.6E+05	-7.6E+05	-4.2E+05	-4.7E+05	-9.7E+05	-5.8E+05
87.9	-7.6E+06	3.7E+07	-3.2E+07	-1.1E+07	6.6E+07	2.3E+06	-8.4E+06	7.8E+07	-6.9E+05	-3.0E+05	-2.9E+05	-7.4E+05	-3.9E+05	-5.1E+05	-8.7E+05	-3.4E+05
97.7	-1.1E+07	3.5E+07	-3.0E+07	-1.1E+07	7.2E+07	2.4E+06	-7.9E+06	8.5E+07	-4.0E+05	-3.0E+05	-1.9E+05	-5.8E+05	-5.5E+05	-5.1E+05	-8.3E+05	-3.9E+05
107.4	-1.5E+07	3.8E+07	-2.6E+07	-1.7E+07	8.0E+07	7.1E+06	-1.1E+07	8.8E+07	-4.0E+05	-3.1E+05	-4.0E+05	-6.9E+05	-4.1E+05	-2.9E+05	-8.4E+05	-5.1E+05
117.2	-2.1E+07	3.6E+07	-2.8E+07	-1.9E+07	8.6E+07	8.0E+06	-1.3E+07	9.8E+07	-1.8E+05	-2.5E+05	-1.9E+05	-4.9E+05	-3.6E+05	-2.2E+05	-5.5E+05	-4.8E+05
127.0	-2.6E+07	4.3E+07	-2.3E+07	-3.0E+07	9.8E+07	1.1E+07	-1.6E+07	1.0E+08	-3.4E+05	-4.5E+05	-3.9E+05	-4.9E+05	-1.1E+06	-3.4E+05	-7.3E+05	-4.0E+05
136.7	-3.0E+07	3.9E+07	-2.8E+07	-2.8E+07	1.1E+08	9.1E+06	-1.9E+07	1.1E+08	-4.9E+05	-4.3E+05	-2.9E+05	-3.2E+05	-7.3E+05	-4.5E+05	-5.9E+05	-7.0E+05

Table 93 Raw data for the test seal at PD=27.6 bar, ω=3 krpm, and inlet GVF=4% with the medium-preswirl insert

Freq.	Re($\boldsymbol{H_{XX}}$)	Re($\boldsymbol{H_{XY}}$)	Re($\boldsymbol{H_{YX}}$)	Re($\boldsymbol{H_{YY}}$)	Im($\boldsymbol{H_{XX}}$)	Im($\boldsymbol{H_{XY}}$)	Im($\boldsymbol{H_{YX}}$)	Im($\boldsymbol{H_{YY}}$)	Re($\boldsymbol{eH_{XX}}$)	Re($\boldsymbol{eH_{XY}}$)	Re($\boldsymbol{eH_{YX}}$)	Re($\boldsymbol{eH_{YY}}$)	Im($\boldsymbol{eH_{XX}}$)	Im($\boldsymbol{eH_{XY}}$)	Im($\boldsymbol{eH_{YX}}$)	Im($\boldsymbol{eH_{YY}}$)
Hz	N/m	N/m	N/m	N/m	N/m	N/m	N/m	N/m	N/m	N/m	N/m	N/m	N/m	N/m	N/m	N/m
9.8	1.2E+07	2.8E+07	-2.2E+07	8.9E+06	3.3E+06	-2.2E+06	-4.8E+05	3.8E+06	-7.8E+05	-1.1E+06	-1.1E+06	-1.2E+06	-4.8E+05	-4.9E+05	-4.9E+05	-1.1E+06
19.5	1.3E+07	2.7E+07	-2.2E+07	8.5E+06	1.1E+07	-2.5E+06	-2.7E+06	1.5E+07	-7.1E+05	-1.0E+06	-1.2E+06	-9.9E+05	-5.8E+05	-4.5E+05	-5.5E+05	-1.2E+06
29.3	1.3E+07	2.4E+07	-2.3E+07	1.0E+07	1.6E+07	2.9E+05	-2.1E+06	2.1E+07	-8.4E+05	-7.5E+05	-1.2E+06	-1.3E+06	-4.9E+05	-5.7E+05	-7.3E+05	-8.3E+05
39.1	1.2E+07	2.6E+07	-2.1E+07	9.7E+06	2.4E+07	3.5E+06	-4.2E+06	3.0E+07	-9.8E+05	-6.9E+05	-1.2E+06	-1.4E+06	-3.4E+05	-6.1E+05	-7.1E+05	-7.1E+05
48.8	7.7E+06	2.7E+07	-2.1E+07	7.9E+06	2.9E+07	4.5E+06	-7.0E+06	3.7E+07	-8.1E+05	-5.8E+05	-8.2E+05	-1.5E+06	-4.0E+05	-5.4E+05	-8.4E+05	-5.2E+05
58.6	4.5E+06	3.0E+07	-2.1E+07	5.3E+06	3.9E+07	4.8E+06	-8.4E+06	4.3E+07	-1.0E+06	-7.9E+05	-8.5E+05	-1.5E+06	-5.0E+05	-7.6E+05	-8.8E+05	-6.1E+05
68.4	2.7E+06	2.7E+07	-2.4E+07	5.0E+06	4.5E+07	8.3E+06	-9.0E+06	5.2E+07	-8.8E+05	-4.0E+05	-6.5E+05	-1.3E+06	-4.5E+05	-6.1E+05	-9.5E+05	-8.0E+05
78.1	3.8E+06	3.0E+07	-2.2E+07	2.7E+06	5.5E+07	5.5E+06	-1.1E+07	5.8E+07	-8.9E+05	-5.3E+05	-4.2E+05	-1.5E+06	-4.9E+05	-6.0E+05	-1.0E+06	-8.2E+05
87.9	2.3E+06	2.9E+07	-2.4E+07	5.1E+05	6.0E+07	5.9E+06	-1.2E+07	6.5E+07	-6.6E+05	-4.2E+05	-3.7E+05	-1.2E+06	-6.9E+05	-5.4E+05	-1.1E+06	-8.9E+05
97.7	-2.0E+06	2.7E+07	-2.5E+07	-3.1E+06	6.5E+07	6.4E+06	-1.4E+07	7.3E+07	-6.2E+05	-2.6E+05	-1.8E+05	-1.1E+06	-6.2E+05	-6.1E+05	-9.7E+05	-1.0E+06
107.4	-7.3E+06	3.0E+07	-2.6E+07	-6.7E+06	7.3E+07	8.3E+06	-1.3E+07	8.0E+07	-7.6E+05	-4.6E+05	-2.0E+05	-1.2E+06	-6.9E+05	-5.9E+05	-1.1E+06	-1.0E+06
117.2	-1.3E+07	3.1E+07	-2.4E+07	-1.2E+07	8.0E+07	9.4E+06	-1.4E+07	8.6E+07	-4.5E+05	-3.0E+05	-5.8E+05	-9.3E+05	-7.1E+05	-5.2E+05	-1.1E+06	-1.6E+06
127.0	-1.8E+07	3.4E+07	-2.0E+07	-2.1E+07	8.9E+07	9.6E+06	-1.9E+07	9.3E+07	-3.7E+05	-3.9E+05	-3.7E+05	-1.5E+06	-8.4E+05	-4.1E+05	-1.4E+06	-1.1E+06
136.7	-2.1E+07	3.1E+07	-2.5E+07	-2.1E+07	1.0E+08	9.0E+06	-2.3E+07	1.1E+08	-4.4E+05	-3.6E+05	-4.5E+05	-8.4E+05	-6.8E+05	-5.5E+05	-1.5E+06	-1.5E+06

Table 94 Raw data for the test seal at PD=27.6 bar, ω=4 krpm, and inlet GVF=4% with the medium-preswirl insert

Freq.	Re($\boldsymbol{H_{XX}}$)	Re($\boldsymbol{H_{XY}}$)	Re($\boldsymbol{H_{YX}}$)	Re($\boldsymbol{H_{YY}}$)	Im($\boldsymbol{H_{XX}}$)	Im($\boldsymbol{H_{XY}}$)	Im($\boldsymbol{H_{YX}}$)	Im($\boldsymbol{H_{YY}}$)	Re($\boldsymbol{eH_{XX}}$)	Re($\boldsymbol{eH_{XY}}$)	Re($\boldsymbol{eH_{YX}}$)	Re($\boldsymbol{eH_{YY}}$)	Im($\boldsymbol{eH_{XX}}$)	Im($\boldsymbol{eH_{XY}}$)	Im($\boldsymbol{eH_{YX}}$)	Im($\boldsymbol{eH_{YY}}$)
Hz	N/m	N/m	N/m	N/m	N/m	N/m	N/m	N/m	N/m	N/m	N/m	N/m	N/m	N/m	N/m	N/m
9.8	8.5E+06	3.1E+07	-2.2E+07	6.1E+06	5.3E+06	-3.4E+06	-3.2E+05	2.9E+06	-8.5E+05	-1.2E+06	-1.2E+06	-1.3E+06	-6.2E+05	-7.0E+05	-6.1E+05	-1.3E+06
19.5	9.9E+06	2.8E+07	-2.1E+07	4.7E+06	1.2E+07	-2.6E+06	-3.2E+06	1.4E+07	-7.7E+05	-9.3E+05	-1.3E+06	-1.1E+06	-5.2E+05	-7.2E+05	-3.7E+05	-1.3E+06
29.3	1.1E+07	2.5E+07	-2.3E+07	5.8E+06	1.7E+07	-1.4E+05	-2.0E+06	2.1E+07	-9.9E+05	-7.0E+05	-1.3E+06	-1.3E+06	-4.1E+05	-6.7E+05	-7.9E+05	-9.9E+05
39.1	9.6E+06	2.6E+07	-2.0E+07	5.2E+06	2.5E+07	2.7E+06	-4.8E+06	3.0E+07	-9.5E+05	-5.0E+05	-1.3E+06	-1.5E+06	-4.1E+05	-8.2E+05	-7.5E+05	-8.0E+05
48.8	5.7E+06	2.6E+07	-2.1E+07	3.8E+06	2.9E+07	3.9E+06	-7.4E+06	3.6E+07	-6.2E+05	-3.4E+05	-1.1E+06	-1.6E+06	-4.8E+05	-6.1E+05	-7.6E+05	-5.5E+05
58.6	2.8E+06	3.1E+07	-2.2E+07	8.4E+05	4.0E+07	4.5E+06	-8.3E+06	4.4E+07	-9.6E+05	-6.6E+05	-9.7E+05	-1.9E+06	-4.7E+05	-6.8E+05	-1.1E+06	-6.3E+05
68.4	-3.9E+05	2.8E+07	-2.3E+07	1.6E+06	4.7E+07	9.1E+06	-9.1E+06	5.3E+07	-1.1E+06	-3.7E+05	-4.4E+05	-1.5E+06	-3.4E+05	-8.4E+05	-1.1E+06	-8.0E+05
78.1	8.3E+05	3.0E+07	-2.4E+07	-1.2E+06	5.7E+07	5.6E+06	-1.2E+07	5.9E+07	-8.8E+05	-4.4E+05	-6.8E+05	-1.6E+06	-5.3E+05	-5.8E+05	-9.3E+05	-6.8E+05
87.9	1.4E+06	3.0E+07	-2.4E+07	-3.2E+06	6.2E+07	4.3E+06	-1.3E+07	6.9E+07	-8.7E+05	-1.1E+05	-4.2E+05	-1.4E+06	-5.3E+05	-6.5E+05	-1.3E+06	-7.8E+05
97.7	-2.9E+06	2.7E+07	-2.6E+07	-7.1E+06	6.7E+07	5.8E+06	-1.4E+07	7.6E+07	-8.1E+05	-1.8E+05	-3.7E+05	-1.6E+06	-6.8E+05	-7.8E+05	-1.2E+06	-1.2E+06
107.4	-8.9E+06	3.0E+07	-2.7E+07	-9.5E+06	7.4E+07	8.4E+06	-1.3E+07	8.4E+07	-5.0E+05	-1.9E+05	-3.0E+05	-1.4E+06	-4.0E+05	-3.2E+05	-1.4E+06	-1.2E+06
117.2	-1.4E+07	3.1E+07	-2.5E+07	-1.3E+07	8.2E+07	8.4E+06	-1.4E+07	9.1E+07	-5.9E+05	-1.7E+05	-2.6E+05	-1.0E+06	-3.7E+05	-3.9E+05	-1.1E+06	-1.2E+06
127.0	-2.0E+07	3.5E+07	-2.1E+07	-2.3E+07	9.1E+07	9.8E+06	-1.8E+07	9.7E+07	-3.9E+05	-3.9E+05	-2.8E+05	-1.7E+06	-7.2E+05	-3.4E+05	-1.7E+06	-1.3E+06
136.7	-2.2E+07	3.2E+07	-2.7E+07	-2.2E+07	1.0E+08	7.6E+06	-2.2E+07	1.1E+08	-7.2E+05	-3.7E+05	-6.4E+05	-5.5E+05	-1.2E+06	-6.4E+05	-9.5E+05	-1.8E+06

Table 95 Raw data for the test seal at PD=20.7 bar, ω=3 krpm, and inlet GVF=0% with the high-preswirl insert

Freq.	Re(H_{XX})	Re(H_{XY})	Re(H_{YX})	Re(H_{YY})	Im(H_{XX})	Im(H_{XY})	Im(H_{YX})	Im(H_{YY})	Re(eH_{XX})	Re(eH_{XY})	Re(eH_{YX})	Re(eH_{YY})	Im(eH_{XX})	Im(eH_{XY})	Im(eH_{YX})	Im(eH_{YY})
Hz	N/m	N/m	N/m	N/m	N/m	N/m	N/m	N/m	N/m	N/m	N/m	N/m	N/m	N/m	N/m	N/m
9.8	1.6E+07	2.1E+07	-2.2E+07	1.7E+07	4.6E+06	1.8E+06	-1.6E+06	3.3E+06	-1.3E+05	-9.6E+04	-1.0E+05	-1.6E+05	-1.1E+05	-9.3E+04	-1.1E+05	-6.7E+04
19.5	1.5E+07	2.2E+07	-2.2E+07	1.6E+07	9.8E+06	3.8E+06	-3.2E+06	9.4E+06	-7.4E+04	-1.0E+05	-1.0E+05	-8.2E+04	-7.2E+04	-7.4E+04	-7.0E+04	-1.0E+05
29.3	1.7E+07	1.8E+07	-2.6E+07	1.8E+07	1.5E+07	5.7E+06	-4.7E+06	1.4E+07	-8.4E+04	-1.1E+05	-6.2E+04	-5.1E+04	-1.1E+05	-6.6E+04	-7.5E+04	-6.7E+04
39.1	1.2E+07	2.2E+07	-2.2E+07	1.3E+07	2.0E+07	6.9E+06	-6.5E+06	2.0E+07	-5.2E+04	-4.0E+04	-6.7E+04	-6.9E+04	-8.6E+04	-6.3E+04	-4.1E+04	-2.7E+04
48.8	9.5E+06	2.2E+07	-2.2E+07	1.0E+07	2.5E+07	8.4E+06	-8.3E+06	2.5E+07	-5.3E+04	-4.0E+04	-4.0E+04	-3.8E+04	-7.0E+04	-6.8E+04	-4.6E+04	-3.2E+04
58.6	6.6E+06	2.2E+07	-2.3E+07	6.7E+06	3.0E+07	1.0E+07	-1.0E+07	3.1E+07	-3.9E+04	-4.8E+04	-4.7E+04	-4.5E+04	-5.2E+04	-7.0E+04	-7.5E+04	-7.7E+04
68.4	2.9E+06	2.3E+07	-2.3E+07	3.7E+06	3.5E+07	1.2E+07	-1.2E+07	3.6E+07	-7.0E+04	-1.0E+05	-4.8E+04	-8.1E+04	-7.1E+04	-7.2E+04	-3.8E+04	-1.7E+04
78.1	-1.3E+06	2.3E+07	-2.3E+07	-9.8E+05	4.0E+07	1.3E+07	-1.4E+07	4.1E+07	-3.8E+04	-3.5E+04	-3.3E+04	-3.7E+04	-2.2E+04	-3.2E+04	-3.3E+04	-2.5E+04
87.9	-6.5E+06	2.3E+07	-2.4E+07	-5.9E+06	4.5E+07	1.5E+07	-1.6E+07	4.6E+07	-2.2E+04	-1.8E+04	-2.4E+04	-1.9E+04	-3.6E+04	-3.5E+04	-1.3E+04	-1.2E+04
97.7	-1.3E+07	2.4E+07	-2.4E+07	-1.2E+07	5.1E+07	1.7E+07	-1.8E+07	5.2E+07	-5.6E+04	-3.5E+04	-3.4E+04	-2.7E+04	-3.4E+04	-4.4E+04	-3.2E+04	-3.3E+04
107.4	-1.9E+07	2.5E+07	-2.5E+07	-1.8E+07	5.6E+07	1.9E+07	-1.9E+07	5.8E+07	-3.1E+04	-2.7E+04	-1.7E+04	-4.4E+04	-2.7E+04	-5.7E+04	-5.0E+04	-5.0E+04
117.2	-2.6E+07	2.6E+07	-2.5E+07	-2.5E+07	6.2E+07	2.1E+07	-2.1E+07	6.4E+07	-2.9E+04	-3.6E+04	-4.8E+04	-5.1E+04	-2.5E+04	-2.2E+04	-4.6E+04	-2.8E+04
127.0	-3.4E+07	2.8E+07	-2.5E+07	-3.3E+07	6.9E+07	2.2E+07	-2.3E+07	7.1E+07	-4.7E+04	-5.9E+04	-2.7E+04	-5.7E+04	-3.8E+04	-3.5E+04	-4.6E+04	-2.8E+04
136.7	-4.1E+07	2.9E+07	-2.7E+07	-4.2E+07	7.5E+07	2.3E+07	-2.5E+07	7.8E+07	-6.0E+04	-3.6E+04	-8.9E+04	-4.5E+04	-9.2E+04	-8.8E+04	-7.7E+04	-1.0E+05

Table 96 Raw data for the test seal at PD=20.7 bar, ω=4 krpm, and inlet GVF=0% with the high-preswirl insert

Freq.	Re(H_{XX})	Re(H_{XY})	Re(H_{YX})	Re(H_{YY})	Im(H_{XX})	Im(H_{XY})	Im(H_{YX})	Im(H_{YY})	Re(eH_{XX})	Re(eH_{XY})	Re(eH_{YX})	Re(eH_{YY})	Im(eH_{XX})	Im(eH_{XY})	Im(eH_{YX})	Im(eH_{YY})
Hz	N/m	N/m	N/m	N/m	N/m	N/m	N/m	N/m	N/m	N/m	N/m	N/m	N/m	N/m	N/m	N/m
9.8	1.6E+07	2.1E+07	-2.2E+07	1.7E+07	4.5E+06	2.0E+06	-1.7E+06	3.0E+06	-9.2E+04	-1.0E+05	-7.5E+04	-8.5E+04	-1.4E+05	-1.4E+05	-1.4E+05	-1.0E+05
19.5	1.5E+07	2.1E+07	-2.2E+07	1.6E+07	9.7E+06	3.6E+06	-3.3E+06	9.4E+06	-8.3E+04	-8.3E+04	-5.1E+04	-8.9E+04	-9.9E+04	-8.5E+04	-1.0E+05	-6.1E+04
29.3	1.7E+07	1.8E+07	-2.5E+07	1.8E+07	1.5E+07	5.6E+06	-4.5E+06	1.4E+07	-8.9E+04	-1.1E+05	-8.8E+04	-9.3E+04	-5.6E+04	-4.8E+04	-5.2E+04	-5.2E+04
39.1	1.2E+07	2.2E+07	-2.2E+07	1.3E+07	2.0E+07	6.8E+06	-6.6E+06	2.0E+07	-6.8E+04	-7.5E+04	-4.5E+04	-6.0E+04	-6.1E+04	-7.6E+04	-4.1E+04	-4.8E+04
48.8	9.5E+06	2.2E+07	-2.2E+07	1.0E+07	2.5E+07	8.4E+06	-8.3E+06	2.5E+07	-8.9E+04	-6.7E+04	-4.9E+04	-5.4E+04	-4.3E+04	-8.1E+04	-8.2E+04	-7.5E+04
58.6	6.6E+06	2.2E+07	-2.2E+07	6.8E+06	3.0E+07	1.0E+07	-1.0E+07	3.1E+07	-5.1E+04	-5.2E+04	-6.1E+04	-7.9E+04	-4.9E+04	-4.3E+04	-7.6E+04	-3.8E+04
68.4	3.0E+06	2.3E+07	-2.3E+07	3.8E+06	3.5E+07	1.2E+07	-1.2E+07	3.6E+07	-4.4E+04	-3.1E+04	-3.6E+04	-4.0E+04	-2.9E+04	-3.0E+04	-2.9E+04	-4.7E+04
78.1	-1.2E+06	2.3E+07	-2.3E+07	-8.7E+05	4.0E+07	1.3E+07	-1.4E+07	4.1E+07	-3.2E+04	-3.4E+04	-3.1E+04	-2.5E+04	-3.6E+04	-3.4E+04	-4.0E+04	-4.0E+04
87.9	-6.5E+06	2.3E+07	-2.4E+07	-5.8E+06	4.5E+07	1.5E+07	-1.6E+07	4.6E+07	-3.1E+04	-2.5E+04	-3.4E+04	-3.3E+04	-2.1E+04	-1.9E+04	-3.1E+04	-2.9E+04
97.7	-1.3E+07	2.4E+07	-2.4E+07	-1.2E+07	5.1E+07	1.7E+07	-1.8E+07	5.2E+07	-2.7E+04	-2.3E+04	-2.8E+04	-3.4E+04	-2.9E+04	-2.9E+04	-3.3E+04	-1.8E+04
107.4	-1.8E+07	2.5E+07	-2.5E+07	-1.8E+07	5.6E+07	1.9E+07	-1.9E+07	5.8E+07	-4.1E+04	-3.8E+04	-5.8E+04	-4.9E+04	-4.5E+04	-2.6E+04	-4.0E+04	-3.5E+04
117.2	-2.6E+07	2.6E+07	-2.6E+07	-2.5E+07	6.2E+07	2.1E+07	-2.1E+07	6.4E+07	-3.8E+04	-2.7E+04	-3.3E+04	-3.0E+04	-2.8E+04	-3.5E+04	-2.2E+04	-2.7E+04
127.0	-3.4E+07	2.8E+07	-2.5E+07	-3.3E+07	6.9E+07	2.2E+07	-2.4E+07	7.1E+07	-5.1E+04	-2.7E+04	-4.6E+04	-6.7E+04	-4.1E+04	-7.0E+04	-3.0E+04	-2.8E+04
136.7	-4.1E+07	2.9E+07	-2.7E+07	-4.2E+07	7.5E+07	2.3E+07	-2.5E+07	7.8E+07	-3.9E+04	-5.2E+04	-6.3E+04	-6.5E+04	-7.0E+04	-3.4E+04	-4.5E+04	-5.9E+04

Table 97 Raw data for the test seal at PD=20.7 bar, ω=5 krpm, and inlet GVF=0% with the high-preswirl insert

Freq.	Re($\boldsymbol{H_{XX}}$)	Re($\boldsymbol{H_{XY}}$)	Re($\boldsymbol{H_{YX}}$)	Re($\boldsymbol{H_{YY}}$)	Im($\boldsymbol{H_{XX}}$)	Im($\boldsymbol{H_{XY}}$)	Im($\boldsymbol{H_{YX}}$)	Im($\boldsymbol{H_{YY}}$)	Re($\boldsymbol{eH_{XX}}$)	Re($\boldsymbol{eH_{XY}}$)	Re($\boldsymbol{eH_{YX}}$)	Re($\boldsymbol{eH_{YY}}$)	Im($\boldsymbol{eH_{XX}}$)	Im($\boldsymbol{eH_{XY}}$)	Im($\boldsymbol{eH_{YX}}$)	Im($\boldsymbol{eH_{YY}}$)
Hz	N/m	N/m	N/m	N/m	N/m	N/m	N/m	N/m	N/m	N/m	N/m	N/m	N/m	N/m	N/m	N/m
9.8	1.5E+07	2.4E+07	-2.4E+07	1.7E+07	5.2E+06	2.5E+06	-1.5E+06	2.9E+06	-1.5E+05	-1.5E+05	-1.2E+05	-1.4E+05	-1.2E+05	-1.3E+05	-1.3E+05	-1.2E+05
19.5	1.4E+07	2.4E+07	-2.4E+07	1.5E+07	1.0E+07	4.4E+06	-3.7E+06	9.4E+06	-8.3E+04	-1.3E+05	-1.1E+05	-1.1E+05	-6.5E+04	-8.3E+04	-1.0E+05	-1.0E+05
29.3	1.6E+07	2.1E+07	-2.8E+07	1.7E+07	1.5E+07	6.7E+06	-5.1E+06	1.4E+07	-1.4E+05	-1.1E+05	-1.3E+05	-1.2E+05	-1.4E+05	-1.1E+05	-1.3E+05	-8.7E+04
39.1	1.1E+07	2.4E+07	-2.4E+07	1.2E+07	2.0E+07	7.9E+06	-7.9E+06	2.0E+07	-6.8E+04	-6.7E+04	-8.2E+04	-8.1E+04	-9.4E+04	-1.0E+05	-5.0E+04	-4.1E+04
48.8	8.7E+06	2.4E+07	-2.4E+07	9.1E+06	2.5E+07	9.4E+06	-9.8E+06	2.5E+07	-4.3E+04	-4.6E+04	-9.8E+04	-7.7E+04	-6.8E+04	-5.0E+04	-5.3E+04	-5.7E+04
58.6	5.6E+06	2.4E+07	-2.5E+07	5.6E+06	3.0E+07	1.2E+07	-1.2E+07	3.1E+07	-3.6E+04	-6.0E+04	-5.2E+04	-3.7E+04	-5.7E+04	-3.8E+04	-6.2E+04	-4.7E+04
68.4	1.9E+06	2.5E+07	-2.5E+07	2.5E+06	3.6E+07	1.4E+07	-1.5E+07	3.7E+07	-6.0E+04	-7.0E+04	-3.8E+04	-5.6E+04	-3.6E+04	-2.4E+04	-5.8E+04	-6.7E+04
78.1	-2.0E+06	2.5E+07	-2.6E+07	-1.6E+06	4.0E+07	1.6E+07	-1.6E+07	4.2E+07	-6.5E+04	-8.9E+04	-4.6E+04	-5.5E+04	-4.3E+04	-3.3E+04	-6.3E+04	-5.4E+04
87.9	-6.9E+06	2.6E+07	-2.7E+07	-6.4E+06	4.5E+07	1.8E+07	-1.9E+07	4.7E+07	-2.3E+04	-3.1E+04	-5.4E+04	-2.4E+04	-2.4E+04	-2.3E+04	-4.1E+04	-5.5E+04
97.7	-1.3E+07	2.7E+07	-2.7E+07	-1.3E+07	5.1E+07	2.1E+07	-2.1E+07	5.3E+07	-4.1E+04	-4.6E+04	-5.2E+04	-7.1E+04	-4.0E+04	-2.4E+04	-6.1E+04	-3.8E+04
107.4	-1.9E+07	2.8E+07	-2.8E+07	-1.8E+07	5.7E+07	2.3E+07	-2.3E+07	5.9E+07	-4.2E+04	-4.8E+04	-3.3E+04	-5.9E+04	-3.3E+04	-4.1E+04	-8.7E+04	-4.0E+04
117.2	-2.7E+07	3.0E+07	-2.9E+07	-2.5E+07	6.3E+07	2.5E+07	-2.4E+07	6.5E+07	-5.5E+04	-4.9E+04	-3.3E+04	-1.7E+04	-2.1E+04	-4.4E+04	-2.3E+04	-4.5E+04
127.0	-3.5E+07	3.2E+07	-2.9E+07	-3.3E+07	7.0E+07	2.7E+07	-2.7E+07	7.2E+07	-7.0E+04	-7.0E+04	-7.2E+04	-8.4E+04	-7.8E+04	-5.8E+04	-5.7E+04	-9.3E+04
136.7	-4.2E+07	3.2E+07	-3.1E+07	-4.2E+07	7.6E+07	2.8E+07	-3.0E+07	7.9E+07	-5.4E+04	-5.8E+04	-6.6E+04	-5.0E+04	-6.6E+04	-4.7E+04	-5.9E+04	-9.5E+04

Table 98 Raw data for the test seal at PD=20.7 bar, ω=3 krpm, and inlet GVF=2% with the high-preswirl insert

Freq.	Re($\boldsymbol{H_{XX}}$)	Re($\boldsymbol{H_{XY}}$)	Re($\boldsymbol{H_{YX}}$)	Re($\boldsymbol{H_{YY}}$)	Im($\boldsymbol{H_{XX}}$)	Im($\boldsymbol{H_{XY}}$)	Im($\boldsymbol{H_{YX}}$)	Im($\boldsymbol{H_{YY}}$)	Re($\boldsymbol{eH_{XX}}$)	Re($\boldsymbol{eH_{XY}}$)	Re($\boldsymbol{eH_{YX}}$)	Re($\boldsymbol{eH_{YY}}$)	Im($\boldsymbol{eH_{XX}}$)	Im($\boldsymbol{eH_{XY}}$)	Im($\boldsymbol{eH_{YX}}$)	Im($\boldsymbol{eH_{YY}}$)
Hz	N/m	N/m	N/m	N/m	N/m	N/m	N/m	N/m	N/m	N/m	N/m	N/m	N/m	N/m	N/m	N/m
9.8	1.7E+07	2.2E+07	-2.2E+07	1.7E+07	4.7E+06	2.2E+06	-2.0E+06	2.9E+06	-1.6E+05	-1.2E+05	-9.8E+04	-9.2E+04	-1.1E+05	-7.0E+04	-1.1E+05	-9.3E+04
19.5	1.6E+07	2.3E+07	-2.2E+07	1.5E+07	9.6E+06	3.7E+06	-3.8E+06	9.5E+06	-1.5E+05	-9.7E+04	-1.1E+05	-9.5E+04	-1.0E+05	-1.3E+05	-1.2E+05	-1.1E+05
29.3	1.8E+07	2.0E+07	-2.6E+07	1.7E+07	1.4E+07	5.6E+06	-4.6E+06	1.3E+07	-6.0E+04	-6.8E+04	-1.1E+05	-1.3E+05	-1.2E+05	-9.8E+04	-7.4E+04	-8.0E+04
39.1	1.3E+07	2.3E+07	-2.2E+07	1.3E+07	1.9E+07	6.0E+06	-6.3E+06	2.0E+07	-1.2E+05	-1.2E+05	-6.2E+04	-6.3E+04	-9.3E+04	-9.0E+04	-9.1E+04	-8.8E+04
48.8	1.0E+07	2.3E+07	-2.3E+07	1.0E+07	2.4E+07	7.4E+06	-7.8E+06	2.5E+07	-1.0E+05	-6.7E+04	-6.3E+04	-4.3E+04	-5.7E+04	-6.8E+04	-8.4E+04	-1.1E+05
58.6	7.6E+06	2.3E+07	-2.3E+07	7.4E+06	2.9E+07	9.3E+06	-9.6E+06	3.1E+07	-8.3E+04	-7.5E+04	-5.7E+04	-6.8E+04	-1.0E+05	-5.7E+04	-7.5E+04	-4.6E+04
68.4	4.4E+06	2.3E+07	-2.4E+07	4.7E+06	3.4E+07	1.0E+07	-1.1E+07	3.7E+07	-1.1E+05	-1.1E+05	-8.9E+04	-1.2E+05	-1.3E+05	-8.7E+04	-1.2E+05	-1.3E+05
78.1	5.6E+05	2.4E+07	-2.3E+07	2.4E+05	3.9E+07	1.2E+07	-1.3E+07	4.2E+07	-4.9E+04	-3.2E+04	-4.1E+04	-6.7E+04	-1.2E+05	-7.7E+04	-1.1E+05	-4.6E+04
87.9	-4.1E+06	2.4E+07	-2.4E+07	-4.2E+06	4.4E+07	1.4E+07	-1.5E+07	4.7E+07	-2.6E+04	-5.0E+04	-5.0E+04	-4.6E+04	-1.2E+05	-6.0E+04	-3.3E+04	-4.5E+04
97.7	-9.7E+06	2.5E+07	-2.4E+07	-9.5E+06	5.0E+07	1.5E+07	-1.7E+07	5.3E+07	-2.8E+04	-5.6E+04	-9.7E+04	-6.5E+04	-1.3E+05	-6.2E+04	-4.1E+04	-4.8E+04
107.4	-1.5E+07	2.5E+07	-2.6E+07	-1.4E+07	5.6E+07	1.6E+07	-1.8E+07	6.0E+07	-4.5E+04	-8.2E+04	-6.9E+04	-9.1E+04	-1.5E+05	-5.4E+04	-5.5E+04	-4.5E+04
117.2	-2.1E+07	2.6E+07	-2.6E+07	-2.1E+07	6.1E+07	1.9E+07	-2.0E+07	6.6E+07	-2.6E+04	-8.4E+04	-8.5E+04	-5.3E+04	-2.2E+05	-5.9E+04	-5.0E+04	-6.5E+04
127.0	-2.8E+07	2.7E+07	-2.7E+07	-2.7E+07	6.7E+07	2.0E+07	-2.1E+07	7.3E+07	-3.1E+04	-9.3E+04	-3.9E+04	-7.8E+04	-1.8E+05	-4.7E+04	-6.3E+04	-3.0E+04
136.7	-3.6E+07	2.9E+07	-2.7E+07	-3.7E+07	7.4E+07	2.1E+07	-2.4E+07	8.1E+07	-7.2E+04	-8.0E+04	-1.3E+05	-7.2E+04	-1.9E+05	-9.0E+04	-8.9E+04	-9.2E+04

Table 99 Raw data for the test seal at PD=20.7 bar, ω=4 krpm, and inlet GVF=2% with the high-preswirl insert

Freq.	Re($\boldsymbol{H_{XX}}$)	Re($\boldsymbol{H_{XY}}$)	Re($\boldsymbol{H_{YX}}$)	Re($\boldsymbol{H_{YY}}$)	Im($\boldsymbol{H_{XX}}$)	Im($\boldsymbol{H_{XY}}$)	Im($\boldsymbol{H_{YX}}$)	Im($\boldsymbol{H_{YY}}$)	Re($\boldsymbol{eH_{XX}}$)	Re($\boldsymbol{eH_{XY}}$)	Re($\boldsymbol{eH_{YX}}$)	Re($\boldsymbol{eH_{YY}}$)	Im($\boldsymbol{eH_{XX}}$)	Im($\boldsymbol{eH_{XY}}$)	Im($\boldsymbol{eH_{YX}}$)	Im($\boldsymbol{eH_{YY}}$)
Hz	N/m	N/m	N/m	N/m	N/m	N/m	N/m	N/m	N/m	N/m	N/m	N/m	N/m	N/m	N/m	N/m
9.8	1.7E+07	2.2E+07	-2.2E+07	1.7E+07	4.8E+06	1.8E+06	-1.8E+06	3.4E+06	-8.7E+04	-8.6E+04	-1.7E+05	-1.5E+05	-1.1E+05	-1.1E+05	-1.5E+05	-1.5E+05
19.5	1.6E+07	2.3E+07	-2.1E+07	1.4E+07	9.9E+06	3.9E+06	-4.3E+06	9.1E+06	-2.0E+05	-1.7E+05	-1.5E+05	-2.1E+05	-6.8E+04	-9.3E+04	-1.1E+05	-1.1E+05
29.3	1.8E+07	2.0E+07	-2.5E+07	1.5E+07	1.4E+07	5.4E+06	-4.7E+06	1.3E+07	-2.1E+05	-2.0E+05	-2.2E+05	-3.0E+05	-9.5E+04	-1.1E+05	-8.9E+04	-9.6E+04
39.1	1.3E+07	2.3E+07	-2.2E+07	1.2E+07	1.9E+07	5.9E+06	-6.5E+06	2.0E+07	-5.9E+04	-2.9E+04	-7.6E+04	-1.3E+05	-5.4E+04	-5.3E+04	-9.1E+04	-1.2E+05
48.8	1.1E+07	2.3E+07	-2.2E+07	9.6E+06	2.4E+07	7.1E+06	-8.0E+06	2.6E+07	-7.6E+04	-1.1E+05	-1.3E+05	-1.8E+05	-9.0E+04	-6.4E+04	-9.8E+04	-1.0E+05
58.6	7.8E+06	2.3E+07	-2.2E+07	6.7E+06	2.9E+07	9.0E+06	-9.8E+06	3.1E+07	-1.0E+05	-1.1E+05	-1.0E+05	-1.7E+05	-7.5E+04	-6.5E+04	-9.7E+04	-5.0E+04
68.4	4.7E+06	2.3E+07	-2.3E+07	4.2E+06	3.4E+07	9.9E+06	-1.2E+07	3.8E+07	-1.2E+05	-1.3E+05	-1.1E+05	-2.4E+05	-1.5E+05	-1.7E+05	-1.7E+05	-2.0E+05
78.1	6.7E+05	2.4E+07	-2.3E+07	-2.3E+04	3.9E+07	1.2E+07	-1.3E+07	4.2E+07	-6.6E+04	-7.1E+04	-5.5E+04	-1.2E+05	-1.1E+05	-8.1E+04	-1.2E+05	-9.7E+04
87.9	-3.8E+06	2.4E+07	-2.3E+07	-4.3E+06	4.4E+07	1.4E+07	-1.5E+07	4.8E+07	-3.7E+04	-6.6E+04	-7.3E+04	-1.7E+05	-1.0E+05	-7.6E+04	-9.7E+04	-7.2E+04
97.7	-9.3E+06	2.5E+07	-2.4E+07	-9.3E+06	5.0E+07	1.5E+07	-1.7E+07	5.4E+07	-3.9E+04	-5.7E+04	-4.4E+04	-9.6E+04	-1.2E+05	-6.4E+04	-9.3E+04	-7.1E+04
107.4	-1.4E+07	2.5E+07	-2.6E+07	-1.3E+07	5.6E+07	1.7E+07	-1.8E+07	6.0E+07	-5.9E+04	-5.6E+04	-1.0E+05	-4.7E+04	-1.3E+05	-1.1E+05	-4.8E+04	-1.5E+05
117.2	-2.1E+07	2.6E+07	-2.6E+07	-2.1E+07	6.2E+07	1.9E+07	-1.9E+07	6.6E+07	-3.9E+04	-7.5E+04	-1.0E+05	-3.4E+04	-1.4E+05	-8.8E+04	-5.0E+04	-1.5E+05
127.0	-2.7E+07	2.7E+07	-2.7E+07	-2.6E+07	6.8E+07	2.0E+07	-2.1E+07	7.3E+07	-9.3E+04	-8.9E+04	-1.3E+05	-9.1E+04	-1.4E+05	-1.6E+05	-5.5E+04	-2.2E+05
136.7	-3.5E+07	2.9E+07	-2.7E+07	-3.5E+07	7.5E+07	2.1E+07	-2.4E+07	8.2E+07	-8.8E+04	-1.0E+05	-1.5E+05	-1.1E+05	-1.6E+05	-1.9E+05	-7.6E+04	-1.9E+05

Table 100 Raw data for the test seal at PD=20.7 bar, ω=5 krpm, and inlet GVF=2% with the high-preswirl insert

Freq.	Re($\boldsymbol{H_{XX}}$)	Re($\boldsymbol{H_{XY}}$)	Re($\boldsymbol{H_{YX}}$)	Re($\boldsymbol{H_{YY}}$)	Im($\boldsymbol{H_{XX}}$)	Im($\boldsymbol{H_{XY}}$)	Im($\boldsymbol{H_{YX}}$)	Im($\boldsymbol{H_{YY}}$)	Re($\boldsymbol{eH_{XX}}$)	Re($\boldsymbol{eH_{XY}}$)	Re($\boldsymbol{eH_{YX}}$)	Re($\boldsymbol{eH_{YY}}$)	Im($\boldsymbol{eH_{XX}}$)	Im($\boldsymbol{eH_{XY}}$)	Im($\boldsymbol{eH_{YX}}$)	Im($\boldsymbol{eH_{YY}}$)
Hz	N/m	N/m	N/m	N/m	N/m	N/m	N/m	N/m	N/m	N/m	N/m	N/m	N/m	N/m	N/m	N/m
9.8	1.8E+07	2.7E+07	-2.8E+07	1.5E+07	5.2E+06	1.2E+06	-2.9E+06	3.6E+06	-3.3E+05	-2.8E+05	-4.5E+05	-3.6E+05	-1.5E+05	-1.5E+05	-2.8E+05	-2.8E+05
19.5	1.4E+07	2.9E+07	-2.3E+07	9.4E+06	1.0E+07	3.7E+06	-5.3E+06	8.5E+06	-2.0E+05	-1.9E+05	-3.8E+05	-3.6E+05	-1.3E+05	-2.0E+05	-1.0E+05	-2.2E+05
29.3	1.6E+07	2.6E+07	-2.8E+07	1.1E+07	1.4E+07	4.7E+06	-6.6E+06	1.4E+07	-3.0E+05	-2.7E+05	-4.1E+05	-4.8E+05	-1.7E+05	-2.0E+05	-1.5E+05	-1.3E+05
39.1	1.2E+07	2.7E+07	-2.5E+07	8.7E+06	2.0E+07	4.9E+06	-7.9E+06	2.2E+07	-1.6E+05	-2.1E+05	-2.2E+05	-2.8E+05	-1.9E+05	-1.4E+05	-2.0E+05	-1.7E+05
48.8	9.4E+06	2.7E+07	-2.6E+07	6.0E+06	2.5E+07	6.8E+06	-9.2E+06	2.8E+07	-1.4E+05	-1.6E+05	-3.0E+05	-3.3E+05	-1.2E+05	-1.0E+05	-2.1E+05	-1.7E+05
58.6	6.4E+06	2.6E+07	-2.5E+07	3.9E+06	3.0E+07	9.1E+06	-1.1E+07	3.4E+07	-1.2E+05	-1.8E+05	-1.8E+05	-3.0E+05	-1.5E+05	-1.1E+05	-2.4E+05	-1.4E+05
68.4	3.7E+06	2.7E+07	-2.6E+07	1.3E+06	3.6E+07	9.7E+06	-1.4E+07	4.2E+07	-9.3E+04	-3.1E+05	-1.4E+05	-3.9E+05	-2.8E+05	-2.0E+05	-3.6E+05	-2.7E+05
78.1	-5.5E+05	2.7E+07	-2.5E+07	-1.9E+06	4.0E+07	1.3E+07	-1.4E+07	4.6E+07	-7.1E+04	-1.6E+05	-9.0E+04	-2.5E+05	-2.1E+05	-1.5E+05	-3.4E+05	-2.2E+05
87.9	-4.6E+06	2.7E+07	-2.6E+07	-5.9E+06	4.6E+07	1.5E+07	-1.7E+07	5.1E+07	-4.6E+04	-2.0E+05	-7.2E+04	-3.0E+05	-2.4E+05	-1.7E+05	-3.2E+05	-2.0E+05
97.7	-1.0E+07	2.9E+07	-2.7E+07	-1.1E+07	5.1E+07	1.7E+07	-1.9E+07	5.8E+07	-5.8E+04	-2.1E+05	-1.2E+05	-3.1E+05	-2.2E+05	-1.7E+05	-3.2E+05	-2.0E+05
107.4	-1.5E+07	2.9E+07	-2.9E+07	-1.4E+07	5.7E+07	1.8E+07	-2.1E+07	6.5E+07	-1.2E+05	-1.8E+05	-1.7E+05	-2.2E+05	-2.3E+05	-2.7E+05	-2.7E+05	-3.0E+05
117.2	-2.2E+07	3.0E+07	-2.8E+07	-2.1E+07	6.4E+07	2.2E+07	-2.2E+07	7.0E+07	-1.0E+05	-1.7E+05	-2.4E+05	-2.0E+05	-1.9E+05	-2.1E+05	-2.3E+05	-2.7E+05
127.0	-2.8E+07	3.0E+07	-3.1E+07	-2.5E+07	6.9E+07	2.2E+07	-2.5E+07	7.8E+07	-1.5E+05	-1.2E+05	-2.8E+05	-2.0E+05	-2.1E+05	-3.0E+05	-2.2E+05	-3.0E+05
136.7	-3.5E+07	3.3E+07	-3.0E+07	-3.5E+07	7.7E+07	2.2E+07	-2.8E+07	8.6E+07	-1.5E+05	-1.2E+05	-3.2E+05	-1.7E+05	-2.1E+05	-2.7E+05	-2.2E+05	-3.8E+05

Table 101 Raw data for the test seal at PD=20.7 bar, ω=3 krpm, and inlet GVF=4% with the high-preswirl insert

Freq.	Re(H_{XX})	Re(H_{XY})	Re(H_{YX})	Re(H_{YY})	Im(H_{XX})	Im(H_{XY})	Im(H_{YX})	Im(H_{YY})	Re(eH_{XX})	Re(eH_{XY})	Re(eH_{YX})	Re(eH_{YY})	Im(eH_{XX})	Im(eH_{XY})	Im(eH_{YX})	Im(eH_{YY})
Hz	N/m	N/m	N/m	N/m	N/m	N/m	N/m	N/m	N/m	N/m	N/m	N/m	N/m	N/m	N/m	N/m
9.8	1.7E+07	2.2E+07	-2.2E+07	1.7E+07	4.6E+06	2.0E+06	-1.7E+06	3.2E+06	-1.7E+05	-1.6E+05	-1.3E+05	-1.4E+05	-1.7E+05	-1.8E+05	-1.3E+05	-1.2E+05
19.5	1.6E+07	2.3E+07	-2.2E+07	1.4E+07	1.0E+07	3.5E+06	-3.9E+06	9.6E+06	-1.3E+05	-1.3E+05	-1.3E+05	-1.5E+05	-9.8E+04	-1.2E+05	-7.5E+04	-8.1E+04
29.3	1.8E+07	2.0E+07	-2.6E+07	1.6E+07	1.5E+07	4.7E+06	-4.6E+06	1.4E+07	-1.4E+05	-1.8E+05	-1.9E+05	-2.8E+05	-9.1E+04	-9.0E+04	-7.2E+04	-1.3E+05
39.1	1.3E+07	2.2E+07	-2.2E+07	1.2E+07	2.0E+07	4.7E+06	-6.7E+06	2.2E+07	-9.0E+04	-6.5E+04	-1.0E+05	-1.6E+05	-9.5E+04	-9.1E+04	-7.9E+04	-5.7E+04
48.8	1.1E+07	2.2E+07	-2.3E+07	1.1E+07	2.5E+07	6.8E+06	-7.6E+06	2.7E+07	-1.0E+05	-4.9E+04	-7.2E+04	-1.5E+05	-7.4E+04	-7.4E+04	-7.5E+04	-6.5E+04
58.6	8.3E+06	2.2E+07	-2.3E+07	8.0E+06	2.9E+07	8.8E+06	-9.5E+06	3.2E+07	-6.7E+04	-6.6E+04	-6.9E+04	-1.4E+05	-5.2E+04	-7.2E+04	-1.0E+05	-7.0E+04
68.4	5.0E+06	2.3E+07	-2.4E+07	5.0E+06	3.5E+07	1.0E+07	-1.1E+07	3.8E+07	-1.3E+05	-6.7E+04	-1.4E+05	-2.2E+05	-1.2E+05	-1.3E+05	-1.7E+05	-2.2E+05
78.1	1.0E+06	2.3E+07	-2.4E+07	1.3E+06	4.0E+07	1.2E+07	-1.2E+07	4.3E+07	-7.3E+04	-6.8E+04	-7.4E+04	-1.3E+05	-9.0E+04	-7.0E+04	-7.2E+04	-5.6E+04
87.9	-2.8E+06	2.3E+07	-2.4E+07	-2.5E+06	4.6E+07	1.4E+07	-1.4E+07	4.9E+07	-4.6E+04	-4.0E+04	-6.1E+04	-1.1E+05	-7.0E+04	-3.6E+04	-4.3E+04	-3.6E+04
97.7	-7.5E+06	2.4E+07	-2.5E+07	-7.8E+06	5.2E+07	1.5E+07	-1.6E+07	5.5E+07	-1.2E+05	-6.2E+04	-6.8E+04	-1.2E+05	-7.5E+04	-8.5E+04	-1.1E+05	-6.0E+04
107.4	-1.2E+07	2.5E+07	-2.7E+07	-1.2E+07	5.8E+07	1.7E+07	-1.7E+07	6.1E+07	-1.1E+05	-3.6E+04	-6.8E+04	-3.8E+04	-7.0E+04	-9.2E+04	-5.9E+04	-1.2E+05
117.2	-1.8E+07	2.5E+07	-2.6E+07	-1.8E+07	6.4E+07	1.9E+07	-1.8E+07	6.7E+07	-1.0E+05	-5.1E+04	-5.7E+04	-7.7E+04	-7.2E+04	-6.2E+04	-8.8E+04	-8.5E+04
127.0	-2.5E+07	2.7E+07	-2.7E+07	-2.3E+07	6.9E+07	2.0E+07	-2.0E+07	7.5E+07	-1.1E+05	-5.2E+04	-6.4E+04	-1.1E+05	-1.2E+05	-1.2E+05	-7.1E+04	-7.0E+04
136.7	-3.2E+07	2.8E+07	-2.8E+07	-3.2E+07	7.6E+07	2.1E+07	-2.2E+07	8.3E+07	-1.1E+05	-1.1E+05	-2.8E+04	-1.1E+05	-1.2E+05	-1.0E+05	-1.2E+05	-4.7E+04

Table 102 Raw data for the test seal at PD=20.7 bar, ω=4 krpm, and inlet GVF=4% with the high-preswirl insert

Freq.	Re(H_{XX})	Re(H_{XY})	Re(H_{YX})	Re(H_{YY})	Im(H_{XX})	Im(H_{XY})	Im(H_{YX})	Im(H_{YY})	Re(eH_{XX})	Re(eH_{XY})	Re(eH_{YX})	Re(eH_{YY})	Im(eH_{XX})	Im(eH_{XY})	Im(eH_{YX})	Im(eH_{YY})
Hz	N/m	N/m	N/m	N/m	N/m	N/m	N/m	N/m	N/m	N/m	N/m	N/m	N/m	N/m	N/m	N/m
9.8	1.6E+07	2.2E+07	-2.2E+07	1.6E+07	5.2E+06	1.9E+06	-1.7E+06	3.6E+06	-1.4E+05	-1.5E+05	-1.4E+05	-1.3E+05	-1.4E+05	-1.6E+05	-1.1E+05	-1.1E+05
19.5	1.5E+07	2.3E+07	-2.1E+07	1.4E+07	1.0E+07	3.2E+06	-3.8E+06	9.6E+06	-1.7E+05	-1.9E+05	-1.3E+05	-1.8E+05	-9.0E+04	-8.7E+04	-1.4E+05	-1.1E+05
29.3	1.7E+07	2.0E+07	-2.6E+07	1.7E+07	1.5E+07	4.5E+06	-4.7E+06	1.5E+07	-1.1E+05	-7.8E+04	-1.5E+05	-2.2E+05	-6.9E+04	-5.0E+04	-6.5E+04	-5.7E+04
39.1	1.2E+07	2.1E+07	-2.2E+07	1.3E+07	2.0E+07	5.0E+06	-6.3E+06	2.2E+07	-8.1E+04	-6.8E+04	-1.1E+05	-1.3E+05	-7.5E+04	-5.6E+04	-4.7E+04	-7.6E+04
48.8	1.0E+07	2.1E+07	-2.2E+07	1.1E+07	2.5E+07	7.2E+06	-7.5E+06	2.6E+07	-8.0E+04	-6.2E+04	-7.4E+04	-1.3E+05	-5.1E+04	-4.0E+04	-7.6E+04	-6.7E+04
58.6	7.3E+06	2.1E+07	-2.3E+07	7.5E+06	3.0E+07	9.1E+06	-9.4E+06	3.1E+07	-6.6E+04	-6.6E+04	-1.0E+05	-1.5E+05	-3.3E+04	-5.8E+04	-8.6E+04	-6.0E+04
68.4	4.1E+06	2.2E+07	-2.4E+07	4.6E+06	3.5E+07	1.0E+07	-1.1E+07	3.8E+07	-9.9E+04	-3.6E+04	-1.0E+05	-1.8E+05	-9.5E+04	-1.6E+05	-1.4E+05	-1.2E+05
78.1	2.1E+05	2.3E+07	-2.4E+07	1.1E+06	4.1E+07	1.2E+07	-1.2E+07	4.3E+07	-3.6E+04	-4.8E+04	-3.9E+04	-8.4E+04	-4.6E+04	-3.1E+04	-5.2E+04	-2.9E+04
87.9	-3.4E+06	2.3E+07	-2.4E+07	-3.0E+06	4.6E+07	1.4E+07	-1.4E+07	4.8E+07	-2.6E+04	-4.6E+04	-5.1E+04	-7.5E+04	-7.1E+04	-3.5E+04	-4.5E+04	-4.2E+04
97.7	-8.2E+06	2.4E+07	-2.5E+07	-8.2E+06	5.2E+07	1.6E+07	-1.5E+07	5.4E+07	-3.8E+04	-5.5E+04	-6.4E+04	-7.1E+04	-5.3E+04	-4.0E+04	-4.2E+04	-7.6E+04
107.4	-1.3E+07	2.5E+07	-2.6E+07	-1.2E+07	5.8E+07	1.7E+07	-1.7E+07	6.1E+07	-3.3E+04	-3.7E+04	-2.2E+04	-3.1E+04	-5.8E+04	-3.3E+04	-3.3E+04	-4.8E+04
117.2	-1.9E+07	2.5E+07	-2.6E+07	-1.9E+07	6.4E+07	1.9E+07	-1.8E+07	6.7E+07	-4.9E+04	-5.3E+04	-4.7E+04	-5.4E+04	-5.6E+04	-4.3E+04	-3.9E+04	-6.6E+04
127.0	-2.6E+07	2.6E+07	-2.7E+07	-2.4E+07	7.0E+07	2.0E+07	-2.0E+07	7.4E+07	-5.6E+04	-4.4E+04	-4.0E+04	-1.0E+05	-5.9E+04	-4.9E+04	-5.5E+04	-5.3E+04
136.7	-3.3E+07	2.8E+07	-2.8E+07	-3.3E+07	7.7E+07	2.1E+07	-2.2E+07	8.2E+07	-8.2E+04	-4.7E+04	-7.8E+04	-7.1E+04	-8.5E+04	-1.3E+05	-4.3E+04	-9.5E+04

Table 103 Raw data for the test seal at PD=20.7 bar, ω=5 krpm, and inlet GVF=4% with the high-preswirl insert

Freq.	Re(H_{XX})	Re(H_{XY})	Re(H_{YX})	Re(H_{YY})	Im(H_{XX})	Im(H_{XY})	Im(H_{YX})	Im(H_{YY})	Re(eH_{XX})	Re(eH_{XY})	Re(eH_{YX})	Re(eH_{YY})	Im(eH_{XX})	Im(eH_{XY})	Im(eH_{YX})	Im(eH_{YY})
Hz	N/m	N/m	N/m	N/m	N/m	N/m	N/m	N/m	N/m	N/m	N/m	N/m	N/m	N/m	N/m	N/m
9.8	1.6E+07	2.8E+07	-2.6E+07	1.2E+07	5.4E+06	8.3E+05	-3.4E+06	3.0E+06	-4.6E+05	-3.5E+05	-7.0E+05	-5.9E+05	-2.1E+05	-2.7E+05	-2.5E+05	-2.4E+05
19.5	1.4E+07	2.9E+07	-2.4E+07	7.5E+06	1.0E+07	2.8E+06	-5.7E+06	8.9E+06	-2.2E+05	-1.6E+05	-4.7E+05	-4.0E+05	-2.3E+05	-2.8E+05	-1.2E+05	-2.9E+05
29.3	1.6E+07	2.5E+07	-2.8E+07	9.7E+06	1.5E+07	4.7E+06	-6.5E+06	1.4E+07	-2.2E+05	-1.7E+05	-3.9E+05	-4.4E+05	-1.6E+05	-1.6E+05	-1.6E+05	-1.6E+05
39.1	1.2E+07	2.6E+07	-2.5E+07	7.7E+06	2.0E+07	3.7E+06	-7.8E+06	2.3E+07	-1.4E+05	-2.4E+05	-3.8E+05	-5.1E+05	-1.4E+05	-9.1E+04	-2.6E+05	-1.9E+05
48.8	9.7E+06	2.6E+07	-2.6E+07	5.0E+06	2.5E+07	6.4E+06	-9.5E+06	2.9E+07	-1.5E+05	-2.5E+05	-3.7E+05	-3.8E+05	-1.5E+05	-9.1E+04	-2.4E+05	-2.1E+05
58.6	6.4E+06	2.5E+07	-2.5E+07	3.1E+06	3.0E+07	8.8E+06	-1.1E+07	3.5E+07	-1.1E+05	-2.5E+05	-2.6E+05	-4.9E+05	-2.5E+05	-1.8E+05	-3.6E+05	-2.2E+05
68.4	3.6E+06	2.7E+07	-2.7E+07	1.4E+05	3.7E+07	9.3E+06	-1.4E+07	4.4E+07	-1.6E+05	-3.9E+05	-3.0E+05	-5.5E+05	-2.8E+05	-1.6E+05	-3.8E+05	-2.5E+05
78.1	-1.6E+05	2.7E+07	-2.6E+07	-2.0E+06	4.1E+07	1.3E+07	-1.4E+07	4.7E+07	-7.9E+04	-2.0E+05	-1.2E+05	-3.6E+05	-2.5E+05	-2.2E+05	-3.6E+05	-2.1E+05
87.9	-3.7E+06	2.7E+07	-2.6E+07	-5.3E+06	4.7E+07	1.5E+07	-1.6E+07	5.3E+07	-1.0E+05	-2.7E+05	-9.0E+04	-3.9E+05	-2.7E+05	-1.7E+05	-3.7E+05	-2.3E+05
97.7	-8.2E+06	2.8E+07	-2.7E+07	-9.9E+06	5.3E+07	1.7E+07	-1.8E+07	5.9E+07	-1.2E+05	-2.2E+05	-1.4E+05	-4.1E+05	-2.6E+05	-1.3E+05	-4.4E+05	-2.1E+05
107.4	-1.2E+07	2.9E+07	-2.9E+07	-1.2E+07	5.9E+07	1.7E+07	-1.9E+07	6.7E+07	-1.1E+05	-2.5E+05	-2.5E+05	-3.8E+05	-2.1E+05	-2.0E+05	-3.9E+05	-3.4E+05
117.2	-1.9E+07	3.0E+07	-2.8E+07	-1.9E+07	6.5E+07	2.0E+07	-2.1E+07	7.2E+07	-1.1E+05	-1.9E+05	-2.6E+05	-3.4E+05	-2.3E+05	-2.4E+05	-3.4E+05	-3.9E+05
127.0	-2.5E+07	2.9E+07	-3.1E+07	-2.2E+07	7.1E+07	2.0E+07	-2.3E+07	8.0E+07	-1.4E+05	-2.2E+05	-3.4E+05	-3.4E+05	-2.7E+05	-3.7E+05	-3.4E+05	-5.2E+05
136.7	-3.1E+07	3.3E+07	-3.1E+07	-3.3E+07	7.9E+07	2.1E+07	-2.7E+07	8.8E+07	-1.1E+05	-1.8E+05	-2.9E+05	-2.0E+05	-2.0E+05	-2.8E+05	-2.3E+05	-4.7E+05

Table 104 Raw data for the test seal at PD=20.7 bar, ω=3 krpm, and inlet GVF=6% with the high-preswirl insert

Freq.	Re(H_{XX})	Re(H_{XY})	Re(H_{YX})	Re(H_{YY})	Im(H_{XX})	Im(H_{XY})	Im(H_{YX})	Im(H_{YY})	Re(eH_{XX})	Re(eH_{XY})	Re(eH_{YX})	Re(eH_{YY})	Im(eH_{XX})	Im(eH_{XY})	Im(eH_{YX})	Im(eH_{YY})
Hz	N/m	N/m	N/m	N/m	N/m	N/m	N/m	N/m	N/m	N/m	N/m	N/m	N/m	N/m	N/m	N/m
9.8	1.7E+07	2.2E+07	-2.3E+07	1.7E+07	4.2E+06	1.5E+06	-1.7E+06	3.8E+06	-1.4E+05	-1.8E+05	-2.0E+05	-2.1E+05	-1.5E+05	-1.6E+05	-2.2E+05	-2.1E+05
19.5	1.6E+07	2.4E+07	-2.2E+07	1.4E+07	1.0E+07	2.7E+06	-3.9E+06	1.0E+07	-1.2E+05	-1.0E+05	-7.7E+04	-4.8E+04	-7.2E+04	-7.1E+04	-7.8E+04	-7.6E+04
29.3	1.9E+07	2.0E+07	-2.7E+07	1.7E+07	1.5E+07	4.4E+06	-4.5E+06	1.4E+07	-1.4E+05	-1.3E+05	-1.1E+05	-8.1E+04	-1.3E+05	-8.2E+04	-1.3E+05	-8.2E+04
39.1	1.4E+07	2.2E+07	-2.2E+07	1.3E+07	1.9E+07	5.5E+06	-5.9E+06	2.1E+07	-7.7E+04	-5.8E+04	-5.9E+04	-4.4E+04	-1.1E+05	-6.8E+04	-6.8E+04	-4.2E+04
48.8	1.1E+07	2.3E+07	-2.4E+07	1.1E+07	2.5E+07	6.8E+06	-7.5E+06	2.7E+07	-8.8E+04	-5.6E+04	-1.4E+05	-7.0E+04	-4.6E+04	-4.0E+04	-5.7E+04	-6.8E+04
58.6	8.5E+06	2.2E+07	-2.4E+07	8.7E+06	3.0E+07	8.2E+06	-8.9E+06	3.2E+07	-5.8E+04	-7.7E+04	-8.2E+04	-8.8E+04	-5.6E+04	-3.7E+04	-8.2E+04	-7.4E+04
68.4	5.9E+06	2.3E+07	-2.4E+07	5.9E+06	3.6E+07	9.3E+06	-1.1E+07	3.9E+07	-1.2E+05	-2.1E+05	-2.0E+05	-1.2E+05	-1.5E+05	-1.0E+05	-1.4E+05	-2.4E+05
78.1	2.2E+06	2.3E+07	-2.4E+07	2.6E+06	4.0E+07	1.1E+07	-1.1E+07	4.3E+07	-4.3E+04	-3.6E+04	-5.6E+04	-6.7E+04	-7.5E+04	-8.0E+04	-5.0E+04	-4.5E+04
87.9	-1.9E+06	2.4E+07	-2.4E+07	-1.2E+06	4.6E+07	1.3E+07	-1.3E+07	4.9E+07	-4.0E+04	-6.0E+04	-4.2E+04	-6.9E+04	-6.8E+04	-2.3E+04	-6.6E+04	-6.2E+04
97.7	-6.7E+06	2.4E+07	-2.5E+07	-6.4E+06	5.2E+07	1.4E+07	-1.5E+07	5.5E+07	-2.9E+04	-5.3E+04	-8.4E+04	-5.5E+04	-9.3E+04	-2.8E+04	-6.8E+04	-4.5E+04
107.4	-1.2E+07	2.5E+07	-2.7E+07	-1.1E+07	5.9E+07	1.6E+07	-1.6E+07	6.3E+07	-4.7E+04	-5.5E+04	-4.0E+04	-5.9E+04	-8.9E+04	-5.3E+04	-1.1E+05	-4.6E+04
117.2	-1.7E+07	2.5E+07	-2.7E+07	-1.7E+07	6.5E+07	1.8E+07	-1.7E+07	6.9E+07	-4.1E+04	-3.7E+04	-5.6E+04	-4.6E+04	-7.0E+04	-2.3E+04	-1.0E+05	-3.8E+04
127.0	-2.4E+07	2.6E+07	-2.8E+07	-2.1E+07	7.2E+07	1.9E+07	-1.8E+07	7.7E+07	-5.4E+04	-5.9E+04	-5.7E+04	-8.6E+04	-6.9E+04	-5.8E+04	-4.7E+04	-5.9E+04
136.7	-3.0E+07	2.9E+07	-2.8E+07	-3.0E+07	8.0E+07	2.0E+07	-2.0E+07	8.6E+07	-5.8E+04	-3.1E+04	-8.0E+04	-1.0E+05	-6.7E+04	-4.2E+04	-7.2E+04	-9.6E+04

Table 105 Raw data for the test seal at PD=20.7 bar, ω=4 krpm, and inlet GVF=6% with the high-preswirl insert

Freq.	Re(H_{XX})	Re(H_{XY})	Re(H_{YX})	Re(H_{YY})	Im(H_{XX})	Im(H_{XY})	Im(H_{YX})	Im(H_{YY})	Re(eH_{XX})	Re(eH_{XY})	Re(eH_{YX})	Re(eH_{YY})	Im(eH_{XX})	Im(eH_{XY})	Im(eH_{YX})	Im(eH_{YY})
Hz	N/m	N/m	N/m	N/m	N/m	N/m	N/m	N/m	N/m	N/m	N/m	N/m	N/m	N/m	N/m	N/m
9.8	1.9E+07	2.3E+07	-2.3E+07	1.6E+07	4.8E+06	1.4E+06	-2.3E+06	3.5E+06	-1.7E+05	-1.5E+05	-2.1E+05	-1.8E+05	-1.9E+05	-1.9E+05	-2.4E+05	-2.4E+05
19.5	1.6E+07	2.4E+07	-2.2E+07	1.3E+07	9.7E+06	2.7E+06	-4.1E+06	9.9E+06	-1.6E+05	-1.3E+05	-2.0E+05	-1.6E+05	-1.0E+05	-1.5E+05	-1.3E+05	-1.3E+05
29.3	1.8E+07	2.1E+07	-2.6E+07	1.6E+07	1.4E+07	3.9E+06	-4.3E+06	1.5E+07	-1.1E+05	-1.1E+05	-1.3E+05	-1.5E+05	-1.7E+05	-7.7E+04	-1.9E+05	-9.9E+04
39.1	1.4E+07	2.2E+07	-2.2E+07	1.3E+07	1.9E+07	5.4E+06	-6.3E+06	2.1E+07	-8.0E+04	-7.3E+04	-9.8E+04	-7.5E+04	-8.9E+04	-8.0E+04	-8.5E+04	-8.0E+04
48.8	1.1E+07	2.3E+07	-2.3E+07	1.0E+07	2.5E+07	6.5E+06	-7.6E+06	2.7E+07	-9.7E+04	-8.5E+04	-1.5E+05	-8.4E+04	-9.6E+04	-7.8E+04	-1.1E+05	-1.2E+05
58.6	8.7E+06	2.3E+07	-2.3E+07	8.2E+06	3.0E+07	8.1E+06	-8.8E+06	3.3E+07	-5.1E+04	-9.7E+04	-1.2E+05	-1.3E+05	-8.0E+04	-5.3E+04	-1.3E+05	-7.5E+04
68.4	6.2E+06	2.3E+07	-2.5E+07	6.5E+06	3.5E+07	8.6E+06	-1.1E+07	4.0E+07	-1.3E+05	-2.3E+05	-1.1E+05	-1.3E+05	-1.0E+05	-8.7E+04	-2.0E+05	-1.7E+05
78.1	2.6E+06	2.4E+07	-2.3E+07	2.7E+06	4.0E+07	1.1E+07	-1.1E+07	4.4E+07	-3.0E+04	-5.9E+04	-7.3E+04	-1.4E+05	-1.0E+05	-6.2E+04	-2.1E+05	-9.4E+04
87.9	-1.9E+06	2.4E+07	-2.4E+07	-1.1E+06	4.6E+07	1.2E+07	-1.3E+07	4.9E+07	-4.1E+04	-5.9E+04	-8.8E+04	-8.3E+04	-1.1E+05	-6.5E+04	-1.4E+05	-1.3E+05
97.7	-6.6E+06	2.4E+07	-2.5E+07	-6.2E+06	5.2E+07	1.4E+07	-1.5E+07	5.5E+07	-3.3E+04	-8.5E+04	-8.0E+04	-1.1E+05	-1.0E+05	-5.2E+04	-1.2E+05	-6.8E+04
107.4	-1.1E+07	2.4E+07	-2.7E+07	-1.0E+07	5.8E+07	1.5E+07	-1.6E+07	6.3E+07	-5.2E+04	-6.9E+04	-6.3E+04	-8.4E+04	-1.4E+05	-9.0E+04	-1.1E+05	-1.5E+05
117.2	-1.7E+07	2.5E+07	-2.6E+07	-1.7E+07	6.4E+07	1.8E+07	-1.7E+07	6.9E+07	-5.3E+04	-7.8E+04	-1.6E+05	-7.3E+04	-1.2E+05	-6.1E+04	-9.1E+04	-1.4E+05
127.0	-2.3E+07	2.6E+07	-2.8E+07	-2.1E+07	7.1E+07	1.9E+07	-1.8E+07	7.7E+07	-5.9E+04	-8.3E+04	-1.8E+05	-6.7E+04	-1.3E+05	-4.5E+04	-8.0E+04	-1.4E+05
136.7	-3.0E+07	2.8E+07	-2.7E+07	-3.0E+07	7.9E+07	2.0E+07	-2.0E+07	8.5E+07	-5.6E+04	-4.6E+04	-1.3E+05	-6.3E+04	-8.2E+04	-7.9E+04	-5.3E+04	-1.4E+05

Table 106 Raw data for the test seal at PD=20.7 bar, ω=5 krpm, and inlet GVF=6% with the high-preswirl insert

Freq.	Re(H_{XX})	Re(H_{XY})	Re(H_{YX})	Re(H_{YY})	Im(H_{XX})	Im(H_{XY})	Im(H_{YX})	Im(H_{YY})	Re(eH_{XX})	Re(eH_{XY})	Re(eH_{YX})	Re(eH_{YY})	Im(eH_{XX})	Im(eH_{XY})	Im(eH_{YX})	Im(eH_{YY})
Hz	N/m	N/m	N/m	N/m	N/m	N/m	N/m	N/m	N/m	N/m	N/m	N/m	N/m	N/m	N/m	N/m
9.8	1.3E+07	3.0E+07	-2.5E+07	6.9E+06	4.6E+06	1.1E+06	-3.8E+06	2.4E+06	-2.7E+05	-2.1E+05	-5.9E+05	-5.2E+05	-2.0E+05	-2.0E+05	-1.6E+05	-2.1E+05
19.5	1.4E+07	2.9E+07	-2.5E+07	4.8E+06	9.6E+06	1.8E+06	-4.8E+06	9.8E+06	-2.1E+05	-2.4E+05	-2.5E+05	-2.2E+05	-2.1E+05	-1.6E+05	-1.5E+05	-1.7E+05
29.3	1.5E+07	2.6E+07	-2.8E+07	7.3E+06	1.5E+07	3.6E+06	-6.0E+06	1.5E+07	-1.9E+05	-1.8E+05	-2.6E+05	-2.3E+05	-2.6E+05	-2.6E+05	-2.8E+05	-2.6E+05
39.1	1.1E+07	2.8E+07	-2.4E+07	4.2E+06	2.0E+07	4.1E+06	-7.5E+06	2.4E+07	-6.7E+04	-1.0E+05	-3.3E+05	-1.9E+05	-1.4E+05	-8.0E+04	-1.6E+05	-2.0E+05
48.8	8.1E+06	2.8E+07	-2.6E+07	1.3E+06	2.6E+07	6.8E+06	-8.7E+06	2.9E+07	-1.7E+05	-1.1E+05	-2.1E+05	-1.8E+05	-8.0E+04	-9.8E+04	-2.0E+05	-1.7E+05
58.6	5.9E+06	2.7E+07	-2.5E+07	-1.8E+05	3.1E+07	8.2E+06	-1.0E+07	3.7E+07	-1.1E+05	-1.2E+05	-2.6E+05	-1.2E+05	-1.0E+05	-1.1E+05	-2.7E+05	-3.2E+05
68.4	3.1E+06	3.0E+07	-2.6E+07	-3.0E+06	3.8E+07	9.9E+06	-1.2E+07	4.5E+07	-1.4E+05	-2.2E+05	-2.5E+05	-3.3E+05	-1.3E+05	-1.3E+05	-3.8E+05	-3.1E+05
78.1	1.3E+06	2.8E+07	-2.6E+07	-3.9E+06	4.2E+07	1.1E+07	-1.2E+07	5.0E+07	-1.1E+05	-5.9E+04	-1.9E+05	-2.2E+05	-5.0E+04	-8.8E+04	-3.9E+05	-2.4E+05
87.9	-3.3E+06	2.9E+07	-2.6E+07	-7.5E+06	4.8E+07	1.3E+07	-1.5E+07	5.6E+07	-6.7E+04	-1.3E+05	-1.5E+05	-2.6E+05	-7.2E+04	-6.2E+04	-3.3E+05	-1.9E+05
97.7	-8.1E+06	2.9E+07	-2.7E+07	-1.1E+07	5.3E+07	1.5E+07	-1.7E+07	6.2E+07	-5.1E+04	-8.0E+04	-1.6E+05	-2.6E+05	-1.3E+05	-6.5E+04	-4.3E+05	-1.7E+05
107.4	-1.2E+07	3.1E+07	-2.9E+07	-1.4E+07	6.0E+07	1.6E+07	-1.8E+07	7.1E+07	-9.3E+04	-1.1E+05	-1.6E+05	-3.5E+05	-7.4E+04	-1.1E+05	-3.5E+05	-1.5E+05
117.2	-1.8E+07	3.1E+07	-2.8E+07	-1.9E+07	6.7E+07	1.9E+07	-1.9E+07	7.7E+07	-7.4E+04	-8.7E+04	-1.2E+05	-2.0E+05	-6.7E+04	-8.7E+04	-3.6E+05	-1.2E+05
127.0	-2.4E+07	3.2E+07	-3.0E+07	-2.3E+07	7.3E+07	1.8E+07	-2.1E+07	8.6E+07	-6.8E+04	-1.5E+05	-2.1E+05	-2.6E+05	-1.3E+05	-1.1E+05	-3.8E+05	-1.4E+05
136.7	-3.0E+07	3.5E+07	-2.8E+07	-3.2E+07	8.1E+07	2.0E+07	-2.3E+07	9.2E+07	-1.1E+05	-1.5E+05	-2.2E+05	-2.6E+05	-1.9E+05	-8.5E+04	-4.7E+05	-4.5E+04

Table 107 Raw data for the test seal at PD=20.7 bar, ω=3 krpm, and inlet GVF=8% with the high-preswirl insert

Freq.	Re($\boldsymbol{H_{XX}}$)	Re($\boldsymbol{H_{XY}}$)	Re($\boldsymbol{H_{YX}}$)	Re($\boldsymbol{H_{YY}}$)	Im($\boldsymbol{H_{XX}}$)	Im($\boldsymbol{H_{XY}}$)	Im($\boldsymbol{H_{YX}}$)	Im($\boldsymbol{H_{YY}}$)	Re($\boldsymbol{eH_{XX}}$)	Re($\boldsymbol{eH_{XY}}$)	Re($\boldsymbol{eH_{YX}}$)	Re($\boldsymbol{eH_{YY}}$)	Im($\boldsymbol{eH_{XX}}$)	Im($\boldsymbol{eH_{XY}}$)	Im($\boldsymbol{eH_{YX}}$)	Im($\boldsymbol{eH_{YY}}$)
Hz	N/m	N/m	N/m	N/m	N/m	N/m	N/m	N/m	N/m	N/m	N/m	N/m	N/m	N/m	N/m	N/m
9.8	1.7E+07	2.3E+07	-2.3E+07	1.4E+07	4.8E+06	7.1E+05	-2.5E+06	4.8E+06	-2.0E+05	-1.6E+05	-2.1E+05	-2.2E+05	-9.6E+04	-1.3E+05	-1.3E+05	-1.3E+05
19.5	1.6E+07	2.5E+07	-2.2E+07	1.1E+07	1.0E+07	2.5E+06	-4.3E+06	1.0E+07	-2.7E+05	-2.1E+05	-3.7E+05	-2.7E+05	-1.1E+05	-1.4E+05	-1.2E+05	-2.0E+05
29.3	1.8E+07	2.0E+07	-2.6E+07	1.5E+07	1.4E+07	4.1E+06	-4.1E+06	1.5E+07	-1.2E+05	-1.9E+05	-1.6E+05	-1.8E+05	-1.8E+05	-1.0E+05	-1.0E+05	-1.2E+05
39.1	1.3E+07	2.2E+07	-2.3E+07	1.1E+07	1.9E+07	4.8E+06	-6.0E+06	2.2E+07	-8.0E+04	-6.1E+04	-8.7E+04	-1.2E+05	-6.3E+04	-5.4E+04	-1.1E+05	-7.4E+04
48.8	1.1E+07	2.3E+07	-2.3E+07	8.5E+06	2.5E+07	6.1E+06	-7.7E+06	2.8E+07	-7.3E+04	-8.3E+04	-1.1E+05	-1.7E+05	-8.7E+04	-7.8E+04	-1.1E+05	-4.6E+04
58.6	8.4E+06	2.3E+07	-2.4E+07	7.1E+06	3.0E+07	7.9E+06	-8.5E+06	3.4E+07	-6.3E+04	-1.0E+05	-1.3E+05	-1.4E+05	-1.0E+05	-1.1E+05	-1.1E+05	-8.4E+04
68.4	5.7E+06	2.3E+07	-2.4E+07	5.0E+06	3.6E+07	8.2E+06	-1.0E+07	4.2E+07	-1.1E+05	-1.7E+05	-1.4E+05	-2.6E+05	-1.2E+05	-1.6E+05	-1.7E+05	-1.9E+05
78.1	2.1E+06	2.4E+07	-2.3E+07	1.7E+06	4.0E+07	1.0E+07	-1.0E+07	4.5E+07	-4.3E+04	-6.3E+04	-5.3E+04	-1.4E+05	-7.4E+04	-4.5E+04	-1.7E+05	-8.5E+04
87.9	-2.1E+06	2.4E+07	-2.4E+07	-2.0E+06	4.6E+07	1.2E+07	-1.2E+07	5.0E+07	-4.3E+04	-5.8E+04	-8.7E+04	-1.7E+05	-8.5E+04	-5.8E+04	-1.0E+05	-6.7E+04
97.7	-6.8E+06	2.4E+07	-2.5E+07	-6.7E+06	5.2E+07	1.4E+07	-1.4E+07	5.7E+07	-6.2E+04	-7.6E+04	-9.8E+04	-1.3E+05	-9.6E+04	-5.5E+04	-2.0E+05	-1.4E+05
107.4	-1.1E+07	2.4E+07	-2.7E+07	-9.8E+06	5.9E+07	1.5E+07	-1.5E+07	6.5E+07	-3.3E+04	-4.7E+04	-1.0E+05	-9.6E+04	-6.2E+04	-2.5E+04	-1.1E+05	-1.1E+05
117.2	-1.6E+07	2.5E+07	-2.6E+07	-1.6E+07	6.6E+07	1.7E+07	-1.5E+07	7.0E+07	-3.5E+04	-3.3E+04	-1.2E+05	-7.4E+04	-7.8E+04	-4.7E+04	-1.1E+05	-1.1E+05
127.0	-2.2E+07	2.5E+07	-2.7E+07	-1.9E+07	7.2E+07	1.8E+07	-1.6E+07	7.8E+07	-9.7E+04	-9.7E+04	-1.6E+05	-1.9E+05	-9.9E+04	-1.3E+05	-1.1E+05	-2.0E+05
136.7	-2.8E+07	2.8E+07	-2.6E+07	-2.8E+07	8.0E+07	1.9E+07	-1.9E+07	8.7E+07	-1.0E+05	-7.4E+04	-1.5E+05	-8.5E+04	-8.3E+04	-1.1E+05	-1.1E+05	-1.8E+05

Table 108 Raw data for the test seal at PD=20.7 bar, ω=4 krpm, and inlet GVF=8% with the high-preswirl insert

Freq.	Re($\boldsymbol{H_{XX}}$)	Re($\boldsymbol{H_{XY}}$)	Re($\boldsymbol{H_{YX}}$)	Re($\boldsymbol{H_{YY}}$)	Im($\boldsymbol{H_{XX}}$)	Im($\boldsymbol{H_{XY}}$)	Im($\boldsymbol{H_{YX}}$)	Im($\boldsymbol{H_{YY}}$)	Re($\boldsymbol{eH_{XX}}$)	Re($\boldsymbol{eH_{XY}}$)	Re($\boldsymbol{eH_{YX}}$)	Re($\boldsymbol{eH_{YY}}$)	Im($\boldsymbol{eH_{XX}}$)	Im($\boldsymbol{eH_{XY}}$)	Im($\boldsymbol{eH_{YX}}$)	Im($\boldsymbol{eH_{YY}}$)
Hz	N/m	N/m	N/m	N/m	N/m	N/m	N/m	N/m	N/m	N/m	N/m	N/m	N/m	N/m	N/m	N/m
9.8	1.7E+07	2.3E+07	-2.3E+07	1.5E+07	4.8E+06	5.7E+05	-2.5E+06	4.7E+06	-2.2E+05	-1.9E+05	-1.9E+05	-1.7E+05	-3.3E+05	-2.7E+05	-2.3E+05	-1.9E+05
19.5	1.5E+07	2.4E+07	-2.2E+07	1.1E+07	1.0E+07	2.5E+06	-4.4E+06	1.0E+07	-1.4E+05	-9.9E+04	-1.8E+05	-1.5E+05	-1.6E+05	-1.4E+05	-1.3E+05	-1.3E+05
29.3	1.8E+07	2.1E+07	-2.6E+07	1.5E+07	1.4E+07	4.4E+06	-3.9E+06	1.4E+07	-7.3E+04	-6.9E+04	-9.9E+04	-8.0E+04	-1.3E+05	-8.5E+04	-8.2E+04	-6.1E+04
39.1	1.3E+07	2.3E+07	-2.2E+07	1.1E+07	2.0E+07	5.0E+06	-6.3E+06	2.2E+07	-9.5E+04	-6.8E+04	-1.1E+05	-8.1E+04	-7.0E+04	-6.4E+04	-6.2E+04	-6.3E+04
48.8	1.1E+07	2.3E+07	-2.3E+07	8.6E+06	2.5E+07	6.0E+06	-7.4E+06	2.8E+07	-6.1E+04	-7.8E+04	-1.4E+05	-1.0E+05	-6.1E+04	-7.8E+04	-6.6E+04	-6.4E+04
58.6	8.5E+06	2.3E+07	-2.4E+07	7.1E+06	3.0E+07	7.9E+06	-8.8E+06	3.4E+07	-4.8E+04	-1.1E+05	-7.4E+04	-6.9E+04	-9.9E+04	-1.0E+05	-1.7E+05	-1.1E+05
68.4	5.8E+06	2.4E+07	-2.4E+07	5.2E+06	3.6E+07	8.3E+06	-1.0E+07	4.1E+07	-7.1E+04	-9.1E+04	-8.4E+04	-1.1E+05	-8.7E+04	-1.2E+05	-1.4E+05	-1.8E+05
78.1	2.2E+06	2.4E+07	-2.3E+07	1.6E+06	4.1E+07	1.0E+07	-1.1E+07	4.5E+07	-4.6E+04	-5.2E+04	-5.2E+04	-9.2E+04	-8.2E+04	-6.4E+04	-8.3E+04	-5.6E+04
87.9	-1.9E+06	2.4E+07	-2.4E+07	-2.1E+06	4.6E+07	1.2E+07	-1.2E+07	5.0E+07	-2.7E+04	-3.6E+04	-6.5E+04	-6.2E+04	-5.4E+04	-3.0E+04	-1.0E+05	-2.7E+04
97.7	-6.8E+06	2.4E+07	-2.5E+07	-6.8E+06	5.3E+07	1.4E+07	-1.4E+07	5.7E+07	-6.5E+04	-4.0E+04	-8.5E+04	-8.0E+04	-5.0E+04	-4.9E+04	-7.9E+04	-5.8E+04
107.4	-1.1E+07	2.5E+07	-2.7E+07	-9.9E+06	6.0E+07	1.4E+07	-1.5E+07	6.5E+07	-4.0E+04	-4.4E+04	-1.3E+05	-1.2E+05	-8.0E+04	-4.1E+04	-1.3E+05	-7.0E+04
117.2	-1.6E+07	2.5E+07	-2.6E+07	-1.6E+07	6.6E+07	1.7E+07	-1.6E+07	7.1E+07	-5.4E+04	-4.9E+04	-6.7E+04	-5.6E+04	-1.0E+05	-4.0E+04	-6.9E+04	-7.1E+04
127.0	-2.2E+07	2.5E+07	-2.7E+07	-1.9E+07	7.2E+07	1.8E+07	-1.7E+07	7.9E+07	-7.5E+04	-7.8E+04	-1.1E+05	-1.1E+05	-9.2E+04	-7.5E+04	-6.6E+04	-1.0E+05
136.7	-2.8E+07	2.8E+07	-2.7E+07	-2.8E+07	8.0E+07	1.9E+07	-1.9E+07	8.7E+07	-7.8E+04	-8.0E+04	-9.7E+04	-1.6E+05	-1.2E+05	-1.1E+05	-1.0E+05	-1.7E+05

Table 109 Raw data for the test seal at PD=20.7 bar, ω=5 krpm, and inlet GVF=8% with the high-preswirl insert

Freq.	Re($\boldsymbol{H}_{XX}$)	Re($\boldsymbol{H}_{XY}$)	Re($\boldsymbol{H}_{YX}$)	Re($\boldsymbol{H}_{YY}$)	Im($\boldsymbol{H}_{XX}$)	Im($\boldsymbol{H}_{XY}$)	Im($\boldsymbol{H}_{YX}$)	Im($\boldsymbol{H}_{YY}$)	Re($\boldsymbol{eH}_{XX}$)	Re($\boldsymbol{eH}_{XY}$)	Re($\boldsymbol{eH}_{YX}$)	Re($\boldsymbol{eH}_{YY}$)	Im($\boldsymbol{eH}_{XX}$)	Im($\boldsymbol{eH}_{XY}$)	Im($\boldsymbol{eH}_{YX}$)	Im($\boldsymbol{eH}_{YY}$)
Hz	N/m	N/m	N/m	N/m	N/m	N/m	N/m	N/m	N/m	N/m	N/m	N/m	N/m	N/m	N/m	N/m
9.8	1.4E+07	3.0E+07	-2.7E+07	6.8E+06	5.0E+06	5.5E+05	-3.5E+06	3.4E+06	-2.4E+05	-2.2E+05	-4.3E+05	-3.5E+05	-2.1E+05	-1.8E+05	-1.8E+05	-1.4E+05
19.5	1.3E+07	3.0E+07	-2.5E+07	3.5E+06	1.0E+07	2.6E+06	-5.4E+06	1.0E+07	-3.3E+05	-3.5E+05	-2.6E+05	-2.7E+05	-1.8E+05	-1.5E+05	-3.1E+05	-3.1E+05
29.3	1.6E+07	2.6E+07	-2.9E+07	8.1E+06	1.5E+07	3.8E+06	-5.2E+06	1.6E+07	-1.4E+05	-1.1E+05	-1.9E+05	-1.3E+05	-1.1E+05	-1.3E+05	-1.9E+05	-1.9E+05
39.1	1.1E+07	2.8E+07	-2.5E+07	4.3E+06	2.0E+07	4.0E+06	-6.8E+06	2.4E+07	-1.5E+05	-1.2E+05	-1.0E+05	-1.2E+05	-1.0E+05	-9.1E+04	-7.3E+04	-9.0E+04
48.8	7.5E+06	2.8E+07	-2.7E+07	1.6E+06	2.6E+07	6.4E+06	-8.5E+06	3.1E+07	-8.5E+04	-5.9E+04	-1.7E+05	-1.5E+05	-8.6E+04	-8.3E+04	-1.2E+05	-1.2E+05
58.6	6.7E+06	2.8E+07	-2.7E+07	6.0E+05	3.2E+07	7.0E+06	-9.6E+06	3.9E+07	-1.2E+05	-1.1E+05	-2.0E+05	-2.5E+05	-1.1E+05	-8.9E+04	-1.3E+05	-8.4E+04
68.4	3.3E+06	3.0E+07	-2.6E+07	-2.0E+06	3.8E+07	9.1E+06	-1.1E+07	4.6E+07	-1.3E+05	-1.6E+05	-2.4E+05	-2.7E+05	-1.2E+05	-1.4E+05	-3.3E+05	-2.4E+05
78.1	1.5E+06	2.8E+07	-2.6E+07	-2.9E+06	4.3E+07	1.0E+07	-1.1E+07	5.0E+07	-1.2E+05	-1.1E+05	-1.0E+05	-1.7E+05	-1.1E+05	-7.9E+04	-1.4E+05	-8.3E+04
87.9	-2.8E+06	2.9E+07	-2.7E+07	-6.0E+06	4.8E+07	1.3E+07	-1.3E+07	5.6E+07	-8.0E+04	-8.6E+04	-1.5E+05	-2.7E+05	-7.8E+04	-1.1E+05	-1.1E+05	-7.0E+04
97.7	-7.7E+06	2.9E+07	-2.7E+07	-9.9E+06	5.4E+07	1.5E+07	-1.5E+07	6.3E+07	-1.1E+05	-9.6E+04	-2.1E+05	-1.3E+05	-5.6E+04	-7.6E+04	-1.4E+05	-1.5E+05
107.4	-1.1E+07	3.0E+07	-2.9E+07	-1.2E+07	6.1E+07	1.5E+07	-1.6E+07	7.1E+07	-8.2E+04	-4.7E+04	-2.4E+05	-1.4E+05	-7.0E+04	-8.2E+04	-1.8E+05	-1.3E+05
117.2	-1.7E+07	3.0E+07	-2.8E+07	-1.6E+07	6.8E+07	1.7E+07	-1.7E+07	7.7E+07	-1.0E+05	-7.0E+04	-1.3E+05	-1.7E+05	-5.9E+04	-5.5E+04	-1.4E+05	-1.4E+05
127.0	-2.2E+07	3.1E+07	-3.0E+07	-1.9E+07	7.5E+07	1.7E+07	-1.9E+07	8.6E+07	-7.0E+04	-1.8E+05	-1.7E+05	-2.9E+05	-7.6E+04	-7.3E+04	-1.2E+05	-9.3E+04
136.7	-2.8E+07	3.4E+07	-2.8E+07	-2.8E+07	8.3E+07	1.9E+07	-2.1E+07	9.2E+07	-8.2E+04	-6.5E+04	-6.6E+04	-1.5E+05	-6.1E+04	-1.5E+05	-2.0E+05	-1.1E+05

Table 110 Raw data for the test seal at PD=20.7 bar, ω=3 krpm, and inlet GVF=10% with the high-preswirl insert

Freq.	Re($\boldsymbol{H}_{XX}$)	Re($\boldsymbol{H}_{XY}$)	Re($\boldsymbol{H}_{YX}$)	Re($\boldsymbol{H}_{YY}$)	Im($\boldsymbol{H}_{XX}$)	Im($\boldsymbol{H}_{XY}$)	Im($\boldsymbol{H}_{YX}$)	Im($\boldsymbol{H}_{YY}$)	Re($\boldsymbol{eH}_{XX}$)	Re($\boldsymbol{eH}_{XY}$)	Re($\boldsymbol{eH}_{YX}$)	Re($\boldsymbol{eH}_{YY}$)	Im($\boldsymbol{eH}_{XX}$)	Im($\boldsymbol{eH}_{XY}$)	Im($\boldsymbol{eH}_{YX}$)	Im($\boldsymbol{eH}_{YY}$)
Hz	N/m	N/m	N/m	N/m	N/m	N/m	N/m	N/m	N/m	N/m	N/m	N/m	N/m	N/m	N/m	N/m
9.8	1.7E+07	2.3E+07	-2.4E+07	1.3E+07	4.6E+06	1.0E+06	-2.1E+06	4.6E+06	-2.8E+05	-2.1E+05	-3.7E+05	-3.2E+05	-1.7E+05	-1.7E+05	-2.1E+05	-1.6E+05
19.5	1.4E+07	2.4E+07	-2.2E+07	1.1E+07	9.9E+06	2.2E+06	-3.9E+06	1.1E+07	-1.3E+05	-1.1E+05	-1.4E+05	-1.1E+05	-1.2E+05	-1.4E+05	-1.3E+05	-1.6E+05
29.3	1.7E+07	2.1E+07	-2.6E+07	1.4E+07	1.5E+07	4.4E+06	-4.3E+06	1.5E+07	-9.0E+04	-1.1E+05	-8.4E+04	-1.5E+05	-8.4E+04	-9.0E+04	-1.3E+05	-1.3E+05
39.1	1.2E+07	2.3E+07	-2.2E+07	1.1E+07	2.0E+07	4.7E+06	-5.8E+06	2.2E+07	-5.7E+04	-4.5E+04	-7.2E+04	-1.0E+05	-4.4E+04	-4.2E+04	-1.1E+05	-7.0E+04
48.8	1.1E+07	2.4E+07	-2.3E+07	7.8E+06	2.6E+07	5.7E+06	-7.3E+06	2.8E+07	-9.0E+04	-1.1E+05	-1.3E+05	-1.7E+05	-1.1E+05	-7.3E+04	-1.1E+05	-3.9E+04
58.6	8.4E+06	2.3E+07	-2.3E+07	6.7E+06	3.0E+07	7.6E+06	-8.4E+06	3.4E+07	-7.4E+04	-1.3E+05	-1.3E+05	-1.5E+05	-6.8E+04	-8.7E+04	-1.4E+05	-9.5E+04
68.4	5.6E+06	2.4E+07	-2.4E+07	4.1E+06	3.6E+07	7.5E+06	-1.1E+07	4.2E+07	-8.3E+04	-1.6E+05	-8.1E+04	-2.3E+05	-9.8E+04	-8.1E+04	-1.8E+05	-2.0E+05
78.1	2.2E+06	2.4E+07	-2.3E+07	1.4E+06	4.1E+07	9.5E+06	-1.0E+07	4.6E+07	-5.5E+04	-5.6E+04	-8.9E+04	-1.1E+05	-5.9E+04	-5.6E+04	-1.8E+05	-8.7E+04
87.9	-1.9E+06	2.4E+07	-2.4E+07	-2.4E+06	4.7E+07	1.2E+07	-1.2E+07	5.1E+07	-7.1E+04	-6.6E+04	-7.7E+04	-1.7E+05	-6.7E+04	-5.9E+04	-1.8E+05	-1.3E+05
97.7	-6.3E+06	2.4E+07	-2.4E+07	-6.9E+06	5.3E+07	1.3E+07	-1.3E+07	5.8E+07	-7.9E+04	-1.2E+05	-1.6E+05	-1.8E+05	-9.3E+04	-5.2E+04	-1.2E+05	-8.6E+04
107.4	-9.3E+06	2.5E+07	-2.6E+07	-8.8E+06	6.0E+07	1.3E+07	-1.4E+07	6.6E+07	-5.0E+04	-7.5E+04	-1.3E+05	-1.4E+05	-6.6E+04	-7.4E+04	-1.5E+05	-1.1E+05
117.2	-1.5E+07	2.5E+07	-2.5E+07	-1.4E+07	6.7E+07	1.6E+07	-1.5E+07	7.1E+07	-5.9E+04	-4.3E+04	-1.1E+05	-8.2E+04	-6.9E+04	-8.0E+04	-8.1E+04	-1.4E+05
127.0	-2.0E+07	2.5E+07	-2.6E+07	-1.7E+07	7.3E+07	1.7E+07	-1.5E+07	8.0E+07	-9.8E+04	-7.3E+04	-9.4E+04	-1.5E+05	-4.2E+04	-1.1E+05	-8.6E+04	-1.0E+05
136.7	-2.5E+07	2.7E+07	-2.6E+07	-2.6E+07	8.1E+07	1.7E+07	-1.8E+07	8.8E+07	-5.3E+04	-9.1E+04	-1.6E+05	-1.2E+05	-7.2E+04	-1.3E+05	-1.9E+05	-2.6E+05

Table 111 Raw data for the test seal at PD=20.7 bar, ω=4 krpm, and inlet GVF=10% with the high-preswirl insert

Freq.	Re(H_{XX})	Re(H_{XY})	Re(H_{YX})	Re(H_{YY})	Im(H_{XX})	Im(H_{XY})	Im(H_{YX})	Im(H_{YY})	Re(eH_{XX})	Re(eH_{XY})	Re(eH_{YX})	Re(eH_{YY})	Im(eH_{XX})	Im(eH_{XY})	Im(eH_{YX})	Im(eH_{YY})
Hz	N/m	N/m	N/m	N/m	N/m	N/m	N/m	N/m	N/m	N/m	N/m	N/m	N/m	N/m	N/m	N/m
9.8	1.6E+07	2.3E+07	-2.2E+07	1.4E+07	4.4E+06	1.2E+06	-2.3E+06	4.5E+06	-1.9E+05	-1.6E+05	-2.7E+05	-3.4E+05	-2.3E+05	-2.3E+05	-2.5E+05	-2.2E+05
19.5	1.5E+07	2.5E+07	-2.1E+07	9.7E+06	1.1E+07	2.4E+06	-4.3E+06	1.1E+07	-1.7E+05	-2.0E+05	-2.3E+05	-2.3E+05	-1.7E+05	-9.7E+04	-1.4E+05	-6.6E+04
29.3	1.7E+07	2.2E+07	-2.5E+07	1.3E+07	1.5E+07	4.7E+06	-4.8E+06	1.5E+07	-1.3E+05	-9.6E+04	-2.0E+05	-1.4E+05	-1.3E+05	-1.2E+05	-1.1E+05	-1.3E+05
39.1	1.2E+07	2.4E+07	-2.2E+07	9.6E+06	2.0E+07	4.4E+06	-6.2E+06	2.3E+07	-7.0E+04	-1.1E+05	-8.1E+04	-1.2E+05	-7.7E+04	-4.3E+04	-7.8E+04	-6.6E+04
48.8	1.0E+07	2.5E+07	-2.3E+07	6.7E+06	2.6E+07	5.9E+06	-8.2E+06	2.9E+07	-1.2E+05	-1.1E+05	-1.7E+05	-1.4E+05	-8.3E+04	-7.9E+04	-1.5E+05	-1.5E+05
58.6	8.5E+06	2.4E+07	-2.3E+07	5.9E+06	3.1E+07	7.1E+06	-9.1E+06	3.5E+07	-4.5E+04	-5.5E+04	-1.4E+05	-1.8E+05	-4.6E+04	-5.1E+04	-1.6E+05	-2.0E+05
68.4	5.6E+06	2.6E+07	-2.4E+07	2.6E+06	3.7E+07	7.1E+06	-1.2E+07	4.3E+07	-6.5E+04	-9.2E+04	-1.5E+05	-2.0E+05	-1.3E+05	-9.7E+04	-2.0E+05	-1.6E+05
78.1	2.5E+06	2.5E+07	-2.4E+07	3.9E+05	4.2E+07	9.3E+06	-1.1E+07	4.7E+07	-5.4E+04	-8.8E+04	-7.3E+04	-1.5E+05	-1.1E+05	-8.3E+04	-2.3E+05	-1.8E+05
87.9	-1.6E+06	2.5E+07	-2.4E+07	-3.2E+06	4.8E+07	1.1E+07	-1.2E+07	5.2E+07	-6.9E+04	-8.1E+04	-1.0E+05	-1.2E+05	-7.7E+04	-4.9E+04	-2.1E+05	-1.4E+05
97.7	-5.8E+06	2.5E+07	-2.5E+07	-7.5E+06	5.5E+07	1.2E+07	-1.4E+07	6.0E+07	-4.0E+04	-5.6E+04	-1.6E+05	-1.5E+05	-1.1E+05	-8.3E+04	-2.1E+05	-1.5E+05
107.4	-8.7E+06	2.5E+07	-2.7E+07	-9.0E+06	6.1E+07	1.3E+07	-1.4E+07	6.8E+07	-7.4E+04	-7.9E+04	-1.4E+05	-1.5E+05	-6.7E+04	-5.6E+04	-1.4E+05	-9.5E+04
117.2	-1.4E+07	2.6E+07	-2.6E+07	-1.5E+07	6.8E+07	1.5E+07	-1.5E+07	7.4E+07	-5.9E+04	-6.7E+04	-1.7E+05	-1.6E+05	-4.7E+04	-3.3E+04	-1.3E+05	-1.2E+05
127.0	-1.9E+07	2.6E+07	-2.7E+07	-1.6E+07	7.4E+07	1.6E+07	-1.6E+07	8.2E+07	-2.7E+04	-1.0E+05	-1.7E+05	-2.1E+05	-6.9E+04	-6.1E+04	-1.1E+05	-1.5E+05
136.7	-2.4E+07	2.8E+07	-2.6E+07	-2.5E+07	8.2E+07	1.6E+07	-1.8E+07	9.1E+07	-5.2E+04	-6.3E+04	-1.9E+05	-1.3E+05	-8.3E+04	-6.9E+04	-7.8E+04	-1.4E+05

Table 112 Raw data for the test seal at PD=20.7 bar, ω=5 krpm, and inlet GVF=10% with the high-preswirl insert

Freq.	Re(H_{XX})	Re(H_{XY})	Re(H_{YX})	Re(H_{YY})	Im(H_{XX})	Im(H_{XY})	Im(H_{YX})	Im(H_{YY})	Re(eH_{XX})	Re(eH_{XY})	Re(eH_{YX})	Re(eH_{YY})	Im(eH_{XX})	Im(eH_{XY})	Im(eH_{YX})	Im(eH_{YY})
Hz	N/m	N/m	N/m	N/m	N/m	N/m	N/m	N/m	N/m	N/m	N/m	N/m	N/m	N/m	N/m	N/m
9.8	1.4E+07	2.9E+07	-2.7E+07	5.5E+06	4.8E+06	3.0E+05	-5.1E+06	2.6E+06	-2.7E+05	-2.2E+05	-4.0E+05	-2.7E+05	-1.2E+05	-1.1E+05	-2.9E+05	-2.7E+05
19.5	1.3E+07	2.9E+07	-2.6E+07	3.4E+06	1.0E+07	1.5E+06	-4.8E+06	1.1E+07	-1.3E+05	-1.8E+05	-4.7E+05	-4.5E+05	-2.0E+05	-1.4E+05	-2.6E+05	-2.4E+05
29.3	1.6E+07	2.5E+07	-3.0E+07	7.1E+06	1.5E+07	3.7E+06	-5.9E+06	1.5E+07	-1.2E+05	-9.7E+04	-2.4E+05	-1.9E+05	-2.4E+05	-2.3E+05	-3.2E+05	-2.7E+05
39.1	1.0E+07	2.8E+07	-2.6E+07	3.7E+06	2.1E+07	4.3E+06	-6.7E+06	2.4E+07	-9.5E+04	-9.4E+04	-3.8E+04	-7.5E+04	-8.9E+04	-6.6E+04	-1.1E+05	-7.5E+04
48.8	7.8E+06	2.8E+07	-2.8E+07	4.6E+05	2.7E+07	6.3E+06	-8.9E+06	3.1E+07	-9.1E+04	-9.2E+04	-1.1E+05	-1.2E+05	-1.1E+05	-9.5E+04	-1.6E+05	-1.1E+05
58.6	6.8E+06	2.7E+07	-2.7E+07	-4.7E+05	3.2E+07	7.4E+06	-9.5E+06	3.9E+07	-1.2E+05	-7.4E+04	-1.5E+05	-1.7E+05	-8.4E+04	-1.6E+05	-2.1E+05	-2.7E+05
68.4	3.9E+06	2.9E+07	-2.7E+07	-2.4E+06	3.9E+07	8.7E+06	-1.1E+07	4.7E+07	-1.2E+05	-1.5E+05	-1.4E+05	-1.5E+05	-9.0E+04	-9.7E+04	-1.5E+05	-1.3E+05
78.1	2.0E+06	2.9E+07	-2.8E+07	-3.1E+06	4.4E+07	1.1E+07	-1.0E+07	5.2E+07	-6.6E+04	-7.3E+04	-7.3E+04	-1.4E+05	-5.0E+04	-5.6E+04	-1.2E+05	-1.1E+05
87.9	-1.8E+06	2.9E+07	-2.7E+07	-6.2E+06	4.9E+07	1.3E+07	-1.2E+07	5.7E+07	-8.6E+04	-1.2E+05	-1.2E+05	-1.9E+05	-8.3E+04	-7.7E+04	-7.2E+04	-1.2E+05
97.7	-6.2E+06	2.9E+07	-2.8E+07	-1.0E+07	5.6E+07	1.4E+07	-1.4E+07	6.4E+07	-8.6E+04	-6.2E+04	-8.2E+04	-1.3E+05	-6.8E+04	-7.5E+04	-2.1E+05	-1.4E+05
107.4	-1.0E+07	3.0E+07	-2.9E+07	-1.2E+07	6.3E+07	1.5E+07	-1.4E+07	7.3E+07	-9.5E+04	-7.5E+04	-1.2E+05	-1.7E+05	-5.9E+04	-1.3E+05	-2.4E+05	-1.9E+05
117.2	-1.5E+07	3.1E+07	-2.8E+07	-1.6E+07	7.0E+07	1.8E+07	-1.5E+07	7.9E+07	-8.2E+04	-7.5E+04	-1.6E+05	-6.3E+04	-4.7E+04	-5.9E+04	-1.1E+05	-1.3E+05
127.0	-1.9E+07	3.1E+07	-2.9E+07	-1.8E+07	7.6E+07	1.7E+07	-1.7E+07	8.8E+07	-8.2E+04	-1.3E+05	-8.4E+04	-2.5E+05	-9.2E+04	-6.4E+04	-1.6E+05	-1.2E+05
136.7	-2.5E+07	3.4E+07	-2.7E+07	-2.7E+07	8.4E+07	1.9E+07	-2.0E+07	9.5E+07	-1.5E+05	-8.8E+04	-2.1E+05	-1.1E+05	-9.2E+04	-1.2E+05	-7.3E+04	-2.2E+05

Table 113 Raw data for the test seal at PD=27.6 bar, ω=3 krpm, and inlet GVF=0% with the high-preswirl insert

Freq.	Re(H_{XX})	Re(H_{XY})	Re(H_{YX})	Re(H_{YY})	Im(H_{XX})	Im(H_{XY})	Im(H_{YX})	Im(H_{YY})	Re(eH_{XX})	Re(eH_{XY})	Re(eH_{YX})	Re(eH_{YY})	Im(eH_{XX})	Im(eH_{XY})	Im(eH_{YX})	Im(eH_{YY})
Hz	N/m	N/m	N/m	N/m	N/m	N/m	N/m	N/m	N/m	N/m	N/m	N/m	N/m	N/m	N/m	N/m
9.8	2.5E+07	2.5E+07	-3.1E+07	2.4E+07	5.9E+06	3.1E+06	6.7E+04	4.5E+06	-1.4E+05	-1.1E+05	-2.1E+05	-1.5E+05	-1.6E+05	-1.7E+05	-2.0E+05	-1.5E+05
19.5	2.1E+07	2.9E+07	-2.9E+07	2.0E+07	1.1E+07	4.7E+06	-2.4E+06	1.1E+07	-1.2E+05	-9.6E+04	-1.0E+05	-8.7E+04	-1.6E+05	-1.5E+05	-8.5E+04	-9.0E+04
29.3	2.3E+07	2.6E+07	-3.2E+07	2.2E+07	1.7E+07	6.2E+06	-4.6E+06	1.6E+07	-1.1E+05	-1.6E+05	-2.0E+05	-1.4E+05	-1.4E+05	-1.3E+05	-1.2E+05	-1.2E+05
39.1	1.7E+07	2.7E+07	-2.9E+07	1.9E+07	2.2E+07	7.9E+06	-5.6E+06	2.3E+07	-1.0E+05	-7.7E+04	-1.1E+05	-1.0E+05	-5.5E+04	-3.9E+04	-1.8E+05	-1.1E+05
48.8	1.7E+07	2.9E+07	-2.9E+07	1.6E+07	2.9E+07	9.2E+06	-7.8E+06	2.9E+07	-1.0E+05	-9.3E+04	-6.8E+04	-1.0E+05	-4.3E+04	-6.9E+04	-8.2E+04	-7.0E+04
58.6	1.2E+07	2.8E+07	-3.0E+07	1.3E+07	3.4E+07	1.1E+07	-9.6E+06	3.5E+07	-9.2E+04	-7.8E+04	-1.0E+05	-8.4E+04	-7.1E+04	-5.0E+04	-1.1E+05	-9.5E+04
68.4	9.7E+06	2.8E+07	-3.1E+07	1.1E+07	3.9E+07	1.2E+07	-1.1E+07	4.2E+07	-1.0E+05	-1.5E+05	-1.5E+05	-2.0E+05	-1.5E+05	-1.5E+05	-1.6E+05	-1.6E+05
78.1	6.2E+06	2.9E+07	-3.0E+07	6.4E+06	4.4E+07	1.4E+07	-1.3E+07	4.6E+07	-1.0E+05	-1.3E+05	-9.0E+04	-9.5E+04	-1.4E+05	-9.7E+04	-9.0E+04	-7.5E+04
87.9	3.9E+05	2.9E+07	-3.1E+07	2.2E+06	5.0E+07	1.7E+07	-1.4E+07	5.3E+07	-8.3E+04	-4.4E+04	-6.4E+04	-1.1E+05	-5.0E+04	-5.1E+04	-9.4E+04	-4.4E+04
97.7	-4.6E+06	3.1E+07	-3.1E+07	-3.3E+06	5.6E+07	1.8E+07	-1.6E+07	5.9E+07	-8.8E+04	-4.1E+04	-4.4E+04	-1.0E+05	-1.2E+05	-8.9E+04	-1.1E+05	-6.1E+04
107.4	-9.7E+06	3.2E+07	-3.2E+07	-8.4E+06	6.3E+07	2.0E+07	-1.8E+07	6.6E+07	-8.0E+04	-4.7E+04	-4.8E+04	-1.1E+05	-8.5E+04	-6.1E+04	-1.0E+05	-4.7E+04
117.2	-1.8E+07	3.2E+07	-3.2E+07	-1.5E+07	6.8E+07	2.3E+07	-2.0E+07	7.2E+07	-6.3E+04	-7.9E+04	-6.0E+04	-6.9E+04	-8.1E+04	-7.1E+04	-1.1E+05	-7.5E+04
127.0	-2.4E+07	3.4E+07	-3.2E+07	-2.3E+07	7.5E+07	2.3E+07	-2.3E+07	7.9E+07	-9.7E+04	-1.1E+05	-7.5E+04	-1.3E+05	-1.3E+05	-5.6E+04	-1.1E+05	-8.6E+04
136.7	-3.3E+07	3.6E+07	-3.3E+07	-3.2E+07	8.2E+07	2.4E+07	-2.5E+07	8.6E+07	-6.1E+04	-6.6E+04	-1.5E+05	-9.4E+04	-1.0E+05	-7.2E+04	-8.5E+04	-1.2E+05

Table 114 Raw data for the test seal at PD=27.6 bar, ω=4 krpm, and inlet GVF=0% with the high-preswirl insert

Freq.	Re(H_{XX})	Re(H_{XY})	Re(H_{YX})	Re(H_{YY})	Im(H_{XX})	Im(H_{XY})	Im(H_{YX})	Im(H_{YY})	Re(eH_{XX})	Re(eH_{XY})	Re(eH_{YX})	Re(eH_{YY})	Im(eH_{XX})	Im(eH_{XY})	Im(eH_{YX})	Im(eH_{YY})
Hz	N/m	N/m	N/m	N/m	N/m	N/m	N/m	N/m	N/m	N/m	N/m	N/m	N/m	N/m	N/m	N/m
9.8	2.5E+07	2.5E+07	-3.3E+07	2.4E+07	5.5E+06	2.5E+06	-4.3E+05	5.2E+06	-1.4E+05	-1.1E+05	-2.3E+05	-2.0E+05	-2.4E+05	-1.9E+05	-2.2E+05	-2.0E+05
19.5	2.1E+07	2.9E+07	-2.9E+07	1.9E+07	1.1E+07	4.4E+06	-2.8E+06	1.1E+07	-2.1E+05	-1.6E+05	-1.8E+05	-1.2E+05	-7.2E+04	-9.4E+04	-1.6E+05	-2.0E+05
29.3	2.3E+07	2.6E+07	-3.2E+07	2.1E+07	1.7E+07	6.6E+06	-4.9E+06	1.6E+07	-2.7E+05	-1.6E+05	-1.3E+05	-1.2E+05	-1.2E+05	-1.1E+05	-1.9E+05	-1.2E+05
39.1	1.7E+07	2.7E+07	-3.0E+07	1.8E+07	2.2E+07	7.7E+06	-5.5E+06	2.4E+07	-2.3E+05	-1.3E+05	-1.6E+05	-5.9E+04	-4.8E+04	-8.1E+04	-2.1E+05	-1.6E+05
48.8	1.6E+07	2.9E+07	-3.0E+07	1.6E+07	2.9E+07	9.2E+06	-7.5E+06	3.0E+07	-1.8E+05	-1.3E+05	-2.0E+05	-8.8E+04	-9.0E+04	-8.9E+04	-2.0E+05	-1.6E+05
58.6	1.2E+07	2.8E+07	-3.0E+07	1.2E+07	3.4E+07	1.1E+07	-9.3E+06	3.6E+07	-1.9E+05	-7.7E+04	-1.6E+05	-6.8E+04	-1.3E+05	-1.3E+05	-1.7E+05	-1.6E+05
68.4	9.4E+06	2.8E+07	-3.1E+07	1.1E+07	3.9E+07	1.2E+07	-1.1E+07	4.3E+07	-2.0E+05	-1.1E+05	-8.0E+04	-1.7E+05	-7.4E+04	-1.1E+05	-2.8E+05	-1.6E+05
78.1	5.9E+06	2.9E+07	-3.0E+07	6.2E+06	4.5E+07	1.4E+07	-1.3E+07	4.7E+07	-1.9E+05	-9.2E+04	-1.9E+05	-3.0E+04	-1.0E+05	-1.4E+05	-2.8E+05	-2.3E+05
87.9	2.2E+05	2.9E+07	-3.1E+07	2.2E+06	5.1E+07	1.7E+07	-1.3E+07	5.4E+07	-1.9E+05	-6.2E+04	-5.9E+04	-1.2E+05	-6.7E+04	-9.9E+04	-2.2E+05	-1.0E+05
97.7	-4.9E+06	3.1E+07	-3.1E+07	-3.2E+06	5.7E+07	1.9E+07	-1.6E+07	6.0E+07	-1.5E+05	-4.6E+04	-1.2E+05	-1.4E+05	-8.8E+04	-1.0E+05	-2.0E+05	-6.2E+04
107.4	-9.7E+06	3.2E+07	-3.2E+07	-8.0E+06	6.3E+07	2.0E+07	-1.7E+07	6.7E+07	-1.9E+05	-4.5E+04	-4.1E+04	-1.3E+05	-1.4E+05	-1.3E+05	-2.6E+05	-8.3E+04
117.2	-1.8E+07	3.2E+07	-3.2E+07	-1.5E+07	6.9E+07	2.3E+07	-1.9E+07	7.2E+07	-2.2E+05	-6.1E+04	-1.0E+05	-1.3E+05	-1.4E+05	-1.3E+05	-2.4E+05	-6.6E+04
127.0	-2.4E+07	3.4E+07	-3.2E+07	-2.2E+07	7.6E+07	2.3E+07	-2.2E+07	8.0E+07	-1.8E+05	-8.3E+04	-1.4E+05	-1.5E+05	-2.4E+05	-1.3E+05	-2.2E+05	-9.2E+04
136.7	-3.2E+07	3.6E+07	-3.3E+07	-3.1E+07	8.3E+07	2.5E+07	-2.4E+07	8.8E+07	-1.8E+05	-1.1E+05	-2.0E+05	-1.3E+05	-2.6E+05	-1.2E+05	-1.3E+05	-1.7E+05

Table 115 Raw data for the test seal at PD=27.6 bar, ω=5 krpm, and inlet GVF=0% with the high-preswirl insert

Freq.	Re(H_{XX})	Re(H_{XY})	Re(H_{YX})	Re(H_{YY})	Im(H_{XX})	Im(H_{XY})	Im(H_{YX})	Im(H_{YY})	Re(eH_{XX})	Re(eH_{XY})	Re(eH_{YX})	Re(eH_{YY})	Im(eH_{XX})	Im(eH_{XY})	Im(eH_{YX})	Im(eH_{YY})
Hz	N/m	N/m	N/m	N/m	N/m	N/m	N/m	N/m	N/m	N/m	N/m	N/m	N/m	N/m	N/m	N/m
9.8	2.4E+07	2.6E+07	-3.2E+07	2.2E+07	5.5E+06	4.0E+06	1.3E+04	4.3E+06	-2.4E+05	-1.9E+05	-2.2E+05	-2.3E+05	-1.2E+05	-1.8E+05	-2.4E+05	-2.3E+05
19.5	1.9E+07	3.2E+07	-3.0E+07	1.8E+07	1.3E+07	6.0E+06	-3.2E+06	1.2E+07	-1.3E+05	-1.7E+05	-1.7E+05	-1.8E+05	-2.1E+05	-1.7E+05	-9.6E+04	-1.5E+05
29.3	2.1E+07	3.0E+07	-3.3E+07	1.9E+07	1.9E+07	7.9E+06	-5.0E+06	1.6E+07	-2.0E+05	-1.9E+05	-2.9E+05	-2.3E+05	-2.9E+05	-2.5E+05	-1.2E+05	-2.4E+05
39.1	1.5E+07	3.0E+07	-3.1E+07	1.5E+07	2.3E+07	8.9E+06	-6.6E+06	2.4E+07	-1.3E+05	-1.0E+05	-8.0E+04	-9.7E+04	-8.4E+04	-8.7E+04	-1.0E+05	-6.9E+04
48.8	1.6E+07	3.2E+07	-3.0E+07	1.4E+07	3.1E+07	9.5E+06	-8.7E+06	3.1E+07	-1.5E+05	-1.6E+05	-1.1E+05	-1.2E+05	-1.0E+05	-6.9E+04	-1.3E+05	-1.2E+05
58.6	1.1E+07	3.0E+07	-3.1E+07	1.0E+07	3.5E+07	1.2E+07	-1.1E+07	3.7E+07	-9.5E+04	-1.2E+05	-1.8E+05	-2.4E+05	-8.6E+04	-7.7E+04	-1.4E+05	-1.1E+05
68.4	8.8E+06	3.1E+07	-3.3E+07	7.9E+06	4.1E+07	1.3E+07	-1.4E+07	4.5E+07	-1.2E+05	-9.7E+04	-1.3E+05	-2.1E+05	-1.1E+05	-1.2E+05	-1.1E+05	-9.7E+04
78.1	4.7E+06	3.2E+07	-3.1E+07	4.2E+06	4.6E+07	1.6E+07	-1.6E+07	4.9E+07	-6.3E+04	-6.4E+04	-1.5E+05	-1.9E+05	-5.8E+04	-5.8E+04	-1.8E+05	-1.5E+05
87.9	-5.0E+05	3.2E+07	-3.3E+07	-1.7E+04	5.3E+07	1.9E+07	-1.7E+07	5.6E+07	-1.2E+05	-6.3E+04	-5.7E+04	-1.1E+05	-8.4E+04	-1.3E+05	-1.6E+05	-1.0E+05
97.7	-5.2E+06	3.3E+07	-3.3E+07	-5.3E+06	5.9E+07	2.0E+07	-2.0E+07	6.2E+07	-5.7E+04	-7.0E+04	-9.5E+04	-1.1E+05	-8.0E+04	-1.2E+05	-1.2E+05	-1.1E+05
107.4	-9.9E+06	3.3E+07	-3.4E+07	-1.0E+07	6.5E+07	2.1E+07	-2.2E+07	6.9E+07	-9.6E+04	-4.2E+04	-8.6E+04	-1.4E+05	-6.4E+04	-1.1E+05	-1.5E+05	-1.0E+05
117.2	-1.8E+07	3.4E+07	-3.5E+07	-1.7E+07	7.0E+07	2.5E+07	-2.4E+07	7.6E+07	-8.4E+04	-7.5E+04	-1.3E+05	-1.2E+05	-7.8E+04	-8.5E+04	-1.1E+05	-1.5E+05
127.0	-2.4E+07	3.6E+07	-3.5E+07	-2.4E+07	7.8E+07	2.5E+07	-2.8E+07	8.4E+07	-1.7E+05	-2.0E+05	-7.7E+04	-1.5E+05	-1.1E+05	-9.5E+04	-1.3E+05	-1.2E+05
136.7	-3.2E+07	3.7E+07	-3.6E+07	-3.2E+07	8.4E+07	2.7E+07	-3.0E+07	9.1E+07	-1.3E+05	-9.5E+04	-1.1E+05	-1.5E+05	-1.0E+05	-7.3E+04	-1.3E+05	-1.8E+05

Table 116 Raw data for the test seal at PD=27.6 bar, ω=3 krpm, and inlet GVF=2% with the high-preswirl insert

Freq.	Re(H_{XX})	Re(H_{XY})	Re(H_{YX})	Re(H_{YY})	Im(H_{XX})	Im(H_{XY})	Im(H_{YX})	Im(H_{YY})	Re(eH_{XX})	Re(eH_{XY})	Re(eH_{YX})	Re(eH_{YY})	Im(eH_{XX})	Im(eH_{XY})	Im(eH_{YX})	Im(eH_{YY})
Hz	N/m	N/m	N/m	N/m	N/m	N/m	N/m	N/m	N/m	N/m	N/m	N/m	N/m	N/m	N/m	N/m
9.8	1.5E+07	2.9E+07	-3.0E+07	6.5E+06	4.3E+06	9.1E+05	-3.6E+06	3.1E+06	-1.2E+05	-1.4E+05	-3.4E+05	-2.6E+05	-2.1E+05	-1.7E+05	-1.8E+05	-2.1E+05
19.5	1.5E+07	3.0E+07	-2.9E+07	4.5E+06	1.1E+07	2.0E+06	-5.2E+06	1.2E+07	-2.5E+05	-1.8E+05	-2.2E+05	-2.3E+05	-1.2E+05	-1.9E+05	-1.5E+05	-9.9E+04
29.3	1.9E+07	2.7E+07	-3.2E+07	6.6E+06	1.7E+07	3.5E+06	-6.7E+06	1.7E+07	-2.0E+05	-1.5E+05	-3.2E+05	-2.0E+05	-1.4E+05	-1.2E+05	-2.2E+05	-2.0E+05
39.1	1.4E+07	3.1E+07	-2.9E+07	3.7E+06	2.4E+07	4.4E+06	-6.7E+06	2.7E+07	-2.8E+05	-1.8E+05	-3.3E+05	-2.4E+05	-1.0E+05	-1.3E+05	-1.4E+05	-2.0E+05
48.8	1.1E+07	3.0E+07	-3.0E+07	4.3E+05	2.9E+07	6.0E+06	-9.7E+06	3.4E+07	-1.1E+05	-8.5E+04	-1.6E+05	-2.1E+05	-9.4E+04	-9.3E+04	-2.4E+05	-1.5E+05
58.6	1.0E+07	3.1E+07	-3.0E+07	-8.9E+05	3.6E+07	7.0E+06	-1.0E+07	4.2E+07	-2.5E+05	-2.0E+05	-2.6E+05	-2.3E+05	-1.4E+05	-1.4E+05	-2.3E+05	-1.8E+05
68.4	6.7E+06	3.1E+07	-3.1E+07	-3.8E+06	4.2E+07	9.2E+06	-1.2E+07	5.1E+07	-2.0E+05	-1.7E+05	-2.2E+05	-1.7E+05	-1.7E+05	-1.7E+05	-3.1E+05	-3.1E+05
78.1	5.6E+06	3.1E+07	-3.1E+07	-4.2E+06	4.9E+07	1.0E+07	-1.1E+07	5.7E+07	-3.1E+05	-2.9E+05	-1.9E+05	-4.9E+05	-3.0E+05	-3.9E+05	-3.6E+05	-2.7E+05
87.9	1.7E+06	3.1E+07	-3.1E+07	-8.3E+06	5.5E+07	1.2E+07	-1.3E+07	6.4E+07	-2.2E+05	-1.3E+05	-2.3E+05	-1.5E+05	-2.0E+05	-1.8E+05	-3.4E+05	-2.3E+05
97.7	-3.1E+06	3.1E+07	-3.1E+07	-1.2E+07	6.1E+07	1.3E+07	-1.6E+07	7.2E+07	-1.6E+05	-9.9E+04	-1.6E+05	-2.8E+05	-2.1E+05	-1.8E+05	-4.1E+05	-1.8E+05
107.4	-7.1E+06	3.2E+07	-3.3E+07	-1.4E+07	6.8E+07	1.5E+07	-1.7E+07	8.1E+07	-1.9E+05	-1.9E+05	-8.9E+04	-2.5E+05	-1.6E+05	-2.2E+05	-4.0E+05	-1.7E+05
117.2	-1.3E+07	3.2E+07	-3.3E+07	-1.9E+07	7.5E+07	1.8E+07	-1.7E+07	8.8E+07	-2.4E+05	-1.3E+05	-8.8E+04	-2.1E+05	-2.2E+05	-1.3E+05	-2.8E+05	-1.4E+05
127.0	-1.9E+07	3.3E+07	-3.4E+07	-2.4E+07	7.9E+07	1.8E+07	-2.0E+07	9.7E+07	-1.8E+05	-2.9E+05	-1.7E+05	-2.1E+05	-3.6E+05	-1.6E+05	-3.7E+05	-2.3E+05
136.7	-2.6E+07	3.5E+07	-3.2E+07	-3.2E+07	8.7E+07	2.1E+07	-2.2E+07	1.0E+08	-1.8E+05	-2.5E+05	-2.0E+05	-1.6E+05	-3.3E+05	-1.6E+05	-2.0E+05	-1.7E+05

Table 117 Raw data for the test seal at PD=27.6 bar, ω=4 krpm, and inlet GVF=2% with the high-preswirl insert

Freq.	Re(H_{XX})	Re(H_{XY})	Re(H_{YX})	Re(H_{YY})	Im(H_{XX})	Im(H_{XY})	Im(H_{YX})	Im(H_{YY})	Re(eH_{XX})	Re(eH_{XY})	Re(eH_{YX})	Re(eH_{YY})	Im(eH_{XX})	Im(eH_{XY})	Im(eH_{YX})	Im(eH_{YY})
Hz	N/m	N/m	N/m	N/m	N/m	N/m	N/m	N/m	N/m	N/m	N/m	N/m	N/m	N/m	N/m	N/m
9.8	1.1E+07	2.9E+07	-3.0E+07	1.7E+06	6.1E+06	2.0E+06	-1.7E+06	4.9E+06	-6.2E+05	-6.1E+05	-6.4E+05	-5.4E+05	-4.3E+05	-1.6E+05	-2.8E+05	-3.1E+05
19.5	1.0E+07	3.0E+07	-3.2E+07	-5.0E+05	1.3E+07	2.7E+06	-4.3E+06	1.4E+07	-6.0E+05	-8.0E+05	-6.1E+05	-4.8E+05	-5.9E+05	-1.2E+05	-1.9E+05	-3.8E+05
29.3	1.2E+07	2.8E+07	-3.5E+07	3.5E+06	2.1E+07	5.8E+06	-4.3E+06	2.0E+07	-9.9E+05	-7.0E+05	-5.2E+05	-2.0E+05	-3.9E+05	-4.0E+05	-3.5E+05	-4.3E+05
39.1	7.3E+06	3.0E+07	-3.1E+07	5.8E+04	2.7E+07	5.5E+06	-4.7E+06	3.0E+07	-8.8E+05	-5.4E+05	-3.9E+05	-2.8E+05	-3.1E+05	-4.6E+05	-3.5E+05	-3.4E+05
48.8	6.9E+06	3.1E+07	-3.1E+07	-2.0E+06	3.5E+07	7.4E+06	-6.9E+06	3.7E+07	-1.2E+06	-6.0E+05	-5.3E+05	-2.8E+05	-2.6E+05	-6.1E+05	-2.7E+05	-3.3E+05
58.6	4.4E+06	2.9E+07	-3.2E+07	-3.5E+06	4.0E+07	8.5E+06	-8.0E+06	4.6E+07	-9.7E+05	-3.4E+05	-4.6E+05	-4.1E+05	-2.7E+05	-6.1E+05	-4.7E+05	-4.2E+05
68.4	3.2E+06	3.1E+07	-3.2E+07	-6.9E+06	4.8E+07	7.8E+06	-9.8E+06	5.4E+07	-9.5E+05	-2.1E+05	-3.3E+05	-3.7E+05	-4.7E+05	-6.9E+05	-5.0E+05	-4.4E+05
78.1	-5.4E+05	3.1E+07	-3.2E+07	-7.3E+06	5.4E+07	1.1E+07	-9.0E+06	6.0E+07	-1.1E+06	-3.1E+05	-3.2E+05	-2.4E+05	-4.3E+05	-6.0E+05	-4.1E+05	-3.3E+05
87.9	-4.4E+06	3.2E+07	-3.1E+07	-1.1E+07	6.1E+07	1.4E+07	-1.1E+07	6.7E+07	-8.5E+05	-1.6E+05	-5.8E+04	-3.8E+05	-5.8E+05	-6.2E+05	-5.6E+05	-1.9E+05
97.7	-7.0E+06	3.3E+07	-3.0E+07	-1.4E+07	6.8E+07	1.5E+07	-1.3E+07	7.4E+07	-7.5E+05	-2.0E+05	-1.8E+05	-4.0E+05	-7.5E+05	-5.3E+05	-4.1E+05	-1.3E+05
107.4	-9.4E+06	3.2E+07	-3.3E+07	-1.7E+07	7.3E+07	1.5E+07	-1.4E+07	8.4E+07	-7.9E+05	-3.4E+05	-2.5E+05	-3.5E+05	-7.7E+05	-5.5E+05	-4.5E+05	-1.5E+05
117.2	-1.5E+07	3.3E+07	-3.2E+07	-2.2E+07	8.0E+07	1.8E+07	-1.5E+07	9.1E+07	-4.7E+05	-3.2E+05	-9.5E+04	-3.2E+05	-8.5E+05	-4.2E+05	-3.9E+05	-2.0E+05
127.0	-2.1E+07	3.3E+07	-3.2E+07	-2.5E+07	8.7E+07	2.0E+07	-1.7E+07	1.0E+08	-7.0E+05	-3.7E+05	-3.0E+05	-3.9E+05	-1.1E+06	-5.6E+05	-4.3E+05	-2.5E+05
136.7	-2.7E+07	3.5E+07	-3.1E+07	-3.3E+07	9.4E+07	2.0E+07	-1.9E+07	1.1E+08	-3.6E+05	-4.2E+05	-2.3E+05	-3.9E+05	-9.1E+05	-3.3E+05	-3.4E+05	-6.4E+04

Table 118 Raw data for the test seal at PD=27.6 bar, ω=5 krpm, and inlet GVF=2% with the high-preswirl insert

Freq.	Re(H_{XX})	Re(H_{XY})	Re(H_{YX})	Re(H_{YY})	Im(H_{XX})	Im(H_{XY})	Im(H_{YX})	Im(H_{YY})	Re(eH_{XX})	Re(eH_{XY})	Re(eH_{YX})	Re(eH_{YY})	Im(eH_{XX})	Im(eH_{XY})	Im(eH_{YX})	Im(eH_{YY})
Hz	N/m	N/m	N/m	N/m	N/m	N/m	N/m	N/m	N/m	N/m	N/m	N/m	N/m	N/m	N/m	N/m
9.8	4.5E+06	3.3E+07	-3.5E+07	-2.0E+06	5.2E+06	1.0E+06	-6.2E+05	2.4E+06	-1.0E+06	-4.1E+05	-5.6E+05	-8.6E+05	-3.7E+05	-1.5E+05	-4.2E+05	-4.5E+05
19.5	4.0E+06	3.4E+07	-3.7E+07	-3.2E+06	1.5E+07	3.7E+06	-2.6E+06	1.4E+07	-1.2E+06	-1.3E+06	-1.0E+06	-1.0E+06	-1.3E+06	-5.7E+05	-6.3E+05	-9.5E+05
29.3	8.4E+06	3.3E+07	-3.9E+07	-1.6E+06	2.3E+07	4.0E+06	-5.0E+06	1.9E+07	-1.1E+06	-1.3E+06	-1.1E+06	-4.2E+05	-1.2E+06	-6.4E+05	-3.7E+05	-9.6E+05
39.1	5.6E+06	3.5E+07	-3.4E+07	-4.9E+06	3.0E+07	4.4E+06	-5.1E+06	3.0E+07	-1.3E+06	-1.1E+06	-1.1E+06	-5.1E+05	-9.5E+05	-1.0E+06	-4.5E+05	-9.1E+05
48.8	4.3E+06	3.5E+07	-3.5E+07	-7.8E+06	3.7E+07	6.2E+06	-8.9E+06	3.7E+07	-1.4E+06	-8.2E+05	-9.3E+05	-7.1E+05	-7.9E+05	-1.1E+06	-5.6E+05	-6.4E+05
58.6	3.5E+06	3.4E+07	-3.6E+07	-8.4E+06	4.3E+07	7.1E+06	-9.0E+06	4.7E+07	-1.4E+06	-5.3E+05	-6.8E+05	-6.8E+05	-5.9E+05	-1.1E+06	-6.8E+05	-5.3E+05
68.4	2.4E+06	3.4E+07	-3.8E+07	-9.4E+06	4.9E+07	8.2E+06	-9.7E+06	5.8E+07	-1.4E+06	-3.0E+05	-6.5E+05	-7.6E+05	-7.2E+05	-1.2E+06	-7.7E+05	-4.9E+05
78.1	1.8E+05	3.5E+07	-3.6E+07	-1.1E+07	5.7E+07	9.7E+06	-8.5E+06	6.4E+07	-1.4E+06	-5.7E+05	-9.5E+05	-6.6E+05	-6.0E+05	-1.2E+06	-4.8E+05	-7.1E+05
87.9	-3.8E+06	3.4E+07	-3.6E+07	-1.5E+07	6.3E+07	1.3E+07	-1.1E+07	7.1E+07	-1.1E+06	-3.3E+05	-2.6E+05	-8.3E+05	-8.5E+05	-9.7E+05	-9.8E+05	-5.0E+05
97.7	-6.9E+06	3.5E+07	-3.5E+07	-1.7E+07	6.9E+07	1.4E+07	-1.3E+07	7.8E+07	-9.7E+05	-4.8E+05	-3.7E+05	-8.4E+05	-1.0E+06	-8.8E+05	-8.9E+05	-3.8E+05
107.4	-1.1E+07	3.5E+07	-3.6E+07	-2.1E+07	7.6E+07	1.6E+07	-1.5E+07	8.8E+07	-8.6E+05	-4.6E+05	-2.8E+05	-8.7E+05	-9.3E+05	-8.5E+05	-5.9E+05	-2.8E+05
117.2	-1.6E+07	3.5E+07	-3.7E+07	-2.3E+07	8.3E+07	1.8E+07	-1.5E+07	9.6E+07	-6.7E+05	-5.8E+05	-1.6E+05	-6.7E+05	-1.1E+06	-7.5E+05	-8.1E+05	-5.0E+05
127.0	-2.1E+07	3.6E+07	-3.4E+07	-2.9E+07	9.0E+07	2.1E+07	-1.9E+07	1.0E+08	-7.6E+05	-6.9E+05	-3.3E+05	-9.1E+05	-1.4E+06	-7.5E+05	-9.4E+05	-6.1E+05
136.7	-2.7E+07	3.7E+07	-3.3E+07	-3.4E+07	9.7E+07	2.3E+07	-1.9E+07	1.1E+08	-4.1E+05	-7.4E+05	-1.0E+05	-8.9E+05	-1.3E+06	-6.5E+05	-8.1E+05	-3.2E+05

Table 119 Raw data for the test seal at PD=27.6 bar, ω=3 krpm, and inlet GVF=4% with the high-preswirl insert

Freq.	Re(H_{XX})	Re(H_{XY})	Re(H_{YX})	Re(H_{YY})	Im(H_{XX})	Im(H_{XY})	Im(H_{YX})	Im(H_{YY})	Re(eH_{XX})	Re(eH_{XY})	Re(eH_{YX})	Re(eH_{YY})	Im(eH_{XX})	Im(eH_{XY})	Im(eH_{YX})	Im(eH_{YY})
Hz	N/m	N/m	N/m	N/m	N/m	N/m	N/m	N/m	N/m	N/m	N/m	N/m	N/m	N/m	N/m	N/m
9.8	7.3E+06	2.9E+07	-3.0E+07	2.7E+05	6.5E+06	1.7E+06	1.4E+05	4.3E+06	-1.1E+06	-4.5E+05	-3.6E+05	-2.0E+05	-4.3E+05	-3.5E+05	-3.6E+05	-3.5E+05
19.5	5.9E+06	3.0E+07	-3.3E+07	-1.0E+06	1.4E+07	2.4E+06	-3.3E+06	1.5E+07	-9.5E+05	-1.1E+06	-3.0E+05	-2.3E+05	-9.5E+05	-3.3E+05	-3.1E+05	-3.8E+05
29.3	1.0E+07	2.7E+07	-3.6E+07	2.6E+06	2.2E+07	3.2E+06	-4.2E+06	2.1E+07	-8.6E+05	-8.2E+05	-4.1E+05	-1.6E+05	-8.3E+05	-6.5E+05	-3.0E+05	-3.7E+05
39.1	6.8E+06	2.9E+07	-3.2E+07	-5.6E+05	2.8E+07	4.5E+06	-4.8E+06	2.9E+07	-1.0E+06	-7.4E+05	-5.3E+05	-3.3E+05	-7.2E+05	-8.8E+05	-2.8E+05	-4.7E+05
48.8	5.2E+06	2.9E+07	-3.3E+07	-2.6E+06	3.5E+07	6.0E+06	-6.9E+06	3.6E+07	-1.0E+06	-4.0E+05	-3.6E+05	-4.5E+05	-5.4E+05	-8.2E+05	-4.6E+05	-3.1E+05
58.6	3.3E+06	2.9E+07	-3.3E+07	-5.6E+06	4.2E+07	7.4E+06	-7.7E+06	4.5E+07	-1.1E+06	-4.8E+05	-3.4E+05	-5.2E+05	-5.0E+05	-7.7E+05	-4.8E+05	-2.4E+05
68.4	2.1E+06	3.0E+07	-3.5E+07	-7.4E+06	4.9E+07	7.8E+06	-8.3E+06	5.4E+07	-9.1E+05	-2.8E+05	-2.2E+05	-4.1E+05	-6.0E+05	-8.6E+05	-4.1E+05	-1.7E+05
78.1	1.2E+05	3.0E+07	-3.4E+07	-8.4E+06	5.6E+07	1.0E+07	-8.1E+06	6.1E+07	-1.1E+06	-1.9E+05	-2.6E+05	-3.9E+05	-5.9E+05	-7.8E+05	-3.3E+05	-2.5E+05
87.9	-3.0E+06	3.0E+07	-3.4E+07	-1.2E+07	6.3E+07	1.2E+07	-8.6E+06	6.8E+07	-1.1E+06	-2.1E+05	-1.7E+05	-4.8E+05	-6.9E+05	-8.4E+05	-4.4E+05	-2.4E+05
97.7	-5.8E+06	3.1E+07	-3.3E+07	-1.4E+07	7.0E+07	1.3E+07	-9.7E+06	7.5E+07	-8.3E+05	-2.5E+05	-1.0E+05	-3.4E+05	-9.0E+05	-7.5E+05	-6.4E+05	-2.1E+05
107.4	-8.5E+06	3.1E+07	-3.5E+07	-1.7E+07	7.6E+07	1.4E+07	-1.2E+07	8.4E+07	-6.3E+05	-2.6E+05	-2.8E+05	-5.1E+05	-8.6E+05	-6.2E+05	-4.5E+05	-1.5E+05
117.2	-1.5E+07	3.0E+07	-3.5E+07	-2.2E+07	8.4E+07	1.7E+07	-1.2E+07	9.3E+07	-6.1E+05	-4.2E+05	-1.3E+05	-3.3E+05	-8.0E+05	-5.4E+05	-2.6E+05	-2.5E+05
127.0	-1.9E+07	3.2E+07	-3.4E+07	-2.6E+07	9.1E+07	1.8E+07	-1.4E+07	1.0E+08	-6.8E+05	-4.8E+05	-2.4E+05	-7.0E+05	-1.0E+06	-6.6E+05	-5.0E+05	-2.9E+05
136.7	-2.3E+07	3.3E+07	-3.3E+07	-3.1E+07	1.0E+08	1.9E+07	-1.4E+07	1.1E+08	-4.6E+05	-4.9E+05	-2.1E+05	-3.6E+05	-1.0E+06	-4.8E+05	-4.0E+05	-2.5E+05

Table 120 Raw data for the test seal at PD=27.6 bar, ω=4 krpm, and inlet GVF=4% with the high-preswirl insert

Freq.	Re(H_{XX})	Re(H_{XY})	Re(H_{YX})	Re(H_{YY})	Im(H_{XX})	Im(H_{XY})	Im(H_{YX})	Im(H_{YY})	Re(eH_{XX})	Re(eH_{XY})	Re(eH_{YX})	Re(eH_{YY})	Im(eH_{XX})	Im(eH_{XY})	Im(eH_{YX})	Im(eH_{YY})
Hz	N/m	N/m	N/m	N/m	N/m	N/m	N/m	N/m	N/m	N/m	N/m	N/m	N/m	N/m	N/m	N/m
9.8	8.8E+06	2.9E+07	-3.0E+07	-3.8E+05	5.9E+06	1.8E+06	-9.1E+05	4.0E+06	-2.9E+05	-2.1E+05	-3.7E+05	-3.5E+05	-1.8E+05	-1.9E+05	-2.3E+05	-2.9E+05
19.5	7.1E+06	2.9E+07	-3.2E+07	-1.4E+06	1.3E+07	2.2E+06	-3.3E+06	1.4E+07	-2.8E+05	-5.1E+05	-3.9E+05	-3.1E+05	-4.8E+05	-2.0E+05	-1.8E+05	-3.1E+05
29.3	1.1E+07	2.7E+07	-3.5E+07	2.0E+06	2.2E+07	3.5E+06	-3.8E+06	2.2E+07	-7.5E+05	-4.7E+05	-4.0E+05	-1.4E+05	-3.1E+05	-3.4E+05	-3.2E+05	-3.4E+05
39.1	6.8E+06	2.9E+07	-3.1E+07	-9.9E+05	2.8E+07	5.2E+06	-4.7E+06	3.0E+07	-7.5E+05	-3.8E+05	-3.1E+05	-1.9E+05	-1.8E+05	-4.0E+05	-2.1E+05	-2.7E+05
48.8	5.3E+06	2.9E+07	-3.3E+07	-3.2E+06	3.6E+07	6.9E+06	-6.9E+06	3.7E+07	-8.6E+05	-3.0E+05	-3.1E+05	-2.6E+05	-2.0E+05	-4.7E+05	-3.1E+05	-2.3E+05
58.6	3.8E+06	2.9E+07	-3.3E+07	-5.6E+06	4.2E+07	7.7E+06	-7.6E+06	4.6E+07	-7.7E+05	-2.3E+05	-2.4E+05	-2.3E+05	-1.7E+05	-4.1E+05	-4.0E+05	-2.1E+05
68.4	2.7E+06	3.0E+07	-3.4E+07	-7.5E+06	4.9E+07	8.0E+06	-8.6E+06	5.5E+07	-7.0E+05	-1.9E+05	-2.5E+05	-2.1E+05	-3.8E+05	-4.8E+05	-3.1E+05	-2.4E+05
78.1	2.3E+04	2.9E+07	-3.4E+07	-8.0E+06	5.6E+07	1.1E+07	-7.9E+06	6.3E+07	-8.8E+05	-1.5E+05	-1.9E+05	-1.7E+05	-4.5E+05	-4.9E+05	-4.0E+05	-2.9E+05
87.9	-3.2E+06	3.0E+07	-3.3E+07	-1.1E+07	6.4E+07	1.3E+07	-8.5E+06	7.0E+07	-6.5E+05	-1.0E+05	-9.4E+04	-2.2E+05	-4.7E+05	-4.1E+05	-3.9E+05	-1.5E+05
97.7	-5.6E+06	3.1E+07	-3.2E+07	-1.3E+07	7.0E+07	1.3E+07	-1.0E+07	7.7E+07	-5.4E+05	-1.4E+05	-1.4E+05	-2.1E+05	-6.2E+05	-3.9E+05	-3.3E+05	-1.1E+05
107.4	-8.1E+06	3.1E+07	-3.4E+07	-1.7E+07	7.7E+07	1.5E+07	-1.2E+07	8.6E+07	-3.9E+05	-1.6E+05	-8.8E+04	-2.2E+05	-6.3E+05	-3.0E+05	-3.4E+05	-9.7E+04
117.2	-1.4E+07	3.1E+07	-3.5E+07	-2.1E+07	8.4E+07	1.7E+07	-1.2E+07	9.4E+07	-3.2E+05	-1.8E+05	-2.2E+05	-3.0E+05	-6.6E+05	-2.5E+05	-3.1E+05	-1.4E+05
127.0	-1.8E+07	3.2E+07	-3.3E+07	-2.6E+07	9.2E+07	1.9E+07	-1.4E+07	1.0E+08	-4.7E+05	-2.4E+05	-2.0E+05	-2.7E+05	-7.2E+05	-4.2E+05	-4.0E+05	-1.8E+05
136.7	-2.3E+07	3.3E+07	-3.2E+07	-3.0E+07	1.0E+08	2.0E+07	-1.5E+07	1.1E+08	-2.5E+05	-3.3E+05	-1.6E+05	-2.6E+05	-7.6E+05	-2.0E+05	-3.7E+05	-2.7E+05

Table 121 Raw data for the test seal at PD=27.6 bar, ω=5 krpm, and inlet GVF=4% with the high-preswirl insert

Freq.	Re(H_{XX})	Re(H_{XY})	Re(H_{YX})	Re(H_{YY})	Im(H_{XX})	Im(H_{XY})	Im(H_{YX})	Im(H_{YY})	Re(eH_{XX})	Re(eH_{XY})	Re(eH_{YX})	Re(eH_{YY})	Im(eH_{XX})	Im(eH_{XY})	Im(eH_{YX})	Im(eH_{YY})
Hz	N/m	N/m	N/m	N/m	N/m	N/m	N/m	N/m	N/m	N/m	N/m	N/m	N/m	N/m	N/m	N/m
9.8	-5.6E+06	3.3E+07	-3.5E+07	1.3E+05	4.1E+06	2.7E+06	1.1E+07	2.0E+06	-9.0E+05	-2.8E+05	-6.1E+05	-4.9E+05	-9.9E+05	-3.9E+05	-2.6E+06	-6.5E+05
19.5	-1.3E+07	3.5E+07	-4.0E+07	-2.6E+06	1.5E+07	1.0E+07	2.6E+05	1.5E+07	-1.7E+06	-3.1E+05	-3.2E+05	-4.6E+05	-4.0E+05	-1.3E+06	-3.6E+05	-3.0E+05
29.3	-9.4E+05	4.2E+07	-3.3E+07	-1.6E+06	3.6E+07	2.5E+06	2.0E+05	1.4E+07	-9.6E+05	-1.8E+06	-1.4E+06	-2.6E+05	-1.9E+06	-3.2E+05	-3.8E+05	-1.2E+06
39.1	1.4E+06	4.1E+07	-3.3E+07	-7.9E+06	4.1E+07	-3.1E+05	-4.4E+06	2.6E+07	-6.1E+05	-1.4E+06	-8.2E+05	-4.9E+05	-1.6E+06	-1.0E+06	-2.4E+05	-7.1E+05
48.8	1.4E+06	3.8E+07	-3.5E+07	-1.2E+07	4.5E+07	1.0E+06	-8.2E+06	3.5E+07	-7.5E+05	-8.2E+05	-8.1E+05	-7.7E+05	-9.5E+05	-9.4E+05	-4.4E+05	-6.7E+05
58.6	8.0E+05	3.6E+07	-3.6E+07	-1.6E+07	5.0E+07	2.5E+06	-1.1E+07	4.6E+07	-7.5E+05	-6.3E+05	-7.9E+05	-1.2E+06	-6.2E+05	-8.8E+05	-7.5E+05	-6.7E+05
68.4	8.7E+04	3.2E+07	-4.2E+07	-1.8E+07	5.4E+07	3.8E+06	-1.2E+07	6.0E+07	-7.7E+05	-1.0E+05	-2.7E+05	-7.4E+05	-2.3E+05	-9.3E+05	-6.1E+05	-4.8E+05
78.1	-1.2E+06	3.2E+07	-4.1E+07	-1.9E+07	6.2E+07	4.0E+06	-1.1E+07	6.7E+07	-1.6E+06	-8.2E+05	-7.3E+05	-2.2E+06	-4.6E+05	-1.8E+06	-1.5E+06	-7.4E+05
87.9	-5.8E+06	3.1E+07	-4.1E+07	-1.7E+07	6.8E+07	8.2E+06	-8.0E+06	7.5E+07	-7.0E+05	-6.0E+05	-4.3E+05	-2.9E+05	-4.6E+05	-6.7E+05	-4.4E+05	-7.5E+05
97.7	-8.1E+06	3.2E+07	-3.8E+07	-1.7E+07	7.6E+07	1.0E+07	-7.1E+06	8.2E+07	-4.8E+05	-3.8E+05	-4.2E+05	-2.1E+05	-4.1E+05	-5.9E+05	-4.2E+05	-8.0E+05
107.4	-1.2E+07	3.5E+07	-3.9E+07	-2.3E+07	8.4E+07	1.2E+07	-1.2E+07	8.7E+07	-5.3E+05	-2.2E+05	-3.8E+05	-2.5E+05	-5.7E+05	-6.2E+05	-1.7E+05	-4.6E+05
117.2	-1.7E+07	3.4E+07	-4.2E+07	-2.4E+07	9.1E+07	1.7E+07	-9.7E+06	1.0E+08	-2.9E+05	-1.5E+05	-3.0E+05	-5.4E+05	-3.6E+05	-3.6E+05	-2.4E+05	-4.2E+05
127.0	-2.0E+07	3.4E+07	-3.9E+07	-3.4E+07	1.0E+08	1.5E+07	-1.4E+07	1.1E+08	-4.9E+05	-4.1E+05	-1.8E+05	-1.4E+06	-4.7E+05	-1.0E+06	-5.7E+05	-4.2E+05
136.7	-2.4E+07	3.9E+07	-3.7E+07	-3.4E+07	1.1E+08	1.8E+07	-1.1E+07	1.1E+08	-3.8E+05	-3.5E+05	-1.6E+05	-7.2E+05	-3.2E+05	-9.5E+05	-3.2E+05	-1.5E+05

Table 122 Raw data for the test seal at PD=27.6 bar, ω=3 krpm, and inlet GVF=6% with the high-preswirl insert

Freq.	Re(H_{XX})	Re(H_{XY})	Re(H_{YX})	Re(H_{YY})	Im(H_{XX})	Im(H_{XY})	Im(H_{YX})	Im(H_{YY})	Re(eH_{XX})	Re(eH_{XY})	Re(eH_{YX})	Re(eH_{YY})	Im(eH_{XX})	Im(eH_{XY})	Im(eH_{YX})	Im(eH_{YY})
Hz	N/m	N/m	N/m	N/m	N/m	N/m	N/m	N/m	N/m	N/m	N/m	N/m	N/m	N/m	N/m	N/m
9.8	3.2E+06	2.8E+07	-3.1E+07	-2.2E+06	6.3E+06	7.7E+05	-5.5E+05	5.0E+06	-1.2E+06	-9.3E+05	-3.8E+05	-4.0E+05	-6.0E+05	-4.7E+05	-2.3E+05	-3.6E+05
19.5	2.5E+06	2.8E+07	-3.4E+07	-2.9E+06	1.4E+07	1.7E+06	-2.4E+06	1.6E+07	-1.1E+06	-1.9E+06	-7.1E+05	-4.5E+05	-1.8E+06	-4.8E+05	-2.6E+05	-5.9E+05
29.3	6.6E+06	2.6E+07	-3.7E+07	2.1E+06	2.2E+07	4.2E+06	-2.5E+06	2.2E+07	-1.5E+06	-1.3E+06	-7.7E+05	-3.4E+05	-1.2E+06	-7.5E+05	-3.2E+05	-5.7E+05
39.1	1.1E+06	2.8E+07	-3.3E+07	-3.5E+06	3.0E+07	5.6E+06	-4.1E+06	3.1E+07	-1.5E+06	-1.0E+06	-6.9E+05	-4.7E+05	-8.1E+05	-9.3E+05	-3.0E+05	-5.4E+05
48.8	4.2E+05	2.9E+07	-3.4E+07	-5.3E+06	3.8E+07	6.7E+06	-6.1E+06	4.0E+07	-1.7E+06	-8.8E+05	-6.3E+05	-5.3E+05	-7.9E+05	-9.5E+05	-4.7E+05	-4.0E+05
58.6	-9.8E+05	2.9E+07	-3.4E+07	-6.4E+06	4.5E+07	7.9E+06	-5.8E+06	4.7E+07	-1.6E+06	-6.2E+05	-6.4E+05	-6.7E+05	-4.7E+05	-9.8E+05	-6.0E+05	-6.6E+05
68.4	-2.7E+06	3.0E+07	-3.6E+07	-7.6E+06	5.2E+07	9.4E+06	-5.9E+06	5.6E+07	-1.7E+06	-3.1E+05	-2.7E+05	-3.7E+05	-6.0E+05	-1.0E+06	-6.3E+05	-2.9E+05
78.1	-5.4E+06	3.0E+07	-3.5E+07	-8.7E+06	6.1E+07	1.1E+07	-6.4E+06	6.4E+07	-1.8E+06	-2.0E+05	-2.1E+05	-6.1E+05	-8.0E+05	-1.2E+06	-5.3E+05	-2.4E+05
87.9	-6.6E+06	3.0E+07	-3.5E+07	-1.1E+07	6.8E+07	1.2E+07	-6.4E+06	7.3E+07	-1.3E+06	-3.9E+05	-1.8E+05	-4.5E+05	-7.9E+05	-9.7E+05	-5.5E+05	-4.6E+05
97.7	-8.5E+06	3.1E+07	-3.3E+07	-1.3E+07	7.6E+07	1.3E+07	-7.3E+06	8.0E+07	-1.1E+06	-3.9E+05	-3.4E+05	-4.1E+05	-7.6E+05	-8.0E+05	-5.9E+05	-3.7E+05
107.4	-1.1E+07	3.1E+07	-3.4E+07	-1.8E+07	8.4E+07	1.4E+07	-1.0E+07	8.9E+07	-1.4E+06	-2.9E+05	-3.4E+05	-7.7E+05	-9.4E+05	-8.8E+05	-4.8E+05	-8.6E+04
117.2	-1.4E+07	3.2E+07	-3.5E+07	-1.9E+07	9.1E+07	1.6E+07	-9.1E+06	9.8E+07	-1.1E+06	-4.0E+05	-2.0E+05	-4.2E+05	-1.3E+06	-7.7E+05	-3.6E+05	-1.8E+05
127.0	-1.9E+07	3.3E+07	-3.5E+07	-2.5E+07	9.9E+07	1.7E+07	-1.2E+07	1.1E+08	-9.0E+05	-6.7E+05	-2.4E+05	-1.1E+06	-1.4E+06	-7.5E+05	-5.1E+05	-4.5E+05
136.7	-2.2E+07	3.5E+07	-3.3E+07	-2.9E+07	1.1E+08	1.8E+07	-1.1E+07	1.1E+08	-4.5E+05	-5.3E+05	-2.2E+05	-4.7E+05	-1.2E+06	-5.0E+05	-3.8E+05	-1.3E+05

Table 123 Raw data for the test seal at PD=27.6 bar, ω=4 krpm, and inlet GVF=6% with the high-preswirl insert

Freq.	Re(H_{XX})	Re(H_{XY})	Re(H_{YX})	Re(H_{YY})	Im(H_{XX})	Im(H_{XY})	Im(H_{YX})	Im(H_{YY})	Re(eH_{XX})	Re(eH_{XY})	Re(eH_{YX})	Re(eH_{YY})	Im(eH_{XX})	Im(eH_{XY})	Im(eH_{YX})	Im(eH_{YY})
Hz	N/m	N/m	N/m	N/m	N/m	N/m	N/m	N/m	N/m	N/m	N/m	N/m	N/m	N/m	N/m	N/m
9.8	-6.8E+05	2.9E+07	-3.1E+07	-2.8E+06	7.5E+06	1.1E+06	-2.2E+05	5.2E+06	-3.6E+05	-5.5E+05	-2.2E+05	-1.7E+05	-4.0E+05	-3.6E+05	-2.0E+05	-2.7E+05
19.5	-2.3E+06	3.4E+07	-3.2E+07	-2.6E+06	2.0E+07	3.6E+06	-1.3E+06	1.5E+07	-7.0E+05	-1.3E+06	-2.5E+05	-3.1E+05	-1.2E+06	-3.0E+05	-2.7E+05	-2.2E+05
29.3	5.8E+06	2.8E+07	-3.6E+07	1.1E+06	2.5E+07	2.8E+06	-2.4E+06	2.1E+07	-8.3E+05	-7.4E+05	-3.3E+05	-1.7E+05	-7.4E+05	-4.1E+05	-1.8E+05	-2.4E+05
39.1	1.1E+06	3.0E+07	-3.1E+07	-5.0E+06	3.2E+07	3.3E+06	-4.4E+06	2.9E+07	-8.0E+05	-4.8E+05	-3.1E+05	-1.3E+05	-4.0E+05	-5.2E+05	-1.5E+05	-2.7E+05
48.8	5.6E+05	3.0E+07	-3.4E+07	-7.0E+06	3.9E+07	4.7E+06	-6.7E+06	3.9E+07	-9.0E+05	-4.6E+05	-3.6E+05	-2.4E+05	-4.7E+05	-4.7E+05	-3.8E+05	-2.9E+05
58.6	-8.6E+05	3.1E+07	-3.3E+07	-8.2E+06	4.7E+07	5.7E+06	-6.1E+06	4.6E+07	-8.0E+05	-4.6E+05	-3.8E+05	-3.5E+05	-3.7E+05	-5.3E+05	-3.3E+05	-3.9E+05
68.4	-2.8E+06	3.0E+07	-3.5E+07	-7.5E+06	5.4E+07	8.1E+06	-5.3E+06	5.6E+07	-1.0E+06	-1.6E+05	-2.3E+05	-1.8E+05	-2.7E+05	-4.8E+05	-4.5E+05	-2.0E+05
78.1	-5.3E+06	3.0E+07	-3.5E+07	-9.9E+06	6.2E+07	9.0E+06	-6.9E+06	6.5E+07	-7.9E+05	-1.9E+05	-1.1E+05	-2.3E+05	-2.2E+05	-4.0E+05	-2.3E+05	-2.0E+05
87.9	-6.2E+06	2.9E+07	-3.5E+07	-1.2E+07	6.8E+07	1.0E+07	-7.1E+06	7.5E+07	-7.8E+05	-2.4E+05	-1.5E+05	-2.0E+05	-4.2E+05	-4.6E+05	-3.5E+05	-2.5E+05
97.7	-7.9E+06	3.0E+07	-3.3E+07	-1.3E+07	7.6E+07	1.1E+07	-6.9E+06	8.1E+07	-7.3E+05	-2.5E+05	-1.6E+05	-1.1E+05	-3.6E+05	-3.8E+05	-2.6E+05	-2.3E+05
107.4	-1.0E+07	3.1E+07	-3.4E+07	-1.9E+07	8.4E+07	1.2E+07	-1.1E+07	8.9E+07	-8.0E+05	-1.2E+05	-1.9E+05	-3.4E+05	-5.0E+05	-5.0E+05	-2.0E+05	-1.3E+05
117.2	-1.4E+07	3.1E+07	-3.5E+07	-2.1E+07	9.2E+07	1.5E+07	-9.1E+06	9.8E+07	-5.1E+05	-2.1E+05	-1.6E+05	-1.6E+05	-7.6E+05	-3.6E+05	-2.5E+05	-7.5E+04
127.0	-1.9E+07	3.2E+07	-3.4E+07	-2.8E+07	1.0E+08	1.6E+07	-1.3E+07	1.1E+08	-7.2E+05	-3.8E+05	-2.5E+05	-3.8E+05	-6.9E+05	-4.6E+05	-3.8E+05	-3.2E+05
136.7	-2.2E+07	3.4E+07	-3.2E+07	-3.1E+07	1.1E+08	1.7E+07	-1.2E+07	1.1E+08	-3.0E+05	-2.3E+05	-2.4E+05	-3.3E+05	-6.7E+05	-3.2E+05	-2.3E+05	-2.1E+05

Table 124 Raw data for the test seal at PD=27.6 bar, ω=3 krpm, and inlet GVF=8% with the high-preswirl insert

Freq.	Re(H_{XX})	Re(H_{XY})	Re(H_{YX})	Re(H_{YY})	Im(H_{XX})	Im(H_{XY})	Im(H_{YX})	Im(H_{YY})	Re(eH_{XX})	Re(eH_{XY})	Re(eH_{YX})	Re(eH_{YY})	Im(eH_{XX})	Im(eH_{XY})	Im(eH_{YX})	Im(eH_{YY})
Hz	N/m	N/m	N/m	N/m	N/m	N/m	N/m	N/m	N/m	N/m	N/m	N/m	N/m	N/m	N/m	N/m
9.8	-7.4E+06	2.5E+07	-3.3E+07	-1.6E+06	6.6E+06	1.6E+05	-1.5E+05	7.0E+06	-2.5E+05	-3.2E+05	-2.2E+05	-2.7E+05	-1.5E+05	-3.6E+05	-1.6E+05	-1.8E+05
19.5	-1.2E+07	2.9E+07	-3.4E+07	-3.1E+06	1.7E+07	5.7E+06	-1.1E+06	1.5E+07	-6.4E+05	-4.4E+05	-2.3E+05	-3.8E+05	-4.0E+05	-5.4E+05	-3.5E+05	-1.9E+05
29.3	-2.6E+06	2.6E+07	-3.7E+07	-2.0E+05	2.4E+07	3.5E+06	-1.2E+06	2.1E+07	-2.5E+05	-4.5E+05	-3.8E+05	-8.5E+04	-5.2E+05	-9.3E+04	-1.2E+05	-2.9E+05
39.1	-7.1E+06	3.1E+07	-3.2E+07	-6.7E+06	3.4E+07	4.3E+06	-3.6E+06	2.9E+07	-5.0E+05	-4.2E+05	-3.2E+05	-1.1E+05	-4.0E+05	-3.1E+05	-9.0E+04	-2.6E+05
48.8	-6.7E+06	2.8E+07	-3.7E+07	-9.0E+06	3.8E+07	4.2E+06	-5.6E+06	4.1E+07	-2.6E+05	-2.7E+05	-2.6E+05	-1.7E+05	-3.0E+05	-2.1E+05	-1.3E+05	-1.7E+05
58.6	-8.4E+06	3.1E+07	-3.5E+07	-9.8E+06	4.9E+07	5.7E+06	-4.6E+06	4.7E+07	-4.7E+05	-4.1E+05	-2.7E+05	-2.3E+05	-3.5E+05	-2.5E+05	-1.7E+05	-1.9E+05
68.4	-1.4E+07	2.9E+07	-3.7E+07	-7.9E+06	5.6E+07	1.1E+07	-2.6E+06	5.6E+07	-4.3E+05	-2.4E+05	-2.1E+05	-2.3E+05	-2.2E+05	-1.6E+05	-2.5E+05	-2.5E+05
78.1	-1.3E+07	3.0E+07	-3.6E+07	-1.2E+07	6.6E+07	9.8E+06	-6.2E+06	6.5E+07	-5.4E+05	-2.6E+05	-2.6E+05	-2.2E+05	-2.5E+05	-3.0E+05	-2.7E+05	-1.5E+05
87.9	-1.2E+07	2.8E+07	-3.6E+07	-1.3E+07	7.4E+07	9.7E+06	-4.5E+06	7.6E+07	-5.1E+05	-1.2E+05	-1.9E+05	-1.3E+05	-1.4E+05	-2.6E+05	-1.0E+05	-1.8E+05
97.7	-1.3E+07	2.9E+07	-3.4E+07	-1.3E+07	8.1E+07	1.1E+07	-4.0E+06	8.3E+07	-3.6E+05	-1.3E+05	-2.5E+05	-1.6E+05	-1.6E+05	-2.8E+05	-2.4E+05	-1.1E+05
107.4	-1.8E+07	3.2E+07	-3.4E+07	-2.0E+07	9.1E+07	1.3E+07	-8.7E+06	8.9E+07	-5.8E+05	-2.3E+05	-2.8E+05	-2.3E+05	-2.1E+05	-3.2E+05	-1.5E+05	-1.5E+05
117.2	-2.0E+07	3.2E+07	-3.5E+07	-2.1E+07	1.0E+08	1.4E+07	-6.3E+06	9.9E+07	-4.3E+05	-1.0E+05	-1.4E+05	-1.1E+05	-2.0E+05	-2.9E+05	-2.3E+05	-1.1E+05
127.0	-2.2E+07	3.4E+07	-3.6E+07	-2.7E+07	1.1E+08	1.5E+07	-9.8E+06	1.1E+08	-3.7E+05	-6.1E+05	-2.6E+05	-3.2E+05	-3.1E+05	-4.7E+05	-2.2E+05	-4.6E+05
136.7	-2.2E+07	3.5E+07	-3.3E+07	-2.9E+07	1.2E+08	1.5E+07	-9.8E+06	1.1E+08	-2.0E+05	-2.6E+05	-1.9E+05	-3.2E+05	-3.1E+05	-3.4E+05	-1.7E+05	-1.8E+05

Table 125 Raw data for the test seal at PD=27.6 bar, ω=4 krpm, and inlet GVF=8% with the high-preswirl insert

Freq.	Re(H_{XX})	Re(H_{XY})	Re(H_{YX})	Re(H_{YY})	Im(H_{XX})	Im(H_{XY})	Im(H_{YX})	Im(H_{YY})	Re(eH_{XX})	Re(eH_{XY})	Re(eH_{YX})	Re(eH_{YY})	Im(eH_{XX})	Im(eH_{XY})	Im(eH_{YX})	Im(eH_{YY})
Hz	N/m	N/m	N/m	N/m	N/m	N/m	N/m	N/m	N/m	N/m	N/m	N/m	N/m	N/m	N/m	N/m
9.8	-7.0E+06	2.5E+07	-3.5E+07	-2.8E+06	6.9E+06	1.6E+04	-7.0E+05	7.6E+06	-1.6E+05	-3.5E+05	-3.2E+05	-1.6E+05	-1.6E+05	-2.5E+05	-1.5E+05	-2.0E+05
19.5	-1.2E+07	2.9E+07	-3.3E+07	-4.5E+06	1.7E+07	5.9E+06	-1.3E+06	1.5E+07	-8.9E+05	-4.4E+05	-2.4E+05	-4.0E+05	-4.6E+05	-8.5E+05	-3.9E+05	-2.1E+05
29.3	-3.3E+06	2.6E+07	-3.7E+07	-1.5E+06	2.4E+07	3.5E+06	-1.1E+06	2.1E+07	-3.4E+05	-6.3E+05	-4.6E+05	-1.0E+05	-7.3E+05	-1.7E+05	-1.1E+05	-3.7E+05
39.1	-7.9E+06	3.1E+07	-3.2E+07	-7.3E+06	3.4E+07	4.3E+06	-3.4E+06	3.0E+07	-5.9E+05	-4.9E+05	-2.8E+05	-1.2E+05	-4.9E+05	-3.4E+05	-1.8E+05	-2.2E+05
48.8	-6.8E+06	2.8E+07	-3.7E+07	-1.0E+07	3.8E+07	3.8E+06	-6.1E+06	4.2E+07	-4.5E+05	-2.9E+05	-3.3E+05	-2.0E+05	-3.8E+05	-3.2E+05	-3.0E+05	-2.3E+05
58.6	-9.4E+06	3.1E+07	-3.6E+07	-9.9E+06	4.9E+07	6.1E+06	-4.2E+06	4.8E+07	-6.0E+05	-3.8E+05	-2.9E+05	-1.9E+05	-3.3E+05	-2.7E+05	-2.1E+05	-1.8E+05
68.4	-1.4E+07	2.9E+07	-3.7E+07	-7.4E+06	5.6E+07	1.1E+07	-1.5E+06	5.6E+07	-7.7E+05	-3.1E+05	-2.0E+05	-1.7E+05	-2.0E+05	-3.0E+05	-3.3E+05	-2.7E+05
78.1	-1.4E+07	3.0E+07	-3.5E+07	-1.1E+07	6.7E+07	9.8E+06	-5.7E+06	6.5E+07	-6.6E+05	-3.9E+05	-3.4E+05	-2.1E+05	-2.6E+05	-3.4E+05	-2.1E+05	-3.3E+05
87.9	-1.2E+07	2.8E+07	-3.6E+07	-1.4E+07	7.4E+07	9.1E+06	-4.8E+06	7.7E+07	-5.4E+05	-6.2E+04	-1.3E+05	-8.8E+04	-1.6E+05	-2.8E+05	-1.2E+05	-1.3E+05
97.7	-1.3E+07	2.8E+07	-3.4E+07	-1.3E+07	8.1E+07	1.0E+07	-3.9E+06	8.4E+07	-3.9E+05	-1.4E+05	-1.5E+05	-1.3E+05	-1.5E+05	-2.4E+05	-1.4E+05	-1.8E+05
107.4	-1.9E+07	3.2E+07	-3.4E+07	-2.1E+07	9.0E+07	1.2E+07	-9.0E+06	9.0E+07	-1.1E+06	-1.9E+05	-2.2E+05	-2.7E+05	-2.2E+05	-5.6E+05	-1.4E+05	-1.7E+05
117.2	-2.0E+07	3.2E+07	-3.4E+07	-2.1E+07	1.0E+08	1.4E+07	-6.3E+06	9.9E+07	-5.7E+05	-7.0E+04	-2.2E+05	-2.4E+05	-2.8E+05	-2.7E+05	-2.0E+05	-1.0E+05
127.0	-2.3E+07	3.3E+07	-3.6E+07	-2.8E+07	1.1E+08	1.4E+07	-1.0E+07	1.1E+08	-6.5E+05	-3.5E+05	-2.3E+05	-3.6E+05	-4.6E+05	-6.9E+05	-1.8E+05	-3.1E+05
136.7	-2.3E+07	3.5E+07	-3.3E+07	-3.0E+07	1.2E+08	1.6E+07	-1.0E+07	1.2E+08	-6.0E+05	-2.3E+05	-2.2E+05	-3.2E+05	-3.9E+05	-3.8E+05	-2.2E+05	-1.7E+05

Table 126 Raw data for the test seal at PD=27.6 bar, ω=3 krpm, and inlet GVF=10% with the high-preswirl insert

Freq.	Re(H_{XX})	Re(H_{XY})	Re(H_{YX})	Re(H_{YY})	Im(H_{XX})	Im(H_{XY})	Im(H_{YX})	Im(H_{YY})	Re(eH_{XX})	Re(eH_{XY})	Re(eH_{YX})	Re(eH_{YY})	Im(eH_{XX})	Im(eH_{XY})	Im(eH_{YX})	Im(eH_{YY})
Hz	N/m	N/m	N/m	N/m	N/m	N/m	N/m	N/m	N/m	N/m	N/m	N/m	N/m	N/m	N/m	N/m
9.8	-3.8E+06	2.6E+07	-4.0E+07	3.2E+06	3.9E+06	5.7E+05	8.3E+06	6.1E+06	-2.9E+05	-6.8E+05	-3.6E+05	-6.4E+05	-7.5E+05	-3.5E+05	-9.1E+05	-3.6E+05
19.5	-1.3E+07	3.3E+07	-3.2E+07	-4.5E+06	1.9E+07	4.0E+06	5.4E+05	1.4E+07	-6.3E+05	-1.0E+06	-2.7E+05	-5.4E+05	-9.4E+05	-6.2E+05	-5.2E+05	-2.5E+05
29.3	-4.9E+06	2.3E+07	-3.9E+07	-3.8E+06	1.7E+07	1.3E+06	-5.0E+05	2.3E+07	-6.9E+05	-5.7E+05	-3.3E+05	-1.9E+05	-7.4E+05	-6.4E+05	-1.8E+05	-2.6E+05
39.1	-1.4E+07	2.8E+07	-3.3E+07	-7.1E+06	2.9E+07	5.5E+06	-8.7E+05	3.1E+07	-2.2E+05	-5.2E+05	-1.4E+05	-1.3E+05	-6.6E+05	-1.3E+05	-1.5E+05	-1.1E+05
48.8	-1.2E+07	2.6E+07	-3.8E+07	-1.1E+07	3.6E+07	3.9E+06	-3.9E+06	4.2E+07	-4.6E+05	-3.5E+05	-2.8E+05	-2.3E+05	-3.6E+05	-2.5E+05	-3.1E+05	-3.3E+05
58.6	-1.5E+07	2.8E+07	-3.7E+07	-1.2E+07	4.5E+07	6.1E+06	-6.2E+06	5.2E+07	-3.9E+05	-1.6E+05	-3.6E+05	-2.8E+05	-1.7E+05	-3.1E+05	-2.6E+05	-2.3E+05
68.4	-2.1E+07	2.6E+07	-4.0E+07	-7.3E+06	5.1E+07	1.1E+07	-2.0E+06	6.1E+07	-3.2E+05	-1.8E+05	-2.9E+05	-3.0E+05	-2.4E+05	-3.1E+05	-4.6E+05	-4.4E+05
78.1	-1.9E+07	3.0E+07	-3.4E+07	-8.4E+06	6.6E+07	1.2E+07	-3.4E+06	6.5E+07	-2.4E+05	-2.7E+05	-1.7E+05	-2.9E+05	-4.5E+05	-2.1E+05	-2.9E+05	-2.0E+05
87.9	-2.0E+07	2.9E+07	-3.7E+07	-1.5E+07	7.5E+07	1.1E+07	-5.5E+06	7.6E+07	-4.4E+05	-2.7E+05	-9.7E+04	-1.6E+05	-4.1E+05	-1.3E+05	-3.5E+05	-1.8E+05
97.7	-2.2E+07	2.8E+07	-4.0E+07	-1.4E+07	8.2E+07	1.0E+07	-2.4E+06	8.9E+07	-5.2E+05	-1.9E+05	-2.6E+05	-2.3E+05	-2.8E+05	-2.7E+05	-3.1E+05	-1.0E+05
107.4	-2.4E+07	3.4E+07	-3.4E+07	-2.3E+07	9.3E+07	1.3E+07	-8.6E+06	9.1E+07	-5.6E+05	-2.2E+05	-3.1E+05	-2.0E+05	-2.9E+05	-2.4E+05	-7.5E+04	-1.7E+05
117.2	-2.9E+07	3.2E+07	-3.8E+07	-2.1E+07	1.0E+08	1.6E+07	-7.2E+06	1.0E+08	-4.2E+05	-1.8E+05	-2.9E+05	-2.1E+05	-4.0E+05	-1.2E+05	-2.1E+05	-2.4E+05
127.0	-2.6E+07	3.1E+07	-3.7E+07	-2.4E+07	1.1E+08	1.4E+07	-9.9E+06	1.1E+08	-3.4E+05	-1.9E+05	-2.1E+05	-2.8E+05	-2.5E+05	-3.2E+05	-2.0E+05	-2.7E+05
136.7	-2.8E+07	3.6E+07	-3.5E+07	-2.9E+07	1.2E+08	1.4E+07	-1.1E+07	1.2E+08	-7.6E+05	-1.7E+05	-4.1E+05	-2.8E+05	-3.1E+05	-4.9E+05	-2.0E+05	-2.1E+05

Table 127 Raw data for the test seal at PR=0.6, ω=5 krpm, and inlet LVF=0% with the zero-preswirl insert

Freq.	Re(H_{XX})	Re(H_{XY})	Re(H_{YX})	Re(H_{YY})	Im(H_{XX})	Im(H_{XY})	Im(H_{YX})	Im(H_{YY})	Re(eH_{XX})	Re(eH_{XY})	Re(eH_{YX})	Re(eH_{YY})	Im(eH_{XX})	Im(eH_{XY})	Im(eH_{YX})	Im(eH_{YY})
Hz	N/m	N/m	N/m	N/m	N/m	N/m	N/m	N/m	N/m	N/m	N/m	N/m	N/m	N/m	N/m	N/m
9.8	6.6E+06	6.6E+05	-2.3E+06	6.1E+06	1.1E+06	7.1E+04	7.7E+04	1.1E+06	-7.0E+04	-5.7E+04	-9.0E+04	-9.0E+04	-8.8E+04	-7.4E+04	-5.0E+04	-6.6E+04
19.5	6.4E+06	7.0E+05	-2.1E+06	5.7E+06	2.4E+06	2.2E+05	6.3E+04	2.6E+06	-5.9E+04	-6.4E+04	-8.6E+04	-3.8E+04	-6.7E+04	-3.7E+04	-4.8E+04	-6.1E+04
29.3	5.9E+06	1.2E+06	-1.5E+06	5.1E+06	2.9E+06	1.1E+06	9.0E+05	3.0E+06	-3.6E+04	-6.2E+04	-1.5E+05	-7.0E+04	-1.1E+05	-5.3E+04	-1.3E+05	-9.0E+04
39.1	6.0E+06	5.9E+05	-2.0E+06	5.5E+06	5.1E+06	1.7E+05	-1.0E+05	5.8E+06	-2.3E+04	-6.2E+04	-3.3E+04	-5.6E+04	-5.5E+04	-6.7E+04	-5.3E+04	-4.5E+04
48.8	6.1E+06	7.2E+05	-1.9E+06	5.2E+06	6.8E+06	2.6E+05	-1.2E+05	7.3E+06	-7.0E+04	-5.0E+04	-1.1E+05	-3.4E+04	-1.3E+05	-8.7E+04	-1.1E+05	-5.2E+04
58.6	6.1E+06	6.3E+05	-1.9E+06	5.3E+06	8.2E+06	3.8E+05	-5.6E+05	8.8E+06	-7.3E+04	-4.5E+04	-1.6E+05	-5.5E+04	-6.0E+04	-8.2E+04	-1.2E+05	-9.2E+04
68.4	5.7E+06	7.3E+05	-1.9E+06	5.4E+06	9.3E+06	3.1E+05	-5.6E+05	1.0E+07	-7.1E+04	-1.1E+05	-2.7E+04	-1.0E+05	-4.3E+04	-5.1E+04	-8.0E+04	-9.0E+04
78.1	5.7E+06	6.0E+05	-2.2E+06	5.1E+06	1.1E+07	5.9E+05	-5.0E+05	1.2E+07	-7.6E+04	-5.3E+04	-4.2E+04	-8.1E+04	-5.0E+04	-5.5E+04	-7.4E+04	-4.8E+04
87.9	5.4E+06	4.5E+05	-2.3E+06	5.0E+06	1.2E+07	4.8E+05	-6.3E+05	1.4E+07	-6.2E+04	-4.8E+04	-7.3E+04	-4.8E+04	-6.1E+04	-7.2E+04	-1.2E+05	-7.3E+04
97.7	5.2E+06	5.0E+05	-2.4E+06	4.8E+06	1.4E+07	5.1E+05	-8.4E+05	1.5E+07	-5.8E+04	-5.3E+04	-3.7E+04	-8.4E+04	-6.7E+04	-4.8E+04	-7.0E+04	-4.3E+04
107.4	4.7E+06	-4.5E+05	-3.1E+06	4.7E+06	1.6E+07	5.2E+05	-8.2E+05	1.7E+07	-4.7E+04	-6.0E+04	-1.1E+05	-6.5E+04	-1.0E+05	-3.5E+04	-1.1E+05	-7.4E+04
117.2	5.3E+06	-8.7E+04	-2.9E+06	5.2E+06	1.7E+07	8.9E+05	-9.5E+05	1.9E+07	-6.8E+04	-5.6E+04	-6.5E+04	-2.9E+04	-5.4E+04	-2.9E+04	-7.8E+04	-7.2E+04
127.0	5.2E+06	6.0E+04	-2.8E+06	5.8E+06	1.8E+07	1.3E+06	-2.7E+05	2.0E+07	-4.7E+04	-6.9E+04	-4.5E+04	-5.6E+04	-4.1E+04	-1.1E+05	-3.7E+04	-8.6E+04
136.7	5.2E+06	-3.9E+04	-3.1E+06	5.6E+06	1.9E+07	1.6E+06	-2.3E+05	2.1E+07	-2.9E+04	-4.1E+04	-4.6E+04	-6.6E+04	-5.8E+04	-6.4E+04	-6.1E+04	-4.4E+04

Table 128 Raw data for the test seal at PR=0.6, ω=10 krpm, and inlet LVF=0% with the zero-preswirl insert

Freq.	Re(H_{XX})	Re(H_{XY})	Re(H_{YX})	Re(H_{YY})	Im(H_{XX})	Im(H_{XY})	Im(H_{YX})	Im(H_{YY})	Re(eH_{XX})	Re(eH_{XY})	Re(eH_{YX})	Re(eH_{YY})	Im(eH_{XX})	Im(eH_{XY})	Im(eH_{YX})	Im(eH_{YY})
Hz	N/m	N/m	N/m	N/m	N/m	N/m	N/m	N/m	N/m	N/m	N/m	N/m	N/m	N/m	N/m	N/m
9.8	6.8E+06	2.7E+06	-3.9E+06	6.4E+06	8.7E+05	4.6E+05	-1.3E+05	1.2E+06	-1.4E+05	-9.0E+04	-1.4E+05	-1.3E+05	-1.2E+05	-1.2E+05	-1.7E+05	-1.4E+05
19.5	6.5E+06	2.8E+06	-3.9E+06	5.7E+06	2.2E+06	3.3E+05	-1.1E+05	2.6E+06	-5.5E+04	-3.6E+04	-4.8E+04	-5.8E+04	-8.1E+04	-3.9E+04	-8.6E+04	-6.3E+04
29.3	6.0E+06	3.0E+06	-3.8E+06	5.7E+06	3.0E+06	1.5E+06	5.5E+05	3.3E+06	-1.1E+05	-7.9E+04	-8.2E+04	-1.0E+05	-8.9E+04	-7.3E+04	-9.3E+04	-5.8E+04
39.1	5.9E+06	2.9E+06	-3.9E+06	5.7E+06	5.0E+06	3.9E+05	-5.9E+05	5.8E+06	-7.7E+04	-7.4E+04	-7.3E+04	-6.0E+04	-6.7E+04	-3.7E+04	-4.1E+04	-8.7E+04
48.8	5.9E+06	3.0E+06	-3.9E+06	5.4E+06	6.6E+06	6.5E+05	-7.4E+05	7.1E+06	-9.5E+04	-3.1E+04	-1.0E+05	-6.4E+04	-4.9E+04	-5.8E+04	-6.9E+04	-6.8E+04
58.6	5.8E+06	2.8E+06	-3.9E+06	5.4E+06	8.1E+06	8.5E+05	-8.3E+05	8.8E+06	-9.8E+04	-3.0E+04	-1.2E+05	-6.4E+04	-6.8E+04	-5.4E+04	-8.9E+04	-7.5E+04
68.4	5.1E+06	3.0E+06	-4.3E+06	5.2E+06	9.6E+06	6.8E+05	-9.6E+05	1.0E+07	-6.7E+04	-6.7E+04	-6.6E+04	-1.2E+05	-4.3E+04	-3.4E+04	-6.2E+04	-9.6E+04
78.1	5.2E+06	2.9E+06	-4.3E+06	4.8E+06	1.1E+07	7.5E+05	-1.1E+06	1.2E+07	-5.6E+04	-4.6E+04	-6.4E+04	-3.3E+04	-7.9E+04	-5.6E+04	-3.7E+04	-5.4E+04
87.9	5.0E+06	2.9E+06	-4.5E+06	4.8E+06	1.3E+07	7.6E+05	-1.3E+06	1.4E+07	-7.9E+04	-6.5E+04	-2.5E+04	-7.6E+04	-4.8E+04	-3.4E+04	-9.8E+04	-4.7E+04
97.7	4.9E+06	2.8E+06	-4.5E+06	4.4E+06	1.5E+07	5.9E+05	-1.7E+06	1.5E+07	-4.7E+04	-4.9E+04	-6.8E+04	-4.7E+04	-2.8E+04	-7.1E+04	-6.6E+04	-7.9E+04
107.4	4.7E+06	1.8E+06	-5.7E+06	4.3E+06	1.7E+07	7.1E+05	-1.1E+06	1.7E+07	-4.3E+04	-2.2E+04	-9.1E+04	-1.0E+05	-9.7E+04	-4.6E+04	-5.7E+04	-5.8E+04
117.2	5.3E+06	2.3E+06	-5.1E+06	5.1E+06	1.8E+07	1.3E+06	-1.6E+06	1.9E+07	-4.6E+04	-6.1E+04	-1.4E+05	-4.2E+04	-9.6E+04	-2.0E+04	-1.2E+05	-6.8E+04
127.0	5.1E+06	2.4E+06	-5.1E+06	5.7E+06	1.9E+07	1.8E+06	-9.6E+05	2.0E+07	-3.6E+04	-7.3E+04	-7.7E+04	-9.9E+04	-6.1E+04	-6.9E+04	-8.2E+04	-1.6E+05
136.7	5.2E+06	2.2E+06	-5.4E+06	5.5E+06	2.0E+07	1.9E+06	-1.0E+06	2.1E+07	-3.6E+04	-5.5E+04	-3.9E+04	-5.2E+04	-5.1E+04	-7.2E+04	-6.8E+04	-3.6E+04

Table 129 Raw data for the test seal at PR=0.6, ω=15 krpm, and inlet LVF=0% with the zero-preswirl insert

Freq.	Re(H_{XX})	Re(H_{XY})	Re(H_{YX})	Re(H_{YY})	Im(H_{XX})	Im(H_{XY})	Im(H_{YX})	Im(H_{YY})	Re(eH_{XX})	Re(eH_{XY})	Re(eH_{YX})	Re(eH_{YY})	Im(eH_{XX})	Im(eH_{XY})	Im(eH_{YX})	Im(eH_{YY})
Hz	N/m	N/m	N/m	N/m	N/m	N/m	N/m	N/m	N/m	N/m	N/m	N/m	N/m	N/m	N/m	N/m
9.8	6.4E+06	5.5E+06	-6.9E+06	6.1E+06	1.1E+06	3.3E+05	-1.3E+04	1.1E+06	-1.1E+05	-1.4E+05	-1.0E+05	-8.8E+04	-6.5E+04	-8.5E+04	-8.8E+04	-1.4E+05
19.5	6.0E+06	5.3E+06	-6.9E+06	5.9E+06	2.5E+06	3.4E+05	-3.2E+05	2.6E+06	-3.9E+04	-6.2E+04	-8.7E+04	-3.4E+04	-6.8E+04	-7.4E+04	-6.1E+04	-7.5E+04
29.3	6.0E+06	5.4E+06	-7.0E+06	5.8E+06	3.4E+06	1.4E+06	2.4E+05	3.2E+06	-6.8E+04	-8.6E+04	-1.1E+05	-6.0E+04	-5.8E+04	-6.5E+04	-8.7E+04	-1.1E+05
39.1	5.8E+06	5.5E+06	-7.0E+06	5.6E+06	5.3E+06	7.0E+05	-6.1E+05	5.9E+06	-5.0E+04	-5.2E+04	-7.1E+04	-8.7E+04	-3.3E+04	-2.8E+04	-6.4E+04	-1.1E+05
48.8	5.5E+06	5.7E+06	-7.2E+06	5.4E+06	6.7E+06	9.7E+05	-7.3E+05	7.2E+06	-1.1E+05	-6.1E+04	-6.7E+04	-4.4E+04	-4.6E+04	-8.8E+04	-7.8E+04	-9.9E+04
58.6	5.4E+06	5.9E+06	-7.2E+06	5.2E+06	8.3E+06	1.2E+06	-1.1E+06	8.7E+06	-4.0E+04	-5.8E+04	-1.1E+05	-5.2E+04	-5.4E+04	-3.1E+04	-7.7E+04	-5.3E+04
68.4	5.0E+06	5.8E+06	-7.4E+06	5.3E+06	9.7E+06	1.2E+06	-1.1E+06	1.0E+07	-9.3E+04	-9.0E+04	-8.0E+04	-4.9E+04	-7.0E+04	-3.6E+04	-5.7E+04	-9.4E+04
78.1	5.0E+06	5.8E+06	-7.5E+06	5.0E+06	1.1E+07	1.2E+06	-1.2E+06	1.2E+07	-3.2E+04	-4.6E+04	-6.4E+04	-3.0E+04	-4.7E+04	-7.2E+04	-4.0E+04	-4.8E+04
87.9	4.7E+06	5.9E+06	-7.6E+06	4.7E+06	1.3E+07	1.1E+06	-1.3E+06	1.4E+07	-3.2E+04	-3.0E+04	-6.0E+04	-7.7E+04	-2.9E+04	-5.4E+04	-7.7E+04	-7.6E+04
97.7	4.5E+06	5.7E+06	-7.5E+06	4.3E+06	1.5E+07	1.1E+06	-1.6E+06	1.6E+07	-6.7E+04	-4.3E+04	-4.9E+04	-4.2E+04	-4.7E+04	-2.5E+04	-8.8E+04	-9.2E+04
107.4	4.3E+06	4.9E+06	-8.4E+06	4.5E+06	1.7E+07	1.1E+06	-1.4E+06	1.8E+07	-3.7E+04	-4.1E+04	-4.5E+04	-4.6E+04	-4.1E+04	-4.8E+04	-6.8E+04	-6.8E+04
117.2	5.2E+06	5.3E+06	-7.6E+06	5.4E+06	1.8E+07	1.6E+06	-1.8E+06	1.9E+07	-4.0E+04	-2.6E+04	-1.2E+05	-7.9E+04	-5.8E+04	-6.8E+04	-1.2E+05	-5.5E+04
127.0	5.3E+06	5.3E+06	-7.9E+06	5.8E+06	1.9E+07	2.0E+06	-1.4E+06	2.0E+07	-5.6E+04	-7.7E+04	-6.4E+04	-6.6E+04	-4.0E+04	-5.6E+04	-5.1E+04	-7.3E+04
136.7	5.3E+06	5.2E+06	-8.0E+06	5.5E+06	2.0E+07	2.4E+06	-1.6E+06	2.1E+07	-2.8E+04	-3.0E+04	-4.7E+04	-5.5E+04	-6.4E+04	-3.9E+04	-4.7E+04	-6.7E+04

Table 130 Raw data for the test seal at PR=0.6, ω=5 krpm, and inlet LVF=2% with the zero-preswirl insert

Freq.	Re(H_{XX})	Re(H_{XY})	Re(H_{YX})	Re(H_{YY})	Im(H_{XX})	Im(H_{XY})	Im(H_{YX})	Im(H_{YY})	Re(eH_{XX})	Re(eH_{XY})	Re(eH_{YX})	Re(eH_{YY})	Im(eH_{XX})	Im(eH_{XY})	Im(eH_{YX})	Im(eH_{YY})
Hz	N/m	N/m	N/m	N/m	N/m	N/m	N/m	N/m	N/m	N/m	N/m	N/m	N/m	N/m	N/m	N/m
9.8	3.5E+06	3.2E+06	-3.2E+06	1.1E+06	1.8E+06	2.2E+05	4.8E+05	2.2E+06	-3.4E+05	-9.7E+04	-2.9E+05	-1.7E+05	-2.1E+05	-9.4E+04	-2.1E+05	-1.1E+05
19.5	3.4E+06	3.4E+06	-3.9E+06	1.4E+06	4.6E+06	7.7E+05	-3.3E+05	4.7E+06	-1.9E+05	-4.3E+04	-1.6E+05	-1.6E+05	-1.7E+05	-9.0E+04	-1.6E+05	-1.8E+05
29.3	3.9E+06	3.3E+06	-4.3E+06	2.4E+06	5.5E+06	1.7E+06	6.8E+05	6.3E+06	-1.7E+05	-1.9E+05	-1.6E+05	-1.7E+05	-1.4E+05	-1.4E+05	-2.3E+05	-2.7E+05
39.1	3.9E+06	3.9E+06	-3.5E+06	2.3E+06	8.1E+06	4.3E+05	-2.6E+05	8.8E+06	-1.8E+05	-6.0E+04	-2.4E+05	-1.1E+05	-1.7E+05	-6.1E+04	-1.7E+05	-8.1E+04
48.8	3.5E+06	3.9E+06	-3.9E+06	2.2E+06	9.8E+06	4.1E+05	-3.6E+05	1.1E+07	-5.4E+04	-4.5E+04	-1.7E+05	-7.2E+04	-8.5E+04	-6.5E+04	-1.5E+05	-1.4E+05
58.6	3.5E+06	3.8E+06	-4.0E+06	2.3E+06	1.2E+07	5.2E+05	-8.1E+05	1.3E+07	-1.3E+05	-4.7E+04	-2.5E+05	-9.8E+04	-1.8E+05	-1.2E+05	-1.1E+05	-1.3E+05
68.4	3.6E+06	3.5E+06	-4.0E+06	2.2E+06	1.4E+07	2.7E+05	-5.8E+05	1.4E+07	-7.2E+04	-1.2E+05	-1.1E+05	-1.9E+05	-4.3E+04	-1.5E+05	-1.5E+05	-2.3E+05
78.1	3.5E+06	3.6E+06	-4.5E+06	2.4E+06	1.5E+07	7.2E+05	-8.4E+05	1.6E+07	-9.8E+04	-6.3E+04	-1.4E+05	-1.9E+05	-5.7E+04	-6.1E+04	-1.4E+05	-4.1E+04
87.9	3.1E+06	3.9E+06	-4.9E+06	2.4E+06	1.7E+07	7.0E+05	-5.9E+05	1.9E+07	-4.9E+04	-7.8E+04	-1.3E+05	-1.4E+05	-8.2E+04	-1.0E+05	-1.2E+05	-1.7E+05
97.7	2.8E+06	4.1E+06	-5.0E+06	2.4E+06	1.9E+07	5.4E+05	-4.3E+05	2.1E+07	-5.7E+04	-7.9E+04	-1.3E+05	-1.8E+05	-5.3E+04	-6.4E+04	-9.7E+04	-6.0E+04
107.4	2.2E+06	3.5E+06	-5.6E+06	2.1E+06	2.2E+07	3.8E+05	-1.6E+05	2.3E+07	-5.2E+04	-1.1E+05	-7.8E+04	-1.7E+05	-1.1E+05	-3.5E+04	-7.6E+04	-9.2E+04
117.2	3.1E+06	3.9E+06	-4.9E+06	2.6E+06	2.3E+07	5.5E+05	-4.4E+05	2.5E+07	-2.1E+05	-1.0E+05	-2.6E+05	-1.2E+05	-1.1E+05	-5.7E+04	-1.3E+05	-6.5E+04
127.0	2.9E+06	3.8E+06	-4.9E+06	2.9E+06	2.5E+07	8.3E+05	3.6E+05	2.7E+07	-1.2E+05	-9.5E+04	-8.7E+04	-1.3E+05	-1.0E+05	-7.5E+04	-1.2E+05	-1.2E+05
136.7	2.8E+06	3.7E+06	-5.2E+06	3.1E+06	2.7E+07	1.0E+06	6.5E+05	2.8E+07	-1.0E+05	-6.3E+04	-1.5E+05	-1.3E+05	-9.5E+04	-8.4E+04	-9.4E+04	-1.1E+05

Table 131 Raw data for the test seal at PR=0.6, ω=10 krpm, and inlet LVF=2% with the zero-preswirl insert

Freq.	Re(H_{XX})	Re(H_{XY})	Re(H_{YX})	Re(H_{YY})	Im(H_{XX})	Im(H_{XY})	Im(H_{YX})	Im(H_{YY})	Re(eH_{XX})	Re(eH_{XY})	Re(eH_{YX})	Re(eH_{YY})	Im(eH_{XX})	Im(eH_{XY})	Im(eH_{YX})	Im(eH_{YY})
Hz	N/m	N/m	N/m	N/m	N/m	N/m	N/m	N/m	N/m	N/m	N/m	N/m	N/m	N/m	N/m	N/m
9.8	3.5E+06	8.4E+06	-9.4E+06	2.8E+06	1.1E+06	6.6E+05	-3.0E+05	3.8E+06	-2.7E+05	-2.7E+05	-5.0E+05	-5.5E+05	-2.6E+05	-3.9E+05	-3.6E+05	-4.9E+05
19.5	3.0E+06	8.6E+06	-9.0E+06	2.8E+06	3.8E+06	7.1E+05	4.6E+05	4.9E+06	-9.5E+04	-8.5E+04	-1.8E+05	-1.4E+05	-1.2E+05	-7.9E+04	-7.8E+04	-9.3E+04
29.3	3.9E+06	8.1E+06	-8.8E+06	3.3E+06	4.8E+06	1.8E+06	6.8E+05	5.2E+06	-9.7E+04	-9.4E+04	-2.2E+05	-9.0E+04	-1.2E+05	-6.2E+04	-2.2E+05	-1.3E+05
39.1	3.2E+06	9.0E+06	-8.2E+06	3.0E+06	7.8E+06	5.5E+05	1.2E+05	8.5E+06	-5.8E+04	-8.5E+04	-5.9E+04	-8.5E+04	-8.7E+04	-9.2E+04	-1.6E+05	-1.1E+05
48.8	3.0E+06	9.0E+06	-7.9E+06	3.1E+06	1.0E+07	6.4E+05	-2.6E+05	1.0E+07	-5.1E+04	-4.5E+04	-1.5E+05	-1.5E+05	-7.1E+04	-4.3E+04	-1.4E+05	-1.6E+05
58.6	3.2E+06	8.9E+06	-8.1E+06	2.8E+06	1.2E+07	7.1E+05	-1.5E+05	1.3E+07	-6.4E+04	-9.4E+04	-2.1E+05	-7.5E+04	-1.6E+05	-1.1E+05	-2.0E+05	-1.2E+05
68.4	3.0E+06	8.6E+06	-8.5E+06	3.0E+06	1.4E+07	5.5E+05	-6.3E+05	1.5E+07	-3.7E+04	-1.1E+05	-1.3E+05	-9.6E+04	-1.4E+05	-9.4E+04	-1.7E+05	-2.0E+05
78.1	3.0E+06	8.9E+06	-8.2E+06	3.1E+06	1.6E+07	8.3E+05	-5.7E+05	1.7E+07	-9.0E+04	-5.1E+04	-1.9E+05	-1.3E+05	-5.4E+04	-6.4E+04	-1.3E+05	-1.0E+05
87.9	2.9E+06	9.0E+06	-8.6E+06	2.9E+06	1.8E+07	9.0E+05	-8.9E+05	1.9E+07	-4.5E+04	-5.4E+04	-1.1E+05	-1.4E+05	-8.2E+04	-1.2E+05	-9.1E+04	-2.0E+05
97.7	2.8E+06	8.9E+06	-8.9E+06	3.0E+06	2.1E+07	8.5E+05	-6.6E+05	2.1E+07	-3.9E+04	-2.5E+04	-7.1E+04	-8.4E+04	-8.0E+04	-5.1E+04	-1.9E+05	-1.2E+05
107.4	2.7E+06	8.3E+06	-9.4E+06	2.6E+06	2.3E+07	1.0E+06	-1.2E+06	2.4E+07	-1.6E+05	-7.3E+04	-2.7E+05	-1.3E+05	-8.2E+04	-6.5E+04	-1.3E+05	-1.6E+05
117.2	3.5E+06	9.1E+06	-9.0E+06	3.4E+06	2.5E+07	1.2E+06	-7.6E+05	2.6E+07	-6.2E+04	-4.2E+04	-1.1E+05	-5.3E+04	-9.5E+04	-3.3E+04	-1.5E+05	-1.9E+05
127.0	3.4E+06	8.8E+06	-9.0E+06	3.5E+06	2.6E+07	1.4E+06	-6.9E+05	2.8E+07	-7.8E+04	-5.6E+04	-1.2E+05	-1.3E+05	-5.0E+04	-1.2E+05	-9.8E+04	-2.5E+05
136.7	3.5E+06	8.7E+06	-8.9E+06	3.7E+06	2.9E+07	1.5E+06	-5.0E+05	2.9E+07	-5.5E+04	-7.6E+04	-1.1E+05	-1.3E+05	-5.2E+04	-8.5E+04	-1.2E+05	-1.1E+05

Table 132 Raw data for the test seal at PR=0.6, ω=15 krpm, and inlet LVF=2% with the zero-preswirl insert

Freq.	Re(H_{XX})	Re(H_{XY})	Re(H_{YX})	Re(H_{YY})	Im(H_{XX})	Im(H_{XY})	Im(H_{YX})	Im(H_{YY})	Re(eH_{XX})	Re(eH_{XY})	Re(eH_{YX})	Re(eH_{YY})	Im(eH_{XX})	Im(eH_{XY})	Im(eH_{YX})	Im(eH_{YY})
Hz	N/m	N/m	N/m	N/m	N/m	N/m	N/m	N/m	N/m	N/m	N/m	N/m	N/m	N/m	N/m	N/m
9.8	5.2E+06	1.3E+07	-1.4E+07	3.9E+06	1.3E+06	2.4E+05	-1.9E+06	2.8E+06	-2.2E+05	-3.6E+05	-2.5E+05	-1.9E+05	-2.0E+05	-1.7E+05	-2.7E+05	-3.6E+05
19.5	4.1E+06	1.4E+07	-1.4E+07	4.4E+06	3.9E+06	2.1E+05	-3.9E+05	4.4E+06	-1.7E+05	-1.5E+05	-2.7E+05	-3.2E+05	-1.2E+05	-1.5E+05	-2.5E+05	-2.6E+05
29.3	4.9E+06	1.3E+07	-1.5E+07	5.1E+06	5.0E+06	1.9E+06	9.7E+05	4.1E+06	-1.0E+05	-4.7E+04	-2.0E+05	-2.0E+05	-1.6E+05	-1.5E+05	-1.8E+05	-1.2E+05
39.1	3.8E+06	1.4E+07	-1.4E+07	4.0E+06	7.9E+06	7.1E+05	3.7E+04	8.6E+06	-5.9E+04	-1.1E+05	-1.2E+05	-1.4E+05	-9.2E+04	-6.6E+04	-1.9E+05	-1.5E+05
48.8	4.0E+06	1.4E+07	-1.4E+07	4.1E+06	9.7E+06	6.4E+05	-2.8E+04	1.0E+07	-4.8E+04	-7.4E+04	-1.1E+05	-9.6E+04	-5.6E+04	-8.0E+04	-1.0E+05	-1.5E+05
58.6	3.9E+06	1.4E+07	-1.4E+07	3.6E+06	1.2E+07	6.6E+05	-4.0E+05	1.2E+07	-9.0E+04	-8.0E+04	-1.5E+05	-1.4E+05	-5.4E+04	-6.2E+04	-1.1E+05	-1.2E+05
68.4	3.7E+06	1.4E+07	-1.4E+07	4.1E+06	1.4E+07	9.0E+05	-1.3E+05	1.5E+07	-9.9E+04	-1.8E+05	-1.5E+05	-1.7E+05	-1.0E+05	-9.3E+04	-1.4E+05	-1.2E+05
78.1	3.6E+06	1.4E+07	-1.4E+07	3.9E+06	1.6E+07	6.7E+05	-4.6E+05	1.7E+07	-5.5E+04	-8.5E+04	-6.9E+04	-9.6E+04	-9.3E+04	-1.1E+05	-1.1E+05	-9.2E+04
87.9	3.6E+06	1.4E+07	-1.4E+07	3.6E+06	1.8E+07	5.5E+05	-4.8E+05	1.9E+07	-5.0E+04	-8.4E+04	-8.8E+04	-1.3E+05	-4.5E+04	-5.4E+04	-1.1E+05	-1.2E+05
97.7	3.3E+06	1.4E+07	-1.4E+07	3.8E+06	2.0E+07	7.7E+05	-6.0E+05	2.2E+07	-7.7E+04	-6.0E+04	-9.0E+04	-8.6E+04	-6.9E+04	-5.2E+04	-1.2E+05	-1.1E+05
107.4	3.1E+06	1.3E+07	-1.5E+07	3.7E+06	2.3E+07	8.2E+05	-9.1E+05	2.4E+07	-1.0E+05	-7.4E+04	-2.4E+05	-1.7E+05	-9.9E+04	-8.5E+04	-1.9E+05	-1.7E+05
117.2	3.8E+06	1.4E+07	-1.5E+07	4.8E+06	2.4E+07	1.3E+06	-8.5E+05	2.7E+07	-3.4E+04	-4.3E+04	-1.5E+05	-1.3E+05	-7.7E+04	-5.4E+04	-1.4E+05	-9.8E+04
127.0	3.6E+06	1.4E+07	-1.5E+07	5.3E+06	2.6E+07	1.7E+06	-3.3E+05	2.8E+07	-4.8E+04	-7.1E+04	-1.3E+05	-1.1E+05	-9.7E+04	-7.7E+04	-1.1E+05	-1.6E+05
136.7	3.5E+06	1.4E+07	-1.5E+07	5.3E+06	2.8E+07	1.9E+06	-4.3E+05	3.0E+07	-7.5E+04	-7.0E+04	-1.0E+05	-9.9E+04	-8.9E+04	-7.2E+04	-1.3E+05	-1.3E+05

Table 133 Raw data for the test seal at PR=0.6, ω=5 krpm, and inlet LVF=4% with the zero-preswirl insert

Freq.	Re($\boldsymbol{H_{XX}}$)	Re($\boldsymbol{H_{XY}}$)	Re($\boldsymbol{H_{YX}}$)	Re($\boldsymbol{H_{YY}}$)	Im($\boldsymbol{H_{XX}}$)	Im($\boldsymbol{H_{XY}}$)	Im($\boldsymbol{H_{YX}}$)	Im($\boldsymbol{H_{YY}}$)	Re($\boldsymbol{eH_{XX}}$)	Re($\boldsymbol{eH_{XY}}$)	Re($\boldsymbol{eH_{YX}}$)	Re($\boldsymbol{eH_{YY}}$)	Im($\boldsymbol{eH_{XX}}$)	Im($\boldsymbol{eH_{XY}}$)	Im($\boldsymbol{eH_{YX}}$)	Im($\boldsymbol{eH_{YY}}$)
Hz	N/m	N/m	N/m	N/m	N/m	N/m	N/m	N/m	N/m	N/m	N/m	N/m	N/m	N/m	N/m	N/m
9.8	4.6E+06	1.7E+06	-3.8E+06	2.0E+06	1.8E+06	1.0E+06	1.4E+06	1.7E+06	-1.5E+05	-1.4E+05	-4.6E+05	-1.9E+05	-3.3E+05	-2.2E+05	-3.5E+05	-1.1E+05
19.5	4.6E+06	3.1E+06	-3.5E+06	2.2E+06	3.9E+06	1.8E+06	7.1E+05	4.6E+06	-1.3E+05	-1.2E+05	-3.9E+05	-2.1E+05	-2.1E+05	-9.7E+04	-2.4E+05	-2.1E+05
29.3	4.5E+06	3.6E+06	-4.0E+06	3.8E+06	5.0E+06	2.5E+06	9.3E+05	5.7E+06	-2.0E+05	-1.0E+05	-2.2E+05	-3.0E+05	-1.5E+05	-2.3E+05	-2.8E+05	-3.5E+05
39.1	4.1E+06	4.0E+06	-3.1E+06	2.9E+06	8.1E+06	1.1E+06	1.6E+05	9.0E+06	-2.0E+05	-1.1E+05	-1.9E+05	-8.4E+04	-1.5E+05	-1.1E+05	-1.2E+05	-1.4E+05
48.8	4.0E+06	4.0E+06	-3.3E+06	2.9E+06	1.0E+07	1.0E+06	4.7E+05	1.1E+07	-8.7E+04	-9.9E+04	-1.9E+05	-1.6E+05	-2.2E+05	-1.7E+05	-3.6E+05	-3.7E+05
58.6	3.8E+06	4.4E+06	-3.7E+06	2.9E+06	1.2E+07	8.7E+05	-3.1E+05	1.3E+07	-6.6E+04	-7.1E+04	-2.5E+05	-2.0E+05	-1.7E+05	-9.6E+04	-2.6E+05	-2.0E+05
68.4	3.6E+06	4.2E+06	-4.0E+06	3.2E+06	1.4E+07	5.7E+05	1.1E+05	1.4E+07	-1.1E+05	-2.4E+05	-1.5E+05	-3.6E+05	-1.2E+05	-1.4E+05	-2.8E+05	-1.9E+05
78.1	3.5E+06	4.1E+06	-4.4E+06	3.0E+06	1.6E+07	8.8E+05	-6.0E+05	1.7E+07	-1.4E+05	-2.2E+05	-1.3E+05	-2.5E+05	-1.1E+05	-2.0E+05	-1.2E+05	-2.0E+05
87.9	3.0E+06	4.1E+06	-4.3E+06	2.6E+06	1.8E+07	9.0E+05	-5.9E+05	1.9E+07	-9.9E+04	-1.3E+05	-1.9E+05	-2.2E+05	-9.9E+04	-1.2E+05	-2.7E+05	-1.1E+05
97.7	3.1E+06	4.4E+06	-4.1E+06	2.6E+06	2.0E+07	9.6E+05	-2.4E+05	2.1E+07	-9.8E+04	-7.6E+04	-2.1E+05	-2.2E+05	-5.8E+04	-1.4E+05	-1.1E+05	-2.7E+05
107.4	2.8E+06	3.5E+06	-4.8E+06	1.7E+06	2.3E+07	5.9E+05	2.1E+05	2.3E+07	-2.4E+05	-1.6E+05	-2.7E+05	-1.9E+05	-2.2E+05	-1.2E+05	-3.1E+05	-1.2E+05
117.2	3.0E+06	4.1E+06	-5.3E+06	2.6E+06	2.5E+07	8.7E+05	-4.1E+04	2.6E+07	-2.0E+05	-7.9E+04	-1.5E+05	-1.1E+05	-1.8E+05	-1.1E+05	-2.4E+05	-1.8E+05
127.0	3.2E+06	4.3E+06	-4.5E+06	3.4E+06	2.6E+07	1.8E+06	4.3E+05	2.8E+07	-1.2E+05	-2.0E+05	-2.9E+05	-1.9E+05	-1.2E+05	-1.8E+05	-1.6E+05	-3.0E+05
136.7	2.8E+06	4.3E+06	-4.9E+06	2.8E+06	2.8E+07	1.0E+06	9.5E+05	2.9E+07	-1.0E+05	-1.8E+05	-1.3E+05	-2.5E+05	-1.3E+05	-6.9E+04	-1.8E+05	-7.2E+04

Table 134 Raw data for the test seal at PR=0.6, ω=10 krpm, and inlet LVF=4% with the zero-preswirl insert

Freq.	Re($\boldsymbol{H_{XX}}$)	Re($\boldsymbol{H_{XY}}$)	Re($\boldsymbol{H_{YX}}$)	Re($\boldsymbol{H_{YY}}$)	Im($\boldsymbol{H_{XX}}$)	Im($\boldsymbol{H_{XY}}$)	Im($\boldsymbol{H_{YX}}$)	Im($\boldsymbol{H_{YY}}$)	Re($\boldsymbol{eH_{XX}}$)	Re($\boldsymbol{eH_{XY}}$)	Re($\boldsymbol{eH_{YX}}$)	Re($\boldsymbol{eH_{YY}}$)	Im($\boldsymbol{eH_{XX}}$)	Im($\boldsymbol{eH_{XY}}$)	Im($\boldsymbol{eH_{YX}}$)	Im($\boldsymbol{eH_{YY}}$)
Hz	N/m	N/m	N/m	N/m	N/m	N/m	N/m	N/m	N/m	N/m	N/m	N/m	N/m	N/m	N/m	N/m
9.8	5.1E+06	8.0E+06	-9.3E+06	2.6E+06	-5.6E+05	3.1E+05	3.3E+05	2.9E+06	-3.0E+05	-2.4E+05	-4.4E+05	-4.7E+05	-2.6E+05	-2.5E+05	-3.8E+05	-3.5E+05
19.5	4.1E+06	8.3E+06	-8.3E+06	2.9E+06	2.7E+06	5.1E+05	5.0E+05	5.3E+06	-1.3E+05	-1.4E+05	-4.3E+05	-2.7E+05	-1.7E+05	-2.1E+05	-4.2E+05	-3.7E+05
29.3	4.4E+06	8.1E+06	-8.7E+06	4.7E+06	4.1E+06	2.1E+06	1.6E+06	5.6E+06	-2.2E+05	-2.1E+05	-3.0E+05	-2.3E+05	-1.8E+05	-2.1E+05	-2.9E+05	-3.0E+05
39.1	3.6E+06	8.2E+06	-7.5E+06	3.2E+06	7.5E+06	1.0E+06	-5.0E+04	9.5E+06	-1.4E+05	-6.4E+04	-1.7E+05	-2.1E+05	-1.3E+05	-1.5E+05	-1.1E+05	-2.4E+05
48.8	3.6E+06	8.4E+06	-7.2E+06	3.8E+06	1.0E+07	6.2E+05	-3.2E+05	1.1E+07	-1.0E+05	-2.6E+05	-1.9E+05	-2.2E+05	-8.1E+04	-7.5E+04	-2.2E+05	-1.6E+05
58.6	3.5E+06	8.1E+06	-7.3E+06	3.7E+06	1.2E+07	1.2E+06	-5.6E+05	1.3E+07	-1.2E+05	-1.8E+05	-1.7E+05	-2.7E+05	-2.3E+05	-1.5E+05	-2.3E+05	-2.6E+05
68.4	3.6E+06	8.6E+06	-8.0E+06	4.8E+06	1.5E+07	1.3E+06	-6.6E+05	1.5E+07	-1.0E+05	-2.1E+05	-1.7E+05	-4.3E+05	-1.0E+05	-9.5E+04	-3.8E+05	-1.9E+05
78.1	3.3E+06	8.8E+06	-7.3E+06	3.5E+06	1.7E+07	1.5E+06	-5.4E+05	1.7E+07	-1.1E+05	-9.7E+04	-2.0E+05	-1.7E+05	-7.2E+04	-1.9E+05	-2.4E+05	-2.3E+05
87.9	3.5E+06	8.8E+06	-7.9E+06	3.6E+06	1.9E+07	1.3E+06	-6.4E+05	1.9E+07	-8.4E+04	-1.5E+05	-1.4E+05	-4.1E+04	-1.1E+05	-9.7E+04	-1.8E+05	-1.7E+05
97.7	3.3E+06	8.6E+06	-8.5E+06	2.9E+06	2.1E+07	1.8E+06	-8.9E+05	2.2E+07	-1.2E+05	-1.3E+05	-2.1E+05	-3.5E+05	-8.4E+04	-1.0E+05	-1.8E+05	-2.5E+05
107.4	3.3E+06	8.1E+06	-8.9E+06	2.6E+06	2.4E+07	1.5E+06	-8.8E+05	2.4E+07	-8.3E+04	-1.1E+05	-1.9E+05	-1.1E+05	-1.0E+05	-5.5E+04	-2.5E+05	-1.1E+05
117.2	4.3E+06	9.0E+06	-8.2E+06	3.6E+06	2.5E+07	1.6E+06	-1.4E+06	2.7E+07	-1.2E+05	-1.3E+05	-3.9E+05	-1.3E+05	-1.5E+05	-1.0E+05	-1.4E+05	-1.3E+05
127.0	3.8E+06	8.7E+06	-8.9E+06	4.3E+06	2.7E+07	2.4E+06	-4.9E+05	2.9E+07	-1.4E+05	-1.8E+05	-2.6E+05	-4.0E+05	-1.5E+05	-3.0E+05	-1.0E+05	-3.5E+05
136.7	3.7E+06	8.3E+06	-8.7E+06	3.6E+06	2.9E+07	2.3E+06	-9.0E+05	3.1E+07	-9.3E+04	-2.4E+05	-2.1E+05	-1.8E+05	-1.4E+05	-1.4E+05	-1.4E+05	-1.3E+05

Table 135 Raw data for the test seal at PR=0.6, ω=15 krpm, and inlet LVF=4% with the zero-preswirl insert

Freq.	Re(H_{XX})	Re(H_{XY})	Re(H_{YX})	Re(H_{YY})	Im(H_{XX})	Im(H_{XY})	Im(H_{YX})	Im(H_{YY})	Re(eH_{XX})	Re(eH_{XY})	Re(eH_{YX})	Re(eH_{YY})	Im(eH_{XX})	Im(eH_{XY})	Im(eH_{YX})	Im(eH_{YY})
Hz	N/m	N/m	N/m	N/m	N/m	N/m	N/m	N/m	N/m	N/m	N/m	N/m	N/m	N/m	N/m	N/m
9.8	7.1E+06	1.3E+07	-1.4E+07	6.0E+06	-1.1E+06	1.1E+06	-1.3E+06	4.0E+06	-3.5E+05	-5.0E+05	-5.5E+05	-5.4E+05	-3.1E+05	-3.2E+05	-3.1E+05	-6.1E+05
19.5	5.8E+06	1.4E+07	-1.5E+07	4.9E+06	1.9E+06	-1.4E+05	-1.0E+04	4.7E+06	-2.5E+05	-2.3E+05	-2.5E+05	-2.1E+05	-2.1E+05	-3.0E+05	-1.9E+05	-2.6E+05
29.3	5.6E+06	1.4E+07	-1.5E+07	5.5E+06	4.0E+06	1.7E+06	1.9E+06	5.1E+06	-1.9E+05	-2.7E+05	-3.5E+05	-4.2E+05	-2.1E+05	-3.3E+05	-3.9E+05	-3.8E+05
39.1	5.1E+06	1.4E+07	-1.4E+07	4.8E+06	7.3E+06	3.1E+05	3.3E+05	9.4E+06	-1.5E+05	-2.0E+05	-2.6E+05	-1.8E+05	-1.5E+05	-2.2E+05	-2.7E+05	-3.4E+05
48.8	4.9E+06	1.3E+07	-1.4E+07	4.3E+06	9.4E+06	8.5E+05	-1.5E+05	1.1E+07	-1.5E+05	-1.6E+05	-2.2E+05	-1.4E+05	-1.5E+05	-1.2E+05	-2.9E+05	-2.0E+05
58.6	4.6E+06	1.4E+07	-1.4E+07	4.4E+06	1.2E+07	6.8E+05	-1.9E+05	1.3E+07	-1.4E+05	-1.8E+05	-2.5E+05	-3.0E+05	-1.5E+05	-1.9E+05	-2.6E+05	-3.7E+05
68.4	5.2E+06	1.4E+07	-1.3E+07	4.1E+06	1.4E+07	5.5E+05	-5.8E+05	1.5E+07	-1.6E+05	-2.7E+05	-2.9E+05	-4.8E+05	-1.5E+05	-2.3E+05	-2.2E+05	-2.9E+05
78.1	4.1E+06	1.4E+07	-1.4E+07	4.2E+06	1.6E+07	1.1E+06	-1.2E+06	1.9E+07	-1.4E+05	-1.7E+05	-1.7E+05	-2.8E+05	-1.8E+05	-2.2E+05	-1.5E+05	-1.6E+05
87.9	4.1E+06	1.4E+07	-1.5E+07	4.6E+06	1.8E+07	9.4E+05	-9.1E+05	2.1E+07	-1.1E+05	-4.3E+04	-1.2E+05	-1.8E+05	-1.0E+05	-2.3E+05	-1.7E+05	-1.4E+05
97.7	4.0E+06	1.4E+07	-1.5E+07	4.6E+06	2.1E+07	1.3E+06	-7.8E+05	2.4E+07	-1.1E+05	-1.1E+05	-8.9E+04	-6.4E+04	-1.2E+05	-2.2E+05	-6.0E+04	-4.6E+04
107.4	3.7E+06	1.3E+07	-1.5E+07	4.5E+06	2.3E+07	1.7E+06	-5.3E+05	2.6E+07	-1.0E+05	-1.3E+05	-2.7E+05	-1.1E+05	-8.8E+04	-1.0E+05	-2.8E+05	-2.1E+05
117.2	4.3E+06	1.4E+07	-1.5E+07	5.8E+06	2.5E+07	2.0E+06	-8.4E+05	2.8E+07	-1.1E+05	-9.1E+04	-1.4E+05	-2.5E+05	-9.1E+04	-1.2E+05	-1.6E+05	-1.8E+05
127.0	3.9E+06	1.4E+07	-1.5E+07	6.0E+06	2.7E+07	2.4E+06	-5.3E+05	3.0E+07	-1.8E+05	-3.1E+05	-2.0E+05	-2.8E+05	-1.7E+05	-1.4E+05	-8.1E+04	-2.6E+05
136.7	3.9E+06	1.4E+07	-1.5E+07	5.7E+06	2.9E+07	2.6E+06	-6.3E+05	3.2E+07	-1.6E+05	-1.4E+05	-1.4E+05	-1.9E+05	-1.1E+05	-1.2E+05	-1.5E+05	-1.7E+05

Table 136 Raw data for the test seal at PR=0.6, ω=5 krpm, and inlet LVF=6% with the zero-preswirl insert

Freq.	Re(H_{XX})	Re(H_{XY})	Re(H_{YX})	Re(H_{YY})	Im(H_{XX})	Im(H_{XY})	Im(H_{YX})	Im(H_{YY})	Re(eH_{XX})	Re(eH_{XY})	Re(eH_{YX})	Re(eH_{YY})	Im(eH_{XX})	Im(eH_{XY})	Im(eH_{YX})	Im(eH_{YY})
Hz	N/m	N/m	N/m	N/m	N/m	N/m	N/m	N/m	N/m	N/m	N/m	N/m	N/m	N/m	N/m	N/m
9.8	6.4E+06	1.5E+06	-6.2E+06	2.3E+06	1.5E+06	1.6E+06	2.1E+06	2.6E+06	-5.7E+05	-1.8E+05	-4.2E+05	-3.9E+05	-2.5E+05	-3.0E+05	-5.4E+05	-2.0E+05
19.5	5.0E+06	3.5E+06	-4.2E+06	2.5E+06	2.8E+06	2.1E+06	7.9E+05	4.9E+06	-2.6E+05	-2.3E+05	-4.3E+05	-1.6E+05	-1.8E+05	-1.8E+05	-1.9E+05	-3.5E+05
29.3	4.9E+06	3.3E+06	-4.5E+06	3.7E+06	4.7E+06	3.3E+06	1.5E+06	6.2E+06	-2.8E+05	-3.0E+05	-2.3E+05	-1.2E+05	-2.5E+05	-2.5E+05	-1.7E+05	-6.9E+05
39.1	4.7E+06	4.2E+06	-3.9E+06	4.0E+06	7.6E+06	1.5E+06	5.3E+05	9.7E+06	-8.7E+04	-1.2E+05	-2.4E+05	-3.3E+05	-1.7E+05	-1.7E+05	-3.2E+05	-2.4E+05
48.8	4.4E+06	4.4E+06	-3.6E+06	3.5E+06	1.0E+07	1.4E+06	-2.6E+05	1.2E+07	-2.0E+05	-1.3E+05	-2.3E+05	-9.1E+04	-1.7E+05	-1.1E+05	-1.9E+05	-1.4E+05
58.6	4.4E+06	4.1E+06	-3.3E+06	3.2E+06	1.3E+07	1.3E+06	-2.1E+05	1.3E+07	-2.1E+05	-2.7E+05	-2.5E+05	-2.9E+05	-2.0E+05	-2.5E+05	-4.3E+05	-2.5E+05
68.4	4.2E+06	4.4E+06	-3.5E+06	3.4E+06	1.4E+07	7.7E+05	1.9E+05	1.5E+07	-2.2E+05	-2.1E+05	-3.0E+05	-4.1E+05	-2.1E+05	-1.5E+05	-1.7E+05	-3.0E+05
78.1	4.0E+06	4.3E+06	-3.7E+06	3.5E+06	1.7E+07	7.9E+05	1.6E+05	1.7E+07	-7.3E+04	-1.6E+05	-2.0E+05	-2.2E+05	-2.4E+05	-1.2E+05	-1.5E+05	-1.3E+05
87.9	3.7E+06	4.0E+06	-4.0E+06	2.2E+06	1.9E+07	9.5E+05	-3.2E+05	2.0E+07	-1.7E+05	-1.6E+05	-1.4E+05	-2.6E+05	-6.3E+04	-1.6E+05	-2.4E+05	-1.4E+05
97.7	3.5E+06	4.2E+06	-4.7E+06	2.8E+06	2.1E+07	7.8E+05	-6.0E+05	2.2E+07	-1.8E+05	-2.0E+05	-1.7E+05	-1.7E+05	-1.0E+05	-9.9E+04	-1.5E+05	-1.8E+05
107.4	2.9E+06	3.8E+06	-5.9E+06	2.6E+06	2.4E+07	1.2E+06	-5.6E+05	2.5E+07	-1.6E+05	-1.3E+05	-3.1E+05	-5.9E+04	-1.9E+05	-7.9E+04	-2.5E+05	-1.9E+05
117.2	3.6E+06	4.1E+06	-5.1E+06	2.3E+06	2.5E+07	1.0E+06	-3.8E+05	2.7E+07	-3.0E+05	-1.6E+05	-1.5E+05	-9.2E+04	-2.1E+05	-1.3E+05	-1.6E+05	-8.1E+04
127.0	3.8E+06	4.1E+06	-5.0E+06	2.6E+06	2.8E+07	1.3E+06	8.1E+05	3.0E+07	-1.2E+05	-1.5E+05	-2.2E+05	-2.1E+05	-1.5E+05	-1.2E+05	-2.8E+05	-2.2E+05
136.7	3.0E+06	4.2E+06	-5.7E+06	2.7E+06	3.0E+07	1.6E+06	6.8E+05	3.1E+07	-1.5E+05	-1.7E+05	-1.6E+05	-1.7E+05	-2.3E+05	-5.3E+04	-1.8E+05	-2.0E+05

Table 137 Raw data for the test seal at PR=0.6, ω=10 krpm, and inlet LVF=6% with the zero-preswirl insert

Freq.	Re(H_{XX})	Re(H_{XY})	Re(H_{YX})	Re(H_{YY})	Im(H_{XX})	Im(H_{XY})	Im(H_{YX})	Im(H_{YY})	Re(eH_{XX})	Re(eH_{XY})	Re(eH_{YX})	Re(eH_{YY})	Im(eH_{XX})	Im(eH_{XY})	Im(eH_{YX})	Im(eH_{YY})
Hz	N/m	N/m	N/m	N/m	N/m	N/m	N/m	N/m	N/m	N/m	N/m	N/m	N/m	N/m	N/m	N/m
9.8	7.3E+06	7.9E+06	-8.0E+06	2.9E+06	-6.4E+05	6.9E+05	3.5E+05	3.2E+06	-3.5E+05	-2.6E+05	-2.5E+05	-3.1E+05	-2.4E+05	-3.8E+05	-6.7E+05	-4.3E+05
19.5	4.9E+06	8.3E+06	-8.1E+06	4.0E+06	2.6E+06	1.0E+06	6.2E+05	5.2E+06	-2.0E+05	-2.2E+05	-3.3E+05	-3.6E+05	-1.3E+05	-3.1E+05	-4.0E+05	-2.7E+05
29.3	5.3E+06	7.1E+06	-8.7E+06	4.3E+06	3.6E+06	2.2E+06	1.3E+06	6.3E+06	-2.2E+05	-3.1E+05	-3.0E+05	-3.1E+05	-1.7E+05	-3.2E+05	-1.8E+05	-3.4E+05
39.1	4.4E+06	8.3E+06	-7.5E+06	4.3E+06	7.1E+06	1.3E+06	6.6E+05	1.0E+07	-1.4E+05	-1.8E+05	-1.7E+05	-3.4E+05	-2.5E+05	-1.9E+05	-2.1E+05	-1.7E+05
48.8	4.2E+06	8.4E+06	-7.6E+06	3.4E+06	9.8E+06	1.3E+06	-2.2E+05	1.3E+07	-1.7E+05	-1.4E+05	-1.7E+05	-1.3E+05	-2.6E+05	-1.9E+05	-2.8E+05	-2.8E+05
58.6	3.9E+06	8.1E+06	-7.5E+06	3.7E+06	1.2E+07	2.1E+06	2.1E+05	1.4E+07	-1.4E+05	-2.2E+05	-2.7E+05	-2.8E+05	-2.8E+05	-2.3E+05	-3.4E+05	-3.0E+05
68.4	4.1E+06	8.5E+06	-7.7E+06	4.6E+06	1.5E+07	2.0E+06	-1.5E+05	1.5E+07	-2.9E+05	-2.8E+05	-3.6E+05	-3.1E+05	-2.2E+05	-2.6E+05	-2.2E+05	-3.5E+05
78.1	4.0E+06	8.2E+06	-7.8E+06	3.5E+06	1.8E+07	1.6E+06	1.3E+05	1.8E+07	-2.2E+05	-1.6E+05	-1.7E+05	-2.7E+05	-2.0E+05	-3.1E+05	-2.8E+05	-2.5E+05
87.9	4.4E+06	8.6E+06	-7.4E+06	3.9E+06	1.9E+07	2.0E+06	-8.2E+05	2.1E+07	-1.3E+05	-1.5E+05	-2.1E+05	-4.3E+05	-2.0E+05	-2.1E+05	-2.3E+05	-2.2E+05
97.7	4.0E+06	8.6E+06	-8.1E+06	4.1E+06	2.2E+07	2.0E+06	-9.5E+05	2.4E+07	-5.2E+04	-1.1E+05	-2.5E+05	-1.5E+05	-1.9E+05	-1.2E+05	-2.8E+05	-4.7E+05
107.4	3.8E+06	8.4E+06	-9.0E+06	3.1E+06	2.5E+07	2.0E+06	-8.7E+05	2.6E+07	-2.6E+05	-2.7E+05	-2.3E+05	-3.8E+05	-1.4E+05	-1.5E+05	-2.8E+05	-4.4E+05
117.2	4.4E+06	9.0E+06	-8.5E+06	3.6E+06	2.6E+07	2.4E+06	-1.4E+06	2.9E+07	-7.9E+04	-9.5E+04	-4.1E+05	-1.9E+05	-2.1E+05	-1.4E+05	-2.3E+05	-1.6E+05
127.0	4.2E+06	9.2E+06	-8.6E+06	3.7E+06	2.8E+07	2.5E+06	-9.0E+05	3.0E+07	-1.5E+05	-1.5E+05	-3.9E+05	-4.8E+05	-1.3E+05	-2.6E+05	-1.9E+05	-3.8E+05
136.7	4.2E+06	8.8E+06	-8.3E+06	4.0E+06	3.1E+07	2.9E+06	-7.8E+05	3.2E+07	-1.2E+05	-1.5E+05	-2.1E+05	-3.2E+05	-1.5E+05	-1.4E+05	-1.0E+05	-3.0E+05

Table 138 Raw data for the test seal at PR=0.6, ω=15 krpm, and inlet LVF=6% with the zero-preswirl insert

Freq.	Re(H_{XX})	Re(H_{XY})	Re(H_{YX})	Re(H_{YY})	Im(H_{XX})	Im(H_{XY})	Im(H_{YX})	Im(H_{YY})	Re(eH_{XX})	Re(eH_{XY})	Re(eH_{YX})	Re(eH_{YY})	Im(eH_{XX})	Im(eH_{XY})	Im(eH_{YX})	Im(eH_{YY})
Hz	N/m	N/m	N/m	N/m	N/m	N/m	N/m	N/m	N/m	N/m	N/m	N/m	N/m	N/m	N/m	N/m
9.8	9.9E+06	1.3E+07	-1.3E+07	4.7E+06	-1.3E+06	-1.1E+05	-1.7E+06	3.2E+06	-6.2E+05	-5.8E+05	-8.4E+05	-1.2E+06	-5.6E+05	-8.9E+05	-1.3E+06	-1.0E+06
19.5	6.9E+06	1.4E+07	-1.5E+07	4.6E+06	1.5E+06	-3.8E+05	6.6E+04	3.2E+06	-3.3E+05	-2.8E+05	-7.1E+05	-9.8E+05	-3.2E+05	-3.5E+05	-5.1E+05	-5.7E+05
29.3	6.0E+06	1.3E+07	-1.5E+07	5.9E+06	2.8E+06	2.7E+06	2.1E+06	4.8E+06	-1.9E+05	-2.5E+05	-3.2E+05	-5.1E+05	-2.2E+05	-3.0E+05	-4.0E+05	-5.2E+05
39.1	4.9E+06	1.3E+07	-1.3E+07	4.4E+06	7.3E+06	3.6E+05	7.9E+05	9.5E+06	-2.6E+05	-1.8E+05	-2.9E+05	-3.0E+05	-2.8E+05	-2.9E+05	-2.5E+05	-2.3E+05
48.8	4.7E+06	1.3E+07	-1.3E+07	5.0E+06	9.8E+06	8.2E+05	6.9E+04	1.2E+07	-1.6E+05	-2.0E+05	-1.9E+05	-2.6E+05	-3.1E+05	-2.8E+05	-1.9E+05	-3.0E+05
58.6	4.8E+06	1.4E+07	-1.3E+07	4.0E+06	1.2E+07	1.1E+06	-9.6E+05	1.5E+07	-1.7E+05	-2.9E+05	-2.5E+05	-2.0E+05	-3.3E+05	-2.4E+05	-2.9E+05	-1.8E+05
68.4	5.3E+06	1.4E+07	-1.3E+07	4.7E+06	1.5E+07	8.1E+05	-7.6E+05	1.6E+07	-2.0E+05	-4.2E+05	-2.9E+05	-1.7E+05	-2.7E+05	-4.9E+05	-1.8E+05	-4.8E+05
78.1	4.6E+06	1.4E+07	-1.3E+07	4.8E+06	1.7E+07	1.1E+06	-6.5E+05	2.0E+07	-9.0E+04	-1.3E+05	-2.6E+05	-3.3E+05	-1.6E+05	-2.1E+05	-2.4E+05	-3.2E+05
87.9	4.7E+06	1.3E+07	-1.3E+07	5.2E+06	1.9E+07	1.9E+06	-6.5E+05	2.2E+07	-1.8E+05	-2.2E+05	-3.4E+05	-1.9E+05	-9.3E+04	-2.7E+05	-2.5E+05	-2.0E+05
97.7	4.2E+06	1.3E+07	-1.4E+07	4.7E+06	2.2E+07	1.9E+06	-1.0E+06	2.5E+07	-1.3E+05	-2.4E+05	-2.1E+05	-2.0E+05	-2.0E+05	-1.7E+05	-2.3E+05	-1.9E+05
107.4	4.1E+06	1.3E+07	-1.4E+07	4.6E+06	2.4E+07	2.1E+06	-9.7E+05	2.7E+07	-1.7E+05	-2.7E+05	-3.2E+05	-3.2E+05	-2.3E+05	-3.0E+05	-1.9E+05	-2.0E+05
117.2	4.7E+06	1.4E+07	-1.3E+07	5.6E+06	2.6E+07	2.7E+06	-1.0E+06	3.0E+07	-1.2E+05	-1.2E+05	-1.3E+05	-1.4E+05	-2.4E+05	-1.7E+05	-2.2E+05	-2.8E+05
127.0	4.2E+06	1.4E+07	-1.4E+07	4.8E+06	2.8E+07	3.1E+06	-1.3E+06	3.2E+07	-1.9E+05	-2.3E+05	-2.0E+05	-3.7E+05	-1.2E+05	-3.6E+05	-2.9E+05	-5.6E+05
136.7	4.2E+06	1.4E+07	-1.4E+07	5.3E+06	3.0E+07	3.0E+06	-1.1E+06	3.3E+07	-2.9E+05	-1.9E+05	-1.5E+05	-2.8E+05	-1.6E+05	-1.7E+05	-2.4E+05	-2.0E+05

Table 139 Raw data for the test seal at PR=0.6, ω=5 krpm, and inlet LVF=8% with the zero-preswirl insert

Freq.	Re(H_{XX})	Re(H_{XY})	Re(H_{YX})	Re(H_{YY})	Im(H_{XX})	Im(H_{XY})	Im(H_{YX})	Im(H_{YY})	Re(eH_{XX})	Re(eH_{XY})	Re(eH_{YX})	Re(eH_{YY})	Im(eH_{XX})	Im(eH_{XY})	Im(eH_{YX})	Im(eH_{YY})
Hz	N/m	N/m	N/m	N/m	N/m	N/m	N/m	N/m	N/m	N/m	N/m	N/m	N/m	N/m	N/m	N/m
9.8	6.2E+06	1.2E+06	-5.4E+06	2.4E+06	1.3E+06	1.8E+06	1.7E+06	1.1E+06	-1.1E+05	-2.2E+05	-3.6E+05	-1.7E+05	-3.7E+05	-1.3E+05	-6.7E+05	-5.0E+05
19.5	5.5E+06	3.1E+06	-4.0E+06	2.6E+06	3.2E+06	2.3E+06	1.7E+06	4.9E+06	-2.4E+05	-1.8E+05	-2.4E+05	-2.9E+05	-2.3E+05	-4.0E+05	-5.8E+05	-1.4E+05
29.3	5.4E+06	3.6E+06	-4.4E+06	3.5E+06	4.4E+06	3.5E+06	2.5E+06	5.6E+06	-4.1E+05	-1.6E+05	-4.3E+05	-2.5E+05	-2.8E+05	-2.8E+05	-2.1E+05	-4.0E+05
39.1	4.8E+06	4.3E+06	-3.1E+06	3.0E+06	8.5E+06	1.5E+06	1.7E+06	1.0E+07	-2.3E+05	-2.1E+05	-3.0E+05	-3.1E+05	-2.8E+05	-1.7E+05	-3.7E+05	-1.4E+05
48.8	4.9E+06	4.3E+06	-3.2E+06	3.0E+06	1.0E+07	1.7E+06	2.3E+05	1.2E+07	-1.7E+05	-1.6E+05	-2.4E+05	-1.3E+05	-3.5E+05	-2.3E+05	-3.7E+05	-3.1E+05
58.6	4.5E+06	4.3E+06	-3.7E+06	2.8E+06	1.2E+07	1.2E+06	6.0E+05	1.4E+07	-2.2E+05	-2.8E+05	-3.8E+05	-2.3E+05	-2.5E+05	-1.4E+05	-3.7E+05	-2.2E+05
68.4	3.7E+06	4.1E+06	-3.9E+06	3.0E+06	1.4E+07	9.6E+05	2.2E+05	1.6E+07	-1.9E+05	-2.2E+05	-2.9E+05	-5.7E+05	-3.2E+05	-1.8E+05	-3.7E+05	-4.9E+05
78.1	3.8E+06	4.5E+06	-4.4E+06	3.3E+06	1.8E+07	9.7E+05	-1.7E+05	1.8E+07	-2.2E+05	-1.1E+05	-2.9E+05	-1.8E+05	-2.6E+05	-1.1E+05	-2.3E+05	-2.5E+05
87.9	3.8E+06	4.5E+06	-4.0E+06	2.7E+06	1.9E+07	1.3E+06	2.1E+05	2.0E+07	-9.5E+04	-2.6E+05	-1.7E+05	-1.7E+05	-2.3E+05	-1.7E+05	-3.7E+05	-1.3E+05
97.7	3.3E+06	4.4E+06	-4.7E+06	2.4E+06	2.2E+07	6.6E+05	-2.6E+05	2.3E+07	-2.0E+05	-2.9E+05	-1.6E+05	-1.4E+05	-1.6E+05	-2.5E+05	-2.5E+05	-1.9E+05
107.4	2.8E+06	3.9E+06	-5.2E+06	1.7E+06	2.5E+07	1.2E+06	-7.1E+05	2.5E+07	-1.1E+05	-2.6E+05	-1.8E+05	-3.5E+05	-2.5E+05	-9.5E+04	-1.8E+05	-1.2E+05
117.2	4.4E+06	3.9E+06	-4.2E+06	2.2E+06	2.7E+07	9.1E+05	8.1E+04	2.8E+07	-9.6E+04	-1.2E+05	-2.4E+05	-1.9E+05	-1.5E+05	-2.0E+05	-5.0E+05	-2.3E+05
127.0	3.5E+06	4.1E+06	-4.8E+06	2.6E+06	2.9E+07	7.1E+05	9.2E+05	3.0E+07	-1.2E+05	-1.0E+05	-3.9E+05	-4.5E+05	-3.2E+05	-1.8E+05	-2.9E+05	-5.7E+05
136.7	3.2E+06	4.1E+06	-4.6E+06	2.1E+06	3.1E+07	9.9E+05	6.8E+05	3.2E+07	-2.6E+05	-1.5E+05	-3.0E+05	-1.9E+05	-2.0E+05	-2.0E+05	-3.0E+05	-3.7E+05

Table 140 Raw data for the test seal at PR=0.6, ω=10 krpm, and inlet LVF=8% with the zero-preswirl insert

Freq.	Re(H_{XX})	Re(H_{XY})	Re(H_{YX})	Re(H_{YY})	Im(H_{XX})	Im(H_{XY})	Im(H_{YX})	Im(H_{YY})	Re(eH_{XX})	Re(eH_{XY})	Re(eH_{YX})	Re(eH_{YY})	Im(eH_{XX})	Im(eH_{XY})	Im(eH_{YX})	Im(eH_{YY})
Hz	N/m	N/m	N/m	N/m	N/m	N/m	N/m	N/m	N/m	N/m	N/m	N/m	N/m	N/m	N/m	N/m
9.8	7.4E+06	6.5E+06	-9.3E+06	3.9E+06	-2.2E+06	1.6E+06	1.5E+06	3.3E+06	-3.2E+05	-2.3E+05	-8.2E+05	-5.3E+05	-3.4E+05	-2.4E+05	-3.0E+05	-5.1E+05
19.5	5.8E+06	8.1E+06	-7.8E+06	3.0E+06	2.3E+06	7.5E+05	1.0E+06	5.3E+06	-2.4E+05	-2.0E+05	-3.1E+05	-5.0E+05	-2.4E+05	-3.0E+05	-5.0E+05	-5.0E+05
29.3	6.7E+06	7.1E+06	-8.3E+06	4.7E+06	3.8E+06	1.0E+06	1.4E+06	6.5E+06	-2.1E+05	-2.9E+05	-3.2E+05	-2.4E+05	-1.7E+05	-3.1E+05	-3.9E+05	-4.2E+05
39.1	5.2E+06	7.9E+06	-7.1E+06	4.1E+06	6.9E+06	9.1E+05	3.8E+04	1.1E+07	-9.2E+04	-2.1E+05	-3.3E+05	-3.0E+05	-3.4E+05	-1.1E+05	-2.2E+05	-1.9E+05
48.8	4.7E+06	8.5E+06	-7.2E+06	4.0E+06	9.6E+06	1.2E+06	-3.4E+05	1.3E+07	-2.8E+05	-1.8E+05	-2.2E+05	-4.5E+05	-1.3E+05	-2.5E+05	-1.9E+05	-2.2E+05
58.6	4.7E+06	7.9E+06	-7.7E+06	4.3E+06	1.2E+07	1.6E+06	-9.1E+05	1.5E+07	-1.4E+05	-3.2E+05	-2.7E+05	-4.3E+05	-3.4E+05	-3.0E+05	-3.1E+05	-4.7E+05
68.4	4.6E+06	8.2E+06	-6.7E+06	3.5E+06	1.5E+07	1.9E+06	-6.5E+05	1.7E+07	-2.5E+05	-2.4E+05	-2.8E+05	-1.9E+05	-2.1E+05	-3.2E+05	-3.0E+05	-3.2E+05
78.1	4.6E+06	8.1E+06	-6.9E+06	4.4E+06	1.8E+07	1.7E+06	-1.1E+06	1.9E+07	-2.6E+05	-2.5E+05	-2.5E+05	-3.7E+05	-3.0E+05	-2.2E+05	-3.9E+05	-4.0E+05
87.9	4.6E+06	8.4E+06	-7.4E+06	4.0E+06	2.0E+07	2.2E+06	-9.0E+05	2.2E+07	-1.2E+05	-1.5E+05	-1.0E+05	-2.2E+05	-1.6E+05	-2.8E+05	-1.4E+05	-3.0E+05
97.7	4.8E+06	8.6E+06	-7.1E+06	3.8E+06	2.3E+07	2.7E+06	-1.5E+06	2.4E+07	-1.5E+05	-1.3E+05	-1.6E+05	-1.7E+05	-1.5E+05	-3.7E+05	-1.4E+05	-3.0E+05
107.4	4.4E+06	8.0E+06	-8.5E+06	2.6E+06	2.6E+07	2.7E+06	-1.5E+06	2.6E+07	-1.8E+05	-2.0E+05	-4.0E+05	-2.4E+05	-2.8E+05	-2.2E+05	-3.9E+05	-2.8E+05
117.2	5.2E+06	9.2E+06	-8.4E+06	3.7E+06	2.6E+07	2.5E+06	-2.1E+06	2.9E+07	-1.1E+05	-2.3E+05	-1.4E+05	-1.9E+05	-2.6E+05	-1.6E+05	-2.3E+05	-1.4E+05
127.0	5.0E+06	9.0E+06	-8.0E+06	3.0E+06	2.8E+07	2.8E+06	-2.0E+06	3.2E+07	-1.8E+05	-1.5E+05	-2.6E+05	-3.0E+05	-2.6E+05	-1.7E+05	-2.7E+05	-4.0E+05
136.7	4.3E+06	8.3E+06	-8.7E+06	3.4E+06	3.1E+07	3.3E+06	-1.8E+06	3.4E+07	-2.2E+05	-1.3E+05	-1.4E+05	-2.7E+05	-1.4E+05	-2.2E+05	-8.1E+04	-2.9E+05

Table 141 Raw data for the test seal at PR=0.6, ω=15 krpm, and inlet LVF=8% with the zero-preswirl insert

Freq.	Re(H_{XX})	Re(H_{XY})	Re(H_{YX})	Re(H_{YY})	Im(H_{XX})	Im(H_{XY})	Im(H_{YX})	Im(H_{YY})	Re(eH_{XX})	Re(eH_{XY})	Re(eH_{YX})	Re(eH_{YY})	Im(eH_{XX})	Im(eH_{XY})	Im(eH_{YX})	Im(eH_{YY})
Hz	N/m	N/m	N/m	N/m	N/m	N/m	N/m	N/m	N/m	N/m	N/m	N/m	N/m	N/m	N/m	N/m
9.8	1.1E+07	1.4E+07	-1.1E+07	5.8E+06	5.4E+05	9.8E+05	-1.5E+06	1.3E+06	-8.3E+05	-8.1E+05	-1.2E+06	-1.0E+06	-8.6E+05	-9.6E+05	-6.5E+05	-7.3E+05
19.5	7.5E+06	1.4E+07	-1.4E+07	3.6E+06	4.5E+05	-1.5E+06	-7.9E+03	5.3E+06	-3.4E+05	-3.1E+05	-3.4E+05	-4.4E+05	-3.4E+05	-4.8E+05	-3.9E+05	-4.3E+05
29.3	6.6E+06	1.3E+07	-1.5E+07	5.3E+06	2.8E+06	2.1E+06	1.6E+06	6.3E+06	-1.9E+05	-4.1E+05	-2.1E+05	-4.3E+05	-3.1E+05	-4.2E+05	-2.8E+05	-4.1E+05
39.1	4.7E+06	1.3E+07	-1.2E+07	4.3E+06	6.9E+06	7.2E+05	8.0E+05	1.1E+07	-2.3E+05	-1.4E+05	-1.9E+05	-1.7E+05	-1.7E+05	-8.4E+04	-3.1E+05	-3.1E+05
48.8	5.5E+06	1.4E+07	-1.2E+07	4.3E+06	1.0E+07	5.1E+05	3.1E+05	1.3E+07	-1.9E+05	-2.2E+05	-2.8E+05	-3.0E+05	-3.8E+05	-3.8E+05	-2.7E+05	-3.2E+05
58.6	5.6E+06	1.3E+07	-1.2E+07	4.3E+06	1.2E+07	1.2E+06	-7.4E+05	1.6E+07	-2.6E+05	-2.3E+05	-2.4E+05	-2.6E+05	-1.3E+05	-2.3E+05	-4.4E+05	-4.0E+05
68.4	5.8E+06	1.4E+07	-1.2E+07	4.2E+06	1.5E+07	1.1E+06	-7.9E+05	1.8E+07	-3.0E+05	-4.5E+05	-2.4E+05	-4.5E+05	-2.1E+05	-2.9E+05	-4.4E+05	-8.7E+05
78.1	4.9E+06	1.3E+07	-1.2E+07	4.9E+06	1.7E+07	1.5E+06	-5.4E+05	2.0E+07	-2.9E+05	-3.0E+05	-2.1E+05	-3.7E+05	-2.7E+05	-3.7E+05	-1.3E+05	-2.2E+05
87.9	5.1E+06	1.3E+07	-1.3E+07	4.4E+06	2.0E+07	1.4E+06	-1.3E+06	2.3E+07	-1.7E+05	-2.1E+05	-2.6E+05	-4.3E+05	-2.6E+05	-2.1E+05	-2.3E+05	-1.5E+05
97.7	4.6E+06	1.3E+07	-1.3E+07	4.9E+06	2.2E+07	2.0E+06	-1.5E+06	2.6E+07	-2.3E+05	-1.1E+05	-4.5E+05	-2.6E+05	-1.8E+05	-3.6E+05	-2.5E+05	-2.6E+05
107.4	4.1E+06	1.2E+07	-1.3E+07	5.3E+06	2.5E+07	2.8E+06	-1.4E+06	2.8E+07	-2.1E+05	-2.0E+05	-2.8E+05	-2.1E+05	-1.9E+05	-1.1E+05	-3.9E+05	-1.9E+05
117.2	5.0E+06	1.3E+07	-1.3E+07	5.5E+06	2.6E+07	3.4E+06	-2.1E+06	3.1E+07	-2.2E+05	-1.8E+05	-2.2E+05	-3.4E+05	-1.4E+05	-3.2E+05	-3.4E+05	-2.0E+05
127.0	4.4E+06	1.4E+07	-1.3E+07	6.1E+06	2.8E+07	3.7E+06	-1.4E+06	3.3E+07	-2.3E+05	-4.1E+05	-3.2E+05	-6.0E+05	-2.2E+05	-4.4E+05	-2.8E+05	-4.3E+05
136.7	4.0E+06	1.4E+07	-1.4E+07	5.8E+06	3.1E+07	3.6E+06	-1.4E+06	3.5E+07	-1.6E+05	-3.7E+05	-3.3E+05	-3.1E+05	-1.5E+05	-2.8E+05	-2.8E+05	-4.2E+05

Table 142 Raw data for the test seal at PR=0.5, ω=5 krpm, and inlet LVF=0% with the zero-preswirl insert

Freq.	Re(H_{XX})	Re(H_{XY})	Re(H_{YX})	Re(H_{YY})	Im(H_{XX})	Im(H_{XY})	Im(H_{YX})	Im(H_{YY})	Re(eH_{XX})	Re(eH_{XY})	Re(eH_{YX})	Re(eH_{YY})	Im(eH_{XX})	Im(eH_{XY})	Im(eH_{YX})	Im(eH_{YY})
Hz	N/m	N/m	N/m	N/m	N/m	N/m	N/m	N/m	N/m	N/m	N/m	N/m	N/m	N/m	N/m	N/m
9.8	5.3E+06	3.2E+05	-2.7E+06	5.1E+06	1.3E+06	3.7E+05	4.2E+04	2.0E+06	-1.1E+05	-1.1E+05	-1.2E+05	-9.2E+04	-1.1E+05	-9.1E+04	-1.0E+05	-1.4E+05
19.5	5.0E+06	3.5E+05	-2.7E+06	4.8E+06	3.0E+06	3.6E+05	2.9E+05	3.1E+06	-5.7E+04	-1.0E+05	-1.4E+05	-8.5E+04	-8.5E+04	-1.3E+05	-4.5E+04	-7.6E+04
29.3	4.6E+06	1.3E+06	-2.4E+06	4.7E+06	4.0E+06	9.5E+05	9.3E+05	3.9E+06	-1.0E+05	-1.3E+05	-6.6E+04	-1.1E+05	-1.2E+05	-1.4E+05	-8.0E+04	-1.1E+05
39.1	4.7E+06	6.2E+05	-2.7E+06	4.6E+06	6.3E+06	4.0E+05	3.7E+04	6.5E+06	-1.3E+05	-5.6E+04	-1.4E+05	-2.9E+04	-7.2E+04	-4.7E+04	-1.1E+05	-4.0E+04
48.8	4.8E+06	6.9E+05	-2.1E+06	4.3E+06	8.2E+06	1.8E+05	6.0E+04	8.3E+06	-6.2E+04	-1.0E+05	-1.1E+05	-1.0E+05	-7.4E+04	-8.6E+04	-1.2E+05	-1.1E+05
58.6	4.8E+06	3.1E+05	-2.1E+06	4.5E+06	1.0E+07	2.6E+05	-4.1E+05	1.0E+07	-6.9E+04	-7.8E+04	-9.8E+04	-6.8E+04	-1.2E+05	-4.8E+04	-1.5E+05	-1.6E+05
68.4	4.6E+06	2.8E+05	-2.5E+06	4.4E+06	1.2E+07	2.2E+05	-1.6E+05	1.2E+07	-9.1E+04	-1.7E+05	-1.4E+05	-2.4E+05	-4.0E+04	-8.4E+04	-8.5E+04	-1.8E+05
78.1	4.7E+06	4.3E+05	-2.7E+06	4.2E+06	1.3E+07	4.7E+05	-4.3E+05	1.4E+07	-7.1E+04	-1.0E+05	-7.6E+04	-7.6E+04	-7.7E+04	-5.1E+04	-5.8E+04	-6.8E+04
87.9	4.5E+06	2.5E+05	-2.7E+06	4.4E+06	1.5E+07	2.3E+05	-5.6E+05	1.6E+07	-9.6E+04	-5.9E+04	-9.2E+04	-5.6E+04	-8.8E+04	-8.8E+04	-1.2E+05	-8.5E+04
97.7	4.5E+06	-4.4E+04	-2.9E+06	4.1E+06	1.7E+07	9.5E+04	-7.8E+05	1.8E+07	-4.2E+04	-6.8E+04	-7.5E+04	-6.5E+04	-4.0E+04	-7.0E+04	-7.4E+04	-1.1E+05
107.4	4.1E+06	-6.1E+05	-3.7E+06	4.1E+06	1.9E+07	4.7E+05	-3.8E+05	2.0E+07	-1.2E+05	-1.0E+05	-1.4E+05	-6.9E+04	-1.2E+05	-7.2E+04	-8.8E+04	-9.7E+04
117.2	4.7E+06	-1.9E+05	-3.1E+06	4.4E+06	2.0E+07	8.6E+05	-5.3E+05	2.2E+07	-8.0E+04	-2.3E+04	-6.2E+04	-6.5E+04	-7.4E+04	-3.6E+04	-1.7E+05	-9.4E+04
127.0	4.6E+06	-3.0E+05	-3.5E+06	4.9E+06	2.1E+07	1.4E+06	-1.8E+05	2.3E+07	-6.2E+04	-1.1E+05	-5.0E+04	-9.6E+04	-7.1E+04	-1.1E+05	-8.3E+04	-1.2E+05
136.7	4.7E+06	-4.6E+05	-3.7E+06	5.1E+06	2.3E+07	1.5E+06	-1.1E+05	2.4E+07	-6.7E+04	-4.9E+04	-7.1E+04	-7.4E+04	-9.6E+04	-8.7E+04	-6.9E+04	-7.0E+04

Table 143 Raw data for the test seal at PR=0.5, ω=10 krpm, and inlet LVF=0% with the zero-preswirl insert

Freq.	Re(H_{XX})	Re(H_{XY})	Re(H_{YX})	Re(H_{YY})	Im(H_{XX})	Im(H_{XY})	Im(H_{YX})	Im(H_{YY})	Re(eH_{XX})	Re(eH_{XY})	Re(eH_{YX})	Re(eH_{YY})	Im(eH_{XX})	Im(eH_{XY})	Im(eH_{YX})	Im(eH_{YY})
Hz	N/m	N/m	N/m	N/m	N/m	N/m	N/m	N/m	N/m	N/m	N/m	N/m	N/m	N/m	N/m	N/m
9.8	4.8E+06	2.7E+06	-5.2E+06	4.6E+06	1.2E+06	1.9E+05	7.5E+04	1.3E+06	-8.0E+04	-1.3E+05	-2.4E+05	-1.5E+05	-8.3E+04	-1.3E+05	-1.9E+05	-1.4E+05
19.5	4.5E+06	3.0E+06	-5.3E+06	4.5E+06	2.9E+06	3.7E+05	-1.0E+05	3.4E+06	-6.8E+04	-6.0E+04	-5.7E+04	-5.5E+04	-6.3E+04	-6.2E+04	-5.2E+04	-1.7E+05
29.3	4.3E+06	3.3E+06	-5.0E+06	4.1E+06	3.9E+06	1.2E+06	7.6E+05	3.8E+06	-1.3E+05	-1.1E+05	-7.8E+04	-1.5E+05	-1.4E+05	-1.5E+05	-5.7E+04	-1.2E+05
39.1	4.2E+06	3.1E+06	-5.1E+06	4.1E+06	6.0E+06	2.3E+05	-1.0E+05	6.5E+06	-4.0E+04	-3.7E+04	-5.9E+04	-9.3E+04	-4.3E+04	-2.9E+04	-1.2E+05	-3.9E+04
48.8	4.0E+06	3.1E+06	-4.7E+06	3.6E+06	7.9E+06	2.9E+05	-3.2E+05	8.4E+06	-6.9E+04	-7.7E+04	-7.7E+04	-6.1E+04	-5.5E+04	-9.7E+04	-1.2E+05	-8.8E+04
58.6	3.8E+06	3.0E+06	-4.8E+06	3.7E+06	9.8E+06	5.0E+05	-3.6E+05	9.9E+06	-3.8E+04	-7.5E+04	-1.7E+05	-1.2E+05	-9.4E+04	-3.7E+04	-1.2E+05	-9.9E+04
68.4	3.8E+06	3.1E+06	-4.9E+06	3.8E+06	1.2E+07	2.1E+05	-3.3E+05	1.2E+07	-7.7E+04	-6.5E+04	-5.9E+04	-1.8E+05	-6.8E+04	-9.2E+04	-7.7E+04	-1.5E+05
78.1	3.7E+06	3.1E+06	-5.0E+06	3.2E+06	1.3E+07	1.6E+05	-5.8E+05	1.4E+07	-6.6E+04	-4.0E+04	-3.3E+04	-8.7E+04	-6.3E+04	-8.2E+04	-6.4E+04	-1.1E+05
87.9	3.8E+06	2.7E+06	-5.0E+06	3.1E+06	1.5E+07	3.3E+05	-8.3E+05	1.6E+07	-7.7E+04	-9.7E+04	-8.2E+04	-8.1E+04	-5.5E+04	-4.6E+04	-7.5E+04	-1.0E+05
97.7	3.9E+06	2.3E+06	-5.5E+06	3.1E+06	1.7E+07	2.9E+05	-1.3E+06	1.8E+07	-8.3E+04	-6.0E+04	-3.1E+04	-6.5E+04	-5.9E+04	-8.6E+04	-7.2E+04	-7.7E+04
107.4	3.7E+06	1.7E+06	-5.8E+06	3.4E+06	1.9E+07	7.4E+05	-6.9E+05	2.0E+07	-5.2E+04	-7.2E+04	-1.1E+05	-4.9E+04	-9.9E+04	-6.1E+04	-6.9E+04	-3.4E+04
117.2	4.4E+06	2.3E+06	-5.5E+06	4.0E+06	2.0E+07	1.0E+06	-1.0E+06	2.2E+07	-1.0E+05	-5.9E+04	-4.9E+04	-6.7E+04	-7.9E+04	-6.5E+04	-4.7E+04	-7.4E+04
127.0	4.2E+06	2.1E+06	-5.6E+06	4.8E+06	2.1E+07	1.4E+06	-5.0E+05	2.4E+07	-4.2E+04	-8.3E+04	-8.8E+04	-9.3E+04	-5.5E+04	-1.2E+05	-8.2E+04	-9.9E+04
136.7	4.5E+06	2.0E+06	-6.1E+06	4.8E+06	2.3E+07	1.7E+06	-3.1E+05	2.5E+07	-6.9E+04	-7.1E+04	-7.4E+04	-7.6E+04	-5.4E+04	-8.8E+04	-5.7E+04	-1.0E+05

Table 144 Raw data for the test seal at PR=0.5, ω=15 krpm, and inlet LVF=0% with the zero-preswirl insert

Freq.	Re(H_{XX})	Re(H_{XY})	Re(H_{YX})	Re(H_{YY})	Im(H_{XX})	Im(H_{XY})	Im(H_{YX})	Im(H_{YY})	Re(eH_{XX})	Re(eH_{XY})	Re(eH_{YX})	Re(eH_{YY})	Im(eH_{XX})	Im(eH_{XY})	Im(eH_{YX})	Im(eH_{YY})
Hz	N/m	N/m	N/m	N/m	N/m	N/m	N/m	N/m	N/m	N/m	N/m	N/m	N/m	N/m	N/m	N/m
9.8	5.5E+06	5.1E+06	-7.6E+06	4.4E+06	1.1E+06	9.2E+04	-1.4E+05	1.4E+06	-7.8E+04	-9.4E+04	-1.3E+05	-1.1E+05	-9.6E+04	-8.6E+04	-7.2E+04	-1.6E+05
19.5	4.9E+06	5.5E+06	-7.8E+06	4.3E+06	2.8E+06	4.6E+05	-6.6E+04	3.2E+06	-1.1E+05	-8.6E+04	-1.1E+05	-1.8E+05	-1.1E+05	-5.1E+04	-1.1E+05	-1.5E+05
29.3	4.9E+06	5.4E+06	-8.0E+06	4.1E+06	3.7E+06	1.5E+06	2.3E+05	3.9E+06	-1.3E+05	-6.3E+04	-1.0E+05	-1.2E+05	-9.8E+04	-1.0E+05	-1.2E+05	-1.2E+05
39.1	4.6E+06	5.3E+06	-7.9E+06	3.9E+06	5.7E+06	8.2E+05	-6.2E+05	6.6E+06	-5.3E+04	-3.4E+04	-7.0E+04	-7.4E+04	-5.6E+04	-5.6E+04	-9.5E+04	-9.1E+04
48.8	4.2E+06	5.6E+06	-7.9E+06	3.6E+06	7.4E+06	1.1E+06	-5.7E+05	8.4E+06	-6.7E+04	-5.8E+04	-5.1E+04	-6.5E+04	-1.1E+05	-1.4E+05	-1.2E+05	-1.5E+05
58.6	4.0E+06	5.8E+06	-8.0E+06	3.6E+06	9.4E+06	1.1E+06	-5.6E+05	1.0E+07	-9.6E+04	-1.1E+05	-1.5E+05	-6.4E+04	-1.0E+05	-9.0E+04	-8.7E+04	-7.7E+04
68.4	3.6E+06	5.8E+06	-8.2E+06	3.4E+06	1.1E+07	8.4E+05	-6.9E+05	1.2E+07	-7.9E+04	-1.3E+05	-1.2E+05	-1.8E+05	-6.2E+04	-1.4E+05	-3.6E+04	-1.0E+05
78.1	3.6E+06	5.8E+06	-8.4E+06	3.1E+06	1.3E+07	8.4E+05	-7.0E+05	1.4E+07	-5.5E+04	-1.1E+05	-6.4E+04	-9.4E+04	-8.0E+04	-7.1E+04	-7.7E+04	-7.6E+04
87.9	3.4E+06	5.8E+06	-8.5E+06	2.9E+06	1.5E+07	6.8E+05	-1.0E+06	1.6E+07	-9.0E+04	-6.7E+04	-1.1E+05	-1.4E+05	-8.2E+04	-4.5E+04	-7.7E+04	-1.1E+05
97.7	3.3E+06	5.6E+06	-8.3E+06	2.7E+06	1.7E+07	5.9E+05	-1.0E+06	1.8E+07	-5.9E+04	-3.3E+04	-1.0E+05	-5.8E+04	-9.0E+04	-7.1E+04	-1.4E+05	-7.6E+04
107.4	3.3E+06	4.8E+06	-8.7E+06	3.3E+06	1.9E+07	7.6E+05	-6.0E+05	2.0E+07	-6.9E+04	-8.0E+04	-1.3E+05	-6.4E+04	-6.6E+04	-5.6E+04	-1.1E+05	-1.3E+05
117.2	4.0E+06	5.1E+06	-8.6E+06	3.8E+06	2.0E+07	1.4E+06	-9.1E+05	2.2E+07	-9.6E+04	-7.9E+04	-8.7E+04	-1.0E+05	-5.9E+04	-6.8E+04	-1.0E+05	-1.1E+05
127.0	4.0E+06	4.9E+06	-8.6E+06	4.6E+06	2.1E+07	1.6E+06	-6.6E+05	2.4E+07	-5.7E+04	-9.7E+04	-9.5E+04	-1.9E+05	-5.7E+04	-1.5E+05	-7.6E+04	-1.5E+05
136.7	4.1E+06	5.0E+06	-8.9E+06	4.7E+06	2.3E+07	2.4E+06	-6.7E+05	2.5E+07	-4.5E+04	-8.1E+04	-3.7E+04	-1.2E+05	-6.9E+04	-8.6E+04	-8.7E+04	-7.0E+04

Table 145 Raw data for the test seal at PR=0.5, ω=5 krpm, and inlet LVF=2% with the zero-preswirl insert

Freq.	Re(H_{XX})	Re(H_{XY})	Re(H_{YX})	Re(H_{YY})	Im(H_{XX})	Im(H_{XY})	Im(H_{YX})	Im(H_{YY})	Re(eH_{XX})	Re(eH_{XY})	Re(eH_{YX})	Re(eH_{YY})	Im(eH_{XX})	Im(eH_{XY})	Im(eH_{YX})	Im(eH_{YY})
Hz	N/m	N/m	N/m	N/m	N/m	N/m	N/m	N/m	N/m	N/m	N/m	N/m	N/m	N/m	N/m	N/m
9.8	3.5E+06	2.9E+06	-4.9E+06	2.4E+06	2.4E+06	6.3E+05	6.5E+05	2.8E+06	-1.8E+05	-1.5E+05	-1.5E+05	-3.0E+05	-1.2E+05	-3.0E+05	-2.3E+05	-2.5E+05
19.5	3.7E+06	3.3E+06	-4.3E+06	2.6E+06	4.5E+06	6.8E+05	3.3E+05	4.8E+06	-2.2E+05	-8.3E+04	-1.8E+05	-1.9E+05	-2.6E+05	-1.5E+05	-1.3E+05	-2.5E+05
29.3	4.2E+06	2.9E+06	-5.1E+06	3.5E+06	5.6E+06	2.0E+06	8.2E+05	6.0E+06	-1.4E+05	-8.4E+04	-2.7E+05	-1.9E+05	-7.7E+04	-1.2E+05	-1.6E+05	-2.1E+05
39.1	3.6E+06	3.6E+06	-4.5E+06	2.8E+06	8.3E+06	7.1E+05	-2.9E+05	9.1E+06	-1.2E+05	-8.0E+04	-1.1E+05	-1.3E+05	-1.5E+05	-1.0E+05	-1.7E+05	-1.3E+05
48.8	4.1E+06	3.8E+06	-4.3E+06	3.2E+06	1.0E+07	5.4E+05	-2.0E+05	1.1E+07	-1.2E+05	-1.5E+05	-9.7E+04	-1.3E+05	-9.6E+04	-1.9E+05	-1.1E+05	-2.2E+05
58.6	3.9E+06	3.8E+06	-4.5E+06	3.0E+06	1.3E+07	7.9E+05	1.3E+05	1.3E+07	-1.5E+05	-1.2E+05	-1.6E+05	-1.3E+05	-1.5E+05	-7.0E+04	-2.0E+05	-1.3E+05
68.4	3.5E+06	4.0E+06	-4.5E+06	3.6E+06	1.4E+07	8.0E+05	-4.8E+05	1.5E+07	-1.2E+05	-1.2E+05	-1.1E+05	-1.1E+05	-1.1E+05	-3.1E+05	-1.6E+05	-3.8E+05
78.1	3.6E+06	3.9E+06	-4.8E+06	3.1E+06	1.7E+07	7.0E+05	-1.9E+05	1.7E+07	-4.1E+04	-5.8E+04	-9.4E+04	-1.2E+05	-5.4E+04	-9.0E+04	-1.4E+05	-1.0E+05
87.9	3.1E+06	4.0E+06	-5.4E+06	2.9E+06	1.9E+07	4.8E+05	-3.9E+05	2.0E+07	-6.9E+04	-4.5E+04	-7.4E+04	-1.1E+05	-9.9E+04	-4.5E+04	-1.5E+05	-1.3E+05
97.7	3.4E+06	3.8E+06	-5.3E+06	3.0E+06	2.1E+07	5.2E+05	-3.7E+05	2.3E+07	-7.7E+04	-1.3E+05	-1.0E+05	-2.0E+05	-8.3E+04	-8.6E+04	-1.3E+05	-1.6E+05
107.4	3.2E+06	3.4E+06	-6.0E+06	3.1E+06	2.4E+07	3.9E+05	8.9E+04	2.4E+07	-1.0E+05	-9.4E+04	-9.2E+04	-1.1E+05	-1.3E+05	-7.7E+04	-1.5E+05	-8.0E+04
117.2	3.9E+06	3.9E+06	-5.6E+06	3.5E+06	2.5E+07	7.2E+05	2.1E+05	2.7E+07	-9.0E+04	-8.0E+04	-9.9E+04	-8.4E+04	-8.0E+04	-8.2E+04	-1.3E+05	-1.2E+05
127.0	3.5E+06	3.9E+06	-5.4E+06	4.3E+06	2.7E+07	8.3E+05	7.2E+05	2.9E+07	-5.7E+04	-1.7E+05	-7.5E+04	-2.0E+05	-4.1E+04	-1.5E+05	-7.2E+04	-2.4E+05
136.7	3.5E+06	3.9E+06	-5.6E+06	4.5E+06	2.9E+07	1.0E+06	9.4E+05	3.0E+07	-9.5E+04	-8.4E+04	-1.3E+05	-9.1E+04	-6.0E+04	-8.3E+04	-7.1E+04	-1.1E+05

Table 146 Raw data for the test seal at PR=0.5, ω=10 krpm, and inlet LVF=2% with the zero-preswirl insert

Freq.	Re(H_{XX})	Re(H_{XY})	Re(H_{YX})	Re(H_{YY})	Im(H_{XX})	Im(H_{XY})	Im(H_{YX})	Im(H_{YY})	Re(eH_{XX})	Re(eH_{XY})	Re(eH_{YX})	Re(eH_{YY})	Im(eH_{XX})	Im(eH_{XY})	Im(eH_{YX})	Im(eH_{YY})
Hz	N/m	N/m	N/m	N/m	N/m	N/m	N/m	N/m	N/m	N/m	N/m	N/m	N/m	N/m	N/m	N/m
9.8	3.7E+06	8.5E+06	-9.7E+06	2.2E+06	1.3E+06	5.1E+05	-2.1E+05	2.7E+06	-2.4E+05	-2.2E+05	-2.2E+05	-2.1E+05	-3.7E+05	-3.8E+05	-3.8E+05	-4.3E+05
19.5	3.3E+06	8.2E+06	-9.1E+06	2.2E+06	3.8E+06	4.4E+05	1.6E+05	5.0E+06	-1.0E+05	-1.0E+05	-1.7E+05	-1.7E+05	-1.7E+05	-1.9E+05	-1.4E+05	-1.4E+05
29.3	4.1E+06	7.9E+06	-9.2E+06	3.3E+06	5.8E+06	2.0E+06	1.3E+06	5.7E+06	-2.2E+05	-7.1E+04	-1.1E+05	-2.1E+05	-2.2E+05	-8.4E+04	-2.8E+05	-1.7E+05
39.1	3.4E+06	9.0E+06	-8.7E+06	3.5E+06	8.7E+06	8.3E+05	6.9E+05	9.5E+06	-1.7E+05	-9.2E+04	-2.3E+05	-8.8E+04	-1.2E+05	-1.1E+05	-1.9E+05	-1.5E+05
48.8	3.4E+06	9.1E+06	-8.3E+06	3.1E+06	1.1E+07	5.9E+05	3.9E+05	1.1E+07	-1.9E+05	-1.1E+05	-1.7E+05	-9.9E+04	-1.2E+05	-1.0E+05	-1.7E+05	-1.1E+05
58.6	3.1E+06	9.3E+06	-9.0E+06	3.3E+06	1.3E+07	8.3E+05	6.6E+05	1.3E+07	-1.8E+05	-1.1E+05	-2.6E+05	-2.4E+05	-1.4E+05	-1.6E+05	-1.8E+05	-2.5E+05
68.4	3.1E+06	8.9E+06	-8.5E+06	3.6E+06	1.5E+07	5.3E+05	2.1E+05	1.5E+07	-1.4E+05	-1.2E+05	-1.1E+05	-2.2E+05	-7.7E+04	-1.5E+05	-2.4E+05	-2.8E+05
78.1	3.4E+06	9.0E+06	-8.5E+06	3.3E+06	1.7E+07	5.3E+05	3.1E+04	1.8E+07	-9.7E+04	-8.4E+04	-2.3E+05	-1.3E+05	-9.3E+04	-9.3E+04	-1.4E+05	-1.3E+05
87.9	3.3E+06	8.9E+06	-9.0E+06	2.9E+06	2.0E+07	6.5E+05	-5.7E+05	2.0E+07	-1.2E+05	-6.8E+04	-1.9E+05	-1.3E+05	-4.5E+04	-9.1E+04	-1.3E+05	-2.0E+05
97.7	3.2E+06	9.0E+06	-9.3E+06	3.0E+06	2.2E+07	9.0E+05	-2.8E+05	2.3E+07	-5.7E+04	-2.6E+04	-1.1E+05	-4.9E+04	-5.3E+04	-9.0E+04	-8.8E+04	-1.2E+05
107.4	3.1E+06	8.4E+06	-1.0E+07	3.1E+06	2.5E+07	7.8E+05	-3.9E+05	2.5E+07	-6.4E+04	-1.2E+05	-1.4E+05	-1.6E+05	-1.3E+05	-6.9E+04	-2.2E+05	-1.5E+05
117.2	4.1E+06	9.1E+06	-9.6E+06	3.4E+06	2.6E+07	8.5E+05	-4.1E+05	2.7E+07	-1.6E+05	-4.9E+04	-1.6E+05	-4.1E+04	-5.0E+04	-4.5E+04	-1.1E+05	-2.1E+05
127.0	4.1E+06	9.0E+06	-9.4E+06	4.4E+06	2.8E+07	1.3E+06	-7.6E+04	3.0E+07	-1.3E+05	-1.1E+05	-1.6E+05	-1.6E+05	-9.8E+04	-1.8E+05	-8.5E+04	-2.3E+05
136.7	4.2E+06	8.7E+06	-9.3E+06	4.1E+06	3.0E+07	1.4E+06	-2.2E+05	3.1E+07	-1.2E+05	-3.6E+04	-2.0E+05	-1.6E+05	-1.2E+05	-8.5E+04	-1.4E+05	-1.1E+05

Table 147 Raw data for the test seal at PR=0.5, ω=15 krpm, and inlet LVF=2% with the zero-preswirl insert

Freq.	Re(H_{XX})	Re(H_{XY})	Re(H_{YX})	Re(H_{YY})	Im(H_{XX})	Im(H_{XY})	Im(H_{YX})	Im(H_{YY})	Re(eH_{XX})	Re(eH_{XY})	Re(eH_{YX})	Re(eH_{YY})	Im(eH_{XX})	Im(eH_{XY})	Im(eH_{YX})	Im(eH_{YY})
Hz	N/m	N/m	N/m	N/m	N/m	N/m	N/m	N/m	N/m	N/m	N/m	N/m	N/m	N/m	N/m	N/m
9.8	5.4E+06	1.4E+07	-1.5E+07	4.7E+06	9.7E+05	-6.8E+04	8.1E+03	2.7E+06	-2.8E+05	-2.6E+05	-3.1E+05	-7.0E+05	-2.5E+05	-3.6E+05	-5.9E+05	-6.0E+05
19.5	4.1E+06	1.4E+07	-1.6E+07	4.5E+06	2.9E+06	4.4E+05	-1.9E+05	5.4E+06	-1.4E+05	-1.4E+05	-2.4E+05	-3.4E+05	-1.1E+05	-1.9E+05	-2.7E+05	-2.5E+05
29.3	4.6E+06	1.4E+07	-1.6E+07	4.7E+06	5.0E+06	1.6E+06	1.4E+06	4.9E+06	-9.1E+04	-7.7E+04	-1.9E+05	-2.2E+05	-1.2E+05	-1.3E+05	-1.7E+05	-2.2E+05
39.1	3.8E+06	1.4E+07	-1.5E+07	4.4E+06	7.6E+06	9.7E+04	5.2E+05	9.0E+06	-1.5E+05	-1.1E+05	-2.6E+05	-2.4E+05	-9.3E+04	-1.0E+05	-2.2E+05	-2.4E+05
48.8	3.6E+06	1.4E+07	-1.5E+07	4.2E+06	1.0E+07	1.1E+05	4.6E+05	1.1E+07	-6.7E+04	-6.9E+04	-1.9E+05	-1.4E+05	-1.5E+05	-1.3E+05	-1.7E+05	-1.2E+05
58.6	3.4E+06	1.4E+07	-1.5E+07	4.2E+06	1.2E+07	1.7E+05	2.4E+05	1.3E+07	-8.6E+04	-6.6E+04	-1.7E+05	-1.7E+05	-7.5E+04	-1.2E+05	-1.9E+05	-1.3E+05
68.4	3.5E+06	1.4E+07	-1.5E+07	4.0E+06	1.5E+07	4.5E+04	1.6E+05	1.6E+07	-1.3E+05	-1.4E+05	-2.7E+05	-2.2E+05	-1.1E+05	-8.9E+04	-2.2E+05	-3.5E+05
78.1	3.5E+06	1.4E+07	-1.4E+07	4.4E+06	1.7E+07	1.7E+04	2.5E+05	1.8E+07	-1.0E+05	-8.3E+04	-1.5E+05	-9.5E+04	-6.3E+04	-1.1E+05	-1.5E+05	-1.4E+05
87.9	3.4E+06	1.4E+07	-1.4E+07	4.0E+06	2.0E+07	1.0E+05	5.1E+04	2.1E+07	-6.0E+04	-5.2E+04	-6.8E+04	-1.1E+05	-8.7E+04	-7.0E+04	-1.4E+05	-1.1E+05
97.7	3.7E+06	1.4E+07	-1.5E+07	4.3E+06	2.2E+07	4.0E+05	-4.3E+05	2.4E+07	-6.0E+04	-9.0E+04	-1.6E+05	-1.1E+05	-9.0E+04	-4.8E+04	-1.8E+05	-1.3E+05
107.4	3.7E+06	1.3E+07	-1.6E+07	4.5E+06	2.4E+07	3.7E+05	9.7E+04	2.6E+07	-1.1E+05	-1.0E+05	-1.2E+05	-8.5E+04	-1.3E+05	-1.3E+05	-1.2E+05	-1.5E+05
117.2	4.1E+06	1.4E+07	-1.5E+07	5.8E+06	2.6E+07	8.4E+05	2.5E+05	2.8E+07	-7.1E+04	-7.7E+04	-7.6E+04	-1.2E+05	-1.0E+05	-6.0E+04	-2.1E+05	-1.3E+05
127.0	4.0E+06	1.4E+07	-1.5E+07	6.2E+06	2.8E+07	1.0E+06	9.6E+04	3.1E+07	-8.9E+04	-7.8E+04	-2.1E+05	-2.7E+05	-1.1E+05	-1.4E+05	-2.4E+05	-3.1E+05
136.7	4.3E+06	1.4E+07	-1.5E+07	5.5E+06	3.0E+07	1.0E+06	-3.2E+05	3.3E+07	-3.5E+04	-5.4E+04	-1.8E+05	-2.0E+05	-5.7E+04	-6.3E+04	-2.1E+05	-1.1E+05

Table 148 Raw data for the test seal at PR=0.5, ω=5 krpm, and inlet LVF=4% with the zero-preswirl insert

Freq.	Re(H_{XX})	Re(H_{XY})	Re(H_{YX})	Re(H_{YY})	Im(H_{XX})	Im(H_{XY})	Im(H_{YX})	Im(H_{YY})	Re(eH_{XX})	Re(eH_{XY})	Re(eH_{YX})	Re(eH_{YY})	Im(eH_{XX})	Im(eH_{XY})	Im(eH_{YX})	Im(eH_{YY})
Hz	N/m	N/m	N/m	N/m	N/m	N/m	N/m	N/m	N/m	N/m	N/m	N/m	N/m	N/m	N/m	N/m
9.8	5.6E+06	1.7E+06	-5.5E+06	3.3E+06	1.3E+06	1.4E+06	1.7E+06	1.6E+06	-3.6E+05	-2.6E+05	-5.6E+05	-4.0E+05	-3.1E+05	-2.2E+05	-5.2E+05	-2.9E+05
19.5	4.4E+06	2.9E+06	-4.4E+06	3.4E+06	3.0E+06	1.7E+06	9.2E+05	4.2E+06	-1.3E+05	-1.6E+05	-9.7E+04	-3.7E+05	-1.7E+05	-3.0E+05	-4.3E+05	-4.1E+05
29.3	5.2E+06	3.0E+06	-4.5E+06	4.9E+06	5.0E+06	2.8E+06	2.0E+06	5.7E+06	-1.9E+05	-1.8E+05	-2.7E+05	-1.4E+05	-9.7E+04	-2.1E+05	-3.0E+05	-2.8E+05
39.1	4.4E+06	4.0E+06	-3.6E+06	3.7E+06	7.8E+06	1.5E+06	6.7E+05	9.1E+06	-9.4E+04	-7.5E+04	-1.5E+05	-1.1E+05	-9.6E+04	-1.2E+05	-6.1E+04	-1.2E+05
48.8	4.2E+06	4.4E+06	-4.0E+06	4.1E+06	1.0E+07	1.3E+06	2.1E+05	1.1E+07	-8.2E+04	-1.3E+05	-1.5E+05	-2.5E+05	-8.8E+04	-1.4E+05	-2.5E+05	-2.3E+05
58.6	4.1E+06	3.9E+06	-4.1E+06	3.8E+06	1.3E+07	9.2E+05	2.8E+05	1.3E+07	-1.1E+05	-7.1E+04	-1.7E+05	-1.5E+05	-1.4E+05	-9.8E+04	-2.0E+05	-2.6E+05
68.4	3.7E+06	4.2E+06	-4.1E+06	3.7E+06	1.4E+07	6.9E+05	1.6E+05	1.5E+07	-9.0E+04	-1.7E+05	-2.6E+05	-2.1E+05	-1.4E+05	-1.4E+05	-2.6E+05	-1.5E+05
78.1	3.8E+06	4.3E+06	-4.4E+06	3.8E+06	1.7E+07	5.4E+05	-1.4E+05	1.7E+07	-1.3E+05	-1.3E+05	-1.4E+05	-2.6E+05	-2.6E+05	-1.7E+05	-3.8E+05	-2.6E+05
87.9	3.6E+06	3.7E+06	-4.6E+06	3.4E+06	1.9E+07	6.3E+05	-1.4E+05	2.0E+07	-1.4E+05	-1.1E+05	-1.7E+05	-1.0E+05	-6.2E+04	-5.7E+04	-1.7E+05	-1.5E+05
97.7	4.0E+06	4.0E+06	-4.3E+06	3.5E+06	2.2E+07	5.4E+05	-2.6E+04	2.2E+07	-1.5E+05	-1.4E+05	-2.0E+05	-1.7E+05	-8.1E+04	-1.6E+05	-7.5E+04	-1.6E+05
107.4	3.5E+06	3.5E+06	-5.5E+06	2.9E+06	2.4E+07	7.3E+05	8.5E+05	2.5E+07	-2.0E+05	-3.0E+05	-2.7E+05	-2.8E+05	-1.2E+05	-1.7E+05	-1.2E+05	-1.1E+05
117.2	4.2E+06	4.4E+06	-5.1E+06	3.8E+06	2.6E+07	1.2E+06	7.9E+05	2.8E+07	-1.6E+05	-8.1E+04	-2.0E+05	-1.7E+05	-1.0E+05	-1.4E+05	-1.9E+05	-1.2E+05
127.0	3.7E+06	4.5E+06	-4.8E+06	4.4E+06	2.8E+07	1.1E+06	1.2E+06	2.9E+07	-1.2E+05	-1.2E+05	-1.1E+05	-1.7E+05	-9.1E+04	-1.8E+05	-6.3E+04	-1.4E+05
136.7	3.4E+06	4.1E+06	-5.4E+06	4.2E+06	3.0E+07	1.3E+06	1.3E+06	3.2E+07	-1.1E+05	-1.4E+05	-3.0E+05	-9.8E+04	-1.1E+05	-1.3E+05	-1.4E+05	-1.4E+05

Table 149 Raw data for the test seal at PR=0.5, ω=10 krpm, and inlet LVF=4% with the zero-preswirl insert

Freq.	Re(H_{XX})	Re(H_{XY})	Re(H_{YX})	Re(H_{YY})	Im(H_{XX})	Im(H_{XY})	Im(H_{YX})	Im(H_{YY})	Re(eH_{XX})	Re(eH_{XY})	Re(eH_{YX})	Re(eH_{YY})	Im(eH_{XX})	Im(eH_{XY})	Im(eH_{YX})	Im(eH_{YY})
Hz	N/m	N/m	N/m	N/m	N/m	N/m	N/m	N/m	N/m	N/m	N/m	N/m	N/m	N/m	N/m	N/m
9.8	6.3E+06	8.2E+06	-9.7E+06	2.8E+06	-1.2E+06	3.3E+04	3.9E+05	3.2E+06	-4.8E+05	-3.3E+05	-5.9E+05	-4.3E+05	-3.4E+05	-3.6E+05	-5.4E+05	-6.5E+05
19.5	5.2E+06	7.9E+06	-8.2E+06	3.0E+06	2.9E+06	8.5E+05	1.2E+06	5.6E+06	-2.3E+05	-1.3E+05	-2.0E+05	-4.3E+05	-2.0E+05	-2.7E+05	-2.8E+05	-5.5E+05
29.3	4.7E+06	7.5E+06	-9.0E+06	4.5E+06	4.3E+06	2.5E+06	2.0E+06	6.9E+06	-1.7E+05	-2.0E+05	-4.4E+05	-3.0E+05	-1.4E+05	-2.5E+05	-4.2E+05	-2.9E+05
39.1	4.2E+06	8.4E+06	-7.6E+06	4.1E+06	7.7E+06	8.8E+05	2.4E+05	9.9E+06	-1.6E+05	-1.2E+05	-2.9E+05	-1.3E+05	-1.1E+05	-1.3E+05	-2.6E+05	-1.1E+05
48.8	3.7E+06	8.6E+06	-7.8E+06	4.3E+06	1.1E+07	1.2E+06	8.1E+05	1.2E+07	-2.7E+05	-1.5E+05	-3.5E+05	-2.5E+05	-2.2E+05	-1.9E+05	-3.1E+05	-3.7E+05
58.6	4.3E+06	9.2E+06	-6.9E+06	4.7E+06	1.3E+07	1.0E+06	-3.5E+05	1.4E+07	-2.5E+05	-2.6E+05	-4.6E+05	-4.3E+05	-1.8E+05	-1.6E+05	-3.8E+05	-2.6E+05
68.4	4.0E+06	8.6E+06	-7.7E+06	4.1E+06	1.5E+07	1.6E+06	2.0E+05	1.7E+07	-2.0E+05	-1.9E+05	-4.3E+05	-2.8E+05	-1.0E+05	-1.9E+05	-4.8E+05	-3.0E+05
78.1	4.0E+06	8.9E+06	-7.6E+06	4.1E+06	1.8E+07	1.2E+06	-2.6E+05	1.8E+07	-1.3E+05	-2.0E+05	-1.8E+05	-2.1E+05	-1.1E+05	-2.0E+05	-1.8E+05	-3.3E+05
87.9	4.1E+06	8.9E+06	-7.5E+06	4.2E+06	2.0E+07	1.7E+06	-8.3E+05	2.1E+07	-2.6E+05	-1.1E+05	-3.2E+05	-1.7E+05	-9.9E+04	-2.3E+05	-2.3E+05	-3.1E+05
97.7	4.7E+06	9.0E+06	-8.1E+06	3.8E+06	2.3E+07	1.1E+06	-8.0E+05	2.4E+07	-1.7E+05	-2.0E+05	-3.6E+05	-2.4E+05	-1.8E+05	-1.5E+05	-2.1E+05	-2.0E+05
107.4	4.8E+06	8.4E+06	-7.9E+06	3.5E+06	2.5E+07	1.2E+06	-4.5E+05	2.6E+07	-1.6E+05	-1.2E+05	-1.4E+05	-2.0E+05	-2.5E+05	-7.1E+04	-3.6E+05	-9.7E+04
117.2	5.2E+06	9.0E+06	-8.4E+06	4.1E+06	2.7E+07	1.3E+06	-8.6E+05	2.8E+07	-1.9E+05	-5.8E+04	-1.1E+05	-1.4E+05	-1.6E+05	-1.5E+05	-3.0E+05	-1.6E+05
127.0	4.8E+06	8.7E+06	-8.5E+06	4.6E+06	2.9E+07	1.7E+06	-4.8E+04	3.1E+07	-2.2E+05	-2.0E+05	-3.9E+05	-3.9E+05	-1.4E+05	-2.9E+05	-2.7E+05	-2.6E+05
136.7	4.8E+06	8.8E+06	-9.2E+06	4.6E+06	3.1E+07	2.0E+06	-5.3E+05	3.3E+07	-1.7E+05	-1.3E+05	-2.1E+05	-2.8E+05	-1.5E+05	-1.9E+05	-2.7E+05	-3.0E+05

Table 150 Raw data for the test seal at PR=0.5, ω=15 krpm, and inlet LVF=4% with the zero-preswirl insert

Freq.	Re(H_{XX})	Re(H_{XY})	Re(H_{YX})	Re(H_{YY})	Im(H_{XX})	Im(H_{XY})	Im(H_{YX})	Im(H_{YY})	Re(eH_{XX})	Re(eH_{XY})	Re(eH_{YX})	Re(eH_{YY})	Im(eH_{XX})	Im(eH_{XY})	Im(eH_{YX})	Im(eH_{YY})
Hz	N/m	N/m	N/m	N/m	N/m	N/m	N/m	N/m	N/m	N/m	N/m	N/m	N/m	N/m	N/m	N/m
9.8	7.3E+06	1.4E+07	-1.5E+07	3.8E+06	-9.0E+05	-1.1E+06	-4.3E+05	3.0E+06	-5.9E+05	-4.0E+05	-6.1E+05	-9.5E+05	-4.0E+05	-6.0E+05	-9.6E+05	-6.9E+05
19.5	6.0E+06	1.4E+07	-1.4E+07	4.2E+06	2.5E+06	-3.9E+05	-1.0E+05	4.1E+06	-4.3E+05	-3.6E+05	-8.6E+05	-4.9E+05	-3.7E+05	-3.9E+05	-3.2E+05	-6.8E+05
29.3	5.5E+06	1.3E+07	-1.6E+07	4.8E+06	4.3E+06	1.2E+06	1.1E+06	6.4E+06	-3.0E+05	-2.3E+05	-3.7E+05	-4.1E+05	-2.6E+05	-1.4E+05	-4.3E+05	-3.3E+05
39.1	4.5E+06	1.4E+07	-1.4E+07	4.5E+06	7.6E+06	-1.1E+05	1.2E+06	1.0E+07	-1.8E+05	-3.1E+05	-5.0E+05	-3.9E+05	-2.7E+05	-1.4E+05	-4.3E+05	-3.2E+05
48.8	3.5E+06	1.4E+07	-1.4E+07	4.6E+06	1.1E+07	7.3E+05	5.7E+05	1.2E+07	-2.8E+05	-2.2E+05	-5.4E+05	-3.0E+05	-1.8E+05	-2.3E+05	-2.9E+05	-2.4E+05
58.6	4.0E+06	1.4E+07	-1.3E+07	4.1E+06	1.3E+07	3.3E+05	5.5E+05	1.5E+07	-1.7E+05	-1.6E+05	-2.7E+05	-3.9E+05	-1.4E+05	-2.4E+05	-2.5E+05	-2.5E+05
68.4	4.0E+06	1.4E+07	-1.3E+07	5.2E+06	1.5E+07	1.0E+06	9.1E+05	1.8E+07	-2.4E+05	-2.2E+05	-3.9E+05	-3.0E+05	-2.5E+05	-3.7E+05	-4.9E+05	-6.0E+05
78.1	4.3E+06	1.4E+07	-1.3E+07	4.8E+06	1.8E+07	8.2E+05	-2.9E+05	2.0E+07	-1.8E+05	-2.2E+05	-3.2E+05	-4.0E+05	-1.6E+05	-2.2E+05	-1.7E+05	-2.0E+05
87.9	4.6E+06	1.3E+07	-1.4E+07	4.8E+06	2.0E+07	7.9E+05	-9.5E+05	2.3E+07	-1.8E+05	-1.1E+05	-1.5E+05	-1.6E+05	-1.6E+05	-2.2E+05	-2.4E+05	-2.4E+05
97.7	4.2E+06	1.4E+07	-1.4E+07	4.9E+06	2.3E+07	1.1E+06	-2.4E+05	2.6E+07	-1.2E+05	-1.8E+05	-4.1E+05	-1.8E+05	-1.4E+05	-1.8E+05	-2.1E+05	-1.6E+05
107.4	4.1E+06	1.4E+07	-1.5E+07	4.9E+06	2.6E+07	1.0E+06	1.1E+05	2.8E+07	-1.4E+05	-2.2E+05	-5.2E+05	-2.8E+05	-2.0E+05	-1.9E+05	-1.3E+05	-2.6E+05
117.2	4.4E+06	1.5E+07	-1.5E+07	6.5E+06	2.7E+07	1.5E+06	-4.3E+04	3.1E+07	-1.0E+05	-1.4E+05	-3.6E+05	-2.5E+05	-1.5E+05	-1.9E+05	-1.8E+05	-2.0E+05
127.0	4.7E+06	1.4E+07	-1.5E+07	7.5E+06	2.9E+07	1.0E+06	-2.8E+04	3.3E+07	-2.4E+05	-1.9E+05	-3.8E+05	-4.0E+05	-2.8E+05	-2.0E+05	-3.1E+05	-4.0E+05
136.7	4.7E+06	1.4E+07	-1.6E+07	7.0E+06	3.2E+07	1.6E+06	3.3E+05	3.5E+07	-1.8E+05	-1.4E+05	-2.7E+05	-1.8E+05	-2.7E+05	-1.4E+05	-1.2E+05	-2.7E+05

Table 151 Raw data for the test seal at PR=0.5, ω=5 krpm, and inlet LVF=6% with the zero-preswirl insert

Freq.	Re(H_{XX})	Re(H_{XY})	Re(H_{YX})	Re(H_{YY})	Im(H_{XX})	Im(H_{XY})	Im(H_{YX})	Im(H_{YY})	Re(eH_{XX})	Re(eH_{XY})	Re(eH_{YX})	Re(eH_{YY})	Im(eH_{XX})	Im(eH_{XY})	Im(eH_{YX})	Im(eH_{YY})
Hz	N/m	N/m	N/m	N/m	N/m	N/m	N/m	N/m	N/m	N/m	N/m	N/m	N/m	N/m	N/m	N/m
9.8	6.7E+06	1.4E+06	-7.9E+06	4.7E+06	1.1E+06	1.8E+06	2.0E+06	1.1E+06	-2.2E+05	-1.8E+05	-4.7E+05	-3.1E+05	-3.4E+05	-3.9E+05	-6.3E+05	-8.8E+05
19.5	6.1E+06	2.7E+06	-4.1E+06	3.5E+06	3.1E+06	2.8E+06	2.2E+06	5.1E+06	-1.1E+05	-3.2E+05	-3.8E+05	-1.8E+05	-3.3E+05	-2.3E+05	-4.4E+05	-4.0E+05
29.3	5.6E+06	3.0E+06	-5.2E+06	4.1E+06	4.7E+06	3.7E+06	2.0E+06	6.5E+06	-2.0E+05	-3.0E+05	-4.2E+05	-4.5E+05	-2.8E+05	-1.2E+05	-2.5E+05	-4.0E+05
39.1	4.9E+06	4.1E+06	-4.3E+06	4.1E+06	7.9E+06	1.8E+06	1.3E+06	9.8E+06	-1.8E+05	-1.8E+05	-1.4E+05	-3.2E+05	-1.2E+05	-1.3E+05	-2.2E+05	-2.2E+05
48.8	4.9E+06	4.8E+06	-3.9E+06	4.7E+06	1.1E+07	1.5E+06	1.2E+06	1.2E+07	-8.6E+04	-2.9E+05	-2.9E+05	-2.0E+05	-1.2E+05	-2.4E+05	-2.6E+05	-1.7E+05
58.6	4.9E+06	4.9E+06	-4.1E+06	4.8E+06	1.3E+07	1.5E+06	5.3E+05	1.5E+07	-2.7E+05	-3.4E+05	-2.1E+05	-4.6E+04	-3.3E+05	-2.6E+05	-2.9E+05	-3.0E+05
68.4	4.2E+06	4.0E+06	-3.9E+06	4.0E+06	1.5E+07	1.4E+06	8.5E+05	1.6E+07	-1.3E+05	-3.4E+05	-2.8E+05	-3.9E+05	-1.8E+05	-4.5E+05	-3.2E+05	-7.2E+05
78.1	4.6E+06	4.2E+06	-4.2E+06	3.9E+06	1.7E+07	4.6E+05	-3.8E+04	1.8E+07	-3.7E+05	-1.1E+05	-2.7E+05	-3.3E+05	-1.6E+05	-2.5E+05	-1.2E+05	-3.7E+05
87.9	3.9E+06	4.4E+06	-4.7E+06	3.6E+06	2.0E+07	7.3E+05	3.2E+05	2.1E+07	-1.4E+05	-1.4E+05	-3.1E+05	-2.4E+05	-2.2E+05	-8.3E+04	-3.7E+05	-2.4E+05
97.7	4.3E+06	3.9E+06	-4.6E+06	3.3E+06	2.3E+07	2.4E+05	-1.3E+05	2.3E+07	-2.9E+05	-1.7E+05	-3.3E+05	-1.8E+05	-3.1E+05	-2.2E+05	-2.2E+05	-3.4E+05
107.4	3.5E+06	3.9E+06	-5.3E+06	3.4E+06	2.6E+07	6.0E+05	1.1E+06	2.6E+07	-1.2E+05	-2.3E+05	-3.7E+05	-2.2E+05	-1.7E+05	-2.5E+05	-3.0E+05	-3.6E+05
117.2	4.4E+06	4.5E+06	-4.9E+06	4.1E+06	2.8E+07	1.2E+06	8.3E+05	2.9E+07	-1.8E+05	-1.9E+05	-1.5E+05	-2.3E+05	-2.9E+05	-2.7E+05	-4.2E+05	-1.8E+05
127.0	4.0E+06	4.0E+06	-5.1E+06	4.6E+06	2.9E+07	8.1E+05	1.3E+06	3.2E+07	-1.7E+05	-2.5E+05	-1.6E+05	-6.2E+05	-1.6E+05	-5.5E+05	-2.8E+05	-5.2E+05
136.7	4.0E+06	4.2E+06	-5.5E+06	4.2E+06	3.2E+07	1.9E+06	1.4E+06	3.4E+07	-1.5E+05	-1.5E+05	-2.5E+05	-1.4E+05	-2.6E+05	-2.1E+05	-3.5E+05	-1.9E+05

Table 152 Raw data for the test seal at PR=0.5, ω=10 krpm, and inlet LVF=6% with the zero-preswirl insert

Freq.	Re(H_{XX})	Re(H_{XY})	Re(H_{YX})	Re(H_{YY})	Im(H_{XX})	Im(H_{XY})	Im(H_{YX})	Im(H_{YY})	Re(eH_{XX})	Re(eH_{XY})	Re(eH_{YX})	Re(eH_{YY})	Im(eH_{XX})	Im(eH_{XY})	Im(eH_{YX})	Im(eH_{YY})
Hz	N/m	N/m	N/m	N/m	N/m	N/m	N/m	N/m	N/m	N/m	N/m	N/m	N/m	N/m	N/m	N/m
9.8	7.7E+06	5.8E+06	-9.7E+06	3.7E+06	-2.9E+06	2.5E+06	2.1E+06	3.0E+06	-6.0E+05	-6.0E+05	-9.7E+05	-6.7E+05	-9.1E+05	-5.4E+05	-6.5E+05	-1.2E+06
19.5	6.0E+06	8.1E+06	-8.5E+06	4.3E+06	2.1E+06	5.1E+05	1.8E+06	5.4E+06	-1.7E+05	-3.7E+05	-2.0E+05	-2.2E+05	-3.0E+05	-4.6E+05	-4.1E+05	-5.4E+05
29.3	5.6E+06	8.1E+06	-1.0E+07	5.7E+06	4.8E+06	1.9E+06	2.5E+06	7.3E+06	-2.4E+05	-3.1E+05	-3.4E+05	-4.9E+05	-2.0E+05	-3.3E+05	-3.0E+05	-5.8E+05
39.1	5.0E+06	8.4E+06	-7.9E+06	5.2E+06	8.3E+06	8.6E+05	8.5E+05	1.0E+07	-3.2E+05	-3.1E+05	-4.3E+05	-2.0E+05	-4.7E+05	-3.0E+05	-3.7E+05	-1.5E+05
48.8	3.6E+06	8.7E+06	-7.8E+06	4.6E+06	1.0E+07	2.0E+06	5.2E+05	1.3E+07	-2.0E+05	-2.8E+05	-3.3E+05	-5.0E+05	-1.5E+05	-2.3E+05	-4.6E+05	-4.5E+05
58.6	4.4E+06	8.0E+06	-7.8E+06	3.8E+06	1.3E+07	1.7E+06	-3.3E+05	1.6E+07	-3.4E+05	-1.5E+05	-7.4E+05	-2.5E+05	-3.3E+05	-1.5E+05	-5.7E+05	-4.7E+05
68.4	5.2E+06	8.5E+06	-7.5E+06	6.0E+06	1.6E+07	1.6E+06	-4.8E+05	1.7E+07	-1.5E+05	-4.5E+05	-4.2E+05	-7.7E+05	-2.4E+05	-2.3E+05	-1.5E+05	-1.3E+05
78.1	4.9E+06	9.5E+06	-7.5E+06	4.2E+06	1.9E+07	1.7E+06	-7.7E+05	1.9E+07	-2.1E+05	-3.0E+05	-3.7E+05	-5.0E+05	-1.5E+05	-1.9E+05	-2.2E+05	-2.1E+05
87.9	4.2E+06	9.4E+06	-8.6E+06	4.4E+06	2.1E+07	1.4E+06	-1.0E+06	2.2E+07	-3.2E+05	-2.0E+05	-6.0E+05	-2.5E+05	-3.8E+05	-3.0E+05	-4.8E+05	-6.2E+05
97.7	5.5E+06	8.9E+06	-7.1E+06	3.8E+06	2.4E+07	1.5E+06	-5.3E+05	2.5E+07	-4.1E+05	-3.2E+05	-1.8E+05	-5.1E+05	-2.6E+05	-2.5E+05	-4.3E+05	-1.9E+05
107.4	4.8E+06	8.5E+06	-9.6E+06	3.5E+06	2.6E+07	1.7E+06	-1.3E+06	2.8E+07	-3.0E+05	-3.1E+05	-5.9E+05	-3.6E+05	-3.2E+05	-1.3E+05	-5.0E+05	-2.9E+05
117.2	5.7E+06	8.7E+06	-9.6E+06	4.0E+06	2.7E+07	1.5E+06	-2.4E+06	3.1E+07	-9.0E+04	-1.8E+05	-4.8E+05	-3.2E+05	-2.9E+05	-1.0E+05	-1.5E+05	-2.8E+05
127.0	5.6E+06	8.1E+06	-8.2E+06	4.7E+06	2.9E+07	1.6E+06	-9.3E+05	3.2E+07	-2.6E+05	-8.8E+04	-3.9E+05	-3.7E+05	-2.9E+05	-3.2E+05	-3.0E+05	-4.9E+05
136.7	5.1E+06	9.3E+06	-1.1E+07	5.6E+06	3.2E+07	2.7E+06	-7.3E+04	3.6E+07	-1.8E+05	-1.2E+05	-2.3E+05	-4.2E+05	-2.2E+05	-2.4E+05	-5.5E+05	-5.1E+05

Table 153 Raw data for the test seal at PR=0.5, ω=15 krpm, and inlet LVF=6% with the zero-preswirl insert

Freq.	Re(H_{XX})	Re(H_{XY})	Re(H_{YX})	Re(H_{YY})	Im(H_{XX})	Im(H_{XY})	Im(H_{YX})	Im(H_{YY})	Re(eH_{XX})	Re(eH_{XY})	Re(eH_{YX})	Re(eH_{YY})	Im(eH_{XX})	Im(eH_{XY})	Im(eH_{YX})	Im(eH_{YY})
Hz	N/m	N/m	N/m	N/m	N/m	N/m	N/m	N/m	N/m	N/m	N/m	N/m	N/m	N/m	N/m	N/m
9.8	9.4E+06	1.5E+07	-1.3E+07	3.8E+06	-4.0E+04	-6.9E+05	-1.5E+06	2.5E+06	-6.0E+05	-6.0E+05	-5.2E+05	-4.7E+05	-4.8E+05	-6.5E+05	-5.8E+05	-6.7E+05
19.5	6.5E+06	1.4E+07	-1.4E+07	4.6E+06	9.1E+05	-4.7E+05	-5.1E+04	6.0E+06	-5.4E+05	-4.0E+05	-6.7E+05	-1.1E+06	-5.3E+05	-8.5E+05	-5.4E+05	-5.8E+05
29.3	6.5E+06	1.4E+07	-1.5E+07	6.1E+06	3.5E+06	1.5E+06	1.9E+06	7.0E+06	-4.5E+05	-5.1E+05	-5.6E+05	-9.7E+05	-2.4E+05	-2.2E+05	-8.2E+05	-8.2E+05
39.1	5.2E+06	1.4E+07	-1.3E+07	5.6E+06	7.5E+06	-2.8E+05	8.7E+05	1.1E+07	-3.8E+05	-4.2E+05	-3.2E+05	-5.1E+05	-5.8E+05	-5.0E+05	-2.2E+05	-3.6E+05
48.8	5.7E+06	1.4E+07	-1.2E+07	4.6E+06	1.1E+07	-5.8E+05	8.2E+05	1.2E+07	-2.9E+05	-2.0E+05	-3.8E+05	-4.5E+05	-1.3E+05	-1.9E+05	-3.2E+05	-2.7E+05
58.6	4.5E+06	1.3E+07	-1.4E+07	4.5E+06	1.3E+07	1.9E+05	9.1E+05	1.6E+07	-2.3E+05	-3.1E+05	-5.0E+05	-5.8E+05	-3.3E+05	-2.7E+05	-2.3E+05	-3.6E+05
68.4	5.4E+06	1.4E+07	-1.3E+07	4.4E+06	1.6E+07	1.1E+06	-7.1E+04	1.9E+07	-2.1E+05	-2.5E+05	-3.6E+05	-6.0E+05	-2.7E+05	-4.4E+05	-5.4E+05	-5.5E+05
78.1	4.9E+06	1.3E+07	-1.2E+07	4.2E+06	1.8E+07	1.3E+06	-1.7E+05	2.1E+07	-3.2E+05	-1.7E+05	-3.9E+05	-5.8E+05	-4.2E+05	-3.6E+05	-3.8E+05	-4.1E+05
87.9	4.6E+06	1.3E+07	-1.2E+07	5.0E+06	2.1E+07	9.6E+05	-7.7E+05	2.4E+07	-4.2E+05	-1.9E+05	-3.2E+05	-3.4E+05	-2.8E+05	-3.0E+05	-1.7E+05	-2.0E+05
97.7	4.8E+06	1.4E+07	-1.3E+07	5.9E+06	2.3E+07	1.7E+06	-9.1E+05	2.7E+07	-1.6E+05	-3.6E+05	-4.5E+05	-3.5E+05	-3.4E+05	-3.3E+05	-3.6E+05	-4.6E+05
107.4	4.5E+06	1.3E+07	-1.4E+07	5.8E+06	2.6E+07	1.8E+06	-4.2E+05	2.9E+07	-2.7E+05	-2.8E+05	-5.0E+05	-2.8E+05	-4.1E+05	-2.9E+05	-3.5E+05	-2.6E+05
117.2	5.1E+06	1.4E+07	-1.4E+07	6.4E+06	2.7E+07	2.2E+06	-1.4E+06	3.2E+07	-2.2E+05	-2.3E+05	-4.0E+05	-4.1E+05	-2.8E+05	-1.1E+05	-3.9E+05	-4.8E+05
127.0	5.4E+06	1.4E+07	-1.4E+07	5.9E+06	3.0E+07	1.6E+06	-1.3E+06	3.4E+07	-2.4E+05	-3.9E+05	-5.4E+05	-7.1E+05	-3.5E+05	-3.6E+05	-4.2E+05	-4.0E+05
136.7	5.8E+06	1.4E+07	-1.4E+07	6.8E+06	3.3E+07	2.7E+06	-2.5E+05	3.6E+07	-3.3E+05	-1.9E+05	-2.1E+05	-3.5E+05	-2.3E+05	-1.9E+05	-3.1E+05	-4.0E+05

Table 154 Raw data for the test seal at PR=0.5, ω=5 krpm, and inlet LVF=8% with the zero-preswirl insert

Freq.	Re(H_{XX})	Re(H_{XY})	Re(H_{YX})	Re(H_{YY})	Im(H_{XX})	Im(H_{XY})	Im(H_{YX})	Im(H_{YY})	Re(eH_{XX})	Re(eH_{XY})	Re(eH_{YX})	Re(eH_{YY})	Im(eH_{XX})	Im(eH_{XY})	Im(eH_{YX})	Im(eH_{YY})
Hz	N/m	N/m	N/m	N/m	N/m	N/m	N/m	N/m	N/m	N/m	N/m	N/m	N/m	N/m	N/m	N/m
9.8	7.5E+06	7.7E+05	-6.6E+06	4.4E+06	8.8E+05	1.8E+06	3.4E+06	1.7E+06	-1.4E+06	-3.3E+05	-1.2E+06	-7.9E+05	-4.8E+05	-5.2E+05	-1.1E+06	-7.4E+05
19.5	7.3E+06	1.8E+06	-4.6E+06	3.1E+06	2.1E+06	2.4E+06	2.4E+06	4.1E+06	-3.2E+05	-3.2E+05	-3.7E+05	-3.6E+05	-4.1E+05	-3.0E+05	-4.3E+05	-4.0E+05
29.3	6.7E+06	2.0E+06	-6.0E+06	4.0E+06	5.0E+06	3.4E+06	2.6E+06	6.4E+06	-3.9E+05	-2.7E+05	-2.9E+05	-6.0E+05	-3.4E+05	-2.7E+05	-2.9E+05	-2.9E+05
39.1	5.4E+06	3.7E+06	-4.1E+06	3.9E+06	8.6E+06	2.3E+06	1.9E+06	1.0E+07	-1.6E+05	-4.1E+05	-3.3E+05	-3.2E+05	-3.3E+05	-1.3E+05	-2.8E+05	-1.3E+05
48.8	4.7E+06	4.3E+06	-4.8E+06	3.9E+06	1.0E+07	2.2E+06	9.1E+05	1.3E+07	-3.2E+05	-1.6E+05	-3.0E+05	-2.0E+05	-4.0E+05	-3.8E+05	-2.1E+05	-4.6E+05
58.6	5.1E+06	4.6E+06	-4.6E+06	3.8E+06	1.3E+07	1.9E+06	2.8E+05	1.5E+07	-2.4E+05	-1.3E+05	-4.3E+05	-3.4E+05	-2.9E+05	-3.5E+05	-3.4E+05	-3.0E+05
68.4	5.3E+06	4.8E+06	-3.8E+06	4.7E+06	1.6E+07	1.2E+06	4.7E+05	1.8E+07	-2.7E+05	-5.5E+05	-2.6E+05	-5.0E+05	-2.9E+05	-1.2E+05	-3.8E+05	-3.7E+05
78.1	5.1E+06	4.2E+06	-4.4E+06	4.5E+06	1.8E+07	1.3E+06	7.2E+05	2.0E+07	-1.8E+05	-1.7E+05	-1.9E+05	-2.7E+05	-3.5E+05	-4.8E+05	-1.7E+05	-5.8E+05
87.9	3.8E+06	4.3E+06	-4.9E+06	3.9E+06	2.1E+07	1.1E+06	2.1E+05	2.2E+07	-1.3E+05	-3.5E+05	-2.4E+05	-3.2E+05	-2.2E+05	-2.8E+05	-3.4E+05	-3.4E+05
97.7	4.2E+06	4.6E+06	-4.7E+06	4.0E+06	2.3E+07	5.3E+05	-7.3E+04	2.4E+07	-2.6E+05	-2.2E+05	-1.9E+05	-4.3E+05	-2.3E+05	-1.4E+05	-3.3E+05	-2.4E+05
107.4	3.7E+06	3.0E+06	-6.0E+06	2.4E+06	2.7E+07	8.4E+05	3.1E+05	2.7E+07	-4.3E+05	-2.5E+05	-2.5E+05	-2.9E+05	-3.6E+05	-2.5E+05	-3.3E+05	-2.7E+05
117.2	4.6E+06	4.6E+06	-4.3E+06	3.9E+06	2.8E+07	7.6E+05	1.6E+04	3.0E+07	-2.1E+05	-1.6E+05	-2.2E+05	-2.0E+05	-2.3E+05	-1.1E+05	-3.0E+05	-3.0E+05
127.0	4.5E+06	4.1E+06	-5.0E+06	3.5E+06	3.0E+07	9.0E+05	1.3E+06	3.2E+07	-3.0E+05	-8.9E+05	-4.2E+05	-6.2E+05	-2.3E+05	-5.1E+05	-3.6E+05	-4.2E+05
136.7	4.8E+06	3.3E+06	-5.2E+06	3.6E+06	3.3E+07	1.7E+06	1.3E+06	3.5E+07	-2.3E+05	-3.8E+05	-4.3E+05	-3.6E+05	-2.0E+05	-2.6E+05	-2.4E+05	-3.7E+05

Table 155 Raw data for the test seal at PR=0.5, ω=10 krpm, and inlet LVF=8% with the zero-preswirl insert

Freq.	Re(H_{XX})	Re(H_{XY})	Re(H_{YX})	Re(H_{YY})	Im(H_{XX})	Im(H_{XY})	Im(H_{YX})	Im(H_{YY})	Re(eH_{XX})	Re(eH_{XY})	Re(eH_{YX})	Re(eH_{YY})	Im(eH_{XX})	Im(eH_{XY})	Im(eH_{YX})	Im(eH_{YY})
Hz	N/m	N/m	N/m	N/m	N/m	N/m	N/m	N/m	N/m	N/m	N/m	N/m	N/m	N/m	N/m	N/m
9.8	8.7E+06	8.3E+06	-9.7E+06	1.9E+06	-1.3E+06	1.6E+06	1.5E+06	3.3E+06	-7.0E+05	-6.6E+05	-7.9E+05	-7.2E+05	-6.3E+05	-3.1E+05	-7.3E+05	-5.0E+05
19.5	6.6E+06	7.5E+06	-8.0E+06	4.3E+06	1.4E+06	1.2E+06	1.0E+06	6.6E+06	-4.2E+05	-3.8E+05	-5.2E+05	-9.4E+05	-4.8E+05	-4.5E+05	-6.6E+05	-3.4E+05
29.3	6.6E+06	7.3E+06	-8.9E+06	3.2E+06	3.5E+06	2.9E+06	1.3E+06	9.0E+06	-2.4E+05	-6.5E+05	-4.3E+05	-3.4E+05	-4.1E+05	-6.5E+05	-6.0E+05	-7.0E+05
39.1	5.6E+06	6.7E+06	-8.0E+06	4.1E+06	7.8E+06	1.2E+06	1.6E+06	1.2E+07	-2.7E+05	-2.6E+05	-2.7E+05	-4.0E+05	-4.5E+05	-3.6E+05	-4.1E+05	-2.7E+05
48.8	6.1E+06	9.1E+06	-7.0E+06	4.6E+06	1.2E+07	1.6E+06	1.6E+06	1.4E+07	-2.3E+05	-2.2E+05	-3.4E+05	-3.8E+05	-5.3E+05	-3.1E+05	-5.3E+05	-5.4E+05
58.6	6.2E+06	8.3E+06	-7.2E+06	4.7E+06	1.4E+07	2.0E+06	-3.0E+05	1.7E+07	-3.7E+05	-2.7E+05	-7.0E+05	-5.4E+05	-3.9E+05	-3.8E+05	-6.5E+05	-4.9E+05
68.4	5.3E+06	7.7E+06	-8.4E+06	5.4E+06	1.7E+07	1.4E+06	-5.4E+04	2.0E+07	-4.2E+05	-4.9E+05	-5.7E+05	-7.1E+05	-1.9E+05	-3.6E+05	-5.4E+05	-4.4E+05
78.1	5.9E+06	9.3E+06	-7.4E+06	4.9E+06	1.9E+07	1.9E+06	-3.3E+05	2.0E+07	-3.0E+05	-3.0E+05	-5.7E+05	-4.3E+05	-1.7E+05	-3.7E+05	-1.7E+05	-4.7E+05
87.9	5.9E+06	8.9E+06	-8.8E+06	4.6E+06	2.2E+07	1.9E+06	-1.2E+06	2.3E+07	-4.8E+05	-1.8E+05	-3.8E+05	-4.2E+05	-4.0E+05	-3.2E+05	-3.9E+05	-2.6E+05
97.7	5.7E+06	9.6E+06	-8.1E+06	4.9E+06	2.4E+07	2.3E+06	-9.2E+05	2.6E+07	-2.1E+05	-3.2E+05	-2.7E+05	-4.7E+05	-2.1E+05	-4.8E+05	-2.4E+05	-3.0E+05
107.4	5.9E+06	8.6E+06	-9.3E+06	4.5E+06	2.7E+07	1.6E+06	-2.1E+06	3.0E+07	-3.7E+05	-3.5E+05	-2.7E+05	-3.7E+05	-3.6E+05	-1.7E+05	-4.0E+05	-3.4E+05
117.2	6.5E+06	9.6E+06	-8.5E+06	4.8E+06	2.9E+07	2.0E+06	-5.3E+05	3.2E+07	-2.0E+05	-8.3E+04	-1.7E+05	-1.7E+05	-3.4E+05	-2.6E+05	-3.3E+05	-2.1E+05
127.0	5.5E+06	9.3E+06	-9.0E+06	4.2E+06	3.1E+07	1.6E+06	-2.2E+06	3.4E+07	-5.3E+05	-3.6E+05	-5.3E+05	-6.0E+05	-2.8E+05	-5.4E+05	-2.9E+05	-4.2E+05
136.7	6.1E+06	9.7E+06	-1.0E+07	5.9E+06	3.3E+07	2.9E+06	-1.1E+06	3.7E+07	-1.8E+05	-1.9E+05	-2.9E+05	-3.4E+05	-1.9E+05	-1.7E+05	-5.5E+05	-6.2E+05

Table 156 Raw data for the test seal at PR=0.5, ω=15 krpm, and inlet LVF=8% with the zero-preswirl insert

Freq.	Re(H_{XX})	Re(H_{XY})	Re(H_{YX})	Re(H_{YY})	Im(H_{XX})	Im(H_{XY})	Im(H_{YX})	Im(H_{YY})	Re(eH_{XX})	Re(eH_{XY})	Re(eH_{YX})	Re(eH_{YY})	Im(eH_{XX})	Im(eH_{XY})	Im(eH_{YX})	Im(eH_{YY})
Hz	N/m	N/m	N/m	N/m	N/m	N/m	N/m	N/m	N/m	N/m	N/m	N/m	N/m	N/m	N/m	N/m
9.8	9.5E+06	1.3E+07	-1.4E+07	5.4E+06	-1.8E+06	6.6E+05	-3.1E+05	7.4E+06	-8.2E+05	-9.8E+05	-8.4E+05	-1.1E+06	-1.1E+06	-1.1E+06	-6.7E+05	-9.2E+05
19.5	7.9E+06	1.7E+07	-1.3E+07	3.4E+06	2.3E+06	-1.3E+06	-8.0E+05	2.9E+06	-7.7E+05	-6.8E+05	-7.9E+05	-6.8E+05	-6.1E+05	-9.5E+05	-7.4E+05	-8.2E+05
29.3	7.1E+06	1.3E+07	-1.5E+07	5.1E+06	3.7E+06	9.9E+05	1.6E+06	8.2E+06	-6.0E+05	-7.2E+05	-4.8E+05	-6.1E+05	-6.4E+05	-4.7E+05	-7.0E+05	-1.1E+06
39.1	5.4E+06	1.4E+07	-1.4E+07	4.3E+06	8.2E+06	-1.2E+05	-4.2E+05	1.2E+07	-5.1E+05	-3.2E+05	-3.9E+05	-6.0E+05	-3.4E+05	-2.7E+05	-5.8E+05	-5.4E+05
48.8	6.0E+06	1.3E+07	-1.3E+07	3.6E+06	9.9E+06	-2.6E+05	6.8E+04	1.4E+07	-7.1E+05	-3.8E+05	-3.4E+05	-3.7E+05	-2.9E+05	-3.0E+05	-7.6E+05	-7.1E+05
58.6	5.4E+06	1.3E+07	-1.2E+07	5.5E+06	1.2E+07	6.6E+04	1.0E+05	1.7E+07	-5.9E+05	-2.9E+05	-5.7E+05	-6.7E+05	-3.2E+05	-2.7E+05	-5.0E+05	-5.2E+05
68.4	5.6E+06	1.4E+07	-1.2E+07	4.3E+06	1.6E+07	9.2E+05	-8.8E+05	2.0E+07	-2.7E+05	-2.0E+05	-7.2E+05	-5.5E+05	-3.9E+05	-6.0E+05	-4.1E+05	-6.0E+05
78.1	5.5E+06	1.3E+07	-1.3E+07	4.1E+06	1.9E+07	6.0E+05	-1.3E+06	2.2E+07	-2.2E+05	-4.1E+05	-5.4E+05	-3.7E+05	-3.8E+05	-2.9E+05	-5.2E+05	-6.4E+05
87.9	5.1E+06	1.3E+07	-1.2E+07	5.7E+06	2.1E+07	2.4E+05	-1.2E+06	2.4E+07	-3.7E+05	-3.1E+05	-4.6E+05	-3.7E+05	-2.7E+05	-3.6E+05	-6.7E+05	-2.5E+05
97.7	4.7E+06	1.3E+07	-1.4E+07	6.4E+06	2.4E+07	1.8E+06	-8.0E+05	2.8E+07	-2.1E+05	-4.3E+05	-4.0E+05	-4.5E+05	-3.5E+05	-4.2E+05	-7.4E+05	-4.4E+05
107.4	5.6E+06	1.2E+07	-1.3E+07	5.7E+06	2.7E+07	1.7E+06	-1.9E+06	3.1E+07	-2.8E+05	-2.3E+05	-4.1E+05	-2.4E+05	-7.0E+05	-2.2E+05	-5.5E+05	-3.2E+05
117.2	5.2E+06	1.4E+07	-1.4E+07	6.5E+06	2.9E+07	2.9E+06	-1.6E+06	3.4E+07	-2.6E+05	-1.7E+05	-5.8E+05	-4.1E+05	-4.5E+05	-3.2E+05	-6.4E+05	-4.1E+05
127.0	5.8E+06	1.5E+07	-1.3E+07	7.8E+06	3.2E+07	1.7E+06	-5.2E+05	3.5E+07	-2.3E+05	-5.5E+05	-4.8E+05	-7.2E+05	-2.3E+05	-3.7E+05	-2.9E+05	-3.6E+05
136.7	5.8E+06	1.5E+07	-1.4E+07	7.1E+06	3.5E+07	3.3E+06	-4.0E+05	3.8E+07	-2.4E+05	-3.1E+05	-3.3E+05	-5.2E+05	-2.9E+05	-2.7E+05	-4.5E+05	-2.7E+05

Table 157 Raw data for the test seal at PR=0.4, ω=5 krpm, and inlet LVF=0% with the zero-preswirl insert

Freq.	Re(H_{XX})	Re(H_{XY})	Re(H_{YX})	Re(H_{YY})	Im(H_{XX})	Im(H_{XY})	Im(H_{YX})	Im(H_{YY})	Re(eH_{XX})	Re(eH_{XY})	Re(eH_{YX})	Re(eH_{YY})	Im(eH_{XX})	Im(eH_{XY})	Im(eH_{YX})	Im(eH_{YY})
Hz	N/m	N/m	N/m	N/m	N/m	N/m	N/m	N/m	N/m	N/m	N/m	N/m	N/m	N/m	N/m	N/m
9.8	1.3E+05	9.5E+05	-2.6E+06	-5.9E+05	1.6E+06	-2.7E+03	-3.3E+04	1.9E+06	-3.0E+04	-6.9E+04	-6.8E+04	-6.5E+04	-5.2E+04	-1.0E+05	-4.0E+04	-3.8E+04
19.5	-1.3E+05	7.9E+05	-2.5E+06	-7.1E+05	3.5E+06	2.2E+05	1.7E+05	3.7E+06	-4.3E+04	-1.7E+04	-2.5E+04	-4.2E+04	-6.6E+04	-6.7E+04	-3.5E+04	-4.7E+04
29.3	3.2E+05	4.9E+05	-3.0E+06	-7.3E+04	5.0E+06	1.2E+06	4.2E+05	5.0E+06	-7.1E+04	-2.8E+04	-6.6E+04	-1.2E+05	-7.2E+04	-7.2E+04	-7.7E+04	-9.4E+04
39.1	-3.4E+05	9.1E+05	-2.4E+06	-8.5E+05	7.5E+06	4.5E+05	8.5E+04	7.5E+06	-2.3E+04	-4.0E+04	-2.8E+04	-6.5E+04	-7.2E+04	-7.9E+04	-7.2E+04	-4.9E+04
48.8	-4.0E+05	1.2E+06	-2.3E+06	-1.2E+06	9.3E+06	3.4E+05	9.4E+03	9.4E+06	-5.1E+04	-6.0E+04	-8.0E+04	-7.7E+04	-8.4E+04	-5.6E+04	-1.2E+05	-5.4E+04
58.6	-1.1E+05	1.4E+06	-2.2E+06	-1.2E+06	1.1E+07	6.0E+05	-1.7E+04	1.1E+07	-8.7E+04	-4.8E+04	-1.0E+05	-9.2E+04	-1.2E+05	-3.7E+04	-1.0E+05	-5.9E+04
68.4	-3.1E+05	1.5E+06	-2.2E+06	-9.1E+05	1.3E+07	4.4E+05	-6.7E+04	1.4E+07	-3.8E+04	-6.7E+04	-5.3E+04	-6.3E+04	-8.6E+04	-1.4E+05	-6.0E+04	-1.1E+05
78.1	-1.6E+05	1.3E+06	-2.4E+06	-1.0E+06	1.5E+07	3.5E+05	-1.7E+05	1.6E+07	-6.3E+04	-4.3E+04	-2.7E+04	-7.4E+04	-3.8E+04	-8.8E+04	-6.8E+04	-1.1E+05
87.9	-1.4E+05	1.2E+06	-2.5E+06	-1.0E+06	1.7E+07	1.7E+05	-3.6E+05	1.8E+07	-2.0E+04	-7.7E+04	-1.2E+05	-5.4E+04	-7.7E+04	-1.2E+05	-6.6E+04	-6.4E+04
97.7	-1.7E+05	7.7E+05	-2.6E+06	-9.7E+05	1.9E+07	1.7E+05	-5.4E+05	2.0E+07	-9.3E+04	-5.9E+04	-9.4E+04	-6.9E+04	-1.1E+05	-3.8E+04	-3.1E+04	-3.1E+04
107.4	-1.2E+05	3.8E+05	-3.1E+06	-7.8E+05	2.1E+07	2.9E+05	-1.4E+05	2.2E+07	-1.1E+05	-3.6E+04	-1.4E+05	-7.9E+04	-9.7E+04	-7.6E+04	-8.6E+04	-3.8E+04
117.2	3.0E+05	9.0E+05	-2.9E+06	-4.1E+05	2.2E+07	6.0E+05	-3.1E+05	2.4E+07	-8.3E+04	-6.1E+04	-8.5E+04	-3.9E+04	-9.3E+04	-4.5E+04	-9.2E+04	-5.6E+04
127.0	-1.4E+05	7.1E+05	-3.1E+06	3.2E+05	2.4E+07	1.0E+06	5.8E+05	2.6E+07	-7.7E+04	-8.0E+04	-3.1E+04	-1.2E+05	-7.5E+04	-5.1E+04	-5.7E+04	-8.6E+04
136.7	2.0E+05	5.3E+05	-3.2E+06	3.8E+05	2.6E+07	1.5E+06	5.3E+05	2.8E+07	-7.1E+04	-5.5E+04	-4.1E+04	-6.8E+04	-2.9E+04	-4.7E+04	-2.0E+04	-8.1E+04

Table 158 Raw data for the test seal at PR=0.4, ω=10 krpm, and inlet LVF=0% with the zero-preswirl insert

Freq.	Re(H_{XX})	Re(H_{XY})	Re(H_{YX})	Re(H_{YY})	Im(H_{XX})	Im(H_{XY})	Im(H_{YX})	Im(H_{YY})	Re(eH_{XX})	Re(eH_{XY})	Re(eH_{YX})	Re(eH_{YY})	Im(eH_{XX})	Im(eH_{XY})	Im(eH_{YX})	Im(eH_{YY})
Hz	N/m	N/m	N/m	N/m	N/m	N/m	N/m	N/m	N/m	N/m	N/m	N/m	N/m	N/m	N/m	N/m
9.8	-1.0E+06	3.9E+06	-5.6E+06	-1.2E+06	1.8E+06	2.6E+05	-1.1E+05	2.0E+06	-5.8E+04	-7.4E+04	-8.3E+04	-1.0E+05	-6.7E+04	-6.0E+04	-9.2E+04	-5.7E+04
19.5	-1.1E+06	3.9E+06	-5.5E+06	-1.4E+06	3.8E+06	3.0E+05	-1.8E+03	3.7E+06	-6.0E+04	-3.1E+04	-6.6E+04	-3.9E+04	-3.5E+04	-6.0E+04	-9.7E+04	-3.6E+04
29.3	-4.1E+05	3.6E+06	-6.2E+06	-7.5E+05	5.5E+06	8.3E+05	5.4E+05	5.0E+06	-9.5E+04	-7.1E+04	-1.2E+05	-1.5E+05	-1.6E+05	-1.2E+05	-5.0E+04	-4.7E+04
39.1	-9.4E+05	4.2E+06	-5.5E+06	-1.4E+06	7.6E+06	2.5E+05	2.3E+05	7.7E+06	-8.2E+04	-3.1E+04	-5.3E+04	-5.8E+04	-8.8E+04	-4.8E+04	-6.4E+04	-4.7E+04
48.8	-1.2E+06	4.4E+06	-5.4E+06	-1.9E+06	9.5E+06	3.5E+05	-1.1E+04	9.8E+06	-5.1E+04	-3.4E+04	-8.1E+04	-6.4E+04	-8.6E+04	-5.7E+04	-6.9E+04	-5.7E+04
58.6	-1.3E+06	4.6E+06	-5.1E+06	-1.7E+06	1.2E+07	4.4E+05	-3.9E+03	1.2E+07	-1.1E+05	-9.8E+04	-8.4E+04	-7.7E+04	-1.5E+05	-7.3E+04	-1.6E+05	-5.0E+04
68.4	-1.2E+06	4.5E+06	-5.3E+06	-2.0E+06	1.4E+07	7.9E+04	-1.7E+05	1.4E+07	-5.0E+04	-9.4E+04	-6.3E+04	-1.6E+05	-1.1E+05	-1.6E+05	-7.4E+04	-1.0E+05
78.1	-1.4E+06	4.3E+06	-5.3E+06	-1.9E+06	1.6E+07	6.5E+04	-1.8E+05	1.6E+07	-1.2E+05	-6.6E+04	-1.1E+05	-1.3E+05	-7.8E+04	-1.1E+05	-1.0E+05	-6.0E+04
87.9	-1.2E+06	4.2E+06	-5.6E+06	-1.8E+06	1.8E+07	-4.2E+04	-3.8E+05	1.9E+07	-1.5E+05	-1.1E+05	-7.7E+04	-7.9E+04	-9.8E+04	-7.5E+04	-1.2E+05	-6.5E+04
97.7	-1.0E+06	3.9E+06	-5.7E+06	-1.5E+06	2.0E+07	1.1E+04	-4.6E+05	2.1E+07	-1.6E+05	-7.6E+04	-4.4E+04	-4.7E+04	-9.9E+04	-8.0E+04	-1.1E+05	-8.0E+04
107.4	-1.1E+06	3.4E+06	-6.4E+06	-1.2E+06	2.2E+07	6.7E+04	-1.7E+04	2.3E+07	-9.1E+04	-7.7E+04	-1.0E+05	-1.1E+05	-1.2E+05	-1.2E+05	-1.3E+05	-1.5E+05
117.2	-3.0E+05	3.8E+06	-5.8E+06	-7.6E+05	2.4E+07	3.1E+05	-2.2E+05	2.5E+07	-1.0E+05	-5.9E+04	-1.4E+05	-6.0E+04	-1.1E+05	-7.8E+04	-1.3E+05	-1.4E+05
127.0	-3.2E+05	3.8E+06	-6.1E+06	3.8E+04	2.5E+07	7.2E+05	5.2E+05	2.7E+07	-6.2E+04	-1.3E+05	-8.0E+04	-1.8E+05	-9.5E+04	-1.1E+05	-9.8E+04	-1.2E+05
136.7	1.4E+05	3.4E+06	-6.5E+06	7.1E+04	2.7E+07	1.1E+06	4.3E+05	2.8E+07	-1.1E+05	-5.2E+04	-9.2E+04	-9.6E+04	-5.9E+04	-7.1E+04	-1.2E+05	-9.8E+04

Table 159 Raw data for the test seal at PR=0.4, ω=15 krpm, and inlet LVF=0% with the zero-preswirl insert

Freq.	Re(H_{XX})	Re(H_{XY})	Re(H_{YX})	Re(H_{YY})	Im(H_{XX})	Im(H_{XY})	Im(H_{YX})	Im(H_{YY})	Re(eH_{XX})	Re(eH_{XY})	Re(eH_{YX})	Re(eH_{YY})	Im(eH_{XX})	Im(eH_{XY})	Im(eH_{YX})	Im(eH_{YY})
Hz	N/m	N/m	N/m	N/m	N/m	N/m	N/m	N/m	N/m	N/m	N/m	N/m	N/m	N/m	N/m	N/m
9.8	-5.9E+05	7.9E+06	-9.3E+06	-1.3E+06	1.7E+06	-1.5E+05	-3.3E+05	1.9E+06	-7.0E+04	-8.1E+04	-4.2E+04	-4.7E+04	-4.8E+04	-8.0E+04	-5.4E+04	-7.5E+04
19.5	-7.6E+05	7.9E+06	-9.4E+06	-1.6E+06	3.7E+06	-1.1E+05	-2.5E+05	3.9E+06	-6.0E+04	-9.9E+04	-6.4E+04	-3.9E+04	-6.5E+04	-5.8E+04	-2.4E+04	-5.8E+04
29.3	-8.4E+05	8.0E+06	-9.9E+06	-1.5E+06	5.6E+06	6.4E+05	-3.8E+04	5.3E+06	-7.2E+04	-6.4E+04	-8.9E+04	-4.7E+04	-1.1E+05	-6.6E+04	-1.1E+05	-9.1E+04
39.1	-1.2E+06	7.9E+06	-9.6E+06	-1.6E+06	7.5E+06	2.6E+05	-2.3E+05	8.1E+06	-7.7E+04	-8.7E+04	-4.2E+04	-4.7E+04	-5.4E+04	-6.3E+04	-5.4E+04	-6.0E+04
48.8	-1.2E+06	8.0E+06	-9.6E+06	-2.0E+06	9.7E+06	1.0E+05	-3.2E+05	1.0E+07	-8.0E+04	-8.6E+04	-3.6E+04	-5.3E+04	-7.9E+04	-7.1E+04	-6.7E+04	-7.7E+04
58.6	-1.3E+06	8.0E+06	-9.7E+06	-2.1E+06	1.2E+07	3.3E+05	-1.9E+05	1.2E+07	-1.5E+05	-1.1E+05	-9.9E+04	-6.2E+04	-1.3E+05	-6.1E+04	-8.5E+04	-4.9E+04
68.4	-1.5E+06	8.2E+06	-9.8E+06	-1.9E+06	1.4E+07	5.3E+04	-1.9E+05	1.5E+07	-1.1E+05	-1.6E+05	-7.4E+04	-7.0E+04	-9.4E+04	-8.3E+04	-5.3E+04	-6.4E+04
78.1	-1.6E+06	8.1E+06	-9.9E+06	-2.0E+06	1.6E+07	2.3E+05	4.7E+04	1.7E+07	-8.9E+04	-8.4E+04	-6.3E+04	-6.2E+04	-5.8E+04	-9.0E+04	-7.7E+04	-7.4E+04
87.9	-1.7E+06	8.1E+06	-1.0E+07	-2.1E+06	1.8E+07	1.4E+04	2.7E+04	1.9E+07	-5.6E+04	-7.9E+04	-8.2E+04	-8.5E+04	-5.4E+04	-4.5E+04	-8.7E+04	-3.2E+04
97.7	-1.8E+06	7.7E+06	-1.0E+07	-2.1E+06	2.0E+07	-3.5E+04	3.6E+04	2.2E+07	-6.1E+04	-7.2E+04	-8.1E+04	-7.5E+04	-9.6E+04	-5.8E+04	-4.6E+04	-6.8E+04
107.4	-1.8E+06	7.5E+06	-1.0E+07	-1.6E+06	2.3E+07	-1.0E+05	4.6E+05	2.4E+07	-3.3E+04	-4.9E+04	-7.8E+04	-6.0E+04	-8.4E+04	-7.1E+04	-4.9E+04	-9.3E+04
117.2	-1.1E+06	7.7E+06	-1.0E+07	-1.2E+06	2.5E+07	2.9E+05	-2.1E+05	2.7E+07	-6.1E+04	-4.9E+04	-1.1E+05	-7.3E+04	-9.8E+04	-3.8E+04	-6.7E+04	-5.0E+04
127.0	-1.5E+06	7.4E+06	-1.0E+07	-3.5E+04	2.7E+07	6.4E+05	7.2E+05	2.9E+07	-4.0E+04	-9.1E+04	-8.6E+04	-9.2E+04	-6.6E+04	-7.2E+04	-6.9E+04	-1.5E+05
136.7	-5.3E+05	7.1E+06	-1.1E+07	1.7E+05	2.9E+07	9.2E+05	5.6E+05	3.0E+07	-1.1E+05	-9.6E+04	-8.5E+04	-6.3E+04	-7.7E+04	-7.7E+04	-1.0E+05	-9.8E+04

Table 160 Raw data for the test seal at PR=0.4, ω=5 krpm, and inlet LVF=2% with the zero-preswirl insert

Freq.	Re(H_{XX})	Re(H_{XY})	Re(H_{YX})	Re(H_{YY})	Im(H_{XX})	Im(H_{XY})	Im(H_{YX})	Im(H_{YY})	Re(eH_{XX})	Re(eH_{XY})	Re(eH_{YX})	Re(eH_{YY})	Im(eH_{XX})	Im(eH_{XY})	Im(eH_{YX})	Im(eH_{YY})
Hz	N/m	N/m	N/m	N/m	N/m	N/m	N/m	N/m	N/m	N/m	N/m	N/m	N/m	N/m	N/m	N/m
9.8	1.7E+06	9.3E+06	-9.9E+06	-8.3E+05	1.2E+06	7.1E+05	2.9E+05	2.1E+06	-2.2E+05	-4.1E+05	-2.8E+05	-2.4E+05	-3.4E+05	-2.4E+05	-2.9E+05	-4.0E+05
19.5	9.0E+05	9.5E+06	-1.0E+07	-3.6E+05	4.3E+06	5.0E+05	2.9E+05	5.4E+06	-1.5E+05	-1.2E+05	-2.9E+05	-2.0E+05	-1.3E+05	-1.0E+05	-1.4E+05	-2.3E+05
29.3	1.9E+06	9.1E+06	-1.0E+07	4.2E+05	6.7E+06	1.2E+06	8.9E+05	6.7E+06	-1.4E+05	-2.6E+05	-1.9E+05	-3.2E+05	-1.3E+05	-1.3E+05	-3.0E+05	-2.9E+05
39.1	1.1E+06	9.9E+06	-9.7E+06	3.3E+05	9.3E+06	6.1E+05	6.2E+05	1.0E+07	-1.5E+05	-9.3E+04	-1.9E+05	-2.2E+05	-9.9E+04	-7.3E+04	-1.9E+05	-1.2E+05
48.8	9.6E+05	1.0E+07	-9.6E+06	3.8E+05	1.2E+07	6.0E+05	2.1E+05	1.3E+07	-9.9E+04	-9.5E+04	-1.8E+05	-2.0E+05	-7.8E+04	-7.8E+04	-1.8E+05	-2.3E+05
58.6	1.0E+06	9.9E+06	-1.0E+07	5.1E+05	1.4E+07	2.8E+05	-2.7E+03	1.5E+07	-1.4E+05	-7.3E+04	-2.9E+05	-1.8E+05	-8.2E+04	-1.6E+05	-2.0E+05	-2.3E+05
68.4	1.4E+06	1.0E+07	-9.4E+06	7.4E+05	1.7E+07	1.0E+05	4.6E+05	1.8E+07	-1.2E+05	-1.5E+05	-2.6E+05	-1.8E+05	-1.6E+05	-1.4E+05	-2.4E+05	-2.8E+05
78.1	1.2E+06	1.0E+07	-1.0E+07	1.1E+06	1.9E+07	6.1E+05	-1.5E+05	2.1E+07	-7.4E+04	-9.5E+04	-2.7E+05	-1.7E+05	-7.1E+04	-1.1E+05	-1.0E+05	-2.7E+05
87.9	1.6E+06	1.0E+07	-9.9E+06	1.2E+06	2.2E+07	3.1E+05	3.7E+05	2.3E+07	-4.3E+04	-6.1E+04	-1.4E+05	-6.4E+04	-1.2E+05	-1.0E+05	-1.3E+05	-2.6E+05
97.7	1.5E+06	9.7E+06	-1.0E+07	7.6E+05	2.4E+07	3.9E+05	4.1E+04	2.6E+07	-1.1E+05	-5.9E+04	-1.7E+05	-1.4E+05	-8.6E+04	-9.8E+04	-1.6E+05	-1.5E+05
107.4	1.7E+06	9.5E+06	-1.0E+07	1.5E+06	2.7E+07	4.2E+05	6.9E+05	2.8E+07	-3.4E+04	-1.4E+05	-3.0E+05	-2.7E+05	-8.6E+04	-4.5E+04	-1.2E+05	-9.3E+04
117.2	2.4E+06	1.0E+07	-1.0E+07	2.0E+06	2.9E+07	6.1E+05	5.4E+05	3.0E+07	-1.6E+05	-9.9E+04	-2.1E+05	-9.4E+04	-1.1E+05	-8.5E+04	-1.4E+05	-2.4E+05
127.0	2.4E+06	1.0E+07	-1.0E+07	2.6E+06	3.1E+07	8.1E+05	9.8E+05	3.3E+07	-9.6E+04	-8.9E+04	-1.9E+05	-2.9E+05	-9.5E+04	-2.0E+05	-2.6E+05	-3.4E+05
136.7	2.8E+06	9.8E+06	-1.1E+07	3.0E+06	3.3E+07	9.8E+05	6.5E+05	3.5E+07	-1.4E+05	-5.2E+04	-1.2E+05	-1.9E+05	-1.3E+05	-7.7E+04	-1.4E+05	-1.5E+05

Table 161 Raw data for the test seal at PR=0.4, ω=10 krpm, and inlet LVF=2% with the zero-preswirl insert

Freq.	Re(H_{XX})	Re(H_{XY})	Re(H_{YX})	Re(H_{YY})	Im(H_{XX})	Im(H_{XY})	Im(H_{YX})	Im(H_{YY})	Re(eH_{XX})	Re(eH_{XY})	Re(eH_{YX})	Re(eH_{YY})	Im(eH_{XX})	Im(eH_{XY})	Im(eH_{YX})	Im(eH_{YY})
Hz	N/m	N/m	N/m	N/m	N/m	N/m	N/m	N/m	N/m	N/m	N/m	N/m	N/m	N/m	N/m	N/m
9.8	1.1E+06	9.3E+06	-1.1E+07	5.4E+05	7.1E+05	1.3E+06	-5.2E+05	3.3E+06	-2.1E+05	-2.1E+05	-5.6E+05	-5.3E+05	-2.2E+05	-2.9E+05	-4.5E+05	-6.5E+05
19.5	1.0E+06	9.6E+06	-1.0E+07	4.8E+05	3.9E+06	8.3E+05	3.7E+05	5.6E+06	-1.6E+05	-1.5E+05	-1.8E+05	-2.5E+05	-1.3E+05	-1.5E+05	-1.9E+05	-1.7E+05
29.3	9.6E+05	1.0E+07	-1.0E+07	1.4E+06	6.3E+06	1.7E+06	1.8E+06	6.3E+06	-9.2E+04	-8.4E+04	-2.5E+05	-2.8E+05	-1.6E+05	-1.3E+05	-4.4E+05	-3.5E+05
39.1	8.7E+05	1.0E+07	-9.8E+06	5.2E+05	9.1E+06	6.8E+05	2.6E+05	1.1E+07	-1.0E+05	-8.4E+04	-1.4E+05	-1.3E+05	-1.3E+05	-1.2E+05	-1.6E+05	-1.6E+05
48.8	8.6E+05	1.0E+07	-9.7E+06	2.4E+05	1.2E+07	2.8E+05	4.5E+05	1.3E+07	-9.2E+04	-5.7E+04	-2.7E+05	-2.1E+05	-6.2E+04	-7.6E+04	-1.7E+05	-2.0E+05
58.6	8.4E+05	1.0E+07	-1.0E+07	7.1E+05	1.4E+07	6.8E+05	2.3E+05	1.6E+07	-1.9E+05	-1.6E+05	-4.3E+05	-1.8E+05	-1.4E+05	-1.6E+05	-1.2E+05	-2.3E+05
68.4	1.1E+06	1.0E+07	-9.5E+06	5.6E+05	1.6E+07	3.0E+05	2.8E+05	1.8E+07	-1.3E+05	-7.0E+04	-2.5E+05	-1.6E+05	-5.9E+04	-1.6E+05	-2.3E+05	-2.8E+05
78.1	1.1E+06	1.0E+07	-9.7E+06	7.6E+05	1.9E+07	1.9E+05	-1.3E+05	2.0E+07	-1.4E+05	-1.6E+05	-2.4E+05	-2.8E+05	-9.5E+04	-1.5E+05	-1.0E+05	-1.7E+05
87.9	1.3E+06	9.9E+06	-1.0E+07	1.1E+06	2.2E+07	4.2E+05	1.9E+05	2.3E+07	-8.9E+04	-6.5E+04	-2.8E+05	-9.3E+04	-1.0E+05	-1.1E+05	-5.5E+04	-1.5E+05
97.7	1.7E+06	9.9E+06	-1.0E+07	1.2E+06	2.4E+07	4.2E+05	2.5E+05	2.6E+07	-9.2E+04	-1.0E+05	-1.6E+05	-2.4E+05	-1.1E+05	-1.1E+05	-1.5E+05	-1.1E+05
107.4	1.7E+06	9.2E+06	-1.1E+07	1.1E+06	2.7E+07	4.7E+05	1.0E+05	2.8E+07	-8.3E+04	-6.5E+04	-1.8E+05	-8.3E+04	-1.1E+05	-8.0E+04	-2.1E+05	-6.7E+04
117.2	2.2E+06	1.0E+07	-1.1E+07	2.2E+06	2.9E+07	8.0E+05	5.2E+05	3.1E+07	-8.2E+04	-6.2E+04	-3.1E+05	-1.7E+05	-5.1E+04	-9.3E+04	-2.9E+05	-1.1E+05
127.0	2.4E+06	1.0E+07	-1.0E+07	3.4E+06	3.1E+07	9.1E+05	1.2E+06	3.3E+07	-1.2E+05	-2.2E+05	-2.0E+05	-1.7E+05	-1.1E+05	-2.4E+05	-1.9E+05	-4.6E+05
136.7	2.6E+06	9.9E+06	-1.1E+07	3.0E+06	3.3E+07	1.1E+06	1.0E+06	3.5E+07	-1.1E+05	-1.1E+05	-2.0E+05	-2.9E+05	-9.8E+04	-5.0E+04	-2.0E+05	-1.1E+05

Table 162 Raw data for the test seal at PR=0.4, ω=15 krpm, and inlet LVF=2% with the zero-preswirl insert

Freq.	Re(H_{XX})	Re(H_{XY})	Re(H_{YX})	Re(H_{YY})	Im(H_{XX})	Im(H_{XY})	Im(H_{YX})	Im(H_{YY})	Re(eH_{XX})	Re(eH_{XY})	Re(eH_{YX})	Re(eH_{YY})	Im(eH_{XX})	Im(eH_{XY})	Im(eH_{YX})	Im(eH_{YY})
Hz	N/m	N/m	N/m	N/m	N/m	N/m	N/m	N/m	N/m	N/m	N/m	N/m	N/m	N/m	N/m	N/m
9.8	2.2E+06	1.5E+07	-1.5E+07	-5.8E+05	9.7E+05	-6.5E+05	-1.9E+06	3.7E+06	-4.3E+05	-3.2E+05	-5.2E+05	-4.4E+05	-3.0E+05	-4.5E+05	-4.0E+05	-5.7E+05
19.5	1.1E+06	1.6E+07	-1.7E+07	6.7E+05	3.6E+06	-4.4E+05	-7.5E+05	5.1E+06	-2.4E+05	-2.5E+05	-4.5E+05	-6.3E+05	-1.9E+05	-2.7E+05	-5.2E+05	-5.0E+05
29.3	1.2E+06	1.6E+07	-1.7E+07	1.4E+06	5.9E+06	1.3E+06	1.2E+06	5.9E+06	-2.3E+05	-1.9E+05	-3.7E+05	-2.3E+05	-1.9E+05	-1.6E+05	-2.9E+05	-2.8E+05
39.1	3.4E+05	1.6E+07	-1.6E+07	1.4E+06	9.0E+06	-3.0E+05	8.6E+05	1.0E+07	-1.9E+05	-1.5E+05	-4.0E+05	-4.4E+05	-1.6E+05	-1.7E+05	-3.8E+05	-2.3E+05
48.8	2.8E+05	1.6E+07	-1.6E+07	5.9E+05	1.2E+07	-7.2E+04	2.8E+05	1.3E+07	-9.5E+04	-1.2E+05	-2.5E+05	-2.7E+05	-1.2E+05	-1.2E+05	-2.2E+05	-2.9E+05
58.6	2.2E+05	1.6E+07	-1.6E+07	8.6E+05	1.4E+07	1.0E+04	8.3E+05	1.6E+07	-1.3E+05	-1.5E+05	-3.2E+05	-1.5E+05	-1.9E+05	-1.7E+05	-3.2E+05	-3.8E+05
68.4	2.7E+05	1.6E+07	-1.6E+07	1.6E+06	1.7E+07	-6.1E+04	1.3E+06	1.8E+07	-1.8E+05	-1.8E+05	-4.7E+05	-5.9E+05	-1.4E+05	-2.0E+05	-3.8E+05	-4.5E+05
78.1	5.4E+05	1.6E+07	-1.6E+07	1.5E+06	2.0E+07	-2.0E+05	1.2E+06	2.1E+07	-2.2E+05	-8.7E+04	-1.6E+05	-3.6E+05	-1.2E+05	-1.3E+05	-3.0E+05	-2.5E+05
87.9	5.3E+05	1.6E+07	-1.6E+07	1.7E+06	2.2E+07	-1.9E+05	1.4E+06	2.4E+07	-1.8E+05	-1.5E+05	-1.2E+05	-2.9E+05	-1.1E+05	-9.4E+04	-3.5E+05	-2.2E+05
97.7	7.5E+05	1.6E+07	-1.7E+07	2.0E+06	2.5E+07	-9.0E+04	1.3E+06	2.7E+07	-1.0E+05	-8.6E+04	-1.6E+05	-2.1E+05	-1.1E+05	-7.4E+04	-2.1E+05	-8.0E+04
107.4	1.2E+06	1.5E+07	-1.6E+07	2.7E+06	2.7E+07	-2.7E+05	1.3E+06	2.9E+07	-1.2E+05	-1.4E+05	-3.1E+05	-3.1E+05	-1.6E+05	-8.9E+04	-4.5E+05	-1.6E+05
117.2	2.0E+06	1.6E+07	-1.7E+07	2.9E+06	3.0E+07	-1.8E+05	1.3E+06	3.2E+07	-1.5E+05	-7.5E+04	-1.5E+05	-9.4E+04	-3.8E+04	-8.3E+04	-1.4E+05	-2.4E+05
127.0	1.8E+06	1.6E+07	-1.7E+07	4.4E+06	3.2E+07	2.2E+05	2.4E+06	3.4E+07	-1.5E+05	-1.2E+05	-2.2E+05	-3.1E+05	-1.4E+05	-1.7E+05	-2.8E+05	-3.7E+05
136.7	2.4E+06	1.6E+07	-1.7E+07	4.3E+06	3.5E+07	4.3E+05	2.3E+06	3.6E+07	-1.4E+05	-1.6E+05	-1.9E+05	-2.4E+05	-1.7E+05	-1.6E+05	-2.8E+05	-3.0E+05

Table 163 Raw data for the test seal at PR=0.4, ω=5 krpm, and inlet LVF=4% with the zero-preswirl insert

Freq.	Re(H_{XX})	Re(H_{XY})	Re(H_{YX})	Re(H_{YY})	Im(H_{XX})	Im(H_{XY})	Im(H_{YX})	Im(H_{YY})	Re(eH_{XX})	Re(eH_{XY})	Re(eH_{YX})	Re(eH_{YY})	Im(eH_{XX})	Im(eH_{XY})	Im(eH_{YX})	Im(eH_{YY})
Hz	N/m	N/m	N/m	N/m	N/m	N/m	N/m	N/m	N/m	N/m	N/m	N/m	N/m	N/m	N/m	N/m
9.8	3.4E+06	2.2E+06	-5.4E+06	2.1E+06	4.9E+05	2.4E+06	3.4E+05	2.0E+06	-4.4E+05	-2.5E+05	-3.5E+05	-4.0E+05	-3.3E+05	-4.3E+05	-2.9E+05	-4.2E+05
19.5	3.2E+06	3.5E+06	-4.3E+06	2.3E+06	3.3E+06	1.3E+06	1.4E+06	4.1E+06	-1.8E+05	-1.7E+05	-2.7E+05	-4.2E+05	-2.0E+05	-1.7E+05	-2.2E+05	-3.1E+05
29.3	3.0E+06	3.5E+06	-5.7E+06	2.9E+06	5.3E+06	2.8E+06	2.7E+06	6.3E+06	-3.1E+05	-2.5E+05	-4.1E+05	-4.1E+05	-2.0E+05	-3.4E+05	-4.2E+05	-6.4E+05
39.1	2.5E+06	4.7E+06	-4.4E+06	2.6E+06	8.9E+06	1.4E+06	1.2E+06	9.8E+06	-1.1E+05	-2.9E+05	-1.8E+05	-3.0E+05	-1.1E+05	-1.3E+05	-2.8E+05	-2.1E+05
48.8	2.4E+06	4.6E+06	-4.0E+06	1.6E+06	1.1E+07	1.2E+06	6.0E+05	1.2E+07	-1.4E+05	-9.0E+04	-2.3E+05	-2.9E+05	-1.6E+05	-2.2E+05	-2.3E+05	-2.1E+05
58.6	2.5E+06	5.3E+06	-3.7E+06	2.7E+06	1.4E+07	9.3E+05	9.2E+05	1.4E+07	-9.6E+04	-1.3E+05	-2.3E+05	-1.6E+05	-8.3E+04	-1.3E+05	-2.6E+05	-2.7E+05
68.4	2.1E+06	4.5E+06	-4.1E+06	2.0E+06	1.6E+07	9.4E+05	7.8E+05	1.7E+07	-1.4E+05	-1.6E+05	-2.0E+05	-2.8E+05	-2.1E+05	-2.9E+05	-2.1E+05	-4.8E+05
78.1	2.2E+06	5.1E+06	-4.3E+06	2.3E+06	1.9E+07	5.4E+05	-3.6E+05	1.9E+07	-2.6E+05	-1.8E+05	-3.8E+05	-2.9E+05	-1.1E+05	-2.9E+05	-3.2E+05	-2.2E+05
87.9	2.0E+06	4.7E+06	-4.5E+06	1.8E+06	2.1E+07	8.8E+05	6.9E+05	2.2E+07	-1.9E+05	-1.0E+05	-2.8E+05	-2.4E+05	-1.8E+05	-2.0E+05	-1.9E+05	-3.1E+05
97.7	2.2E+06	4.5E+06	-4.7E+06	1.4E+06	2.4E+07	7.8E+05	9.7E+05	2.5E+07	-2.5E+05	-1.1E+05	-2.4E+05	-1.5E+05	-7.3E+04	-9.5E+04	-1.8E+05	-2.5E+05
107.4	1.9E+06	4.4E+06	-5.1E+06	2.0E+06	2.7E+07	8.9E+05	1.4E+06	2.7E+07	-2.4E+05	-1.6E+05	-2.5E+05	-1.3E+05	-2.3E+05	-1.2E+05	-4.0E+05	-2.4E+05
117.2	2.3E+06	5.0E+06	-5.1E+06	2.6E+06	2.9E+07	1.1E+06	8.9E+05	3.0E+07	-5.3E+04	-1.8E+05	-1.4E+05	-2.5E+05	-3.6E+05	-1.0E+05	-3.6E+05	-1.6E+05
127.0	2.4E+06	4.8E+06	-4.8E+06	3.3E+06	3.1E+07	1.2E+06	1.7E+06	3.2E+07	-2.6E+05	-2.1E+05	-3.3E+05	-1.8E+05	-2.0E+05	-4.5E+05	-3.3E+05	-2.7E+05
136.7	2.4E+06	4.9E+06	-5.0E+06	2.8E+06	3.4E+07	1.8E+06	1.6E+06	3.5E+07	-1.3E+05	-2.3E+05	-1.8E+05	-3.0E+05	-1.7E+05	-2.2E+05	-3.4E+05	-3.2E+05

Table 164 Raw data for the test seal at PR=0.4, ω=10 krpm, and inlet LVF=4% with the zero-preswirl insert

Freq.	Re(H_{XX})	Re(H_{XY})	Re(H_{YX})	Re(H_{YY})	Im(H_{XX})	Im(H_{XY})	Im(H_{YX})	Im(H_{YY})	Re(eH_{XX})	Re(eH_{XY})	Re(eH_{YX})	Re(eH_{YY})	Im(eH_{XX})	Im(eH_{XY})	Im(eH_{YX})	Im(eH_{YY})
Hz	N/m	N/m	N/m	N/m	N/m	N/m	N/m	N/m	N/m	N/m	N/m	N/m	N/m	N/m	N/m	N/m
9.8	3.8E+06	7.4E+06	-1.1E+07	4.9E+05	-4.5E+05	1.4E+06	6.5E+05	3.9E+06	-4.0E+05	-2.9E+05	-6.2E+05	-6.3E+05	-5.1E+05	-4.3E+05	-4.8E+05	-5.4E+05
19.5	1.5E+06	8.7E+06	-9.5E+06	4.2E+05	2.7E+06	2.1E+06	7.4E+05	6.0E+06	-1.7E+05	-1.6E+05	-3.4E+05	-4.1E+05	-1.5E+05	-3.9E+05	-2.3E+05	-2.8E+05
29.3	2.6E+06	8.5E+06	-9.7E+06	2.0E+06	4.6E+06	3.2E+06	1.9E+06	7.4E+06	-3.2E+05	-3.2E+05	-5.7E+05	-2.4E+05	-3.2E+05	-3.0E+05	-3.9E+05	-5.1E+05
39.1	1.7E+06	9.9E+06	-8.1E+06	1.3E+06	9.2E+06	1.1E+06	1.2E+06	1.0E+07	-2.3E+05	-2.7E+05	-3.4E+05	-3.2E+05	-1.7E+05	-1.0E+05	-3.8E+05	-1.9E+05
48.8	1.7E+06	9.7E+06	-8.4E+06	9.9E+05	1.2E+07	9.3E+05	5.9E+05	1.3E+07	-3.1E+05	-1.9E+05	-1.9E+05	-2.5E+05	-2.8E+05	-2.6E+05	-3.2E+05	-1.4E+05
58.6	2.1E+06	1.0E+07	-7.9E+06	1.4E+06	1.5E+07	1.0E+06	8.3E+05	1.6E+07	-2.8E+05	-2.4E+05	-4.5E+05	-3.3E+05	-3.5E+05	-2.4E+05	-6.5E+05	-2.9E+05
68.4	1.9E+06	9.7E+06	-7.7E+06	2.5E+06	1.7E+07	8.3E+05	1.0E+06	1.8E+07	-2.6E+05	-8.4E+04	-4.6E+05	-3.8E+05	-2.8E+05	-2.9E+05	-4.0E+05	-7.1E+05
78.1	1.9E+06	1.0E+07	-8.4E+06	2.2E+06	1.9E+07	1.4E+06	4.2E+05	2.1E+07	-1.2E+05	-1.7E+05	-4.1E+05	-4.2E+05	-1.4E+05	-2.1E+05	-3.5E+05	-2.4E+05
87.9	2.7E+06	1.0E+07	-8.0E+06	2.4E+06	2.2E+07	1.1E+06	1.9E+05	2.4E+07	-1.3E+05	-9.8E+04	-2.4E+05	-1.7E+05	-1.7E+05	-1.6E+05	-3.8E+05	-2.1E+05
97.7	2.6E+06	9.9E+06	-9.2E+06	1.6E+06	2.5E+07	7.0E+05	-4.3E+05	2.6E+07	-1.6E+05	-2.3E+05	-1.8E+05	-4.4E+05	-1.4E+05	-2.4E+05	-3.6E+05	-4.2E+05
107.4	2.3E+06	9.7E+06	-9.6E+06	2.2E+06	2.8E+07	9.4E+05	1.4E+05	2.9E+07	-1.6E+05	-2.9E+05	-6.0E+05	-3.6E+05	-3.9E+05	-2.7E+05	-3.3E+05	-3.9E+05
117.2	3.8E+06	1.0E+07	-8.6E+06	2.3E+06	2.9E+07	9.9E+05	-3.3E+04	3.1E+07	-1.3E+05	-1.9E+05	-2.6E+05	-1.4E+05	-2.0E+05	-2.0E+05	-3.8E+05	-1.7E+05
127.0	3.4E+06	9.7E+06	-8.9E+06	2.7E+06	3.2E+07	1.4E+06	6.7E+05	3.3E+07	-1.1E+05	-2.5E+05	-2.1E+05	-5.7E+05	-3.2E+05	-1.9E+05	-2.7E+05	-3.7E+05
136.7	3.2E+06	1.0E+07	-9.8E+06	3.5E+06	3.4E+07	1.9E+06	6.3E+05	3.6E+07	-2.1E+05	-2.1E+05	-3.2E+05	-3.1E+05	-2.3E+05	-2.0E+05	-4.5E+05	-2.9E+05

Table 165 Raw data for the test seal at PR=0.4, ω=15 krpm, and inlet LVF=4% with the zero-preswirl insert

Freq.	Re(H_{XX})	Re(H_{XY})	Re(H_{YX})	Re(H_{YY})	Im(H_{XX})	Im(H_{XY})	Im(H_{YX})	Im(H_{YY})	Re(eH_{XX})	Re(eH_{XY})	Re(eH_{YX})	Re(eH_{YY})	Im(eH_{XX})	Im(eH_{XY})	Im(eH_{YX})	Im(eH_{YY})
Hz	N/m	N/m	N/m	N/m	N/m	N/m	N/m	N/m	N/m	N/m	N/m	N/m	N/m	N/m	N/m	N/m
9.8	3.4E+06	1.4E+07	-1.5E+07	2.5E+05	-7.5E+05	-1.2E+05	-1.8E+05	3.5E+06	-3.6E+05	-2.5E+05	-7.3E+05	-7.8E+05	-4.1E+05	-4.6E+05	-8.9E+05	-7.6E+05
19.5	1.7E+06	1.5E+07	-1.5E+07	1.7E+06	2.9E+06	2.4E+05	1.0E+06	6.3E+06	-3.2E+05	-3.2E+05	-5.7E+05	-6.0E+05	-3.8E+05	-4.9E+05	-7.0E+05	-7.6E+05
29.3	2.1E+06	1.5E+07	-1.6E+07	3.6E+06	5.3E+06	2.0E+06	3.2E+06	7.5E+06	-2.7E+05	-3.1E+05	-3.5E+05	-3.9E+05	-2.5E+05	-3.7E+05	-4.2E+05	-6.6E+05
39.1	1.5E+06	1.5E+07	-1.4E+07	2.1E+06	8.8E+06	2.9E+04	9.3E+05	1.0E+07	-2.5E+05	-2.2E+05	-3.0E+05	-3.6E+05	-2.2E+05	-2.9E+05	-3.1E+05	-1.7E+05
48.8	1.7E+06	1.5E+07	-1.4E+07	2.0E+06	1.2E+07	2.2E+05	1.5E+06	1.4E+07	-1.9E+05	-1.7E+05	-5.4E+05	-4.0E+05	-2.8E+05	-2.0E+05	-4.7E+05	-5.4E+05
58.6	1.2E+06	1.5E+07	-1.4E+07	1.0E+06	1.4E+07	2.0E+05	3.7E+05	1.6E+07	-2.5E+05	-2.0E+05	-5.7E+05	-3.5E+05	-2.9E+05	-2.7E+05	-4.0E+05	-4.9E+05
68.4	2.1E+06	1.5E+07	-1.2E+07	3.1E+06	1.8E+07	-4.3E+05	9.6E+05	1.9E+07	-2.7E+05	-2.4E+05	-5.5E+05	-4.1E+05	-2.1E+05	-2.6E+05	-4.7E+05	-6.2E+05
78.1	2.0E+06	1.5E+07	-1.3E+07	2.9E+06	2.1E+07	4.3E+05	1.2E+06	2.2E+07	-2.4E+05	-2.0E+05	-5.8E+05	-2.5E+05	-2.9E+05	-2.0E+05	-5.1E+05	-4.2E+05
87.9	2.0E+06	1.5E+07	-1.3E+07	3.3E+06	2.2E+07	6.9E+05	-1.4E+05	2.5E+07	-3.4E+05	-2.3E+05	-4.9E+05	-5.5E+05	-1.6E+05	-2.7E+05	-6.0E+05	-4.8E+05
97.7	2.3E+06	1.5E+07	-1.4E+07	3.5E+06	2.5E+07	4.4E+05	1.0E+06	2.7E+07	-2.4E+05	-1.5E+05	-1.1E+05	-3.1E+05	-2.0E+05	-2.9E+05	-3.3E+05	-2.7E+05
107.4	2.8E+06	1.5E+07	-1.5E+07	3.2E+06	2.7E+07	5.4E+04	-3.5E+05	3.0E+07	-1.9E+05	-1.6E+05	-4.3E+05	-3.1E+05	-2.0E+05	-1.7E+05	-3.4E+05	-2.7E+05
117.2	2.8E+06	1.6E+07	-1.4E+07	4.6E+06	3.0E+07	5.2E+05	7.8E+05	3.3E+07	-2.2E+05	-1.9E+05	-4.0E+05	-4.2E+05	-3.2E+05	-1.9E+05	-3.7E+05	-5.2E+05
127.0	2.4E+06	1.6E+07	-1.4E+07	5.8E+06	3.2E+07	5.7E+05	1.7E+06	3.5E+07	-1.4E+05	-1.6E+05	-3.5E+05	-4.8E+05	-1.6E+05	-1.8E+05	-4.3E+05	-4.8E+05
136.7	2.5E+06	1.5E+07	-1.5E+07	6.1E+06	3.5E+07	1.9E+06	1.8E+06	3.8E+07	-2.8E+05	-2.0E+05	-3.5E+05	-2.3E+05	-2.2E+05	-1.9E+05	-3.4E+05	-3.8E+05

Table 166 Raw data for the test seal at PR=0.4, ω=5 krpm, and inlet LVF=6% with the zero-preswirl insert

Freq.	Re(H_{XX})	Re(H_{XY})	Re(H_{YX})	Re(H_{YY})	Im(H_{XX})	Im(H_{XY})	Im(H_{YX})	Im(H_{YY})	Re(eH_{XX})	Re(eH_{XY})	Re(eH_{YX})	Re(eH_{YY})	Im(eH_{XX})	Im(eH_{XY})	Im(eH_{YX})	Im(eH_{YY})
Hz	N/m	N/m	N/m	N/m	N/m	N/m	N/m	N/m	N/m	N/m	N/m	N/m	N/m	N/m	N/m	N/m
9.8	4.5E+06	1.8E+06	-6.6E+06	2.5E+06	2.0E+06	1.6E+06	2.2E+06	1.0E+06	-5.4E+05	-3.4E+05	-7.9E+05	-4.9E+05	-5.5E+05	-4.9E+05	-8.9E+05	-6.0E+05
19.5	3.7E+06	3.7E+06	-5.5E+06	1.9E+06	3.5E+06	2.9E+06	2.2E+06	4.9E+06	-1.4E+05	-1.1E+05	-3.2E+05	-4.1E+05	-3.2E+05	-2.5E+05	-5.1E+05	-6.2E+05
29.3	4.1E+06	3.6E+06	-5.1E+06	1.7E+06	5.4E+06	3.9E+06	2.9E+06	6.6E+06	-2.0E+05	-1.9E+05	-3.0E+05	-4.3E+05	-2.6E+05	-2.4E+05	-3.8E+05	-4.9E+05
39.1	3.4E+06	4.8E+06	-3.5E+06	1.9E+06	8.9E+06	1.1E+06	1.8E+06	9.8E+06	-2.0E+05	-2.7E+05	-2.7E+05	-2.1E+05	-1.3E+05	-9.2E+04	-1.6E+05	-2.9E+05
48.8	2.5E+06	6.0E+06	-3.6E+06	2.7E+06	1.2E+07	1.2E+06	1.2E+06	1.2E+07	-2.5E+05	-3.5E+05	-4.9E+05	-4.2E+05	-1.6E+05	-1.6E+05	-3.1E+05	-3.1E+05
58.6	2.6E+06	4.7E+06	-3.4E+06	2.0E+06	1.4E+07	8.4E+05	1.0E+06	1.5E+07	-2.7E+05	-3.2E+05	-4.7E+05	-3.4E+05	-1.9E+05	-1.4E+05	-3.7E+05	-6.2E+05
68.4	2.6E+06	6.2E+06	-3.5E+06	2.8E+06	1.7E+07	3.9E+05	1.2E+06	1.8E+07	-1.0E+05	-4.1E+05	-5.9E+05	-5.3E+05	-3.3E+05	-2.3E+05	-2.6E+05	-2.8E+05
78.1	2.4E+06	5.2E+06	-3.9E+06	3.0E+06	1.9E+07	5.3E+05	6.9E+05	2.0E+07	-2.9E+05	-2.1E+05	-3.3E+05	-4.0E+05	-2.9E+05	-3.5E+05	-2.2E+05	-4.2E+05
87.9	2.6E+06	5.3E+06	-3.9E+06	2.2E+06	2.2E+07	5.3E+05	7.3E+05	2.3E+07	-1.8E+05	-2.4E+05	-2.5E+05	-2.9E+05	-1.5E+05	-3.2E+05	-3.3E+05	-3.3E+05
97.7	3.1E+06	4.4E+06	-3.5E+06	1.9E+06	2.5E+07	6.7E+05	5.2E+05	2.6E+07	-3.8E+05	-3.3E+05	-5.8E+05	-5.6E+05	-2.9E+05	-1.9E+05	-2.7E+05	-2.5E+05
107.4	2.5E+06	4.2E+06	-4.7E+06	2.2E+06	2.8E+07	3.8E+05	1.8E+06	2.9E+07	-2.8E+05	-2.3E+05	-2.4E+05	-3.4E+05	-3.2E+05	-1.6E+05	-2.8E+05	-1.3E+05
117.2	2.1E+06	4.4E+06	-5.7E+06	1.9E+06	3.0E+07	7.7E+05	2.1E+05	3.1E+07	-2.6E+05	-2.4E+05	-2.0E+05	-3.2E+05	-2.8E+05	-2.4E+05	-4.3E+05	-3.8E+05
127.0	3.1E+06	3.7E+06	-4.0E+06	2.0E+06	3.2E+07	7.4E+05	1.8E+06	3.3E+07	-1.1E+05	-4.0E+05	-1.7E+05	-5.8E+05	-2.0E+05	-2.6E+05	-2.5E+05	-5.3E+05
136.7	3.7E+06	5.1E+06	-4.7E+06	3.7E+06	3.5E+07	9.4E+05	1.7E+06	3.6E+07	-3.3E+05	-5.9E+05	-1.8E+05	-4.0E+05	-1.9E+05	-3.7E+05	-1.4E+05	-4.8E+05

Table 167 Raw data for the test seal at PR=0.4, ω=10 krpm, and inlet LVF=6% with the zero-preswirl insert

Freq.	Re(H_{XX})	Re(H_{XY})	Re(H_{YX})	Re(H_{YY})	Im(H_{XX})	Im(H_{XY})	Im(H_{YX})	Im(H_{YY})	Re(eH_{XX})	Re(eH_{XY})	Re(eH_{YX})	Re(eH_{YY})	Im(eH_{XX})	Im(eH_{XY})	Im(eH_{YX})	Im(eH_{YY})
Hz	N/m	N/m	N/m	N/m	N/m	N/m	N/m	N/m	N/m	N/m	N/m	N/m	N/m	N/m	N/m	N/m
9.8	5.9E+06	8.7E+06	-9.5E+06	4.5E+05	7.1E+05	2.1E+06	2.2E+06	3.5E+06	-7.0E+05	-7.1E+05	-6.8E+05	-7.4E+05	-8.9E+05	-5.6E+05	-7.1E+05	-5.4E+05
19.5	3.1E+06	8.5E+06	-8.6E+06	2.7E+05	2.1E+06	1.4E+06	1.0E+06	5.9E+06	-1.2E+05	-2.4E+05	-3.9E+05	-2.8E+05	-3.3E+05	-3.6E+05	-2.5E+05	-4.9E+05
29.3	3.0E+06	8.1E+06	-8.6E+06	1.9E+06	4.7E+06	3.2E+06	2.6E+06	7.3E+06	-3.0E+05	-3.9E+05	-3.6E+05	-3.8E+05	-2.6E+05	-2.8E+05	-3.1E+05	-5.0E+05
39.1	2.1E+06	9.5E+06	-7.5E+06	1.6E+06	8.8E+06	1.3E+06	7.9E+05	1.2E+07	-2.5E+05	-1.3E+05	-3.4E+05	-2.2E+05	-8.2E+04	-2.6E+05	-2.7E+05	-3.0E+05
48.8	1.8E+06	9.8E+06	-8.5E+06	1.0E+06	1.2E+07	1.4E+06	3.8E+05	1.5E+07	-3.9E+05	-3.2E+05	-3.0E+05	-4.5E+05	-1.1E+05	-2.1E+05	-2.7E+05	-3.2E+05
58.6	2.6E+06	1.0E+07	-7.7E+06	1.5E+06	1.5E+07	1.6E+06	-4.7E+05	1.7E+07	-3.4E+05	-3.2E+05	-6.1E+05	-5.8E+05	-2.1E+05	-3.3E+05	-2.9E+05	-2.1E+05
68.4	2.5E+06	1.0E+07	-6.8E+06	2.3E+06	1.8E+07	1.6E+06	3.8E+05	2.0E+07	-3.5E+05	-2.4E+05	-4.4E+05	-6.4E+05	-3.7E+05	-3.6E+05	-5.4E+05	-5.6E+05
78.1	2.6E+06	1.0E+07	-8.3E+06	2.8E+06	2.0E+07	1.2E+06	-4.0E+05	2.2E+07	-2.2E+05	-1.2E+05	-4.5E+05	-3.8E+05	-2.2E+05	-2.1E+05	-5.0E+05	-6.5E+05
87.9	2.9E+06	1.0E+07	-7.9E+06	2.1E+06	2.3E+07	9.8E+05	-1.0E+06	2.5E+07	-2.0E+05	-1.8E+05	-2.4E+05	-5.0E+05	-1.6E+05	-1.8E+05	-2.8E+05	-3.2E+05
97.7	3.2E+06	9.8E+06	-8.7E+06	1.9E+06	2.6E+07	1.4E+06	-1.5E+05	2.9E+07	-2.0E+05	-1.9E+05	-3.4E+05	-3.5E+05	-2.6E+05	-1.7E+05	-3.1E+05	-3.1E+05
107.4	3.2E+06	9.9E+06	-9.4E+06	2.5E+06	2.9E+07	1.1E+06	6.6E+05	3.1E+07	-2.4E+05	-2.6E+05	-3.4E+05	-3.3E+05	-1.3E+05	-1.9E+05	-2.5E+05	-2.5E+05
117.2	3.7E+06	1.0E+07	-8.9E+06	2.3E+06	3.1E+07	1.7E+06	-9.5E+05	3.4E+07	-1.4E+05	-1.7E+05	-2.3E+05	-8.9E+04	-2.8E+05	-1.4E+05	-4.3E+05	-3.6E+05
127.0	3.6E+06	1.0E+07	-8.9E+06	3.7E+06	3.3E+07	1.3E+06	3.8E+05	3.6E+07	-1.6E+05	-1.2E+05	-4.2E+05	-2.6E+05	-1.8E+05	-2.6E+05	-2.1E+05	-7.1E+05
136.7	4.0E+06	1.0E+07	-9.4E+06	3.6E+06	3.6E+07	1.5E+06	5.1E+05	3.8E+07	-2.0E+05	-4.4E+05	-2.0E+05	-5.9E+05	-3.0E+05	-2.2E+05	-3.8E+05	-3.6E+05

Table 168 Raw data for the test seal at PR=0.4, ω=15 krpm, and inlet LVF=6% with the zero-preswirl insert

Freq.	Re(H_{XX})	Re(H_{XY})	Re(H_{YX})	Re(H_{YY})	Im(H_{XX})	Im(H_{XY})	Im(H_{YX})	Im(H_{YY})	Re(eH_{XX})	Re(eH_{XY})	Re(eH_{YX})	Re(eH_{YY})	Im(eH_{XX})	Im(eH_{XY})	Im(eH_{YX})	Im(eH_{YY})
Hz	N/m	N/m	N/m	N/m	N/m	N/m	N/m	N/m	N/m	N/m	N/m	N/m	N/m	N/m	N/m	N/m
9.8	6.9E+06	1.6E+07	-1.4E+07	3.2E+05	-4.6E+05	-4.5E+05	-1.2E+06	4.6E+06	-1.1E+06	-1.1E+06	-7.7E+05	-6.9E+05	-1.1E+06	-9.9E+05	-9.5E+05	-9.2E+05
19.5	2.1E+06	1.6E+07	-1.5E+07	3.1E+06	2.6E+06	7.3E+05	1.9E+06	6.5E+06	-2.4E+05	-4.5E+05	-5.5E+05	-8.1E+05	-4.3E+05	-5.5E+05	-4.8E+05	-5.7E+05
29.3	2.9E+06	1.5E+07	-1.6E+07	3.1E+06	4.1E+06	1.5E+06	2.8E+06	7.9E+06	-4.3E+05	-2.8E+05	-4.9E+05	-3.7E+05	-3.4E+05	-6.9E+05	-4.4E+05	-7.1E+05
39.1	1.8E+06	1.5E+07	-1.4E+07	3.0E+06	8.6E+06	3.1E+04	1.6E+06	1.2E+07	-2.7E+05	-4.7E+05	-2.4E+05	-3.5E+05	-4.2E+05	-3.4E+05	-4.6E+05	-5.5E+05
48.8	2.0E+06	1.4E+07	-1.4E+07	2.5E+06	1.1E+07	-1.5E+04	4.2E+05	1.4E+07	-1.7E+05	-1.9E+05	-3.0E+05	-4.8E+05	-1.9E+05	-2.5E+05	-6.2E+05	-3.9E+05
58.6	2.4E+06	1.5E+07	-1.4E+07	2.3E+06	1.5E+07	3.2E+05	1.1E+06	1.8E+07	-5.3E+05	-3.0E+05	-3.2E+05	-6.1E+05	-3.1E+05	-4.6E+05	-6.5E+05	-2.9E+05
68.4	1.9E+06	1.5E+07	-1.4E+07	3.7E+06	1.8E+07	3.3E+05	5.6E+05	2.0E+07	-4.4E+05	-2.8E+05	-5.7E+05	-7.1E+05	-4.7E+05	-4.8E+05	-6.8E+05	-6.4E+05
78.1	2.3E+06	1.4E+07	-1.3E+07	3.3E+06	2.0E+07	4.6E+05	-1.2E+05	2.3E+07	-2.6E+05	-3.8E+05	-4.1E+05	-3.7E+05	-2.1E+05	-4.7E+05	-6.3E+05	-3.8E+05
87.9	2.0E+06	1.6E+07	-1.4E+07	3.3E+06	2.4E+07	8.0E+05	3.5E+05	2.6E+07	-3.0E+05	-3.7E+05	-5.2E+05	-4.5E+05	-2.8E+05	-2.9E+05	-4.7E+05	-5.3E+05
97.7	2.6E+06	1.5E+07	-1.4E+07	3.4E+06	2.7E+07	8.8E+05	-1.2E+05	2.9E+07	-2.3E+05	-3.1E+05	-4.1E+05	-4.4E+05	-1.7E+05	-2.4E+05	-6.5E+05	-2.8E+05
107.4	2.5E+06	1.5E+07	-1.6E+07	3.0E+06	2.9E+07	4.8E+05	-7.6E+05	3.3E+07	-3.9E+05	-3.5E+05	-6.2E+05	-3.5E+05	-5.2E+05	-2.3E+05	-2.0E+05	-4.0E+05
117.2	3.5E+06	1.5E+07	-1.4E+07	4.1E+06	3.1E+07	9.9E+05	-1.6E+06	3.5E+07	-2.1E+05	-2.6E+05	-5.4E+05	-5.2E+05	-4.0E+05	-2.3E+05	-3.5E+05	-4.2E+05
127.0	2.8E+06	1.6E+07	-1.5E+07	6.2E+06	3.5E+07	1.7E+06	1.6E+06	3.8E+07	-4.0E+05	-4.0E+05	-5.5E+05	-4.5E+05	-2.7E+05	-4.7E+05	-3.6E+05	-3.3E+05
136.7	3.7E+06	1.6E+07	-1.5E+07	5.8E+06	3.7E+07	1.6E+06	1.0E+06	4.0E+07	-2.1E+05	-2.9E+05	-5.0E+05	-3.9E+05	-2.6E+05	-3.2E+05	-5.6E+05	-3.6E+05

Table 169 Raw data for the test seal at PR=0.4, ω=5 krpm, and inlet LVF=8% with the zero-preswirl insert

Freq.	Re(H_{XX})	Re(H_{XY})	Re(H_{YX})	Re(H_{YY})	Im(H_{XX})	Im(H_{XY})	Im(H_{YX})	Im(H_{YY})	Re(eH_{XX})	Re(eH_{XY})	Re(eH_{YX})	Re(eH_{YY})	Im(eH_{XX})	Im(eH_{XY})	Im(eH_{YX})	Im(eH_{YY})
Hz	N/m	N/m	N/m	N/m	N/m	N/m	N/m	N/m	N/m	N/m	N/m	N/m	N/m	N/m	N/m	N/m
9.8	5.0E+06	2.4E+06	-8.0E+06	3.0E+06	2.0E+06	1.6E+06	4.0E+06	2.2E+06	-6.5E+05	-1.9E+05	-4.5E+05	-3.4E+05	-6.7E+05	-6.0E+05	-8.2E+05	-3.6E+05
19.5	4.0E+06	3.2E+06	-5.2E+06	1.5E+06	3.6E+06	2.8E+06	2.5E+06	4.3E+06	-2.6E+05	-2.0E+05	-4.2E+05	-4.1E+05	-4.6E+05	-2.0E+05	-8.9E+05	-2.8E+05
29.3	3.7E+06	3.7E+06	-5.9E+06	1.9E+06	5.6E+06	4.0E+06	3.3E+06	7.7E+06	-1.4E+05	-1.4E+05	-3.9E+05	-5.6E+05	-2.2E+05	-2.2E+05	-3.5E+05	-3.7E+05
39.1	3.3E+06	4.9E+06	-4.2E+06	2.0E+06	8.8E+06	1.7E+06	2.0E+06	1.1E+07	-2.6E+05	-1.7E+05	-2.7E+05	-2.9E+05	-2.7E+05	-2.4E+05	-3.9E+05	-2.4E+05
48.8	3.5E+06	5.2E+06	-4.1E+06	1.7E+06	1.2E+07	1.8E+06	2.2E+06	1.5E+07	-2.6E+05	-3.2E+05	-4.4E+05	-5.6E+05	-3.2E+05	-1.1E+05	-3.1E+05	-4.0E+05
58.6	2.4E+06	4.8E+06	-3.9E+06	2.2E+06	1.5E+07	9.4E+05	1.7E+06	1.7E+07	-2.7E+05	-5.5E+04	-3.2E+05	-2.1E+05	-3.5E+05	-2.0E+05	-3.4E+05	-2.9E+05
68.4	2.8E+06	4.2E+06	-3.8E+06	1.7E+06	1.8E+07	1.1E+06	1.5E+06	1.8E+07	-1.5E+05	-4.3E+05	-3.6E+05	-3.9E+05	-4.0E+05	-3.8E+05	-5.2E+05	-2.6E+05
78.1	2.9E+06	5.3E+06	-3.7E+06	2.7E+06	2.1E+07	7.3E+05	1.4E+06	2.2E+07	-3.6E+05	-2.9E+05	-2.7E+05	-6.3E+05	-2.9E+05	-3.0E+05	-3.2E+05	-3.3E+05
87.9	2.9E+06	5.6E+06	-3.7E+06	2.9E+06	2.4E+07	-3.7E+04	1.3E+06	2.5E+07	-2.5E+05	-3.4E+05	-3.7E+05	-3.6E+05	-1.7E+05	-3.6E+05	-4.1E+05	-3.2E+05
97.7	2.8E+06	5.4E+06	-4.8E+06	2.3E+06	2.7E+07	5.2E+05	1.2E+06	2.7E+07	-1.5E+05	-3.3E+05	-3.0E+05	-5.0E+05	-1.7E+05	-3.2E+05	-3.0E+05	-1.7E+05
107.4	2.9E+06	5.2E+06	-4.9E+06	2.6E+06	3.1E+07	-2.7E+05	1.8E+06	3.0E+07	-2.0E+05	-2.8E+05	-3.6E+05	-3.5E+05	-3.4E+05	-1.7E+05	-2.8E+05	-1.9E+05
117.2	3.1E+06	4.9E+06	-4.4E+06	2.4E+06	3.2E+07	4.7E+05	1.8E+06	3.3E+07	-4.5E+05	-2.1E+05	-4.8E+05	-2.2E+05	-2.4E+05	-9.6E+04	-3.8E+05	-2.1E+05
127.0	3.2E+06	3.9E+06	-4.7E+06	2.8E+06	3.5E+07	9.8E+04	2.3E+06	3.6E+07	-2.1E+05	-5.5E+05	-2.0E+05	-3.1E+05	-4.6E+05	-3.8E+05	-4.8E+05	-2.7E+05
136.7	3.9E+06	4.7E+06	-4.5E+06	3.2E+06	3.7E+07	1.0E+06	1.9E+06	3.9E+07	-3.7E+05	-2.9E+05	-3.0E+05	-3.0E+05	-3.8E+05	-4.9E+05	-3.5E+05	-5.6E+05

Table 170 Raw data for the test seal at PR=0.4, ω=10 krpm, and inlet LVF=8% with the zero-preswirl insert

Freq.	Re(H_{XX})	Re(H_{XY})	Re(H_{YX})	Re(H_{YY})	Im(H_{XX})	Im(H_{XY})	Im(H_{YX})	Im(H_{YY})	Re(eH_{XX})	Re(eH_{XY})	Re(eH_{YX})	Re(eH_{YY})	Im(eH_{XX})	Im(eH_{XY})	Im(eH_{YX})	Im(eH_{YY})
Hz	N/m	N/m	N/m	N/m	N/m	N/m	N/m	N/m	N/m	N/m	N/m	N/m	N/m	N/m	N/m	N/m
9.8	5.7E+06	7.4E+06	-9.9E+06	-1.0E+05	-3.1E+05	2.7E+06	7.5E+05	3.9E+06	-9.1E+05	-6.4E+05	-9.6E+05	-7.2E+05	-1.0E+06	-5.4E+05	-9.1E+05	-4.2E+05
19.5	3.9E+06	8.8E+06	-7.5E+06	6.8E+05	1.7E+06	1.5E+06	1.5E+06	6.1E+06	-3.8E+05	-4.6E+05	-3.2E+05	-2.6E+05	-3.2E+05	-3.6E+05	-4.8E+05	-4.4E+05
29.3	3.9E+06	8.1E+06	-8.5E+06	2.4E+06	4.4E+06	2.7E+06	2.6E+06	8.4E+06	-2.9E+05	-4.2E+05	-2.4E+05	-3.2E+05	-2.7E+05	-2.9E+05	-3.8E+05	-4.1E+05
39.1	2.7E+06	9.2E+06	-8.1E+06	1.8E+06	9.5E+06	1.3E+06	1.3E+06	1.2E+07	-1.7E+05	-1.5E+05	-2.4E+05	-3.2E+05	-2.3E+05	-3.1E+05	-3.0E+05	-2.9E+05
48.8	2.7E+06	9.8E+06	-7.3E+06	1.4E+06	1.3E+07	2.2E+06	4.4E+05	1.6E+07	-3.0E+05	-4.3E+05	-1.8E+05	-2.6E+05	-2.6E+05	-4.6E+05	-3.9E+05	-2.2E+05
58.6	3.3E+06	9.6E+06	-7.5E+06	2.2E+06	1.6E+07	2.3E+06	1.1E+06	1.8E+07	-2.5E+05	-3.8E+05	-2.3E+05	-4.2E+05	-1.3E+05	-3.5E+05	-6.4E+05	-3.5E+05
68.4	3.4E+06	9.5E+06	-7.1E+06	2.2E+06	1.8E+07	2.0E+06	-3.8E+05	2.1E+07	-2.6E+05	-4.8E+05	-4.1E+05	-5.5E+05	-4.0E+05	-4.6E+05	-4.2E+05	-6.0E+05
78.1	3.5E+06	1.1E+07	-7.3E+06	2.8E+06	2.2E+07	1.9E+06	-7.5E+04	2.3E+07	-1.7E+05	-2.6E+05	-1.5E+05	-3.9E+05	-4.1E+05	-2.4E+05	-5.3E+05	-4.4E+05
87.9	3.8E+06	1.0E+07	-8.0E+06	2.9E+06	2.4E+07	1.2E+06	1.5E+05	2.5E+07	-2.6E+05	-3.5E+05	-4.6E+05	-4.3E+05	-1.4E+05	-1.4E+05	-4.3E+05	-6.2E+05
97.7	4.9E+06	1.0E+07	-8.0E+06	2.0E+06	2.7E+07	1.7E+06	-1.5E+06	2.9E+07	-2.0E+05	-1.5E+05	-4.3E+05	-3.3E+05	-2.4E+05	-1.2E+05	-4.9E+05	-3.0E+05
107.4	3.9E+06	9.6E+06	-8.4E+06	2.4E+06	2.9E+07	1.2E+06	-4.6E+05	3.1E+07	-2.2E+05	-4.3E+05	-6.7E+05	-3.0E+05	-2.2E+05	-3.8E+05	-6.5E+05	-5.5E+05
117.2	5.1E+06	1.0E+07	-8.3E+06	2.8E+06	3.1E+07	1.3E+06	-1.2E+06	3.5E+07	-3.2E+05	-3.2E+05	-5.6E+05	-3.7E+05	-4.2E+05	-3.3E+05	-3.7E+05	-3.4E+05
127.0	4.5E+06	1.0E+07	-9.2E+06	4.4E+06	3.4E+07	1.8E+06	1.9E+05	3.7E+07	-2.3E+05	-5.3E+05	-3.9E+05	-5.6E+05	-2.1E+05	-3.5E+05	-4.7E+05	-7.8E+05
136.7	4.4E+06	1.0E+07	-9.6E+06	3.2E+06	3.7E+07	2.2E+06	4.5E+05	4.0E+07	-2.1E+05	-3.6E+05	-3.1E+05	-3.0E+05	-3.4E+05	-3.4E+05	-2.2E+05	-3.0E+05

Table 171 Raw data for the test seal at PR=0.4, ω=15 krpm, and inlet LVF=8% with the zero-preswirl insert

Freq.	Re(H_{XX})	Re(H_{XY})	Re(H_{YX})	Re(H_{YY})	Im(H_{XX})	Im(H_{XY})	Im(H_{YX})	Im(H_{YY})	Re(eH_{XX})	Re(eH_{XY})	Re(eH_{YX})	Re(eH_{YY})	Im(eH_{XX})	Im(eH_{XY})	Im(eH_{YX})	Im(eH_{YY})
Hz	N/m	N/m	N/m	N/m	N/m	N/m	N/m	N/m	N/m	N/m	N/m	N/m	N/m	N/m	N/m	N/m
9.8	9.1E+06	1.6E+07	-1.5E+07	4.0E+05	-1.5E+06	-2.0E+05	-2.8E+06	2.4E+06	-1.5E+06	-1.0E+06	-1.2E+06	-1.0E+06	-8.9E+05	-1.1E+06	-1.0E+06	-1.1E+06
19.5	5.4E+06	1.4E+07	-1.5E+07	3.4E+06	1.1E+06	1.1E+05	5.6E+05	7.7E+06	-3.0E+05	-5.6E+05	-7.9E+05	-9.1E+05	-5.1E+05	-6.8E+05	-6.5E+05	-1.0E+06
29.3	5.5E+06	1.4E+07	-1.5E+07	2.6E+06	3.5E+06	2.0E+06	3.3E+06	7.4E+06	-3.4E+05	-4.7E+05	-5.4E+05	-6.2E+05	-4.1E+05	-7.2E+05	-4.7E+05	-7.2E+05
39.1	4.0E+06	1.5E+07	-1.4E+07	3.0E+06	9.3E+06	-3.4E+05	1.9E+06	1.3E+07	-3.8E+05	-3.9E+05	-5.0E+05	-2.7E+05	-4.2E+05	-4.2E+05	-2.8E+05	-4.7E+05
48.8	4.1E+06	1.4E+07	-1.4E+07	2.8E+06	1.2E+07	1.8E+05	1.6E+06	1.7E+07	-5.0E+05	-5.3E+05	-7.1E+05	-4.0E+05	-3.6E+05	-3.5E+05	-5.3E+05	-5.5E+05
58.6	3.9E+06	1.4E+07	-1.4E+07	3.4E+06	1.6E+07	9.0E+05	9.4E+05	1.9E+07	-3.5E+05	-5.8E+05	-4.3E+05	-5.0E+05	-5.7E+05	-3.2E+05	-6.8E+05	-5.7E+05
68.4	3.9E+06	1.4E+07	-1.3E+07	3.7E+06	1.8E+07	1.2E+05	7.3E+05	2.1E+07	-5.2E+05	-7.7E+05	-5.6E+05	-8.5E+05	-4.0E+05	-6.9E+05	-4.7E+05	-6.3E+05
78.1	4.6E+06	1.4E+07	-1.4E+07	5.5E+06	2.0E+07	2.4E+05	7.1E+05	2.6E+07	-5.9E+05	-4.8E+05	-5.2E+05	-3.5E+05	-2.5E+05	-5.5E+05	-7.0E+05	-5.7E+05
87.9	5.4E+06	1.4E+07	-1.3E+07	3.5E+06	2.4E+07	4.3E+05	-5.6E+05	2.8E+07	-2.4E+05	-5.2E+05	-4.8E+05	-6.1E+05	-3.2E+05	-1.5E+05	-5.8E+05	-7.3E+05
97.7	4.5E+06	1.4E+07	-1.3E+07	4.5E+06	2.8E+07	8.0E+05	-9.3E+05	3.2E+07	-2.5E+05	-3.5E+05	-3.3E+05	-1.9E+05	-3.0E+05	-3.9E+05	-4.3E+05	-6.3E+05
107.4	3.4E+06	1.2E+07	-1.4E+07	4.3E+06	3.0E+07	1.5E+06	-6.0E+05	3.4E+07	-5.3E+05	-4.9E+05	-6.1E+05	-7.1E+05	-2.8E+05	-3.4E+05	-6.2E+05	-4.5E+05
117.2	5.5E+06	1.5E+07	-1.3E+07	6.6E+06	3.3E+07	1.5E+06	2.3E+05	3.7E+07	-5.0E+05	-1.5E+05	-6.7E+05	-2.3E+05	-2.3E+05	-1.7E+05	-7.5E+05	-6.5E+05
127.0	4.6E+06	1.5E+07	-1.4E+07	6.0E+06	3.5E+07	2.3E+06	-4.8E+05	3.9E+07	-3.5E+05	-7.4E+05	-6.6E+05	-1.0E+06	-4.7E+05	-4.6E+05	-2.9E+05	-8.0E+05
136.7	5.2E+06	1.5E+07	-1.4E+07	7.3E+06	3.8E+07	2.1E+06	1.1E+05	4.2E+07	-5.5E+05	-3.5E+05	-3.5E+05	-7.4E+05	-2.7E+05	-5.5E+05	-3.5E+05	-9.3E+05

Table 172 Curve-fitted results of real parts at PD=27.6 bar for the test seal with the zero-preswirl insert in pure- and mainly-oil conditions

Inlet GVF	ω	K_{xx}	M_{xx}	eK_{xx}	eM_{xx}	R^2_{xx}	K_{yy}	M_{yy}	eK_{yy}	eM_{yy}	R^2_{yy}	K_{xy}	M_{xy}	eK_{xy}	eM_{xy}	R^2_{xy}	K_{yx}	M_{yx}	eK_{yx}	eM_{yx}	R^2_{yx}
%	krpm	N/m	kg	N/m	kg		N/m	kg	N/m	kg		N/m	kg	N/m	kg		N/m	kg	N/m	kg	
0	3	4.0E+6	60.53	6.6E+5	1.84	0.998	4.8E+6	60.92	8.7E+5	2.43	0.996	1.5E+7	1.52	6.9E+5	1.91	0.199	-2.2E+7	3.85	5.7E+5	1.59	0.699
2	3	6.2E+6	52.30	7.8E+5	2.16	0.996	4.2E+6	51.13	8.3E+5	2.32	0.995	1.9E+7	4.16	9.4E+5	2.62	0.501	-1.6E+7	6.66	7.0E+5	1.93	0.824
4	3	6.5E+6	49.79	7.5E+5	2.07	0.996	4.4E+6	49.15	8.3E+5	2.31	0.994	2.0E+7	2.52	7.8E+5	2.18	0.345	-1.6E+7	7.13	8.1E+5	2.25	0.798
6	3	6.7E+6	47.98	6.7E+5	1.79	0.997	3.1E+6	46.37	6.5E+5	1.74	0.997	2.1E+7	3.08	8.4E+5	2.26	0.450	-1.5E+7	6.23	9.6E+5	2.57	0.721
8	3	6.4E+6	43.68	6.2E+5	1.66	0.997	2.2E+6	40.74	6.9E+5	1.86	0.995	2.3E+7	4.42	9.4E+5	2.53	0.574	-1.4E+7	4.59	1.1E+6	2.86	0.530
10	4	6.5E+6	41.68	6.1E+5	1.63	0.997	1.3E+6	37.86	9.6E+5	2.57	0.990	2.3E+7	4.84	8.4E+5	2.25	0.672	-1.5E+7	3.56	1.2E+6	3.22	0.349
0	4	4.6E+6	62.29	5.2E+5	1.45	0.999	4.7E+6	59.76	8.1E+5	2.24	0.996	1.6E+7	2.32	7.5E+5	2.09	0.328	-2.1E+7	4.13	6.0E+5	1.67	0.709
2	4	6.7E+6	51.44	6.8E+5	1.89	0.997	4.7E+6	51.16	9.2E+5	2.56	0.994	2.0E+7	3.93	8.9E+5	2.48	0.499	-1.6E+7	7.72	5.3E+5	1.48	0.915
4	4	7.6E+6	51.13	7.7E+5	2.14	0.996	3.8E+6	49.11	8.4E+5	2.34	0.994	2.0E+7	3.64	8.1E+5	2.26	0.507	-1.5E+7	6.91	7.0E+5	1.95	0.833
6	4	6.6E+6	47.35	7.3E+5	1.95	0.996	2.8E+6	45.15	5.5E+5	1.47	0.998	2.1E+7	3.54	9.2E+5	2.46	0.478	-1.5E+7	5.58	9.8E+5	2.62	0.667
8	4	6.3E+6	43.59	5.7E+5	1.53	0.997	1.9E+6	40.47	6.0E+5	1.61	0.996	2.3E+7	4.51	8.0E+5	2.15	0.660	-1.5E+7	4.75	1.1E+6	3.05	0.516
10	4	6.5E+6	41.32	6.4E+5	1.71	0.996	1.0E+6	37.37	8.7E+5	2.34	0.991	2.3E+7	4.76	6.8E+5	1.83	0.749	-1.5E+7	4.43	1.2E+6	3.10	0.473
0	5	4.1E+6	60.24	5.6E+5	1.55	0.998	4.2E+6	61.12	5.4E+5	1.50	0.998	2.4E+7	2.76	6.6E+5	1.84	0.470	-2.3E+7	9.00	6.1E+5	1.70	0.917
2	5	7.0E+6	50.93	7.5E+5	2.08	0.996	4.1E+6	49.13	7.9E+5	2.21	0.995	2.6E+7	3.13	7.8E+5	2.16	0.453	-2.1E+7	8.97	5.2E+5	1.44	0.939
4	5	6.4E+6	49.72	8.7E+5	2.43	0.994	4.1E+6	48.15	7.8E+5	2.18	0.995	2.6E+7	2.20	6.7E+5	1.86	0.357	-2.1E+7	7.80	7.3E+5	2.03	0.854
6	5	6.6E+6	46.66	7.6E+5	2.11	0.995	3.3E+6	44.81	4.5E+5	1.25	0.998	2.7E+7	1.43	7.5E+5	2.10	0.155	-2.1E+7	6.34	8.1E+5	2.26	0.756
8	5	7.0E+6	43.16	6.1E+5	1.64	0.997	1.8E+6	39.19	4.6E+5	1.24	0.998	2.9E+7	2.04	9.7E+5	2.59	0.214	-2.1E+7	5.45	1.1E+6	2.99	0.594
10	5	6.0E+6	38.67	7.1E+5	1.92	0.994	9.4E+4	34.22	9.3E+5	2.50	0.988	2.9E+7	1.84	6.8E+5	1.82	0.310	-2.1E+7	4.65	1.1E+6	2.97	0.519

Table 173 Curve-fitted results of imaginary parts at PD=27.6 bar for the test seal with the zero-preswirl insert in pure- and mainly-oil conditions

Inlet GVF	ω	C_{xx}	eC_{xx}	R^2_{xx}	C_{yy}	eC_{yy}	R^2_{yy}	C_{xy}	eC_{xy}	R^2_{xy}	C_{yx}	eC_{yx}	R^2_{yx}
%	krpm	N-s/m	N-s/m		N-s/m	N-s/m		N-s/m	N-s/m		N-s/m	N-s/m	
0	3	1.1E+5	7.3E+2	0.999	1.2E+5	1.2E+3	0.999	1.5E+4	1.2E+3	0.940	-1.4E+4	7.5E+2	0.969
2	3	1.1E+5	1.5E+3	0.998	1.2E+5	1.6E+3	0.998	8.5E+3	1.0E+3	0.858	-1.6E+4	8.2E+2	0.974
4	3	1.2E+5	1.8E+3	0.997	1.2E+5	2.0E+3	0.997	7.7E+3	9.9E+2	0.815	-1.6E+4	8.1E+2	0.968
6	3	1.2E+5	1.9E+3	0.997	1.2E+5	2.1E+3	0.996	6.2E+3	7.6E+2	0.835	-1.5E+4	3.7E+2	0.992
8	3	1.2E+5	1.9E+3	0.997	1.3E+5	2.4E+3	0.996	4.5E+3	6.2E+2	0.796	-1.4E+4	5.9E+2	0.977
10	4	1.2E+5	1.7E+3	0.997	1.3E+5	2.2E+3	0.997	4.0E+3	8.2E+2	0.532	-1.4E+4	6.2E+2	0.977
0	4	1.1E+5	8.8E+2	0.999	1.2E+5	9.9E+2	0.999	1.4E+4	1.2E+3	0.930	-1.5E+4	1.1E+3	0.950
2	4	1.1E+5	1.2E+3	0.999	1.2E+5	1.4E+3	0.998	8.7E+3	1.2E+3	0.835	-1.7E+4	7.4E+2	0.978
4	4	1.1E+5	1.6E+3	0.998	1.2E+5	1.9E+3	0.997	7.2E+3	1.0E+3	0.799	-1.6E+4	8.1E+2	0.972
6	4	1.2E+5	1.8E+3	0.997	1.2E+5	2.2E+3	0.996	5.7E+3	7.2E+2	0.832	-1.5E+4	4.0E+2	0.990
8	4	1.2E+5	1.8E+3	0.997	1.3E+5	2.3E+3	0.996	4.7E+3	6.5E+2	0.797	-1.4E+4	5.8E+2	0.976
10	4	1.2E+5	1.7E+3	0.997	1.3E+5	2.2E+3	0.996	4.0E+3	7.9E+2	0.623	-1.4E+4	5.6E+2	0.979
0	5	1.2E+5	7.0E+2	1.000	1.2E+5	1.1E+3	0.999	1.6E+4	1.3E+3	0.927	-2.3E+4	8.5E+2	0.985
2	5	1.1E+5	1.2E+3	0.999	1.2E+5	1.4E+3	0.998	1.2E+4	1.1E+3	0.904	-2.0E+4	7.1E+2	0.986
4	5	1.2E+5	1.6E+3	0.998	1.2E+5	1.7E+3	0.998	1.1E+4	1.1E+3	0.890	-1.9E+4	8.2E+2	0.980
6	5	1.2E+5	1.9E+3	0.997	1.2E+5	2.1E+3	0.996	1.0E+4	1.1E+3	0.848	-1.7E+4	7.8E+2	0.977
8	5	1.2E+5	1.8E+3	0.997	1.3E+5	1.9E+3	0.997	8.4E+3	9.0E+2	0.862	-1.6E+4	5.5E+2	0.984
10	5	1.2E+5	1.4E+3	0.998	1.3E+5	2.0E+3	0.997	7.4E+3	8.6E+2	0.772	-1.4E+4	6.2E+2	0.978

Table 174 Curve-fitted results of real parts at PD=34.5 bar for the test seal with the zero-preswirl insert in pure- and mainly-oil conditions

Inlet GVF	ω	K_{xx}	M_{xx}	eK_{xx}	eM_{xx}	R^2_{xx}	K_{yy}	M_{yy}	eK_{yy}	eM_{yy}	R^2_{yy}	K_{xy}	M_{xy}	eK_{xy}	eM_{xy}	R^2_{xy}	K_{yx}	M_{yx}	eK_{yx}	eM_{yx}	R^2_{yx}
%	krpm	N/m	kg	N/m	kg		N/m	kg	N/m	kg		N/m	kg	N/m	kg		N/m	kg	N/m	kg	
0	3	6.1E+6	57.99	7.7E+5	2.06	0.997	9.2E+6	63.62	1.3E+6	3.48	0.993	2.7E+7	6.49	6.4E+5	1.73	0.862	-1.1E+7	12.11	7.3E+5	1.96	0.944
2	3	9.0E+6	49.64	9.4E+5	2.52	0.994	7.9E+6	49.03	1.2E+6	3.21	0.990	2.7E+7	7.98	8.8E+5	2.36	0.834	-1.1E+7	10.03	8.5E+5	2.28	0.895
4	3	8.4E+6	44.20	9.7E+5	2.59	0.992	7.9E+6	45.17	1.0E+6	2.76	0.992	2.8E+7	5.77	9.4E+5	2.53	0.696	-1.1E+7	9.77	8.4E+5	2.25	0.892
6	3	6.7E+6	39.36	7.4E+5	1.99	0.994	6.9E+6	38.60	8.7E+5	2.33	0.992	2.9E+7	6.26	8.0E+5	2.15	0.789	-1.1E+7	6.88	9.6E+5	2.58	0.758
8	3	6.2E+6	35.33	8.2E+5	2.20	0.991	5.2E+6	31.36	1.0E+6	2.68	0.984	2.9E+7	5.83	6.0E+5	1.60	0.854	-1.2E+7	4.80	1.1E+6	2.83	0.559
10	4	5.1E+6	33.11	1.0E+6	2.67	0.985	5.4E+6	32.32	2.3E+6	6.06	0.926	2.8E+7	3.65	1.2E+6	3.34	0.344	-1.4E+7	1.62	1.5E+6	4.07	0.065
0	4	7.8E+6	60.07	9.0E+5	2.42	0.996	5.3E+6	60.17	1.3E+6	3.45	0.993	2.7E+7	7.23	7.7E+5	2.06	0.845	-1.2E+7	11.99	8.6E+5	2.30	0.923
2	4	9.1E+6	49.27	8.5E+5	2.27	0.995	8.4E+6	49.18	1.1E+6	3.00	0.992	2.8E+7	8.15	8.7E+5	2.32	0.845	-1.1E+7	10.19	6.3E+5	1.69	0.942
4	4	7.2E+6	43.86	7.6E+5	2.03	0.995	7.7E+6	44.96	1.1E+6	3.02	0.990	2.8E+7	6.04	1.0E+6	2.70	0.688	-1.1E+7	9.09	7.1E+5	1.89	0.910
6	4	7.2E+6	39.57	7.2E+5	1.92	0.995	6.5E+6	39.09	8.7E+5	2.34	0.992	2.9E+7	6.29	9.0E+5	2.40	0.751	-1.1E+7	7.47	9.2E+5	2.48	0.801
8	4	5.6E+6	35.51	9.9E+5	2.65	0.987	4.9E+6	30.91	9.8E+5	2.64	0.984	2.9E+7	5.93	7.0E+5	1.88	0.814	-1.3E+7	3.24	1.3E+6	3.44	0.281
10	4	4.8E+6	35.15	1.6E+6	4.38	0.966	2.1E+6	28.94	1.0E+6	2.80	0.979	2.7E+7	-0.14	9.9E+5	2.65	0.001	-1.5E+7	-1.64	2.0E+6	5.37	0.040
0	5	8.9E+6	60.70	6.9E+5	1.84	0.998	1.6E+6	54.55	5.0E+5	1.34	0.999	3.3E+7	6.88	7.8E+5	2.10	0.825	-1.9E+7	10.07	8.4E+5	2.26	0.898
2	5	7.5E+6	48.62	7.3E+5	1.94	0.996	7.4E+6	47.05	7.7E+5	2.06	0.996	3.4E+7	6.85	8.8E+5	2.37	0.786	-1.8E+7	9.95	1.1E+6	2.84	0.844
4	5	7.1E+6	43.57	6.7E+5	1.80	0.996	7.4E+6	41.88	6.8E+5	1.82	0.996	3.4E+7	3.75	1.1E+6	2.95	0.417	-1.8E+7	9.94	8.8E+5	2.36	0.887
6	5	5.8E+6	38.46	8.9E+5	2.40	0.991	5.1E+6	33.57	7.3E+5	1.96	0.992	3.5E+7	3.59	8.2E+5	2.19	0.542	-2.0E+7	6.44	1.2E+6	3.09	0.656
8	5	4.0E+6	35.37	8.3E+5	2.23	0.991	4.0E+6	29.37	1.4E+6	3.78	0.964	3.6E+7	4.75	1.1E+6	2.96	0.531	-2.1E+7	5.27	1.2E+6	3.25	0.537
10	5	1.4E+6	33.24	1.6E+6	4.42	0.961	2.5E+5	26.38	1.6E+6	4.28	0.943	3.1E+7	-3.11	1.3E+6	3.45	0.264	-2.4E+7	-0.16	1.6E+6	4.38	0.001

Table 175 Curve-fitted results of imaginary parts at PD=34.5 bar for the test seal with the zero-preswirl insert in pure- and mainly-oil conditions

Inlet GVF	ω	C_{xx}	eC_{xx}	R^2_{xx}	C_{yy}	eC_{yy}	R^2_{yy}	C_{xy}	eC_{xy}	R^2_{xy}	C_{yx}	eC_{yx}	R^2_{yx}
%	krpm	N-s/m	N-s/m		N-s/m	N-s/m		N-s/m	N-s/m		N-s/m	N-s/m	
0	3	1.3E+5	8.6E+2	0.999	1.2E+5	1.3E+3	0.999	5.8E+3	1.2E+3	0.640	-2.4E+4	6.0E+2	0.991
2	3	1.3E+5	1.2E+3	0.999	1.3E+5	1.6E+3	0.998	3.0E+3	1.2E+3	0.429	-2.1E+4	4.8E+2	0.993
4	3	1.3E+5	1.7E+3	0.998	1.3E+5	2.5E+3	0.996	2.4E+3	9.4E+2	0.402	-1.9E+4	5.0E+2	0.990
6	3	1.3E+5	1.6E+3	0.998	1.4E+5	2.4E+3	0.996	1.3E+3	9.8E+2	0.093	-1.6E+4	4.9E+2	0.988
8	3	1.4E+5	1.5E+3	0.999	1.4E+5	2.1E+3	0.997	7.5E+2	1.2E+3	0.000	-1.4E+4	4.1E+2	0.989
10	4	1.4E+5	1.4E+3	0.999	1.5E+5	2.6E+3	0.996	2.5E+3	1.4E+3	0.000	-1.1E+4	7.7E+2	0.952
0	4	1.2E+5	7.6E+2	1.000	1.3E+5	1.1E+3	0.999	4.4E+3	1.4E+3	0.498	-2.4E+4	7.3E+2	0.987
2	4	1.3E+5	1.2E+3	0.999	1.3E+5	1.6E+3	0.998	2.8E+3	1.3E+3	0.380	-2.1E+4	4.0E+2	0.996
4	4	1.3E+5	1.7E+3	0.998	1.3E+5	2.4E+3	0.996	2.2E+3	9.3E+2	0.390	-1.9E+4	5.0E+2	0.990
6	4	1.3E+5	1.6E+3	0.998	1.4E+5	2.6E+3	0.996	1.0E+3	1.0E+3	0.071	-1.7E+4	5.0E+2	0.988
8	4	1.4E+5	1.6E+3	0.998	1.4E+5	1.9E+3	0.998	7.0E+2	1.2E+3	0.000	-1.2E+4	7.1E+2	0.965
10	4	1.4E+5	2.0E+3	0.997	1.4E+5	2.1E+3	0.997	6.4E+3	2.0E+3	0.000	-7.5E+3	1.1E+3	0.840
0	5	1.2E+5	8.5E+2	0.999	1.3E+5	7.8E+2	1.000	8.5E+3	1.4E+3	0.757	-2.5E+4	7.3E+2	0.990
2	5	1.3E+5	1.1E+3	0.999	1.3E+5	1.3E+3	0.999	6.4E+3	1.3E+3	0.681	-2.2E+4	5.4E+2	0.993
4	5	1.3E+5	1.9E+3	0.998	1.4E+5	2.1E+3	0.997	6.4E+3	1.1E+3	0.794	-1.8E+4	4.0E+2	0.994
6	5	1.4E+5	1.7E+3	0.998	1.4E+5	2.0E+3	0.998	5.7E+3	1.5E+3	0.310	-1.4E+4	6.8E+2	0.972
8	5	1.4E+5	1.6E+3	0.998	1.5E+5	2.3E+3	0.997	4.9E+3	1.8E+3	0.007	-1.1E+4	9.9E+2	0.931
10	5	1.4E+5	2.3E+3	0.997	1.5E+5	2.5E+3	0.996	1.1E+4	2.5E+3	0.000	-6.0E+3	1.2E+3	0.741

Table 176 Curve-fitted results of real parts at PD=41.4 bar for the test seal with the zero-preswirl insert in pure- and mainly-oil conditions

Inlet GVF	ω	K_{xx}	M_{xx}	eK_{xx}	eM_{xx}	R^2_{xx}	K_{yy}	M_{yy}	eK_{yy}	eM_{yy}	R^2_{yy}	K_{xy}	M_{xy}	eK_{xy}	eM_{xy}	R^2_{xy}	K_{yx}	M_{yx}	eK_{yx}	eM_{yx}	R^2_{yx}
%	krpm	N/m	kg	N/m	kg		N/m	kg	N/m	kg		N/m	kg	N/m	kg		N/m	kg	N/m	kg	
0	3	1.1E+7	58.34	9.9E+5	2.66	0.995	9.9E+6	57.50	1.1E+6	2.89	0.994	3.3E+7	7.94	8.0E+5	2.16	0.857	-8.0E+6	11.14	8.4E+5	2.24	0.916
2	3	9.3E+6	42.47	1.1E+6	3.02	0.987	9.8E+6	38.48	8.9E+5	2.46	0.990	3.2E+7	5.45	7.2E+5	2.01	0.744	-9.4E+6	8.73	1.1E+6	3.07	0.761
4	3	3.8E+6	32.96	1.6E+6	4.43	0.961	3.9E+6	25.57	8.2E+5	2.24	0.983	3.0E+7	1.49	1.0E+6	2.81	0.110	-1.9E+7	-1.29	1.7E+6	4.55	0.034
6	3	4.5E+6	31.29	1.7E+6	4.64	0.947	3.1E+6	24.19	8.9E+5	2.47	0.974	3.0E+7	3.28	1.1E+6	3.09	0.309	-1.8E+7	-1.00	1.8E+6	4.87	0.017
8	3	3.3E+6	29.45	3.8E+6	10.70	0.750	-3.0E+6	27.35	2.5E+6	6.83	0.864	2.6E+7	0.11	3.6E+6	10.01	0.000	-2.2E+7	-0.97	2.8E+6	7.65	0.006
10	4	-4.7E+6	26.97	2.6E+6	7.80	0.856	2.0E+6	24.52	2.3E+6	6.87	0.864	2.4E+7	1.90	3.1E+6	9.31	0.020	-2.5E+7	-1.05	2.7E+6	8.12	0.008
0	4	1.1E+7	58.04	7.6E+5	2.12	0.997	1.0E+7	57.52	1.0E+6	2.88	0.994	3.3E+7	7.83	6.6E+5	1.84	0.877	-7.6E+6	11.78	6.2E+5	1.73	0.948
2	4	9.5E+6	41.87	9.1E+5	2.52	0.991	7.9E+6	39.58	1.9E+6	5.30	0.957	3.2E+7	4.84	1.0E+6	2.82	0.539	-1.1E+7	6.85	1.2E+6	3.22	0.641
4	4	4.3E+6	33.94	1.6E+6	4.28	0.965	4.4E+6	26.45	9.5E+5	2.58	0.979	3.1E+7	3.13	9.8E+5	2.67	0.377	-1.8E+7	-0.67	1.8E+6	5.00	0.008
6	4	3.5E+6	32.64	1.2E+6	3.48	0.978	3.8E+6	25.30	1.4E+6	4.10	0.950	3.0E+7	3.58	1.4E+6	4.13	0.272	-1.8E+7	1.95	1.3E+6	3.90	0.110
8	4	-6.5E+6	24.83	1.2E+6	3.53	0.961	4.8E+6	21.52	1.8E+6	5.22	0.894	2.6E+7	0.99	2.0E+6	6.11	0.013	-2.5E+7	-2.18	2.4E+6	7.09	0.045
10	4	-6.8E+6	24.42	9.8E+5	2.72	0.970	2.0E+5	23.89	1.9E+6	5.26	0.891	1.9E+7	-2.36	1.3E+6	3.75	0.135	-2.7E+7	-0.42	1.8E+6	4.90	0.003
0	5	8.8E+6	56.71	7.8E+5	2.10	0.997	8.4E+6	54.63	9.2E+5	2.46	0.995	3.9E+7	7.43	8.6E+5	2.31	0.820	-1.7E+7	12.25	8.3E+5	2.22	0.931
2	5	6.5E+6	39.75	1.0E+6	2.78	0.988	5.1E+6	31.61	9.4E+5	2.61	0.983	3.7E+7	1.36	7.0E+5	1.93	0.164	-2.3E+7	4.76	1.4E+6	3.97	0.363
4	5	1.7E+6	33.91	1.4E+6	3.70	0.974	8.6E+5	26.26	1.2E+6	3.10	0.969	3.5E+7	-1.12	1.6E+6	4.16	0.031	-2.7E+7	2.77	1.3E+6	3.43	0.222
6	5	-1.5E+6	27.23	1.4E+6	3.84	0.952	3.1E+5	21.51	1.1E+6	3.13	0.949	3.2E+7	-4.09	1.0E+6	2.86	0.447	-2.9E+7	1.40	1.3E+6	3.70	0.054
8	5	-4.6E+6	24.59	9.4E+5	2.61	0.972	-3.6E+5	20.73	1.6E+6	4.54	0.892	2.9E+7	-5.11	1.5E+6	4.30	0.359	-3.2E+7	1.29	1.4E+6	3.92	0.041
10	5	-5.6E+6	23.31	1.2E+6	3.44	0.948	4.0E+5	22.78	1.3E+6	3.55	0.942	2.6E+7	-6.66	1.3E+6	3.66	0.567	-3.1E+7	0.42	1.6E+6	4.33	0.004

Table 177 Curve-fitted results of imaginary parts at PD=41.4 bar for the test seal with the zero-preswirl insert in pure- and mainly-oil conditions

Inlet GVF	ω	C_{xx}	eC_{xx}	R^2_{xx}	C_{yy}	eC_{yy}	R^2_{yy}	C_{xy}	eC_{xy}	R^2_{xy}	C_{yx}	eC_{yx}	R^2_{yx}
%	krpm	N-s/m	N-s/m		N-s/m	N-s/m		N-s/m	N-s/m		N-s/m	N-s/m	
0	3	1.4E+5	1.0E+3	0.999	1.4E+5	1.3E+3	0.999	1.7E+2	1.1E+3	0.000	-2.7E+4	4.6E+2	0.996
2	3	1.4E+5	1.9E+3	0.998	1.5E+5	1.6E+3	0.999	1.6E+1	1.6E+3	0.000	-1.8E+4	9.2E+2	0.971
4	3	1.5E+5	2.3E+3	0.998	1.6E+5	2.5E+3	0.997	2.9E+3	2.9E+3	0.000	-4.2E+3	2.0E+3	0.521
6	3	1.5E+5	2.3E+3	0.997	1.6E+5	2.2E+3	0.998	2.2E+3	2.5E+3	0.000	-4.3E+3	1.7E+3	0.547
8	3	1.6E+5	4.5E+3	0.990	1.6E+5	4.5E+3	0.991	6.8E+3	5.7E+3	0.018	-8.8E+2	3.0E+3	0.004
10	4	1.7E+5	3.8E+3	0.995	1.7E+5	4.8E+3	0.993	6.3E+3	4.3E+3	0.171	2.7E+3	2.8E+3	0.000
0	4	1.4E+5	1.1E+3	0.999	1.4E+5	1.7E+3	0.998	3.9E+2	1.6E+3	0.000	-2.7E+4	6.2E+2	0.994
2	4	1.4E+5	1.9E+3	0.998	1.5E+5	2.4E+3	0.997	6.5E+2	2.1E+3	0.000	-1.6E+4	9.2E+2	0.966
4	4	1.5E+5	2.2E+3	0.998	1.6E+5	2.2E+3	0.998	1.6E+3	2.7E+3	0.000	-5.2E+3	2.0E+3	0.579
6	4	1.5E+5	2.9E+3	0.997	1.6E+5	2.7E+3	0.997	2.4E+3	2.5E+3	0.000	-4.1E+3	2.0E+3	0.525
8	4	1.6E+5	2.7E+3	0.998	1.6E+5	3.1E+3	0.997	5.5E+3	2.9E+3	0.000	2.3E+3	2.2E+3	0.000
10	4	1.6E+5	2.5E+3	0.997	1.7E+5	4.3E+3	0.993	8.3E+3	1.3E+3	0.791	1.9E+2	2.1E+3	0.000
0	5	1.4E+5	1.0E+3	0.999	1.4E+5	9.3E+2	0.999	5.4E+3	1.6E+3	0.468	-2.7E+4	6.9E+2	0.992
2	5	1.5E+5	1.8E+3	0.998	1.6E+5	1.9E+3	0.998	5.8E+3	2.5E+3	0.000	-9.5E+3	1.8E+3	0.785
4	5	1.5E+5	2.3E+3	0.997	1.6E+5	2.6E+3	0.997	7.4E+3	2.1E+3	0.000	-5.4E+3	1.2E+3	0.656
6	5	1.6E+5	1.8E+3	0.998	1.7E+5	3.0E+3	0.996	9.1E+3	3.2E+3	0.000	-2.7E+3	1.3E+3	0.212
8	5	1.6E+5	2.0E+3	0.998	1.7E+5	3.5E+3	0.995	1.1E+4	2.4E+3	0.000	-1.3E+3	1.0E+3	0.000
10	5	1.6E+5	2.1E+3	0.998	1.7E+5	3.8E+3	0.994	1.2E+4	1.5E+3	0.723	-1.4E+3	1.1E+3	0.000

Table 178 Curve-fitted results of real parts at PD=20.7 bar for the test seal with the medium-preswirl insert in pure- and mainly-oil conditions

Inlet GVF	ω	K_{xx}	M_{xx}	eK_{xx}	eM_{xx}	R^2_{xx}	K_{yy}	M_{yy}	eK_{yy}	eM_{yy}	R^2_{yy}	K_{xy}	M_{xy}	eK_{xy}	eM_{xy}	R^2_{xy}	K_{yx}	M_{yx}	eK_{yx}	eM_{yx}	R^2_{yx}
%	krpm	N/m	kg	N/m	kg		N/m	kg	N/m	kg		N/m	kg	N/m	kg		N/m	kg	N/m	kg	
0	3	1.8E+7	76.87	6.2E+5	1.89	0.999	2.0E+7	78.84	6.0E+5	1.84	0.999	1.7E+7	-8.82	5.3E+5	1.62	0.929	-1.7E+7	6.29	5.9E+5	1.80	0.843
2	3	1.8E+7	72.04	6.1E+5	1.86	0.998	2.0E+7	73.31	5.5E+5	1.69	0.999	1.6E+7	-8.38	5.1E+5	1.55	0.927	-1.7E+7	6.61	5.8E+5	1.78	0.859
4	3	1.9E+7	64.55	5.6E+5	1.69	0.998	2.1E+7	66.96	7.0E+5	2.14	0.998	1.6E+7	-6.99	5.9E+5	1.81	0.868	-1.7E+7	7.04	5.5E+5	1.66	0.888
6	3	1.9E+7	63.78	8.0E+5	2.24	0.997	2.1E+7	65.66	6.4E+5	1.78	0.998	1.6E+7	-6.98	7.2E+5	2.00	0.829	-1.7E+7	6.30	8.5E+5	2.36	0.738
8	3	1.8E+7	57.45	6.5E+5	1.99	0.997	2.0E+7	59.58	6.0E+5	1.81	0.998	1.7E+7	-6.79	7.1E+5	2.15	0.815	-1.8E+7	5.74	6.1E+5	1.84	0.810
10	3	1.7E+7	54.92	6.5E+5	1.99	0.997	1.9E+7	56.91	5.7E+5	1.74	0.998	1.7E+7	-5.97	7.1E+5	2.16	0.770	-1.7E+7	5.71	6.0E+5	1.83	0.811
0	4	1.8E+7	76.85	6.5E+5	1.96	0.999	2.0E+7	79.37	6.3E+5	1.91	0.999	1.6E+7	-8.90	5.5E+5	1.67	0.926	-1.7E+7	6.58	6.3E+5	1.92	0.838
2	4	1.8E+7	70.82	6.0E+5	1.81	0.999	2.0E+7	72.31	5.9E+5	1.80	0.999	1.6E+7	-8.76	5.3E+5	1.61	0.929	-1.7E+7	5.83	6.3E+5	1.91	0.804
4	4	1.9E+7	64.63	5.6E+5	1.72	0.998	2.1E+7	66.84	7.5E+5	2.28	0.997	1.6E+7	-7.57	6.4E+5	1.93	0.871	-1.7E+7	6.85	5.5E+5	1.66	0.882
6	4	1.9E+7	63.46	7.8E+5	2.18	0.997	2.1E+7	65.17	6.7E+5	1.87	0.998	1.6E+7	-7.13	7.2E+5	1.99	0.835	-1.7E+7	6.37	8.9E+5	2.48	0.723
8	4	1.8E+7	56.91	6.1E+5	1.85	0.998	2.0E+7	59.77	6.0E+5	1.81	0.998	1.7E+7	-7.40	6.0E+5	1.82	0.879	-1.8E+7	5.89	6.4E+5	1.94	0.803
10	4	1.8E+7	54.37	6.0E+5	1.82	0.997	1.9E+7	56.29	6.2E+5	1.87	0.997	1.8E+7	-5.16	7.1E+5	2.17	0.714	-1.7E+7	6.87	5.9E+5	1.81	0.864
0	5	1.7E+7	75.27	7.1E+5	2.16	0.998	1.9E+7	77.99	5.6E+5	1.69	0.999	1.9E+7	-10.77	6.4E+5	1.96	0.930	-2.0E+7	8.12	7.8E+5	2.37	0.838
2	5	1.7E+7	67.58	7.0E+5	2.13	0.998	1.9E+7	70.40	7.6E+5	2.31	0.998	2.1E+7	-8.16	8.4E+5	2.55	0.818	-2.0E+7	8.08	8.8E+5	2.67	0.801
4	5	1.6E+7	58.83	6.8E+5	2.08	0.997	1.8E+7	61.35	1.2E+6	3.77	0.992	2.2E+7	-4.43	9.9E+5	3.02	0.487	-2.1E+7	7.81	8.9E+5	2.70	0.787
6	5	1.5E+7	58.37	9.4E+5	2.61	0.995	1.5E+7	57.19	1.2E+6	3.31	0.992	2.4E+7	-3.67	1.1E+6	3.15	0.349	-2.0E+7	6.33	1.1E+6	2.93	0.649
8	5	1.4E+7	53.38	9.7E+5	2.70	0.994	1.3E+7	52.36	1.1E+6	3.19	0.991	2.6E+7	-3.73	1.2E+6	3.37	0.327	-2.1E+7	4.48	1.0E+6	2.80	0.502
10	5	9.8E+6	46.25	8.6E+5	2.50	0.994	6.9E+6	45.77	8.7E+5	2.53	0.994	3.0E+7	0.97	1.1E+6	3.14	0.045	-2.0E+7	5.05	7.2E+5	2.10	0.741

Table 179 Curve-fitted results of imaginary parts at PD=20.7 bar for the test seal with the medium-preswirl insert in pure- and mainly-oil conditions

Inlet GVF	ω	C_{xx}	eC_{xx}	R^2_{xx}	C_{yy}	eC_{yy}	R^2_{yy}	C_{xy}	eC_{xy}	R^2_{xy}	C_{yx}	eC_{yx}	R^2_{yx}
%	krpm	N-s/m	N-s/m		N-s/m	N-s/m		N-s/m	N-s/m		N-s/m	N-s/m	
0	3	8.5E+4	2.1E+3	0.994	2.5E+4	8.9E+2	0.984	-2.7E+4	1.6E+3	0.971	8.3E+4	2.3E+3	0.992
2	3	8.3E+4	2.4E+3	0.992	2.4E+4	1.0E+3	0.977	-2.6E+4	1.4E+3	0.972	8.1E+4	2.5E+3	0.991
4	3	8.5E+4	2.4E+3	0.992	2.2E+4	8.4E+2	0.984	-2.5E+4	1.5E+3	0.966	8.2E+4	2.5E+3	0.991
6	3	8.8E+4	2.9E+3	0.988	2.1E+4	7.4E+2	0.984	-2.3E+4	1.3E+3	0.967	8.6E+4	3.0E+3	0.986
8	3	9.1E+4	3.6E+3	0.985	1.9E+4	1.3E+3	0.947	-2.1E+4	1.6E+3	0.946	8.8E+4	3.7E+3	0.983
10	3	9.3E+4	3.7E+3	0.985	1.7E+4	1.4E+3	0.917	-2.1E+4	1.6E+3	0.942	8.9E+4	3.5E+3	0.985
0	4	8.5E+4	2.2E+3	0.994	2.5E+4	8.4E+2	0.986	-2.7E+4	1.5E+3	0.972	8.3E+4	2.3E+3	0.992
2	4	8.4E+4	2.4E+3	0.992	2.3E+4	9.9E+2	0.978	-2.5E+4	1.6E+3	0.965	8.2E+4	2.7E+3	0.989
4	4	8.5E+4	2.4E+3	0.992	2.3E+4	7.8E+2	0.986	-2.4E+4	1.6E+3	0.963	8.3E+4	2.6E+3	0.990
6	4	8.8E+4	2.9E+3	0.989	2.1E+4	7.1E+2	0.985	-2.3E+4	1.2E+3	0.968	8.6E+4	3.0E+3	0.987
8	4	9.1E+4	3.8E+3	0.984	1.9E+4	1.3E+3	0.943	-2.1E+4	1.7E+3	0.935	8.9E+4	3.6E+3	0.984
10	4	9.4E+4	3.9E+3	0.984	1.7E+4	1.5E+3	0.896	-2.2E+4	1.6E+3	0.941	9.0E+4	3.4E+3	0.986
0	5	8.6E+4	2.2E+3	0.993	3.0E+4	8.7E+2	0.991	-3.3E+4	1.9E+3	0.970	8.5E+4	2.4E+3	0.992
2	5	8.8E+4	2.9E+3	0.990	2.6E+4	1.3E+3	0.970	-3.1E+4	2.1E+3	0.961	8.5E+4	2.9E+3	0.989
4	5	9.1E+4	2.7E+3	0.991	2.2E+4	1.3E+3	0.968	-2.9E+4	2.0E+3	0.954	8.8E+4	2.6E+3	0.991
6	5	9.7E+4	2.9E+3	0.990	1.9E+4	1.2E+3	0.961	-2.8E+4	1.8E+3	0.957	9.2E+4	3.0E+3	0.988
8	5	1.0E+5	3.3E+3	0.989	1.6E+4	1.2E+3	0.947	-2.6E+4	2.0E+3	0.940	9.6E+4	3.1E+3	0.989
10	5	1.1E+5	3.7E+3	0.989	1.2E+4	1.9E+3	0.856	-2.5E+4	1.8E+3	0.948	9.9E+4	2.8E+3	0.992

Table 180 Curve-fitted results of real parts at PD=27.6 bar for the test seal with the medium-preswirl insert in pure- and mainly-oil conditions

Inlet GVF	ω	K_{xx}	M_{xx}	eK_{xx}	eM_{xx}	R^2_{xx}	K_{yy}	M_{yy}	eK_{yy}	eM_{yy}	R^2_{yy}	K_{xy}	M_{xy}	eK_{xy}	eM_{xy}	R^2_{xy}	K_{yx}	M_{yx}	eK_{yx}	eM_{yx}	R^2_{yx}
%	krpm	N/m	kg	N/m	kg		N/m	kg	N/m	kg		N/m	kg	N/m	kg		N/m	kg	N/m	kg	
0	3	2.5E+7	73.43	8.8E+5	2.44	0.997	2.5E+7	73.13	1.2E+6	3.23	0.995	2.3E+7	-7.50	8.2E+5	2.28	0.811	-2.0E+7	7.45	1.1E+6	3.04	0.704
2	3	1.4E+7	51.96	1.4E+6	3.84	0.986	1.5E+7	47.41	2.0E+6	5.44	0.968	2.5E+7	-10.78	1.4E+6	3.96	0.746	-2.4E+7	-2.21	1.3E+6	3.67	0.125
4	3	1.3E+7	45.45	1.6E+6	4.89	0.974	1.1E+7	41.43	1.4E+6	4.20	0.977	2.7E+7	-6.53	1.4E+6	4.36	0.498	-2.2E+7	6.00	9.1E+5	2.77	0.675
0	4	2.3E+7	69.64	8.4E+5	2.57	0.997	2.3E+7	68.47	1.3E+6	4.09	0.992	2.4E+7	-7.43	5.6E+5	1.71	0.893	-2.0E+7	8.74	9.4E+5	2.87	0.804
2	4	8.5E+6	46.18	2.0E+6	6.10	0.962	9.8E+6	36.34	2.4E+6	7.24	0.917	2.5E+7	-13.34	1.8E+6	5.42	0.727	-2.7E+7	-4.84	1.3E+6	3.84	0.411
4	4	1.0E+7	42.21	1.9E+6	5.73	0.960	7.0E+6	37.58	9.6E+5	2.92	0.986	2.8E+7	-4.97	1.7E+6	5.28	0.281	-2.1E+7	8.71	9.4E+5	2.86	0.803
0	5	1.5E+7	64.08	1.3E+6	4.01	0.991	1.2E+7	56.80	2.0E+6	5.95	0.976	3.2E+7	-4.32	1.2E+6	3.73	0.372	-2.6E+7	2.14	8.1E+5	2.46	0.250
2	5	3.5E+6	44.07	1.4E+6	3.89	0.981	3.8E+5	40.03	2.7E+6	7.47	0.919	3.7E+7	-4.08	2.1E+6	5.96	0.157	-3.0E+7	-4.94	1.8E+6	4.87	0.289

Table 181 Curve-fitted results of imaginary parts at PD=20.7 bar for the test seal with the medium-preswirl insert in pure- and mainly-oil conditions

Inlet GVF	ω	C_{xx}	eC_{xx}	R^2_{xx}	C_{yy}	eC_{yy}	R^2_{yy}	C_{xy}	eC_{xy}	R^2_{xy}	C_{yx}	eC_{yx}	R^2_{yx}
%	krpm	N-s/m	N-s/m		N-s/m	N-s/m		N-s/m	N-s/m		N-s/m	N-s/m	
0	3	9.8E+4	2.0E+3	0.995	2.0E+4	1.1E+3	0.964	-3.0E+4	1.5E+3	0.972	9.1E+4	2.4E+3	0.993
2	3	1.1E+5	1.9E+3	0.996	1.5E+4	2.0E+3	0.768	-2.0E+4	2.4E+3	0.896	1.1E+5	3.0E+3	0.991
4	3	1.2E+5	1.8E+3	0.998	1.2E+4	2.3E+3	0.779	-2.2E+4	2.0E+3	0.929	1.1E+5	3.8E+3	0.989
0	4	1.0E+5	1.8E+3	0.997	2.0E+4	1.2E+3	0.956	-2.8E+4	1.9E+3	0.959	9.4E+4	2.8E+3	0.992
2	4	1.2E+5	3.4E+3	0.990	1.6E+4	2.8E+3	0.639	-1.4E+4	3.2E+3	0.786	1.1E+5	4.2E+3	0.988
4	4	1.2E+5	2.6E+3	0.996	1.1E+4	2.8E+3	0.681	-2.2E+4	1.9E+3	0.934	1.1E+5	3.8E+3	0.989
0	5	1.1E+5	2.4E+3	0.995	1.7E+4	2.1E+3	0.901	-3.0E+4	2.4E+3	0.935	1.0E+5	3.8E+3	0.988
2	5	1.3E+5	2.9E+3	0.994	9.5E+3	2.2E+3	0.716	-1.7E+4	3.6E+3	0.783	1.2E+5	3.2E+3	0.992

Table 182 Curve-fitted results of real parts at PD=20.7 bar for the test seal with the high-preswirl insert in pure- and mainly-oil conditions

Inlet GVF	ω	K_{xx}	M_{xx}	eK_{xx}	eM_{xx}	R^2_{xx}	K_{yy}	M_{yy}	eK_{yy}	eM_{yy}	R^2_{yy}	K_{xy}	M_{xy}	eK_{xy}	eM_{xy}	R^2_{xy}	K_{yx}	M_{yx}	eK_{yx}	eM_{yx}	R^2_{yx}
%	krpm	N/m	kg	N/m	kg		N/m	kg	N/m	kg		N/m	kg	N/m	kg		N/m	kg	N/m	kg	
0	3	1.7E+7	78.59	5.2E+5	1.40	0.999	1.8E+7	79.37	5.7E+5	1.53	0.999	2.1E+7	-10.32	4.5E+5	1.22	0.969	-2.2E+7	6.52	2.7E+5	0.72	0.973
2	3	1.7E+7	71.44	2.8E+5	0.75	1.000	1.7E+7	70.85	6.5E+5	1.74	0.999	2.2E+7	-8.01	4.9E+5	1.32	0.942	-2.2E+7	6.84	4.0E+5	1.08	0.947
4	3	1.7E+7	66.07	3.8E+5	1.01	0.999	1.7E+7	64.41	8.9E+5	2.39	0.997	2.2E+7	-7.49	7.2E+5	1.92	0.870	-2.2E+7	8.30	4.1E+5	1.11	0.961
6	3	1.7E+7	64.18	2.3E+5	0.62	1.000	1.7E+7	61.38	9.2E+5	2.48	0.996	2.2E+7	-7.19	7.6E+5	2.05	0.845	-2.2E+7	7.59	4.8E+5	1.30	0.938
8	3	1.7E+7	61.69	8.6E+5	2.40	0.996	1.5E+7	55.29	1.2E+6	3.37	0.991	2.2E+7	-5.62	9.9E+5	2.74	0.624	-2.3E+7	4.72	9.1E+5	2.53	0.578
10	3	1.6E+7	57.36	9.6E+5	2.67	0.995	1.4E+7	51.03	1.1E+6	3.17	0.990	2.3E+7	-5.06	7.8E+5	2.18	0.682	-2.3E+7	4.30	9.5E+5	2.65	0.510
0	4	1.7E+7	78.83	5.1E+5	1.36	0.999	1.8E+7	79.58	6.0E+5	1.60	0.999	2.1E+7	-10.23	4.1E+5	1.10	0.975	-2.2E+7	6.81	2.4E+5	0.65	0.980
2	4	1.7E+7	70.08	2.7E+5	0.72	1.000	1.6E+7	67.43	8.6E+5	2.31	0.997	2.2E+7	-7.71	5.3E+5	1.41	0.929	-2.2E+7	7.54	4.5E+5	1.19	0.946
4	4	1.7E+7	66.24	4.1E+5	1.10	0.999	1.6E+7	65.12	8.4E+5	2.25	0.997	2.1E+7	-8.11	7.1E+5	1.90	0.890	-2.2E+7	8.53	3.4E+5	0.91	0.975
6	4	1.8E+7	65.11	7.7E+5	2.14	0.997	1.7E+7	60.46	1.1E+6	2.94	0.994	2.2E+7	-6.50	8.5E+5	2.38	0.747	-2.3E+7	6.10	9.6E+5	2.68	0.673
8	4	1.7E+7	61.53	8.1E+5	2.25	0.997	1.5E+7	55.58	1.2E+6	3.22	0.992	2.2E+7	-5.68	8.7E+5	2.41	0.687	-2.3E+7	5.61	9.2E+5	2.55	0.658
10	4	1.6E+7	55.21	8.2E+5	2.28	0.996	1.2E+7	49.23	1.3E+6	3.48	0.988	2.4E+7	-5.00	8.7E+5	2.41	0.631	-2.2E+7	6.29	8.8E+5	2.44	0.725
0	5	1.6E+7	78.19	5.9E+5	1.59	0.999	1.7E+7	78.46	4.8E+5	1.30	0.999	2.3E+7	-12.29	7.5E+5	2.01	0.943	-2.4E+7	9.17	3.3E+5	0.87	0.980
2	5	1.7E+7	69.87	8.6E+5	2.40	0.997	1.3E+7	61.93	1.2E+6	3.47	0.992	2.6E+7	-6.64	1.0E+6	2.87	0.679	-2.5E+7	6.33	1.3E+6	3.59	0.552
4	5	1.6E+7	63.82	7.0E+5	1.93	0.998	1.1E+7	55.08	1.4E+6	3.82	0.988	2.6E+7	-6.21	1.2E+6	3.29	0.585	-2.5E+7	7.82	1.1E+6	2.95	0.735
6	5	1.5E+7	60.51	8.3E+5	2.30	0.996	7.0E+6	49.12	1.1E+6	3.19	0.989	2.7E+7	-7.76	1.2E+6	3.42	0.671	-2.5E+7	5.73	9.8E+5	2.72	0.637
8	5	1.4E+7	56.93	9.9E+5	2.75	0.994	6.8E+6	43.81	1.4E+6	3.89	0.980	2.8E+7	-5.89	1.2E+6	3.35	0.550	-2.6E+7	3.77	1.1E+6	2.96	0.391
10	5	1.4E+7	53.26	1.0E+6	2.91	0.993	5.8E+6	40.69	1.4E+6	3.81	0.978	2.7E+7	-6.64	1.1E+6	3.00	0.659	-2.7E+7	1.29	1.1E+6	2.92	0.071

Table 183 Curve-fitted results of imaginary parts at PD=20.7 bar for the test seal with the high-preswirl insert in pure- and mainly-oil conditions

Inlet GVF	ω	C_{xx}	eC_{xx}	R^2_{xx}	C_{yy}	eC_{yy}	R^2_{yy}	C_{xy}	eC_{xy}	R^2_{xy}	C_{yx}	eC_{yx}	R^2_{yx}
%	krpm	N-s/m	N-s/m		N-s/m	N-s/m		N-s/m	N-s/m		N-s/m	N-s/m	
0	3	8.7E+4	1.9E+3	0.995	2.7E+4	4.1E+2	0.997	-2.9E+4	4.7E+2	0.997	8.4E+4	1.6E+3	0.996
2	3	8.9E+4	2.2E+3	0.993	2.5E+4	4.6E+2	0.996	-2.7E+4	4.7E+2	0.996	8.2E+4	1.7E+3	0.995
4	3	9.1E+4	2.2E+3	0.994	2.5E+4	6.6E+2	0.991	-2.5E+4	4.9E+2	0.995	8.5E+4	1.6E+3	0.996
6	3	9.4E+4	2.7E+3	0.991	2.4E+4	4.8E+2	0.995	-2.3E+4	5.5E+2	0.992	8.7E+4	2.5E+3	0.991
8	3	9.6E+4	2.4E+3	0.993	2.2E+4	6.3E+2	0.991	-2.2E+4	8.7E+2	0.975	8.8E+4	2.4E+3	0.991
10	3	9.7E+4	2.4E+3	0.993	2.0E+4	6.2E+2	0.989	-2.1E+4	9.1E+2	0.970	8.9E+4	2.2E+3	0.993
0	4	8.6E+4	1.9E+3	0.995	2.8E+4	3.9E+2	0.997	-2.9E+4	4.9E+2	0.997	8.4E+4	1.6E+3	0.996
2	4	9.0E+4	2.3E+3	0.993	2.5E+4	5.2E+2	0.994	-2.7E+4	4.8E+2	0.996	8.3E+4	1.7E+3	0.995
4	4	9.1E+4	2.2E+3	0.993	2.5E+4	5.8E+2	0.994	-2.5E+4	4.4E+2	0.996	8.6E+4	1.7E+3	0.995
6	4	9.3E+4	2.5E+3	0.992	2.3E+4	5.5E+2	0.993	-2.3E+4	6.1E+2	0.990	8.6E+4	2.3E+3	0.992
8	4	9.6E+4	2.5E+3	0.992	2.2E+4	6.1E+2	0.991	-2.2E+4	8.8E+2	0.976	8.8E+4	2.4E+3	0.992
10	4	1.0E+5	2.7E+3	0.992	1.9E+4	6.7E+2	0.985	-2.2E+4	1.2E+3	0.946	9.0E+4	2.1E+3	0.994
0	5	8.8E+4	1.9E+3	0.995	3.3E+4	5.5E+2	0.997	-3.4E+4	4.5E+2	0.998	8.5E+4	1.6E+3	0.996
2	5	9.6E+4	2.4E+3	0.993	2.7E+4	1.1E+3	0.980	-3.1E+4	8.6E+2	0.990	8.6E+4	1.8E+3	0.995
4	5	9.8E+4	2.5E+3	0.993	2.5E+4	1.3E+3	0.973	-3.0E+4	1.1E+3	0.978	8.7E+4	1.7E+3	0.996
6	5	1.0E+5	2.6E+3	0.993	2.4E+4	8.8E+2	0.985	-2.7E+4	1.1E+3	0.975	9.0E+4	2.2E+3	0.993
8	5	1.0E+5	2.2E+3	0.995	2.2E+4	8.4E+2	0.984	-2.4E+4	1.2E+3	0.958	9.1E+4	2.2E+3	0.994
10	5	1.1E+5	2.6E+3	0.993	2.2E+4	8.9E+2	0.983	-2.3E+4	1.8E+3	0.878	9.3E+4	2.1E+3	0.994

Table 184 Curve-fitted results of real parts at PD=27.6 bar for the test seal with the high-preswirl insert in pure- and mainly-oil conditions

Inlet GVF	ω	K_{xx}	M_{xx}	eK_{xx}	eM_{xx}	R^2_{xx}	K_{yy}	M_{yy}	eK_{yy}	eM_{yy}	R^2_{yy}	K_{xy}	M_{xy}	eK_{xy}	eM_{xy}	R^2_{xy}	K_{yx}	M_{yx}	eK_{yx}	eM_{yx}	R^2_{yx}
%	krpm	N/m	kg	N/m	kg		N/m	kg	N/m	kg		N/m	kg	N/m	kg		N/m	kg	N/m	kg	
0	3	2.4E+7	75.60	1.0E+6	2.89	0.996	2.4E+7	72.55	1.1E+6	2.92	0.996	2.6E+7	-12.01	9.1E+5	2.53	0.899	-3.0E+7	3.55	8.9E+5	2.46	0.451
2	3	1.7E+7	55.33	1.3E+6	3.38	0.992	6.2E+6	48.89	1.2E+6	3.29	0.990	3.0E+7	-5.58	5.6E+5	1.51	0.858	-2.9E+7	5.83	7.9E+5	2.12	0.769
4	3	9.3E+6	42.72	1.3E+6	3.52	0.983	1.5E+6	43.31	1.1E+6	2.94	0.988	2.9E+7	-4.90	6.9E+5	1.93	0.719	-3.3E+7	2.55	1.3E+6	3.55	0.170
6	3	4.2E+6	35.38	1.2E+6	3.29	0.979	-5.8E+5	37.08	1.4E+6	4.02	0.971	2.7E+7	-9.05	7.0E+5	1.95	0.895	-3.4E+7	-0.07	1.4E+6	3.77	0.000
8	3	-6.4E+6	23.13	2.2E+6	6.17	0.848	-2.5E+6	36.31	1.9E+6	5.19	0.951	2.7E+7	-9.85	1.5E+6	4.28	0.677	-3.5E+7	-1.26	1.4E+6	3.92	0.039
10	3	-1.0E+7	29.61	3.3E+6	9.07	0.808	-3.0E+6	34.95	2.8E+6	7.79	0.888	2.7E+7	-10.13	2.3E+6	6.48	0.491	-3.7E+7	-0.70	2.5E+6	6.90	0.004
0	4	2.3E+7	75.02	1.0E+6	2.86	0.996	2.3E+7	70.37	1.1E+6	3.07	0.995	2.6E+7	-12.00	8.4E+5	2.34	0.913	-3.1E+7	2.33	9.6E+5	2.67	0.232
2	4	1.2E+7	50.78	9.6E+5	2.66	0.993	2.7E+6	45.64	1.3E+6	3.52	0.985	2.9E+7	-6.48	7.0E+5	1.95	0.814	-3.2E+7	-0.05	1.0E+6	2.92	0.000
4	4	9.9E+6	43.12	1.1E+6	2.93	0.988	9.7E+5	40.62	1.1E+6	3.16	0.985	2.8E+7	-5.77	6.0E+5	1.68	0.823	-3.3E+7	1.46	1.4E+6	3.78	0.055
6	4	2.7E+6	31.77	2.0E+6	5.54	0.929	-1.2E+6	39.07	1.7E+6	4.86	0.962	3.0E+7	-3.51	1.4E+6	3.91	0.242	-3.3E+7	1.16	1.4E+6	3.84	0.035
8	4	-6.7E+6	23.66	2.2E+6	6.14	0.854	-3.3E+6	35.18	1.9E+6	5.42	0.944	2.7E+7	-8.94	1.6E+6	4.41	0.619	-3.5E+7	-1.56	1.4E+6	3.82	0.062
0	5	2.2E+7	73.08	1.2E+6	3.36	0.995	2.1E+7	70.00	9.8E+5	2.71	0.996	2.9E+7	-9.71	1.3E+6	3.50	0.752	-3.1E+7	6.72	7.4E+5	2.05	0.810
2	5	8.4E+6	44.18	1.9E+6	5.29	0.965	-1.9E+6	42.01	9.9E+5	2.77	0.989	3.4E+7	-3.89	6.6E+5	1.84	0.639	-3.7E+7	-2.72	1.3E+6	3.54	0.189
4	5	2.6E+5	28.07	4.7E+6	13.15	0.643	-4.8E+6	41.48	3.4E+6	9.41	0.885	3.6E+7	2.47	3.2E+6	8.78	0.030	-3.6E+7	5.62	2.5E+6	7.05	0.201

Table 185 Curve-fitted results of imaginary parts at PD=20.7 bar for the test seal with the high-preswirl insert in pure- and mainly-oil conditions

Inlet GVF	ω	C_{xx}	eC_{xx}	R^2_{xx}	C_{yy}	eC_{yy}	R^2_{yy}	C_{xy}	eC_{xy}	R^2_{xy}	C_{yx}	eC_{yx}	R^2_{yx}
%	krpm	N-s/m	N-s/m		N-s/m	N-s/m		N-s/m	N-s/m		N-s/m	N-s/m	
0	3	9.8E+4	1.4E+3	0.998	3.0E+4	8.0E+2	0.990	-2.7E+4	1.0E+3	0.985	9.3E+4	1.1E+3	0.998
2	3	1.2E+5	2.3E+3	0.996	2.2E+4	9.9E+2	0.980	-2.5E+4	1.4E+3	0.948	1.0E+5	1.1E+3	0.999
4	3	1.2E+5	1.7E+3	0.998	2.2E+4	8.0E+2	0.985	-1.7E+4	1.1E+3	0.945	1.1E+5	6.4E+2	1.000
6	3	1.3E+5	1.4E+3	0.999	2.2E+4	5.2E+2	0.993	-1.4E+4	1.0E+3	0.924	1.2E+5	8.6E+2	0.999
8	3	1.3E+5	2.0E+3	0.997	1.9E+4	1.6E+3	0.904	-1.1E+4	1.6E+3	0.780	1.3E+5	1.6E+3	0.998
10	3	1.4E+5	2.5E+3	0.996	1.9E+4	1.8E+3	0.893	-1.0E+4	3.5E+3	0.602	1.3E+5	4.6E+3	0.987
0	4	9.9E+4	1.4E+3	0.998	3.0E+4	7.7E+2	0.991	-2.6E+4	1.0E+3	0.984	9.4E+4	1.1E+3	0.998
2	4	1.2E+5	1.5E+3	0.998	2.4E+4	9.9E+2	0.978	-2.1E+4	8.8E+2	0.976	1.1E+5	6.6E+2	1.000
4	4	1.3E+5	1.5E+3	0.998	2.2E+4	7.6E+2	0.987	-1.8E+4	1.0E+3	0.953	1.1E+5	6.7E+2	1.000
6	4	1.3E+5	2.0E+3	0.997	1.9E+4	9.6E+2	0.972	-1.4E+4	1.3E+3	0.901	1.3E+5	1.9E+3	0.997
8	4	1.3E+5	1.9E+3	0.997	1.8E+4	1.7E+3	0.893	-1.1E+4	1.9E+3	0.731	1.3E+5	1.6E+3	0.998
0	5	1.0E+5	1.6E+3	0.997	3.3E+4	1.3E+3	0.976	-3.3E+4	1.3E+3	0.984	9.6E+4	1.2E+3	0.998
2	5	1.3E+5	2.7E+3	0.995	2.4E+4	1.5E+3	0.959	-2.2E+4	1.3E+3	0.954	1.1E+5	1.6E+3	0.997
4	5	1.3E+5	5.0E+3	0.985	1.7E+4	4.1E+3	0.625	-1.6E+4	4.8E+3	0.582	1.3E+5	5.6E+3	0.972

Table 186 Curve-fitted results of imaginary parts at PR=0.6 for the test seal with the zero-preswirl insert in pure- and mainly-air conditions

PR	Inlet LVF	Speed	C_{xx}	eC_{xx}	R^2_{xx}	C_{yy}	eC_{yy}	R^2_{yy}	C_{xy}	eC_{xy}	R^2_{xy}	C_{yx}	eC_{yx}	R^2_{yx}
	%	krpm	N-s/m	N-s/m		N-s/m	N-s/m		N-s/m	N-s/m		N-s/m	N-s/m	
0.6	0	5	2.2E+4	4.7E+2	0.995	2.5E+4	6.3E+2	0.993	1.3E+3	3.6E+2	0.471	-8.1E+2	4.3E+2	0.346
0.6	2	5	3.1E+4	3.2E+2	0.999	3.4E+4	4.2E+2	0.998	1.1E+3	5.2E+2	0.000	-3.1E+2	5.8E+2	0.000
0.6	4	5	3.3E+4	4.6E+2	0.998	3.5E+4	4.6E+2	0.998	1.8E+3	9.6E+2	0.000	2.5E+2	7.0E+2	0.000
0.6	6	5	3.4E+4	8.0E+2	0.994	3.7E+4	5.4E+2	0.997	2.1E+3	1.3E+3	0.000	1.7E+2	9.4E+2	0.000
0.6	8	5	3.5E+4	9.5E+2	0.992	3.7E+4	6.3E+2	0.997	1.9E+3	1.4E+3	0.000	6.1E+2	1.2E+3	0.000
0.6	0	10	2.3E+4	6.7E+2	0.991	2.5E+4	6.3E+2	0.993	1.8E+3	4.7E+2	0.303	-1.8E+3	4.3E+2	0.581
0.6	2	10	3.3E+4	5.7E+2	0.997	3.4E+4	7.4E+2	0.994	1.7E+3	5.3E+2	0.000	-9.8E+2	4.2E+2	0.461
0.6	4	10	3.4E+4	1.2E+3	0.987	3.6E+4	6.6E+2	0.996	2.8E+3	5.5E+2	0.378	-1.1E+3	6.4E+2	0.394
0.6	6	10	3.5E+4	1.5E+3	0.982	3.8E+4	7.7E+2	0.995	3.6E+3	6.4E+2	0.054	-9.3E+2	7.0E+2	0.339
0.6	8	10	3.6E+4	1.9E+3	0.972	4.0E+4	5.9E+2	0.997	3.9E+3	4.7E+2	0.722	-2.1E+3	8.8E+2	0.560
0.6	0	15	2.4E+4	5.8E+2	0.993	2.5E+4	6.9E+2	0.992	2.4E+3	4.0E+2	0.594	-2.2E+3	2.8E+2	0.834
0.6	2	15	3.3E+4	4.9E+2	0.997	3.5E+4	9.0E+2	0.992	1.8E+3	5.6E+2	0.171	-7.6E+2	7.0E+2	0.000
0.6	4	15	3.3E+4	1.5E+3	0.981	3.8E+4	9.8E+2	0.992	2.6E+3	5.9E+2	0.543	-9.2E+2	8.1E+2	0.141

Table 187 Curve-fitted results of imaginary parts at PR=0.5 for the test seal with the zero-preswirl insert in pure- and mainly-air conditions

PR	Inlet LVF	Speed	C_{xx}	eC_{xx}	R^2_{xx}	C_{yy}	eC_{yy}	R^2_{yy}	C_{xy}	eC_{xy}	R^2_{xy}	C_{yx}	eC_{yx}	R^2_{yx}
	%	krpm	N-s/m	N-s/m		N-s/m	N-s/m		N-s/m	N-s/m		N-s/m	N-s/m	
0.5	0	5	2.7E+4	4.2E+2	0.997	2.8E+4	6.0E+2	0.995	1.1E+3	4.3E+2	0.250	-4.9E+2	4.1E+2	0.240
0.5	2	5	3.4E+4	3.4E+2	0.999	3.6E+4	4.4E+2	0.998	1.2E+3	6.4E+2	0.000	2.6E+2	5.4E+2	0.000
0.5	4	5	3.5E+4	8.3E+2	0.994	3.7E+4	6.0E+2	0.997	1.7E+3	1.1E+3	0.000	1.1E+3	8.7E+2	0.000
0.5	6	5	3.6E+4	1.1E+3	0.990	3.9E+4	6.8E+2	0.996	2.0E+3	1.6E+3	0.000	1.5E+3	1.2E+3	0.000
0.5	8	5	3.8E+4	1.3E+3	0.988	4.0E+4	5.3E+2	0.998	2.2E+3	1.5E+3	0.000	1.3E+3	1.6E+3	0.000
0.5	0	10	2.7E+4	5.3E+2	0.996	2.9E+4	7.7E+2	0.992	1.3E+3	4.6E+2	0.346	-9.6E+2	4.2E+2	0.403
0.5	2	10	3.6E+4	5.0E+2	0.998	3.7E+4	5.5E+2	0.997	1.6E+3	5.8E+2	0.000	-1.1E+2	5.7E+2	0.000
0.5	4	10	3.6E+4	1.4E+3	0.984	3.8E+4	4.4E+2	0.998	2.4E+3	7.5E+2	0.000	-4.5E+2	8.8E+2	0.079
0.5	6	10	3.7E+4	1.9E+3	0.973	4.1E+4	5.8E+2	0.997	2.9E+3	9.6E+2	0.000	-1.0E+3	1.4E+3	0.155
0.5	8	10	3.9E+4	2.0E+3	0.974	4.4E+4	9.0E+2	0.994	3.3E+3	1.0E+3	0.000	-1.2E+3	1.3E+3	0.240
0.5	0	15	2.7E+4	7.0E+2	0.992	2.9E+4	7.5E+2	0.993	2.0E+3	5.5E+2	0.227	-1.2E+3	2.9E+2	0.461
0.5	2	15	3.5E+4	8.9E+2	0.993	3.8E+4	8.2E+2	0.994	8.8E+2	5.1E+2	0.083	1.5E+2	5.1E+2	0.000
0.5	4	15	3.6E+4	1.5E+3	0.983	4.1E+4	6.5E+2	0.997	1.7E+3	5.4E+2	0.557	1.8E+2	6.9E+2	0.000

Table 188 Curve-fitted results of imaginary parts at PR=0.4 for the test seal with the zero-preswirl insert in pure- and mainly-air conditions

PR	Inlet LVF	Speed	C_{xx}	eC_{xx}	R^2_{xx}	C_{yy}	eC_{yy}	R^2_{yy}	C_{xy}	eC_{xy}	R^2_{xy}	C_{yx}	eC_{yx}	R^2_{yx}
	%	krpm	N-s/m	N-s/m		N-s/m	N-s/m		N-s/m	N-s/m		N-s/m	N-s/m	
0.4	0	5	3.1E+4	3.2E+2	0.999	3.2E+4	4.8E+2	0.997	1.0E+3	4.3E+2	0.128	1.8E+1	3.6E+2	0.000
0.4	2	5	3.9E+4	5.7E+2	0.997	4.1E+4	4.9E+2	0.998	9.8E+2	4.4E+2	0.000	7.8E+2	3.8E+2	0.000
0.4	4	5	3.8E+4	1.0E+3	0.993	4.0E+4	6.6E+2	0.997	1.9E+3	1.2E+3	0.000	1.8E+3	9.4E+2	0.000
0.4	6	5	4.0E+4	9.6E+2	0.994	4.2E+4	7.0E+2	0.997	1.4E+3	1.5E+3	0.000	2.1E+3	1.3E+3	0.000
0.4	8	5	4.3E+4	1.3E+3	0.990	4.5E+4	6.1E+2	0.998	1.2E+3	1.7E+3	0.000	3.1E+3	1.7E+3	0.000
0.4	0	10	3.2E+4	3.1E+2	0.999	3.3E+4	5.2E+2	0.997	6.2E+2	3.8E+2	0.000	2.7E+1	3.4E+2	0.001
0.4	2	10	3.9E+4	6.9E+2	0.996	4.1E+4	6.1E+2	0.997	1.1E+3	6.8E+2	0.000	8.3E+2	6.3E+2	0.020
0.4	4	10	4.0E+4	1.4E+3	0.987	4.2E+4	5.7E+2	0.998	2.1E+3	1.2E+3	0.000	7.6E+2	8.1E+2	0.000
0.4	6	10	4.1E+4	1.5E+3	0.986	4.5E+4	6.5E+2	0.997	2.4E+3	1.2E+3	0.000	1.8E+2	1.2E+3	0.000
0.4	8	10	4.3E+4	1.9E+3	0.981	4.7E+4	6.7E+2	0.997	3.0E+3	1.3E+3	0.000	-4.7E+1	1.2E+3	0.000
0.4	0	15	3.3E+4	4.8E+2	0.998	3.5E+4	6.5E+2	0.996	4.9E+2	3.2E+2	0.180	2.4E+2	3.4E+2	0.144
0.4	2	15	4.0E+4	8.5E+2	0.995	4.3E+4	8.0E+2	0.996	-5.5E+0	5.0E+2	0.000	2.4E+3	7.9E+2	0.582
0.4	4	15	4.0E+4	1.4E+3	0.987	4.4E+4	5.6E+2	0.998	9.6E+2	7.2E+2	0.059	1.7E+3	1.1E+3	0.000